NASA Engineering and Safety Center
Technical Assessment Report

Volume I

Pilot Breathing Assessment

November 19, 2020

Report Approval and Revision History

NOTE: This document was approved at the November 19, 2020, NRB. This document was submitted to the NESC Director on November 23, 2020, for configuration control.

Approved:	*Original Signature on File*	11/23/20
	NESC Director	Date

Version	Description of Revision	Office of Primary Responsibility	Effective Date
1.0	Initial Release	Clint Cragg, NESC Principal Engineer's Office, LaRC	11/19/2020
1.1	Minor changes made to Section 1.4.2 and Appendix 6 (Vol. II)	Clint Cragg, NESC Principal Engineer's Office, LaRC	12/03/2020
1.2	Volumes I and II: Export Control deemed report has no restrictions. Removed SBU cover, EAR statement, and adjusted footer.	Clint Cragg, NESC Principal Engineer's Office, LaRC	2/03/2021

Table of Contents

Technical Assessment Report

List of Figures

List of Tables

Technical Assessment Report

Signature Page

Submitted by:

Team Signature Page on File – 11/23/20

Mr. Clinton H. Cragg Date

Significant Contributors:

Dr. W. Lance Richards Date	Dr. David J. Alexander Date
Col. Kevin “Sonar” Hall Date	Dr. Craig S. Schallhorn Date
Dr. John C. Graf Date	Dr. Daniel L. Dietrich Date
Mr. Jon P. Haas Date	Mr. David L. Iverson Date
Ms. Kellie D. Kennedy Date	Mr. Mark W. Hodge Date
Mr. Christopher M. Matty Date	Dr. Joachim D. Pleil Date
Ms. Marta B. Shelton Date	Dr. Jon R. Sobus Date
Mr. Phillip J. Wellner Date	Mr. James “Clue” Less Date

Signatories declare the findings, observations, and NESC recommendations compiled in the report are factually based from data extracted from program/project documents, contractor reports, and open literature, and/or generated from independently conducted tests, analyses, and inspections.

Abstract

This report represents the third in a series of studies conducted by the NASA Engineering and Safety Center (NESC) to help shed light on Physiological Episodes (PEs) that pilots have been experiencing while flying high performance aircraft. Building on experiences gained with the USAF's F-22 in 2012 and the USN's F/A-18 in 2017, the NESC initiated its Pilot Breathing Assessment (PBA) at NASA Armstrong Flight Research Center in 2018 to gather what was defined in previous studies as the missing element in the PE problem: a robust dataset to quantify how the complex human system interacts with the complex aircraft system operating in the complex flight environment. Before PBA, it was generally accepted that providing adequate oxygen (O_2) line pressure and mask flow was sufficient to meet pilot breathing requirements for all high-performance aircraft operations. PBA has shown that the subtleties in parameter stability, timing and sequencing of the pilot-machine interface are critical. An aircraft breathing system begins to deliver air when it senses pilot inhalation and stops when exhalation is sensed. Lags in response make breathing more difficult despite nominal delivery of O_2, pressure and flow. In PBA, all such timing and sequencing mismatches, collectively designated as Breathing Sequence Disruptions (BSDs), revealed system/pilot interactions that had not been previously documented. Cabin pressure fluctuations were found to interfere with pilot breathing signals, and mask valves response could become erratic over time; both situations caused regulators to deliver air out of step with pilot demands. Certain flight maneuvers such as high-G turns and rapid altitude changes were found to stress the system's response to pilots' immediate air demands. In short, these small, subtle disruptions often go unnoticed but can accumulate to transform simple breathing into complex disrupted patterns, which in turn, forces the pilot to subconsciously adapt or consciously compensate to meet their physiological needs. All PBA flights experienced BSDs, however, disruptions were greater in magnitude and frequency with the use of safety pressure. Cabin pressure fluctuations as small as a few mmHg can cause measurable BSDs. Other features of this report are a Pilot Breathing Almanac which documents the breadth and variety of pilot breathing metrics under various flight conditions. New insights into pilot physiology are presented; for example, pilots may suffer pulmonary decrements during flight that can lower their threshold for developing hypoxia. Specific post-flight results revealed that blood O_2 saturation can regularly drop below 95%, the threshold defining mild hypoxia. In separate ground tests, F-35 breathing systems analysis showed BSDs based on unpredictable pressures and flow within breaths, and between adjacent breaths. PBA also designed, developed, and flight-tested a new sensor integrated within the mask that accurately monitors CO_2 and water vapor concentrations at high temporal resolution (83 Hz). These new miniaturized sensors produced nearly clinical-quality results, yielding new physiological insights. To support follow-on work by the military, this report presents a standardized flight test procedure for the services to adapt and use to establish a baseline of aircraft breathing system performance.

Key recommendations for users and manufacturers of high-performance aircraft include: **1.** Measuring pilot breathing, *in situ*; that should be used in the creation of future hardware and system specifications to meet pilot physiological needs, throughout all relevant flight envelopes. **2.** Reconsidering safety pressure's benefits in light of the problems it introduces to pilot breathing. **3.** Trusting subjective pilot reports of breathing as a significant indication of breathing system performance and following up in a methodical investigative manner with objective data. **4.** Investigating the F-35 Breathing System's BSDs. **5.** Performing standardized flight test procedures to establish and evaluate an aircraft's pilot breathing system performance.

Executive Summary

In early 2017, the Navy requested the NASA Engineering and Safety Center (NESC) provide an independent review of their efforts to address an increased occurrence of physiological episodes (PEs) across their F/A-18 fleet. As a part of this review, the NESC team noted that the Navy's understanding of key pilot physiological parameters was lacking, primarily because data needed to make informed decisions about Human System Integrations (HSI) did not exist. **To shed some light on this important area and by using NASA-owned F-18s and F-15s, the NESC set out to examine pilot physiological responses in high performance aircraft in an effort, aptly named, the Pilot Breathing Assessment (PBA).** Additionally, Admiral Sara Joyner, then head of the Navy's PE Action Team, challenged the NESC to come up with a way to identify problems with 'bad-actor' jets.

Flying began in late-spring 2018 to measure pilot respiratory rates, tidal volumes, and air composition at Armstrong Flight Research Center (AFRC). Using five NASA test pilots, flying six different flight profiles in an F-18A/B or an F-15D, the assessment logged over 100 flights and gathered over 4,750 minutes of analyzable data on pilot-machine-environment states. Measurements were made on both the inhale and exhale lines, as well as in the pilot's mask itself. Spirometry tests were performed before and after many of the flights. Pilot questionnaires helped round out the 'per flight' data collection.

Test profiles were chosen to be challenging, but still within a moderate envelope to avoid risk of Physiological Episodes (PEs). As such, they did not reach the full extent of extreme USAF/USN combat operations. Despite these limitations, breathing issues occurred and are described in this report.

When the PBA team was developing plans for flight tests, suitable pilot breathing was thought about in terms of pressure and flow. The prevailing assumption was that if the inhale line pressure was sufficient and measured flow was adequate, pilot breathing requirements would be met. As PBA flight test data became available, it was realized that the timing and sequencing of the pilot-machine interface was also of prime importance. If a pilot breathing system delivered air to the pilot at the wrong time, breathing was difficult, even with nominal delivery pressure and flow. **Detailed investigations into these Breathing Sequence Disruptions (BSD) (i.e., specific instances of timing mismatch), revealed system interactions and pilot effects that had not been previously recognized.** Cabin pressure fluctuations, for instance, can cause regulators to deliver air out of step with pilot demands. Other examples include pilot mask valves operating incorrectly and the F-35 Breathing System (which, although from limited data, caused more BSDs than any other breathing system reviewed in this report).

BSDs transform simple breathing into complex disrupted patterns, forcing subconscious adaptation or conscious compensation by the pilot. Disruptions cause extra exertional effort and physical compensation during every breath to overcome, like running on a rocky beach instead of a treadmill, and can divert attention from flying, depending on severity. BSDs are frequently subtle enough to go undiagnosed, often violating assumptions and complicating analysis, such as when flow goes the wrong way for just a fraction of a second at the beginning of a breath. They also reduce the volume of air exchanged within the lungs. If this reduced volume persists and if the pilot is unable to compensate by taking deep breaths or by dropping his/her mask, the result can be inadequate ventilation regardless of O_2 levels. BSDs are likely contributors to PEs. The in-flight measurements of breathing system interactions and breathing

system timing, and what they revealed about the pilot-machine-environment interaction, were the most important discoveries of the PBA team.

Overall, PBA was successful for a number of significant reasons: i) PBA developed test methods with a focus on repeat measures, ii) PBA focused on pilot breathing demands with a pilot performing tasks in an actual flight environment, iii) PBA linked real-world flight events to pilot physiological behavior, and iv) PBA established a baseline of pilot pulmonary function and the effect of flying on pilot physiology:

- PBA developed test methods with a focus on repeat measures: A major objective was to develop a process and methodology to measure key physiological parameters that was standardized, systematic, and relatively easy to perform. Using these new methods, PBA was able to make conclusions of pilot breathing under a wide variety of flight conditions with a focus on repeat measures. That is, PBA was designed to have each pilot fly each profile in each type of aircraft and breathing equipment at least twice. Such repeat measures allowed calculations that helped understand if flight-to-flight differences were more likely due to differences among pilot or aircraft or flight environment parameters.

- PBA focused on pilot breathing demands with a pilot performing tasks in an actual flight environment: Flight testing provides a real environment and unique data that cannot be duplicated anywhere else. While individual components have been thoroughly scrutinized (e.g., On-Board Oxygen Generation System (OBOGS)), only a full system of systems assessment like PBA was able to capture the critical interactions in flight. Individual elements of the breathing system, most importantly the pilot, are highly variable with critical interactions that only occur when all elements are present. Additionally, coupling pilot breathing metrics with aircraft data (acceleration, pressures, altitude change) allowed PBA to put the life support data in perspective. Finally, by using only jets with LOX, complications from OBOGS were avoided, enabling a baseline for breathing in configurations that historically has had lower proportions of PEs.

- PBA linked real-world flight events to pilot physiological behavior: PBA acquired in-flight, in situ breathing data and linked these data to pilot physiological responses. When pilots had comments about adverse breathing system performance, there was <u>always</u> objective support in the data corresponding to their subjective observations. When pilots were impacted enough to report an adverse breathing dynamic, the PBA team trusted their reports and took actions to understand and mitigate the breathing dysfunction which led to key findings.

- PBA established a baseline of pilot pulmonary function and the effect of flying on pilot physiology: A key feature of PBA was the inclusion of pulmonary function testing of pilots at four points on a PBA flight day: one hour before and after each flight while the pilot was sitting at rest just prior to donning and just after doffing his flight suit, and the same tests repeated in the chokes while strapped in the jet just minutes prior to take-off and just after returning. These measurements showed a significant negative impact that flying had on the pilot.

<u>PBA Advances:</u>

<u>Breathing Sequence Disruptions (BSDs)</u>. The most critical interaction discovered by PBA was the identification of BSDs. The importance of the delivery of the proper airflow at the proper pressure and at the proper time to meet the pilots breathing requirements cannot be

overstated. Objective measures of breathing disruptions were developed characterizing pressure and flow relationships giving unprecedented insight into pilot breathing dynamics. The characterization of the Pressure/Flow Phase Shift, the Hysteresis of individual breaths (i.e., Pressure vs. Flow), and Pressure-No-Flow (PNF) analyses were three of these measures. Some causes/amplifiers of BSDs include:

BSDs and Safety Pressure: While all breathing systems tested in PBA experienced BSDs, breathing sequence disruptions were significantly greater in magnitude and frequency in the presence of safety pressure. Safety pressure introduced an additional and multi-factorial level of complexity into what was already a highly dynamic and variable environment. This added complexity greatly increased the breathing system's difficulty in responding to pilot breathing demands quickly and appropriately in the CRU-103 specifically). Safety Pressure exacerbated or induced 11 of the 13 adverse interactions identified by PBA.

BSDs and Pilot Mask Valves: The critical importance of the Mask Breathing Unit (MBU)-20/23 valves to the proper function of this dynamic system of systems, when safety pressure is present, was identified and led to the first preliminary briefing to the USAF/USN in early 2019. For proper function, the regulator and the mask's valves (inhalation and exhalation) need to sequence properly; data suggests this is not always true in flight. In some cases, degraded performance of the exhalation valve will lead to the inhale and exhalation valves remaining simultaneously open at times, disrupting proper regulator function, and allowing constant flow through the mask. In other cases, the exhalation valve becomes overly difficult to unseat as in the event of an inhalation valve that leaks during exhalation. Either of these conditions lead to BSDs.

BSDs and Cabin Pressure Fluctuations: The impact of cabin pressure fluctuations (even as little as a few mmHg) was also explored and documented. Cabin pressure fluctuations have been of particular interest to the Navy, and PBA data show that even small-scale cabin pressure instabilities can have disproportionate impact, causing BSDs. Enabling this analysis was the development of time-synchronized data analysis processes and techniques permitting the visualization of the relationships between pressures, flows and locations for every single breath, as well as overall metrics that reflected the relative levels of dysfunction during breathing. Cabin pressure micro-oscillations depend on the state of cabin-pressure control (including the health of the exit valve). Out of 6 distinct tail numbers utilized in PBA, 2 airframes had micro-oscillations throughout entire sorties, close to the frequency and amplitude of breathing. A third airframe had situational under-damped oscillations, meaning that the cabin pressure was only disturbed by a pressure insult (e.g., *post* combat descent), after which it took at times 2 minutes for 0.4 Hz oscillations to reach steady state.

Pilot Breathing Almanac: In flight, PBA data showed that pilot-induced mask pressure (i.e., the instantaneous flow rate demand) and the sustained average by-the-minute ventilation (specifically during recovery breathing) are much greater and often more chaotic than baseline ground breathing or the regular sinusoidal breathing pattern historically simulated for testing. Data consolidated in the Pilot Breathing Almanac serves to document the breadth and variety of pilot breathing metrics under various conditions of flight. This data base includes multiple flight profiles, aircraft (F-15 and F-18), pilot breathing parameters, and flight parameters that can be used to identify problematic flight issues. In combination, these parameters describe the interaction between two complex systems: the human pilot and the machine/aircraft.

Identifying Emerging Life Support Problems: By measuring in-flight mask pressure and flow, and applying the several tools the PBA has developed, degraded life support components can be identified. For example, analytical tools can recognize improperly operating pilot mask valves or regulators not holding safety pressure, prompting a maintenance check. PBA developed a standardized flight test procedure to evaluate an aircraft's breathing system performance. This test can be used to compare a single airframe across its service life or even across a class of jets.

Updated Oxygen Transport Model (OTM): The OTM was introduced in the NESC's report to the Navy on F/A-18 PEs in 2017. Because of PBA, pilot breathing was measured, and new data is available. It is therefore beginning to be possible to assess system interactions with in-flight data and propose more detailed explanations to the complex system interactions previously identified. For example, it is believed that some F/A-18 hypoxia PEs were caused by a combination of cabin pressure surges and a regulator that overcorrects for deep inhalation and large demands for air. Another example is some F/A-18 hypoxia PEs may have been caused by a combination of a tight harness, a breathing system that suffers hysteresis and delivers air late, and pilot compensation resulting in smaller and smaller breaths.

Flight Physiology: PBA provided some keen insights to Pilot Physiology. On the basis of physiological testing and analysis of in-flight parameters, pilots are suffering physiological decrements in pre-flight operations and in flight that degrade the physiological reserve and lower the threshold for developing hypoxia. Preflight results of pilots, wearing ALSE (Aircrew Life Support Equipment) and strapped into ejection seats showed a reduction of FVC (Forced Vital Capacity) and of O_2 saturations. This effect is present in both the USAF and USN ALSE configurations, but more prominent in the USN torso harness system. The post flight and post doffing values data also revealing concerning impacts. Specific results post flight revealed that O_2 saturation drops below 95%, representing mild hypoxia. The synergistic combination of these reductions in FVC, the BSDs and inconsistent O_2 delivery leads to decreased lung ventilation (decreased amount, pressure, and flow of air resulting in decreased gas exchange in the lung).

F-35: Using PBA developed tools, data from two F-35 ground tests suggested that the breathing system causes BSDs by delivering an unpredictable amount of flow at the beginning, middle, and end of each breath and that it changed from breath-to-breath. Such rapid changes in the breath-to-breath supply forces the pilot to continually compensate by adjusting breathing rate, volume, and exhalation/inhalation force. Pilots who have suffered PEs in the F-35, interviewed by the PBA team, fault the breathing system for acute and chronic health conditions that have caused impairment for days, weeks, months, or longer. The available data, though limited, does not support that the F-35 breathing system protects the pilot from adverse effects. Additional ground and in-flight measurements of F-35 life support system performance is a key recommendation.

JPL Mask: As part of the PBA project, NASA modified an MBU-20P pilot mask with a unique sensor. The sensor, inside the mask and at the actual source of the breath, provides the most accurate real-time measure of the pilot's breathing. The Sensor measures pressure, temperature, and CO_2 concentration and its data sampling rate is fast (83 Hz). Its accuracy compares well with measurements made in a medical doctor's office. After successfully testing the mask in flight, the mask project was turned over to the Department of Defense (DoD) for continued development.

Key Recommendations for the US Military Services/manufacturers of high-performance Aircraft:

1. Recommend acquiring quantitative measures of pilot breathing, in situ, that should be used in the creation of future hardware and system specifications to meet pilot physiological needs, throughout all relevant flight envelopes.
2. Recommend a standardized flight test procedure to evaluate an aircraft's pilot breathing system performance.
3. Recommend reconsidering safety pressure's purpose and cost/benefit tradeoff in light of the problems it introduces to pilot breathing.
4. Recommend trusting subjective pilot reports of breathing as a significant indication of breathing system performance and followed up in a methodical investigative manner with objective data.
5. Recommend that the F-35 Breathing System's BSDs be investigated.

Introduction

Overview

Piloting jet fighters is mentally and physically demanding. Unlike simulated ground activities, flying is performed in an artificial, enclosed environment with external cabin pressure, G-force, temperature, orientation, and velocity stressors. The pilot relies on the aircraft systems to provide adequate environmental control (pressures and temperature) and breathing gas (flow and O_2 concentration). If these systems underperform, the pilot may experience discomfort and a decrease in cognition which could ultimately lead to a physiological episode (PE) resulting in an aborted mission or serious mishap.

Although they are relatively rare, PEs are of extreme concern in military aircraft operations as they appear at random and have resulted in loss of aircraft and life. Detailed studies of PE occurrences have been performed by branches of the US military that have focused on engineering of onboard O_2 gas supplies, personal gear, and environmental control systems. Some progress has been made in reducing PE's occurrence, but to date, the incidence rates are still deemed unacceptably high. The root cause(s) have not been satisfactorily identified and mitigated.

Previously, NASA/NESC evaluated USAF F-22 PEs in 2012, and USN F/A-18 PEs in 2017. The root cause corrective action (RCCA) efforts by USAF and USN were inconclusive; NASA investigators concluded that PEs defy purely engineering explanations because they are likely due to a complex interaction between pilot physiology and aircraft systems. NASA investigators found that certain combinations of flight activities could adversely affect the operation of the OBOGS and the bleed air gas supply from the environmental control system (ECS), but there was no specific "smoking gun" explanation from the aircraft engineering side for predicting PEs. NASA researchers proposed an "oxygen transport model" that described the progression of viable breathing gas from the aircraft to pilot mask, to the lungs, to the blood, and ultimately to organs and brain. NASA concluded that empirical data for calculating O_2 transport based on pilot demand were unavailable.

PBA Concept

To further investigate the concept of the pilot – aircraft interaction, NASA/NESC embarked on the PBA to focus on pilot breathing needs and responses to complement the previous engineering systems (RCCA) investigations.

In contrast to the two previous NASA/NESC observational studies, PBA is a designed scientific study that produced new datasets of simultaneous pilot and aircraft performance. All PBA flights were scripted for flight maneuvers, altitudes, G-force, etc., and repeated for aircraft, pilots, and breathing systems to allow best possible statistical comparisons. Details of PBA study design are provided in Technical Section 1.

The PBA team also delved further into the physiological activity of human respiration on the ground at 1 atmosphere pressure and 21% O_2 concentration; a detailed contrast about how "on-demand" breathing using masks and regulators could influence pilot breathing response via conscious and subconscious adjustments is presented in Technical Section 2.

PBA Flight Profiles

The goal of PBA was to understand the pilots' breathing requirements with a series of reproducible parameters, but to avoid complications from random flight profiles and aircraft constraints, especially from OBOGS and ECS. As such, the PBA used only liquid oxygen (LOX) jets that were available at the NASA Armstrong Flight Research Center, located on Edwards AFB, Edwards, CA, and a series of different scripted flight profiles, each of which were flown multiple times by each of the five NASA test pilots.

Later in the study, PBA added a few more scripted flights with certain maneuvers designed to test observations derived from the standard suite of profiles.

Using scripted flight profiles was considered to be a primary factor distinguishing PBA from previous observational studies. Although this approach reduces the total number of flights to just those designed for the study, it allows direct comparisons across aircraft and pilots. Five specific flight profiles were constructed to assess a variety of "real-world" military flight segments that are encountered by jet fighter pilots such as high altitude, aerobatics, and low altitude flight.

Details of PBA flight profiles and all scripted flights are provided in Technical Section 1.

Individual Pilot Differences

The PBA was specifically designed to investigate response variance caused by individual pilot differences; this is one of the crucial factors missing from the current knowledge base of PE research. There is little value in setting across-the-board engineering targets for aircraft breathing systems without understanding the likelihood of an individual pilot's adverse response. Individual differences in response to common stimuli are well-known in human subject research. These are best investigated using within- and between-subjects variance statistics. The important issue is to understand the apparently random pilot response found in similar flights. The PBA was specifically designed to investigate response variance caused by such differences and provide guidance as to how to apply safety factors. Details of repeat measures (individual variance) of pilots' physiological and subjective response are provided in Technical Sections 1, 5, and 7.

Breathing Gear Differences

Personal breathing gear (masks), attendant regulators, and other air supply hardware serve as the "front-line" interface between the aircraft and the pilot. Even small differences in individual components, and the related complex interactions between multiple components, can become critical. Within the PBA study, gear configurations were categorized as "USAF/Air Force" and "USN/Navy" types (Section 1.1.1.3). These were not identical to all setups used by active USAF or USN pilots, but rather representative of key differences in equipment setup; in the repeat measures design, most PBA pilots flew across service platforms.

Within PBA, these differences break down into the following types:

1. Regulator Type (Demand, Diluter Demand, Safety Pressure)
2. Mask Type (USAF or USN)
3. Physical placement of hardware on pilot

The effects of breathing gear on pilot breathing and performance are discussed in detail in the ensuing report, especially in Technical Sections 1, 2, and 6, and in the supplemental discussion regarding some limited ground tests of F-35 aircraft.

Subjective Pilot Assessments

Like individual differences in physiology, there are individual differences in subjective experience. Muscular discomfort, headache, nausea, changes in perception, or other symptoms do not generally become part of the official record, yet they may portend more severe symptoms leading to PEs in the future.

There are two paths for acquiring subjective data. The first is to informally interview pilots about their general experiences on a regular basis, the second is to develop a formal questionnaire to gain a broader understanding of the linkage between aircraft and pilot performance. Both have been implemented within the overall PBA construct.

Informal interviews: These interviews are comprised of open-ended questions from researchers such as "How do you feel now? Did you have any discomfort during the flight? If so, what were you doing at the time? Follow-up questions as necessary.

Formal questionnaires: The formal questionnaires serve the purpose of deducing what pilots do in the cockpit, what their histories are, and how they perceive their flights. For PBA, these are only applied to NASA test-pilots and have limited generalizability. However, this first trial will provide reference material for future broader investigations. Once implemented across USN and USAF, the questionnaires will provide a database for assessing how pilots perceive their breathing demands/response, and then developing new test procedures to align aircraft ECS with pilot needs.

Details of PBA subjective study design are provided in Appendix 9.

PBA Data Collection Sensors

Cobham VigilOX brand sensing systems were used as the primary pilot breathing monitoring system for PBA. Other systems also exist for measuring pilot breathing, however the VigilOX equipment was considered the most advanced at the time and had been flight approved.

Sensor configurations: PBA was designed to empirically measure pilot breathing parameters during flights and to couple these directly with scripted flight activities. This was accomplished with sensor arrays monitoring the inhalation and exhalation flows, pressures, and O_2 concentrations on either side of the pilot's mask. Pilots were tasked to notate specific flight activities and their perceptions.to serve as complementary information to the sensors. Breathing flow/pressure/concentration measurement equipment was acquired from VigilOX comprised of inhalation sensor block (ISB) and exhalation sensor block (ESB). The ISB probe was inserted into the inlet flow between the regulator and mask inlet valve; the ESB was inserted into the exhalation tube downstream of the mask exhalation valve. ISB and ESB sensor arrays were shown to be non-invasive with respect to regulator/mask performance.

The list below identifies ISB and ESB sensor channels:

ISB		**ESB**
Partial pressure, O_2		Partial pressure, O_2
Inhalation Flow		Exhalation Flow
Cabin pressure		Cabin pressure
Inlet gas temperature		Exhaled gas temperature
Inlet gas pressure		Exhaled gas pressure
Inlet gas humidity		Exhaled gas humidity
Cabin temperature		Cabin temperature
3-axis accelerometer		3-axis accelerometer
		Partial pressure, Exhaled CO_2
		Mask pressure

The pilot sensor blocks were installed on both USN and USAF style mask/regulator combinations. From these, investigators could assess breathing rates, per breath (tidal) volumes, changes in mask pressure, and total flows. For some flights, Madgetech brand data sensors were used in-cabin as a supplement to record altitude and acceleration data from the flight profile. These data streams were post-processed mathematically to provide aircraft position, velocity, and acceleration as needed. In addition, native sensors in the aircraft were used to provide altitude data and redundant cabin pressure data to complement the VigilOX data streams.

Rationale for choosing VigilOX systems: As PBA was performed on an accelerated timescale and with a limited scope, a readily available and quickly fieldable system was required. VigilOX systems were chosen for PBA based primarily on the following factors:

1. VigilOX currently exists as a high-TRL fieldable system.
2. VigilOX hardware is readily available from the supplier.
3. The DoD and US Military are currently testing VigilOX systems in some field applications, thus the opportunity exists to share data and combine learned knowledge.
4. VigilOX systems have been wind-blast tested and qualified for use in fighter aircraft.
5. VigilOX systems delivered data in an understood format, facilitating quick and ready assessment of the data.

PBA researchers understand that there are some inherent limitations to the VigilOX system, as will be discussed in the subsequent technical sections. The VigilOX system was updated and revised by Cobham based on direct input from lessons learned in PBA.

Details of PBA study design with respect to VigilOX sensor systems are provided in Technical Sections 3, 4, and 9.

Aircraft and Flight Parameters

Aircraft types: PBA used NASA jets and test pilots to fly pre-determined sorties out of the AFRC at Edwards Air Force Base, CA. The six aircraft used for data collection were: two F/A-18A models (single-seat), two F/A-18B models (dual-seat), and two F-15D models (dual seat). The F/A-18s were flown and acquired from the USN and the F-15s were flown and acquired from the USAF. PBA utilized the F/A-18A, F/A-18B, F-15D aircraft with LOX breathing systems deliberately to demonstrate the performance and parameters prior to OBOGS modifications in later models. These data provide insight as a baseline observation of breathing

behaviors in jet aircraft operation across various maneuvers in the absence of perturbations from ECS and OBOGS.

Aircraft Instrumentation: The aircraft described in the previous section were outfitted with flight data instrumentation systems referred to in this report as "TTC recorders", systems manufactured by Teletronics Technology Corp for recording aircraft parameters with two removable solid-state recorder cartridges to facilitate the process of downloading flight data after every sortie. The TTC recorded the aircraft Memory Unit (MU) data and derived parameters of interest to PBA.

Test Pilots: The Pilots subjects used for this assessment were recruited from the test pilot pool at NASA AFRC. A basis set of five pilots comprised all the front-seat flight crew and the majority of the back-seat flight crew during data collection runs. Each of the pilots flew each of the 5 flight profiles and performed the non-flying Ground Profile G, at least twice each for 115 PBA missions. On occasion, additional pilots were rotated in to serve as "back-seat" controls.

Pilot Breathing Gear: Test flights were performed with different configurations of USAF and USN breathing regulators and masks using different protocols of safety pressure and dilution demand. There were two basic configurations to reflect USN and USAF gear. The USN configuration utilized a CRU-103 and the USAF utilized a NASA/AFRC EDOX regulator with the matching spec to a CRU-60; pilots tended to use their own personal masks as much as possible. Within these designators, PBA flew different variants to examine effects of safety pressure and demand dilution. Details of all flight gear are discussed in Technical Section 1.

PBA Flight Profiles: A key objective of PBA was to fly scripted flight profiles to produce comprehensive, time-synchronized datasets of pilot breathing together with key aircraft state parameters in a consistent, systematic, methodical, and repeatable way. This was important for the PBA team to be able to develop a statistical baseline for comparison across aircraft, equipment configuration, and pilots, and to provide a template for other organizations for future comparison. These scripted flight profiles were considered to be a primary factor distinguishing PBA from previous observational studies. Although scripting reduces the total number of flights to just those designed for the study, this approach allows direct comparisons across aircraft and pilots within the study.

Originally, five specific flight Profiles A through E were constructed to assess a variety of "real-world" military flight segments that are encountered by jet fighter pilots. Each of these are comprised of individual maneuvers (flight segments) that could be further partitioned for analysis. Later, PBA added two flight activities, Profiles F and G as to follow-up with specific tests. A final profile designated Profile H was created at the end of the study to incorporate all of the main features of Profiles A-G into a single flight. This was flown a total of three times during PBA prior to the end of flight operations at NASA AFRC due to COVID-19. Technical Section 10 provides details about this profile, which is offered as a combination test and check-out for future diagnostics.

Briefly, they are referred to by mnemonic single-letter descriptors A-H as follows:

Profile A: High **Al**titude
Profile B: Aero**B**atics
Profile C: **C**ontrol
Profile D: **D**own low
Profile E: for future **E**xpansion

Profile F: **F**unction Check Flight
Profile G: **G**round only
Profile H: **H**ealth Check - Standardized Flight Test Profile

Although these profiles partially overlap in particular flight segments (e.g., altitudes, velocity, climbs, descents), they were designed to represent broad classes of flight types. Subsequent data curation allowed further partitioning and rearrangements of flight segments to test specific short-term flight activities, as discussed later.

Details of PBA study design, profiles, flights statistics, and pilots are provided in Technical Sections 1, 5, and 7.

PBA Pulmonary Function Assessment

The pre- and post-flight status of pilot pulmonary function tests (PFT) has been considered an important clue of low-level inflammation, hypoxia, and oxidative stress. The normal range of PFT is highly variable and so repeat measures are required to establish central tendencies and within-and between-pilot variance components. The current procedure includes four measurements per flight: a measurement prior to donning of equipment and prior to entry into the jet (pre-don), post-donning in the jet (pre-flight), post-flight in the jet (post-flight), and post-doffing on the ground (post-doff). The difference between pre- and post-flight measures are indicative of that particular flight impact on the pilot PFT.

PBA provides a standardized method designed for jet-fighter pilots to collect this information as well as a small sample baseline of data to compare other samples against. In terms of a within-subject samples, each pilot is observed multiple times across several conditions to provide a longitudinal data set. Pre-post flight variations may inform the current equipage and impact to the pilot breathing. Further investigation may include indications of increased hazardous event potential projections. For example, variations in pre-flight values may provide a potential indication of a predisposition to an adverse breathing event, and post-flight values and indication of a hazardous event in-flight.

The extra time and disruption to normal operations incurred with pilot PFT monitoring is of concern. Furthermore, flight-line PFT monitoring is very difficult to accomplish in windy, bright sun, and hot conditions as the handheld instrumentation is designed for indoor use. As such, this type of investigation is recommended for periodic discovery and assessment, not as a routine procedure for all flight-sorties across the military. PBA successfully conducted detailed spirometry testing for 44 flights, and pulse oximetry for 43 flights, across all PBA pilots. Results are discussed in Technical Section 7.

PBA Pilot Questionnaires and Interviews

Often pilots will not volunteer personal feelings or observations unless asked; this part of the report describes how to get such probative information. Objective measurements can only tell a part of the story; it was crucial that the PBA study also addressed pilot perceptions and observations. To identify the parameters of a subjective experience, data must be gathered, analyzed, and interpreted. A questionnaire is the primary method of measurement for self-report psychological phenomena. These subjective data are based entirely on the individual's perspective. Objective data are those collected using an outside measurement. When combined, subjective data can provide context for trends observed in the objective data. For example, an individual might subjectively report experiencing symptoms they perceive to be an altitude

fluctuation. The actual altitude of the cockpit can be measured objectively by way of altimeter readings. These altitude measurements can confirm or refute the subjective report of an altitude change. This information can help guide the appropriate mitigation strategy.

NASA/NESC implemented a detailed scientific questionnaire to collect self-reported psychological phenomena. These questionnaires were used to collect psychophysiological and individual difference data not otherwise available in the objective data-streams. These self-report data include observations of minor physiological effects such as "ears popping", brief nausea, slight dizziness, and other discomforts, as well as more severe (temporary) disturbances such as disorientation, headache, tunnel vision, and air hunger that could affect flight performance. Such individual and subjective differences are expected to help understand data variations not otherwise explainable by objective measures within the study. These data establish a baseline for subjective experience in the flight deck, improve outlier identification, and enable advanced observation interpretations. These additional data may help to provide insight into data patterns beyond the basic VigilOX and aircraft sensors.

Data Curation: Data Types

Briefly, the PBA data-streams represent continuous data for two distinct categories of variables:

1. ***Dependent variables***: continuous measurements and calculations of pilot physiological response parameters, including breathing rates, breath volumes, breath flows, breathing pressure, O_2 usage, etc.

2. ***Independent variables***: continuous measurements of aircraft parameters, including altitude, speed, acceleration (G-force), cabin pressure, etc.

Together, these two categories represent the class of "random effects" continuous data that change within flights.

Additionally, the random effects datasets are tagged with meta-data including date, time, flight#, pilot#, aircraft i.d., flight profile, regulator type, mask type, etc.; these are referred to as "fixed effects" data that do not change within flights.

Data Curation: VigilOX Data

The VigilOX ISB data and ESB data were recorded in a tabular format as separate files. In case of a 2-seater aircraft, there were four separate files, with the Aircraft recorded parameters being the fifth file. Although the VigilOX equipment does have a clock capable of outputting time to the thousandth of a second, its precision as far as setting and keeping accurate time, were not designed to remain drift-free and accurate to 1/20th of a second. Thus, the data received was not true 20-Hz data, but rather the PBA team received 1,200 readings per minute most of the time. In the process of aligning inhalation flow with exhalation flow it was discovered that 6-10 times within an hour the system recorded anywhere from 10 to 18 readings at random times, just enough to make time-base alignments impossible. Instead a dynamic signal signature of mask pressure and flow rate-of-change to align the ISB and ESB data streams was chosen, after the time-skips have been interpolated. Data range control was an important part of this process. Cobham, the VigilOX vendor has built-in "Bit" records identifying different out-of-range events, so users can search for the presence of such keywords. In some cases, unrealistic flow values were tagged by the "DFRL" code, marking reverse flow conditions. Based on manufacturer and other services inputs, these were caused by the presence of condensation in the ESB hose.

Certain flights had to be removed from summary statistics due to excessive DFRL, while in others, PBA researchers developed algorithms to work around infrequent occurrences using neighboring un-impacted segments.

Data Curation: 20-Hz Data Processing

The PBA uses multiple data streams from systems with independent time bases. The VigilOX ISB and ESB data are acquired at a 200 Hz rate and subsequently processed to 20 Hz in real time within the data loggers; other aircraft parameters, especially altitude and velocity, are derived from additional sensors from the aircraft. The ISB and ESB required near perfect alignment (within 0.03 seconds) to allow accurate assessment of within-breath flow and pressure profiles.

Each individual flight was curated as a master list of all VigilOX and aircraft sensor data streams, and then processed to assure that they were aligned in time. Secondly, each flight's data streams were tagged with meta-data data including date, time, flight#, pilot#, aircraft i.d., flight profile, regulator type, mask type, etc. This was a difficult procedure as different aircraft, VigilOX units, and mask/regulator data had to be individually curated initially until a common framework was established.

The VigilOX and Aircraft data alignment was also based on similar dynamic data signatures. 3-axis accelerometer data was not useful in its raw format, due to different reference frames of the systems. However, a composite acceleration vector was sufficient to apply a signal-alignment tool (Matlab), which is focusing on aligning peak events to reduce the difference between the two signals.

Because PBA focuses on pilot breathing in-flight, the data sets were trimmed to weight off/on wheels. Not all the aircraft used had this parameter available, so velocity and angle were used to automate this process (the altimeter fluctuations were too great to be used alone). Then the pilot-actuated "event marks" were extracted, and augmented by the captured event descriptions (e.g., 5 G's Wind-up Turn, etc.). The resulting "Unified" file was the basis of future analyses. As these individual flight files were later merged in some cases, metadata identifying the flight number, pilot ID, flight profile, Safety Pressure applied Y/N and others were added.

As a derived product, the 20-Hz data was collapsed into 1-minute segments characterized by statistical descriptive data for all raw, and some derived parameters (e.g., O_2 concentration).

Data Curation: 1-min Flight Segments

The aligned 20 Hz data streams were recalculated into consecutive 1-min flight segments for each flight to facilitate subsequent modeling and calculation of physiological breathing parameters. Each parameter was expressed as minimum, maximum, average, and standard deviation within each flight minute. Additional columns were constructed as independent variables, including total acceleration vector (G_3), and dependent variables defined as differential mask pressure (DMP in mmHg), tidal volume (V_T in liters/breath), and breathing rate (BR in BPM).

This data curation was especially important for the dependent variables, as these are generally only used as 1-minute segments. As an example, consider that there are instantaneous measures of inhalation flow; to determine the breathing rate (BR) in breaths per minute (BPM), the number of "peaks" of inhalation flow are counted within a specific minute. Similarly, the BR BPM is

divided by the average of the inhalation flow in liters/minute within that minute to estimate V_T in liters/breath.

Data Curation: Flight Segments

The PBA had planned from the beginning to implement push-button actuated segment markings, with the foresight that attention to specific maneuvers, and tying the aircraft provided conditions to pilot breathing will be important. These "event marks" were then augmented by criteria definitions using Altitude, Velocity, angle of attack (AOA) angles as needed.

Because flight profiles are created based on repeating segments, such as take-off, climb, high-G maneuvers, descents, etc., the PBA used digital Event Markers and parametric definitions to define such segments, dramatically increasing the statistical significance of the results. The results of segment analysis with respect to breathing and air consumption aids characterizing pilot needs for various real mission profiles. Of note are the contrasts between ground breathing rates of 11 BPM, contrasting with in-flight breathing rates of 18 to 21 BPM, underlying the importance of "test-as-you-fly." High-G maneuvers while G-breathing are also noted as higher effort segments (higher mask pressures), but even more informative is the need for 20% higher tidal volume by the pilots, in the minutes immediately following these high-G segments, with Minute Ventilation nearly twice the amount of that on the ground. Lastly, long duration high-altitude flights show one of the higher mask-pressures (effort of breathing), with a moderate return in air volume.

The following flight segments were considered for further correlation analyses, independent of the flight profile under which they occurred:

Flight Segment	**Descriptions**
Ground	On tarmac, Mask On, mostly pre-flight
Takeoff	From Weight-off-wheels to 2.1 kft AGL
Mil Power Ascent	Post Take-off, 5.5 kft per minute, 27 deg max pitch
Max AB Climb	12.6 kft per minute with After Burner, 47 deg pitch
Low Boom dive	14 kft dive, with the purpose of reaching > Mach 1
High G	Criteria > 3.5 G's. Max measured 5.2 G's
Post G	Recovery, first 2-3 minutes after G breathing
40 Kft	High Altitude, low pressure, long 1 hour duration
Sonic	Criteria > 0.9 Mach, to as high as 1.3 Mach
OBOGS Descent	Long duration descent from 40 kft, > 10 minutes
Combat Descent	Fast descent at 45 deg, dropping 17 kft/minute
Airline Descent	Slow descent, 11 degrees, 3 kft/minute

These flight segments represent a form of hybrid 1-minute data stream; technically, they might be considered "fixed effects" for modeling purposes, however, in a practical sense they represent a multi-level variable across all data that could be treated as a "random effect" as well. These flight segment categories were identified from the original 20-Hz data-streams, and subsequently assigned to their respective flight minutes within the 1-minute curated data sets.

This serves as finer resolution of the airplane independent variable called "Profile"; consider that Profile B (aerobatics) may represent most G-maneuvers, however, these are not restricted just to

Profile B as Profiles D and F also include G-maneuvers. As such, an analysis using only the profile fixed effect might lose statistical power if G-force is an important parameter for pilot response.

Detailed information regarding data curation and flight segment analysis are provided in Technical Sections 4, 5, and 6.

Data Interpretation

Data Interpretation: 20-Hz data

High resolution data are the basis for all subsequent breathing observations. They were used to calculate a variety of "per minute" parameters for assessing pilot breathing. Before data reduction into 1-miunte smoothed blocks, 20-Hz data have the advantage of showing short-term anomalies and instantaneous rates of breathing parameters. However, they are subject to detector noise, electrical interference, and sample acquisition irregularities. Furthermore, at this data rate, 1,200 values/minute are dealt with for ~25 sensor streams (depending on exact configuration) for typical 60-minute-long flights. This results in about 1.8 million measurements per flight, which is an overwhelming amount of information to process. As such, 20-Hz data observation were generally relegated to investigating short sections of flights (a minute or so at a time), that had been flagged as "interesting", and had been curated for sensor dropouts.

Specifically, 20-Hz data were used to explore instantaneous flow demands, mask valve sequencing, within-breath volume changes, regulator response, and other fast phenomena. These data also demonstrated where sensor placement could be improved, especially for exhaled water, O_2 and CO_2 that were subject to mixing and delays in the tubing leading to the ESB detectors.

Data Use: 1-minute Data Blocks

A 1-minute resolution data provided the common baseline in that all sensor streams can be compared in the same format. Furthermore, no information is lost, so despite the common (lower) resolution, any anomalies found at 1-minute resolution can be reinvestigated at higher resolution if necessary. There are three distinct uses of the 1-minute data: Summary statistics, data visualization, and mixed-effects models.

1. ***Summary statistics:*** Herein, all flight-minutes are treated equally, regardless of metadata such as flight profile, pilot, aircraft type, etc. The purpose is to understand the central tendencies and extrema (min, max, 95^{th} percentiles, etc.) of pilot breathing needs. The primary application of summary statistics is for the dependent (pilot breathing) parameters that show how much air a pilot actually requires during a wide range of real-world flight minutes.
2. ***Data visualization:*** It is important to see data beyond complex tables of statistics. Two forms of data visualization were used to explain patterns, trends, and comparisons. The first was the "QQ-plot" which is a hybrid graphical tool that shows the distribution of continuous variables and also the location of outlier measurements. The second is the "Heat Map" which is a color-coded array of all individual data points organized by flight-minute on the x-axis, and by flight/pilot/profile, etc. blocks on the y-axis. This pictorial form allows the reader to quickly see trends based on color code, as well as pick-out individual data points of interest according to their labeled x-y coordinates.

3. ***Mixed-effects models:*** Herein, all independent data (aircraft data including altitude, G-force, cabin pressure, etc.) are used in separate multivariate models to assess how they influence each of the breathing outcome parameters such as liters/min, BPM, liters/breath, and differential mask pressure. These analyses provide two functions: first, they assess how important specific independent (aircraft) parameters are in changing breathing behavior, and second, they estimate the amount of variance in pilot breathing behavior that is intrinsic to the pilot, and how much variance is attributable to the aircraft.

For this report, a set of 50 flights were curated and used to develop these summary statistics, data graphs, and mixed effects models. Flights were selected to represent at least 45 flight minutes, a full dataset of both ISB and ESB sensors, and to have completed all of the maneuvers of the particular scripted profile. Selection details have been described in Technical Section 1.

Data Use: Improving Instrumentation

As certain aspects of the VigilOX sensor blocks were still in development throughout the PBA study; researchers constantly evaluated the quality of sensors and respective data acquisition. Results from 20-Hz data streams indicated a variety of intermittent data anomalies, time-base mismatches, and other sensor disruptions. This prompted an ancillary route of inquiry into specific issues regarding real-time data processing as well as evaluations for data acquisition frequency needed to assess different within-breath parameters and the accuracy of flow data integrations. Sensor issues were addressed and corrected as possible. Subsequent mixed effects models showed that differences in sensors did not affect the global results of the study or summary statistics. Furthermore, observations about physical sensor issues such as proximity to the pilot and humidity accumulation in the ESB indicated that additional engineering changes may be required.

An important outgrowth of this part of the investigation revolved around the recognition that the ESB sensor channels for O_2, water, and CO_2were not capable of resolving the changes within individual breaths. This was not a flaw in the sensors, but rather a physical mixing issue dictated by the required distance in the tubing run from the mask exhalation valve to the ESB. This exhalation tubing needed sufficient width and volume to avoid downstream breathing back pressure that then became a mixing chamber. The overall smoothed data were sufficient to monitor longer term fluctuations in these exhaled parameters.

In response to these results, the PBA team initiated a collaborative program with the NASA Jet Propulsion Laboratory (JPL) in Pasadena, CA to develop miniaturized “in-mask” sensors. To date, PBA has developed a sensor system for CO_2 and water vapor capable of rapid within-breath sampling, have flight-qualified a new mask that includes the sensor array, and have successfully flight-tested a prototype. PBA is in the process of turning this new technology over to US Department of Defense for further development and deployment.

Details of PBA data interpretation and statistical results for Pilot breathing data are provided in Technical Sections 4, and 5. Future sensor modifications and development are discussed in Technical Section 9.

Physiological Interpretation: Background

The ultimate goal of PBA was to understand how the human and aircraft interaction may lead to precursors of PEs and to develop data to inform future standards for breathing systems. This part of the study developed a medical/physiological model for assessing the stresses encountered by

the pilots during realistic flight conditions. The empirical measurements and questionnaire data were combined in this section to address the probabilities of developing cognitive dysfunction due to hypoxia, atelectasis, inflammation, barotrauma, oxidative stress, nausea, or other breathing/pressure related effects.

The previous NESC F/A-18 report concludes that PEs are primarily a human-based phenomenon. Secondly, the report concluded that hypoxia is not solely a condition of insufficient levels of O_2 in breathing gas; it is insufficient delivery of oxygen to tissues in the body. An additional factor that was revealed in the Airway Breathing evaluations was that a restriction of volume, regardless of oxygen concentration, can lead to hypoxia. Thirdly, a key to reliable OBOGS and supply system performance is uniform operating conditions. Fourthly, the previous reports from the various aircraft programs have a large amount of aircraft performance data, but a shortage of evidence directly related to the Human System. This gap of information is examined in the present PBA. As emphasized in previous reports, aircraft systems that support human health are complex, dynamic, and should be interactive; this requires a well-coordinated, "systems approach" to design requirements, interfaces and operations.

Physiological Interpretation: Human Response

Physiologically, the areas that were previously identified as increasing human susceptibility to PEs are hyperoxia, absorption and acceleration atelectasis, and also increased external pressure on the chest wall limiting inhaled volumes (previously equated as increased work of breathing). All of these lead to tissue hypoxia and the related moderate to severe symptoms. The PBA evaluation was designed to specifically look at the human machine interactions, specifically measuring the breathing dynamics and the inferences to lung parameters. There were numerous physiological impacts elucidated in the PBA study. Exceedances, both excessive and insufficient, of normal physiological pressure, flow, volume, and concentration of O_2 at the mask were delineated. Exceeding high inspiratory and expiratory pressures were noted, that decreased the inspiratory and expiratory volumes and ultimately the vital capacity. These can all lead to hypoxia if left uncorrected. Also, exceedingly high expiratory pressures can cause CO_2 retention and result in circulatory depression and lung injury from over distention leading to cumulative trauma and altered breathing patterns. Elevated peak inspiratory pressures and mean airway pressures have been shown to cause a reduction in cardiac output. Other issues in regulator and mask interactions have revealed decreasing tidal volumes supplied to the human. System hysteresis leads to distinct increases in work of breathing as well as limited tidal volumes. These will be discussed in detail in the Physiology section, Technical Section 7.

Some common misperceptions were refuted in the study. One is that the O_2 concentration that is produced by the system is the same as in the mask. Alterations in pressures and volumes at the mask can decrease the amount of O_2 delivered to the pilot and result in hypoxia. Specifically, if the aircraft is not able to provide adequate flow, volume or concentration of O_2 to compensate for the lower partial pressure of O_2 at altitude, tissue hypoxia results. Another is that pilots will hyperventilate. No indications of exceedingly high minute volumes were delineated, but exactly the opposite was found.

Details of PBA study design with respect to pilot physiological response and health effects are provided in Technical Section 7.

Subjective Data Analysis

Informal Interviews

Throughout the PBA study, the PBA team conducted a series of informal interviews with pilots on a random basis; some of these were volunteered by the pilots themselves, others were requested by team members. This also included interviews with F-35 pilots who were not part of the designed PBA program but were available on an *ad hoc* basis. These interviews were informal, and queried pilots' state of mind and recent flight experiences. Some of the most important information came from these interviews in the sense that the PBA team gained insight into the smaller perturbations that occurred in flight, that pilots generally regard as too minor to report. These included comments that some jets are "bad breathers", that there were times when exhaling was more difficult, that there was some slight "air hunger" on inhalation, etc. After compilation of these comments, the PBA team found commonality in low-level effects from the pilot-aircraft interaction and could begin to investigate associations with flight activities and breathing gear type.

Formal Questionnaires

The PBA questionnaire included three sections: pre-study, pre-flight, post-flight. Results from questionnaires were coded using Likert scales and composited similarly to the empirical summary measurement data in that meta-data was attached. In addition, verbal descriptions from interviews were included as available. Questionnaires were compiled and assessed in composite to evaluate differences in pilot experience between subjects (e.g., same pilot, different profile) and within subjects (e.g., different pilot, same profile). Features of interest include pilot, profile, equipage, aircraft position, and transient individual differences (e.g., sleep, nutrition, hydration, and other recent flight activity).

Details of PBA subjective data study design and questionnaire results are provided in Appendix 9.

Beyond PBA – Application of Data

The data collected throughout PBA correspond to a relatively narrow and specific set of pilot/aircraft/flight environment interactions. The PBA aircraft breathing systems were all supplied with LOX; specific configurations including diluter demand and safety pressure are discussed in Technical Sections 1, 2 and 6. All flight tests were conducted at the NASA Armstrong Flight Research Center (AFRC) at Edwards, CA. There were two basic configurations for aircrew equipment and harness configuration tested, representing USN and USAF style gear.

This relatively narrow set of test conditions limits the scope for generalization, but it affords an opportunity to serve as a reference of comparison for other pilot/aircraft/flight environment configurations. Because the PBA maneuvers were scripted, and repeat tests were made, the PBA data can be used for comparison purposes in a statistically rigorous way. Because the PBA data is collected, compiled, and archived in an annotated database, specific flight segments from PBA can be compared to data collected from different aircraft flying similar flight segments.

PBA data may be useful for understanding complex pilot/aircraft/flight environment interaction issues for other types of military aircraft if they fly similar profiles. Baseline breathing parameters from PBA can be used to put future flights into context within the PBA framework.

Some examples of possible cross platform comparisons include:

- Comparing regulator hysteresis trends collected during PBA to regulator hysteresis trends from different types of regulators – particularly electronically controlled regulators.
- Comparing breathing cadences, breathing inhalation/exhalation ratios, and breathing flow profiles collected during PBA to breathing data collected on trainer aircraft with smaller engines and reduced ECS "muscle pressure."
- Comparing the maximum inhalation velocity and maximum inhalation breathing volume collected during PBA to peak breathing collected with different aircrew equipment and different harness configurations.
- Comparing the variability of partial pressure of O_2, ppO_2, and O_2 percentage, pO_2, collected during PBA to the respective variability during tests of aircraft systems that use OBOGS.

Details of PBA study outcomes that are applicable to other aircraft, environmental control systems, and breathing gear are provided in Technical Sections 8 and 9.

OBOGS Breathing Systems

Any possible effects of the OBOGS breathing system were removed from the PBA study with the implementation of LOX breathing gas available in the NASA AFRC aircraft. The PBA explored what has been deemed a best "case scenario", or at least a scenario wherein fluctuations in aircraft bleed air and OBOGS timing cannot change the breathing gas supply. As such, flows and pressures that are required by the pilot were able to be defined when breathing a stable known supply, and then provide guidance for concentrations, flows and pressures to be supplied by aircraft actually using OBOGS.

Other Aircraft Types

The information gleaned from the PBA study reflects new insights into pilot breathing requirements, and the interaction between pilot and aircraft gear. As such, this work can be translated to assess other aircraft types using different mask/regulator configurations. In fact, an addendum reporting ground-tests data for breathing gear in two F-35 jets is provided. Additionally, the application of PBA derived metrics to tests of any military jets when collecting VigilOX style breathing data have been discussed. These tests are described in detail in Technical Sections 6 and 10.

Other Masks and Regulator Configurations

Although not discussed in detail, any other mask/regulator configurations could be tested as long as they can be retrofitted for VigilOX equipment.

Holistic Aircraft Flight Evaluations

PBA has documented some anomalies that are likely caused by pilot breathing equipment that was broken, contaminated, or otherwise out of specification. Without PBA data, these kinds of anomalies in pilot breathing equipment could not be verified or documented, nor would it be possible to collect reliable data about the severity or frequency of such problems. These data have provided a series of potential failure modes of mask and regulator components that are investigated in detail.

Such failures are subtle, and so NESC/NASA proposes a concept for mitigating adverse outcomes by using periodic breathing-aircraft interaction test flights with full PBA

instrumentation. These tests would provide a benchmark for breathing gear performance, much like current check-out flights document aircraft performance.

Details of PBA study outcomes are discussed for developing pilot-aircraft interaction "check-out" flights for all military aircraft, environmental control systems, and breathing gear. Results are provided in Technical Section 10.

Description of Technical Sections

After this introduction, the next major part of this report is comprised of a series of technical sections. The first 10 sections provide descriptions, analyses and results for specific PBA topics. In addition, a detailed PBA almanac of relevant measurement data and metadata is provided as a separate Technical Section 11, and an annotated summary of findings, observations, and NESC recommendations (FORs) are listed in Technical Section 14. Finally, Technical Section 13 provides an overview of how PBA methodology was applied to two F-35 ground tests, the details of which are discussed in Appendix 7. The technical sections are meant to each stand alone; that is, they each tell individual stories from implementation to ultimate results.

The following topics, as organized by Technical Section number, comprise the main body of the PBA report:

1. PBA Study Design: Description of PBA study design; provides metadata, pilot parameters, aircraft specifications, mask and regulator specifications, flight profiles, and breakdown of all flights and respective categories.
2. Fundaments of Pilot Breathing: Description of "normal" human breathing at atmospheric pressures and O_2 concentrations and the relationship with pilot "on-demand" breathing systems at altitude.
3. PBA-Unique Sensor Systems: The selection, history, complexity, accuracy, and precision of VigilOX system sensors (and other aircraft sensors) to evaluate their probative value for different breathing assessment needs.
4. Data Curation and Alignment: Curation and alignment of all data streams; removal of errors, identification of dropouts, and synchronization of timing from disparate sensor systems.
5. Statistical Analysis of Pilot Breathing: Presentation of summary information, data visualization, and statistical analyses of pilot breathing needs within the context of 1-min resolution breathing data.
6. Engineering Analysis of Pilot Breathing: Detailed investigation of observed anomalies in pilot breathing response, especially in 20 Hz resolution to identify stressful flight conditions and diagnose breathing gear abnormalities or failures.
7. Pilot Physiology and Medical Outcomes: Interpretation of all human response data within the context of human physiology and medical outcomes, including pre- and post-flight pulmonary function testing.
8. Non-PBA Aircraft Analysis and Lessons of PBA Data for Other Breathing Systems: Interpretation of PBA results within the context of other aircraft types and other breathing supplies/gear.
9. Sensor Status and Future Development: Evaluation the current state of the sensor systems and provide guidance for future changes in hardware and software, especially for VigilOX ESB.

10. Development of a Diagnostic Test of In-Flight Breathing System Performance: Develop flight testing protocols for identifying potential "bad-actor" jets and breathing gear routinely before more serious problems arise.
11. Almanac of Pilot Breathing: Compilation of all flights and resultant data.
12. Oxygen Transport Model (OTM): Exploration of oxygen transport from regulator to mask to lungs to pilot organs and brain.
13. Case Example Application – The F-35 Lightning II: Ancillary report describing breathing parameters collected from two ground tests of F-35 jets.
14. Findings, Observations and Recommendations (FORs): Annotated list of all FOR's resulting from the PBA study.
15. Acronyms and Abbreviations

Appendices (Volume II)

The PBA report includes a series of appendices that provide additional detailed information and data for the interested reader; they are called out for reference within the technical sections as appropriate. The following list provides the topics for the appendices:

1. Additional information for Technical Section 1; PBA Study design
2. Additional information for Technical Section 2; Fundamentals of Pilot Breathing
3. Additional information for Technical Section 3; VigilOX sensors
4. Additional information for Technical Section 7; Pilot Physiology
5. Additional information for Technical Section 9; Development of JPL Mask
6. Additional information for Technical Section 10; Standardization of test flights
7. F-35 Pilot Interviews and Ground Test Data
8. Pilot Breathing Assessment (PBA) Considerations on NESC's F/A-18 PE Report (2017) and Other Issues
9. Results of Pilot Questionnaires and interviews
10. Description of PBA Machine Learning software tools
11. Glossary of PBA terms

Summary of Introduction

The preceding introductory materials serve to outline the overall PBA project. They are organized by sections that reflect the different segments of the readership; that is, the early sections refer to the logic behind the study design (planners), the middle sections describe the implementation (engineering), and the later sections describe the use of the curated data and ultimately to make modifications (mitigation). These different aspects of the study described in this introduction are left deliberately broad, and do not provide specific outcome information. The introduction is intended to give the readership a feel for the concepts, complexity, and scope of embarking on such a difficult problem. In the next major section of the report entitled "Technical Sections", the topics mentioned in the Introduction are each dissected in detail and results presented. All ultimate results are then presented in tabular form within the major Section entitled "PBA Findings and NESC Recommendations" to provide guidance for future interpretation and ultimate reduction in PE occurrences.

Team List

Name	Discipline	Organization
Core Team		
Clint Cragg	NESC Lead	NASA
Lance Richards	Deputy Lead, Principal Investigator	NASA
David Alexander	Medical Officer	NASA
Daniel Dietrich	Analysis Team	NASA
John Graf	Instrumentation Lead	NASA
Jon Haas	Engineering Lead	NASA
Kevin “Sonar” Hall	F-35 Test Pilot/Analysis Team Co-lead	USAF
Mark Hodge	AFRC Project Lead (2019-2020)	NASA
David Iverson	Data Systems Analysis	NASA
James “Clue” Less	AFRC Project Pilot Lead	NASA
Kellie Kennedy	Human Factor	NASA
Jack Ly	Aircraft Operations Engineer	NASA
Christopher Matty	Analysis Team Co-Lead	NASA
Robert Navarro	AFRC Project Lead (2018-2019)	NASA
Joachim Pleil	Physicist	US EPA
Craig Shallhorn	Navy Flight Surgeon	USN
Marta Shelton	Analysis Team	NASA
Mark Smith	Analysis Team	NASA
Jon Sobus	Research Physical Scientist	US EPA
Phillip Wellner	Senior Technician of Air Crew Life Support	NASA
JPL In-Mask Sensor		
Ryan Briggs	JPL Engineer	NASA
Lance Christensen	JPL Engineer	NASA
Kim Simpson	NESC Chief Engineer, JPL	NASA
Consultants		
John Camperman	NSWC Engineer	NAVSEA
Tim Krall	Flight Operations Engineer	NASA
Kurtis Long	Aerospace Life Support Engineer	NASA
Andy Ramlatchan	Machine Learning	NASA
Alston Rush	NAVAIR Engineer	NAVAIR
Pete Zingarelli	NAVAIR Engineer	NAVAIR
Matthew Zu	Aerospace Engineer	NASA
Business Management		
Tricia Johnson	Program Analyst	LaRC/MTSO
Assessment Support		
Kylene Kramer	Project Coordinator	LaRC/AMA
Tina Dunn Pittman	Project Coordinator	LaRC/AMA
Jocelyn Santos	Project Coordinator	LaRC/AMA
Linda Burgess	Planning and Control Analyst	LaRC/AMA
Jessica Malara	Scheduling Analyst	AFRC/Millennium
Erin Moran	Technical Editor	LaRC/AMA
Pricilla Taylor-Percival	Flight Data Coordinator	AFRC/Peerless

Acknowledgements

Armstrong Flight Research Center (AFRC): Without the enthusiastic support and dedication of so many at AFRC, this assessment would not have been possible. Specifically the PBA team would like to thank the following: AFRC Senior Leadership, Flight Operations Directorate (AFRC Pilots, Life Support, Operations Engineering, Aircraft Maintenance, Avionics, and Engineering Support), Mission Support Directorate (Medical/Health), Programs Directorate (Aeronautics Projects), Research Engineering Directorate (Flight Instrumentation, Aerodynamics, Systems); Mission Operations (Range Operations, Range Engineering, Safety and Mission Assurance Directorate

X-59 Low Boom Flight Demonstration - Quiet Supersonic Flight 2018 (QSP18) Project: PBA gratefully acknowledges QSP18 (Project Manager Heather Maliska) for support of additional pilot breathing datasets during ride-along sorties in 2018

Many organizations and individuals helped make PBA possible. These included:

- **Cobham Mission Systems** (VigilOX): Rob Schaeffer, Zoe Rabinowitz, Bill Siska, Lucas Mesmer, Jim Talty, and Ryan Edmonds, and Aaron Rood.
- **Masimo Corporation** (Rad-97): Raul Rosales and Philip Weber
- **Medical International Research USA** (Spirodoc): Bruce Morgan
- **Naval Air Weapons Station, China Lake**: Behzad Lessany, Michael Sorenson, Jacob Dunken, Robert Keathley, John Zipp, Joseph Kumm, Britt Wheatley, Douglas Karnes, Samuel Schoenhals, and Ceasor Santiago
- **Naval Air Systems Command, Patuxent River**: Peter Zingarelli, Alston Rush, Matthew Pack, A. Buckler, Dennis Goss, Christine Brown, Matthew Pack, Charles Nelson, and Dennis Goss
- **NASA JPL** (In-Mask Sensor): Lance Christensen, Ryan Briggs, and Kim Simpson
- **NASA JSC**: David Knerr, the Piston Breather Developer
- **NASA Langley**: Jon Levy, PBA Animations
- **PBA Final Report Peer Reviewers**: Kathy Hughes, Chuck Campbell, Alston Rush, Steve Gentz, Lloyd Trip, Matt Stein, Thomas Massa, and John Camperman

F-35 Review

The PBA team would like to express gratitude and appreciation to the F-35 pilots who agreed to be interviewed for this report. Their stories were the impetus for PBA's examination of the F-35.

Technical Section 1: PBA Study Design

Scientific study design of PBA

1.0 Introduction

1.1 Rationale for PBA

F-22 and F/A-18 investigations conducted by the NESC indicated that PEs are a result of complex pilot-aircraft interactions (NESC, 2012; NESC, 2017). Both studies reported that there was a dearth of in-flight breathing data available (e.g., breathing frequency, flow rates, air consumption, and mask pressures) to shed light on the complex O_2 delivery process to the pilot while flying high performance aircraft. In addition, key aircraft parameters such as cabin pressure, inlet regulator pressure, instantaneous flow rates, etc. were also not measured or recorded.

PBA was initiated in 2018 to use commercially available instruments to measure pilot breathing, aircraft performance parameters, and to combine aircraft data and breathing data in a single, time synchronized data set. The three main goals of PBA were to develop processes and methods to measure these parameters that is standardized, systematic, and relatively easy to perform; develop new instrumentation systems that are smaller, lighter, more capable, and more energy-efficient; and assist in better understanding the causes of PEs. An important consideration of PBA was to develop and apply data collection and analysis methods that other organizations could adopt for widespread use.

1.2 Literature Comparisons for PBA

There are a number of published articles that describe the breathing parameters and physiological workload of pilots; most are based on simulator or centrifuge measurements, and many tend to focus on commercial aircraft. However, there are four studies that address PBA style instrumentation and observations for military applications. Lauritzen and Pfitsner (2003) and Travis and Morgan (1994) discuss the issues surrounding pressure breathing, and Delgado et al. (2018) and West (2013) discuss in-flight breathing sensor development. Only two publications were found wherein the authors document in-flight pilot breathing measurements from jet aircraft. The earliest is a 1987 NATO report based on the British RAF Hawker-Hunter T7 trainer wherein the authors make inflight measurements of breathing frequency, inspiratory minute volume, inhalation peak (instantaneous) flow, and end-tidal carbon dioxide (CO_2) tension (Harding 1987). Of particular interest in this report are estimates of the "metabolic cost of flying" as calculated by the conversion of O_2 to CO_2. This work represents 46 flights and 18 different pilots. The second publication is a USN report that studied a variety of aircraft including F-14, F/A-18, A6, A7, and S-3 (Gordge 1993). This work presents data from 51 flights and 41 different pilots with measurements of inhalation peak (instantaneous) flow, breath tidal volume, and breathing frequency.

While these studies represent important contributions to scientific literature, neither study provided detailed analyses of data, nor was capable of allowing repeat measures analysis due to the apparent random assignments of pilots, aircraft, and flight profiles. Notably, the Harding and Gordge data do not provide distributions, confidence levels, or other statistical descriptors beyond the 97.5 percentile, which were also incomplete.

PBA was uniquely designed to investigate timing, pressure, volume and flow parameters at high-resolution (20 Hz) sufficient to resolve the shape of individual breaths and perform frequency analyses. This capability enabled a number of new phenomena regarding pressure/flow hysteresis, inhalation/exhalation mismatches, and other small systemic perturbations to be the identified in in-flight breathing data. These phenomena can all contribute to pilot fatigue, distraction, and hypoxia. PBA also used the detailed flight-minute data to assess the distributions, trends, and outliers for a comprehensive set of pilot breathing parameters beyond these early studies. Furthermore, the intentional repeat measures design wherein pilots repeat the same profiles, etc. allow additional detailed analyses with mixed effects models that provide additional insights into assessing variance components which will ultimately help decide which pilot-aircraft interactions have the most effect on pilot breathing stress. The Gordge and Harding studies, while novel and important, could not be used for these kinds of analyses.

1.3 Oxygen Transport Model (OTM)

How do PEs occur? There are multiple etiologies, most likely causing some form of reduced O_2 delivery to organs, most importantly the brain. Previous NESC work evaluating fleet PEs in the F/A-18 and E/A-18 developed an OTM to identify the O_2 losses that occur along the circuitous path from the breathing system source all the way to the tissues of the pilot's brain (Figure 1.1; NESC, 2017). A key finding of this study was recognizing the lack of specific in-flight human breathing data to quantitatively pinpoint where the transport of O_2 breaks down along this path. PBA was designed to provide hard evidence for elusive pieces of the PE puzzle and to better understand how the pilot's physiology interacts with airplane systems, and how these interactions may influence O_2 transport.

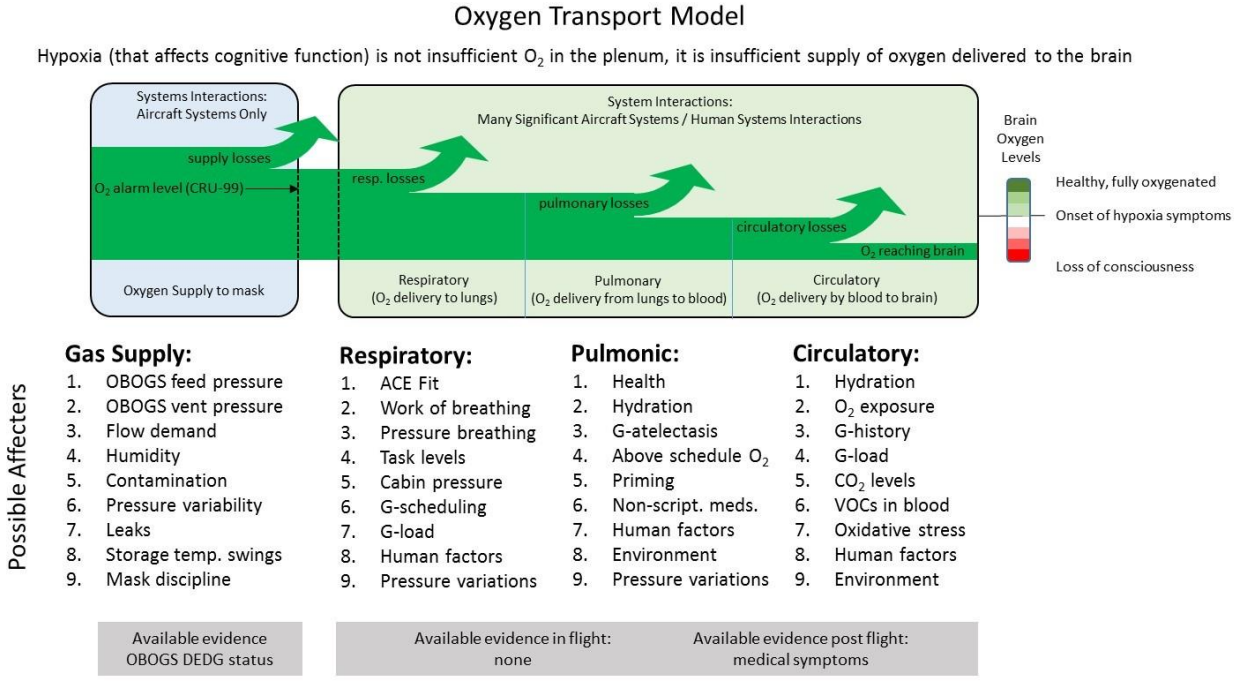

Figure 1.1. The OTM (NESC, 2017)
The concept describes the potential loss mechanisms of O_2 starting with the gas supply, and progressing through inhalation, pulmonary uptake, and distribution to the organs and brain by the circulatory system.

1.4 Unique Features of PBA Design

1.4.1 Aircraft

Figure 1.2 shows the aircraft types, models, and tail numbers flown at NASA AFRC in support of PBA. Two F/A-18A models (single-seat), two F/A-18B models (dual-seat), and two F-15D models (dual seat) were used to fly 115 dedicated sorties. A unique feature of these aircraft is they are equipped with LOX supply systems rather than more recent fighter aircraft that use On-board OBOGS. The use of LOX jets is key in reducing the confounding factors associated with OBOGS performance in identifying the cause of PEs. LOX jets were able to provide a steady flow of O_2 independent of the variables that have affected OBOGS outputs (e.g., Throttle position, limited plenum volume, O_2 level). This allowed the PBA team to concentrate more on the pilot physiology without the variability an OBOGS would introduce to the data.

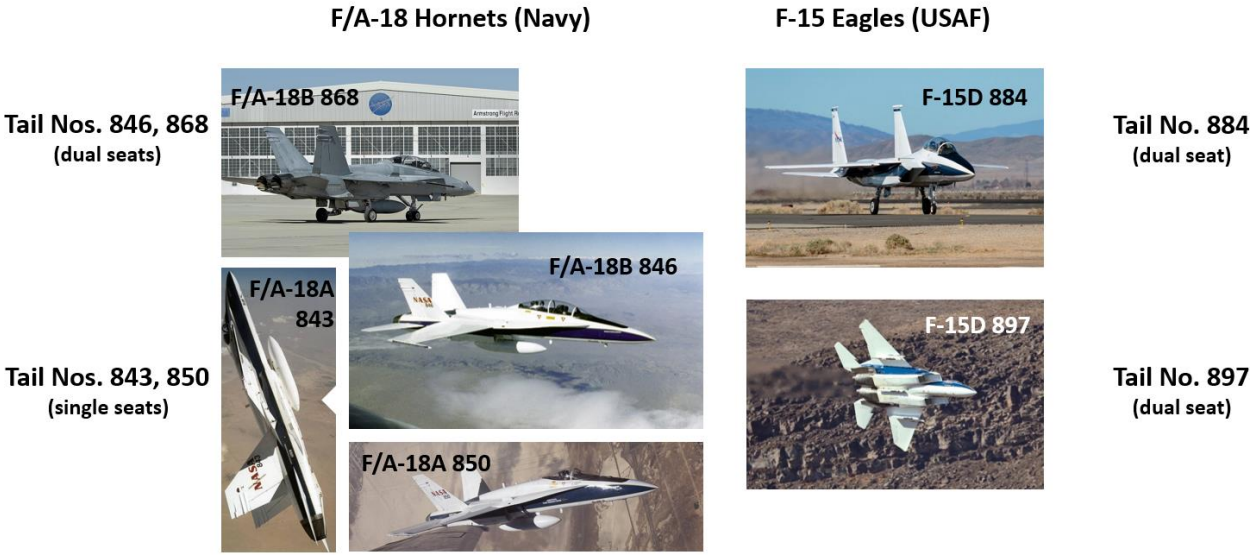

Figure 1.2. NASA AFRC Aircraft used in PBA (Legacy, LOX breathing systems)

1.4.2 Pilots

The PBA pilots were all highly experienced and well-educated. All have engineering degrees (most with master's degrees) and are graduates of the USAF Test Pilot School. Each pilot has an average of 22 years of flight test experience and 26 years as flight instructors. Each pilot has flown an average of 7220 hours across a variety of aircraft, 3158 hours of which have been in high performance jets in various configurations. All PBA research pilots were male, and self-identified as Caucasian. The average age of pilots was 54.8 years (SD = 2.56), height was 72 inches (SD = 1.73), and weight in lbs was 186.6 (SD = 18.28).

Each of the five NASA AFRC pilots flew an average of 22 sorties for the PBA, flying multiple sorties following six scripted flight profiles. Additional data were also gathered on so called "ride-along" flights, in which aircraft- and breathing- data were recorded on a non-interference basis by another project. Flights were conducted using both USAF and USN Aircrew Flight Equipment (AFE) to discover if the equipment impacted the pilot's physiological response.

Although limiting the study to five pilots sacrificed some generalizability to the overall pilot population, it allowed the unique ability for within- and between-parameter statistical analyses of

the various profiles, flight activities, and aircrew equipment configurations as they could all be repeated by the same individuals within the logistical constraints of the study.

The pilots proved to be a valuable resource for both gathering and interpreting the data collected. Their training and experience helped them to recognize the subtle effects of the different AFE configurations and minor equipment malfunctions as well as the differences in breathing needs while flying different profiles.

An important recommendation coming out of the NESC briefings to USN leadership in 2017 was the admonition to "Listen to your pilots" (NESC, 2017). In many instances during PBA the pilots gave immediate feedback on the effects or anomalies they experienced during flight. This feedback was captured at times through in-flight communication between the pilot and the control room staff. Detailed in-flight comments were also noted on their flight cards, relayed in post-flight debriefs and captured in their post-flight written reports. This information was instrumental in guiding PBA analysts to a more focused investigation. With pilots serving as a first-alert system, analysts could quickly evaluate what the aircraft was doing, where it was in the air, and how the pilot's breathing parameters were affected. In one such example, two different pilots flying the same profile experienced breathing difficulties on two different days. They flew the same jet, the same maneuvers, but each one independently experienced the same phenomena at the same place in the profile. These experienced test pilots, who were not expecting issues during the flight, both experienced the same problem with their breathing. Well-trained PBA pilots served as the first line of communication for bad -breathing jets or faulty AFE by noting unexpected breathing results. They were often able to report subtleties in breathing dynamics by stating that "something wasn't right when I did my second squirrel cage", or "I felt like I was over-breathing the regulator and couldn't get enough air". The following excerpt from a PBA pilot's post-flight report serves as an example of important "data" used by PBA to focus on particular features in the measured data:

> *Flight 69: Event Mark 3 at 13:38:16 - 2 min of relaxed normal breathing - noticed slight stickiness of valve on inhalation; required slightly more than normal effort on inhalation (however, it's not unusual for the mask valve to exhibit this behavior).*
>
> *Event Mark 4 at 13:40:53 - Time to take 10 normal breaths: 86 sec - it felt as if the slight restriction to airflow caused by the mask and hose slowed down my breathing and resulted in it taking longer for 10 breaths than earlier with the mask down.)*

Such feedback was extremely helpful to data analysts as it could alert them quickly to a potential problem and help them to identify precisely when in the flight profile the problem happened. This information gave analysts detailed information on where to look in the flight data and helped them better understand what specific anomalies, like sticky inhalation valves, look like in the breathing data.

1.4.3 Life Support Specialists (LSS)

A significant consequence of modern fighter aircraft design is they can easily produce conditions that are well beyond the limits of what the human flying these machines can safely endure. The Life Support Specialist has the important job, among many, of maintaining the pilot's Aircrew Flight Equipment (AFE). This equipment comprise the essential pieces of hardware designed to meet the pilot's physiological needs during the highly dynamic conditions produced by these high-performance aircraft.

The AFRC-PBA Life Support team consisted of three highly experienced Life Support Specialists (LSS). The LSS team was able diagnose subtle post-flight anomalies in pilot AFE and aircraft life support systems and could confirm pilot observations of breathing discomfort encountered during flight. They were an important resource for the PBA team to better understand factors in the AFE that might have affected the test results. The LSS team has an average of 36 years of experience in the field, 30 years of which was in direct support of DoD high performance aircraft and have taught the discipline for over 22 years.

In addition to the traditional AFE worn by PBA pilots, an in-flight in-situ portable physiological monitoring system, called VigilOX (Cobham Missions Systems, Orchard Park, NY), was used to monitor breathing and aircraft parameters. Technical details about VigilOX are provided in Technical Section 3. VigilOX was designed to be worn by pilots as part of their AFE. Integrating and flying these one-of-a-kind developmental units, along with conventional gear, required a high level of life support expertise. AFRC LSS expertise was instrumental for the integration of VigilOX within both USN and USAF AFE to achieve the stringent DoD AFE requirements as well as to gather a reliable, consistent, and robust dataset for PBA. LSS kept the AFE in good working condition throughout the program and, as the list below shows, they performed a myriad of functions for the assessment. In addition to the day of flight activities, the LSS conducted bench-level testing, continually swapped USAF and USN AFE on the pilot and in the jets and played an important role in achieving successful results of AFE during wind-blast testing.

The LSS team were also technically trained by a team of medical doctors to play an essential role in gathering important physiological parameters, like spirometry, capnography, and pulse-oximetry, before and after each flight. (Specific details on the LSS training is provided in Technical Section 7). These data were gathered to help assess the effect that the gear and flight profile had on pilot physiology. LSSs gathered this information from the pilot (or two pilots if a dual-seat aircraft was used) at four key times for every flight. The first dataset was gathered approximately one hour before the sortie with the pilot sitting in plain clothes in an office environment. The second and third datasets were gathered immediately before and after the sortie with the pilots suited-up in flight gear while strapped in the cockpit. The fourth and final data were taken at approximately one hour after flight, matching the first set of test conditions. (Section 1.6.2.4 provides details about the types of physiological testing and equipment used. Technical Section 7 for additional details about test protocols and results).

The LSS team supported each of the flights, from outfitting the pilots prior to each flight, to mastering the use of physiological test equipment, administering the tests, creating LSS reports to document all the associated metadata for flight, and uploading the data from each of the systems to a project server. Figure 1.3 shows examples of some of the roles performed by the life support team.

(a) *(b)* *(c)* *(d)*

Figure 1.3. NASA AFRC Life Support Specialists
(a) Pilot AFE fit checks, (b-d) assisting pilot acquire spirometry and capnography measurements on ramp under real-world weather conditions at Edwards AFB, CA.

The list of tasks the LSSs perform for PBA on a daily basis is remarkably comprehensive and varied. The following procedural list provides a snapshot of "a day in the life" of the LSS in support of a typical PBA flight.

Day of flight

Pre-Flight

Pre-Crew Brief

- Identify mission pilot(s) and determine flight equipment status
- Identify mission aircraft and verify aircraft is in proper mission configuration (USN, USAF)
- Inspect and prepare all flight AFE for each pilot flying PBA for the day: masks, helmets, harnesses, breathing regulators, parachutes and survival kits
- Clean, repair, replace as necessary
- Inspect and prepare all PBA hardware, systems, sensors, (PBA hardware and data systems, VigilOX, MadgeTech, Spirodocs, Rad-97s etc.)
- Calibrate systems as necessary, charge batteries, manage and verify capacity of data cards for flights
- Configure flight equipment per mission profile (USN, USAF)
- Document all hardware metadata used for PBA through a Life Support Metadata report

Crew Brief

- Support Crew brief; give life support status report

Post-Crew Brief

- Administer 1st round of spirometry, capnography for each pilot (in conference room)
- Upload Pulmonary Function Testing (PFT) data to server, maintain and manage disk space

At Life Support Ready-Room

- Help each pilot don AFE and fit check
- Walk out with pilot and assist in the jet

At Jet

- Configure aircraft with cockpit Madge Tech
- Assist pilots with aircraft integration
- Administer 2nd round of spirometry and capnography for each pilot (at jet-side)

Post-Flight

At Jet

- Meet aircraft in the chocks
- Administer 3rd round of spirometry and capnography for each pilot (at jet-side)
- Assist pilots will normal aircraft egress
- Return to the pilot's ready room

At Life Support Ready-Room

- Help each pilot doff AFE and debrief pilot on AFE fit and issues, if any
- Inspect AFE hardware, clean and repair as appropriate
- Download VigilOX ISB/ESB data to Life Support Computer
- Upload to PBA data server

Crew Debrief

- Support Crew brief; give life support status report

Post- debrief

- Administer 4th round of spirometry, capnography for each pilot (in conference room)
- Collate all remaining PBA data and Upload data to server, maintain and manage disk space
- Compete Life Support Metadata report and upload to PBA data server

1.4.4 Scripted Flight Profiles

A key design feature of PBA was the use of scripted flight profiles to produce comprehensive, time-synchronized datasets of pilot breathing together with key aircraft state parameters in a consistent, systematic, methodical, and repeatable way. This was important not only for the PBA team to be able to develop a statistical baseline for comparison across aircraft, AFE configuration, and pilots, but also to provide a template for U.S. military services to consider adapting.

The list below provides the names and single-letter descriptor for the scripted profiles A-H developed and flown in PBA. Each profile was designed with specific detailed instructions for the pilot to gather a comprehensive dataset of breathing response across a broad set of flight conditions. These instructions were captured on a set of flight cards that were executed for each PBA sortie.

PBA Scripted Flight Profiles

- Profile A: High Altitude
- Profile B: AeroBatics
- Profile C: Control
- Profile D: Down low
- Profile E: Elimination of Cabin Pressure
- Profile F: Functional Check Flight
- Profile G: Ground only
- Profile H: Health Check – Standardized Flight Test Profile

These profiles are described in detail in subsequent Section 1.6.1.2. Profile H, described in Technical Section 10, represents a compilation of maneuvers the PBA team believes will challenge a breathing system and help to identify anomalies and deficiencies. The project offers

this profile as a standardized means to baseline specific aircraft and fleet performance as well as to troubleshoot breathing system anomalies and verify corrective actions. In addition, this profile could be used to verify a new design against specifications and provide a measure for production acceptance of new aircraft.

Figure 1.4 shows an example of a scripted maneuver to further illustrate the detail associated with PBA profile scripting and documentation. The "dance card" for Profile D, the low altitude profile is shown, along with the specific flight card detailing some of the low-level maneuvering. The flight card contains annotations taken by the back-seat crew member during the flight. For all sorties, the flight cards were discussed step by step in a pre-flight crew briefing, annotated during flight by the pilot (and back seat aircrew, if applicable), and discussed after each flight in a crew debrief. Figure 1.5 shows a PBA Pilot ready for flight with the flight cards strapped to his leg.

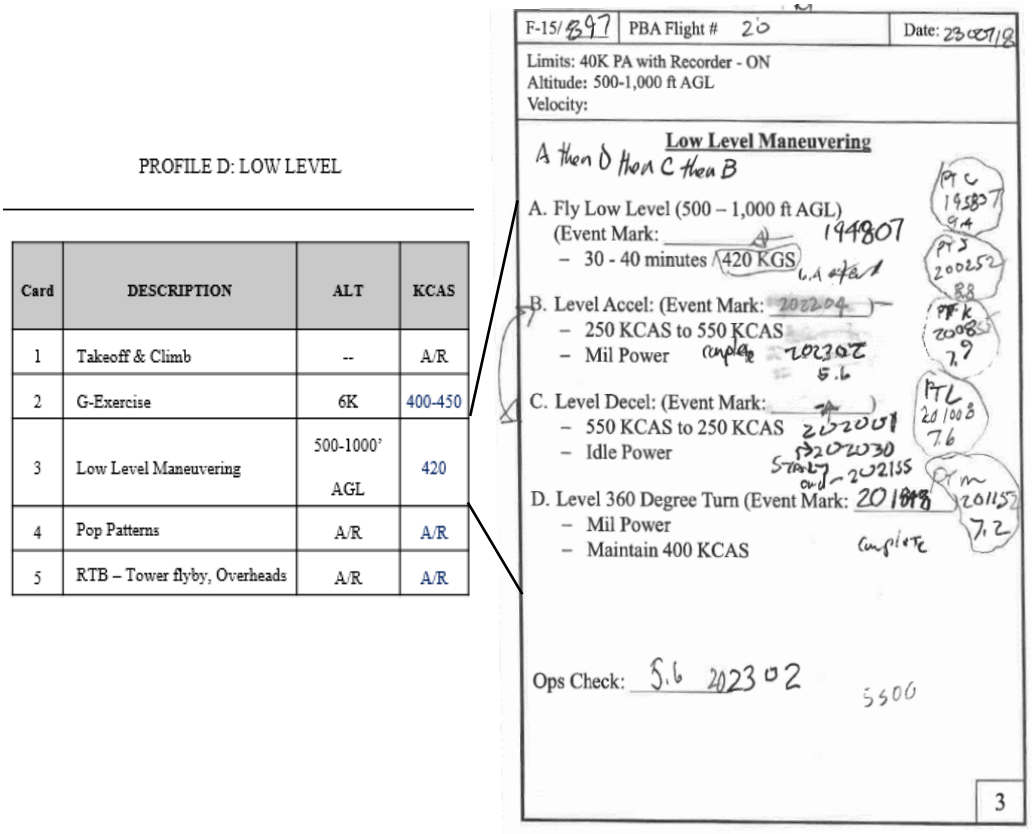

PROFILE D: LOW LEVEL

Card	DESCRIPTION	ALT	KCAS
1	Takeoff & Climb	--	A/R
2	G-Exercise	6K	400-450
3	Low Level Maneuvering	500-1000' AGL	420
4	Pop Patterns	A/R	A/R
5	RTB – Tower flyby, Overheads	A/R	A/R

F-15/ 897 | PBA Flight # 20 | Date: 23 OCT 18

Limits: 40K PA with Recorder - ON
Altitude: 500-1,000 ft AGL
Velocity:

Low Level Maneuvering

A then D then C then B

A. Fly Low Level (500 – 1,000 ft AGL)
(Event Mark: A 194807)
– 30 - 40 minutes 420 KGS

B. Level Accel: (Event Mark: 202204)
– 250 KCAS to 550 KCAS
– Mil Power complete 202302

C. Level Decel: (Event Mark: A 202001)
– 550 KCAS to 250 KCAS
– Idle Power 202030 start 202155

D. Level 360 Degree Turn (Event Mark: 201848)
– Mil Power
– Maintain 400 KCAS complete

Ops Check: 5.6 202302

3

Dance Card for Profile D Card 3

Figure 1.4. Example of Scripted Flight Profile
Dance card for Profile D (left) and notes for low level maneuvers on Card 3 (right).

Figure 1.5. PBA Pilot Ready for Flight
VigilOX ISB hose visible in front; flight cards strapped to pilot's leg.

1.5 Innovation in PBA Study

The PBA study developed a scientific experimental design that generated sufficiently distributed data to make a number of important, and heretofore unknown, statements about pilot breathing interactions with aircraft parameters. Below a series of design protocols are discussed that are novel to such studies.

1.5.1 Novel Repeat Measures Design

PBA was the first known attempt to draw meaningful conclusions of pilot breathing under a wide variety of flight conditions with a focus on repeat measures. That is, PBA was designed to have each pilot fly each profile in each type of aircraft at least two times. Such repeat measures allow calculations to be made of important parameters to better understand if flight to flight differences are more likely due to differences among pilot or aircraft parameters, or if the variability is just intrinsic to flying in general. Table 1.1 list types of repeat measures, referred to as "segments" captured during PBA. In some cases, a segment is a maneuver flown as part of a scripted profile, or an in-flight activity, such as a "talking script" that the pilots performed during the flight. The table shows these segments, a brief description, and the number of segments gathered during the PBA flight program. The compilation of these repeat segments across all flight profiles are the basis for the Pilot Breathing Almanac presented in Technical Section 11.

Table 1.1. List of Repeat Measures for Development of an Almanac of Pilot Breathing

Segment	Descriptions	No. of Segments
Ground	On tarmac, Mask On, mostly pre-flight	7
Takeoff	From Weight-off-wheels to 2.1 kft AGL	35
Military Power Climb	Post Take-off, 5.5 kft per minute, 27 deg Maximum pitch	29
Maximum AB Climb	12.6 kft per minute with After Burner, 47 deg pitch	16
Pop Pattern	Climb to Altitude, then drop 3,000 ft; pull up	20
Low Boom dive	14 kft dive, with the purpose of reaching > Mach 1	18
HighG	Criteria > 3.5 G's. Maximum measured 5.2 G's	93
PostG	Recovery, first 2-3 minutes after G breathing	18
40 Kft	High Altitude, low pressure, long 1 hour duration	7
Sonic	Includes Transonic and Supersonic. Criteria > 0.9 Mach, up to 1.3 Mach	33
Combat Descent	Fast descent at 45 deg, dropping 17 kft/minute	26
Post Combat Descent	2 minutes of recovery breathing, after Combat Descent	25
OBOGS Descent	Long duration descent from 40 kft, > 10 minutes	7
Post OBOGS descent	Recovery period of 2 minutes, immediately following OBOGS descent	10
Airline Descent	Slow descent, 11 degrees, 3 kft/minute	15
Flight Baseline	<1.5 G's, 500 ft ALT delta, <7 deg Pitch	13
Talking Script	Pilots talked in-flight with mask on, following 2x 30 second scripts	40
Maximum Breath	Taken during Velocity < 300 KCAS, straight and level, usually 3x repeat	35

PBA developed and used an *in-situ* technique to parse data from the eight different profiles into these segments. An "Event mark" was a digital mark in the VigilOX data which could later be read automatically by analysis software to locate the beginning and/or end of a data segment. An event mark was introduced simultaneously to the ISB and ESB when the pilot pressed a button on a splitter cable connected to both sensor blocks. Event marks made it easier for analysts to segment and compare like flight maneuvers and events from different profiles.

The flight cards specified an Event Mark immediately prior to the start of each maneuver or event in the cards. In some cases, a second Event Mark was specified at the end of a maneuver (usually long duration maneuvers) to bound the end of the data. Figure 1.6 shows (a) the event mark cable with the button and two ends of the splitter cable going to the VigilOX ISB and ESB, (b) the location of the event mark cable on the USN harness, (c) the list of event markers associated with the 10 different events in a Profile A flight, and (d) where the event marks exist during the flight time history.

(a) Event Mark Cable

(b) PBA Test Pilot in Navy AFE and breathing measurement systems

Event Mark Number	Flight Segment Description
1	Mask Up
2	Level accel 1.25M
3	Talking Script 1
4	Talking Script 2
5	360 Turn 2.2g
6	Maintain Alt, 60 mins
7	Decel
8	Descent 5k
9	RTB
10	Mask off

(c) Event Mark Table

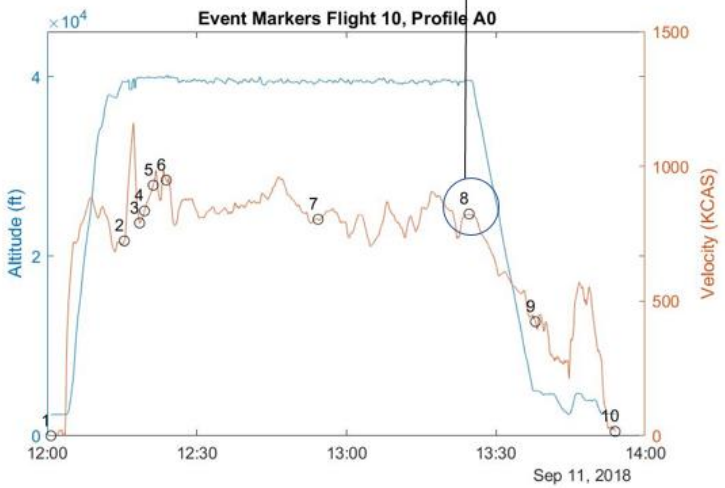

(d) Event Mark Number at time and condition during an example PBA flight

Figure 1.6. Event Mark Cable and its Location, List of Event Markers, and Event Marks Location During Flight Time History
(a) Event Mark Cable with Button and Two Ends of Splitter Cable Going to VigilOX ISB and ESB, (b) Location of Event Mark Cable on USN Harness, (c) List of Event Markers Associated with 10 Different Events in Profile A Flight, and (d) Where Event Marks Exist During Flight Time History

Figure 1.7 shows the segmented data associated with event markers 1 – 9 as listed within the figure.

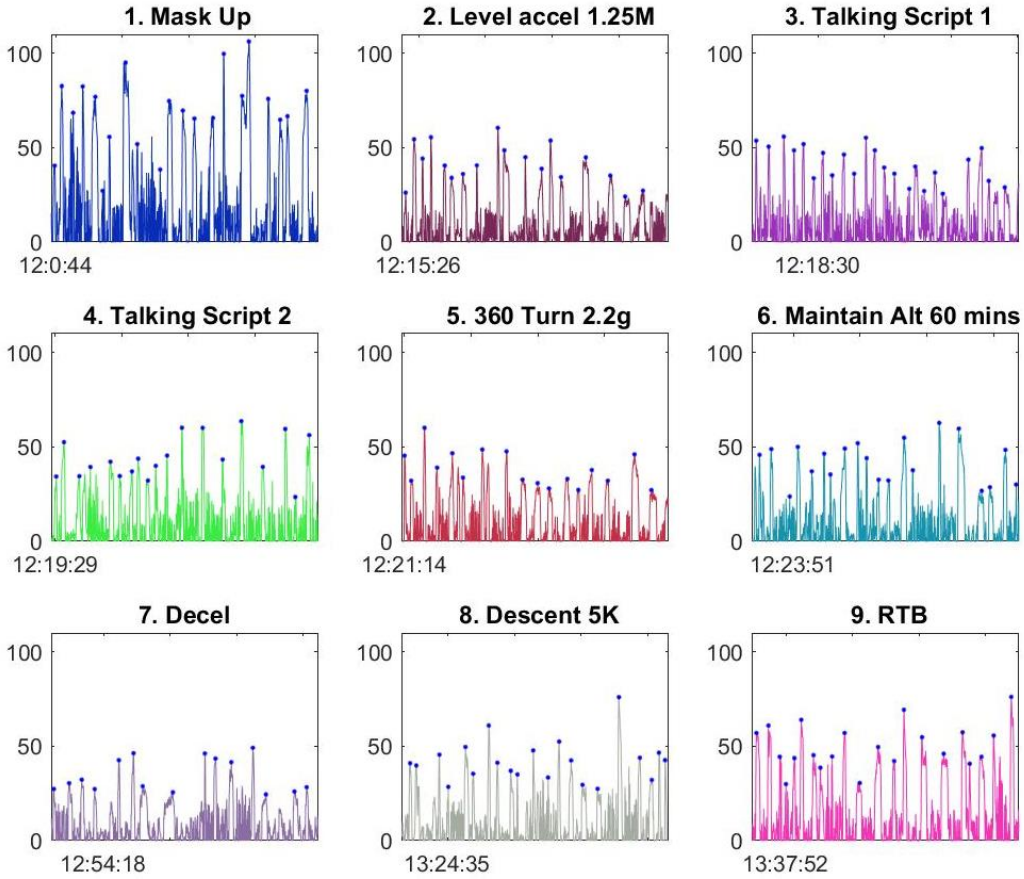

Figure 1.7. Example of Data Segmented by Event Markers 1 – 9 as Identified Previously in Figure 1.6 Note that event marker 10 (mask off) is not included.

1.5.2 Comprehensive Breathing Datasets in Broad Spectrum of Flight Conditions

Flight testing provides real environmental conditions and gathers unique data that cannot be duplicated anywhere else. Very few reports have been found in the literature where human breathing data have been acquired in a flight environment, as described in Section 1.2 in this Technical Section (Harding, 1987 and Gordge, 1993 are exceptions). Most testing of AFE, such as masks and regulators, are conducted in ground test laboratories and using ideal breathing machines that simulate breathing. While important and necessary, these machines cannot capture physiological factors that significantly affect breathing dynamics. Such factors include the subtlety and wide variability in human physiology and the interaction that occurs between the human and the machine, the latter of which includes the compliance of lungs, airways and diaphragm muscles that both affect and are affected during the process of breathing. Most importantly, these machines do not factor in human's innate ability to compensate, sometimes subconsciously, to less-than ideal breathing conditions. Ground breathing machines provide highly repeatable breathing dynamics in closely controlled environments, but the conditions they produce are often a poor representation of in-flight breathing.

1.5.3 Real-world Flight Segments Linked to Pilot Physiological Behavior

A large body of seminal research on human physiology for aircraft and spacecraft was conducted in the 1950s and 1960s. However, in the post-cold war period, severe funding cuts to the research infrastructure and expertise that undergirded these studies have impacted the ability of the nation to keep pace with the advances in aeronautics design, engineering and modern technology. (Lyon, 2013; Martin, 2013). Despite this negative impact, a few organizations still exist (although significantly diminished) and continue to pursue human-systems integration (HSI) research in government laboratories or ground test facilities.

Although some observations of in-flight pilot breathing parameters have been published (Gordge 1993, Harding 1987), PBA is the first designed study to acquire comprehensive in-flight, in-situ breathing data and link these data to pilot physiological response. One of the central questions PBA was designed to answer is *"What does realistic, real-world breathing look like for a pilot operating a high performance jet and undergoing a variety of common flight maneuvers?* Previous work sheds little light on this question. For the PE problem, this has dire consequences. Causal factors due to gaps in the OTM (Figure 1.1) will remain an enigma until Pilot Breathing data can be acquired (NESC, 2017).

An Almanac of pilot breathing is presented in Technical Section 11. This almanac links the repeat measures, or flight segments, listed in Table 1.1 to pilot breathing response.

1.5.4 Focus on Pilot Breathing Demands

The process that humans use to exchange $CO_2$and O_2 is one of the most fundamental of all physiological processes in life. And yet, as the PBA team has grown to appreciate over the past eight years and three assessments, the process involved in human breathing is deceptively subtle and complex. The pressures involved in normal, open air breathing at 1g are small. In contrast, the pressures a pilot is subjected to in flight by a modern aircraft breathing system can be large, variable, and at times, chaotic and unpredictable. Very little is known about what effects these pressure changes have on the human and what the human really needs while flying modern high-performance aircraft.

PBA was designed to focus on the breathing demands of human in the machine. In an effort to better understand the complexity of breathing dynamics, these were reviewed, and animations were developed to characterize the basics of ideal human breathing at 1 atm. Technical Section 2 reviews these fundamentals. PBA returned to the basics of breathing physiology before addressing more complex questions, for example: *"How is a person's breathing affected while breathing under positive-pressure- vs. non-positive-pressure breathing systems?"* Conversely, *"How is a breathing system affected when a human is intentionally breathing with an unnatural cadence, such as "G-breathing" under high G's?"*, and *"How does a human breathe and how does this change in flight with a pressure regulator?)"* These basic primers were essential in understanding the complex questions of pilot breathing.

1.5.5 Design and Observational Study Elements

PBA consisted of aspects of both observational and designed studies. Designed studies apply "a treatment (or a protocol, procedure, or methodology) to individuals (e.g., pilots) and attempts to isolate the effects of these treatments on a response variable." (Sullivan, 2015). An example of such methodologies employed in PBA was the use of scripted profiles discussed earlier. The intent was to gather breathing data from all five pilots, who flew the same profiles multiple

times, to control and monitor variables that affect pilot breathing. Examples of the methodologies and protocols used in PBA are summarized below and discussed in greater detail in subsequent portions of this report. Specifically, the aircraft and pilot response variables and the data summaries are discussed in Technical Section 5, and detailed engineering analyses are explored in Technical Section 6. The underlying data set for summary statistical analysis is based on 50 flights with an aggregate of 3275 flight minutes. Other specialty flights were conducted to explore specific issues including cabin pressure variance and mask configuration modifications.

An observational aspect in the form of pre- and post-flight pilot surveys was also an important part of PBA. As the name implies, observational studies "observe the characteristics of a population by studying individuals in a sample but do not attempt to manipulate or influence the variables of interest." (Sullivan, 2015). Two examples of observational elements used in PBA involved pilot surveys. Pre- and post-assessment surveys were conducted to help correlate effects on pilot physiology that may have occurred during flight. In addition, day-of-flight pilot surveys were also conducted before and after each sortie to understand any changes associated with that particular flight. Pilot interviews and survey results are presented and discussed in Appendix 9.

1.5.6 Wide Array of Inflight Pilot Physiological Data

Figures 1.8 and 1.9 show two data analysis products and the wide array of inflight pilot physiological data acquired and calculated from a single PBA flight. Figure 1.8 presents tile data in a format that allows quick visualization and characterization of unified flight data and pilot breathing at a glance. Parameters include inhalation and exhalation flows, mask pressure and O_2 concentration together with aircraft parameters of O_2 delivery or line pressure, aircraft altitude, position (latitude/longitude), and G-level.

Figure 1.9 shows the metabolic products for a given PBA flight. The metabolic analysis processing provides a standard format for pilot physiological activity. This standardized format provides a detailed look at what the pilot and aircraft are experiencing and how the pilot's breathing and metabolic activity are changing at all phases of flight. Metabolic parameters include respiration rate, ppO_2, ventilation rate, O_2 supply rate, inspired O_2 flow rates, and tidal volumes.

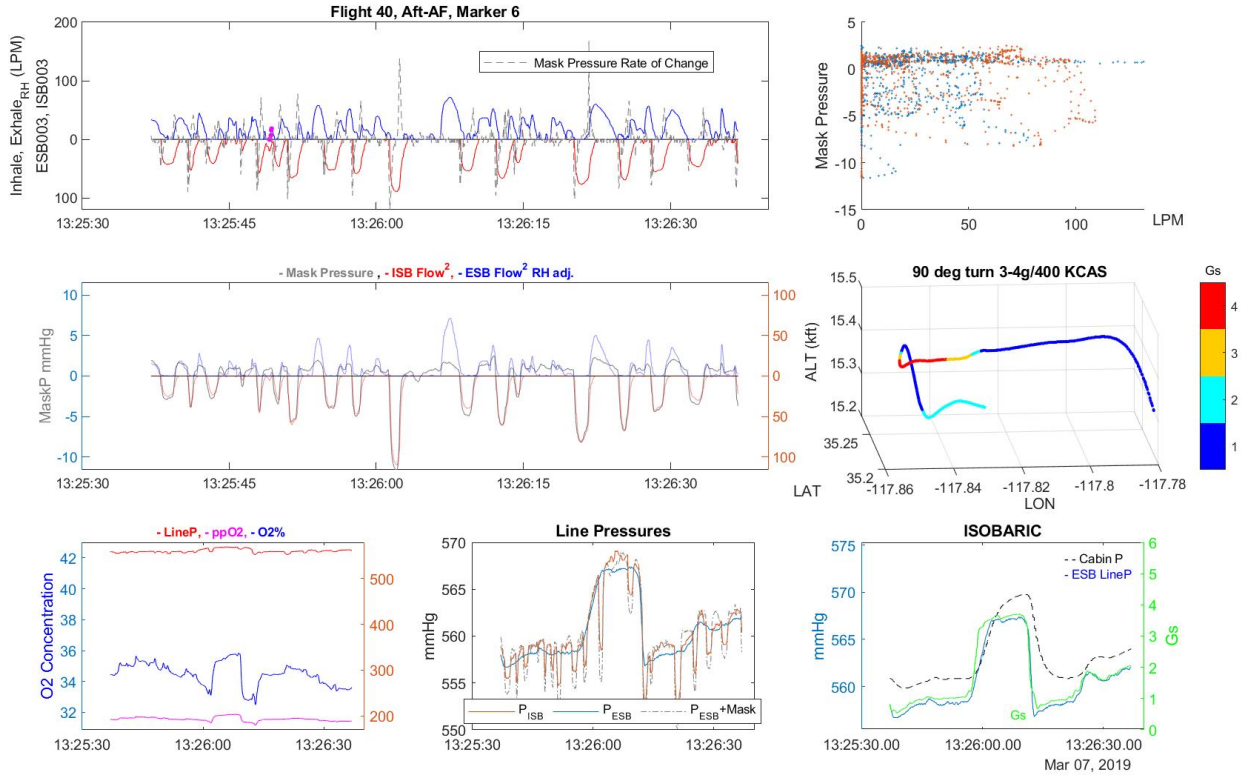

Figure 1.8. Analysis Data "Tiles"
Consisting of data formatted for quick visualization and characterization of unified flight data at a glance.

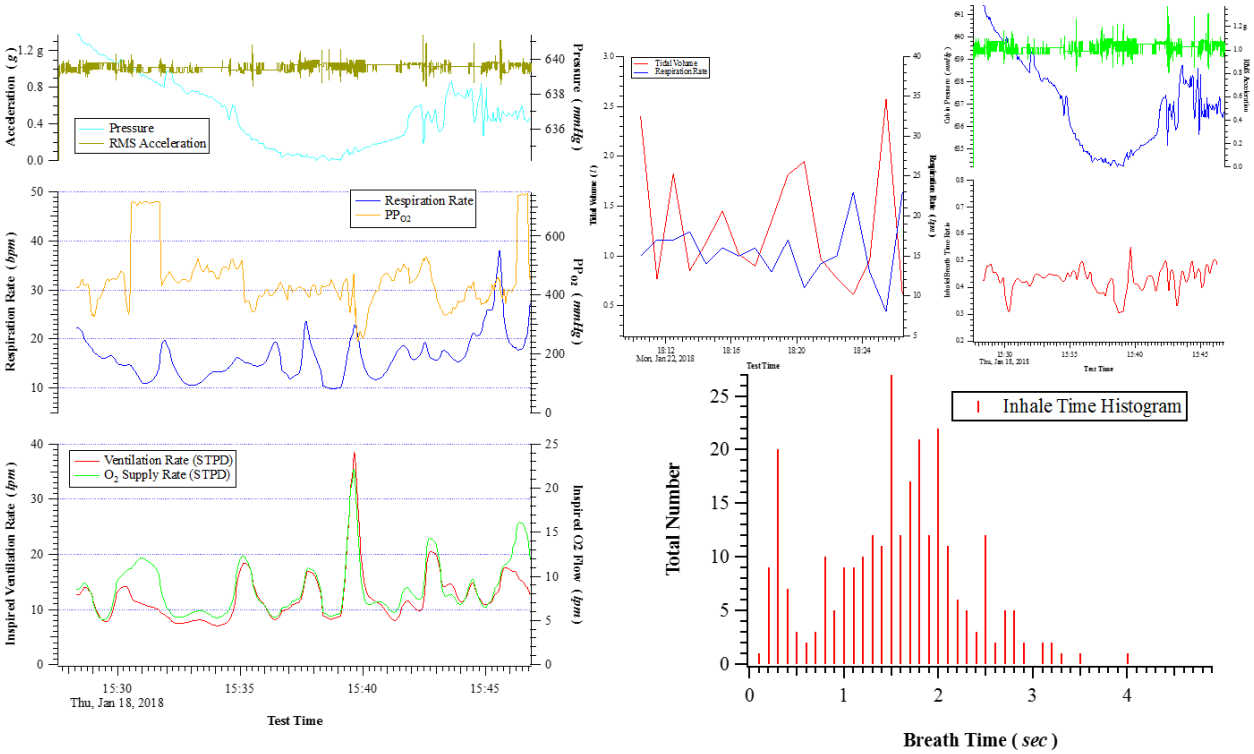

Figure 1.9. Metabolic Products for Single PBA Flight

1.5.7 Pilot Physiological Data Acquired Before and After Flying

A key feature of PBA was the inclusion of tests to gather the pilot's physiological data (e.g., spirometry and capnography) at four points on a PBA flight day, as show in Figure 1.10. The first set of tests were administered at approximately one hour prior to flight, while the pilot was sitting at rest and prior to donning his AFE. The same tests were repeated after donning AFE and while strapped in the jet just minutes before engine start, generally 30 to 40 minutes prior to take-off. Any effect of the AFE and position in the cockpit could be assessed with these measurements. The third set of measurements were collected immediately after the flight, with the pilot still strapped in the cockpit, under the same conditions as the second set of tests. These measurements were gathered to assess what effect, if any, the flying of a given sortie had on the pilot's physiology. The fourth and final set of data were gathered post-flight, under the same conditions as the first set. The equipment used and the parameters measured are introduced later in Section 1.6.2.4 and results presented in Technical Section 7: Pilot Physiology and Medical Outcomes.

Pilot physiological testing helped the project discern the differences among and within pilots as well as to see how high-performance flights could affect short-term breathing capability. In previous work, NASA NESC had suggested that PEs could be related to pre-flight "priming" from exposures and other activities unrelated to the flying activity, and additionally that the flight itself could exacerbate mild pulmonary inflammatory response.

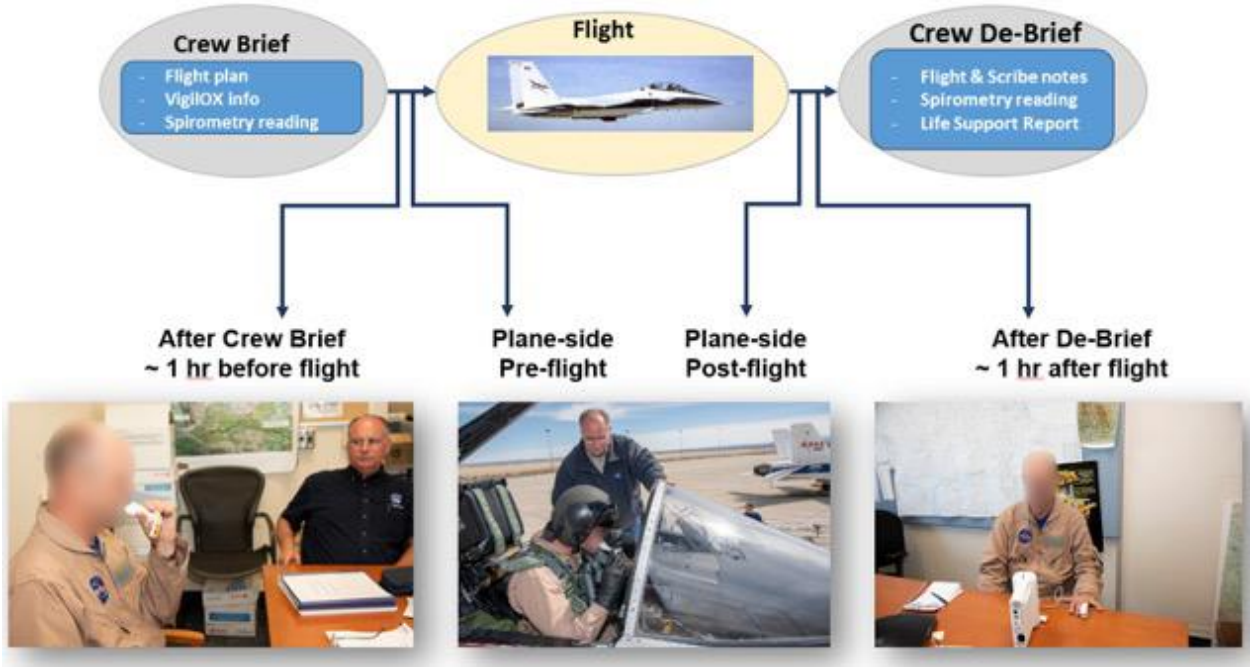

Figure 1.10. Physiological Testing of Pilots During Crew Brief
Pre- and post-flight in flight gear and strapped in the cockpit, and during flight debrief.

1.6 Technical Descriptions and Overview

This section provides the technical description and overview of the aircraft flown, the equipment used, and the data collected for PBA.

1.6.1 Metadata

Included in this section is a description of the metadata of the aircraft, flight profiles, AFE, pilot de-identification approach, the data systems used, and pilot observations.

1.6.1.1 Aircraft

Two F/A-18A models (single-seat), two F/A-18B models (dual-seat), and two F-15D models (dual seat) were used to fly 131 sorties, 65 of which were used by PBA analysts. Figure 1.2 shows the aircraft flown at NASA AFRC in support of PBA. Table 1.2 shows the tail numbers, models, serial numbers, BUNOs, production numbers and years on the PBA aircraft at AFRC. The F/A-18 Hornets and the F-15 Eagles were acquired from the USN and USAF, respectively, as the services upgraded their fleet with newer models. All the jets in the AFRC support aircraft fleet are early production models, equipped with LOX systems that pre-date the conversion of systems to OBOGS. The use of LOX jets is key in reducing the confounding factors associated with OBOGS and helped the project focus instead on pilot breathing needs, breathing dynamics, and subtle interactions of other parts (regulators, masks) of the breathing system.

Table 1.2. PBA Aircraft Metadata
Tail numbers, models, serial numbers, BUNOs, production numbers and years, tail numbers, hours flown, and hours of total life.

F-15D			
Tail No.	Model (MDS)	Serial No.	Production Year
N884NA	F-15D	78-0564	1978
N897NA	F-15D	79-0007	1979

F/A-18A/B				
Tail No.	Model	BUNO	Production #	Year /Lot / Block
N843NA [1]	F/A-18A [2]	161519	A-027	1982 / Lot IV / Block 6
N850NA [1]	F/A-18A	161703	A-038	1982 / Lot V / Block 8
N846NA	TF/A-18 [2,3]	161355	B-006	1981 / Lot IV / Block 5
N868NA	F/A-18B	161938	B-022	1983 / Lot VI / Block 11

[1] Aircraft retired during PBA [2] Previous Blue Angel aircraft [3] Lot IV upgraded to Lot V (TF/

1.6.1.2 Flight Profiles

Profile Design Philosophy

Five different flight profiles (A, B, C, D, F) were initially developed to provide data for a variety of typical fighter-type missions. They were designed to be executable with a single load of fuel in an F-18B configured with a centerline fuel tank. Limitations at AFRC which drove the content of these profiles included:

- AFRC support fleet aircraft are limited to 5 G's.
- A second aircraft would rarely be available, so missions were designed single-ship.
- Air refueling assets were rarely available, so missions needed to be flown un-refueled.

- AFRC pilots were not current in Air Combat Maneuvering or Weapons Delivery, so generic fighter-like maneuvers were employed.

A ground-only, Profile G, was developed which could be accomplished on its own or in conjunction with a flight.

Even though the test aircraft all had LOX-based breathing systems, the flight profiles were designed with the anticipation they would later be flown in aircraft with OBOGS-based breathing systems and the data would be compared. Some of the maneuvers were specifically chosen based on current evidence which suggested they would stress OBOGS. It was not expected that any of the maneuvers or profiles would result in any physiological incidents when flown with LOX systems.

After data analysis of the initial phase of flight test, Profile E was added to explore the effects of the aircraft cabin pressure regulation system on pilot breathing dynamics. Finally, near the end of the assessment, a "Breathing System Functional Check Flight", Profile H, was developed and flown as a deliverable of the project.
Each of the profiles was designed to study different factors which might affect the pilot's physiology or breathing dynamics differently. Many of the maneuvers and events were repeated in at least two different profiles to investigate whether the results were affected by the overall profile in which a specific occurred. The seven flight profiles and one ground profile were as follows:

- Profile A: High Altitude
- Profile B: AeroBatics
- Profile C: Control
- Profile D: Down low
- Profile E: Elimination of Cabin Pressure
- Profile F: Function Check Flight
- Profile G: Ground only
- Profile H: Health Check - Standardized Flight Test Profile

The content of these profiles is discussed in more detail below.

Profile A: High Altitude

This profile was designed to represent a cross-country flight in which the pilot climbs to high altitude and cruises for a long duration before descending to land. The breathing effort on this type of flight was low, but the pilot's physiology was subjected to a cabin altitude at or above 15,000 ft. The intent of Profile A was to investigate the effects of this high-altitude exposure on the pilot's breathing dynamics. The specific events were as follows:

- Military Power Takeoff
- Military Power climb to 45,000 ft
- Level Acceleration – Maximum After Burner (AB) (0.90 – 1.25 Mach)
- Level Deceleration – Idle (1.25 Mach – 0.90 Mach)
- Talking Scripts (1 min)
- 45,000 ft level 360-degree turn (0.90 Mach)
- Remain at or above 15,000 ft Cabin Altitude (CA) for 60 minutes
- 'OBOGS Descent' – 45,000 ft to 5000 ft Pressure Altitude (PA), (no lower than 2000 ft AGL) - Idle/250 KCAS

- Return to Base (RTB) – Straight-In approach (ILS or TACAN) then Initial for full-stop

Profile B: AeroBatics

This profile was designed to require a higher breathing effort from the pilot. Within the limitations explained above, this profile used aerobatics and elevated G maneuvers to represent the breathing dynamics a pilot would experience on a Basic Fighter Maneuvers (BFM) training sortie, while providing single-ship maneuvers which could be executed precisely and repeatably. Profile B was intended to be the most physically challenging of all the profiles. The specific events were as follows:

- Maximum Power Takeoff
- Maximum AB Climb from 5,000 ft to 30,000 ft PA/0.90 Mach
- Talking Script
- 'Combat Descent' – 30,000 ft to 5000 ft PA (no lower than 2000 ft AGL)
    - Idle/SB
    - 0.85 Mach until 420 KCAS, hold KCAS
- G-Exercise: 90 turn at 3 to 4 G, 90 turn at 4 to 5 G @ 15,000 ft PA
- Level 360-degree 5-G turn @ 15,000 ft 5,000 ft/450 KCAS)
- Check 6 assessment (left & right)
- 3 x Squirrel Cage
    - Start 15,000 ft PA, 450 KCAS
    - Consecutive Loop, ½ Cuban 8, Immelmann, Split-S
    - Recover @ 300 KCAS for 2 min between sets
- 5-G Wind Up Turn (WUT) – start 20,000 ft PA/450 KCAS, hold 1 min
- Spiral Descent – start 20,000 ft PA/350 KCAS, Military Power
    - Pull 4 G's to decelerate to 300 KCAS, relax to 2 G's to accelerate back to 350 KCAS
    - Simultaneously descend 5 to 10 degrees Flight Path Angle (FPA) while alternating G/airspeed, stop after 3 minutes
- Talking Script - 5,000 ft PA
- RTB – Tower Fly-By @ 450 KCAS then sim-single engine touch & go followed by normal overhead for Full stop

Profile C: Control

This profile was designed to be a benign profile flown at a relatively constant, medium altitude with low breathing effort. Effects of different settings for the aircraft Environmental Control System (ECS) were investigated and the ECS was characterized at various speeds. Profile C was intended as the initial baseline profile to gather the first data from the VigilOX and as the first sortie for each of the pilots. The specific events were as follows:

- Military Power Takeoff & Climb to 20,000 ft PA
- Level 360-degree 3-G turn @ 20,000 ft PA/400 KCAS
- Level Acceleration/Deceleration – 250 KCAS to 0.95M to 250 KCAS @ 20,000 ft PA
- Defog – MIN/MAX/MID – 20,000 ft PA/350 KCAS (3 min @ each setting)
- Cockpit Temperature – Full Cold to Full Hot to Full Cold (over 2 min)

- ECS Characterization @ 20,000 ft PA – 2 min @ each speed
  170 KCAS (w/flaps)/300 KCAS/0.90M/0.98M/1.10M
- Talking Scripts
- Barrel Roll/Wingover/Aileron Roll
- Slow Flight (Gear/Flaps) – On Speed – 2 minutes
- Airline descent – 5 degrees FPA/300 KCAS from 20,000 ft to 5,000 ft PA
- RTB – Instrument approach then Initial for overhead full stop

Profile D: Down Low

This profile was designed to stay below 8,000 ft PA so that the cabin pressure remained equal to outside atmospheric pressure. The maneuvers are similar to those a military pilot would execute on a low-altitude tactical training sortie. This profile was intended to investigate breathing dynamics at a cabin altitude below that at which supplemental O_2 is normally required while demanding a moderate breathing effort from the pilot. The specific events were as follows:

- Military Power Takeoff
- G Exercise: 90 turn @ 3 to 4 G's/400 KCAS then 90 turn @ 4 to 5 G's/450 KCAS
- Low Level for 20 to 30 minutes
- Level Military Power Acceleration from 250 KCAS to 550 KCAS
- Level Idle Power Deceleration 550 KCAS to 250 KCAS
- Level 360 Military Power maintaining 400 KCAS
- 2 x 15 degree Pop patterns
- RTB
  - Tower Fly-By @ 450 KCAS
  - Instrument Approach
  - Overhead to Full stop

Profile E: Elimination of Cabin Pressure

Profile E was initially designated an Extra profile for a use to be determined later in the program. After the first phase of flight test and subsequent data analysis, the team observed that the F-18 cabin pressure fluctuated from its designed schedule under a variety of conditions. The cabin pressure is an input to the function of the O_2 regulator and also has a physiological effect on the pilot. To investigate the impact of these effects, the team recognized the need for a profile which eliminated off-schedule fluctuation, but which otherwise duplicated the airspeeds, G's, and maneuvering of one of the previously flown profiles. To accomplish this, the profile was flown with the Cabin Pressure Switch set to RAM DUMP, which equalized the cabin pressure with outside atmospheric pressure. Profile B was chosen as the profile to duplicate. The actual aircraft altitude in Profile E was kept equal to the cabin altitude scheduled by the cabin pressurization system at the same point in a Profile B sortie. For example, the cabin altitude during a typical Squirrel Cage should be constant at 8,000' PA, so in Profile E, the Squirrel Cage was flown in the horizontal plane at 8,000 ft PA, instead of climbing and diving in the vertical

plane. Profile E was intended to replicate the cabin pressure time history of a Profile B sortie while flying at the same airspeeds and G level. The specific events were as follows:

- Maximum Power Takeoff
- Maximum AB Climb 5,000 to 8,000 ft PA, level off 1 min, 10-degree climb at 350 KCAS to 12,000 ft PA
- Talking Scripts at 12,000 ft PA
- Combat Descent: 10-degree descent at 420 KCAS, level off at 8,000 ft PA for 40 sec, then continue 15-degree descent at 420 KCAS to 5,000 ft PA
- G-Exercise: 90 turn at 3 to 4 G's, 90 turn at 4 to 5 G's @ 8,000 ft PA
- Level 360-degree 5-G turn @ 8,000 ft/450 KCAS
- Check 6 assessment (left & right) @ 8,000 ft PA
- 3 x "Squirrel Cage"
    - Start 450 KCAS; entire maneuver level at 8,000 ft PA
    - "Loop": level turn in Idle for 180 deg to slow to ~220 KCAS, then Min AB for next 180 degrees to accelerate to ~450 KCAS; G's to match a vertical Loop
    - "½ Cuban 8": level turn like Loop above but after 225 degrees of turn, roll opposite direction and continue 45 degrees more turn; G's to match a vertical Cuban 8
    - "Immelmann": level turn Loop above but after 180 degrees of turn, roll opposite direction, pause
    - "Split-S": continue another 180 degrees of turn accelerating back to ~450 KCAS
    - Recover @ 300 KCAS for 2 min between sets
- Level 5-G turn at 8000 ft PA; start at 0.85 to 0.90 Mach; hold 5 G's for 1 min
- Level turn at 8000 ft PA; pull 4 to 5 G's in level flight to decelerate to 300 KCAS. Relax to 2 G's and accelerate back to 350 KCAS using 1 eng MIN AB/1 eng MIL. Alternate between 4- and 5-G-level pull and 2-G Acceleration for 3 minutes.
- Talking Script @ 5,000 ft PA/300 KCAS
- RTB – Sim-single engine touch & go followed by normal overhead for Full stop

Profile F: Functional Check Flight

Profile F was designed to cover most of the flight envelope in altitude and airspeed. It includes some systems checks, as can be found in a Functional Check Flight (FCF) profile, as well as breathing exercises conducted with a variety of ECS and regulator settings. Profile F was intended to investigate the effects of the aircraft breathing system settings on pilot breathing dynamics with only a low level of breathing effort from the pilot, but while also covering a larger part of the aircraft envelope than the other profiles. The specific events were as follows:

- Military Power Takeoff
- Military Power Climb from 5,000 to 40,000 ft PA/350 KCAS then 0.85 Mach
- Talking Script
- Baseline breathing, regulator effects @ 40,000 ft PA/250 KCAS
- Combat Descent – 40,000 to 15,000 ft PA, Idle/SB, 0.85 Mach then 420 KCAS

- Baseline breathing, cabin pressurization, ECS, and regulator systems effects @ 15,000 ft PA/250 KCAS
- Talking Scripts
- Check 6 assessment
- Maximum AB Climb from 15,000 to 45,000 ft PA
- Low Boom Dive: start @ 49,000 ft PA/0.96 Mach, roll and pull to achieve 53-degree dive/1.10 Mach @ 40,000 ft PA, then pull 3.5 G's until nose above the horizon
- Full aft stick stall: start above 30,000 ft AGL, recover NLT 25,000 ft AGL
- Cabin pressurization transition: 300 KCAS/2000 FPM climb from 22,000 to 26,000 ft PA then 300 KCAS/2000 FPM descent from 26,000-22,000 ft PA
- Airline Descent – 20,000 to 5,000 ft PA, 5-degree FPA/300 KCAS, power as required
- RTB for Instrument approach, then Overhead for a Full stop

Profile G: Ground only

Profile G was designed to be accomplished on the ground with the engines running to eliminate any effects caused by altitude, airspeed, G, or high power settings. The profile can be conducted independent of a PBA flight, or in conjunction with one. When executing Profile G, the team generally proceeded directly to Profile F in flight. Profile G was intended to provide a baseline of pilot breathing with regulator effects for comparison to inflight measurements. The specific events were as follows:

- Mask Off/Mask On Breathing
- Ground System Operation
- Breathing Exercises
- Talking Scripts
- Canopy Operations
- Check-6 assessment

Profile H: Health Check - Standardized Flight Test Profile

Profile H was designed as a compilation of maneuvers the PBA team believes will challenge a breathing system and help to identify anomalies and deficiencies. This profile is explained in more detail in Technical Section 10. Profile H was intended as a standardized means to baseline specific aircraft and fleet performance as well as to troubleshoot breathing system anomalies and verify corrective actions. In addition, this profile could be used to verify a new design against specifications and provide a measure for production acceptance of new aircraft. The specific events were as follows:

- Ground Block I
- Military Power Takeoff/Military Power Climb 5,000 to 15,000 ft PA
- Breathing Baseline – 15,000 ft PA
- Mask On/Off Comparison – 15,000 ft PA
- Talking Script – 15,000 ft PA
- Military Power Climb 15,000 to 30,000 ft PA
- OBOGS Descent 30,000 to 7,000 ft PA
- Military Power Climb 7,000 to 15,000 ft PA

- Breathing Baseline – 25,000 ft PA
- Combat Descent and Zoom Climb 25,000 to 7,000 to 12,000 ft PA
- G-Exercise – 12,000 ft PA
- 5 G's Descending Turn for 1 minute, start 15,000 ft PA
- Maximum AB Climb 7,000 to 30,000 ft PA
- Breathing Baseline – 30,000 ft PA
- Cruise Descent 30,000 to 20,000 ft PA – DEFOG HIGH
- Descending turn – 20,000 to 12,000 ft PA – alternating 4 to 5 G's, then 2 G's for 3 minutes
- RTB
- Ground Block II

1.6.1.3 Aircrew Flight Equipment

The Life Support Specialist has the important job of maintaining the pilot's AFE. AFE is safety equipment that keeps the pilot safe and healthy throughout all nominal and off-nominal events that occur during a wide variety of planned and unforeseen mission scenarios. USAF AFE includes the pilot's helmet, mask, harness, G-suit, parachute, and survival kit. The USN AFE includes the pilot's helmet, mask, integrated survival vest/harness, G-suit, parachute, survival kit, and O_2 regulator. Unlike the USAF, the USN includes many survival items in the integrated survival vest/harness including a life preserver in case of an overwater ejection. The USN AFE is attached to a larger and tighter safety harness. These essential pieces of equipment are designed to meet the pilot's physiological needs during the highly dynamic and extreme conditions of flight as well as protect the pilot during ejection and provide resources for land/sea survival.

For commonality of equipment, training, and support, the F/A-18s operated at NASA AFRC have long been modified to use a CRU-73 panel-mounted regulator and a USAF-style harness for attaching the pilot into the seat, to the survival kit, and to the parachute. In this report, that configuration is referred to as the "USAF configuration" of the F-18. To support PBA's requirement to better mimic a more typical USN configuration, the F/A-18s were converted back to their original USN configuration to use a CRU-103 harness-mounted regulator, and to accept a USN-style harness for attaching the pilot into the seat, to the survival kit, and to the parachute. In this report, that configuration is referred to as the "USN configuration". When NASA F-15s were used for PBA flights, only their original USAF configuration was flown; they were not modified to accept USN flight gear.

The two AFE configurations, USN and USAF, were used throughout the PBA project to determine the effect the AFE has on pilot breathing dynamics. Switching between configurations required changing both the parachute and survival kit located in the ejection seat for compatible O_2 and parachute riser connections with the pilot's harness.

AFE metadata were captured before and after every flight in a Life Support Metadata Report (see LSS Report example in Appendix 1. For the day-of-flight, the LSS report documented the AFE configuration assembled by life support specialists to support a given sortie. Such data included the following for the flight:

- Name of Life Support Specialist
- Flight AFE Config

- Pre-flight LS Metadata for both FCP and RCP (if applicable)
    - ISB Serial No/Software Version/Sync Time
    - ESB Serial No/Software Version/Sync Time
    - O2 Connector (e.g., EDOX)
    - Regulator Used (e.g., CRU-103 for USN, CRU-73 for USAF)
    - Madgetech Cockpit Pressure Sensor, Serial No.
    - Madgetech Sensor for In-line Supply pressure on CRU-103, Serial No.
    - Special Hardware, e.g., Flow Straighteners, Moisture Trap
- Post-Flight LS Metadata for both FCP, RCP (if applicable)
    - ISB, Data file name
    - ESB, Data file name
    - Post-flight observations/anomalies, if any
        - e.g., Spirometry difficulties
        - Weather: high/low temperatures, high winds
        - Other environmental factors that affect data

1.6.1.3.1 Mask: MBU-20/P

COMBAT EDGE MBU-20/P O_2 masks (Gentex Corporation, Carbondale, Pennsylvania) were used exclusively throughout PBA by all five test pilots (Figure 1.11). The masks and mask components are discussed in greater detail in Technical Section 2 (Fundamentals of Pilot Breathing) and Technical Section 8 (Non-PBA Aircraft Analysis and Lessons of PBA Data for Other Breathing Systems).

Figure 1.11. MBU-20/P Mask, Exterior and Interior Photographs Showing Hose Connections and Non-Rebreathing Valves, Respectively
The MBU-20/P mask is described in greater detail in Technical Sections 2 and 8.

Five sizes are available for the MBU-20/P mask. For PBA, two pilots wore medium narrow, two wore medium wide, and 1 wore a large wide mask size. Based on the differences in mask sizes, and the geometric differences in faces between pilots, the mask volumes, sometimes referred to as "dead space" in the mask can vary slightly from pilot to pilot – within a few ml. These differences were considered to be negligible in PBA analysis. If a pilot's mask was required to be replaced, it was replaced with the same style and size. Because an individual pilot used the same size mask throughout the program, the dead space in the mask remained consistent for a given pilot throughout the program.

1.6.1.3.2 USN Configuration

Figure 1.12a shows a PBA pilot suited up with AFE in the "USN configuration". Figure 1.12b shows the components of the USN configuration with PBA instrumentation. A MadgeTech in-

line pressure sensor was connected between the O_2 supply line and the CRU-103 regulator. The VigilOX ISB was connected between the CRU-103 and the pilot's O_2 hose. An extra flexible O_2 hose was connected to the MBU-20P mask at the normal exhalation port to route the pilot's exhaled breath to the VigilOX ESB. A U-shaped moisture trap with absorbent material was connected between the exhalation hose and the ESB to collect moisture in the pilot's breath which would tend to corrupt the ESB data. (Note: the Madgetech in-line pressure sensor and the moisture trap were added after Flight 59, courtesy of NAVAIR). The Event Mark cable is connected to both the ISB and ESB to allow the pilot to simultaneously place an Event Mark in the ISB and ESB data.

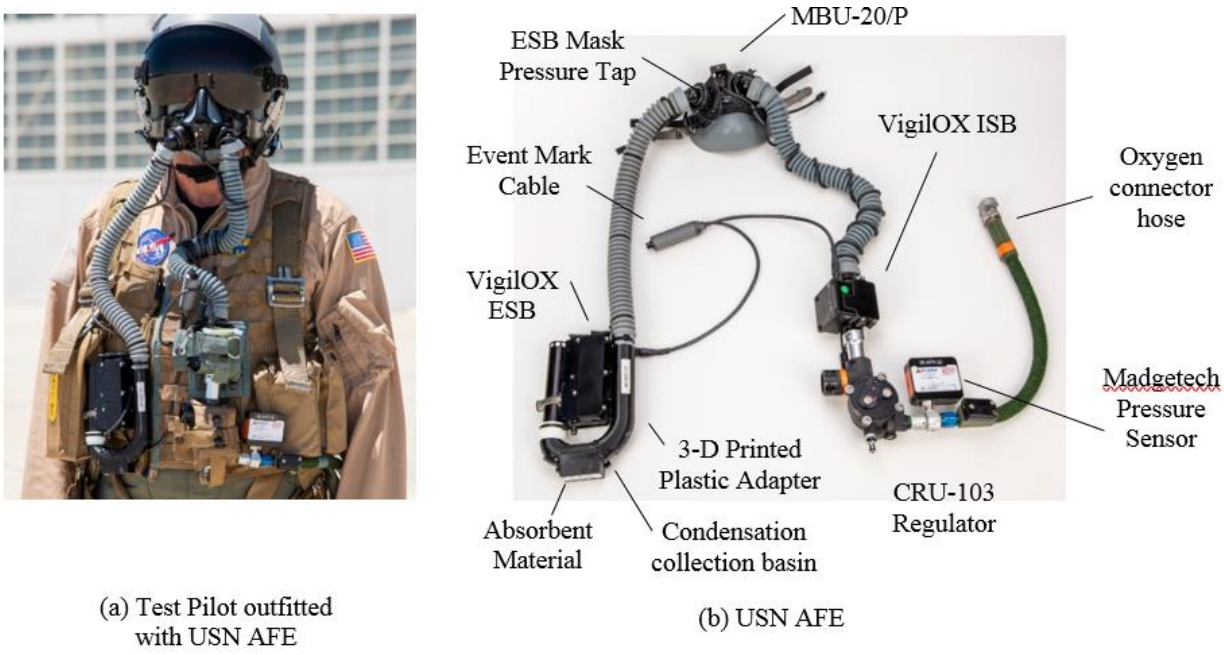

Figure 1.12. (a) PBA Pilot Wearing USN AFE, (b) USN AFE Components Corresponding to Starting at Beginning of Flow
The O_2 connector, MadgeTech in-line pressure sensor, CRU-103 Breathing Regulator, the VigilOX ISB, Mask inhalation hose, MBU-20/P Mask, the ESB Mask Pressure port, the exhalation hose, 3-D printed U-shaped moisture trap, condensation basin, absorbent, VigilOX ESB, and the event mark cable.

1.6.1.3.3 USAF AFE

Figure 1.13a shows a PBA test pilot wearing AFE referred to in this assessment as "USAF configuration", which was flown in both the F/A-18 and the F-15. In this configuration, the O_2 supply hose is on the pilot's right and comes from the aircraft side panel, controlled by the CRU-73 panel-mounted regulator shown. The O_2 supply hose is attached to the pilot's harness at the EDOX connector. The MadgeTech pressure sensor was not installed as there was no attach point available. The VigilOX ISB was connected between the EDOX and the pilot's O_2 hose going to the MBU-20P mask. An extra flexible O_2 hose was connected to the mask at the normal exhalation port to route the pilot's exhalation breath to the VigilOX ESB, mounted on the left side of the harness. This configuration did not permit installation of the moisture trap used with the USN AFE. The Event Mark cable is connected to both the ISB and ESB to allow the pilot to simultaneously place an Event Mark in the ISB and ESB data.

(a) *(b)*

Figure 1.13. (a) USAF AFE Configuration as Worn by Pilot and (b) Photograph of CRU-73 Panel-Mounted Breathing Regulator used for USAF AFE (F-15 and F/A-18)

1.6.1.4 Pilot Identification

A pilot identification number was randomly assigned to each aircrew member to maintain pilot anonymity through the assessment. A pilot identification table was developed and privately maintained by a single person so that the identity of the pilot could not be easily traced to the data and comments produced on a given sortie. The unique pilot identification number was part of the flight identification descriptor that was used to define sorties, data file names, directory structures, metadata reports, and analysis products. As an example, every PBA flight was assigned a unique name according to the following convention.

Table 1.3. Flight ID key code

Flight ID Key:	
"001-5-884-0605188-B2-XX"	
001	Flight No.
5	Aircraft: 5=F-15; 8=F/A-18
884	tail number
060518	date of flight
B2	Nomenclature for flight profile
	(second digit is version no. where no

Breathing data collected via VigilOX, SpiroDoc, Rad-97 systems were keyed to the Flight ID above to protect pilot identity. Similarly, survey data collected from the pilots before and after every flight were also referenced only by the Flight ID.

1.6.2 Data-Streams

1.6.2.1 VigilOX

There are enormous challenges in getting scientific systems to work in the rigors of high-performance flight. The design, development, test, and flight validation of flight systems are expensive, time consuming, and necessarily results in reduced system capability compared to their ground test counterparts. Flight system designers have often traded channel count, measurement uncertainty, power consumption, storage capacity, sensor sample rates and other important features to work safely and reliably in the flight environment. Flight integration and testing often requires close partnership with the sensor/system vendors who are often required to provide specialized training and product support for field applications.

Figure 1.14 shows the Cobham VigilOX chest mounted flight system integrated with the USN AFE. The figure also shows, the location of the event marker), the ISB, the ESB, and the various parameters acquired and calculated, along with their respective engineering units and data acquisition rates.

VigilOX represents a break-through for physiological flight testing. Though not without issues, VigilOX has enabled access to data that has not been available before. Some of the salient features of VigilOX, its heritage, version numbers, and its limitations are discussed in greater detail in Technical Section 3.

Exhalation Sensor Block **(ESB)**
Line P (mmHg)
Line T (°C)
Mask Pressure (mmHg)
PPO_2 (mmHg)
$PPCO_2$ (mmHg)
*Rate 20 hz**

Cabin P (mmHg)
Cabin T (°C)
*Rate 2.5 hz**

VigilOX ESB

VigilOX ISB

Inhalation Sensor Block (ISB)
Line P (mmHg)
Line T (°C)
PPO_2 (mmHg)
*Rate 20 hz**

Cabin P (mmHg)
Cabin T (°C)
*Rate 2.5 hz**

Calculated Data Values

- Flow (all flows are calculated from pressure differentials and approximated gas density)
- Inhalation/Exhalation (differential between ISB and ESB)

Figure 1.14. Description of VigilOX Instrumentation and Attachment Points On Pilot Gear

1.6.2.2 Madgetech Pressure Sensors

In-line Supply Pressure Sensors

(a) *(b)* *(c)*

Figure 1.15. MadgeTech Pressure Sensor Integrated In-line with CRU-103 Breathing Regulator (a) as worn by the pilot, (b) shown connected on the bench, and (c) magnified to show details.

Cabin Pressure Sensors

Figure 1.16. MadgeTech Pressure Sensor Mounted in Cockpit Map Case to Measure Cabin Pressure for PBA Flights After Flight 60, Both USN and USAF Configurations

1.6.2.3 Aircraft Data

The aircraft data systems used in PBA were set up to record MIL-STD-1553 channels in a format called “Chapter 10”. Chapter 10 refers to the IRIG 106 Chapter 10 which was defined to standardize data formats for telemetered and multi-streamed data from military aircraft. This section describes the two aircraft data systems used.

1.6.2.3.1 AFRC TTC Recorders

The aircraft described in the previous section were each outfitted with flight data instrumentation systems for the collection of research quality flight datasets. The instrumentation systems used for several PBA aircraft (F/A-18 T/N 843/846/850, F-15 T/N 884/897) were TTC MUX-3005R (Teletronics Technology Corp, a Curtiss-Wright Defense Solutions, Davidson, North Carolina,

USA). These systems, referred to in this report as “TTC recorders”, record flight data from various sources into IRIG 106 Chapter 10 standard format. The TTC recorders are comprised of an MUX-3005R flight data recorder with 5 input/output (I/O) slots, an internal recorder slot that takes removable storage media that supports IRIG 106 Chapter 10, 4-channel 20-Mpbs PCM card, and an 8-channel MIL-STD-1553 Bus Card for capturing bus data. The removable solid-state recorder cartridges were used to facilitate the process of downloading flight data after every sortie and allow a quick turnaround for further flights. The TTC recorders acquired the aircraft Memory Unit (MU) data from the various streams on the 1553 databus as well as derived parameters of interest to PBA.

1.6.2.3.2 NAVAIR QIK System

Figure 1.17 shows one of the aircraft recorders used in PBA, referred as the “QIK System”, courtesy of the USN NAVAIR China Lake, CA. F/A-18 850 used such a system, which was designed, built, and flight tested by NAVAIR. The QIK system used standard communication and power protocols that interfaced efficiently with the F/A-18 aircraft systems.

Figure 1.17. USN QIK System on F-18, TN850

1.6.2.4 Medical/Physiological Instruments

As stated, PBA is primarily a methods development activity with the goal of gathering information and developing techniques that previously did not exist. One such embodiment of this goal was the development of methods to assess the impact of flight on pulmonary function of pilots. New methods and protocols were developed by NASA and USN flight surgeons, in concert with LSSs and instrument vendors. The scientific equipment was designed for use in benign indoor laboratory environments but was repurposed for use in the extreme environment of the California high desert flight line. The goal was to measure pulmonary function parameters before and after instrumented flights using handheld portable medical devices with the pilot strapped into the cockpit just before and after a flight. The results were used to help assess possible correlations between pulmonary function and flight activity and fit of the AFE.

Pre and post flight data were collected and labeled to ensure that the data analyst did not know the name or identification of the person.

The two devices used in PBA to assess pulmonary function are shown in Figure 1.18. The SpiroDoc handheld spirometer (MIR - Medical International Research USA, Inc., New Berlin,

WI, USA) and the Rad-97 (Masimo Corp., 52 Discovery, Irvine, CA, USA) are shown in Figure 1.19(a) and (b), respectively.

For the SpiroDoc, the most pertinent parameters used in assessing pilot breathing were FEV1, PEF, FEF 25-75, which establish a baseline as to how fast one can exhale. FVC was also useful in determine the volume of biggest breath one can take. The SpiroDoc was used to acquire the following spirometric parameters: FVC, FEV1, FEV1/FVC%, FEV3, FEV3/FVC%, FEV6, FEV1/FEV6%, PEF, FEF25%, FEF50%, FEF75%, FEF25%-75%, FET, Estimated Lung Age, Extr. Vol., FIVC, FIV1, FIV1/FIVC%, PIF, VC, IVC, IC, ERV, FEV1/VC%, VT, VE, Rf, ti, te, ti/t-tot, VT/ti, MVV measured, MVV calculated. For Pulse-oximetry, the spirodoc measured the following parameters: SpO2 [Baseline, Min, Max, Mean], Pulse rate [Baseline, Min, Max, Mean], T90% [SpO25%], ΔIndex [12s], SpO2 Events, Pulse rate events [Bradycardia, Tachycardia], Recording time, Analysis time.

The Rad-97 was used to perform pulse CO-Oximetry and capnography or noninvasive blood pressure (NIBP) measurement for PBA. Of special interest was the pilot's SpO2 (O_2 saturation), PR (pulse rate), Pi (perfusion index), and PVi (Pleth variability index).

(a) ***(b)***

Figure 1.18. (a) The MIR Corp Spirodoc Handheld Spirometer and Pulse-Oximeter, and (b) Masimo Corp, Rad-97.

(a) ***(b)***

Figure 1.19. (a) In Situ Capnography Immediately Pre- and Post-Flight in Cockpit Suited in AF, and (b) 1 Hour Pre- and Post-Flight without AFE
(Note: spirometry and capnography were performed at all four times, as described in 1.0.4.7., and 7.4.1).

1.6.2.5 Pilot Breathing Data

As discussed in Section 1.5.6, the metabolic products for a given flight were calculated and analyzed. Pilot breathing parameters such as breathing rate, O_2 concentrations, inhalation and exhalation flows, and tidal volumes were measured.

1.6.2.6 Aircraft Data

Table 1.4 provides a list of aircraft data parameters, including aircraft altitude, air speed, position (INS Lat/Lon), 3-axis acceleration, and cabin pressure. The aircraft data are discussed in greater detail in Technical Section 4.

Table 1.4. Key Aircraft Data Parameters, Engineering Units (20 Hz sample rates)

Aircraft Parameters		
Label	**Description**	**Unit**
TIME	UTC Time given in POSIX format, with a 10E-6 second precision	HH:mm:ss.00
INBIALT	INS BARO Inertial Altitude	ft
INLNACC	INS Longitudinal Acceleration	ft/s^2
INLTACC	INS Lateral Acceleration	ft/s^2
INNMACC	Aircraft Normal Acceleration	ft/s^2
INPITCH	Pitch (torque movement around the cross axis)	angle [-90:90]
ADPALT	Pressure Altitude	ft
INVACC	INS Vertical Acceleration	ft/s^2
ENPLA1	Engine Power Lever Angle (1=Left Engine)	angle (1:100)
INLAT	INS Latitude	degree
INLON	INS Longitude	degree
INNVEL	Inertial North Velocity	ft/s
INEVEL	Inertial East Velocity	ft/s
INVVEL	Inertial Vertical Velocity	ft/s
INROLL	Roll (torque movement around the body long axis)	angle [-180:180]
INTHDG	True Heading	degree

1.6.2.7 Flight Cards

Another important source of PBA metadata were aircrew flight cards as shown below in Figure 1.20. The pilots used these cards to record Event Marks, deviations from the script, comments, and observations for review in the flight debrief and for inclusion in the flight report.

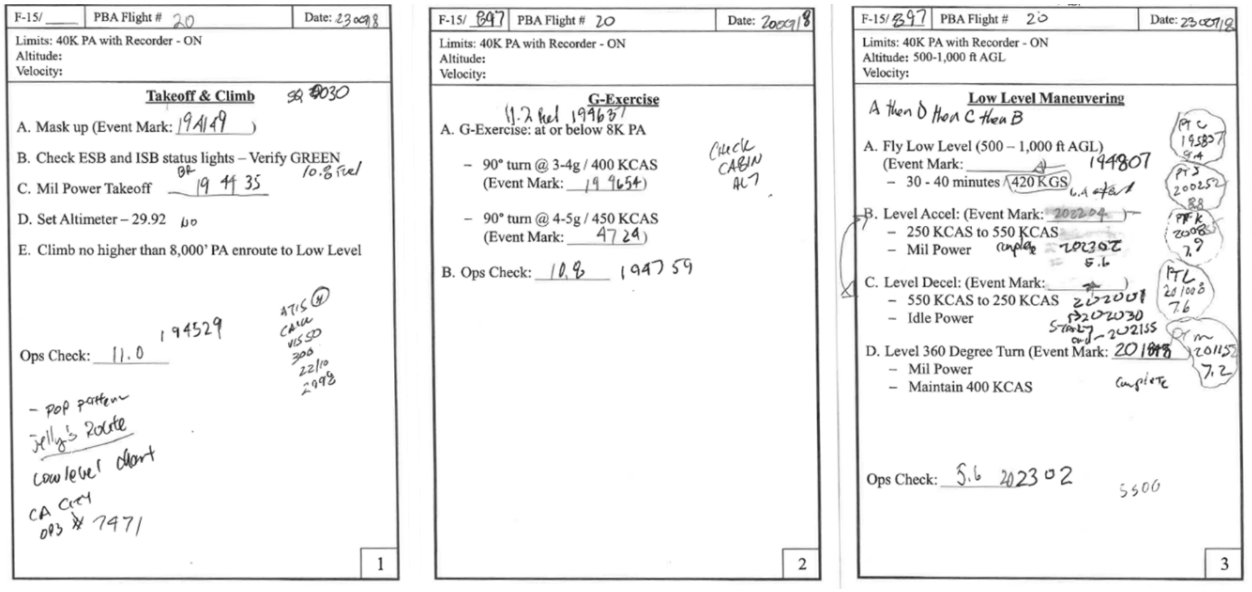

Figure 1.20. Flight Card Examples Showing In-Flight Hand-Written Notes

1.6.2.8 Pilot Post-Flight Test Reports

As mentioned earlier, pilot observations can be one of the most valuable sources of diagnostic information for understanding breathing phenomena. PBA pilots captured their observations about their respective flights through verbal post-flight debriefings of their flight cards and written post flight test reports. By design, the profiles were not intended to stress a pilot to the point of causing a PE. However, as is the case many times in flight test, the unexpected occurs without warning. Flight Test reports were often the first written evidence that a problem occurred and could point the analyst to the right location in the data for in-depth quantitative analysis.

1.6.2.9 In-Flight and Post-Flight Debriefing Audio Recordings

Audio recordings captured the communication during a sortie between the pilot and the control room for nearly all the PBA flights. If all other sources of data failed to clarify the events of a flight, the com files could be accessed and the events that transpired could be reviewed. Post-flight debriefings were also recorded and uploaded to the project servers for reference.

1.6.3 Flight Sortie Summary

A rigorous screening process was used to ensure that the PBA analysis products were of the highest quality and that a common dataset was used consistently by all analysts. This screening process is described in greater detail in Technical Section 4. Table 1.5 summarizes the number of flight hours, and sorties in various categories. PBA dedicated sorties and "ride along" sorties (defined below) are shown in blue highlights; the number of *ad hoc* sorties for troubleshooting and diagnostics, as well as the total number of completed sorties are shown in green highlights; Subgroups of sorties used for detailed high resolution analyses, and those used to develop summary statistics are shown in orange highlights.

Table 1.5. Flight Sortie Summary

PBA Dedicated Sorties	Ride-Along Sorties	Partial and Checkout Sorties	Fully Completed Sorties	Specialized Sorties for Detailed Analyses	Specialized Sorties for Statistical Analyses
115	12	20	107	87	50

PBA flew 115 dedicated sorties at NASA AFRC over a two years period, and accumulated a total of 160 flight hours, where each sortie took an average of 1.3 hours/sortie. An additional 12 so-called "ride-along" flights were conducted by another flight project that permitted VigilOX data to be gathered during a scripted profile. Both aircraft and breathing data from these flights were generously provided to PBA for follow-on analyses. Five of these ride-along flights were included in the PBA analysis database. Of the 127 sorties flown (Dedicated and Ride-along), 107 were operationally complete in that the pilot performed the entire profile and aircraft data were acquired during the entire sortie and were provided as a project deliverable.

Table 1.5 also includes 20 "Checkout" sorties, which were reasonable due to challenges that are inherent in developing and implementing a complex set of flight-test methods. Most of these sorties occurred in the early phases of the assessment and were considered as "pathfinder" or "shake-out" flights. Projects that seek to develop new ground- and flight test methodologies, like PBA, require more checkout sorties to work out flight integration and operational issues. Such issues stemmed from developing new flight test procedures and protocols with multiple pilots, multiple aircraft, two aircraft types, two types of AFE configurations, and three disparate data systems (VigilOX ISB, VigilOX ESB, and aircraft instrumentation) that all had to work together in flight. The integration and flight testing with VigilOX were major sources of the operational challenges that needed to be worked through. Each flight of the 115 flights was valuable and assisted in the implementation of this complex endeavor.

There were 87 sorties contained subsets of flights that served specific needs for the report. In some of these sorties, especially the early ones, the VigilOX data contained errors in certain segments of the sortie (such as DFRL errors described in Technical Section 3). The adversely affected flight segments were excluded from the dataset. The remaining data were used in the various analyses presented this report (see Technical Section 4 for a complete listing of data used for analyses and demonstration studies). The DFRL errors were minimized mid-way through the program (in Flight 59) after a USN-designed device was provided to the project and integrated within the USN AFE (Section 1.6.1.3.2, Figure 1.12). As a subset of these specialized sorties, 45 flights were selected to represent the primary Profiles A through E; these included 5 back seat pilot datasets deemed independent, resulting in a total of 50 fully completed independent pilot breathing flights. This reduced dataset was produced from five of the eight profiles (Profiles A-E) that all contained physiologically reasonable breathing data. This was done to ensure the mixed modeling efforts were as balanced and as physiologically relevant as possible. Other profiles, such as Profiles F and G were designed to stress the aircraft breathing system and contained extreme breathing exercises that were outside the bounds of normal breathing that a pilot would normally produce during flight. For example, pilots were instructed to take maximum breaths to tax the breathing systems but were not a realistic representation of pilot breathing. Additionally, pilots flying these profiles followed procedures to drop their masks to evaluate the impact on aircraft O_2 delivery. These types of actions from Profiles F and G would unrealistically bias the 1-minute statistics. The data for this analysis needed physiological

relevant data to be acquired throughout the entire sortie to ensure each of the one-min summary statistics were statistically meaningful.

1.6.4 PBA Test Summary at Glance

The entire list of PBA flights flown are shown in Table 1.6. Relevant metadata associated with the flight, such as the Flight ID., date, systems meta data, profile ID for Front Cockpit (FCP) and Rear Cockpit (RCP), if applicable, the AFE configuration, etc.

PBA overall flight statistics parsed by different metadata groups.

Tables 1.7 a, b, c, d, e, and f provides a summary of all the metadata distribution of PBA flights at a glance. Further details of all flights and all measurement data are provided in the comprehensive "Flight Almanac" in Technical Section 11.

Of the 65 fully successful flights indicated in Table 1.5, 5 of the profiles (A-E) were down-selected for 1-min statistical analysis (Section 1.6.4). Table 1.7a shows the distribution of these 50 sorties by pilot and profile.

Table 1.6. Total PBA Flights at a Glance

Test Name	Test Date	Plane type	Single / Dual Seat	Flight Profile	FCP	RCP	Front Cockpit (FCP)		Rear Cockpit (RCP)		Front Cockpit (FCP)			Rear Cockpit (RCP)		
							VigilOX ISB	VigilOX ESB	VigilOX ISB	VigilOX ESB	AFE	Aircraft Regulator Type	Oxygen Connector	AFE	Aircraft Regulator Type	Oxygen Connector
001-5-884-060518-P0-71-09	6/5/2018	F-15	Dual	Prof	71	9	DEV003	DEV004	n/a	n/a	AF/AFRC	CRU98	CRU60/P	AF/AFRC		
002-8-850-080318-C-28-00	8/3/2018	F-18	Single	C0	28	n/a	DEV003	n/a	n/a	n/a	AF/AFRC	CRU73	EDOX	AF/AFRC		
003-8-850-080918-C-12-00	8/9/2018	F-18	Single	C0	12	n/a	DEV003	n/a	n/a	n/a	AF/AFRC	CRU73	EDOX	AF/AFRC		
004-8-850-081618-C1-71-00	8/16/2018	F-18	Single	C1	71	n/a	DEV003	n/a	n/a	n/a	AF/AFRC	CRU73	EDOX	AF/AFRC		
005-5-884-081718-C1-21-18	8/17/2018	F-15	Dual	C1	21	18	No Data	n/a	n/a	n/a	AF/AFRC	CRU98	CRU60/P	AF/AFRC		
006-5-884-082118-C1-71-18	8/21/2018	F-15	Dual	C1	71	18	DEV003	n/a	n/a	n/a	AF/AFRC	CRU98	CRU60/P	AF/AFRC		
007-5-884-090418-A0-71-45	9/4/2018	F-15	Dual	A0	71	45	DEV003	EDEV08	n/a	n/a	AF/AFRC	CRU98	CRU60/P	AF/AFRC		
008-8-846-090518-C1-21-XX	9/5/2018	F-18	Dual	C1	21	XX	DEV003	EDEV08	n/a	n/a	AF/AFRC	CRU73	EDOX	AF/AFRC		
009-5-884-090618-A0-55-18	9/6/2018	F-15	Dual	A0	55	18	DEV003	EDEV08	n/a	n/a	AF/AFRC	CRU98	CRU60/P	AF/AFRC		
010-5-884-091118-A0-21-23	9/11/2018	F-15	Dual	A0	21	23	DEV003	EDEV08	n/a	n/a	AF/AFRC	CRU98	CRU60/P	AF/AFRC		
011-5-884-091218-C1-55-68	9/12/2018	F-15	Dual	C1	55	68	DEV003	EDEV08	n/a	n/a	AF/AFRC	CRU98	CRU60/P	AF/AFRC		
012-5-884-091918-B0-21-18	9/19/2018	F-15	Dual	B0	21	18	DEV006	EDEV04	n/a	n/a	AF/AFRC	CRU98	CRU60/P	AF/AFRC		
013-8-846-100318-B0-12-21	10/3/2018	F-18	Dual	B0	12	21	DEV003	EDEV05	DEV006	EDEV04	AF/AFRC	CRU73/9682	EDOX	AF/AFRC	CRU73/12370	EDOX
014-8-846-100318-D0-12-21	10/3/2018	F-18	Dual	D0	12	21	DEV003	EDEV05	DEV006	EDEV04	AF/AFRC	CRU73/9682	EDOX	AF/AFRC	CRU73/12370	EDOX
015-8-846-100418-D0-28-55	10/4/2018	F-18	Dual	D0	28	55	DEV006	EDEV04	DEV003	EDEV05	AF/AFRC	CRU73/9682	EDOX	AF/AFRC	CRU73/12370	EDOX
016-5-884-100918-D0-21-64	10/9/2018	F-15	Dual	D0	21	64	DEV003	EDEV04	n/a	n/a	AF/AFRC	CRU98/404243	CRU60	AF/AFRC	CRU98/4030321	CRU60
017-8-850-101118-D0-71-00	10/11/2018	F-18	Single	D0	71	n/a	DEV003	EDEV05	n/a	n/a	USN	n/a	CRU103/P Ser#	n/a	n/a	n/a
018-8-846-101718-F0-28-68	10/17/2018	F-18	Dual	F0	28	68	DEV003	EDEV05	DEV006	EDEV04	AF/AFRC	CRU73/9682	EDOX	AF/AFRC	CRU73/12370	EDOX
019-8-846-101818-F0-28-68	10/18/2018	F-18	Dual	F0	28	68	DEV006	EDEV05	DEV003	EDE004	AF/AFRC	CRU73/9682	EDOX	AF/AFRC	CRU73/12370	EDOX
020-5-897-102318-D0-71-28	10/23/2018	F-15	Dual	D0	71	28	DEV003	EDEV05	DEV006	EDEV04	AF/AFRC	CRU98/479XMC3	CRU60	AF/AFRC	CRU98/467033	CRU60
021-5-897-102418-D0-55-64	10/24/2018	F-15	Dual	D0	55	64	DEV006	EDEV05	DEV003	EDEV04	AF/AFRC	CRU98/479XMC3	CRU60	AF/AFRC	CRU98/467033	
022-8-850-102918-A0-28-00	10/29/2018	F-18	Single	A0	28	n/a	DEV003	EDEV04	n/a	n/a	USN	n/a	CRU103/20303	n/a	n/a	n/a
023-8-850-103018-F0-12-00	10/30/2018	F-18	Single	F0	12	n/a	DEV003	EDEV04	n/a	n/a	USN	n/a	CRU103/20294	n/a	n/a	n/a
024-8-850-112118-B0-28-00	11/21/2018	F-18	Single	B0	28	n/a	ISB001	ESB002	n/a	n/a	USN	n/a	CRU103/20288	n/a	n/a	n/a
025-8-850-112618-F0-21-00	11/26/2018	F-18	Single	F0	21	n/a	ISB001	ESB002	n/a	n/a	USN	n/a	CRU103/20303	n/a	n/a	n/a
026-8-850-112718-A0-55-00	11/27/2018	F-18	Single	A0	55	n/a	ISB003	ESB003	n/a	n/a	USN	n/a	CRU103/20292	n/a	n/a	n/a
027-8-850-112718-A0-12-00	11/27/2018	F-18	Single	A0	12	n/a	ISB002	ESB001	n/a	n/a	USN	n/a	CRU103/20294	n/a	n/a	n/a
028-8-850-112818-C1-12-00	11/28/2018	F-18	Single	C0	12	n/a	ISB001	ESB001	n/a	n/a	USN	n/a	CRU103/20294	n/a	n/a	n/a
029-8-850-121018-B0-55-00	12/10/2018	F-18	Single	B0	55	n/a	ISB002	ESB004	n/a	n/a	USN	n/a	CRU103/20294	n/a	n/a	n/a
030-8-850-121118-C1-28-00	12/11/2018	F-18	Single	C0	28	n/a	ISB002	ESB004	n/a	n/a	USN	n/a	CRU103/20294	n/a	n/a	n/a
031-5-884-121218-F1-71-12	12/12/2018	F-15	Dual	F1	71	12	ISB001	ESB001	No Data	ESB003	AF/AFRC	CRU98/404243	CRU60	AF/AFRC	CRU98/4030321	CRU60
032-5-884-121718-B0-55-28	12/17/2018	F-15	Dual	B0	55	28	ISB001	ESB001	ISB002	ESB003	AF/AFRC	CRU98/404243	CRU60	AF/AFRC	CRU98/4030321	CRU60
033-8-850-021119-C1-55-00	2/11/2019	F-18	Single	C1	55	n/a	ISB001	ESB001	n/a	n/a	AF/AFRC	CRU73/507551	EDOX	n/a	n/a	n/a
034-8-850-021219-C1-28-00	2/12/2019	F-18	Single	C1	28	n/a	ISB001	ESB001	n/a	n/a	AF/AFRC	CRU73/507551	EDOX	n/a	n/a	n/a
035-8-850-021519-F1-55-00	2/15/2019	F-18	Single	F1	55	n/a	ISB001	ESB001	n/a	n/a	AF/AFRC	CRU73/507551	EDOX	n/a	n/a	n/a
036-8-850-021919-C1-71-00	2/19/2019	F-18	Single	C1	71	n/a	ISB003	ESB003	n/a	n/a	AF/AFRC	CRU73/507551	EDOX	n/a	n/a	n/a
037-8-850-022619-B0-21-00	2/26/2019	F-18	Single	B0	21	n/a	ISB002	ESB004	n/a	n/a	AF/AFRC	CRU73/507551	EDOX	n/a	n/a	n/a
038-8-846-022819-B0-21-71	2/28/2019	F-18	Dual	B0	21	71	ISB002	ESB004	ISB003	ESB003	USN	n/a	CRU103/20303	AF/AFRC	CRU73/12307	EDOX
039-8-850-030419-A0-71-00	3/4/2019	F-18	Single	A0	71	n/a	ISB002	ESB004	n/a	n/a	USN	n/a	CRU103/20292	n/a	n/a	n/a
040-8-846-030719-B0-71-21	3/7/2019	F-18	Dual	B0	71	21	ISB002	ESB004	ISB003	ESB003	USN	n/a	CRU103/20292	AF/AFRC	CRU73/12370	EDOX
041-8-846-031519-GF-28-12	3/15/2019	F-18	Dual	GF	28	12	ISB002	ESB001	ISB004	ESB003	USN	n/a	CRU103/20292	AF/AFRC	CRU73/12370	EDOX
042-8-846-031519-B0-21-71	3/15/2019	F-18	Dual	B0	21	71										
043-8-850-032619-GF-21-00	3/26/2019	F-18	Single	GF	21	n/a	ISB004	ESB004	n/a	n/a	USN	n/a	CRU103/20303	n/a	n/a	n/a
044-8-850-032619-D0-55-00	3/26/2019	F-18	Single	D0	55	n/a	ISB002	ESB001	n/a	n/a	USN	n/a	CRU103/20292	n/a	n/a	n/a
045-8-846-032919-GF-12-28	3/29/2019	F-18	Dual	GF	12	28	ISB002	ESB001	ISB004	ESB003	USN	n/a	CRU103/20303	AF/AFRC	CRU73/12370	EDOX
046-8-846-041019-B0-21-71	4/10/2019	F-18	Dual	B0	12	21	ISB004	ESB001	ISB003	ISB003	USN	n/a	CRU103/20292	AF/AFRC	CRU73/12370	EDOX
047-8-850-041019-C1-21-00	4/10/2019	F-18	Single	C0	21	n/a	ISB001	ESB004	n/a	n/a	USN	n/a	CRU103/20292	n/a	n/a	n/a
048-8-850-041119-GF-55-00	4/11/2019	F-18	Single	GF	55	n/a	ISB004	ESB004	n/a	n/a	USN	n/a	CRU103/20292	n/a	n/a	n/a
049-8-850-041119-D0-28-00	4/11/2019	F-18	Single	D0	28	n/a	ISB003	ESB001	n/a	n/a	USN	n/a	CRU103/20303	n/a	n/a	n/a
050-8-850-041219-A0-28-00	4/12/2019	F-18	Single	A0	28	n/a	ISB003	ESB001	n/a	n/a	USN	n/a	CRU103/20303	n/a	n/a	n/a
051-8-850-041519-B0-12-00	4/15/2019	F-18	Single	B0	12	n/a	ISB003	ESB001	n/a	n/a	USN	n/a	CRU103/20292	n/a	n/a	n/a
052-8-850-041619-FG-71-00	4/16/2019	F-18	Single	FG	71	n/a	ISB003	ESB003	n/a	n/a	AF/AFRC	CRU73/507551	EDOX	n/a	n/a	n/a
053-8-850-041719-B0-28-00	4/17/2019	F-18	Single	B0	28	n/a	ISB003	ESB003	n/a	n/a	AF/AFRC	CRU73/507551	EDOX	n/a	n/a	n/a
054-8-850-041719-C1-12-00	4/17/2019	F-18	Single	C1	12	n/a	ISB004	ESB001	n/a	n/a	AF/AFRC	CRU73/507551	EDOX	n/a	n/a	n/a
055-8-850-041819-A0-12-00	4/18/2019	F-18	Single	A0	12	n/a	ISB004	ESB001	n/a	n/a	AF/AFRC	CRU73/507551	EDOX	n/a	n/a	n/a
056-8-850-042219-A0-28-00	4/22/2019	F-18	Single	A0	28	n/a	ISB004	ESB001	n/a	n/a	AF/AFRC	CRU73/507551	EDOX	n/a	n/a	n/a
057-8-850-042319-GF-28-00	4/23/2019	F-18	Single	GF	28	n/a	ISB004	ESB001	n/a	n/a	AF/AFRC	CRU73/507551	EDOX	n/a	n/a	n/a
058-8-850-042419-GF-12-00	4/24/2019	F-18	Single	GF	12	n/a	ISB004	ESB001	n/a	n/a	AF/AFRC	CRU73/507551	EDOX	n/a	n/a	n/a
059-8-850-042619-B0-71-00	4/26/2019	F-18	Single	B0	71	n/a	ISB004	ESB001	n/a	n/a	AF/AFRC	CRU73/507551	EDOX	n/a	n/a	n/a
060-8-850-050119-C1-71-00	5/1/2019	F-18	Single	C1	71	n/a	ISB003	ESB003	n/a	n/a	USN	n/a	CRU103/19647	n/a	n/a	n/a
061-8-850-050119-A0-21-00	5/1/2019	F-18	Single	A0	21	n/a	ISB004	ESB002	n/a	n/a	USN	n/a	CRU103/19647	n/a	n/a	n/a
062-8-850-050219-D0-21-00	5/2/2019	F-18	Single	D0	21	n/a	ISB003	ESB003	n/a	n/a	USN	n/a	CRU103/19647	n/a	n/a	n/a
063-8-850-050619-GF-71-00	5/6/2019	F-18	Single	GF	71	n/a	ISB003	ESB003	n/a	n/a	USN	n/a	CRU103/19647	n/a	n/a	n/a
064-8-850-050619-D0-28-00	5/6/2019	F-18	Single	D0	28	n/a	ISB004	ESB001	n/a	n/a	USN	n/a	CRU103/19647	n/a	n/a	n/a
065-8-850-050819-B0-12-00	5/8/2019	F-18	Single	B0	12	n/a	ISB001	ESB002	n/a	n/a	USN	n/a	CRU103/19647	n/a	n/a	n/a
066-8-850-050919-D0-12-00	5/9/2019	F-18	Single	D0	12	n/a	ISB001	ESB002	n/a	n/a	USN	n/a	CRU103/19647	n/a	n/a	n/a
067-8-850-050919-B0-55-00	5/9/2019	F-18	Single	B0	55	n/a	ISB004	ESB003	n/a	n/a	USN	n/a	CRU103/19647	n/a	n/a	n/a
068-8-846-051319-B0-71-21	5/13/2019	F-18	Dual	B0	71	21	ISB004	ESB001	ISB003	ESB002	AF/AFRC	CRU73/9682	EDOX	USN	n/a	CRU103/19647
069-8-850-051519-GF-21-00	5/15/2019	F-18	Single	GF	21	n/a	ISB001	ESB001	n/a	n/a	AF/AFRC	CRU73/507551	EDOX	n/a	n/a	n/a
070-8-843-093019-A0-12-00	9/30/2019	F-18	Single	A0	12	n/a	ISB003	ESB004	n/a	n/a	AF/AFRC	CRU73/103305	EDOX	n/a	n/a	n/a
071-8-843-102219-B1-12-00	10/22/2019	F-18	Single	B1	12	n/a	ISB001	ESB001	n/a	n/a	USN	n/a	CRU103/19517	n/a	n/a	n/a
072-8-843-110619-D1-12-00	11/6/2019	F-18	Single	D1	12	n/a	ISB001	ESB001	n/a	n/a	USN	n/a	CRU103/19517	n/a	n/a	n/a
073-8-843-110819-B1-71-00	11/8/2019	F-18	Single	B1	71	n/a	ISB001	ESB001	n/a	n/a	USN	n/a	CRU103/19517	n/a	n/a	n/a
074-8-843-111219-B1-12-00	11/12/2019	F-18	Single	B1	12	n/a	ISB001	**No Data**	n/a	n/a	USN	n/a	CRU103/19517	n/a	n/a	n/a
075-8-843-111919-D1-21-00	11/19/2019	F-18	Single	D1	21	n/a	ISB003	ESB004	n/a	n/a	AF/AFRC	CRU73/103305	EDOX	n/a	n/a	n/a
076-8-843-112019-D1-28-00	11/20/2019	F-18	Single	D1	28	n/a	ISB003	ESB004	n/a	n/a	AF/AFRC	CRU73/103306	EDOX	n/a	n/a	n/a
077-8-843-112119-B1-71-00	11/21/2019	F-18	Single	B1	71	n/a	ISB003	ESB004	n/a	n/a	AF/AFRC	CRU73/103307	EDOX	n/a	n/a	n/a
078-8-843-112619-B1-55-00	11/26/2019	F-18	Single	B1	55	n/a	ISB001	ESB001	n/a	n/a	USN	n/a	CRU103/20292	n/a	n/a	n/a
079-8-843-112619-D1-28-00	11/26/2019	F-18	Single	D1	28	n/a	ISB001	ESB001	n/a	n/a	USN	n/a	CRU103/20292	n/a	n/a	n/a
080-8-843-120219-F-55-00	12/2/2019	F-18	Single	F	55	n/a	ISB003	ESB001	n/a	n/a	USN	n/a	CRU103/20292	n/a	n/a	n/a
081-8-843-120319-D1-12-00	12/3/2019	F-18	Single	D1	12	n/a	ISB003	ESB001	n/a	n/a	USN	n/a	CRU103/20292	n/a	n/a	n/a
082-8-843-120519-B1-12-00	12/5/2019	F-18	Single	B1	12	n/a	ISB003	ESB001	n/a	n/a	USN	n/a	CRU103/20292	n/a	n/a	n/a
083-8-843-120619-D1-28-00	12/6/2019	F-18	Single	D1	28	n/a	ISB003	ESB001	n/a	n/a	USN	n/a	CRU103/20292	n/a	n/a	n/a
084-8-843-120919-D1-21-00	12/9/2019	F-18	Single	D1	21	n/a	ISB003	ESB001	n/a	n/a	USN	n/a	CRU103/20292	n/a	n/a	n/a
085-8-843-121019-A0-55-00	12/10/2019	F-18	Single	A0	55	n/a	ISB001	ESB004	n/a	n/a	AF/AFRC	CRU73/103305	EDOX	n/a	n/a	n/a
086-8-843-121119-A0-71-00	12/11/2019	F-18	Single	A0	71	n/a	ISB001	ESB004	n/a	n/a	AF/AFRC	CRU73/103305	EDOX	n/a	n/a	n/a
087-8-843-121619-F0-21-00	12/16/2019	F-18	Single	F1	21	n/a	ISB001	ESB004	n/a	n/a	AF/AFRC	CRU73/103305	EDOX	n/a	n/a	n/a
088-8-843-121719-B1-12-00	12/17/2019	F-18	Single	B1	12	n/a	ISB001	ESB004	n/a	n/a	AF/AFRC	CRU73/103305	EDOX	n/a	n/a	n/a
089-8-843-121819-B1-12-00	12/18/2019	F-18	Single	B1	12	n/a	ISB003	ESB001	n/a	n/a	USN	n/a	CRU103/20292	n/a	n/a	n/a
090-8-843-121919-B1-71-00	12/19/2019	F-18	Single	B1	71	n/a	ISB001	ESB004	n/a	n/a	AF/AFRC	CRU73/103305	EDOX	n/a	n/a	n/a
091-8-843-010820-F1-55-00	1/8/2020	F-18	Single	F1	55	n/a	ISB001	ESB004	n/a	n/a	AF/AFRC	CRU73/103305	EDOX	n/a	n/a	n/a
092-8-843-011420-F1-21-00	1/14/2020	F-18	Single	F1	21	n/a	ISB003	ESB001	n/a	n/a	USN	n/a	CRU103/20292	n/a	n/a	n/a
093-8-843-011620-B1-12-00	1/16/2020	F-18	Single	B1	12	n/a	ISB003	ESB001	n/a	n/a	USN	n/a	CRU103/20293	n/a	n/a	n/a
094-8-843-012320-H0-21-00	1/23/2020	F-18	Single	H0	21	n/a	ISB003	ESB001	n/a	n/a	USN	n/a	CRU103/20294	n/a	n/a	n/a
095-8-843-012720-H0-12-00	1/27/2020	F-18	Single	H0	12	n/a	ISB003	ESB001	n/a	n/a	USN	n/a	CRU103/19647	n/a	n/a	n/a
096-8-846-021220-E0-12-00	2/12/2020	F-18	Dual	E0	12	55	ISB003	ESB001	n/a	n/a	USN	n/a	CRU10319647	n/a	n/a	n/a
097-8-868-021320-H1-55-00	2/13/2020	F-18	Dual	H1	55	n/a	ISB003	ESB001	n/a	n/a	USN	n/a	CRU103/19647	n/a	n/a	n/a
098-8-868-021820-H1-12-00	2/18/2020	F-18	Dual	H1	12	71	ISB003	ESB001	n/a	n/a	USN	n/a	CRU103/19647	n/a	n/a	n/a
099-8-846-021920-E0-71-21	2/19/2020	F-18	Dual	E0	71	21	ISB003	ESB001	ISB001	ESB004	USN	n/a	CRU103/19820	USAF	CRU73/05858	EDOX
100-8-868-022020-H1-28-00	2/20/2020	F-18	Dual	H1	28	45	ISB003	ESB001	n/a	n/a	USN	n/a	CRU103/19820	n/a	n/a	n/a
101-8-846-022420-E1-28-00	2/24/2020	F-18	Dual	E1	28	96	ISB003	ESB001	n/a	n/a	USN	n/a	CRU103/19820	n/a	n/a	n/a
102-8-868-022520-H1-55-00	2/25/2020	F-18	Dual	H1	55	53	ISB001	ESB001	n/a	n/a	USN	n/a	CRU103/19647	n/a	n/a	n/a
103-8-846-022620-E1-21-XX	2/26/2020	F-18	Dual	E1	21	88	ISB001	ESB001	ISB002	n/a	USN	n/a	CRU103/19647	USAF	CRU73/12370	EDOX
104-8-846-022820-E2-12-00	2/28/2020	F-18	Dual	E2	12	53	ISB003	ESB001	n/a	n/a	USN	n/a	CRU103/19820	n/a	n/a	n/a
105-8-846-030920-E2-12-21	3/9/2020	F-18	Dual	E2	12	21	ISB003	ESB001	ISB001	ESB004	USN	n/a	CRU103/19820	USAF	CRU73/12370	EDOX
106-8-868-031620-F2-28-00	3/16/2020	F-18	Dual	F2	28	96	ISB003	ESB001	n/a	n/a	USN	n/a	CRU103/20294*(mod	USAF	n/a	n/a
107-8-868-031720-B1-12-00	3/17/2020	F-18	Dual	B1	12	53	ISB003	ESB001	n/a	n/a	AF/AFRC	CRU73	EDOX	n/a	n/a	n/a
108-8-868-031820-F2-28-00	3/18/2020	F-18	Dual	F2	28	53	ISB003	ESB003	n/a	n/a	AF/AFRC	CRU73	EDOX	n/a	n/a	n/a
109-8-868-070120-H1-21-12	7/1/2020	F-18	Dual	H1	28	12	ISB003	ESB003	ISB002	ESB001	USN	n/a	CRU103/	USAF	CRU73	EDOX
110-8-868-080420-A-12-00	8/4/2020	F-18	Dual	A0	12	n/a	ISB001	n/a	n/a	n/a	USAF	CRU73	EDOX	n/a	n/a	n/a
111-8-868-080620-A-12-00	8/6/2020	F-18	Dual	A0	12	n/a	ISB001	n/a	n/a	n/a	USAF	CRU73	EDOX	n/a	n/a	n/a
112-8-868-081120-A-12-21	8/11/2020	F-18	Dual	A0	12	21	ISB001	n/a	ISB003	ESB001	USAF	CRU73	EDOX	USAF	CRU73	EDOX
113-8-868-081720-H-21-45	8/17/2020	F-18	Dual	H1	21	45	ISB001	ESB001	ISB003	ESB003	USN	n/a	CRU103/19820	USAF	CRU73	EDOX
114-8-868-081820-H-21-00	8/18/2020	F-18	Dual	H1	21	n/a	ISB001	ESB001	n/a	n/a	USN	n/a	CRU103/19820	n/a	n/a	n/a
115-8-868-082020-H-21-12	8/20/2020	F-18	Dual	H1	21	12	ISB001	ESB003	ISB003	n/a	USN	n/a	CRU103/19820	USAF	CRU73	EDOX

Table 1.7. Summary of all Metadata Distribution of PBA Flights

(a) Number of PBA flights for each pilot and profile, repeat measures

Pilot	Profile_Group					
	A	B	C	D	E	Total
12	2	4	2	1	3	12
21	1	4	2	3	2	12
28	2	2	0	3	0	7
55	2	1	2	2	0	7
71	2	5	2	2	1	12
Total	9	16	8	11	6	50

Table 1.7b shows the distribution of the 50 down-selected sorties between the type of aircraft and AFE used in the flight. "F18_USN" refers to an F/A-18 configured in USN AFE. The types of regulators used for a given flight, along with the O_2 connector and the number of flights analyzed are shown.

(b) Number of PBA flights for each pilot and AFE Configuration

Configuration	AFE	Regulator	O2 Connector	Plane	#
"F18_USN"	USN	--	CRU-103	F-18	24
"F18_AF"	AF/AFRC	CRU-73	EDOX	F-18	20
"F15_AF"	AF/AFRC	CRU-98	CRU-60	F-15	6

Table 1.7c shows the distribution of the 50 down-selected sorties by pilot, profile, and aircraft/AFE configuration.

(c) Number of PBA flights for each pilot, profile, and airframe, AFE Configuration

F-15 AF

Pilot	Profile_Group					
	A	B	C	D	E	Total
12	0	0	0	0	0	0
21	1	1	0	0	0	2
28	0	0	0	1	0	1
55	0	0	1	1	0	2
71	0	0	0	1	0	1
Total	1	1	1	3	0	6

F-18 AF

Pilot	Profile_Group					
	A	B	C	D	E	Total
12	1	2	1	0	0	4
21	0	2	1	1	2	6
28	1	1	0	1	0	3
55	1	0	1	0	0	2
71	1	3	1	0	0	5
Total	4	8	4	2	2	20

F-18 USN

Pilot	Profile_Group					
	A	B	C	D	E	Total
12	1	2	1	1	3	8
21	0	1	1	2	0	4
28	1	1	0	1	0	3
55	1	1	0	1	0	3
71	1	2	1	1	1	6
Total	4	7	3	6	4	24

Data for five of the 50 down-selected sorties were obtained for the pilot occupying the rear cockpit (RCP). The distribution of the data between front and rear cockpit is shown in Table 1.7(d).

(d) Number of PBA flights for profile and aircrew in FCP and RC)

Profile	Description	# FCP	# RCP	# Total
A	High Altitude	9	0	9
B	AeroBatics	14	2	16
C	Control	8	0	8
D	Down low	10	1	11
E	Isobaric G-Exercises	4	2	6
	Total	45	5	50

Table 1.7e provides the distributions of VigilOX ISB versions that gathered data across the three combinations of aircraft and AFE configurations. The VigilOX serial numbers, for example DEV03, DEV06, etc.) changed during the course of PBA. Statistical analysis was performed with the data from this table used as input. The results of these analyses are presented and discussed in TS04.

(e) Distributions of VigilOX ISB across configurations

Configuration	Vigilox_ISB						
	DEV003	DEV006	ISB001	ISB002	ISB003	ISB004	Total
F15_AF	3	3	0	0	0	0	6
F18_AF	2	0	7	1	5	5	20
F18_USN	1	0	4	5	14	0	24
Total	6	3	11	6	19	5	50

1.7 Summary

Technical Section 1 provided the overall implementation of the NASA-NESC PBA. It serves as a reference for the detailed technical analyses performed in the ensuing sections. This section presented all aspects of the study starting with the technical rationale and descriptions of instrumentation, flight activities, aircraft measurement, physiological measurements, and study design and balance. Probably the most important concept developed herein are the unique features of this study with respect to the development of new test methods for gathering pilot physiological data in a real-world flight environment in a high-performance aircraft.

The incidence of PEs has been attributed to complex pilot-aircraft interactions. The information developed from this study provides a baseline against which all flights, including those with PE outcomes, can ultimately be assessed. Furthermore, the accumulation of empirical data serves as a guide for future improvements in aircrew equipment and aircraft breathing systems.

1.8 References

Anon, Advanced Concept Ejection Seat ACES II. Report MDC J4576 Revision D, March l988.

Anon, Telemetry Standards, IRIG Standard 106-15 (Part 1), Chapter 10, July 2015.

Delgado J, Chullen C, Berry D, Guzman N, Mottino S, Hellstern G, Soto A, Tripp L. Sensor Integrated Pilot Mask for On-Board, Real-Time, Monitoring of Pilot Breathing Gas. 48th International Conference on Environmental Systems. https://ttu-ir.tdl.org/bitstream/handle/2346/74266/ICES_2018_334.pdf?sequence=1&isAllowed=y

Gordge DN. In-Flight Measurement of Aircrew Breathing in Navy Aircraft. NAVAL AIR WARFARE CENTER AIRCRAFT DIV PATUXENT RIVER MD; 1993 Sep 20. https://apps.dtic.mil/sti/pdfs/ADA271811.pdf

Harding, R.M., *Human Respiratory Responses During High Performance Flight,* AGARDOGRAPH No. 312. Advisory Group for Aerospace Research and Development (AGARD), Nov. 1987. https://apps.dtic.mil/sti/pdfs/ADA191601.pdf

Lauritzsen LP, Pfitzner J. Pressure breathing in fighter aircraft for G accelerations and loss of cabin pressurization at altitude—a brief review. Canadian Journal of Anesthesia. 2003 Apr 1;50(4):415-9.

Lyon, Maj Gen Charles W. *F–22 Pilot Physiological Issues,* Hearing Before the Subcommittee on Tactical Air and Land Forces of the Committee on Armed Services House of Representatives, One Hundred Twelfth Congress, Second Session, Hearing Held September 13, 2012, US Government Printing Office, Washington, 2013 (pp 21).

Martin, Gen Gregory S., USAF (Ret.), *F–22 Pilot Physiological Issues,* Hearing Before the Subcommittee on Tactical Air and Land Forces of the Committee on Armed Services House of Representatives, One Hundred Twelfth Congress, Second Session, Hearing Held September 13, 2012, US Government Printing Office, Washington, 2013 (pp 46-54).

Military Standard for Adjustable, Upward, Aircraft Ejection Seat Systems. MIL-S-9479B(USAF), 24 March 1971

Naval Air and Training and Operating Procedures Standardization (NATOPS) General Flight and Operation Instructions Manual, CNAF, M-3710.7, Dept. of the Navy, Naval Air Forces, May 5, 2016.

NESC F/A-18 Final Report, NESC-RP-17-01205. 2017

NESC F/A-18 Final Presentation, NESC-RP-17-01205. 2017

NESC F-22 Final Report, NESC-RP-12-00792. 2012

Sullivan, Michael, *Statistics: Informed Decisions Using Data*, (4th Edition), Pearson, Education Inc. 2013. (ISBN: 0321757270)

Travis TW, Morgan TR. US Air Force positive-pressure breathing anti-G system (PBG): subjective health effects and acceptance by pilots. Aviation, space, and environmental medicine. 1994 May; 65(5 Suppl): A75-9.

West JB. A strategy for in-flight measurements of physiology of pilots of high-performance fighter aircraft. Journal of Applied Physiology. 2013 Jul 1; 115(1):145-9. https://journals.physiology.org/doi/pdf/10.1152/japplphysiol.00094.2013

Technical Section 2: Fundamentals of Pilot Breathing

2.0 Introduction

Breathing, or human respiration, is the process that moves air in and out of the lungs so O_2 can be absorbed into the blood during inhalation, and waste CO_2 can be removed during exhalation. O_2 reactions with food and nutrients provide the energy for life at the cellular level; the human system ceases to function without a sufficient supply of O_2 in the blood.

There are three basic scenarios for human respiration:

- Autonomic (normal) breathing
- Supplied air (external gas supply)
- Mechanical (ventilator) breathing

Autonomic (or autonomous) breathing is what people experience in normal living. One does not really think about the next breath unless there is an unusual circumstance, perhaps an odd smell, or while swimming, or during high exertion exercise, or periods of anxiety, or singing, or breath-holding. Supplied air is necessary when the surrounding environment does not provide sufficient clean air and O_2. Activities like firefighting, working with infectious agents, scuba diving, mountain climbing, confined space work, and jet piloting all fall into this category wherein an external air supply is required. Supplied air comes in generally two different supplies. One is continuous, in which there is a constant supply of air or O_2 and on-demand or pulse flow. On-demand or pulse flow devices sense when you breathe in, and they supply you with air or O_2 with each inhalation. Finally, there are times when the human body cannot breathe for itself at all, for example during surgery, illness recovery, paralysis, or coma when external ventilation is mechanically applied with a medical ventilator. A medical ventilator enables the delivery or movement of air or O_2 into the lungs of a patient whose breathing has ceased, is failing, or is inadequate. These devices not only supply the air or O_2, but perform the function of moving the air, taking over autonomous breathing.

Human physiology literature presents in-depth research on “normal” breathing at rest and during various exercise scenarios. At the other extreme, the clinical research literature presents detailed methods and technology of appropriate mechanical ventilation. In scenarios where high O_2 is demanded for increased metabolism, the needs are derived from exercise physiology. Although a valuable resource overall, the knowledge of normal breathing does not properly address all the unique requirements of the fighter pilot environment.

PBA was designed to better understand the complexity of human breathing dynamics under the stress of piloting in modern high-performance aircraft. Unlike normal autonomous breathing at 21% O_2 and 1-atmosphere pressure, this jetfighter environment imposes physical strains on the pilot from altitude, acceleration and orientation, as well as physiological challenges from changing pressures and O_2 concentration. To maintain life support under such adverse conditions, the aircraft provides on-demand breathing gear in the form of a gas supply, regulator, and non-rebreathing mask.

In an effort to better understand the complexity of breathing dynamics, this section presents a fundamental perspective on the basics of ideal human breathing at 1 atm as the foundation for remaining sections of the report wherein details of on-demand breathing are studied. The ultimate goal is to tie together empirical data from pilot breathing measurements with the associated aircraft data. These findings and recommendations will serve to understand how the

human breathes in fighter aircraft while strapped in with complicated components that serve to keep him or her healthy during a wide variety of physiologically demanding scenarios.

First, the physiology of breathing and the associated terminology, units, and graphical conventions are presented as a precursor to subsequent sections. Second, key pieces of pilot breathing equipment, the O_2 regulator and mask, are described in an idealized way and salient features of these complex pieces of hardware are discussed. Next, an in-flight breathing time-history is presented and discrete points along the path are analyzed are highlighted. At each snapshot, the state of the O_2 regulator, the positions of mask valves, and the associated regulator outlet pressure and mask pressure are interpreted. The intent of these snapshots is to introduce the variety of states and sequencing present "behind the scenes" in two key pieces of aircrew equipment that a pilot depends on during dynamic flight conditions.

2.1 Mechanics of Breathing

2.1.1 Breathing as an Active Element in a Pilot Breathing System

Breathing is part of the pilot breathing system. Breathing interacts with the mechanical parts of the breathing system (e.g., regulator, mask, ECS system). There, interactions are mutually dependent; mechanical elements cause changes in breathing and breathing changes mechanical response.

2.1.2 Forces that Drive Breathing

The pilot's respiratory or breathing muscle work drives the flow of air. Two groups of muscles are involved. For natural regular open-air breathing, the two muscle groups are the chest wall muscles and the diaphragm. These muscles of respiration contribute to inhalation and exhalation, by aiding in the expansion and contraction of the thoracic cavity. When these muscles contract, they expand the rib cage, then the volume of the lungs increases and the pressure inside the lungs drops. When the pressure in the lungs is lower than the pressure in the room, inhalation occurs. When the muscles relax the chest wall contracts, the volume of the lungs decreases, and the pressure inside the lungs rises. If the pressure in the lungs is higher than the pressure in the room, exhalation occurs. If the airway pressure on exhalation is high enough, the resulting action of the breathing muscles is to contract as opposed to relaxing to drive exhalation. Pilot reports of soreness in the chest wall is a diagnostic clue that the chest wall muscles are driving against a higher than normal external pressure. Also, if the pilot has an increased demand of air, all the respiratory muscles are maximally engaged to repeat the cycle faster and supply that demand. Again, this produces some muscle fatigue and soreness.

2.1.3 General Trends for Breathing

All breathing has inhalation and exhalation. The inhalation and exhalation cycle can be defined by duration, volume, pressure difference, and cadence. Breathing is highly variable, but it is helpful to note general trends for unrestricted breathing while resting or light exercise in the open atmosphere. The duration of a single breath is generally about 3 seconds (20 BPM). Breathing frequency changes as a function of activity level, and environment. Pilot breathing system interactions generally cause the average fighter pilot to take fewer, deeper breaths. The standard clinical range for pilot breathing is 3 to 5 seconds per breath (12 to 20 BPM.

Volume of a single breath is generally 1 liter, but the maximum volume change in the lungs between fully expanded and fully contracted can be 5 liters. The pressure difference that drives a

resting breath is 2–3 mmHg. The difference between the lung and the room during inhalation while at rest is 2–3 mmHg (the lung pressure is at most 2-3 mmHg lower than the room). The difference between lung pressure and room pressure during exhalation while at rest is 2-3 mmHg (the lung pressure is 2–3 mmHg higher than room pressure. Pressure differences increase when exercise levels increase and breathing becomes faster and deeper.

As discussed in Technical Section 5.1.3.5, the maximum amount of pressure difference a person can achieve under no-flow conditions is about 120 mmHg (e.g., the difference between blowing up a balloon and sucking a really thick milkshake through a straw). The maximum amount of pressure difference a person typically develops under flowing exercise inhalation/exhalation conditions is about 20 mmHg. Cadence is highly variable – people are constantly adapting their breathing patterns to receive the necessary amounts of air for the minimum effort. But as a general rule, inhalation is symmetric. When inhaling normally, about 50% of the inhaled breath occurs at the approximate mid-point of inhalation, and peak inhalation velocity occurs during the mid-point of inhalation. Exhalation is asymmetric: the beginning of the exhalation is marked with high velocities and large amounts of exhalation, while exhalation velocity tapers off to very low values at the end of exhalation. Breathing is highly variable and breathing through a pilot breathing system is different from unrestricted open-air breathing, but it is helpful to have some general trends to provide some context.

2.1.4 Breathing Variability

The duration, volume, pressure differences, flow profiles, and cadence of breathing is constantly changing. People in open air unrestricted breathing conditions are constantly adjusting their breathing to receive the necessary amount of air with the minimum amount of effort. This is sometimes referred to as “finding the breathing solution”. These adjustments are generally unconscious – people are not generally aware of adjustments in their breathing when they transition from walking to jogging to running to sprinting. Pilots also change their breathing patterns to find their breathing solution, but pilots need to adjust to two different factors: 1) the amount of physical activity and the amount of air they need, and 2) the nature of the mechanical parts of the pilot breathing system.

For instance, if the pilot breathing system has a lag in the delivery of air, the pilot breathing solution may involve fewer bigger breaths or may involve faster smaller breaths depending on several factors including the physical activity or resistance of the system.

2.1.5 Breathing System Interactions

Pilots interact and directly control the mechanical elements of a pilot breathing system. When a pilot inhales, the line pressure drops, which triggers the demand regulator to deliver flow. Mechanical aspects of the pilot breathing system influence pilot breathing. People are always adjusting their breathing patterns to receive the necessary amount of air with the minimum effort. If, for instance, the breathing system cannot deliver breathing air in extremely high velocity/short duration bursts – the pilot will unconsciously adjust breathing to a different profile. Pilot urges to drop their mask provides a strong diagnostic clue. If the pilot has the urge to drop their mask, the mechanical aspects of the breathing system might not be supplying sufficient airflow, and the unconscious adjustments of breathing cadences are not producing a “breathing solution”. Measurements of pilot breathing patterns can provide diagnostic clues about much the pilot is adjusting their breathing to fit the system. Ideal systems have mechanical elements adapting and

responding to meet the needs of the human, and human breathing patterns seek to match unrestricted open-air breathing (for equivalent metabolic workloads).

2.1.6 Sensitivities to Environmental Conditions

Pilots are breathing in a cabin environment with a variable atmospheric pressure. Based on new PBA data, the frequency of breathing ranges from 0.3 – 0.6 Hz (20 BPM to 40 BPM). Each inhalation lasts approximately 0.75 – 1.5 seconds. During that 0.75- to 1.5-second time of inhalation, the diaphragm is working to expand the lung and drop the pressure until it is 2–5 mmHg lower than the cabin pressure. Based on PBA data, the cabin pressure fluctuation trends can range in frequency from 0.1–1.0 Hz (6 to 60 fluctuations per minute). The magnitude of these cabin pressure fluctuations can range from 0.5–5.0 mmHg in 1 second. A pilot inhaling in a cabin environment needs to compensate for cabin pressure surges. The magnitude of these cabin pressure surges can be greater than the total amount of pressure change needed for inhalation in an open-air environment. When the frequency of the cabin pressure surges and the frequency of breathing nearly align – cabin pressure surges will have a profound effect on breathing.

2.2 Physiology of Breathing: Flow, Pressure, and Volume

Breathing is deceptively complex. Future sections of this report will introduce findings, observations, and recommendations that are based on a detailed understanding of how masks and regulators work and how human breathing looks with demand and diluter demand regulators. Many people with variety of backgrounds and disciplines analyze breathing data (physiologists, medical doctors, researchers, etc.). With so many analyzing breathing patterns, the small multidiscipline PBA team had to decide on a standard way of analyzing and plotting data. This section defines the common terms, axis, labels and units and conventions associated with pilot data.

This section highlights three main points:

1. Peak breathing is different than average breathing.
2. The regulators are complex mechanical devices and the interfaces matter.
3. Masks are complex systems and we need to pay attention to the valves.

Figure 2.1 shows the physiology of breathing in terms of flow, pressure, and volume. A single breathing cycle is schematically shown on the left, with inhalation and exhalation velocities show as a function of breathing volumes for both a large breath and a resting breath. The corresponding breathing cycle is shown on the right with the lung pressures involved for a resting breathing and a maximum breath.

The breathing cycle begins with the inhalation shown on the top left from A-E. It is uniform and symmetric while the exhalation, shown from E- A is asymmetric and non-uniform. The exhalation stage begins at point E with a large rate of change in velocity output that reaches a maximum velocity at point G and tapers off exponentially from points G to A.

Although the profile of a maximum breath and a resting breath are qualitatively similar, this schematic shows a large difference between the magnitudes of the velocities, volumes, and pressures. One of the key takeaways from Figure 2.1 is *peak breathing is very different than nominal breathing*. Figure 2.1 clearly illustrates how dynamic the flows – and how relatively small the pressures are involved in nominal breathing. Normal breaths at rest only involve about 3 mmHg while maximum breaths are an order of magnitude larger. The difference to cycle the

air in and out the lungs is a very small amount given the peak amount of flows. In-flight breathing systems need to accommodate this very large range in dynamic and non-uniform measurements. PBA learned to appreciate how small the forces are, how large the flows are, and how variable the entire breathing mechanics can be.

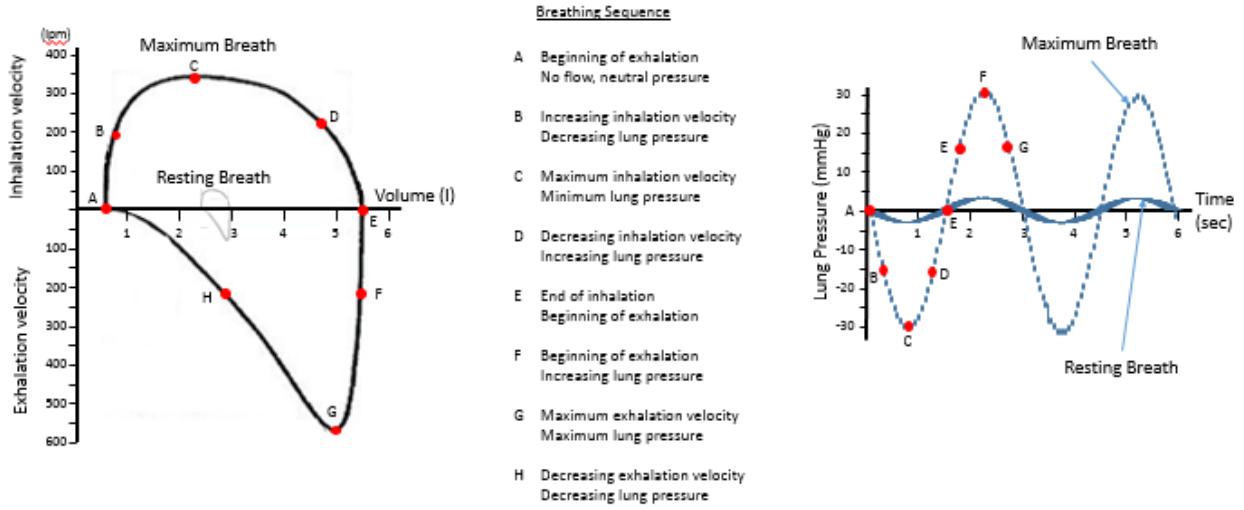

Figure 2.1. Physiology of Breathing in Terms of Flow, Pressure, and Volume
A single breathing cycle is schematically shown on the left, with inhalation and exhalation velocities show as a function of breathing volumes for both a large breath and a resting breath. The corresponding breathing cycle is shown on the right with the lung pressure time history.

For future graphs, inhalation will nominally be denoted by a red curve above the x-axis and exhalation will be denoted in blue and shown below the x-axis. Pressure plots in future sections will be presented like the figure on the right, with positive pressure above the line and negative pressure below it. Figure 2.1 shows idealized sinusoidal waveform of lung pressure.

2.3 Pilot Breathing Equipment

Modern demand breathing regulators were invented in the 1940s for underwater diving applications, and are, by now, ubiquitous and very well understood. This section presents several aspects of regulator breathing relevant to PBA and to the overall PE problem.

2.3.1 Regulators

Figure 2.2 presents simplified schematics of a demand regulator and a diluter demand regulator. The demand regulator senses two different pressures. The demand regulator is a sealed system with a plugged supply air hose which is feeding a moderate pressure air supply into the breathing tube that connects to the pilot's mask. When the pilot is resting or exhaling, this system is at rest and sealed. This system references the cabin pressure, which is on the other side of the diaphragm. The demand system remains closed until there is demand for air made by the pilot. At this point, the right side of the schematic reaches a low pressure, the diaphragm moves, the small mechanical lever amplifies the force to allow this very small demand signal to push against the high pressure. The lever arm opens the plug letting the high-pressure supply gas in.

The demand regulator is more complex when there is a requirement to maintain a mask "safety" pressure, or more precisely, "positive pressure". (Note, the terms, "Safety Pressure" and "Positive Pressure" are discussed at the end of this Technical Section, 2.3.2). The job of the

regulator is not to balance the system to neutral pressure but bias it so that it always maintains a slight positive pressure. Therefore, a safety pressure regulator always has an extra constant mechanical force produced either by a mechanical spring or an aneroid. This mechanism always exerts pressure on that side of regulator and is another component in the breathing system that must be designed to operate with precision.

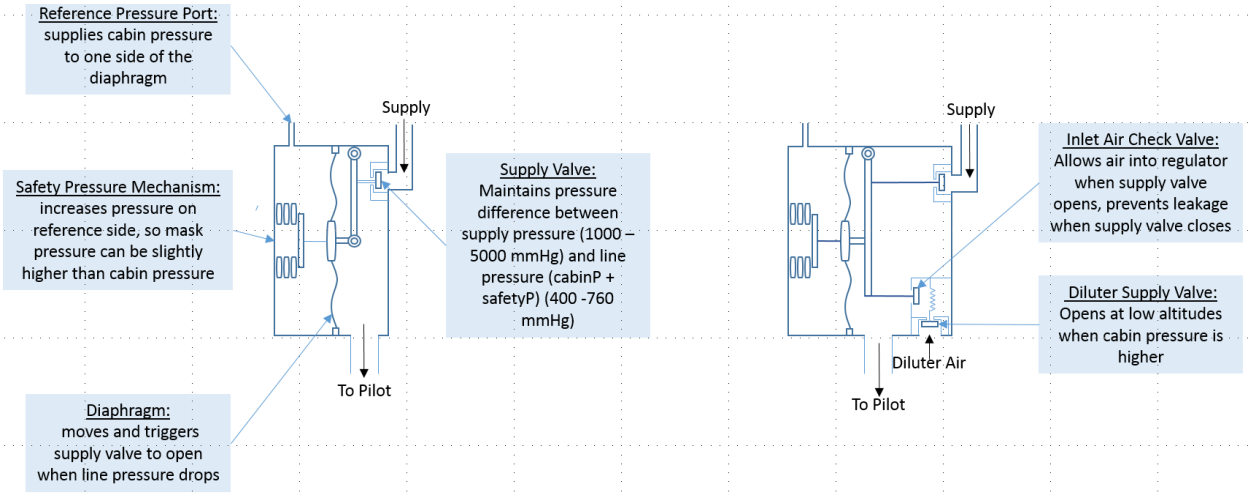

Figure 2.2. Pilot Breathing Equipment: Regulators

By way of comparison, Figure 2.2 (right) shows a diluter demand regulator. This regulator is comprised of the same mechanical design elements as the demand regulator: the aneroid, diaphragm, reference pressures and supply ports but it has a second source of air. If the cabin altitude is low and cabin pressure is relatively high, when the diaphragm moves and the supply is flowing in, a second source of air feeds directly from the cabin into the pilot breathing system.

Notes about Regulators and Pilot Breathing

The following list offers a summary of important axioms regarding pilot breathing through regulators. A more complete list is provided in (Appendix 2).

- During nominal breathing, the air supply is unlimited and always at the same pressure. In contrast, during regulator breathing, a demand regulator will not open without a small drop in pressure.
- Nominal breathing rates vary from 0 to >200 lpm. Regulators need to match breathing rates, and the volume of the mask/line is very small.
- Supply pressure ranges from 1000 mmHg to 5000 mmHg. Regulators control pressure to <2 mmHg.
- Regulators are mechanical devices, with thin diaphragms. Inspection cycle is <90 days.
- The job of regulation is more difficult when:
    - Supply pressure is variable
    - Pilot breathing demand large
    - Pilot breathing demand is variable
    - Regulators with safety pressure components are involved
    - Cabin pressure is variable
    - Mechanical loads like G-forces are involved

2.3.2 Masks

As with pressure regulators, mask designs are also a complex component in the breathing system; a complexity which is not often full appreciated given how common they are and how robust they appear. Figure 2.3 shows a photograph of an MBU-20/P mask and a simplified schematic of a generic mask with pressure compensation (Rainford and Gradwell, 2016). The schematic of the generic mask design highlights the differences between the inhalation and exhalation valve designs.

Photograph of MBU-20/P

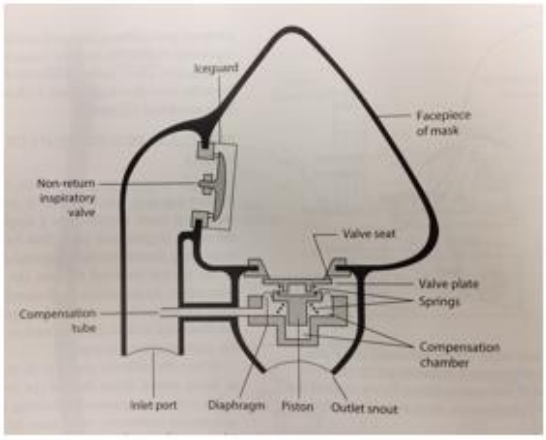

Schematic of a generic mask with pressure compensation

Figure 2.3. Pilot Breathing Equipment: Masks

The MBU-20/P pilot breathing mask has two sets of valves: one for inhalation which opens when the pilot breathes in, and another for exhalation that opens when the pilot breathes out. As designed, these two valves should open and close mutually exclusive to one another. When the pilot breathes in, the inhalation valve opens, and the exhalation valve closes. Conversely, when the pilot breathes out, the inhalation valve closes, and the exhalation valve opens. In order for the mask to function as designed, this process needs to happen < 50 ms during every breathing cycle, with only one valve open at a time enabling the air provided by the aircraft to be supplied, and exhausted in a synchronized pattern with the pilot's breathing.

The inhalation valve consists of a very thin, flexible piece of rubber-like material that is optimized to allow air to flow in with the least amount of breathing resistance. The inhalation valve is designed to fully seal and prevent back flow during exhalation. By design, the forces of air involved are small. The inhalation valve being inherently thin and flexible sometimes fails to re-seat, which can allow air to free-flow through the system, exhaled breath to backflow into the supply line, or both. These failures can adversely affect system timing. The inhalation valve is also prone to contamination. A wet or sticky inhalation valve can require greater forces to open – this can also adversely system timing.

For safety pressure systems, with a design architecture of the MBU-20/P, there are three different pressure elements and three different forces that all work in balance on the exhalation side. A static, pneumatic force of the pressure is produced on the pressure compensation bladder. There is also a dynamic pressure element to this bladder because the inlet to the bladder references the line pressure through a pressure compensation tube. When flow is at a maximum, an extra force

is produced on the bladder to keep the valve closed. The third force is produced by a thin mechanical spring in the compensation chamber. This spring forces the exhalation valve closed when there are no active exhalation forces. These three forces need to work in concert, in a system where the total pressure budget is only a few mmHg.

The compensation tube is thin, flexible, and prone to blockage due to contamination. As will be shown later, a common failure mode occurs when the tube is blocked, valve system timing can be disrupted.

Figure 2.4 shows a schematic of the regulator and mask (left-hand side) and a photograph of exhalation valve components. The pressure compensation tube is pneumatically connected to the line side and faces directly into the supply air. Again, the three forces described are listed in this figure: the mechanical springs, the static pressure within the compensation bladder, and the dynamic pneumatic pressure applied to the exhalation valve system. These are the three forces that must work with precision to keep the exhalation valve closed during inhalation, and open quickly and easily during exhalation. The components of the external spring, exhalation valve housing, valve plate, pressure compensation tube, the piston, and the pressure compensation bladder are shown on the right. Note: the exhalation bladder is informally referred to as a "balloon". This term is used to emphasize the fact that pressure applied on the valve changes as the quantity of air inside the bladder changes. The cross-sectional area of the bladder in the exhalation valve does not change as the pneumatic pressure inside the bladder changes.

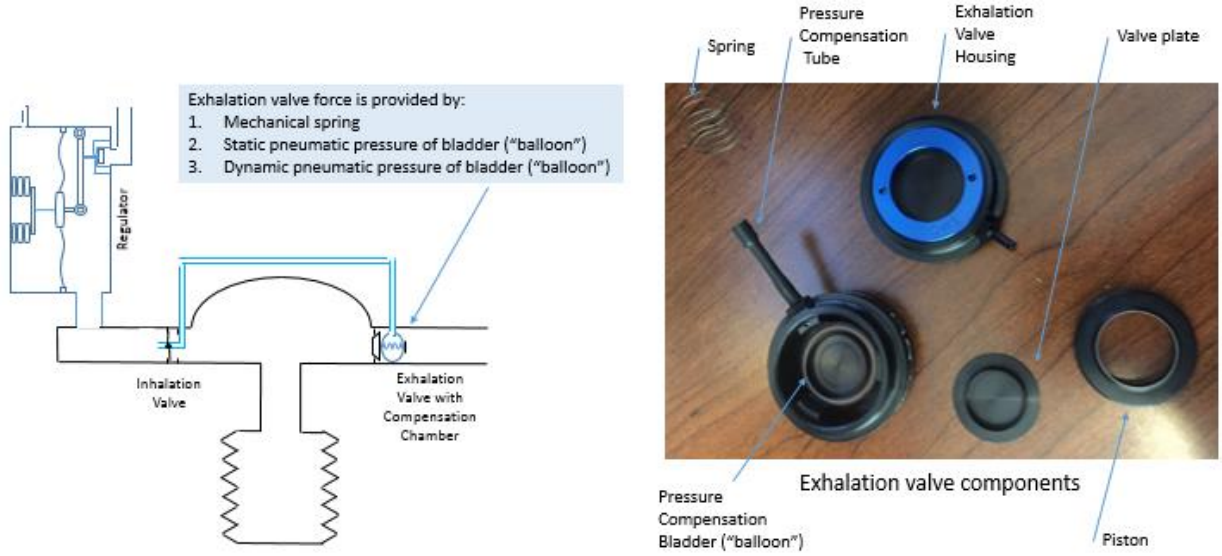

Figure 2.4. Pilot Breathing Equipment: Masks

Notes about Masks and Pilot Breathing

- Total pressure change for normal breathing is less than 10 mmHg. Masks need to route airflow into, and out of a mask with very little delta-pressure.
- Masks with a design architecture like the MBU-20/P are more mechanically complex than masks with a simple "reed valve" type exhalation valve.
- Exhalation valves that need to maintain safety pressure (generally less than 5 mmHg) use three different types of forces
- Pressure compensation tubes have a small diameter – airflow through the tube can delay system response. Transfer of air through the pressure compensation tube can adversely

affect the timing and sequence of valve function, if there is a large, sudden change in cabin pressure.

- The inhalation check valve is thin, flexible, and prone to sticking closed if contaminated. Valve sticking can adversely affect system timing.

Notes about the terms "Positive Pressure" and "Safety Pressure" in Masks

Mask pressure terminology is complex, and can lead to considerable confusion, especially as it relates to delivery of positive pressure, or so-called "Safety Pressure" to the mask. Although "Safety Pressure" is more widely used terminology; from an analytical and physics standpoint, the term "positive pressure" is more descriptive. Any breathing system that maintains a mask pressure that is greater than cabin pressure can be defined as one with "positive mask pressure." The term positive mask pressure does not define intent, or map to a specific requirement – it simply defines the relative pressure between the inside of the mask, and the cabin. Ernsting (Rainford and Gradwell, 2016) notes that maintaining positive pressure in the mask can mitigate some of the effects of mask leakage and can reduce the amount of inhalation of cabin air, which is especially important when the cabin atmosphere is contaminated. Ernsting and Miller (Ernsting and Miller, 1996) also describe the benefits of providing additional mask pressure at high altitudes, and during conditions of pressure breathing for G (PBG). (Note that PBG was not active for PBA). Positive mask pressure could be maintained with a relatively simple mechanical spring in the mask. PBA flights used an MBU-20/P mask, which uses a comparatively complex set of components that includes mechanical springs, a pneumatic bladder, and a pressure compensation tube. The added complexity of the MBU-20/P enables this mask to support more complex pressure control requirements, where different amounts of mask pressure are applied under different flight conditions. When different pressure environments are compared, this report uses the term "positive mask pressure. The term "safety pressure" is used in this report when describing specific components and component interactions. When different pressure signals are compared, this report uses the term "positive mask pressure."

2.4 Nominal Pilot Breathing Profile

PBA created animations to better illustrate the complex human system interactions that occur during pilot breathing. Links to these animations are provided here (enter URL to view) and in Appendix 2. Figure 2.5 shows a screen-capture of one of the animations highlighting all the various systems that must work in harmony to meet the breathing demands of pilot breathing through a mask and regulator.

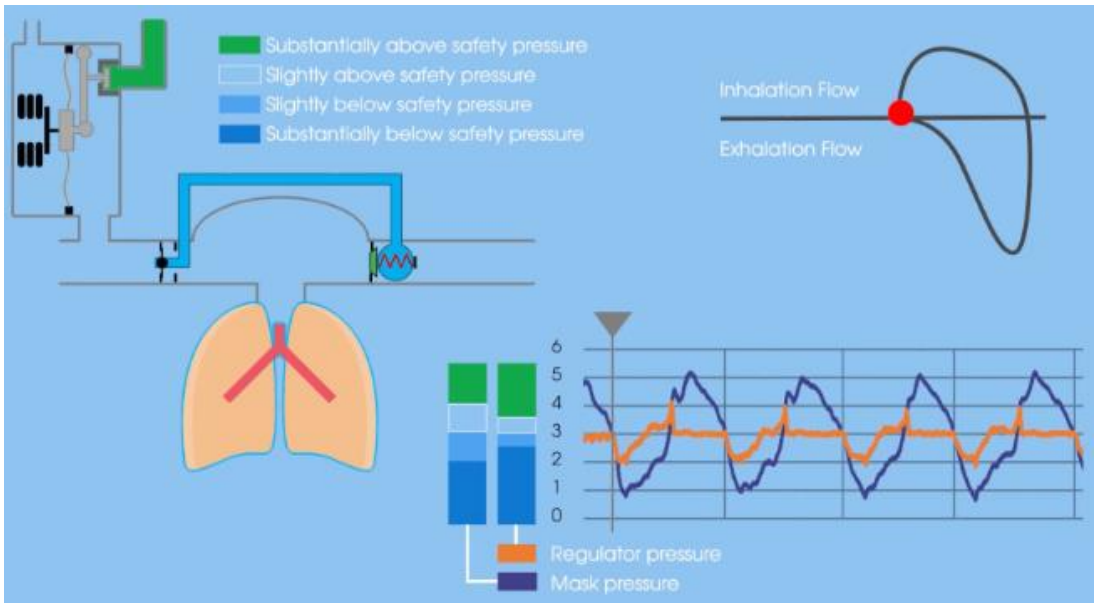

Figure 2.5. Screen Capture of Animation of Pilot Breathing (breathing data courtesy of NSWCPCD/J. Camperman, used with permission)

A representative waveform of pilot breathing data for a safety pressure system is shown for two sources of data: the regulator outlet pressure, also referred to in this report as "line pressure" (shown in red), and the mask pressure (shown in blue), both in units of mmHg.

Figure 2.6 shows an enlarged view of six steps during inhalation.

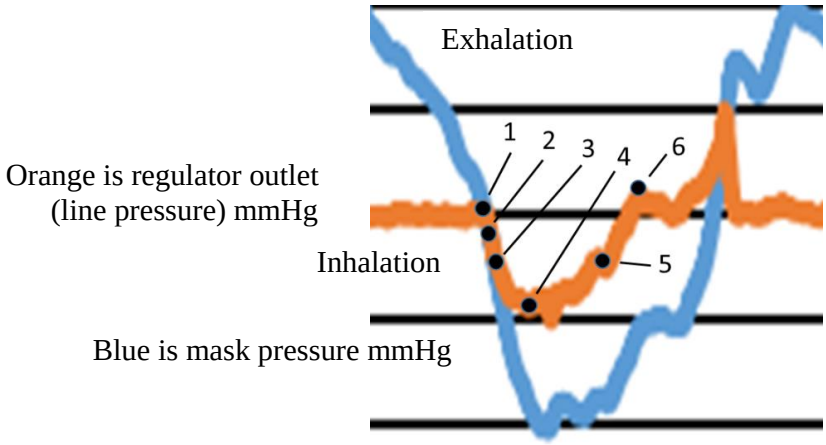

Figure 2.6. Nominal Breathing Pressure Profile

Point 1 highlights the time in the breathing cycle in which inhalation begins. Point 2 shows the time immediately after the pilot starts to inhale, and the corresponding pressure drop that occurs in both the line and the mask pressure. At Point 3, the pilot continues to draw air in, the regulator valve opens, line pressure feed starts, and the pressure decrease slows. The pilot is still calling for air, so both pressures continue to drop, with the mask pressure dropping to a greater extent. At Point 4, the regulator flow matches pilot demand and line pressure starts to rise.

This figure also illustrates a key point. Figure 2.6 shows that the line pressure at points 3 and 5 is the same. Therefore, one would expect that for an ideal regulator, where the flow responds

instantly and in proportion to the pressure (demand), the flow at the two points in time would be the same. Actual measurements, however, indicate that the flow at the two points is very different. As will be seen in a following section, all regulators have a pressure-flow lag due to the finite time for the mechanical components in the regulator, like the springs, pressure diaphragms, etc., to actuate. There is relatively less air flow at the beginning of the inhalation cycle when the regulator flows and relatively more flow at the end of the regulator sequence.

From Point 5 to 6 in Figure 2.6 the regulator pressure continues to rise and then over-shoots regulator cracking pressure (safety pressure here) before the inhalation valve closes and the regulator responds to the increased pressure and stops flow.

2.4.1 Hysteresis

Hysteresis is an indication of a non-conservative effect in a mechanical system which causes the loading and unloading of the system to become path dependent. For breathing systems, this means that the loading, or increased pressure that occurs during exhalation, and the unloading, or decreased pressure that occurs during inhalation, can follow different paths. A system demonstrates hysteresis if it does not return to its original rest state along the same path on which it went out, or if the system takes longer to return from a dynamic state than it did to reach the state initially.

Ideally, the aircraft breathing system will respond to pilot demand pressure quickly, reliably, and in proportion to the demand. Figure 2.7 shows three consecutive inhalation breaths from a PBA test flight in an F/A-18 aircraft (Flight 68). The jet breathing system was in a USAF CRU-73 diluter demand panel mounted configuration, so it did not have safety pressure. The graph shows the inhalation flow as a function of the differential pressure of the regulator outlet and the cabin,

$$\Delta P_{(l - c)} = (P_{line} - P_{cabin}).$$

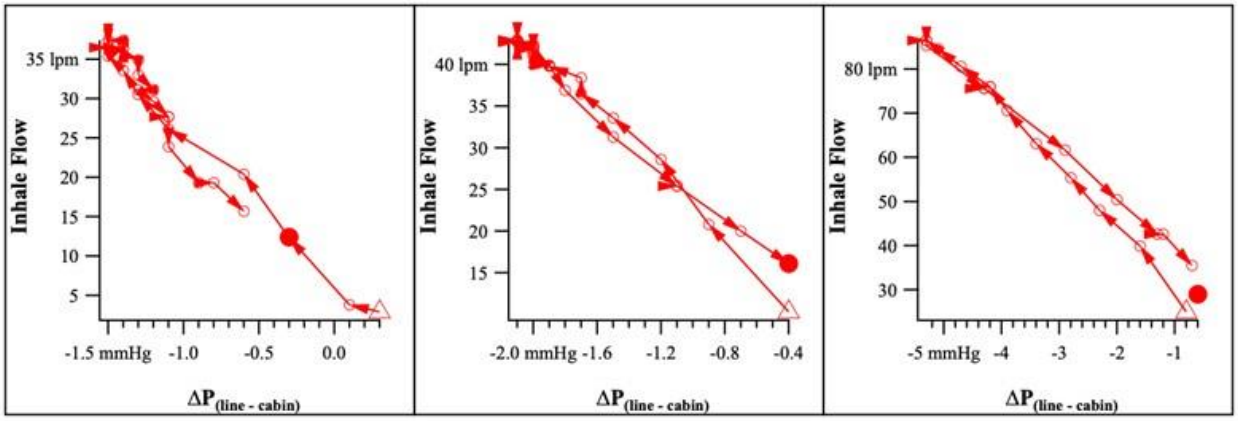

Figure 2.7. Inhalation Flow vs Regulator Outlet Differential Pressure for NASA F/A-18 with Diluter Demand Regulator; Showing Minimal Hysteresis
Note the linear relationship between flow and demand pressure over time. The start and end of inhalation are indicated by the open triangle and closed circle, respectively. Each datum point represents a time increment of 0.05 sec and the arrows represent the path taken from the start of the breath to the end of the breath. The three breaths are from a part of the test while the F/A-18 aircraft was still on the tarmac before takeoff.

Note the linear relationship between flow and demand pressure over time. The start and end of inhalation are indicated by the open triangle and closed circle, respectively. Each datum point represents a time increment of 0.05 sec and the arrows represent the path taken from the start of the breath to the end of the breath. The three breaths are from a part of the test while the F/A-18 aircraft was still on the tarmac before takeoff.

These breath plots illustrate several points. First, breathing flow varies very linearly with the pressure differential. The flow from the regulator is in direct proportion to the demand signal on the regulator. Further, the regulator response is the same from breath to breath; the system reliably produces the same flow for a given demand. Finally, there is no appreciable lag or hysteresis in the system; the flow from the regulator is only a function of the demand signal and not dependent on whether it is in the beginning, middle, or end of the pilot inhalation cycle.

This figure also shows that the flow does not return to zero for each cycle in Figure 2.7. This offset was observed in many flights throughout the assessment. This offset occurs because, at the end of an inhalation breath, there is frequently some inhalation flow from the regulator when exhalation flow starts. This represents the exhalation valve opening before the inhalation flow stops and is the result of a small overshoot on the regulator and some overlap between the handoff between the valves.

In contrast, Figure 2.8 shows a sequence of three breaths during relaxed breathing (the same pilot as in Figure 2.7) in an F/A-18 only this time in a USN chest mounted CRU-103 configuration with safety pressure. In this case there is an offset in the differential line pressure (x-axis) corresponding to the safety pressure. The data show that the path for the inhalation is oblong (non-linear) rather than a line (linear), and does not trace the same path back and forth as the pilot's breath pressure changes with time, with a different return path than the "out" path; in other words the breathing pattern is displaying hysteresis.

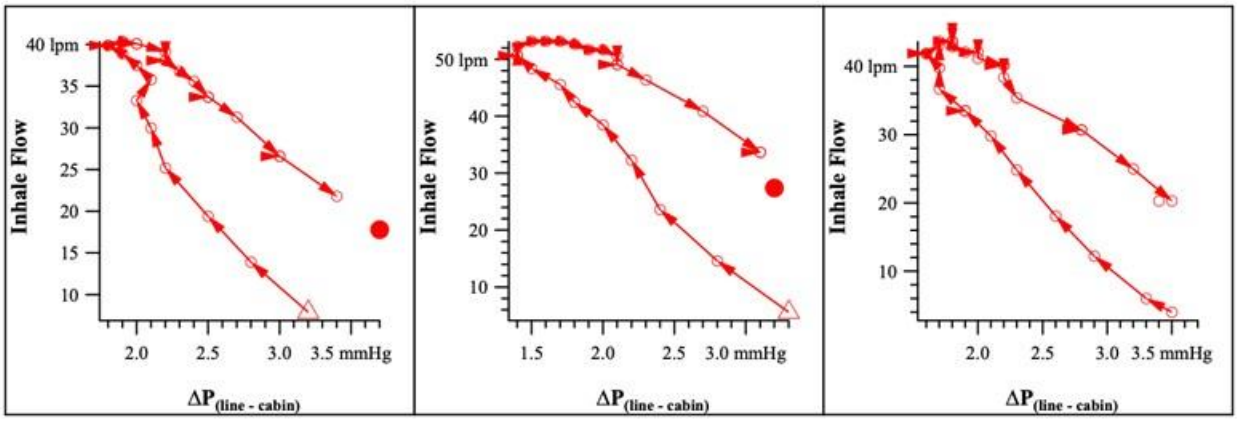

Figure 2.8. Inhalation Flow as Function of Line-Cabin Differential Pressure for NASA F/A-18 with Safety Pressure Regulator; showing pressure and flow hysteresis, with flow lagging behind pressure early. Later in the breath, flow exceeds demand.

While the breathing system in Figure 2.8 is not ideal, the path traced by the breath is still very smooth. Further, there is still a reliable and predictable relationship between the flow of air supplied to the pilot, and the pilot's demand. The PBA data show that pilots can breathe on a demand safety pressure system like that in Figure 2.8 safely if the hysteresis in the system remains relatively low.

This oblong path is indicative of the inherent lag in a demand system without a diluter functionality. Because the regulator is sensing the signal from a finite distance away from the pilot (the length of the mask and hose), and has mechanical springs and bellows regulating the mass flow response, it cannot respond instantly to changes in the demand signal. In a demand regulator system, unlike normal breathing on the ground, there will always be a delay between the initiation (the request for air), the regulator response, and the resulting flow reaching the pilot's mask. Diluter systems fundamentally minimize this problem. The dilution functionality allows instant access to a large volume of unrestricted air (the cockpit) to backfill for any delay or minor regulator restriction to flow. Some delay is unavoidable in any regulator where the pressure sensor and flow source are physically displaced from the demand signal. When a pilot first starts to breathe in and lung pressure drops, the pilot's demand signal must first open the inhalation valve, travel through the mask, down the hose, and activate the regulator's physical mechanism, and the resulting flow must traverse back to the mask. Significant loss or delay in this process results in flow that is not directly proportional. During the first half of the breath where demand is increasing, a delay results in less flow than demanded in any given instant, which is why the oblong path is lower at first. Conversely, when a pilot is decreasing their breathing demand during the second half of the breath, the lag causes the regulator to proportionally provide more flow until the responding flow drops to match the decreased demand for flow. The pilot has to work against the aircraft, being slightly undersupplied during the first part of the breath and being slightly oversupplied during the second half of the breath.

PBA used the concept of hysteresis as a metric to help identify and characterize disharmony in the breathing system. Figure 2.9 further illustrates the impact that a breathing system with hysteresis can have on the pilot. The beginning, middle, and end of the flow follows the nonlinear pressure-flow curve from (x to y) where the beginning of the flow is down at the bottom and the end of the flow loops around to the backside. Notice the two points of interest. For this part of that breath, delta pressure at the beginning of the inhalation flow give you about 1.3 lps of flow. The same delta pressure at the end of the flow, gives you about 2.6 lps of flow. Same $\Delta P_{(l-c)}$, or pilot demand, two very different flow rates. The difference between the beginning and end of the breath shows the lag of the regulator and can be clearly shown in a metric for "bad breathing" system as hysteresis.

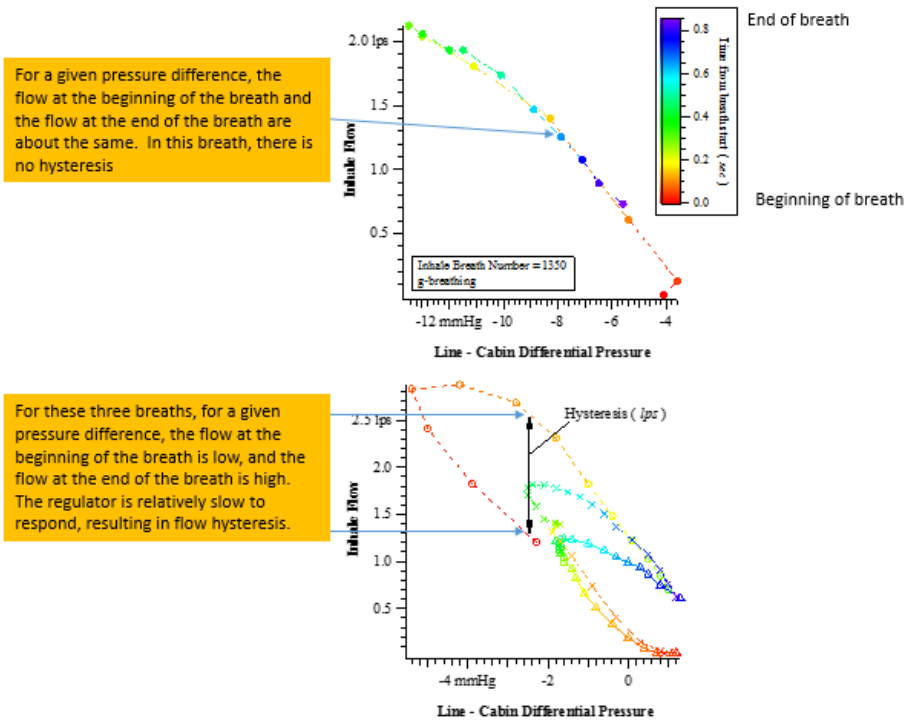

Figure 2.9. Illustrates Impact that Breathing System with Hysteresis Can Have on Pilot The beginning, middle, and end of the flow follows the nonlinear pressure-flow curve from (x to y) where the beginning of the flow is down at the bottom and the end of the flow loops around 2 to the backside.

2.4.2 G-Breathing

Figure 2.10 shows an example of "G-breathing". This is a special breathing technique that pilots use as part of the Anti-G Straining Maneuver (AGSM) to increase their tolerance to sustained G forces. According to Bates et al., 1990, this breathing technique

> … involves a forced exhalation against a… closed glottis… just before and during high sustained G's. The exhalation (increased intrathoracic pressure) is maintained for 3–4 sec and is interspersed with rapid inspirations less than 1 sec; the process is repeated cyclically.

Pressure and flow data are presented from a mid-level-G maneuver during PBA Flight 68. For this sortie, Profile B (aeroBatics) was performed in a two-seat F/A-18 in USAF configuration (CRU-73 diluter demand regulator). Data from the front seat pilot shows the pilot's breathing in terms of flow rates in lpm (top), and mask pressure in mmHg (bottom), as functions of time.

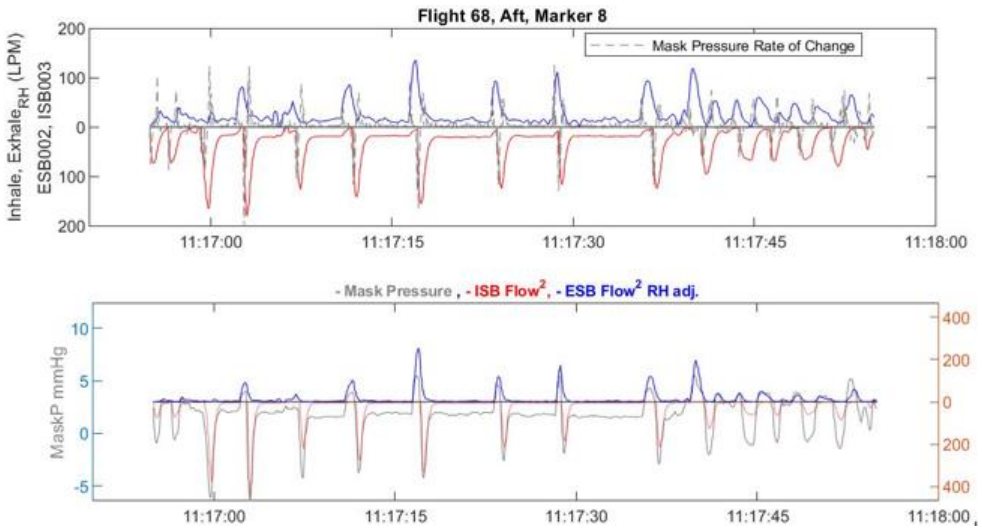

Figure 2.10. In-Flight Data Showing G-Breathing in Terms of Flow Rates in lpm, and Mask Pressure in mmHg

Notice how different G-breathing looks in contrast to smooth steady 1-G laboratory breathing. This figure shows that for a fast exhalation breath, the pressure needed to push the exhaled breath out is relatively small. Immediately after the exhaled breath, there's a big gulp of inhaled air, and the pressures are low compared to exhaled breath. During G-breathing, the pilot needs to work to get a big breath in a short amount of time.

This figure also shows that the sequencing and the times of the breathing cycles are completely different. A normal breathing cadence has smooth, continuous flow on the order of 3 seconds per breath. The total amount of time between the beginning of the fast exhalation and the end of the inhalation for some of these short breaths is on the order of 500 msec.

Notes about G-Breathing

G-Breathing has a fast valve sequencing cadence

- The process begins with a fast exhalation (the pressure needed to exhale is about 3 mmHg)
- Immediately after exhalation, there is a fast inhalation (inhalation delta P is large, about 7 mmHg)
- PPG: all the valve and regulator sequencing occurs in less than 500 ms
- Nominal breathing: valve sequencing takes 3000 ms

2.5 Analysis of Regulator and Mask Valve Sequencing

2.5.1 Nominal Breathing

Figure 2.11 shows the sequencing that occurs with the regulator and mask values during normal breathing. The top figure presents in-flight measured pressure profiles during exhalation (blue) and inhalation (red). The bottom figure is the time-aligned regulator/valve actuation schedule (no velocity data available).

The data streams shown on the top capture mask (blue) and line (red) pressures from three breathing consecutive cycles from a PBA flight. The figure below shows the actuation schedule of the inhalation and exhalation valves that are time synchronized to the breathing data. Starting with the start of the exhalation.

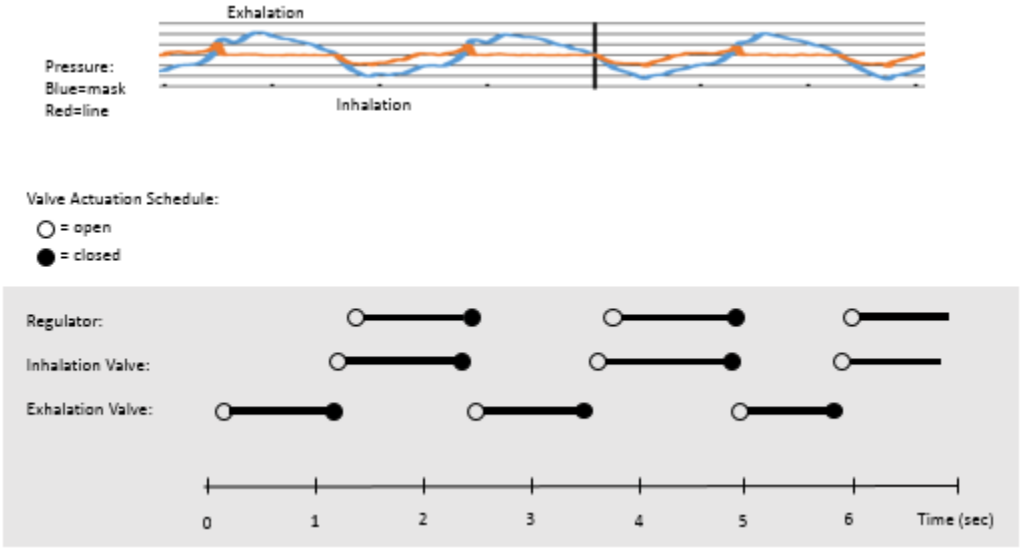

Figure 2.11. Regulator and Mask Valve Sequencing During Normal Breathing
Top: Pressure profiles during exhalation (blue) and inhalation (red); and bottom: corresponding regulator/valve actuation schedule

This figure shows that when the exhalation starts, the exhalation valve first opens to allow breath out and then closes after 1 approximately 1 second. After the exhalation valve closes during the beginning of the inhalation cycle, first the inhalation valve opens and shortly after that, the regulator valve cracks. The inhalation valve and the regulator are synchronized and mapped resulting in a long slow steady inhalation breath that tapers down as the flows go to zero and the exhalation begins. Notice the long breaths and the long durations and the valves perform as expected during this nominal breathing example.

2.5.2 G-Breathing

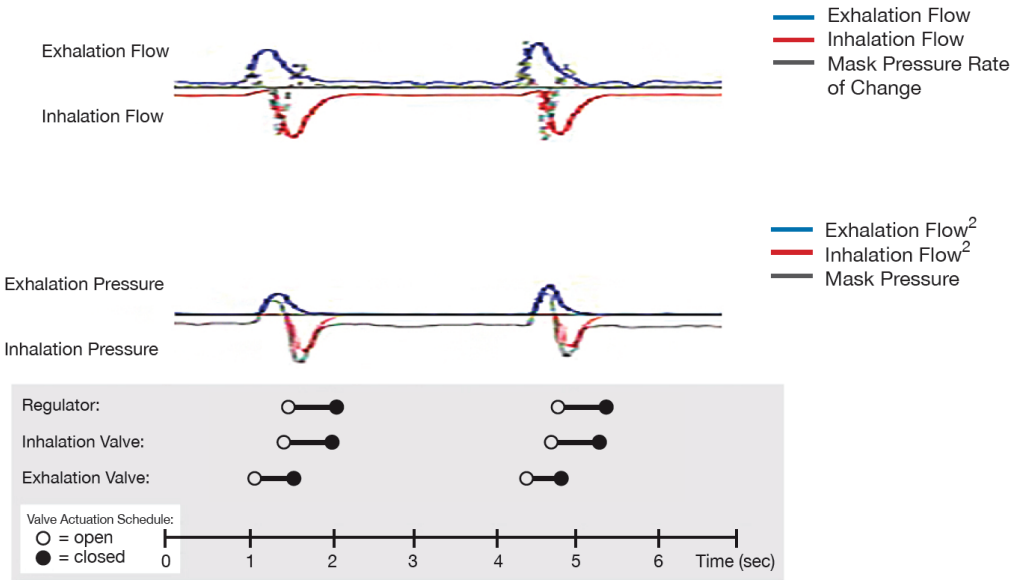

Figure 2.12. Regulator and Mask Valve Sequencing During "G-Breathing"
Top: Flow profiles during exhalation flow (blue), inhalation flow (red), Middle: Pressure profiles during exhalation (blue) and inhalation (red); and Bottom: corresponding regulator/valve actuation schedule

Figure 2.13 presents G-Breathing from Flight 68. The pilot in this case exhales at a high rate, followed quickly by an inhaled breath and a long pause. The time between the inhalation valve closing until to the end of the exhalation is short. The inhalation valve cadence is also short. The valve opens and closes in a short amount of time followed by a long pause. G-breathing produces a significantly greater dynamic demand on the system.

To further illustrate the disharmony in the pilot breathing system, Figure 2.13 takes the pressure data from the figure, along with the system response, for further analysis.

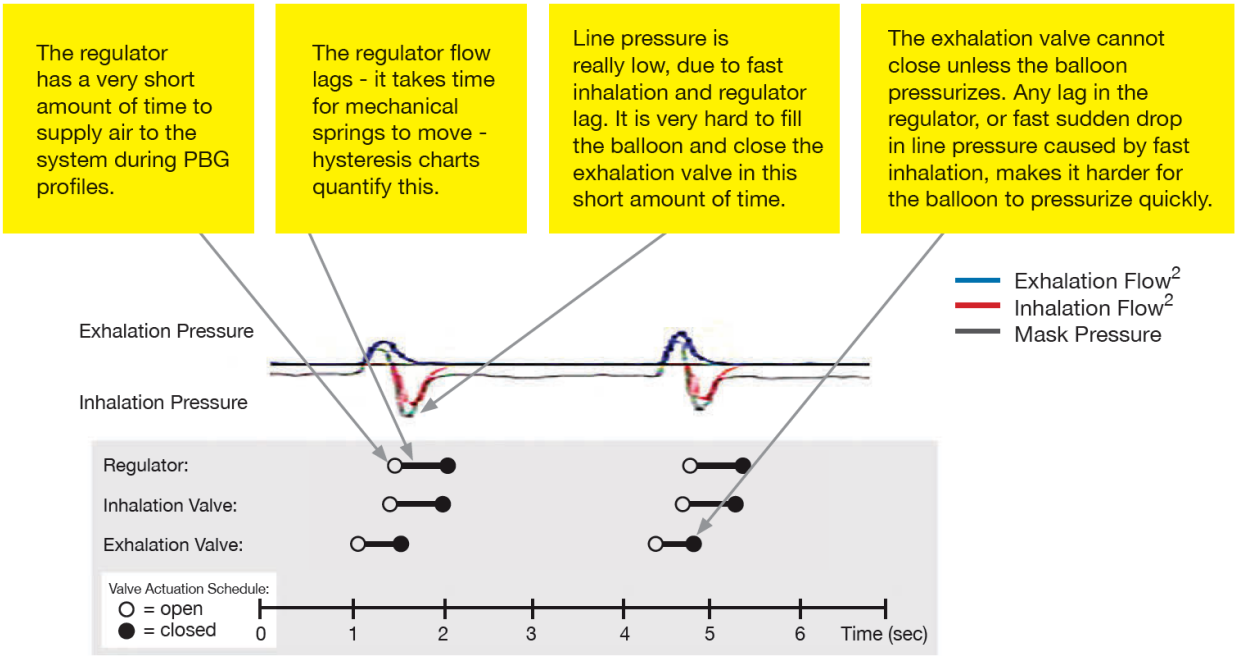

Figure 2.13. Nominal G-Breathing, Pressure profiles, Regulator/Valve Actuation Schedule, and Valve Sequencing Notes (from Flight 68)

Notice that at the regulator has a very short amount of time to supply a big volume of air. Notice that the inhalation pressure is very low, which is a symptom of the regulator lagging. The mechanical springs respond relatively slowly to this large demand for air (i.e., hysteresis). The pilot is suddenly demanding a large breath, but the regulator cannot respond in time. Notice that the line pressure is low because of the fast inhalation and the regulator drag. Remember the compensation tube described in Section 2.3.2, is designed to close the exhalation valve and is tied to the line pressure, which during this part of the inhalation is low and the compensation bladder is under-inflated. For exhalation valve closure, the exhalation valve cannot close until the bladder pressurizes. The bladder cannot pressurize until the regulator catches up. The regulator for this example becomes overwhelmed with this fast sequence.

2.5.3 A Comparison of Normal Breathing and G-Breathing

To further elucidate the complexity of the component response in these highly dynamic conditions, Figure 2.14 shows the sequencing side-by-side with a consistent time scale to see the difference in the valve sequencing at critical points in the breathing cycle.

These critical points in time is the lag of the minimum line pressure when the inhalation is at its peak and the exhalation valve should be closed. These systems struggle during especially dynamic times, such as during the G-breathing maneuvers that are a routine occurrence in high

performance flight. Conversely, these subtle timing issues are often not experienced in laboratory breathing systems.

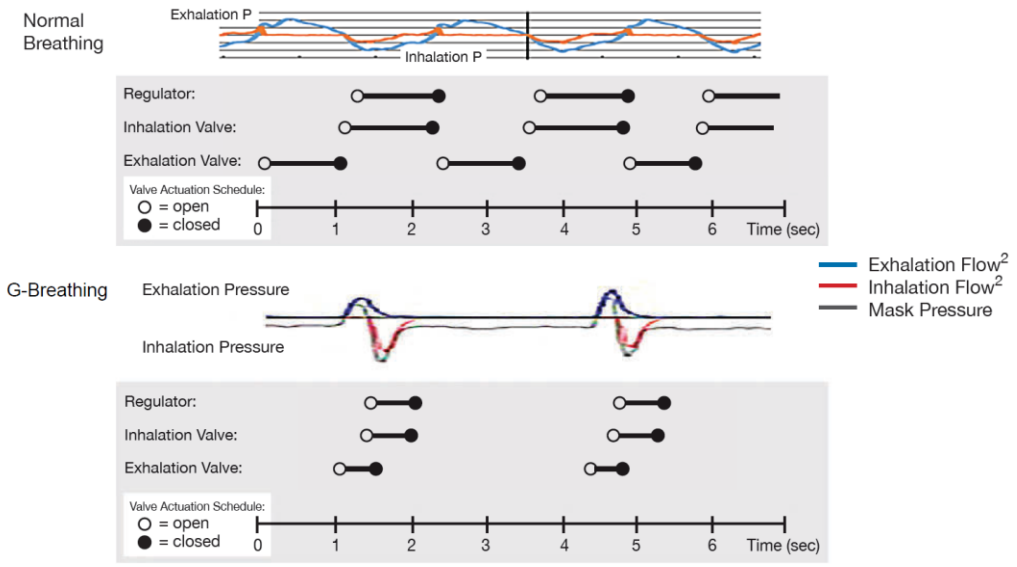

Figure 2.14. A Comparison of Valve Actuation Schedules for Normal Breathing and G-Breathing

2.5.4 Flight 29 Breathing

Figure 2.15 presents the pressure profiles, flow profiles, regulator/valve actuation schedule, and notes about valve sequencing as example of breathing system disharmony. These data illustrate what bad breathing looks like from a flight that will be exhaustively analyzed in the sections to come. This flight was an aerobatics profile flown in USN gear, which included the USN AFE and CRU-103 demand regulator.

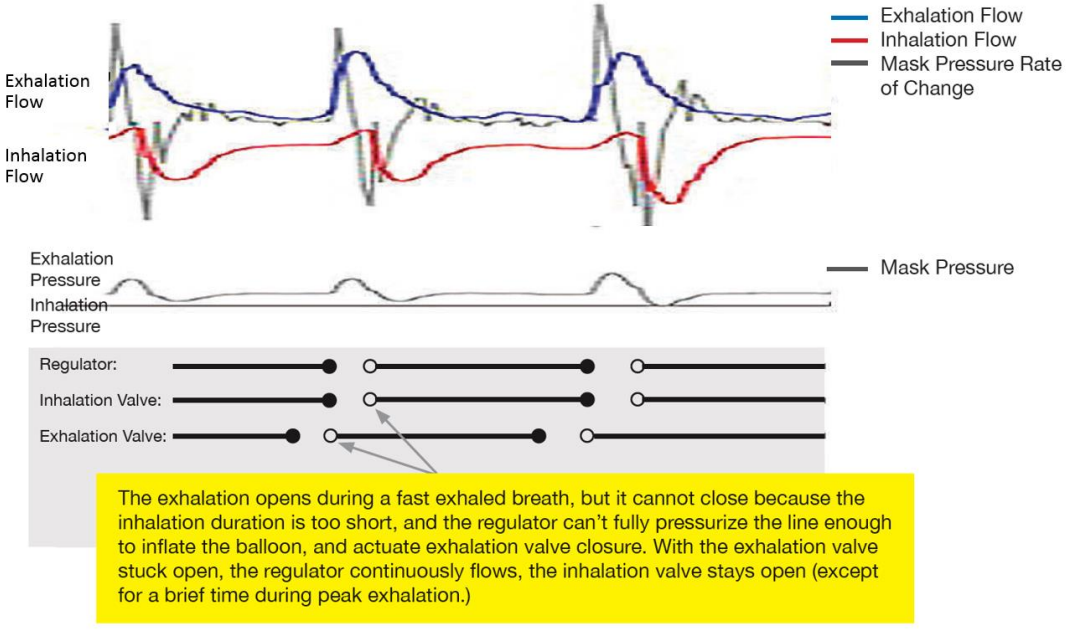

Figure 2.15. Pressure Profiles, Flow Profiles, Regulator/Valve Actuation Schedule, and Valve Sequencing Notes (example of breathing system disharmony)

This shows an extent of valve disharmony that the exhalation valve never had a chance to close because the compensation bladder (i.e., balloon) never had a chance to inflate. With the exception of a short pause at the time of peak exhalation at the beginning of the PBG cycle, (where the pilot rapidly exhales at the beginning) that is the only time when the inhalation is closed, and the regulator flow has stopped. The rest of the time the exhalation valve cannot find the pressure to inflate the balloon, to close the exhalation valve and there is flow through the whole system. The PBA team suspects that this disharmony causes other problems that will be addressed later.

2.6 Summary

This subsection presents an overview of breathing fundamentals that puts the jetfighter pilot on-demand air supply into context between normal autonomic respiration (without conscious effort) and the other extreme, the medical ventilator. The goal of this introductory material, and the remaining PBA report, is to develop an understanding as to how "normal" breathing is affected by imposed on-demand breathing gear. All topics described in this Technical Section are explained in detail in the subsequent Technical Section 6 of this report.

The take home message from this part of the report is that stressors from flying require modifications to normal breathing that are implemented by regulators and masks that turn the regime to on-demand breathing. This imposes challenges to the human part of the whole system. The human can only signal with relatively small pressure differences to open and close mask valves, and to trigger flow from the regulator. At times, these human applied changes in mask pressure compete with safety pressure, cabin pressure fluctuations, valve hysteresis, and other mechanical interactions, as shown in some of examples above.

There are three basic issues that arise in the adaptation to on-demand breathing.

- Safety pressure interactions. In some regulators, the safety pressure may create a situation wherein the pilot has difficulty exhaling or may interfere with the smooth cycling of valves. This approaches the realm of forced ventilator breathing, and the pilot ends up competing with the system.
- Mismatches between pressure and flow. These include disharmony or hysteresis, as well as increased pressure and reduced volume, with respect to the expected pulmonary functions for unrestricted normal breathing. These can accumulate over time in creating breathing fatigue or trauma. The system does not supply air to the pilot at the right time, volume, pressure, or O_2 concentration to meet the pilot's demands.
- Compensation for high G-force stress. This radically changes the breathing response forcing the pilot to consciously modify the breathing pattern and may also tax the breathing supply beyond its design function. G-breathing takes the pilot out of the normal breathing regime and requires conscious effort.

In conclusion, ease of breathing in the cockpit is best achieved by understanding how normal unrestricted, 1 atmosphere, and 1-G breathing is accomplished in the real world, and then diagnosing situations wherein on-demand breathing deviates from this baseline. On-demand breathing always requires additional effort, but minimizing this effort is only possible through a complete understanding of detailed pilot interactions with the aircraft.

References

Bates et al. High G Physiological Protection Training, AGARDograph No. 322, AMP Working Group 14, AGARD-AG-322, Dec 1990.

Rainford, D, and DP Gradwell, Ernsting's Aviation and Space Medicine, Boca Raton Chapman and Hall/CRC, 2016.

Ernsting, J; and RL Miller (Editors), *Advanced Oxygen Systems for Aircraft*, Advisory Group for Aerospace Research and Development (AGARD), Apr 1996.

Findings

F.2-1. Pilots subconsciously adjust their breathing to accommodate to changes in the mechanical supply system.

F.2-2*. *Lung pressure changes of 2-3 mmHg drive normal inhalation and exhalation. Cabin pressures can change up to 5 mmHg during the course of a single inhalation and can have a profound effect on breathing.*

Technical Section 3: PBA-Unique Sensor Systems: VigilOX

3.0 Introduction

The PBA utilized unique sets of sensor systems as required by the data demands associated with measuring different aspects of aircraft system performance and mechanical interaction on the pilot's breathing. The full suite of available monitoring systems is discussed in Technical Section 1.

The distinctive feature of PBA is the simultaneous collection of aircraft flight/performance parameters and pilot physiological breathing response. The latter (breathing monitoring) was implemented using commercially available instrumentation comprised of VigilOX sensing systems designed by Cobham Missions Systems (Orchard Park, NY). PBA incorporated both inhale sensor block (ISB) and exhale sensor block (ESB) components for in-flight breathing data acquisition.

The PBA team collected data with different versions of Cobham's VigilOX system that evolved over the course of the study. Differences were comprised of software upgrades and small technical improvements. The particular VigilOX system for any given flight was based on the system's availability at the NASA Armstrong Flight Research Center at Edwards Air Force Base, CA. The VigilOX sensor suite includes multiple sensors across two independent and physically separate units (the ISB and the ESB) to provide data on essential factors necessary to understand pilot breathing. This system redundancy provides robust error detection through comparative analysis between the sensors to examine cabin pressure, line pressure, mask pressure, flow, and O_2.

3.0.1 VigilOX System Description

The VigilOX system combines multiple data collection sensors to provide preliminary insight into pilot physiology that was previously unknown and essential to understanding pilot breathing. PBA selected the VigilOX prototype system for data collection due to the availability and technical readiness of the device. This selection process and determination is consistent with other research teams conducting similar in-flight research; and follows a similar process to that used by the Royal Australian Air Force (RAAF).

Briefly, two fundamental questions are explored:

What does VigilOX do?

- VigilOX provides a suite of synchronized measurement sensors designed to collect numerous aspects of human breathing during flight that is unique and beneficial as a flight test capability.

What is the accuracy and validity of VigilOX?

- The VigilOX includes multiple sensors across two independent and physically separate units (the ISB and the ESB). This system redundancy provides allows for robust error analysis and detection through comparative analysis.

A description and photographs of ISB and ESB sensors and their attachment points on pilot flight gear is provided in Technical Section 1.1.2.1. For reference, Table 3.1 shows the sensor lists for ISB and ESB, respectively.

Table 3.1. List of ISB and ESB VigilOX Sensors

ISB		ESB
Partial pressure, O_2		Partial pressure, O_2
Inhalation Flow		Exhalation Flow
Cabin pressure		Cabin pressure
Inlet gas temperature		Exhaled gas temperature
Inlet gas pressure		Exhaled gas pressure
Inlet gas humidity		Exhaled gas humidity
Cabin temperature		Cabin temperature
3-axis accelerometer		3-axis accelerometer
		Partial pressure, Exhaled CO_2
		Mask pressure

3.0.2 Choosing VigilOX System

A review of the market indicated this device as the most suitable for PBA due to commercial availability and approval for use in military jet fighters. There are numerous other systems in various stages of research and development that are designed to identify physiological or environmental aspects of the human and the aircraft environment. A non-exhaustive list includes Elbit's Canary Physiological Monitoring and Warning System, Holistic Modular Aircrew Physiologic Status Monitoring System (HMAPS) manufactured by Athena GTX, Physiologic Health Status of Isolated Personnel (PHYSIO), MAsk SEnsor System (MASES), Theratactics SpO_2, INSTA Mask, Equivital, Slam Sticks, Sorbent Tubes, and Garmin Watches.

However, among these systems, the VigilOX was considered the best choice due to a preponderance of existing baseline data compiled by previous efforts, ease of access, and technical readiness level. The PBA team remains hopeful that continued interest in the pilot during jet aircraft operation will enable further development to the current state of overall technology capable of serving this operational environment.

The VigilOX is currently in testing at USAF School of Aerospace Medicine (USAFSAM), Naval Medical Research Unit – Dayton (NAMRU-D), USAF 711th Human Performance Wing (HPW), Naval Air Systems Command (NAVAIR), PAX River, and Royal Australian Air Force (RAAF). This is not an exhaustive list and the exact version numbers of the VigilOX software and hardware systems for each of these locations is changing over time.

3.0.3 VigilOX System Caveats and Solutions

Specifically, the intention of the PBA task was not to provide laboratory grade accuracy of human breathing but instead to provide early insight regarding potential inconsistencies between the predicted human breathing patterns and those actually observed during jet aircraft operation. The PBA team is confident that the quality of the data collected using this system is suitable to provide both an awareness of the pilot experience and to support the need for increased improvements in data collection technology to enable rigorous assessments of human breathing during flight. Two important questions are addressed:

Why are we confident in the conclusions based on VigilOX data?

- Self-consistency checks. The PBA analysis of VigilOX data does not rely solely on a single sensor for any conclusion, but rather multiple sensor readings, coupled with aircraft data and pilot feedback.

- Many metrics do not depend on the absolute value of the sensor reading but the trend and relative trend (i.e., how flow and pressure changes during G-breathing compared to relaxed breathing).
- The values are physiologically relevant (i.e., tidal volumes, respiration rates) and in the narrow range one would expect for pilot breathing.

What are the known issues?

- The ESB VigilOX sensors may have interference from condensing water vapor from exhaled breath, especially the exhaled gas flow and exhaled gas temperature sensors.
- The ESB VigilOX sensors may experience a "washout" effect due to the tube volume at the exhalation port, especially for the O_2 and CO_2 channels.
- The data channels from ISB and ESB may not be accurately aligned due to separate time-base and internal time drifts.
- Different versions of data acquisition software may default to different sensitivity limits.

All of these topics are explored in detail in the ensuing technical analyses of this report using the results of real-world flights performed by NASA test pilots. Overall, the PBA team has confidence that the VigilOX systems met the general research goals of providing a series of pilot breathing parameters within the context of a designed and controlled military flight environment.

3.1 Technical History of VigilOX

In May 2018, VigilOX was considered a prototype system and listed as TRL 6. Since this time, there have been several software and hardware updates. As of today, VigilOX development has reached a fixed point and the system is mid-way through the four-step verification and validation testing by the joint efforts of the USN and USAF laboratories. The VigilOX system has undergone extensive testing across various DoD and collaborative partners (USAFSAM, NAMRU-D, 711th HPW, NAVAIR, RAAF) which included sensor Verification and Reliability Testing, SpO_2 evaluation, manned centrifuge testing, and altitude chamber testing. Testing has occurred throughout the development history of this device. Testing data depends on the state and build of the device which is not readily available or reported.

From study initialization to current date, VigilOX has undergone several improvement cycles. These changes were in response to DoD and NASA customer interactions. The NASA study has collected data on three updated builds, including most recent build as of writing. Corrected errors from the ISB are related to O_2 sensing, humidity sensing, status information, improved circuit boards, and reduced bit collisions. Corrected errors from the ESB include voltage instability, improved CO_2 sensor, and mask pressure sensor. Data drop-outs due to post-processing time-out were present in two of the three builds used in the PBA testing.
There are known variations in naming structures and device versions across testing.

- VigilOX contains two sensor system suites: the ISB and the ESB.
- VigilOX started as AMPSS (Aircrew Physiologic Monitoring Sensor Suite).
- AMPSS 1.0 to 2.5 system versions were developed by Orbital Research with DoD guidance and only contained the ISB.
- Cobham purchased AMPSS 2.5 (briefly known as AIMS).
- Cobham conducted a complete redesign featuring sensor and software replacements.
- Cobham released AMPSS 2.6 = AMPSS 3.0 = VigilOX. Cobham selected VigilOX as the final name.

The ISB and ESB both have a software version and hardware version. There are four known ISB software and hardware pairs that have flown: (V0.24, DEV), (V0.26, DEV), and (V0.34, DEVA). The most recent delivered systems with associated information that have not flown are (V1.01, A). There are known updated systems V1.02, V1.03 and V1.04 but change information has not yet been provided. There are three known ESB software and hardware pairs that have flown: (V0.12, DEV) and (V0.27, DEV(-)). The most recent delivered systems with associated information are (V1.01, A), and show the timing issue fixed. There are known updated systems V1.02, V1.03 and V1.04 but change information has not yet been provided.

3.2 Rationale for Implementing VigilOX for PBA

During previous work with the USN on F/A-18 PEs, the NESC team identified a deficiency in information about the fundamental human breathing patterns observed during jet aircraft operation. The NESC recognized that knowledge of pilot physiology during flight was critical to confirm or refute potential factors contributing to PEs and reported that information of this type would be beneficial. The NESC PBA task initiated to examine parameters of human breathing during jet aircraft operation.

The PBA required a sensor suite capable of detecting and recording several components of human inhalation and exhalation data simultaneously during jet aircraft operation. The extreme environment inside the jet aircraft during operation precluded traditional, research-grade, laboratory equipment. This data collection system had to be small, self-contained, self-powered, and unobtrusive while also being robust to temperature, altitude, and windblast testing. The NESC was made aware of several physiological collection systems during the F/A-18 investigation.

The PBA data collection device selection process was informed using the criteria of availability, technology readiness, and amount of data provided. This information was collected via market survey and DoD working groups. The DoD Technology Readiness Level (TRL) is used to indicate the maturity of a developmental technology. The USAF listed the Cobham VigilOX Integrated Aircrew Equipment Physiologic Monitoring System at TRL 6 in May 2018. TRL 6 corresponds to: “System/subsystem model or prototype demonstration in a relevant environment” (See Appendix 3 for the TRL table). TRL 7 indicates “Prototype near, or at, planned operational system” and relies on demonstration in operational environment. A system is not considered near-final or determined as meeting design specifications until TRL 8: “Actual system completed and qualified through test and demonstration. Technology has been proven to work in its final form and under expected conditions.” The VigilOX system prototype was selected for this study above other potential device options due to the technical maturity and system availability. Although imperfect, no other system was identified as more or equally mature enough to meet the required data collection needs within the realm of jet aircraft operation environments.

VigilOX provides a suite of synchronized measurement sensors designed to collect numerous aspects of human breathing during flight that is unique and beneficial as a flight test capability. A review of the market indicated this device as the most suitable. Potential alternative sensors devices were excluded due to singular data specialization (e.g., devices specializing in only one data stream), inability to provide the necessary range or dynamic capability during flight conditions (e.g., flow sensors), inability to integrate into the existing aircrew flight equipment

(e.g., large, cumbersome, or non-self-powered), and inability to measure both inhale and exhale characteristics (e.g., mask pressure).

The VigilOX also combines multiple data collection sensors to provide data on essential factors necessary to understand pilot breathing. The VigilOX suite includes multiple sensors across two independent and physically separate units (the ISB and the ESB). This system redundancy provides allows for robust error analysis and detection through comparative analysis between the sensors to examine cabin pressure, line pressure, mask pressure, flow, and O_2. The pressure sensors have varied designs, and therefore slightly different strengths and weaknesses. For example, the mask pressure is a differential pressure sensor allowing for much higher precision when measuring small changes, whereas the cabin pressure sensor is an absolute pressure sensor that is not as sensitive to small changes or drift, and the O_2 sensor is an optical sensor which is more sensitive and optimized in the middle range. While this makes data analysis tedious at times, the redundant overlapping of independent sensing capability allows for increased error detection of single sensor malfunctions, sensor bias, and sensor drift. Additionally, for complex phenomena that behave in non-linear and unpredictable manners VigilOX offers multiple partially overlapping data streams to observe an event across multiple data streams to assist in isolating errors, such as a rogue sensor, a leak in the mask, or a malfunctioning valve.

The normal development path for a mid-TRL prototype system includes many hardware and software advancements as new data becomes available. As in PBA, many other research efforts in this similar environment also chose this device for testing. The high visibility of data collection efforts using this system during prototype development has caused confusion. There are known inconsistencies in naming structures and device versions which leads to confusion. In the current iteration, VigilOX contains two sensor system suites: the ISB and the ESB. In the earliest phases of prototype development, this system began as AMPSS (Aircrew Physiologic Monitoring Sensor Suite). The AMPSS 1.0 to 2.5 system versions were developed by Orbital Research with DoD guidance and only contained the ISB. Cobham purchased AMPSS 2.5 (briefly known as AIMS) conducted a complete redesign including hardware and software replacements. The new system was known by multiple names: AMPSS 2.6, AMPSS 3.0, and VigilOX. Cobham selected VigilOX as the final name.

The VigilOX system has undergone prior testing across various DoD and collaborative partners (USAFSAM, NAMRU-D, 711th HPW, NAVAIR, RAAF) including sensor verification and reliability testing, SpO_2 evaluation, manned centrifuge testing, and altitude chamber testing. However, testing was concurrent with device development. Data collected during testing has depended on the device hardware and software builds, information which is not readily available. Cobham continued to update and improve this prototype system prior to and throughout the PBA data collection time period. Cobham provided the PBA team with customer support in the form of technical communication and system improvements in the form of physical, mechanical, and software. See Appendix 3 to review several ISB and ESB build schedules and change logs showing the modification across versions.

3.3 Technical Evaluations

3.3.1 Software revisions

The PBA data collection included all three of the VigilOX software versions. See Table 3.2 to identify which runs were flown with which VigilOX system.

Table 3.2. VigilOX Configurations

Set	Flight Runs Collected	ISB Versions	ESB Versions
Phase 1	1–23	ISB V0.26, DEV	ESB V0.12, DEV
Phase 1a	24–69	ISB V0.34, DEVA	ESB V0.27, DEV(-)
Phase 2	Proficiency Flight P01	ISB V1.01, A	ESB V1.01, A
Phase 3 *provisional		ISB V1.02/3/4, A?	ESB V1.02/3/4, A?

Several VigilOX device issues were identified during the development cycle. These issues were consistent with the current state of technology capable of addressing the needs of this study while operating within the limitations of the extreme environment. Previous verification testing by the USAF revealed few data concerns with the ISB sensors of O_2, flow, pressure, temperature, and humidity. However, the ESB has been shown to be highly problematic in terms of flow rate, temperature, and humidity primarily due to data failure, low test-retest reliability, the O_2 sensor error increasing with altitude. Over the course of VigilOX technical improvements, the data dropout and data syncing problems have largely been overcome. However, operational flight testing also revealed several similar ESB data issues.

3.3.2 Individual sensors

Part of the PBA strategy related to the VigilOX assessment during in-flight data collection is to evaluate parameters individually. PBA analysis showed that the VigilOX differential mask pressure measurement is accurate, precise and not prone to error. From this single measurement PBA can get reasonable estimates of critical physiological metrics such as breath count (respiration rate) and breath timing given the sensors response and sampling rate of 20 Hz. Through analysis, both the ISB and ESB line pressure measurements were shown to be within the manufacturer's stated specifications. These ISB line pressure sensor tracks pilot breathing patterns well and has shown, for example, that it is possible to detect a malfunctioning inhalation valve in the mask. While the ISB and ESB line pressure measurements are accurate and precise and within the manufacturer's specifications, the complexity involved with using them in conjunction to make differential line pressure measurement still presents some technical challenges.

Statistical calculation shows the ISB flow sensor to be a relatively robust measurement. PBA analysis did indicate problems with the inhalation flow measurement during exhalation and when there is a malfunctioning inhalation valve (causing reverse flow or pressure gradient). This problem was mostly remedied with a software update. The tidal volumes calculated from the flow measurement are physiologically reasonable. Further, the sensor is robust enough to track trends in flow and volume (integrated flow) over the course of a flight. This allows the sensor to provide breath counts (respiration rate) and other man/machine metrics such as flow hysteresis that do not depend on the absolute accuracy of the sensor.

The PBA team has used multiple independent analyses of the VigilOX data to provide pilot breathing metrics. These include custom-developed algorithms for peak definition, industry-standard tools for signal processing and custom-developed breath-by-breath analysis for metabolic analysis. While these analysis tools use the same VigilOX data set, they provide independent analyses of the data providing another layer of confidence in the conclusions of PBA. The majority of PBA analysis has relied on mask differential pressure, ISB and ESB line pressures and ISB flow. ISB and ESB line temperatures are deemed accurate and precise and are

only used to convert flows and volumes to standard temperature and pressure (dry) conditions (STPD).

Extensive testing throughout the research community has shown other measurements provided by the VigilOX system to be less reliable and are found almost exclusively on the ESB. PBA preliminary analysis agree with this ongoing work and hold reduced confidence in ESB ppO_2, ESB $ppCO_2$, and ESB flow. A primary issue for the ESB has been reported as humidity in the form of liquid water and condensation from exhaled breath. This issue is not a problem for the ISB as the source air to the ISB is dry, however, this is a serious problem for the ESB.

Analysis shows the ESB $ppCO_2$ measurement to be accurate and precise, providing physiologically relevant values. PBA analysis does show, however, that the ESB $ppCO_2$ is a volume-averaged measurement meaning that it cannot track breath-to-breath changes in $ppCO_2$ or within-breath $ppCO_2$ measurements (e.g., it cannot provide a true end-tidal $ppCO_2$). Within these limits though the sensor is useful as a self-consistency check in the data. For instance, ESB $ppCO_2$ values track changes in pilot tidal volume providing confidence in the tidal volume data.

The current ESB flow has been visibly problematic and frequently produces unrealistically low volumes when referenced to the ISB flow. The error in ESB flow inaccuracies are likely related to way the ESB flow is measured. The ESB outlet is exposed to the cockpit cabin and the combination of cabin pressure fluctuations (mmHg) and the condensing water likely impacts the ESB flow sensor. Due to the inaccuracies, PBA rarely uses this metric with the exception of assisting in the production of trumpet curve graphics. Condensing water can cause “reverse flow” conditions which are well depicted in these graphical representations. Another issue with flow is calibration offset and drift. In early flights, VigilOX protocol usage was unclear related to system taring. Pre-flight tare improves data accuracy but does not exclude drift and it remains possible for offsets to develop during flight. Unfortunately, if there is an offset and it is negative, Cobham has designed the utility to be unable to display a negative number, thus providing truncated data that cannot be corrected in post-processing. The features of the sensor drift are currently unknown and unable to be considered correctable.

Another member of the flight research community with extensive knowledge and use of the VigilOX system, the RAAF, has decided against the use of any VigilOX flow data. The absence of flow data prevents tidal volume and minute ventilation calculations. PBA is taking this under consideration during analysis particularly due to the individual sensor measurement errors compounding when integrated together. PBA incorporated alternative methods to utilize these data while avoiding conclusions that extend beyond the existing data quality. In particular, the sensor appears to have reduced accuracy in lower readings but has also provided results supported by physiology and physics, such as higher flow and narrower breath of G-breathing having reduced area under the curve.

The O_2 sensors exhibit a considerable amount of high frequency noise that is unlikely to be physical. The O_2 measurement is capable of tracking overt O_2 fluctuations but lacks the precision to track the small changes in O_2 consumption by the pilot. The O_2 measurement should not be dismissed entirely but the subsequent conclusions should be limited and conscientiously assessed. The O_2 sensor outputs Partial Pressure (ppO_2) values. O_2 concentration, an important metric to track for human physiology, is calculated as the ratio of the reported ppO_2 and the Line Pressure from the same unit (ISB or ESB). Thus, transients in either output, or changes not recorded in the same 1/20 of a second output, can cause this ratio to compound its error.

The ISB line pressure follows the expected increase and decrease during inhalation. PBA line pressure measurements were observed ranging 370–720 mmHg absolute, which corresponds appropriately to the expected range of pressures given the altitude measured by independent aircraft sensors. This system accuracy was calculated to be less than a 1% error (5 mmHg) which is below the threshold of mask change values that are determined as relevant. However, a simultaneous 1% compounding error in both ISB and ESB line pressures would require manual offset of one data set. The recorded absolute value occasional fails to equal the independent measure of cabin pressure in the aircraft; however, observations indicate the delta or relative changes match the changes observed in mask pressure. The ESB line observations show little variation with breath but it can be used as a reference.

Aircraft cabin pressure is sampled at a lower frequency and averaged so changes are detected slower and potentially reduced as compared to those observed in line pressure. Because aircraft cabin pressure is an active result of aircraft pressure control system function, the aircraft cabin pressure cannot be considered a linear analog for ambient pressure, and likewise may or may not be a stable reference value depending on aircraft function. For this reason, cabin pressure may be used as a loose reference when examining pressure scheduling, but not for pressure transients. Observed data can be considered the modified version of a true event, meaning, if there is an extreme change in cabin pressure, the actual change may have occurred earlier, faster, or with higher amplitude. Cobham reports testing to show that the cabin pressure reading is unaffected by G.

3.3.3 Pilot/Aircraft Interaction Data

During the course of the PBA, the team identified several aspects of pilot/aircraft interactions that can potentially have severely negative physiological consequences. The pilot/aircraft issues identified during PBA were not an artifact of the known limitations of VigilOX, but instead were a product of the unique interactions of the pilot and the life support equipment during flight. Identification was enabled, in part, due to post-processing for data handling, data stream combination, advanced data cleaning, and outlier identification.

Although there are known issues with this data collection system, as a result of the rigorous analysis of the VigilOX data during the PBA project, the team remains confident that the system fulfills the needs outlined in the charter of the assessment. Specifically, the intention of the PBA task was not to provide laboratory grade accuracy of human breathing, but instead to provide early insight regarding potential inconsistencies between the predicted human breathing patterns and those actually observed during jet aircraft operation. Thus, the quality of the data collected using this system is suitable to provide both an increase in understanding of the pilot experience and to support the need for increased improvements in data collection technology that will enable increasingly rigorous assessments of human breathing during flight.

3.4 VigilOX Systems Summary

The VigilOX system, combined with the aircraft and other data acquisition systems used by the Pilot Breathing Assessment, provided a unique and promising opportunity to gather dedicated datasets associated with pilot performance. While the VigilOX began PBA as relatively developmental in nature, it improved immeasurably over the course of the assessment as the NESC worked with Cobham. The analysis conducted by the PBA team, using VigilOX provided data, has fundamentally changed the current understanding of Pilot Physiology in high performance aircraft.

Technical Section 4: Data Curation and Alignment of Continuous Variables

4.0 Introduction

The incorporation of breathing data alongside the aircraft data is a unique feature of the PBA. To carry out high fidelity analysis, the PBA data team had to curate and align all data streams, remove errors, identify dropouts, and synchronize timing from disparate sensor systems.

In general, this section serves to illustrate the importance and complexity of using disparate high frequency PBA measurement data. The data generally cannot be used as is, but instead, needs to be carefully assessed to avoid spurious correlations. Even small shifts in time between two sensors can introduce large errors when interpreting.

As described in the Introduction Section 1.4.1, continuous variables were categorized as dependent (pilot) variables and independent (aircraft/flight) variables as derived from VigilOX ESB, ISB, and aircraft-based sensors. In the PBA, raw data-streams were acquired at 20 Hz from a variety of different sensors with different time-bases and reliabilities. As such, there is no *a priori* confidence that data are consistent and simultaneous when overlaid.

Specifically, the properties and structures of pilot breathing, and aircraft data are described, and examples are provided as to how complex data-streams were curated for accuracy and aligned in time.

The goal of this technical Section is to develop a dataset of VigilOX ISB and ESB data streams, identify data dropouts and other obvious sensor problems, and then incorporate all other random variables into one consistent master dataset. The sensor systems are described in Technical Section 1.1.2.

4.1 Curation of Data

4.1.1 Timing

To characterize pilot respiration, it is important to study mask pressure and inhalation/exhalation flow. The inhalation and exhalation sensor block (ISB and ESB) parameters are sampled at a higher rate (e.g., 200 Hz), then post-processed in real time and output at a target 20 Hz data rate. Throughout this report, Inhalation Flow, Exhalation Flow and Mask Pressure are often referenced, as they are important breathing parameters for pilots. The inhalation and exhalation flow come from two separate sensors, the ISB and ESB block. Because the time to inhale may take as little as 0.5 seconds, it is crucial that the 20 Hz streams are aligned to the highest possible precision (0.05 seconds).

Initial alignment inconsistencies pointed the PBA team to examine the timestamp intervals, and multiple, random large time-skips up to 0.4s (an error of 8 measurement points) were found in units ISB002 and ESB004 with software version 1.01 (Figure 4.1). The ISB/ESB manufacturer, Cobham Missions Systems was kept appraised of the issue.

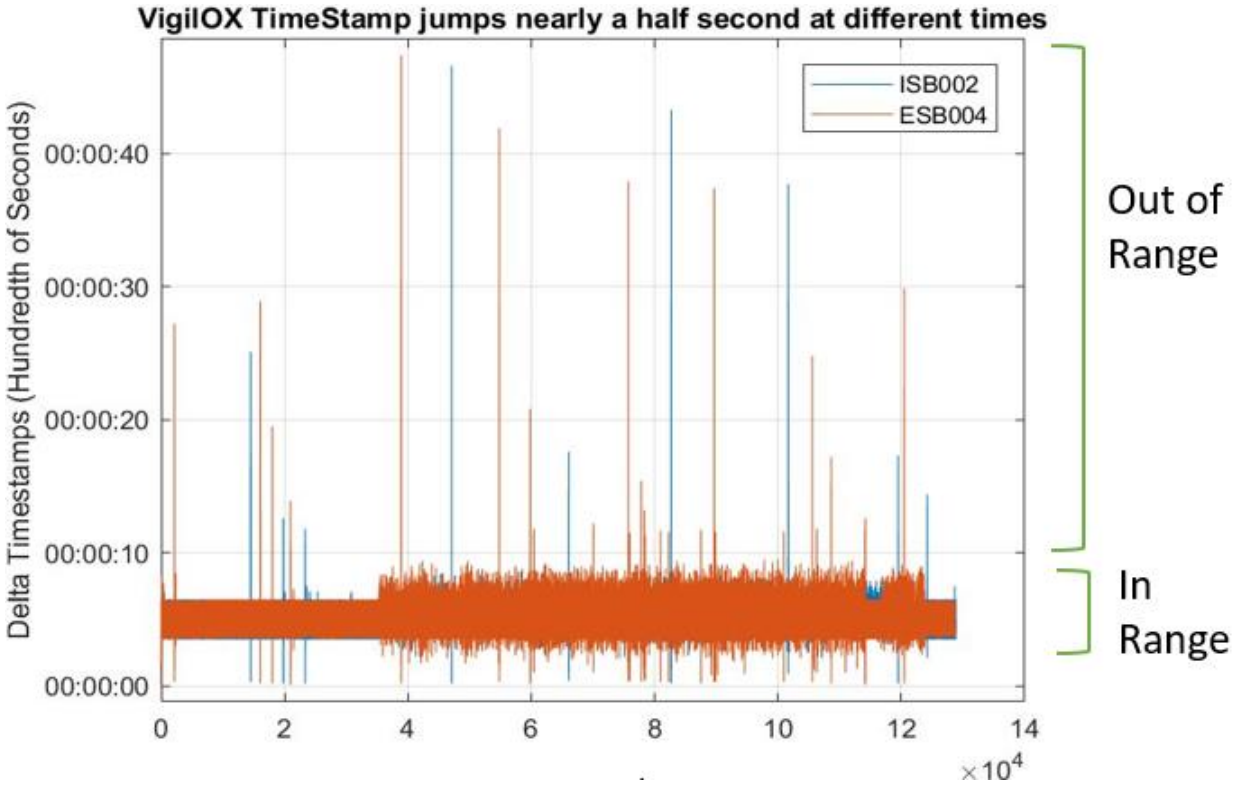

Figure 4.1. Visual Representation of ISB/ESB Time Output Swings
Precise time stamps are on the horizontal line at 00:00:05 (0.05 seconds)

NASA has filled the out-of-range timestamps and interpolated the data using the Piecewise Cubic Hermite Interpolating Polynomial (PCHIP) technique (Figure 4.2). The small timestamp jitter in the in-range band is attributed to instrument "write" time. Cobham, working with NASA, ultimately resolved these processing issues.

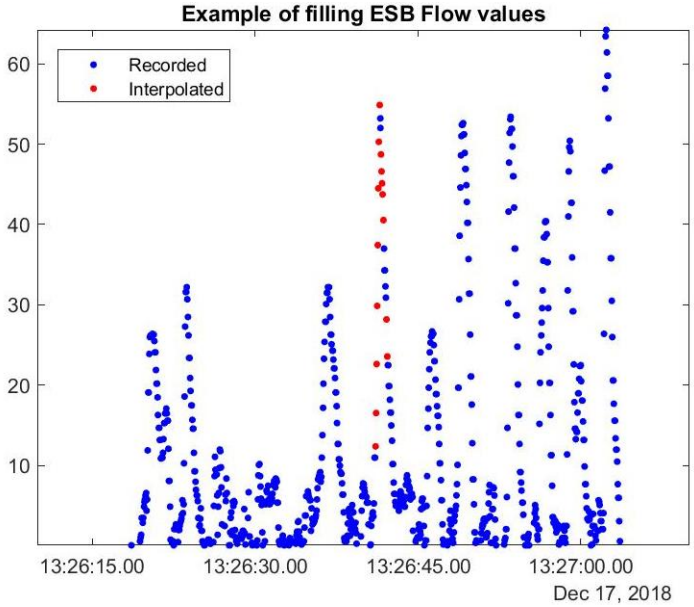

Figure 4.2. Example of Interpolated Data (red points) Based on PCHIP Technique

4.1.2 Alignment of ISB and ESB

Alignment of the ISB and ESB data starts by selecting the optimum channels from each block. After testing alignment between the ISB and the ESB using cabin pressure, acceleration, or even time common to both, the PBA found that these channels lack the precision sought. It is shown in Section 5 that the Cabin Pressure is averaged over a longer period, and that dynamic changes characteristic to fighter jets are reported dampened and with a significant lag.

The ESB mask pressure sensor is a differential pressure transducer that directly measures the differential pressure between the mask and the cabin. It is the most precise and reliable parameter, both because it encompasses inhalation and exhalation pressure in one channel, and because of the low bounds of its range.

The closest correlation among parameters is between the fall in Mask Pressure (ESB) and the Inhalation flow (ISB); flow being a parameter derived from pressures. When inhalation commences, the Mask Pressure decreases, and so does the pressure in the line supplying the air. These two signals represent the same process (Figure 4.3).

To bring these two pressure signals to the same scale, their rate of change is used, as a sharp inhale would display both as a change in mask pressure and flow. Matlab's Alignsignals function from the Signal Processing Toolbox aligns the instantaneous Delta Mask Pressure (iDMP) from the ESB and Delta Line Pressure (DLP) and outputs an offset, which then are applied to all the channels of the sensor blocks. The rise and fall of the aligned iDMP and DLP signals are shown in Figure 4.4.

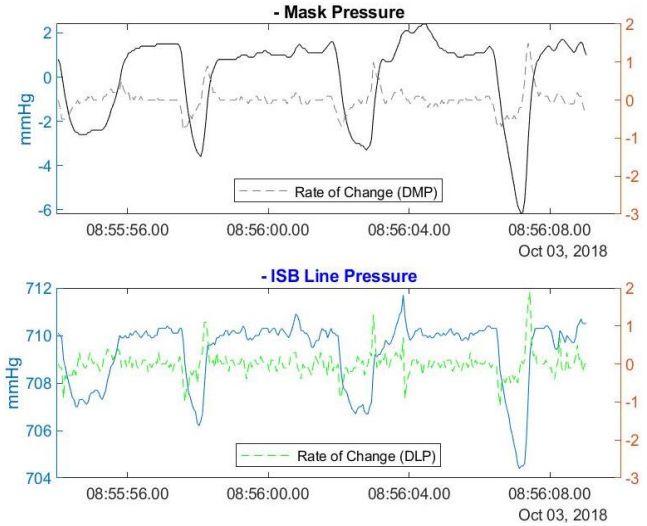

Figure 4.3. Mask Pressure and Inhale Supply Line Pressure
Mask pressure and inhale supply line pressure are synchronous channels, which unite the ISB and ESB instruments through Inhalation.

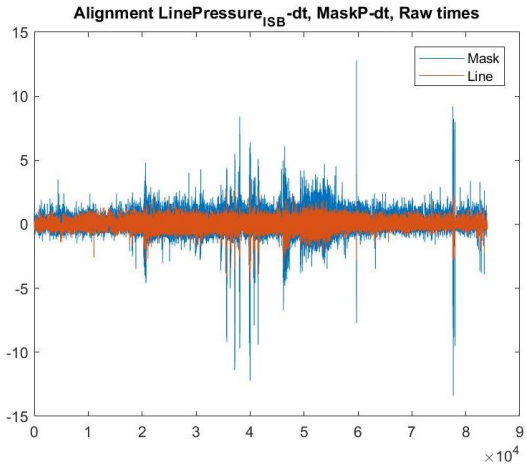

Figure 4.4. The Rate of Change (dt) Derived Parameter of Each Key Channel
The rate of change (dt) derived parameter of each of the key channels creates a sharp feature in the signals at the start of each inhale and brings one absolute and one differential signal onto the same scale for correlation.

4.1.3 Aircraft Data

Pilot breathing is affected by the aircraft, ambient pressures and maneuvers. Therefore, to study cause and effect, it is important to link pilot breathing to aircraft dynamics. Through the 2 phases of the PBA several types of aircraft were used (F-15 and five F/A-18 legacy LOX aircrafts, single and dual seat), 16 key parameters which were commonly available to all were selected (Table 4.1).

Table 4.1. Lists Aircraft Channels Available through Auxiliary Instrumentation (20 Hz)

Aircraft Parameters		
Label	**Description**	**Unit**
TIME	UTC Time given in POSIX format, with a 10E-6 second precision	HH:mm:ss.00
INBIALT	INS BARO Inertial Altitude	ft
INLNACC	INS Longitudinal Acceleration	ft/s^2
INLTACC	INS Lateral Acceleration	ft/s^2
INNMACC	Aircraft Normal acceleration	ft/s^2
INPITCH	Pitch (torque movement around the cross axis)	angle [-90:90]
ADPALT	Pressure Altitude	ft
INVACC	INS Vertical Acceleration	ft/s^2
ENPLA1	Engine Power Lever Angle (1=Left Engine)	angle (1:100)
INLAT	INS Latitude	degree
INLON	INS Longitude	degree
INNVEL	Inertial North Velocity	ft/s
INEVEL	Inertial East Velocity	ft/s
INVVEL	Inertial Vertical Velocity	ft/s
INROLL	Roll (torque movement around the body long axis)	angle [-180:180]
INTHDG	True Heading	degree

A similar signal-alignment technique was used to align the aircraft parameters with the unified ISB/ESB data table, based on 3-axis acceleration derived from both systems. Later in the campaign, courtesy of the USN, a 4^{th} instrument was added made by MadgeTech, at 0.5 Hz, which, in USN configurations, measured the breathing air regulator pressure.

4.1.4 Start and End of Flight

While weight-on-wheels (on the tarmac, not air-borne) baseline breathing is important, the need to separate and characterize in-flight breathing was required, therefore the flight data was further processed to trim the data from take-off to landing. A “weight-on-wheels” parameter would have been useful, but since it was not an instrumented output on all test aircraft, a combination of velocity and pitch angle were used, together with Altitude to extract the flight portion. Later, an “ischange” function was used to find subtler changes differentiating between take-off and climb segments. On certain flight profiles, the PBA scripted a “ground” segment. Breathing recorded during the ground segment serves as an important baseline and comparison between on-the-ground and in-flight metrics.

4.1.5 Data Errors

In all complex systems, there are occurrences of sensor and/or acquisition failures that needed to be identified and corrected before being used for statistical analysis. These failures include intermittent data dropouts (sensor reporting zero), noise/interference (sensor reporting noise), or other sensor (data acquisition losses).

The PBA was rigorous about identifying flights with sensor problems and omitted entire or partial flights as necessary. Prevalent issues were low range in Mask Pressure (+/– 1 mmHg), and extreme values and patterns of (mostly exhale) flow.

The most important data streams for breathing analysis are Mask Pressure from the ESB device and Flows from both Inhalation and Exhalation sensor blocks. The VigilOX instrument converted the differential of two pressures (components are not part of the output) to flow, in real time. There was an expected order to the magnitudes of the two reference pressures. If this order reversed, and it surpasses a pre-determined threshold, it would be equivalent to "Reverse Flow" (e.g., it would appear that there is air pushing in on the exit path). VigilOX by convention does not publish negative flow values, so if this occurs, a value of 0 is reported. Cobham has built in self-diagnosis "bits" which alert the user to warnings and failures during which the validity of these data points should be questioned or discarded. The code that was most prevalent in altering the data was the "DFRL" bit associated with the above described Reverse Flow.
The DFRL BIT is triggered when the flow differential sensor records a pressure magnitude larger than –10 Pascals. It will remain ON until the sensor reads a magnitude smaller than –5 Pascals. In order for this to occur:

1. Gas must be moving backwards through the system at roughly 30 slpm (equivalent to –10 Pascals) when the system is tared (zeroed) at 0 slpm.
2. If the system is incorrectly tared, or the tare drifts during flight, the statement 1 still applies, but the required backward flow decreases.

The system requires 5 non-reverse flow measurements before the warning is cleared. This means the system must measure 5 pressure samples > –5 Pascals. There can be DFRL BITs indicated during some positive flow measurements. Figures 4.5 and 4.6 show examples of flights with Reverse Flow. (Both flights 22 and 46 were removed from the list of approved flights for the final analysis).

The mechanism for reverse flow on the ESB is better understood and it is attributed to humidity (see the pink dots on Figures 4.5 and 4.6). The warning persists for a few samples post the negative-direction flow, which is appropriate, since these initial values post DFRL are not trustworthy (with a constant inhalation flow <50 lpm, it is not humanly possible to maintain an exhale >200 lpm). Note that in Figure 4.6 at 15:00 the ESB flow is irregular, yet the DFRL warning is on the ISB side. For these reasons, flight data with DFRL interwoven throughout have been removed from the modeling and statistical pool. Figure 4.7 is a close-up of a segment containing "DFRL" error/warning code.

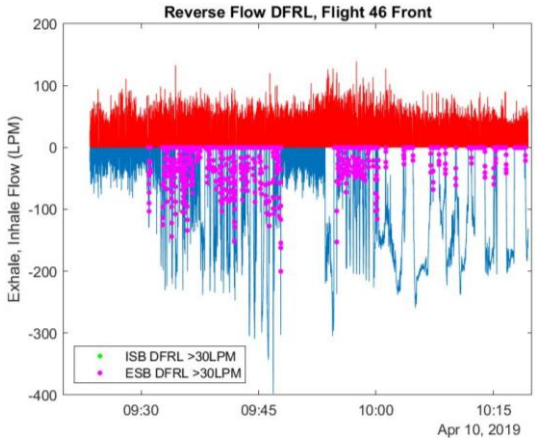

Figure 4.5. Examples of DFRL Reverse Flow Error Bits Flight 46

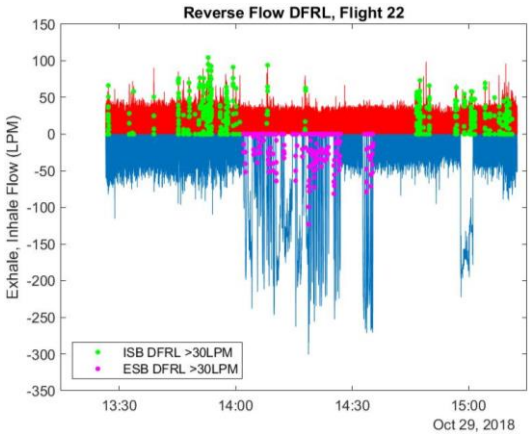

Figure 4.6. Example of DFRL Reverse Flow Error Bits Flight 22

Magenta dots on the exhalation block side, and green dots over the Inhalation block. The reverse flow, possibly induced by moisture, manifests at times in unrealistic amplitudes. Note, ESB flow (blue) is also reported positive, and it is only plotted negative for visual separation.

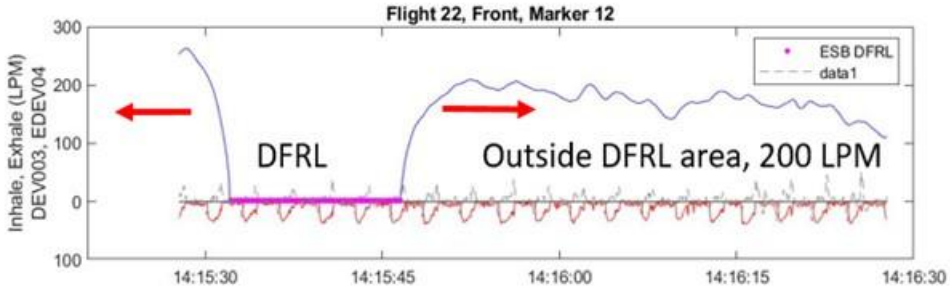

Figure 4.7. Close-Up of Segment Containing "DFRL" Error/Warning Code
The red line is the Inhalation flow, and the blue is exhalation. Erroneous output in the ESB flow exist outside of the Magenta dots where DFRL was reported.

The significance of Figure 4.7 is that removing the section marked by DFRL is not sufficient. As shown, before and after the DFRL bit, the blue exhalation flow line does not complete the red line as a sinusoidal flow, but presents an unrealistic 280 liters per minute, also not in line with the mask pressure rate-of-change (data1). As the PBA shared this finding with Cobham and USN analysts working on validating the Cobham instrument suite, this was attributed to condensed moisture in the hose. By mid-campaign, the USN devised a design-to-print simple aperture to catch the moisture, and dramatically reduce otherwise unusable DFRL occurrences.

Other data issues included Mask pressure lower than the valid range or shifted away from the 0–3 mmHg axis. For this reason, a Flight Health Check quad tile was developed (Figure 4.8).

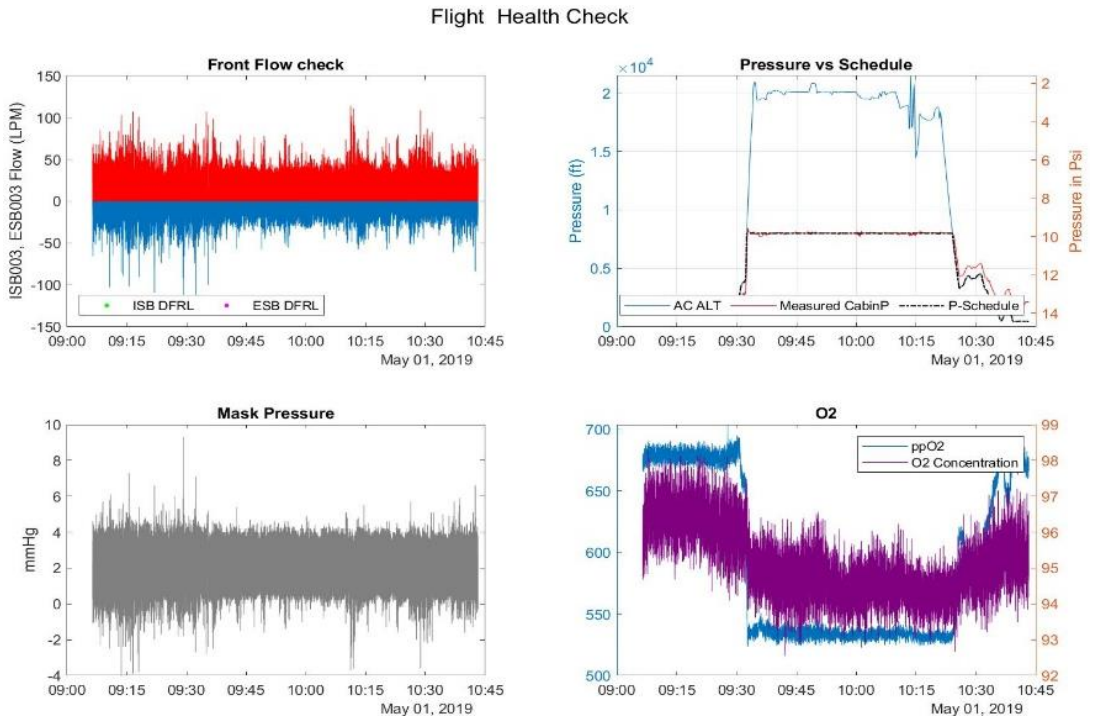

Figure 4.8. Flight Health Check
In clockwise order, tile 1 checks for flow extrema, as well as DFRL. Tile 2 shows if there were deviations from the cabin pressure schedule. Tile 3 confirms if the Mask Pressure is within the expected range. The O_2 concentration's range is verified in Tile 4.

The Health Check plot tiles 1, 3 and 4 are from the VigilOX, while Tile 2 is from the aircraft instrumentation. Thus, the health check plot tells analysts at a glance if data from 3 sensors is nominal to approve the flight for further analysis. Secondly, if the data is nominal, it reveals areas of extrema to zoom in on during the investigation.

4.1.6 Data Accuracy

It was not within the PBA scope to validate the VigilOX instrument. However, to understand pilot breathing, the volume output (lpm) to calculate Tidal Volume and Minute Ventilation is often integrated. The integral of the inhaled flow compared to the exhalation flow for the same unit period are not in synch. This finding prompted a PBA analyst to carry out a laboratory test in which 3 liters of air was pumped through the VigilOX ISB. This was done repeatedly with different velocities, resulting in a range of Peak Flow (lpm) values (recorded on the X-axis of Figure 4.9). When all flow data points are integrated, the expected result should have equaled 3 liters, as the input volume was controlled by a metered syringe.

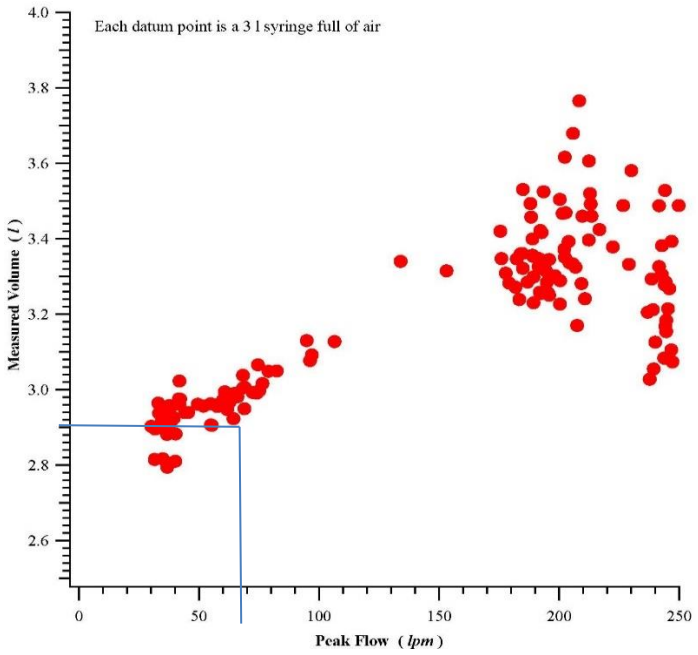

Figure 4.9. VigilOX ISB004 Flow Test Shows Positive Increasing Bias with Increasing Peak Flow Rates, Relative to 3L Input

The test results are illustrated in Figure 4.9 and reveal that between 50–80 lpm, the integral validates close to the 3L volume pushed through. At 200–250 lpm, two items are evident. First, the bias in measured volume is almost linearly increases with increasing peak flow, yielding 3.8 liters post integration, instead of 3L. Second, the standard deviation is much greater in this area, integrals ranging from 3 to 3.8 liters. The standard deviation is much greater in this area, integrals ranging from 3 to 3.8 liters. To put these results in perspective, non-aerobatic breathing mean peak flows are in the 50 lpm range, where the integrals are valid. Aerobatic breathing has been recorded around 100 lpm, while "max inhalations" reach over 200 lpm. As a result, the PBA will use in its findings timing and trends of inhalation/exhalation flow, rather than relying on absolute values of flow integrals in the high flow rate regions.

Table 4.2. Cobham-Provided Offsets Measured at Higher 360 lpm Rate
The ISB004 offset is proportional to the NASA finding.

ISB/ESB FlowLPM offsets measured by Cobham			
ISB001 (1.04)	4.8	ESB001 (1.04)	–8.1
ISB002 (1.01)	10.6	ESB002 (1.01)	–3.0
ISB003 (1.04)	4.4	ESB003 (1.04)	0.7
ISB004 (1.04)	1.2	ESB004 (1.04)	13.1

4.2 Event Markers (repeatable per profile) and Flight Segments

The VigilOX suite has the option to manually mark the time. This was intended for time synchronization, but the PBA added the extra functionality of marking key maneuvers (start, end, or unexpected event). The Event Marker codeword is embedded in the data, while Event Descriptions from flight cards are incorporated post flight. Having the event marks and descriptions greatly helped analysts to compare like segments of flights, and also helped in segmentation for compiling the Almanac of pilot breathing metrics during various ascent and descent types, high-G maneuvers etc. (See Section 11 for the Pilot Breathing Almanac).

4.3 Data Products

4.3.1 "Breath-slicing Algorithm"

BPM is an important metric, and analysts used a Signal Processing Toolbox to mark the location and peak amplitude of breaths. Figure 4.10 shows a noisy floor from a 1st generation instrument, an effect which was filtered out in the 2nd generation but caused other small rounding effects.

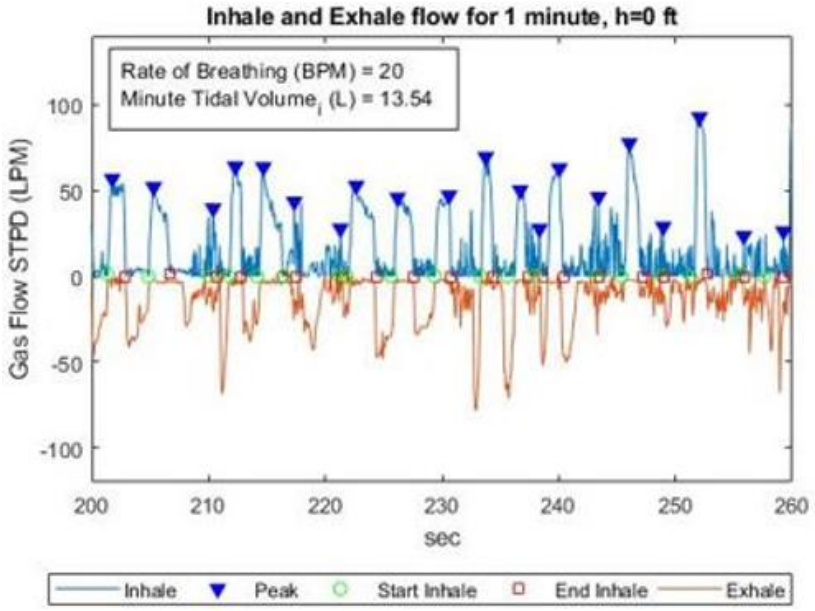

Figure 4.10. The Signal Processing Toolbox Correctly Identifies Peaks for Breath per Minute Calculation

Matlab detects the minimums nearest to the peaks, which could be used as marks of the beginning and end of inhale and exhale. Due to noise or filtering effects, a more reliable method is presented, by correlating two channels: the mask pressure change, and the flow of breath. Instances when both channels undergo maximum change, define the start and end points of integration under the flow curve for the breath volume. To illustrate the technique, the mask pressure and the resulting flow rate are overlapped in Figure 4.11. Under high flow rates, (change of tube diameters or branching), the flow is considered turbulent and governed by the squared law (J. Nunn, *Nunn's applied respiratory physiology*).

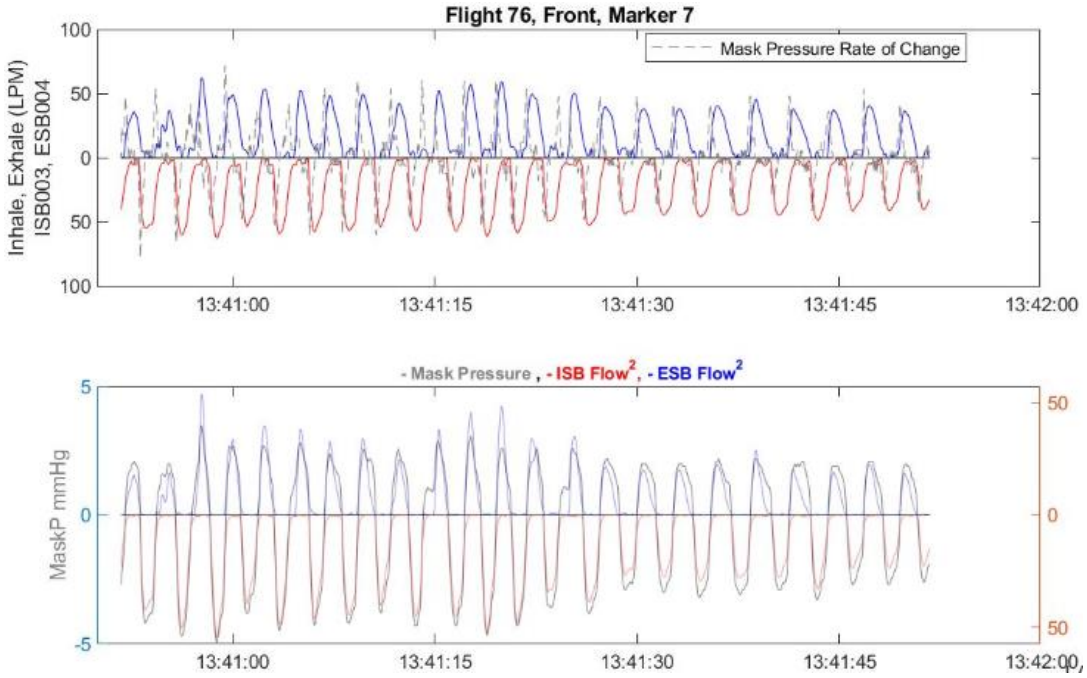

Figure 4.11. In Turbulent Flow Driving Pressure is Proportional to Square of Gas Flow Rate The inhalation/exhalation flow rates are perfectly aligned with the driving pressure.

The start of the draw-down of the pressure overlaps with the start of the flow (Figure 4.12). By using the mask pressure as demarcation, it is known from physiology that the drop-in pressure (negative mask pressure) ties in with the inhalation and inhalation flow, while positive mask pressure correlates to the exhalation flow.

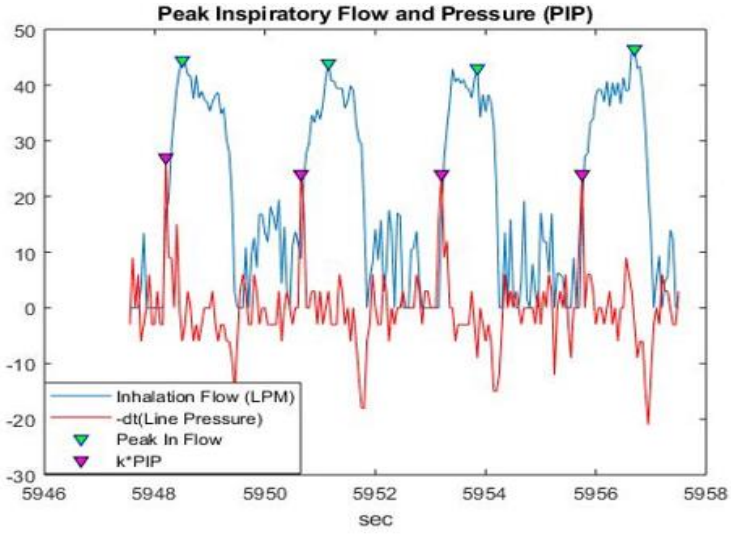

Figure 4.12. Peak Inspiratory Pressure (PIP) Marks Start of Inhalation Flow for Alignment

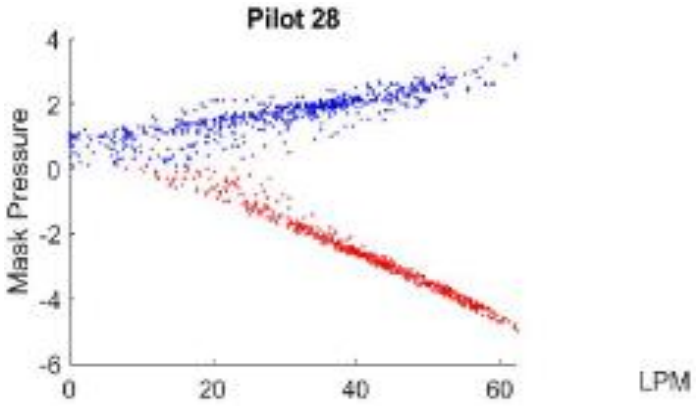

Figure 4.13. Modified "Trumpet Curve" Relating Mask Pressure and Inhalation and Exhalation Flow Rate
Shown are 1200 data pairs from 20 Hz, 1-minute data.

Relating the peak mask pressure to peak flow produces another important metric often referred to as the trumpet curve (Figure 4.13). The expected Liters-per-minute flow, per mask pressure is prescribed in an important document that serves as a guideline, the MIL-STD 3050. In the 1-minute data tile visualization product in Section 4.3.2, all pairs of pressure and flow data are plotted, not just the peaks.

4.3.2 Data Visualization

The PBA has identified the importance of systems interactions when studying pilot breathing. The pilots do not breathe in a bubble, but their breathing is affected by G's, AOA angles, pressure changes and other parameters. It is necessary to create a snapshot of all these interactions. Because pilots breathe an average of 18–20 BPM, 1-minute intervals are ideal for a window of analysis. The analysis was started with 9 individual tiles describing the same 1-minute window, which ended up as 7 tiles by extending the tiles depicting the inhale/exhalation flows and mask pressure, for easier visualization (Figure 4.14). The PBA heavily utilized the VigilOX sensor's capability to create a digital marker actuated by the push of a button by the user. Since NASA was using scripted flights with 20 to 40 events per profile, the analysts were able the zoom in on specific events of interest. Shown above is a 360-degree turn with high velocity and a sustained 3 G's.

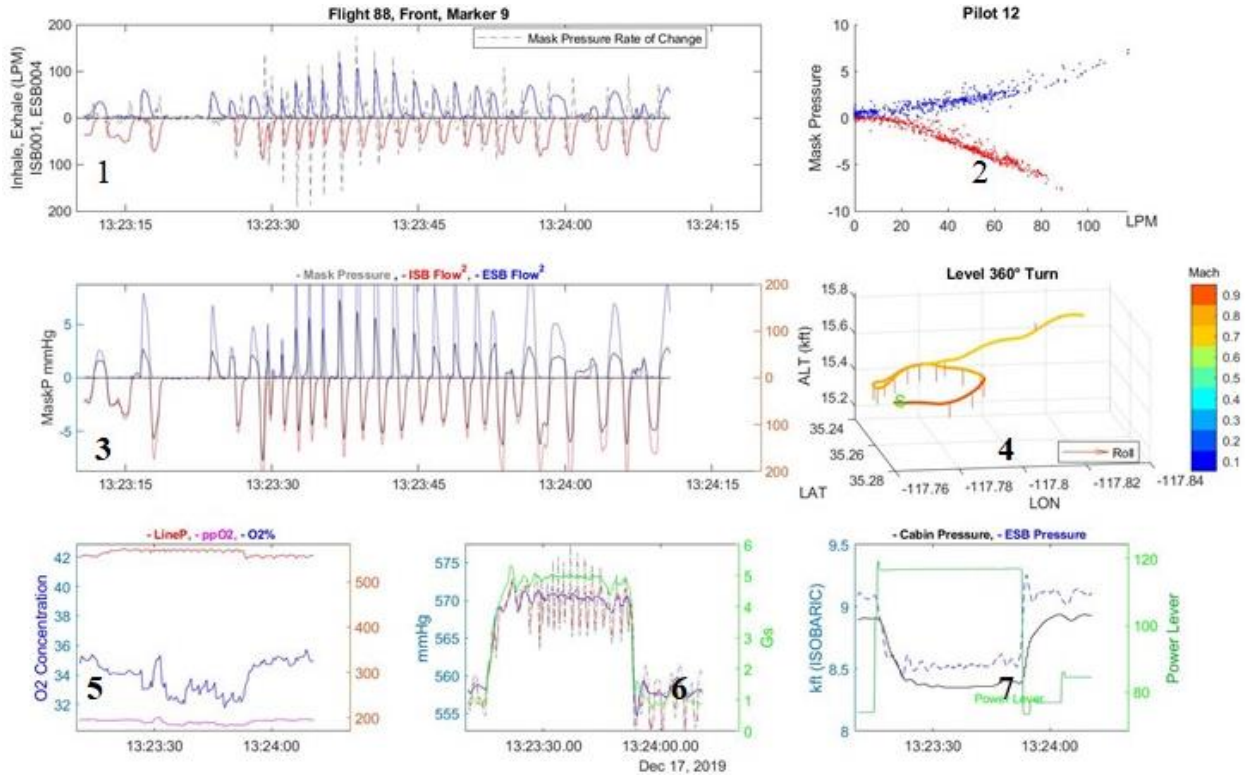

Figure 4.14. at-a-glance representation of 1 minute of 20-Hz flight data, Aligned to show correlations between aircraft dynamics and breathing parameters. Numbered Tiles, 1 through 7 are shown.

Tile 1 in Figure 4.14 plots the inhalation flow (red) and the exhalation flow (blue), with gray dashed lines marking the rate-of-change of the mask pressure (iDMP). The last parameter proved useful to correctly mark the start of each breathing segment, as well as the pressure demand and flow return relationship. Note that the last 5 breaths were taken with forces below 2 G's at a much slower pace (5 breaths in 15 seconds) amounting to 20 BPM, while during the 5 G portion, the rate of breathing increased to 15 breaths in 30 seconds, or 30 BPM. Also, there was much faster initial exhalation in the 5 G period (higher gray bars in Tile 1, compared to the flow rate).

Tile 2 displays a pressure-flow diagram, a variation of a graph referred to as a "trumpet curve." The difficulty or effort required by the pilot can be judged by the slope of the inhalation (red) and exhalation (blue). The MIL-STD-3050 document with design criteria standards for Aircraft Crew Breathing Systems (published 2015, under revision in 2019) prescribes mask pressure minimums, maximums and swings for given peak flow rates. Interpolating these values, for systems without safety pressure 50 lpm should be drawn with a –2-mmHg mask pressure excursion. The team data is out of bounds at this point, showing a driving pressure of –3.5 mmHg, translating to a higher effort.

Tile 3 overlays the driving mask pressure signal and the resulting inhale and exhalation flows. As mask pressure (grey) draws down into the negative domain, the inhalation cycle takes place, and the positive mask pressure lines up with the exhalation. For this reason, the inhalation flow rate is drawn inverted, below the Mask Pressure base line. The mask base line is 0 mmHg for a no-positive pressure system, and 3 mmHg for a positive pressure system. The level of correlation

between mask pressure (grey) and flow squared were examined, appropriate for turbulent flow. Areas where the curves do not overlap are indicative of greater resistance.

Tile 4 creates a grid based on Latitude and Longitude and represents altitude and velocity/Mach changes in 3D, which correlate back to changes in breathing patterns. The vertical heat bar in version one of this product was based on INS velocity, and changed to a Mach scale, as more conversions were necessary for the Mach level, and the high Mach region is an area of interest. In this case the turn involved medium-high roll angles, which are plotted as whiskers mimicking the aircraft wings. Longer the whisker, greater the roll.

Tile 5 shows the two collected parameters, ISB Line pressure and ppO_2, from which O_2 concentration is calculated. O_2 concentration is of key interest in the diluter demand configuration. In this case it can be seen that a 4% drop in O_2 concentration (within requirement) occurred, solely because the pressure changes due to dynamic maneuvering.

Tile 6 shows both ISB and ESB line pressures changing together. This illustrates that the change is affecting both inhale and exhale simultaneously, and therefore is a global change in the cabin. In this plot, the pressure change is 15 mmHg, while in Isobaric region. Also, the 3-axis G's were plotted, showing the maneuver in this example reaching 5 G's. Note the near perfect overlay of the G's signal with the increased pressure curves.

Tile 7 provides the explanation for the pressure signature in Tile 6. The G value increased from 1 to 5, as soon as the craft started banking. Note the velocity remains close to the same. Also, the altitude change is not significant ("level turn"), and the craft is in the isobaric region, yet the Cabin Pressure changes in accordance with the G's. The hypothesis is that the F/A-18s pressure reference is located in the Nose Wheel Well (NWW), where higher pressures are experienced under dynamic conditions (change of AOA, G's, etc.), and the plane's pressure scheduling is affected accordingly. Boeing in a separate study had identified the governing factors to be ambient pressure, Mach number and AOA; G's were not mentioned in this preliminary study, but they are a resultant of one or more of the independent parameters and/or their derivatives.

In version 2 of the Tile product, the Power Lever Angle was added, as pressure changes or oscillations later were tied to this parameter.

4.3.3 Inhale Volume Histogram

Inhale volume is an important physiological parameter, which is varied in a dynamic flight, such as in Profile B. The volume is calculated by integrating the Flow Rate parameter (FlowLPM). This is a useful tool for inter-pilot breathing comparisons, comparisons between positive-pressure supply and no-positive pressure systems, and the range of breath volumes shows the dynamic range of a flight. The Inhale Volume can be displayed on a timeline, or as a histogram (Figure 4.15).

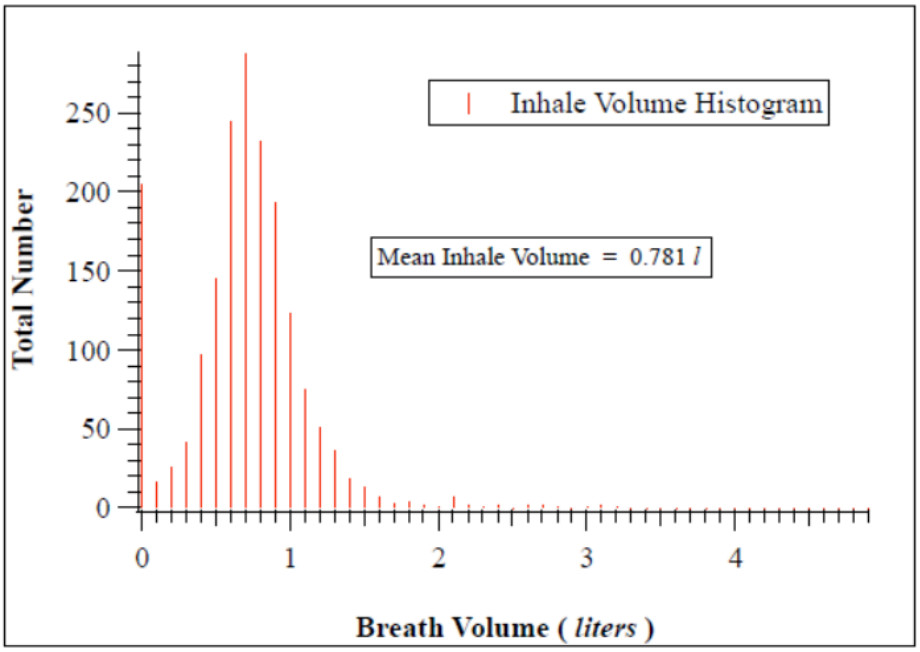

Figure 4.15. Example Flight 59, Profile B; Majority of Inhale Volumes range from 0.25L to 1.5 L with a mean of 0.78 L. The histogram is symmetric, which indicates no unusual resistance during the deeper breaths.

4.3.4 Inhalation Time

Another important metric is the inhalation time, or rather the inhalation over the full breath time. The inspiratory expiratory ratio (I:E) at rest is usually about 1:2, meaning that one exhales more slowly than inhales. This ratio drops toward 1:1, however, with exertion. This makes the Inhalation/Total Breath time ratio 1/3 at rest, and closer to ½ during exertion. Figure 4.16 shows results from a dynamic flight profile.

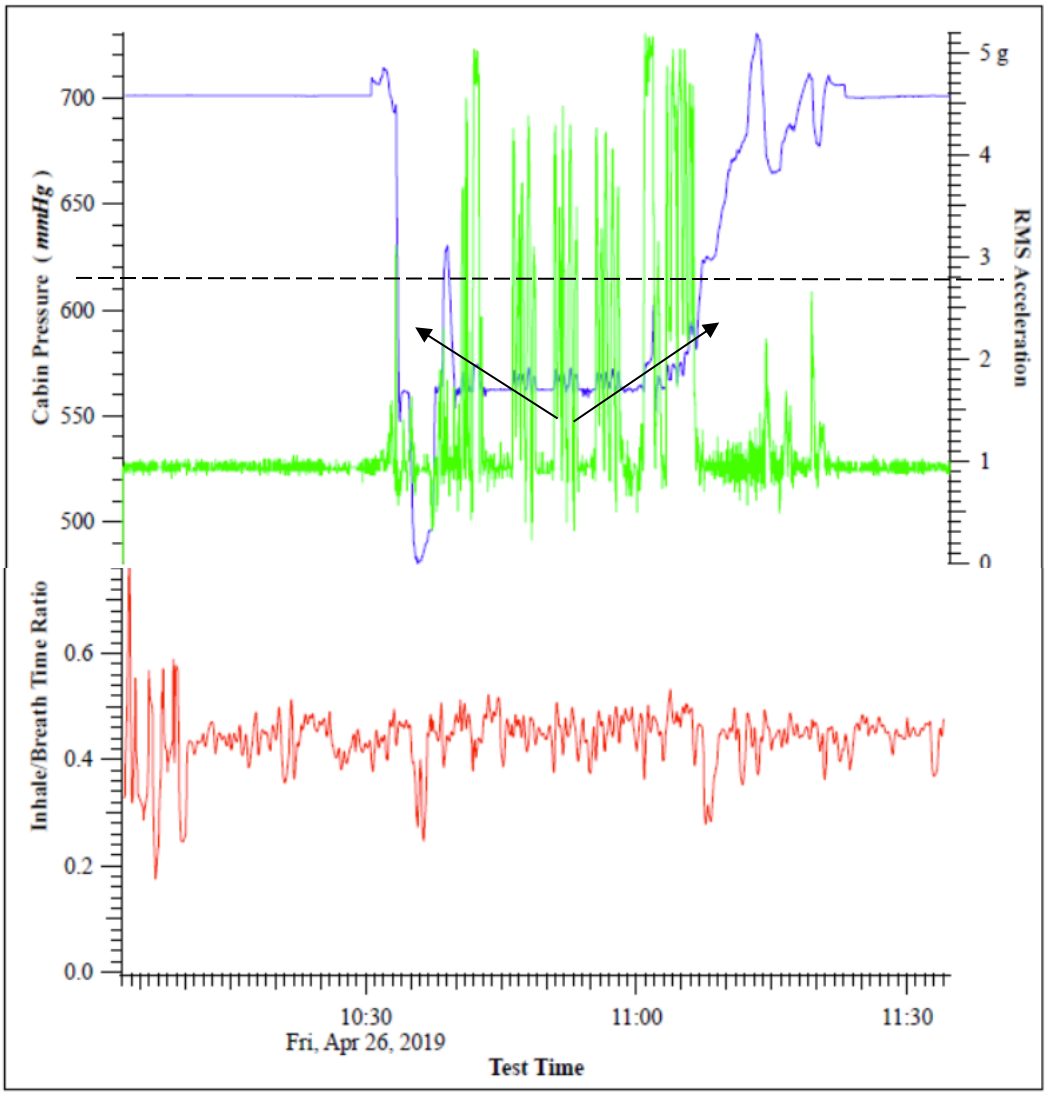

Figure 4.16. Profile B Example; Two "Restful Breathing" Times Line Up with Recovery Periods from "Combat Descent" After Series of High-G Maneuvers

4.3.5 Hysteresis

During open-air breathing, the lung creates a demand, reducing pressure that results in inhalation flow. The flow responds instantly, independent of when in the breath cycle it occurs, and is directly proportional to the demand (lung-ambient pressure differential).

Ideal pilot breathing (through a mask and air supply), should strive to be similar – a demand from the lung should result instantly in a proportional flow from the regulator, independent of when it occurs during the breath cycle. In such a case, Pilot and Supply are 'in sync'.

- ***Data*** show that ideal pilot breathing is seldom achieved
    - Early in inhale demand exceeds supply
    - Later in inhale supply exceeds demand
    - Pilot and Supply are 'out of sync'
    - The difference between the two at the breath mid-pressure is *defined* as the ***Hysteresis***

Figures 4.17 and 4.18 plot the Inhale flow as a function of line-cabin differential pressure for a single inhale breath per graph, with the hysteresis represented by the magnitude of the blue arrows.

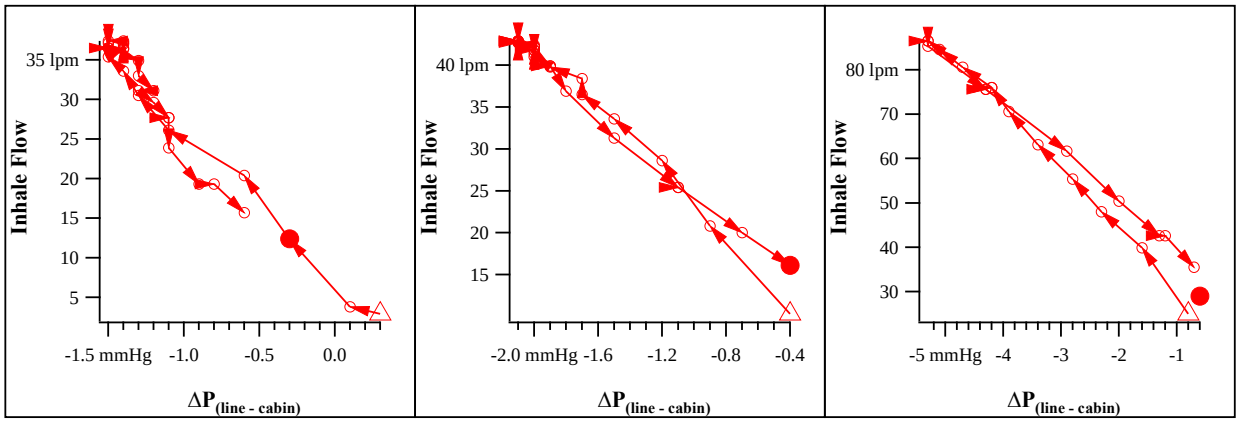

Figure 4.17. Three Consecutive Breaths with almost No Hysteresis (USAF configuration, FLT-058)

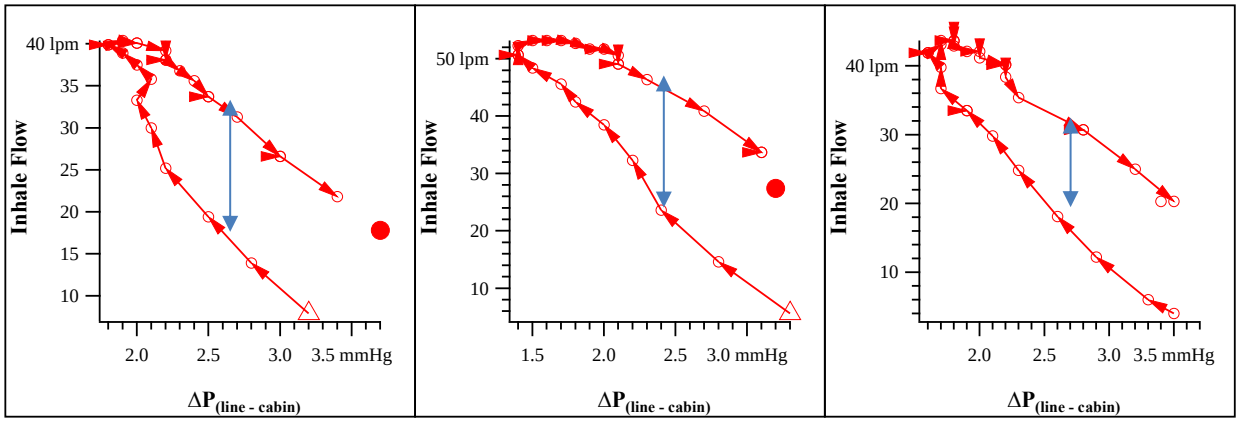

Figure 4.18. Three Consecutive Breaths with Moderate Hysteresis (USN configuration, FLT-045) The hysteresis is the difference in flow as indicated by the arrows are 0.25, 0.42 and 0.23 lps (converting from lpm to lps), respectively, at the mid-point pressure in the breath (halfway between the minimum and maximum pressure).

The hysteresis is calculated for each breath during a test and expressed in lps. For each flight, it can be seen how the hysteresis is distributed (Figure 4.19).

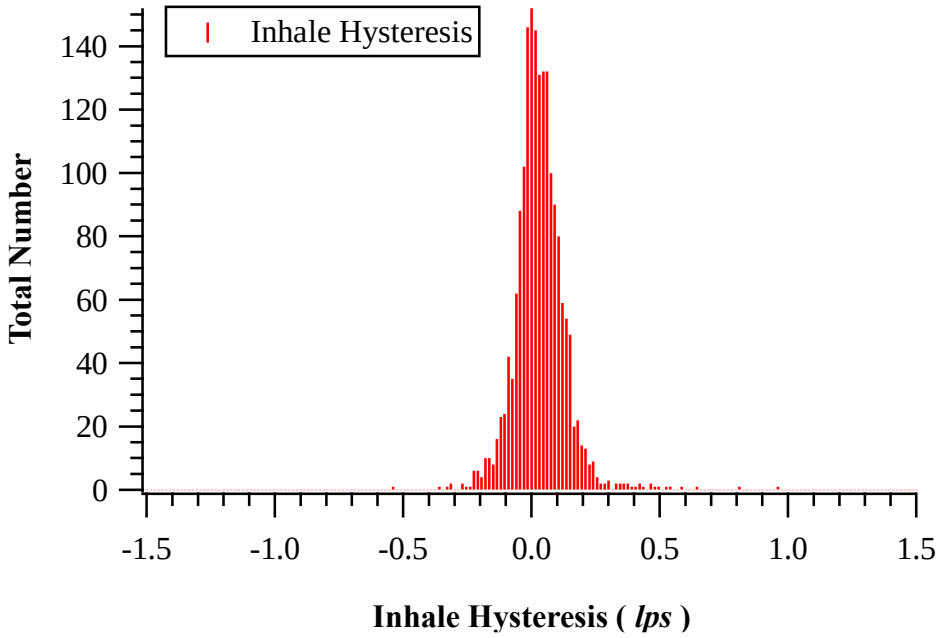

Figure 4.19. Hysteresis Histogram for PBA FLT-059 in USAF Configuration
Values close to 0 are ideal. Low negative values in this example are due to noise, while high negative values are a possibility and a concern when supply and demand are not in synch.

4.3.6 Breath Effort

The calculation of the breath effort is the work required to move gas in and out of the lungs. The breath effort ε of the j^{th} breath is calculated as:

$$\varepsilon^{j} = \int_{\tau_s^j}^{\tau_f^j} (MP)\ dV_i^j$$

(Formula 4.1)

The integral is over the cumulative volume of the breath, given as $V^{j} = \int_{\tau_s^j}^{\tau_f^j} \dot{V}(t)dt$.

(Formula 4.2)

The integration occurs from the start to end of the inhale (or exhale). The value at the end of the breath is the tidal volume (Tv). For a visual representation, see Figure 4.20. In the breath portrayed, the calculated effort is 5.62 mJ. While this is not comparable to other studies detailed measurements of work-of-breathing as an absolute value, it is a great tool to compare breath effort for different pilots, with different air supply systems, and in varying dynamic conditions.

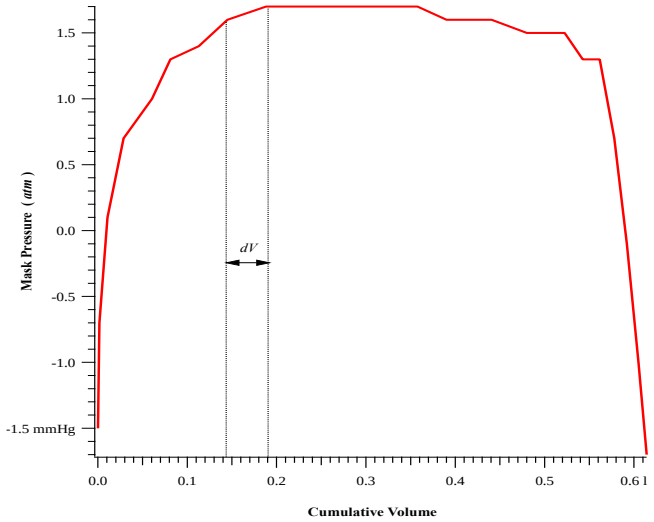

Figure 4.20. Area Under Curve Represents Effort of Breathing in an Ideal Case
The effort of inhale in this case, following formula 5.1, is 5.62 mJ.

4.3.7 Phase Shift

In open-air breathing, exhalation is reflexive. During exhalation through a mask though, flow is expected to lag behind pressure due to exhalation valve cracking-pressure and finite valve resistance. Pressure-Flow Disharmony is a mismatch between the pressure profile and the flow profile, including start/stop and time it takes to reach the peak.

In the Figure 4.21 example, a **mismatch** between the grey Mask Pressure and the blue ESB (Exhalation) Flow^2 is shown. Pilots often report difficulty exhaling in certain systems. Quantifying the driving pressure-resulting flow disharmony over a flight can be a metric of the pilot-system interaction (the system's ability to supply the pilot with the *volume* of air needed, *when* needed), and on a larger scale can characterize differences between air delivery systems applied by services on different aircraft.

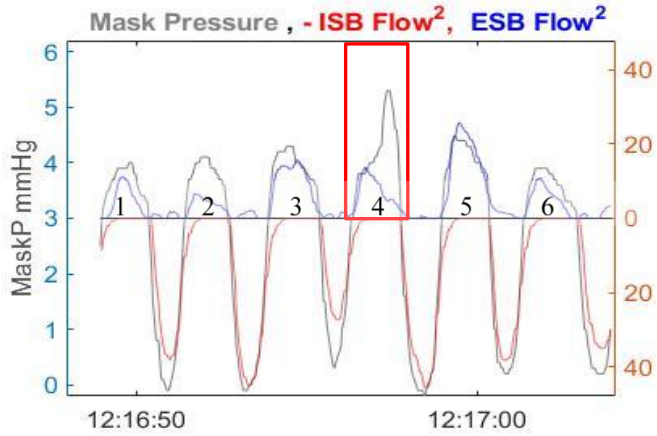

Figure 4.21. Example of Mismatch Between Mask Pressure and ESB (Exhalation) Flow
Exhalation Pressure and Flow are in the top half of the graph. In exhales 1, 3, 5 and 6, the flow responds appropriately to the driving pressure; the grey and blue lines nearly overlap, as they should. In exhale #4 the pressure and flow start out the same, but the mask pressure peaks at the end, as flow trends down, resulting in a mismatch. The line at 3 mmHg represents the positive pressure provided.

To illustrate the concept, exhale breaths #4 and #5 from Figure 4.21 are enlarged and shown in Figure 4.22.

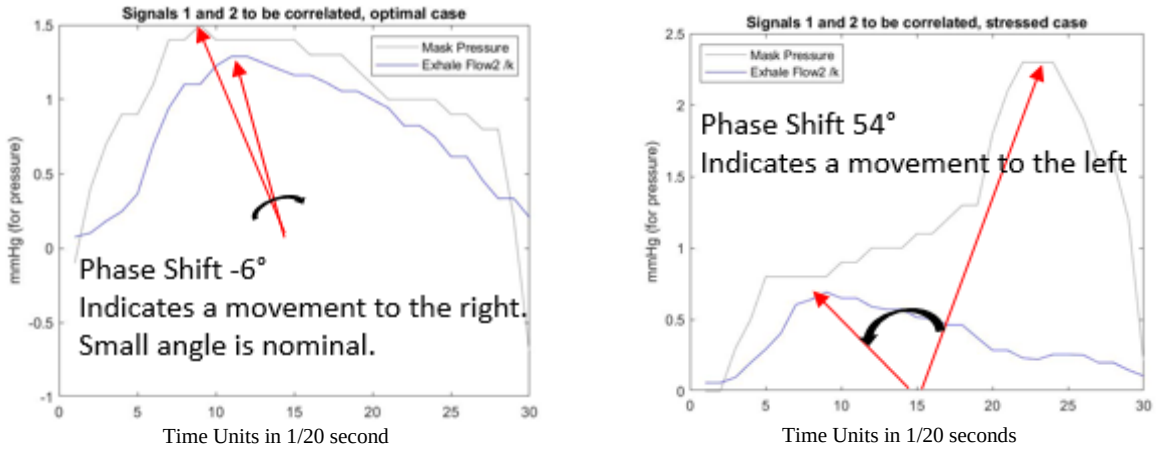

(a) Nominal Exhale #5 ***(b) A Pressure-Flow Mismatch Found in Exhale #4***

Figure 4.22. Exhale Breaths #4 and #5 from Figure 4.21

- Negative phase shifts (Figure 4.22a) are the result of pressure leading flow
- The smaller the lag, the more ideal the system. (Small negative numbers are expected)
- The larger the lag, the more resistance in the system (e.g., when a valve is sticky or "slow to open"), the pressure builds up, the valve opens with a delay, then flow peaks
- Positive phase shifts (Figure 4.22b), indicate a reverse order of flow peaking before the pressure peaks $T_{\text{Peak Pressure}} - T_{\text{Peak Flow}} > 0$
- This happens when the exhalation flow is pinched off. As a result, flow cannot exit, and pressure rises
- Imagine a valve that closes too early, pinching off flow (e.g., due to safety pressure in the compensation valve)

Both of these sensations are experienced regularly in mask breathing, and pilots adjust to small phase shifts routinely.

4.3.7.1 Metrics

The PBA devised 3 metrics to characterize Pressure-Flow Mismatch, using the industry-validated Matlab Signal Processing Toolbox.

1. Shift in Time. This can be a + or – time lag. The VigilOX instrument used in this experiment has a 1/20 second output rate, thus given the physics and the instrument, a "0" or (–1) in this category is good mark.
2. Phase Shift in degrees. This builds on the Shift in Time and takes in consideration the length of the exhale. Since breath time varies every breath, each breath is normalized by its length such that the breath length equals 180°, giving a metric independent of those constantly varying times. A 20 Hz sample rate means that if the optimal alignment is off by one sample, there will be a phase shift of around 6° (depending on the breath time). A "0" or (–6) for this metric is a good mark. This is the single most meaningful metric.
3. Normalized Correlation (R). Compares paired points of the signals. This characterizes how the ***shape*** of the pressure and flow of the *entire* exhale (not just the timing) compare. The output is [0, 1], 1 being a perfect match. Table 4.3 lists the numerical results from the six exhales in Figure 4.22b.

Table 4.3. Metrics calculated on the Exhale Data from Figure 4.22b
These metrics give numerical meaning to the perceived pressure-flow timing, phase and correlation mismatch. This is highlighted in red, in row 4. A nominal example is in green, in row 5.

Nr	Exhale Starts	Exhale Stops	Shift in Time 1/20 s	Phase Shift Degree	Correlation Normalized
1	'12:16:49.03'	'12:16:50.33'	0	0.00	0.922
2	'12:16:51.44'	'12:16:52.63'	0	0.00	0.979
3	'12:16:53.89'	'12:16:55.33'	–1	–6.00	0.975
4	'12:16:56.39'	'12:16:57.74'	9	57.86	0.759
5	'12:16:58.99'	'12:17:00.33'	–1	–6.43	0.979
6	'12:17:01.44'	'12:17:02.89'	0	0.00	0.980

Histograms display the phase shift distribution for an entire sortie (Figure 4.23).

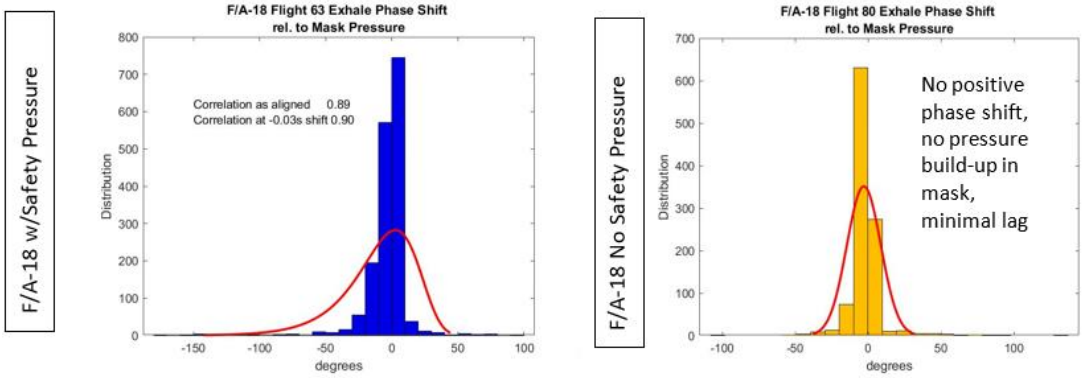

Figure 4.23. Histograms Displaying Phase Shift Distribution for an Entire Sortie
Shows greater negative phase shifts (delayed response) during exhalation for the positive pressure setup (left), than the F/A-18 flown with no positive pressure supply (right).

The same method is applied to the inhale process, and Inhale Histograms are in Figure 4.24.

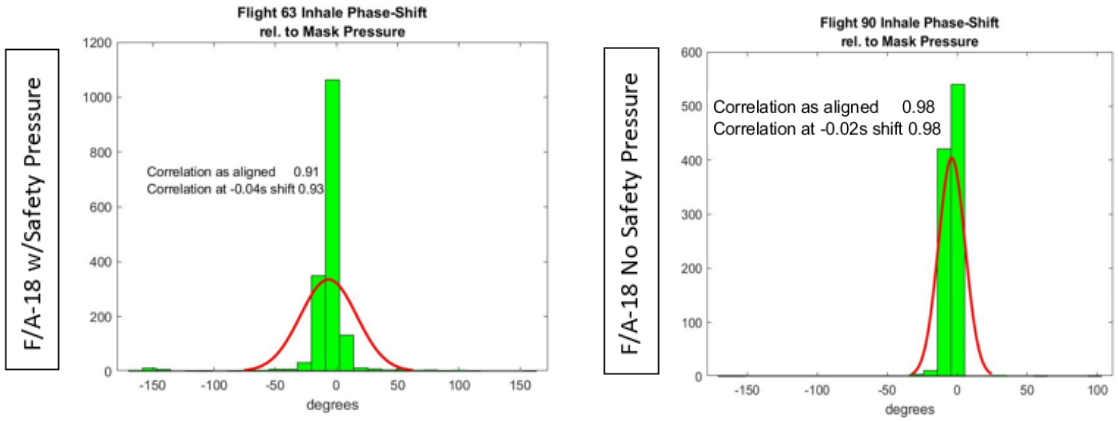

Figure 4.24. F/A-18 USAF Configuration Inhale Histograms
The F/A-18 USAF configuration without Safety Pressure (NOSP, right) shows an unencumbered inhale profile, while on the left, 30% of inhales show phase lags of 10°–20° with the F/A-18 legacy USN configuration with Safety Pressure (SP, left). Note the near-perfect 98% correlation achieved with NOSP.

A 98% correlation means that inhaling on that particular flight with the mask was nearly as effortless as breathing in open air. The correlation as flown on the left is 91%. The algorithm finds the shift for optimum alignment between driving-pressure and flow and calculates the

hypothetical outcome. A score of 93% means, that even if it could adjust the time response, the shape of inhales is still slightly off, resulting in a lower number than on the right. These two examples are both "good" flights. In some, correlations in the 70–80% range, or even lower in other aircraft can be seen.

4.3.8 Development of empirical 1-minute data from the aligned dataset

Summary Statistics were calculated on 1-minute data segments on sensor provided channels and derived parameters and were tabulated for all approved flights. See section 4 for an in-depth discussion.

4.4 Summary

The PBA made every effort to ensure the highest scientific standards for the ensuing analysis and findings, and therefore imposed stringent requirements on data selection.

Data Selection Requirements
Common Data set to serve various analyses, machine learning, STATs, 1-minute data
Complete data set: ISB, ESB, Aircraft data
Healthy Data Set (Remove flights with ESB DFRL, Bad or no Mask Pressure)
Minimum 50 minutes of flight time
This is necessary for
Quality of the data set
Accuracy of the analysis output
High confidence/ low error
Unified voice and results

Table 4.4 shows the PBA data set with the breakdown of scripted profiles flown. Though 115 sorties were flown, 87 were used to support a variety of analyses as discussed in Section 1.19 and presented in subsequent Technical Sections of this report. Sixty-five were down-selected to develop a common database for detailed engineering analyses and machine learning. Fifty sorties were used for the 1-minute summary statistics presented in Technical Section 5. In addition, five of these flights provided front-seat/aft-seat dual data streams. During flight testing, PBA also encountered aircraft system- or flight breathing- irregularities that were of special interest. These sorties provided additional learning opportunities to explore pilot breathing in special "off-nominal" cases. In Table 4.4, these are listed under Special Demonstrations and presented in Technical Section 6. In some cases, these flights had fewer requirements (only the ISB block data intact), thus a total of 17 sorties were made available for these special studies.

Table 4.4. PBA Data Set with Breakdown of Variety of Profiles

Category	Description	Sorties used in PBA Analysis
1	Profiles A, B, C, D	41
2	Profile E, Pressure effects/no pressurization	4
3	Ride-along flights with Aircraft data	5
4	Profiles F	12
5	Profile H, Unified test profile for Pilot Breathing	3
6	Special Demonstrations	17
7	JPL Mask Flights	5
		87

Technical Section 5: Summary Information and Statistical Analyses based on 1-minute Data Compilations

5.0 Introduction

This section details the use of VigilOX and other aircraft data that have been collapsed to 1-min flight blocks to summarize pilot responses and to identify important parameters that influence pilot breathing. There are two technical parts to this section: *1. Summary Statistics and Data Visualization* and *2. Mixed Effects Models*. Both sections depend on a main database comprised of 50 flights of which 5 are backseat pilots with an aggregate of 3275 flight minutes curated for quality and completeness. These have been calculated from the 20-Hz data-streams as described in Technical Sections 3 and 4.

The 1-minute data compilations serve to assess changes in effort of breathing in response to the external environment (the aircraft) and the level of activity required of the pilot. In the following discussions, it is important to always consider that all parameters are linked to some extent. For example, as pilots perform more strenuous activity, they require more O_2 and will respond by breathing more frequently, breathing deeper, and breathing with more force. These parameters are all measurable, and each individually reflects the level of effort on the part of the pilot. Furthermore, external forces from the aircraft breathing system and aircraft maneuvers can influence the breathing parameters as well. As the cockpit pressure is lower with altitude, the pilot requires more airflow at the same concentration of O_2. As the external G-forces increase, the pilot needs to expend more force to move air in and out of the lungs. The stress of complex flight maneuvers can increase the required mental vigilance. In short, there are complex factors that influence the amount of effort required by the pilot simply to breathe and maintain the capability to fly the mission successfully.

The following investigations relate measurable pilot breathing parameters with external aircraft flight effects to determine what activities, conditions, and breathing hardware could push the pilot's physiological response towards higher effort. Ultimately, it is hoped to provide guidance as to how to mitigate the stresses that could lead to pilot discomfort, excessive effort, and fatigue, and distraction.

The first section looks at various pilot parameters individually to assess their distribution, range, and character and link them to physiology. A summary description of the aircraft flight parameters is also provided that were used to elicit pilot responses. The second section relates the pilot breathing responses with the external aircraft parameters using multivariate statistical models to discern the interactions of variables, and to understand the variance components within and between pilots.

5.1 Part 1: Summary Statistics and Data Visualization

The PBA was based on a wide variety of flights designed to explore different pilot/aircraft interactions and implementation/evaluation of sensor systems. In aggregate, there were 104 total flights performed to explore a wide variety of scenarios. From these, 50 flights were selected for developing summary statistics based on the following criteria:

- Real world scenario: flight represents one of five profiles designed to simulate actual military sorties.
- All sensor systems performed properly: no mechanical, electronic, or acquisition losses.

- Flights were at least ~45 minutes long: no flights shortened by weather, air-traffic, or other safety concerns were included.

These data are the most complete and robust for linking pilot parameters to specific aircraft maneuvers. Many other flights were performed wherein scripted activities such cabin pressure dump, mask removal, deep breaths, breath holding, emergency O_2, etc. and different configurations of breathing gear were tested, however these would have skewed the summary statistics.

5.1.1 Summary Statistics: Construction and Evaluation of PBA Variables

The aligned 20-Hz data streams were parsed into 1-min flight segments to facilitate subsequent modeling and calculation of physiological breathing parameters and aircraft parameters. Each individual parameter was expressed as the "within minute" minimum, maximum, average, and standard deviation for each flight minute. Additional hybrid parameters were calculated from the raw data as well.

Certain parameters were developed to quantify pilot breathing; these are designated as the primary PBA dependent variables. Recall from Section 1.4.1 that dependent variables are defined as:

> ***Dependent variables***: continuous measurements and calculations of pilot physiological response parameters, including breathing rates, breath volumes, breath flows, breathing pressure, O_2 usage, etc.

For the purposes of this Technical Section, the focus is on the dependent variables listed below. Note, there are calculations possible to extract additional variables for specific physiological or health-based investigations, however, these six are thought to be the most important.

- Breathing frequency: (BPM)
- Average flow volume (liters/min)
- Maximum flow volume (liters/min)
- Breath volume, mean (liters/breath)
- Differential mask pressure, DMP (mmHg)
- Standard deviation mask pressure std. dev. MP

The first four dependent variables were extracted or calculated from the VigilOX ISB flow sensor; the mask pressure parameters (DMP and std. dev. MP) were extracted from the VigilOX ESB pressure sensor. For convenience, all sensors within ISB and ESB are listed in Table 5.1. Notably, that ESB also has flow and pressure sensors that could also have been used for assessing average flow volume (liters/min), maximum flow volume (liters/min), breathing frequency: (BPM), breath volume, mean (liters/breath), however, the ISB represents more mature technology and was therefore chosen as the source for these parameters.

Calculating 1-min data streams from the 20-Hz raw data was especially important for the dependent variables, as these are generally only used as 1-minute segments in real-world applications. As an example, consider that there are instantaneous measures of inhalation flow; to determine the breathing rate (BR) in BPM, the number of "peaks" of inhalation flow were counted within a specific minute. Similarly, the BR BPM were divided by the average of the inhalation flow in liters/minute within that minute to estimate V_T in liters/breath. DMP was calculated by subtracting the within-minute minimum pressure value from the within-minute

maximum pressure value and st. dev. MP was calculated as the standard deviation of the 20 Hz data within each minute.

Table 5.1. List of ISB and ESB VigilOX Sensors

ISB		ESB
Partial pressure, O_2		Partial pressure, O_2
Inhalation Flow		Exhalation Flow
Cabin pressure		Cabin pressure
Inlet gas temperature		Exhaled gas temperature
Inlet gas pressure		Exhaled gas pressure
Inlet gas humidity		Exhaled gas humidity
Cabin temperature		Cabin temperature
3-axis accelerometer		3-axis accelerometer
		Partial pressure, Exhaled CO_2
		Mask pressure

Table 5.2 shows an excerpt example of the dependent variables for the first 20 flight minutes of Flight #20 with the following metadata (fixed effects):

Date: 10/23/18
Aircraft: F-15
Flight #: 20
Pilot #: 71
Profile: D
Mask: AF/AFRC
Regulator: CRU-98

Each flight's dataset is tagged with these respective metadata for future reference.

Each row in the table represents 1-minute flight time; the column labels are defined as:

UniqueID: n^{th} minute of all PBA flights in sequence for all flight minutes
Group: j^{th} minute of that individual flight
mean_FlowLPM_I: ISB flow sensor values (liters/min) averaged for that minute
max_FlowLPM_I: ISB flow sensor maximum (liters/min) within that minute
Breaths_per_min: Breathing frequency (BPM) within that minute, as counted from ISB flow sensor peaks
Breath_Vol_mean: Average inhaled volume for each breath (liters/breath) as calculated by dividing column "mean_FlowLPM_I" by column "Breaths_per_min" for that minute
DMP: Differential mask pressure (mmHg) calculated by subtracting "Min_maskpress" column from "Max_maskpress" columns of original data within each minute.
st. dev. MP Standard deviation of mask pressure (mmHg) of original data within each minute.

Table 5.2. Example of 1-min Pilot (dependent variables) Data for 20 Minutes of PBA Flight #20 in Units as Described in Text

UniqueID	Group	mean_FlowLPM_I	max_FlowLPM_I	Breaths_per_min	liters/breath	DMP_minute
500	8	22.51	97.6	19	1.185	14
501	9	19.40	102.4	17	1.141	9.8
502	10	20.20	95.7	22	0.918	11.3
503	11	20.66	85.8	22	0.939	9.6
504	12	24.70	106.7	21	1.176	15.6
505	13	22.70	99.2	20	1.135	9
506	14	22.28	106.2	17	1.310	12.9
507	15	22.00	100.2	18	1.222	11.8
508	16	19.90	75.5	18	1.105	9.1
509	17	21.68	99	17	1.275	14
510	18	24.78	104.2	19	1.304	13.1
511	19	22.73	109.9	18	1.263	12.8
512	20	19.93	95.8	17	1.173	8.6
513	21	20.03	97.8	18	1.113	8.7
514	22	22.87	88.3	20	1.144	10.2
515	23	21.00	93.9	18	1.166	11.6
516	24	21.58	114	16	1.349	17.7
517	25	19.43	81.8	18	1.080	9.3
518	26	21.47	80.2	21	1.022	8
519	27	19.52	67.8	18	1.085	7.3
520	28	20.98	95.6	20	1.049	9.9

This is an example of the data structure for a few of the important dependent variables. Many more data-streams (columns) are available from the ISB, ESB and other aircraft sensors and can be used for more detailed analyses as necessary. The complete datasets for all ISB, ESB and aircraft sensors, their minima, maxima, standard deviations, and a variety of other calculations are provided in the Supplemental sections of this report.

Like the dependent (pilot) variables described in the previous section, the analogous 1-min data-streams for the independent (aircraft) variables can be constructed. These are defined as:

> ***Independent variables*:** flight meta-data (pilot#, flight# etc.) and continuous measurements of aircraft parameters, including altitude, speed, acceleration (G-force), cabin pressure, orientation, etc.

The fixed effects variables are later used in the models in Section 5.2, also as "independent". For this section, only with the basic VigilOX and Aircraft MU sensor data-streams associated with a particular flight are used; these have calculated specific useful parameters in the 1-min format to serve as the independent continuous variables.

The primary independent (flight) parameters considered for initial summary statistics are:

G-force vector (G3): Composite G-force vector calculated from VigilOX ISB 3-directional accelerometer in units of G.
Aircraft velocity: Airspeed of aircraft in miles/hour
Aircraft Altitude: Vertical altitude of aircraft as derived from aircraft sensors in feet
Change Altitude: Within minute change in altitude calculated as max-min, in ft.
Cabin altitude: Based on cabin pressure as derived from VigilOX ISB sensor, in mmHg
Change cabin alt.: Within minute change in cabin altitude calculated as max-min, in mmHg

Table 5.3. Example of 1-min Aircraft (independent variables) Data for 20 Minutes of PBA Flight #20 in Units as Described in Text

UniqueID	Group	mean_G3	max_G3	mean_ALT	delta Alt	mean_Velocity	mean_Cabin	delta Cabin
500	8	1.0	1.5	3695	430	712.5	686.8	10.9
501	9	1.0	1.4	3329	790	738.7	695.2	19.3
502	10	1.0	1.5	3476	840	722.0	692.3	19.3
503	11	1.0	1.6	3866	496	724.0	682.1	14.1
504	12	1.3	2.7	4213	818	736.3	676.4	13.5
505	13	1.4	3.5	4271	274	804.5	678.0	10.7
506	14	1.0	1.4	4061	192	841.7	682.9	6.7
507	15	1.5	2.5	4047	368	782.3	682.8	6.4
508	16	1.0	1.5	4493	1638	758.8	670.4	38.0
509	17	1.2	2.2	5618	636	732.3	642.6	13.8
510	18	1.4	3.2	3663	3181	674.4	684.7	69.9
511	19	1.2	2.0	1984	331	699.1	727.1	15.1
512	20	1.0	1.4	2346	316	719.7	718.1	8.8
513	21	1.0	1.5	2147	390	736.6	722.8	9.0
514	22	1.0	1.6	2735	854	791.7	711.3	22.4
515	23	1.1	1.6	3451	580	776.4	692.5	16.1
516	24	1.0	1.4	2781	1324	738.7	705.1	29.8
517	25	1.2	2.1	2413	624	712.4	715.6	18.3
518	26	1.1	2.1	3038	820	727.0	701.1	19.3
519	27	1.0	1.6	3569	266	744.8	687.3	6.3
520	28	1.2	2.3	3814	1140	729.8	682.3	26.7

This is an example of the data structure for a few important independent variables in a format similar to Table 5.2. Many more data-streams are available from the ISB, ESB and other aircraft sensors and can be used for more detailed analyses as necessary in other sections.

5.1.2 Summary Statistics for all Selected PBA Variables

The summary statistics of pilot breathing parameters were calculated for all PBA flights to gain insight into real-world physiological responses and needs under a wide range of flying activities. Below, Table 5.4 shows results for 3,275 flight minutes across 50 PBA flights. These are data summaries based on flights curated to represent "real-world" sorties as selected on the criteria described in Section 5.1; the overall concept for this kind of data interpretation is based on assessing empirical, not distribution-based percentiles (Pleil 2015).

Table 5.4. Summary Statistics Across All Available Flight Data for Selected Dependent (pilot) Variables these are not yet triaged for physiological outliers.

Parameter	units	n	average	s.d.	median	GM	GSD	2.50%	5%	95%	97.5%	99.0%
breath freq.	breaths/min	3275	18.18	4.70	18.00	17.51	1.34	9.00	11.00	26.00	28.00	31.00
flow vol. (mean)	liters/min	3275	18.58	5.32	17.84	17.89	1.32	9.87	11.13	27.35	30.46	35.10
flow vol. (max)	liters/min	3275	78.42	25.65	74.40	74.47	1.38	39.10	42.27	123.2	136.8	152.8
breath vol. (mean)	liters/breath	3275	1.06	0.39	0.98	1.02	1.30	0.68	0.72	1.64	1.82	2.04
DMP min	mmHg	3275	8.10	3.93	7.20	7.45	1.48	3.70	4.20	14.40	16.72	22.45
st. dev. MP	mmHg	3275	1.76	0.44	1.68	1.71	1.27	1.07	1.14	2.59	2.80	3.14

In the ensuing sections, these parameters are each discussed in more detail.

Similarly, the summary statistics were calculated for the independent (aircraft) continuous variables. Table 5.5 is the independent data analog of the previous Table 5.4 for important aircraft parameters.

Table 5.5. Summary Statistics Across All Available Flight Data for Selected Independent (aircraft) Variables

Parameter	units	n	average	s.d.	median	GM	GSD	2.50%	5%	95%	97.5%	99.0%
G3 (mean)	G	3275	1.32	0.58	1.06	1.24	1.38	0.98	0.99	2.73	3.20	3.59
G3 (max)	G	3275	2.04	1.22	1.46	1.76	1.67	1.01	1.02	4.77	5.07	5.21
altitude (mean)	feet	3275	17252	15064	14260	10863	2.79	2278	2419	44338	44444	44816
delta altitude	feet	3275	1638	2766	479	404	7.36	5	9	8469	10046	12213
velocity (mean)	feet/sec	3275	673	202	707	623	1.62	209	263	947	998	1065
cabin press. (mean)	mmHg	3275	576	112	569	563	1.24	377	380	713	719	731
delta cabin press.	mmHg	3275	16.64	20.76	9.60	8.74	3.29	0.90	1.20	59.80	75.68	102.1

In the ensuing sections, these parameters are each discussed in more detail.

5.1.3 Individual Analyses of Pilot (Breathing) Variables

The summary statistics presented in Table 5.4 are a valuable tool to assess how pilots respond to "real-world" military maneuvers in aggregate. They demonstrate the breathing gas requirements in a statistical framework as well as indicating relative stress level. The next steps are to evaluate these parameters in detail to understand and visualize their empirical distributions, as well as to identify any outlier data. In biological and physiological studies, the outliers may tell an important story highlighting unexpected events, and the ensuing analyses focus on interpreting such anomalies.

In the following subsections, the six pilot-dependent variables are analyzed in the order they appear in summary Table 5.4 by row. The process is as follows:

- Create QQ-plots to assess distribution
- Compare PBA results to published values
- Identify and interpret outlier points
- Demonstrate main effects with heat map visualization
- Recalculate statistics if necessary

The *a priori* assumption for these datasets is that they are lognormally distributed (Pleil et al. 2014). As such, the first step is to confirm this notion, and to observe how individual data points align within their overall distribution. Log-normality is a safe assumption; if the data were actually Gaussian distributed instead, the lognormal transformation would give the same ultimate statistical results. In contrast, erroneously assuming Gaussian distribution for a log-normal character will give skewed results.

The "QQ-plot" method was used to visualize the transformed data and find outliers (Pleil 2016 a,b). Here, the x-axis scale represents the "z-score" of the relative position of each data point wherein z=0 is the median value, z = 1 or -1 is one standard deviation distance from 0, z = 1.664 or -1.664 is the 95^{th} or 5^{th} percentile, etc. When the data (real space, or transformed) fall on a straight line, then one has chosen the appropriate distribution. Certainly, all real-world data have

bumps and outliers, so the straight line will never be perfect, however, the r-squared (r^2) value of the linear regression is close to the Shapiro-Wilk parameter for test of normality. The r^2 metric can range from 0 to 1, the closer r^2 is to 1, the better is the approximation of lognormality.

The "Heat Map" visualization tool serves to tell a story of the overall pattern as selected by the researcher. The concept is to develop a rectangular array with two chosen parameters, and then color-in the interstitial boxes based on a quantitative scheme ranging from dark blue (low values) through the rainbow to dark red (high values). Heat map visualization is commonly used to view complex genetic data but has been adapted for environmental and biomonitoring datasets as well (Pleil et al. 2011). Typically, the x-axis represents a sample designator (e.g., flight minutes) and the y-axis represents a sample category (e.g., flight-profile, pilot#, etc.). In contrast to QQ-plots, heat maps are statistically agnostic; they serve to show patterns based on a color coding.

5.1.3.1 Analysis of Breathing Frequency Dependent Variable (Breaths/Min)

Breathing frequency, or respiratory rate, is a count of how many times an individual breathes in and out during one minute; the normal resting respiratory rate for adults is 12 to 16 breaths/min, but can range up to 20 breaths/min with age and health state. Different studies have reported that the respiratory rate in adults can reach up to 40-60 breaths/min as a response to different levels of exercise, with a 95% confidence maximum of ~54 breaths/min (Blackie et al. 1991).

Summary statistics for this parameter was assessed across 3,275 flight minutes as shown in Table 5.4, row 1. For the PBA pilots, the breathing rate is found to be well within the "normal" ranges, with 95% of all values between 9 and 28 breaths/min. One caveat for these comparisons is that the comparison data were developed in the laboratory/clinic at 1 atmosphere pressure and nominal 21/79 O_2 /nitrogen ratio; fighter pilots experience a range of pressures below 1 atm in the cockpit, and generally breathe O_2 concentrations ranging up to 100%. These confounding conditions may affect "normal" breathing frequency interpretations. As these data are to be used to model the pilot/aircraft interaction, it is important to assess the "shape" of the data values might influence the validity of such interpretations.

The first step for interpreting distribution and outliers in a dataset is to observe how individual data points align within their overall distribution. Figure 5.1 shows the log-transformed BPM data from all flight minutes. Here the y-axis shows the log-transformed values. The straight line represents the linear regression; the 95% of the measurements (shown in the highlighted area) are lognormally distributed. There is a slight "light-tailed" set of values beyond 28 breaths/min that may or may not be considered outliers. The rapid fall-off below 9 breaths/min bears further scrutiny. Overall, even including the points outside the linear range, the r-squared value of the regression is $r^2 = 0.9221$, which means that the lognormal model explains more than 92% of the variance. For convenience, some important values are annotated in real-world space.

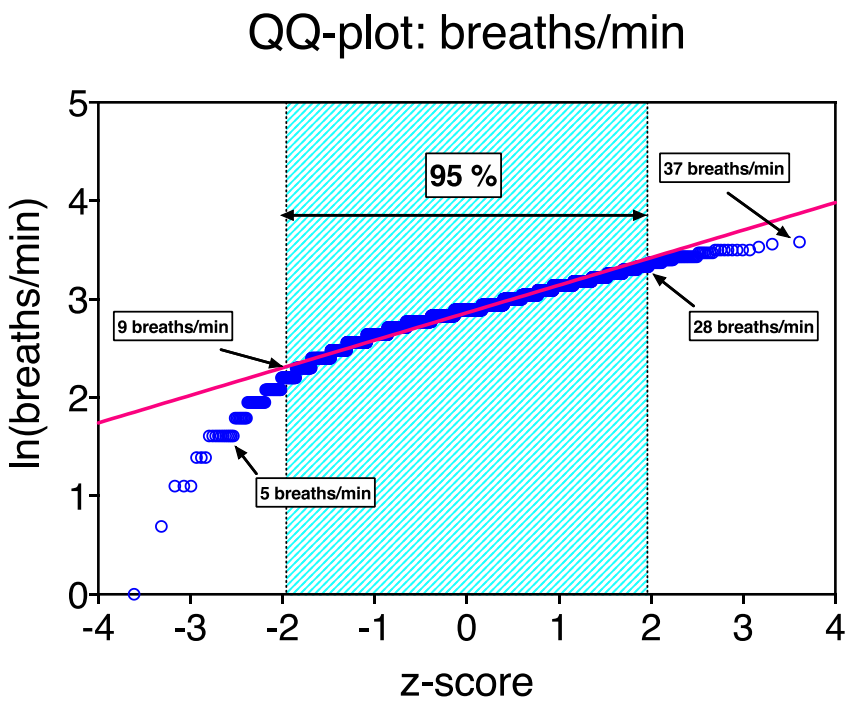

Figure 5.1. Standard QQ-plot of log-Transformed BPM Data
The highlighted center section represents 95% of the breaths/min values where the distribution is definitely lognormal. There is a "high-end" set of values from 28 to 37 breaths/min that may or may not be considered outliers. The rapid fall-off below 9 breaths/min bears further scrutiny.

The high-end deviations from the regression line are modest and may be perfectly reasonable. However, the advantage of a QQ-plot with respect to the more standard frequency distribution plot is that each individual point is identified. As such, the reader can quickly discern the high-end and low-end outliers by flight number and minute within the respective flight. These data could then be subjected to further examination beyond this summary statistics evaluation.

- High-end data, 79 flight minutes:

These were defined as breathing rates above 28 BPM with a maximum of 37 breaths /minute. Of these, most occur in a few flights. As examples, Flight 24 (B-profile) is dominant with 37 of 62 flight minutes in this high range; Flight 53 (B-profile) is second with 21 of 60 flight minutes in the range, with Flights 29, 40, 59, 68, 82, 90 (B-profiles); 76, 83, and 99 each contributing 1 to 4 flight minutes to this group. Pilot #28 had 60 of the total flight minutes in the range; Pilot #71 had 15 flight minutes in the range.

- Low-end data, 72 flight minutes:

These were defined as breathing rates below 9 BPM. Of these, most occur in a few flights. Briefly, Flight 85 (A-profile) is dominant with 38 of 85 flight minutes in this low range; Flight 54 (C-profile) is second with 24 of 62 flight minutes in the range, with Flights 11 (C-profile), 21 (D-profile), and 33 (C-profile) each contributing a few flight minutes to this group. Overall, most low-end flight minutes were contributed by the high-altitude A-profile (38 of 72) and by the "control" C-profile (23 of 72). Pilot #55 had 49 of total flight minutes in the range and Pilot #12 had 23 flight minutes in the range.

Based on the QQ-plot and outlier analyses, it appears that flight profile and pilot# are two important parameters creating differences in respiratory rate. The heat map can be designed to identify the pattern of all data with the goal of interpreting how profile and pilot affect this independent variable.

As seen in the QQ-plot analyses, most of the extreme values are between B-profile and A&C-profile flights. The heat maps in Figure 5.2 shows this pattern at the individual data point level. The x-axis (columns) represents the minute within a particular flight and the y-axis (rows) represents each flight as annotated by profile, flight#, pilot#. The right-side color scale shows the breaths/min quantitation.

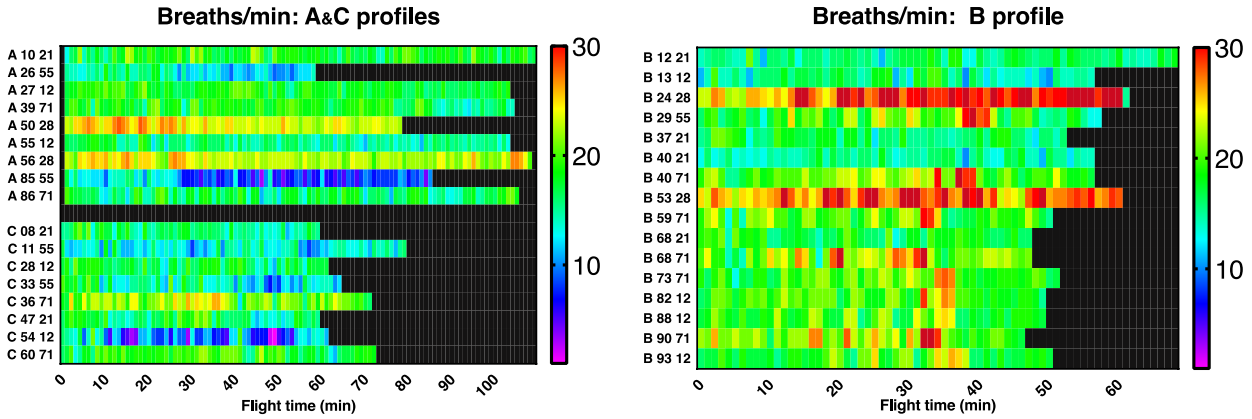

Figure 5.2. Heat Map Visualization Showing Differences in BPM for A&C Profile Flights vs. B Profile Flights
X-axis denotes the ordinal flight minutes; Y-axis shows individual flights annotated by: profile, flight#, pilot#. As found in the QQ-plot statistical analyses, the left panel (A&C profiles) trend towards blue-green indicating lower breaths/min, whereas the right panel (B profiles) trend towards yellow-red indicating higher breaths/min.

The heat maps comparison reinforces the statistical analyses from the QQ-plot in Figure 5.1. Briefly, there is a definite bias toward overall higher respiration rate for the aggressive combat maneuver flights, and also that some pilots trend towards higher respiratory response than others under similar flight conditions.

For overall context, Figure 5.3 shows all of the breaths/min data for all flights ordered by profile.

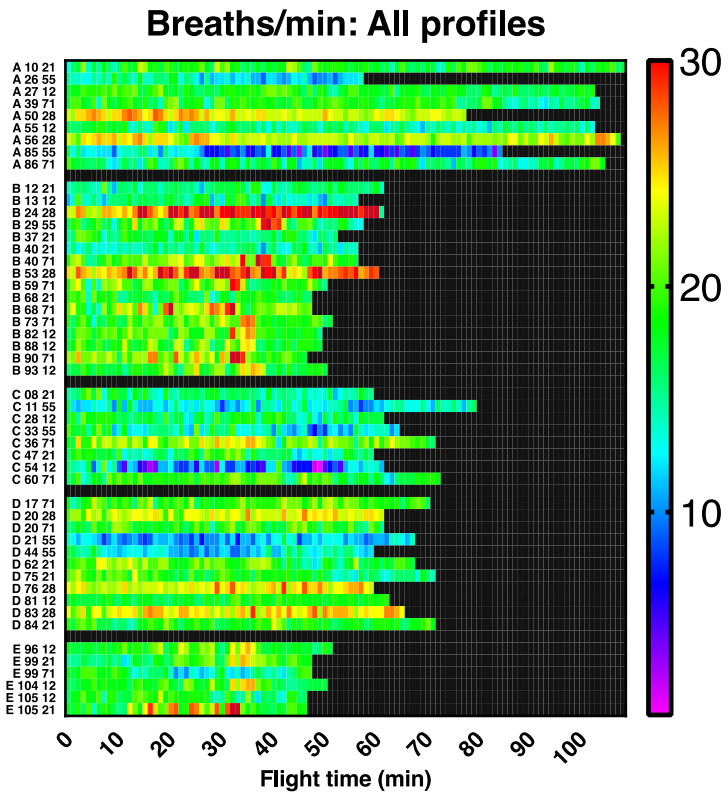

Figure 5.3. Heat Map Visualization Showing Differences in BPM Breathing Frequency for all Flights in Blocks of Rows Ordered by Profile
X-axis denotes the ordinal flight minutes; Y-axis shows individual flights annotated by: profile, flight#, pilot#. As found in the QQ-plot statistical analyses, the highest values (red) are found in B profile flights, especially flights 29 and 24. A and C profile flights trend towards the lowest values overall. D and E profiles are moderate with some mixture of higher and lower values.

5.1.3.2 Analysis of "Mean Flow Volumes" Dependent Variable

Mean flow volume as used here is defined as the total amount of breathing gas the pilot uses within each minute. It is calculated from the 20 Hz data profiles of the ISB representing the per minute total positive flow from the regulator to the mask in liters/min. In physiology, this is referred as "minute ventilation" or "respiratory minute volume". For context, an adult at rest typically exchanges 0.50 liters/min to maintain body function, which, when coupled with a resting breathing rate of 12 to 16 breaths/min, results in mean minute volumes from 6 to 8 liters/min. As activity increases, the body demands more air; this has been estimated as ranging from 60 to 91 liters/min depending on study parameters, with the highest levels reaching ~124 liters/min at the 95th percentile (Coyne et al. 2006). These measurements are not corrected for tracheal dead space in the publication.

Summary statistics for this parameter were assessed across 3,275 flight minutes as shown in Table 5.4, row 2. For the PBA pilots, the minute ventilation has a central tendency of about 18 liters/min, with 95th percentile confidence limits from 9.8 to 30.5 liters/min, and a 99th percentile at 35 liters/min. These values are well within the "normal" ranges discussed, in fact, they lie well below the values expected during heavy exercise. Again, there is a caveat that the reference data come from laboratory settings at ambient atmospheric conditions.

Figure 5.4 shows the log-transformed mean flow rate data from all flight minutes. Here the y-axis represents the log-transformed values. The straight line represents the linear regression; notice 99.4% of the measurements (shown in the highlighted area) are lognormally distributed. There is a slight "heavy-tailed" set of values beyond 38 liters/min that may or may not be considered outliers. The low end of the plot is along the line and as such is unremarkable. Overall, even including the points outside the linear range, the r-squared value of the regression is $r^2 = 0.9901$, which means that the lognormal model explains more than 99% of the variance. For convenience, some important values are annotated in actual space.

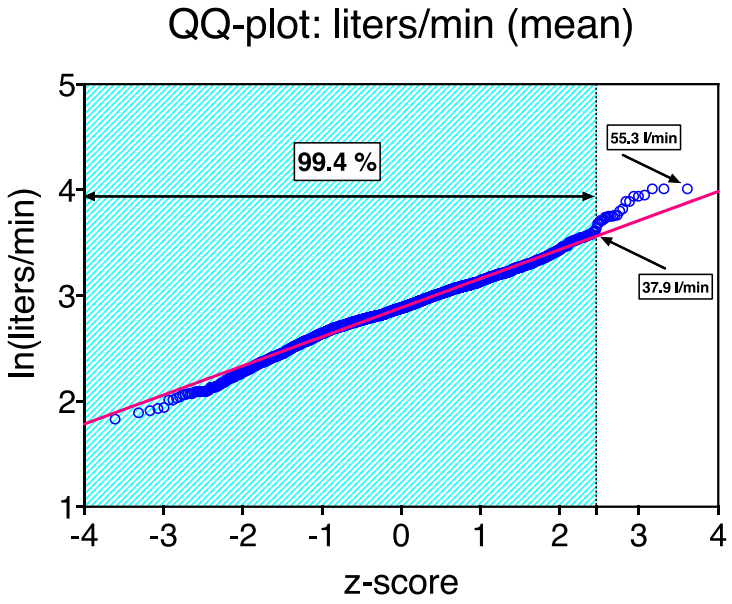

Figure 5.4. Standard QQ-plot of Log-Transformed Mean Flow from ISB (ventilation rate) The highlighted represents 99.4% of the minute ventilation values where the distribution is definitely lognormal. There is a slight "heavy-tailed" set of values beyond 38 liters/min that are probably not outliers, as they fall well within normal exercise parameters.

The high-end deviations from the regression line are modest and may be perfectly reasonable. However, the advantage of a QQ-plot with respect to the more standard frequency distribution plot is that each individual point is identified. As such, the high-end and low-end outliers by flight number and minute can be quickly discerned within the respective flight. These data could then be subjected to further examination beyond this summary statistics evaluation.

- High-end data, 23 flight minutes:

These were defined as ventilation rates above 37.9 liters/min with a maximum of 55.3 liters/min only because they trended off the line slightly. Of these, 17 values occurred in Flight #29 (pilot #55), and 6 in Flight #24 (pilot #28). These represented 0.7% of the values and were not considered remarkable.

- Low-end data:

The lowest 5 values are well within normal resting ventilation rates for adults from 6 to 8 l/min and fall on the distribution line. These are totally unremarkable.

As seen from the QQ-plots and the physiology interpretation, mean flow rates are unremarkable in value and distribution. However, there was a distinct trend for the highest values to occur in B

profiles. Figure 5.5 shows the heat map for all flights. As expected, B-profile flights 29 and 24 contain the highest (red) values and Profiles A and C flights contain some of the lowest values.

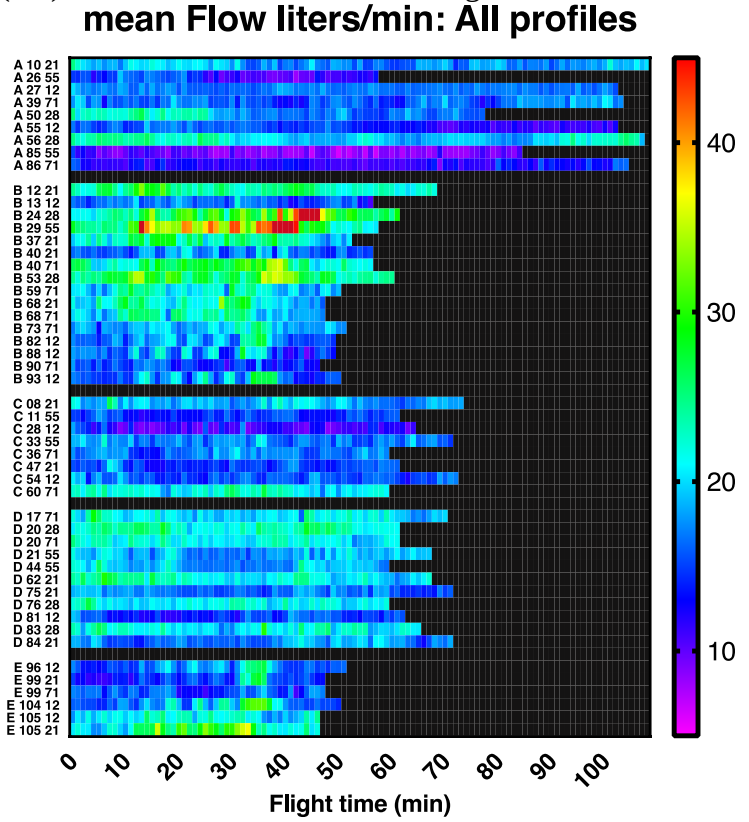

Figure 5.5. Heat Map Visualization Showing Differences in Mean Minute Ventilation for all Flights X-axis denotes the ordinal flight minutes; Y-axis shows individual flights annotated by: profile, flight#, pilot#. As seen in the QQ-plot statistical analyses, the highest values (red) are found in B profile flights, especially flights 29 and 24. A and C profile flights trend towards the lowest values. Overall, these values are unremarkable with respect to human physiological statistics.

5.1.3.3 Analysis of "Max Flow Volumes" Dependent Variable

Maximum flow volume as used here is defined as the highest instantaneous flow rate measured within each flight minute based on the 20 Hz data stream from the ISB flow sensor. In physiology, this is often referred to as the "peak instantaneous inhalation airflow". In the previous section for mean flow rate, a value results from a combination of breath volumes and breath frequency sustained over each flight minute; for this section, the values represent the instantaneous highest slope of the single fastest inhalation within each flight minute. High values are not expected to be sustained for a minute but are important for setting parameters for instantaneous pilot mask valve and on-demand regulator response.

For context, the normal at rest "peak nasal inhalation flow" or PNIAF has been measured in the laboratory to be about 300 ml/sec per nostril resulting in about 3.6 liters/min (Rennie et al. 2011). At high exertion levels, the "peak instantaneous inhalation airflow" through the mouth has been measured in two different studies as ranging from 196 to 248 liters/min, and 166 to 262 liters/min respectively (Coyne et al. 2006, Berndtsson 2004).

Summary statistics for this parameter in PBA were assessed across 3,275 flight minutes as shown in Table 5.4, row 3. For the PBA pilots, the max flow volume has a central tendency of

about 74 liters/min, with 95th percentile confidence limits from 39 to 137 liters/min and a 99th percentile at 153 liters/min. This indicates that pilots are sometimes very relaxed in the cockpit and that even their highest values under stress are well below laboratory exertion tests that have upper values around 250 liters/min.

Figure 5.6 shows the log-transformed max Flow rate data from all flight minutes. Here the y-axis shows the log-transformed values and the straight line represents the linear regression confirming the almost perfect lognormal character of this parameter with $r^2 = 0.9981$. The only discernible deviation is at the low end where a few points are around 27 to 30 liters/min but these values are very close to the expected resting rate in the literature. For convenience, the extrema values are annotated in real-world space.

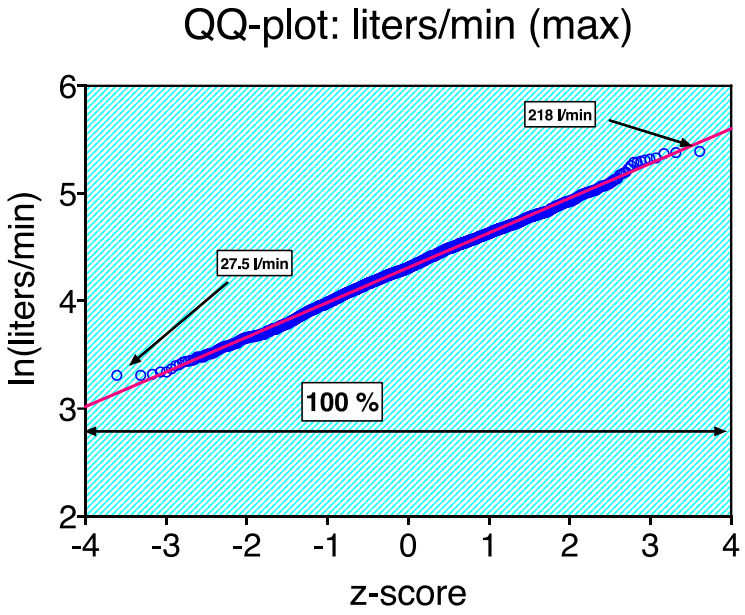

Figure 5.6. Standard QQ-plot of Log-Transformed Max Flow from ISB (instantaneous peak flow rate) The highlighted represents 100% of the values where the distribution is definitely lognormal with regression $r^2 = 0.9981$. There is a slight low-end deviation of as few values at ~27 liters/min.

As seen in the QQ-plot in Figure 5.6, there are only a few values deviating from the perfect regression line at the low-end at ~27.5 liters/min. These values occur in Profile A, Flight #55, but they are reasonable as resting, easy breathing at nominal 0.5 liters/breath tidal volume. At the high-end, the extreme value is 218 liters/min which unremarkable within the context of laboratory measurements of subjects exercising aerobatically**.**

As seen from the QQ-plots and the physiology interpretation, max Flow rates are unremarkable in value and distribution from the perspective of summary statistics. Figure 5.7 shows the heat map for all flights visualizing the internal distribution of values as driven by profile, flight# and Pilot#.

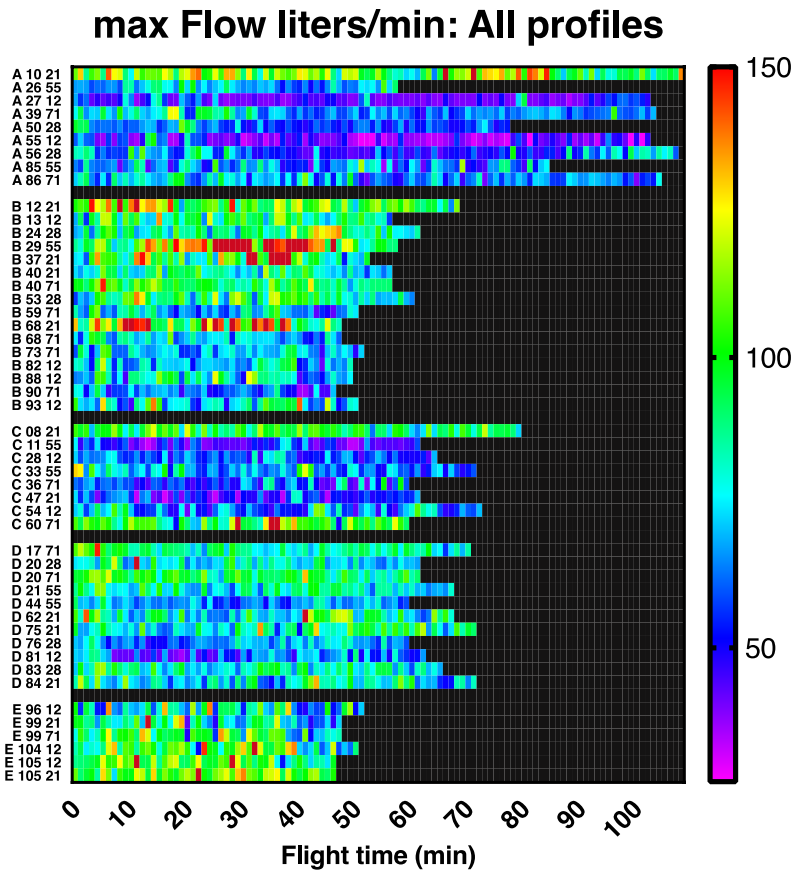

Figure 5.7. Heat Map Visualization Showing Differences in Max Flow Rate for all Flights X-axis denotes the ordinal flight minutes; Y-axis shows individual flights annotated by: profile, flight#, pilot#. As seen in the QQ-plot statistical analyses, the highest values (red) are found in B profile flights, especially flights #'s 12, 29 and 68. A and C profile flights trend towards the lowest values. Overall, these values are unremarkable with respect to human physiological statistics.

5.1.3.4 Analysis of "Breath Volume (mean)" Dependent Variable

This dependent variable is defined as the average volume per breath (liters/breath) within each flight minute based on the 20 Hz data stream from the ISB flow sensor. It is a hybrid variable in the sense that it is calculated from the "counts" of breathing frequency and the average flow volume parameters from each minute.

In physiology, this is often referred to as the "tidal volume" measured in liters/breath and includes tracheal dead volume. The human response of increasing tidal volume (breathing more deeply) is attributed to a feeling of "air hunger", a perception that one cannot get enough air. In clinical settings, this is referred to as dyspnea, or "shortness of breath" generally instigated by an underlying disease state. For pilots, this sensation can occur from more metabolic need of O_2 in response to more strenuous activity, or from some restriction of normal flow (easy breathing) imposed by the mask or regulator (Lansing et al. 2000, Nicolo et al. 2018).

For context, the default assumption for adult tidal volume at rest is ~0.5 liters/breath. The maximum tidal volume for a single breath is referred to as the "forced vital capacity" or "forced expiratory volume" ranges from 3 to 6 liters depending on the subject's gender, age, size and health state. According to the American Lung Association, the mean value is about 4.8 liters for

adult males. This level is not generally sustainable for a full minute. In a laboratory study, tidal volumes at the end of aerobatic exercise were measured at 2.7 ± 0.48 liter/breath for adult males, resulting in an estimated 95th percentile of 3.64 liters/breath for sustained breathing (Blackie et al. 1991).

Summary statistics for this parameter in PBA were assessed across 3,275 flight minutes as shown in Table 5.4, row 4. For the PBA pilots, the central tendency was ~1 liter/breath with a 95$^{\%}$ confidence range of 0.68 to 1.82 liters/breath, and a 99th percentile of 2.04 liters/breath. These values are well within normal ranges found in the laboratory and indicate a relatively modest level of exertion in comparison to maximum aerobatic exercise.

Figure 5.8 shows the log-transformed tidal volume (liter/breath) data from all flight minutes. Here the y-axis shows the log-transformed values and the straight line represents the linear regression indicating the expected values under perfect lognormal distribution, with 99.6% of the values representing lognormal character. For convenience, the extreme values are annotated in real-world space.

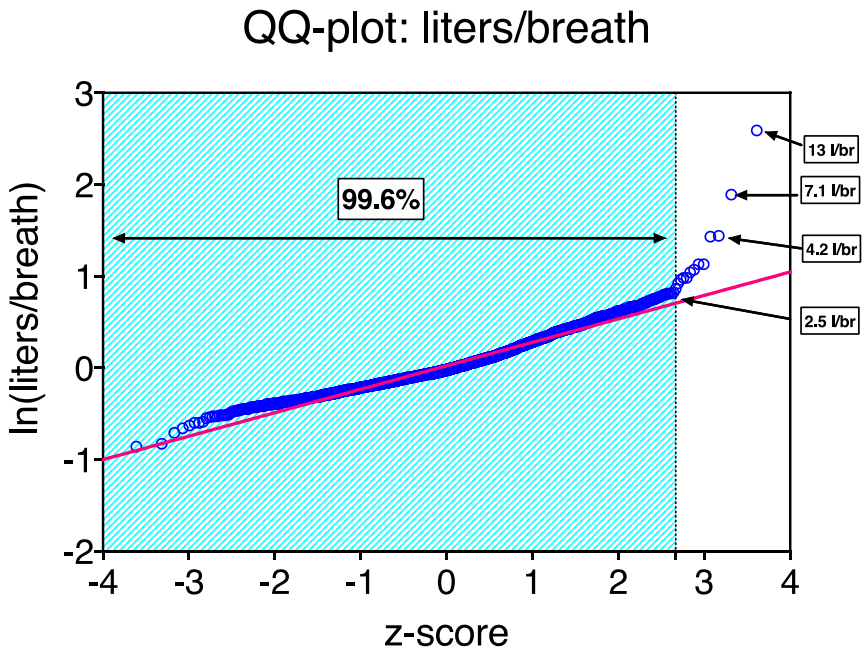

Figure 5.8. Standard QQ-plot of Log-Transformed Tidal Volume Data in Liters/Breath Calculated from ISB within Minute BPM and Liters/Min Values
The highlighted represents 99.6% of the values where the distribution is definitely lognormal with regression $r^2 = 0.9719$. There is a heavy tailed deviation at the high-end representing values not likely physiologically possible; these are annotated in real-world space.

As seen in the QQ-plot in Figure 5.8, there are a series of extreme measurements above ~2.5 liters/breath showing a heavy-tailed character at the high-end. Most of these values occur throughout Profile C, Flight #54. Although it is highly unlikely that values between 2.5 and 4.2 liters/breath could be sustained over a minute, it is physiologically possible. Other possibilities are that there are only a few very large breaths within that minute, or that there was free-flow in the mask. This can be explored further using multivariate analysis, or by interrogating data streams at the 20 Hz resolution level. Overall, this is a "well-behaved"

parameter and should be useful in identifying flight segments wherein the pilot may have experienced breathing discomfort.

As seen from the QQ-plots and the physiology interpretation, tidal volume measurements are unremarkable in value and distribution with the exception of some high values. Figure 5.9 shows the heat map for all flights visualizing the internal distribution of tidal volume (liters/breath) values as driven by profile, flight# and Pilot#.

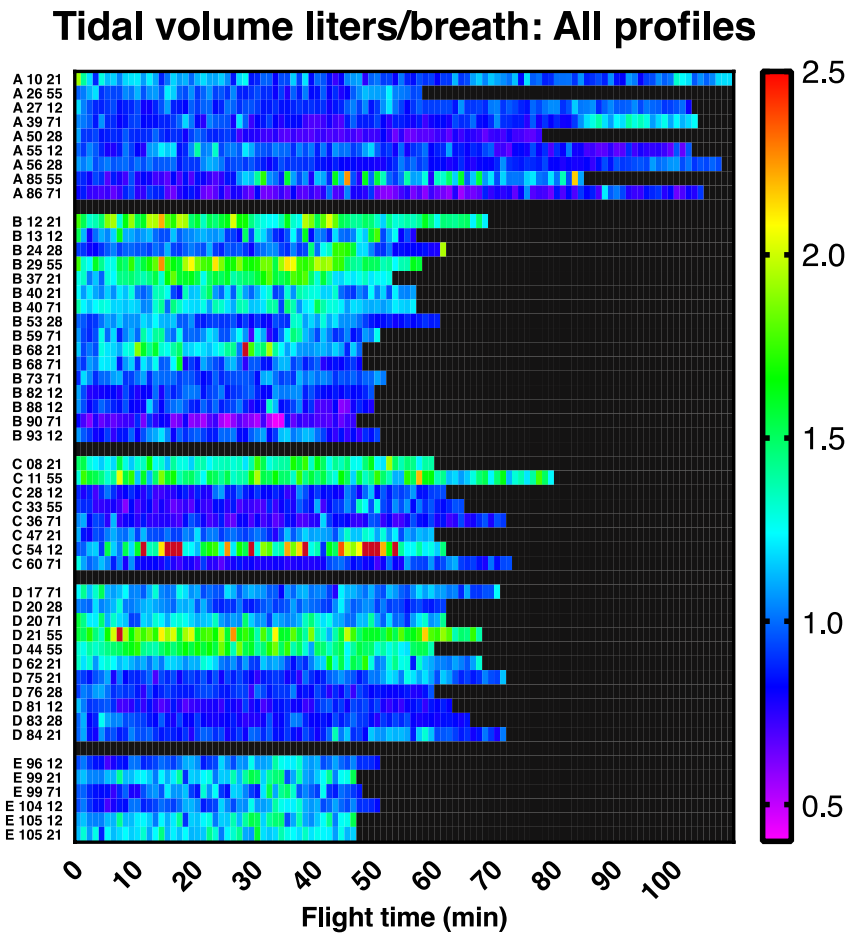

Figure 5.9. Heat Map Visualization Showing Differences in Tidal Volumes for all Flights X-axis denotes the ordinal flight minutes; Y-axis shows individual flights annotated by: profile, flight#, pilot#. As observed from the QQ-plot statistical analyses, the highest values (red) are found in C profile flight #54; some B and C profile flights have relatively high trending values (yellow and green). A and E profile flights trend towards the lowest values. Overall, these values are unremarkable with respect to human physiological statistics.

The few values above 2.5 liters/breath are physiologically unlikely and could be caused by an interaction of the two data streams; for example, if the pilot drops the mask briefly, the mask could free-flow, yet no breaths could be counted. Such conjectures can be resolved with detailed study of the 20 Hz data streams.

5.1.3.5 Analysis of Differential Mask Pressure (DMP) Dependent Variable

This is a "constructed" variable designed to interpret changes in effort the pilot might be requiring to breathe and has a much more complex nature than the preceding four dependent

breathing variables. Furthermore, DMP is derived from the ESB pressure channel, not from the ISB flow sensors, and is highly dependent on the fit of the mask and the response of the non-rebreathing valves and regulator. Although created by the pilot's breathing activity, DMP is probably the best empirical measurement describing the pilot-aircraft interaction. As such, this ensuing discussion requires a higher level of interpretation than the other more standard breathing parameters.

The concept of "mask pressure" is not encountered in normal experience. When one breathes in and out, the pressure in the room does not change. However, in non-rebreathing systems as in SCUBA diving, firefighting, and other supplied air respirators, an inhalation triggers incoming gas flow, and exhalation shuts off this flow and allows a valve to vent. As such, if working properly, very small changes in pressure exerted by the human trigger a smooth transition between new incoming air and outgoing breath. If subjects require more air faster, then they may exert more negative pressure during inhalation and more positive pressure during exhalation against the non-rebreathing system's mechanics. If the system does not respond quickly, or has restrictions in the valves, the subject also has to exert more pressure. In either case, higher pressure swings are directly related to the effort exerted for breathing in response to the aircraft systems.

In PBA, these pressure changes were monitored at a high sampling rate (20 Hz) and converted to 1-minute blocked data. The DMP variable is calculated as the difference between the highest and lowest recorded mask pressure value within each flight minute. A cursory inspection of the DMP variable in row 5 of Table 5.4 shows a natural space coefficient of variation (cv) defined as: cv = s.d./average = 3.53/7.82 = 0.45. It has been documented that if the cv is greater than 0.2, then the underlying distribution is not normal (Gaussian) but more likely lognormal (Pleil 2016a). As such, DMP data were lognormally transformed for further analysis in this report.

The summary statistics indicate a central tendency of 7.2 mmHg, with a 95% confidence range of 3.7 to 16.7 mmHg and a 99^{th} percentile of 22.4 mmHg. These values are highly dependent on mask fit, but that they do allow relative comparisons within and between flights and pilots.

For context, imagine one is blowing up a balloon or drinking a thick milkshake through a straw; there is a maximum amount of positive or negative pressure that a human can exert, after which the activity fails. The question is how this relates to the pressures required for the pilot to open and close the non-rebreathing systems providing airflow to the mask.

According to the literature, laboratory tests have shown that maximum expiratory pressures are in the range from 60 to 120 cmH_2O (44 to 88 mmHg) and maximum inspiratory pressures are bit lower in the range from 40 to 100 cmH_2O (29–74 mmHg) for adult males, and is highly dependent on respiratory health and age (Lausted et al. 2006, Evans and Whitelaw 2009). Assuming mid-range values from these laboratory tests, the equivalent DMP values at full exertion would be around 120 mmHg. Despite the wide ranges, these estimates indicate that the pilots do not ever experience exertion levels beyond ~20% of their presumed maximum threshold, and for half the time are below 6% of this maximum. However, it is important to note that under normal breathing conditions at ambient pressure (without a mask), the DMP equivalent is zero, and so any use of non-rebreathing systems adds to the effort of breathing.

Figure 5.10 shows the log-transformed differential mask pressure (mmHg) data from all flight minutes. Here the y-axis shows the log-transformed values and the straight line represents the linear regression indicating the expected values under perfect lognormal distribution, with 99.6%

of the values representing lognormal character. For convenience, the extreme values are annotated in real-world space.

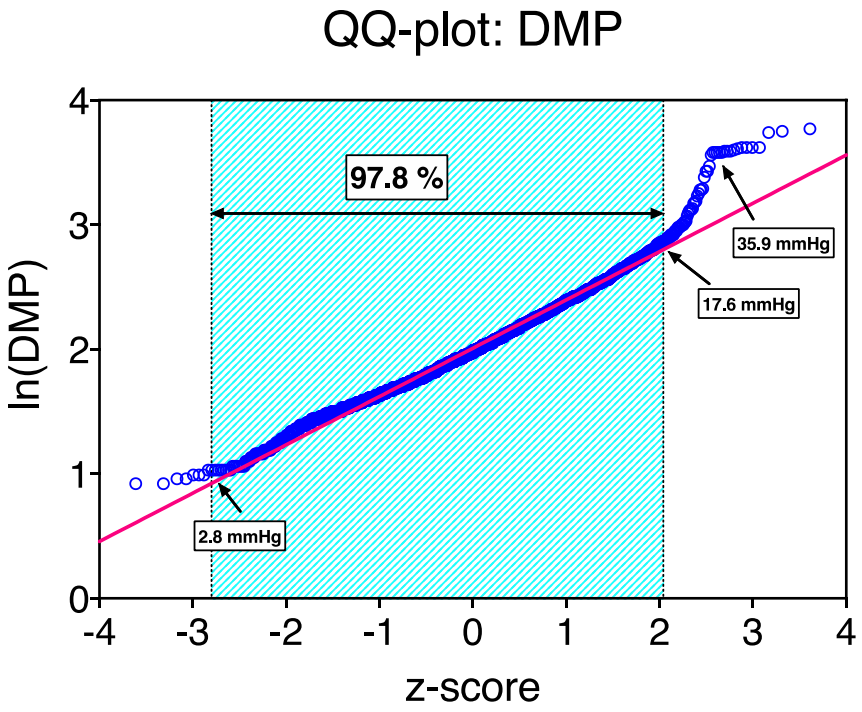

Figure 5.10. Standard QQ-plot of Log-Transformed DMP Data in mmHg Calculated from ESB Pressure Channel
The highlighted area represents 97.8% of the values where the distribution is definitely lognormal with regression $r^2 = 0.9806$. There is a heavy tailed deviation at the high-end and some tailing off at the low-end.

As seen in the QQ-plot in Figure 5.10, there are a series of extreme measurements above 17.6 mmHg (67 of 3275 comprising ~2% of the measurements) showing a heavy-tailed character at the high-end. There is no particular pattern to these high values, they occur in all flight profiles, with an emphasis in B, D and E. The low-end deviations are unremarkable; here the values are around 2.5 mmHg and could reflect subtraction related measurement noise. These QQ-plot results are somewhat different than those from the other dependent variables that showed definite relationships with fixed effects like profile, pilot# and flight#. However, as mentioned, the absolute values are relatively low within the context of maximal exertion, although his could be an artifact due to mask leakage at higher DMP.

The QQ-plots and the physiology interpretation show that DMP measurements are unremarkable in value and distribution with the exception of some high values. Figure 5.11 shows the heat map for all flights visualizing the internal distribution of DMP (mmHg) values as driven by profile, flight# and Pilot#. Overall, Profile A representing altitude level flight seems to perturb the pilots the least, whereas Profile B representing aerobatics and Profile D representing low level aerobatics have the greatest excursions of DMP.

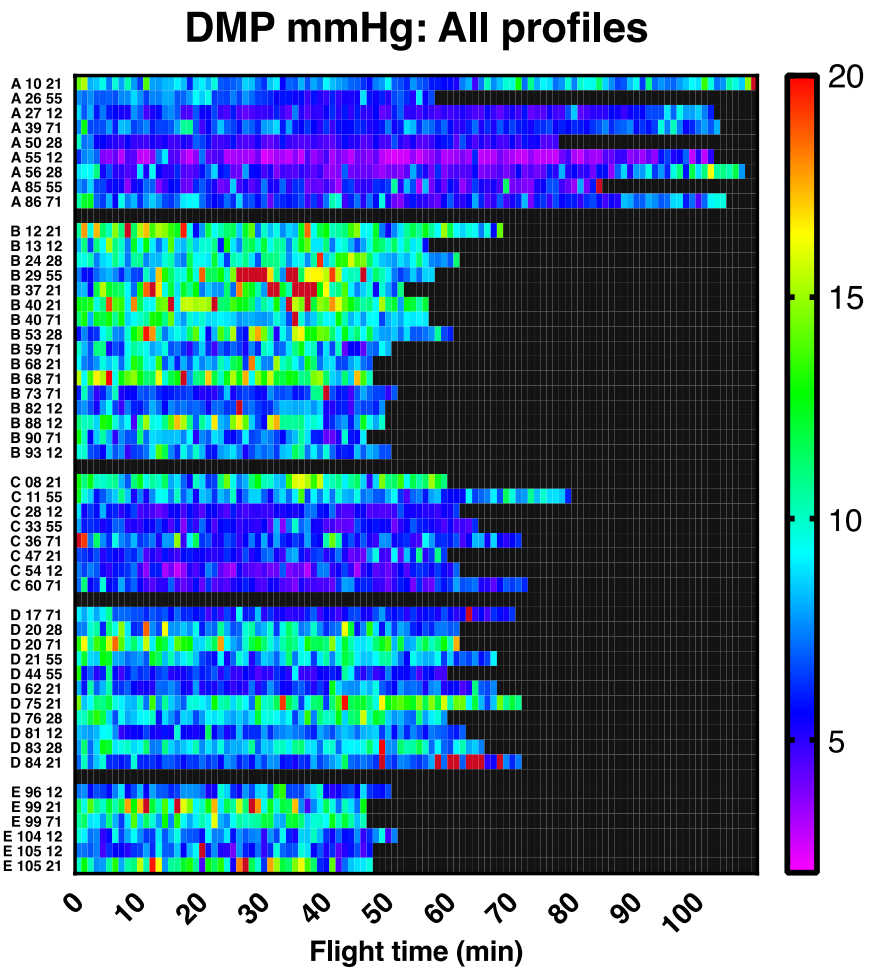

Figure 5.11. Example of Heat Map Visualization of Flight Comparisons Showing DMP Measurements

X-axis denotes the ordinal flight minutes; Y-axis shows individual flights annotated by: profile, flight#, pilot#. As observed from the QQ-plot statistical analyses, the highest values (red) are found in the B profile flight and also scattered about in the other profiles. Overall, DMP is lowest in the A profile and highest in the C profile, but in general, these values are unremarkable with respect to human physiological statistics.

#54; some B and C profile flights have relatively high trending values (yellow and green). A and E profile flights trend towards the lowest values. Overall, these values are unremarkable with respect to human physiological statistics.

5.1.3.6 Analysis of Standard Deviation Mask Pressure (st. dev. MP) Dependent Variable

This calculation provides similar information as DMP, but captures the overall variability within each minute, rather than the extreme values. The physiological effects are thought to be different in that DMP tends to capture very brief extreme events, whereas st. dev. MP is designed to capture longer term stresses from continuous fluctuations that may cause fatigue.

Here the central tendency is 1.68 mmHg with 95% confidence of 1.7 to 2.80 mmHg, and a 99th percentile of 3.14 mmHg. The data suggest that the higher values in st. dev. MP reflect times when the system is working well but the pilot requires more flow, or when fluctuations from the regulator and mask valves are affecting the response, or when the cabin pressure control

becomes erratic. As such, this is a complex parameter and the anomalies will require detailed analysis using the 20 Hz data. The low-end deviation shows some flattening at very low easy breathing comprising 53 flight minutes of which 52 are Profile A, mostly with pilot #12, and some with pilot #55. This is an expected result; the Profile A is considered an easy breathing high-altitude flight without aerobatics. The range displayed in the QQ-plot in Figure 5.12 is considered reasonable considering the DMP values shown in Figure 5.10 where the highest deviations are greater than 17.6 mmHg.

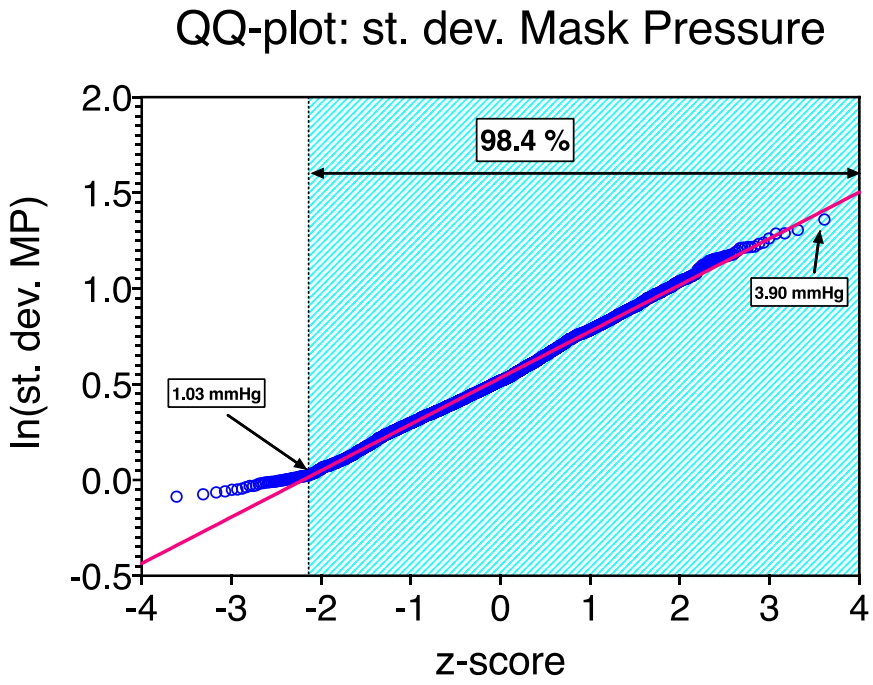

Figure 5.12. Standard QQ-plot of Log-Transformed Standard Deviations of Mask Pressure Variable (st. dev.MP) Data within Each Minute in mmHg Calculated from ESB Pressure Channel The highlighted area represents 98.6% of the values where the distribution is definitely lognormal with an overall regression $r^2 = 0.9996$. There is some tailing off at the low-end representing very smooth easy breathing from A profile flights.

The QQ-plots show that st. dev. MP are lognormally distributed with the exception of some tailing at the low-end. Figure 5.13 shows the corresponding heat map for all flights visualizing the internal distribution of st. dev. MP (mmHg) values as driven by profile, flight# and Pilot#. Overall, Profile A representing altitude level flight seems to perturb the pilots the least, whereas Profile B representing aerobatics and Profile D representing low level AeroBatics have the greatest excursions of DMP.

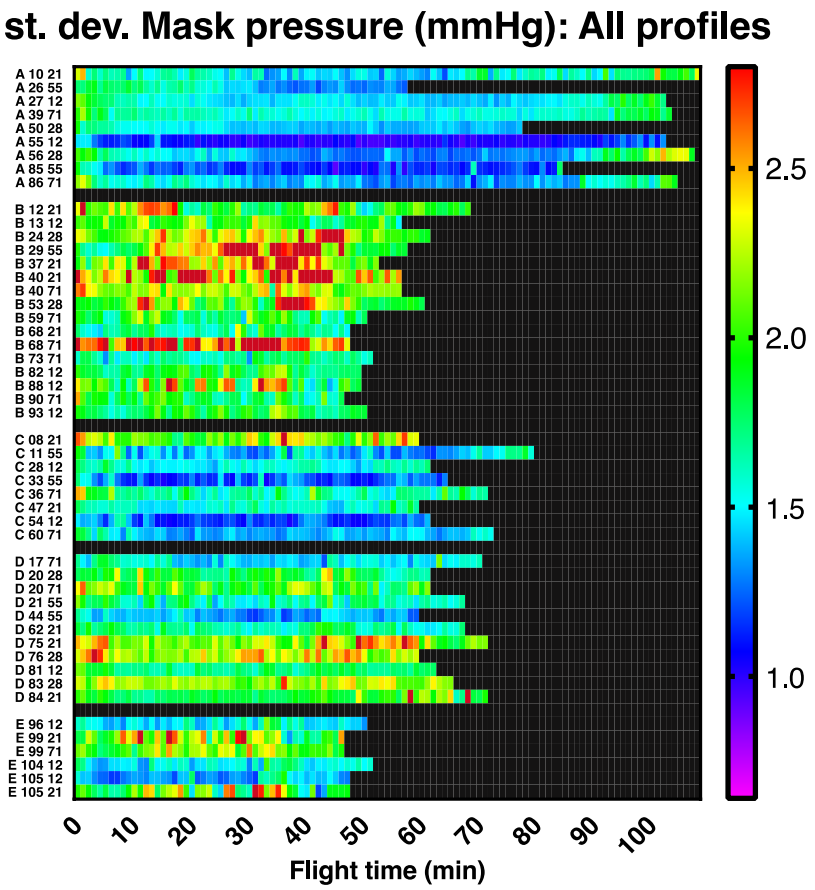

Figure 5.13. Example of Heat Map Visualization of Flight Comparisons Showing Standard Deviation of Mask Pressure Within Each Flight Minute Measurements
X-axis denotes the ordinal flight minutes; Y-axis shows individual flights annotated by: profile, flight#, pilot#. The highest values (red) are found in the B profile flight and also scattered about in the other profiles. Overall, st. dev. MP is lowest in the A profile.

5.1.4 Context of Dependent (pilot) Variables Interpretation:

Overall, the six selected pilot breathing parameters appeared to be within reasonable ranges of human physiology when compared to available literature values. The QQ-plots were useful in identifying extreme values and outlier values and the heat maps allowed us to quickly discern patterns and to find which flights and flight minutes were most affected. There were a few obvious measurements that fell into the realm of "impossible", and some others that were improbable.

5.1.4.1 Review of Outliers

The first observation of "improbable" values occurred in the evaluation of tidal volume constructed from ISB flow sensors as shown in Figure 5.8. Sustained breath volumes from 2.5 to 4.2 liters/breath as found in C profile Flight #54 (see heat map in Figure 5.9) are highly unlikely, but physiologically possible; values above that are impossible. Summary statistics are not affected, but there is still a need to explore what may have caused these readings.

Breathing frequency (BPM) also shows potential physiological outliers at the low-end in the QQ-plot in Figure 5.1 where there is a roll-off of values below 9 BPM. These values are unlikely

under normal conditions as the accepted resting range for adults is 12 – 16 BPM, although high-altitude chamber tests have shown such values. The heat map in Figure 5.2 indicates that these low values occur primarily in A profile Flight #85 from flight minute 28 until the end at flight minute 85, and in C profile flight #54 from flight minutes 10 to 55. It is possible that using high O_2 levels in the breathing gas could slow breathing rate under some conditions, but sustained rates at 9 (or less) BPM are suspect. Similarly, some of the higher breathing rates (above 30 BPM) seen in the QQ-plot in Figure 5.1 are suspect as they are reminiscent of sustained exercise, but they are possible, and still well below the laboratory levels found for aerobatic tests.

The DMP variable is difficult to assess physiologically from purely a summary statistical perspective as it is a function of mask fit and valve/regulator function. The DMP's experienced overall are all well below what is considered to be the straining or maximal values. The highest values occur in B profile and D profile flights (heat map Figure 5.11) which seems reasonable as these profiles have high-stress combat maneuvers.

5.1.4.2 Caution about PBA Pilot Comparisons with Laboratory Data

PBA pilot breathing results provide the empirical measurements for flow, volume, pressure, and timing experienced in a very specialized cockpit environment. Pilots wear restrictive flight gear and are harnessed into their seat; they experience changing pressures, O_2 concentrations, accelerations, and on-demand breathing gas supply variability that all affect their breathing response. However, there is value in providing context to the scale of these measurements from the peer-reviewed literature describing the general population. Such comparisons are summarized in Table 5.6.

The main caution for interpreting this table is that laboratory measurements, typically for exercise physiology, are performed at ambient pressure, 21% O_2, room temperature, and 1-G, with the subjects spontaneously breathing and wearing unrestrictive clothing. There are monitoring masks employed in such studies, but these are designed to be as non-invasive to normal breathing as possible.

As such, direct numerical comparisons between the specialized cockpit environment and laboratory studies are subject to some caution. For example, does a modest range of tidal volume for pilots reflect the actual needs of the pilot, or is it influenced by harness and gear constriction that prevent full inhalation? Regardless of the additional underlying factors that influence PBA data, the information derived from the peer-reviewed literature shown in Table 5.6 provides some overall context for normal aerobatic breathing.

Table 5.6. Comparison of PBA Pilot Breathing Statistics with Available Literature Values

Variable	units	PBA results			literature values		
		Central	95th CI	99th %	resting	exercise	max
Breath Freq.	br/min	18	9 - 28	31	12 - 16	40 - 60	
mean flow	liters/min	17.8	9.9 - 30.5	35.1	6 - 8	60 - 91	124
max flow	liters/min	74.4	39 - 137	153	3.6	166 - 262	
tidal volume	liters/breath	0.98	0.68 - 1.82	2.04	0.5	2.2 - 3.2	4.8
DMP	mmHg	7.2	3.7 - 16.7	22.5	0		120

5.1.4.3 Summary Statistics

Summary statistics of 1-min collapsed data and their more detailed analyses are a powerful tool to get an appreciation of the overall data structure. Tables 5.4 and 5.5 show how to interpret pilot breathing parameters across real flights For example, as seen in from Table 5.4, at the high-end, during the top 2.5% of the flight minutes (or ~145 flight minutes), the pilot requires an average flow of 30.5 liters/min, and there are instantaneous flow requirements exceeding 137 liters/min. If the aircraft/mask/regulator cannot provide these levels of flow, the pilot will feel discomfort. This was not known prior to PBA in-flight testing.

Other pilot breathing parameters can be observed at the extremes as well. For example, BPM describes physiological effects related to hyperventilation, and liters per breath may indicate pressure issues in the mask. Again, the summary data in Table 5.4 of the statistical distributions show how often such stressors occur. The parameter st. dev. MP was left off Table 5.6 as the PBA team could find no comparable literature values.

5.1.5 Discussion of Independent (aircraft) Parameters

Aircraft flight profiles were designed to capture a variety of flight activities as discussed in Technical Section 1. As these were chosen as "independent", their individual distributions (QQ-plots) are not particularly probative, and their between-profile summary statistics will be skewed due to the *a priori* design choices that were made, not from unknown outcomes. Certainly, these characteristics, especially distribution, will be tested when building interaction models in Part 2 of this Technical Section, but for the purposes here, the aircraft parameters individually are reviewed as a way to explain the differences among flights.

What is important for this summary and visualization section is how consistent the within-profile performances are. For example, if the particular test prescribes high-altitude but non stressful A profile flights as a group, then each flight within that profile can be consistently evaluated for pilot response to altitude, velocity, and G force, etc. As seen in Table 5.5, the summary statistics for some of these preselected parameters can be evaluated across the board for all flights.

Some representative aircraft variables were chosen to visualize the different profiles by group, but caution that there are different ways to use the same complex 20 Hz data streams to create new independent variables, if deemed necessary, for mixed effects modeling in Part 2 of this Technical Section. Note that all flights will have relatively similar take-off and landing parameters and so only the center sections will be representative of the particular profile.

5.1.5.1 Independent (aircraft) Parameters – G3 mean and G3 max

Acceleration is considered the most taxing of the aircraft parameters; it is expressed in G units that represent a multiplier of 1 gravity experienced at the earth's surface. In a high-performance aircraft, G-force is experienced as a vector and for PBA is calculated from the 3-D axis accelerometer built into the ISB. For the purposes of this section, G-force is considered as a sustained within-minute average (G3 mean) and also as an instantaneous maximum (G3 max) within each minute. The former is more likely to have effects on breathing whereas the latter is more likely related to barotrauma. Notably, G3 can be experienced as less than 1.0 G during a sharp descent, but this uncommon. For the PBA study, G-force was designed to be limited to 5 G's for pilot safety; In general, F-15 jets are safety rated for a maximum of 9 G's and F-18 jets are safety rated for a maximum of 7.5 G's although the aircraft are capable of higher G-loads in extreme combat circumstances.

The various profiles were designed to assess the effects of G-force from combat maneuvers and from different turns, ascents and descents. For G3 mean, the summary statistics in Table 5.5 show a central tendency of 1.06 G with 95% confidence interval of 0.98 to 3.2 G and 99th percentile of 3.2 G. G3 max has a central tendency of 1.46 G with 95% confidence interval of 1.02 to 5.07 G and 99th percentile of 5.2 G.

Figures 5.14 and 5.15 show the G3 mean and G3 max heat maps for all flights annotated as profile, flight #, and pilot #. The main feature of these heat maps is to show the consistency within profiles, and visualize the differences among profiles.

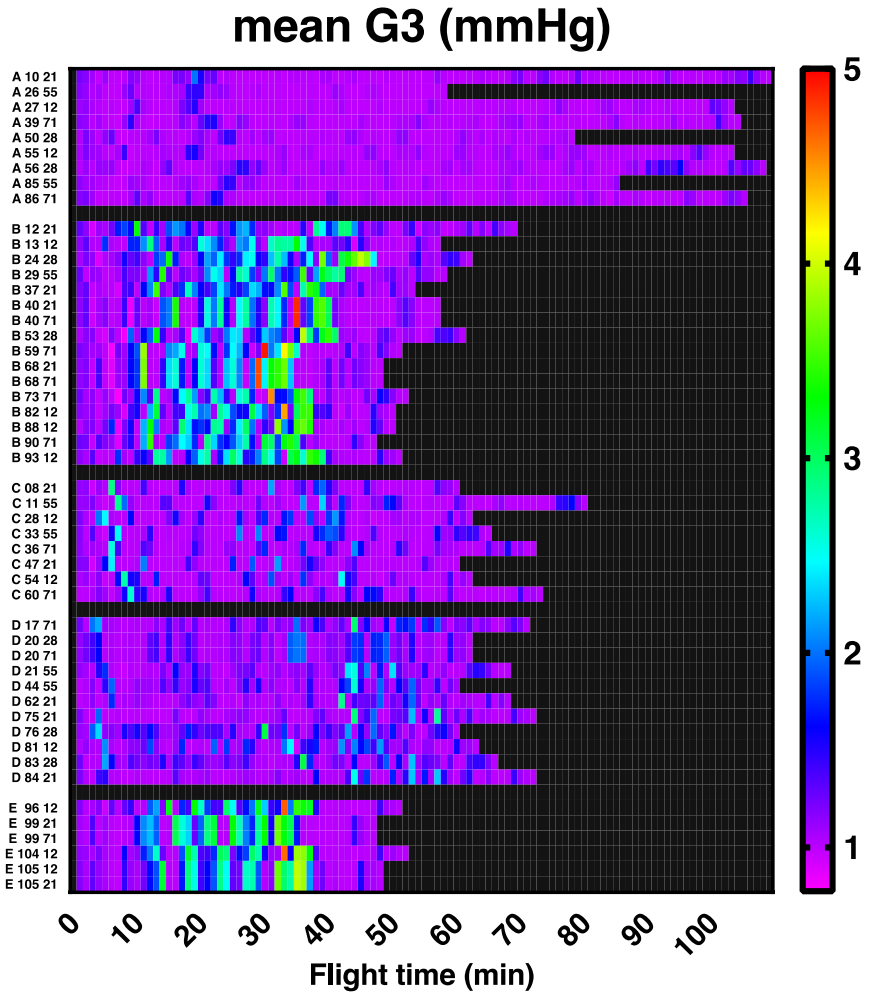

Figure 5.14. Heat Map Visualization of G-force Vector (G3 mean) as Averaged for Each Flight Minute (x-axis) and all PBA Flights (y-axis) by Profile, Flight#, Pilot#
Most high averaged G3 occur in flight Profiles B and E. Visualization of the within-profile rows indicate excellent consistency making profile an important fixed effect.

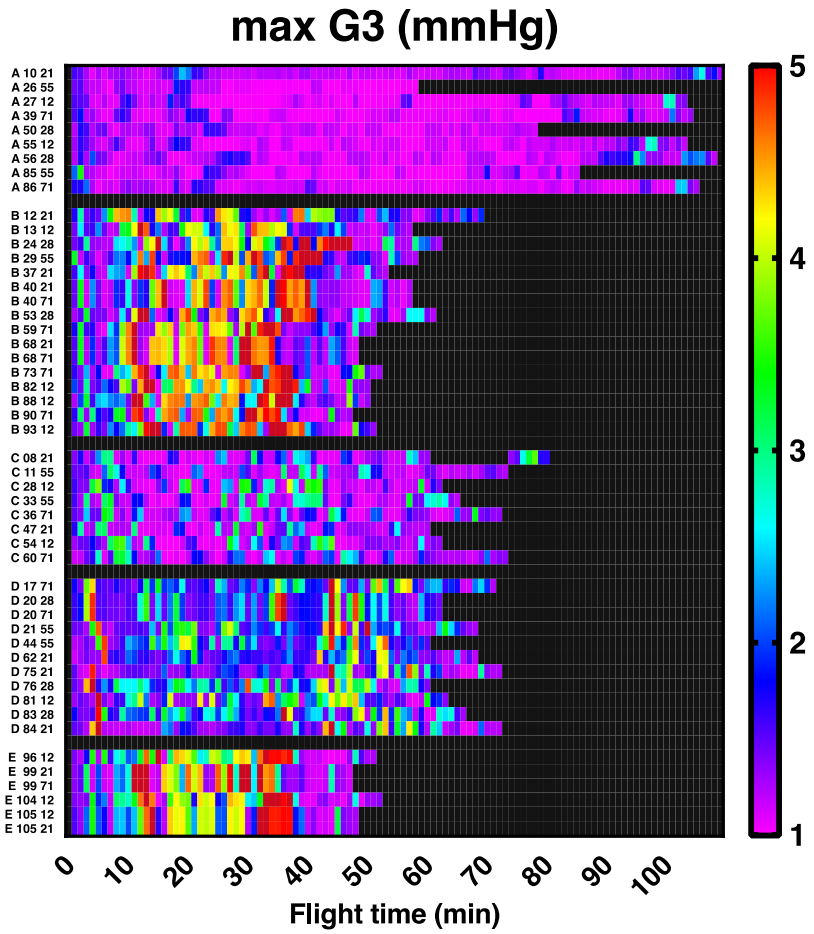

Figure 5.15. Heat Map Visualization of G-force Vector (G3 max) as Maximum G Experienced for Each Flight Minute (x-axis) and all PBA Flights (y-axis) by Profile, Flight#, Pilot# Most high G3 max measures occur in flight profile B and E, but C and D profiles also demonstrate some higher value. Flight Profile A does not show overall G3 extremes. Visualization of the within-profile rows indicate excellent consistency making profile an important fixed effect.

5.1.5.2 Independent (aircraft) Parameter: altitude – "Alt mean" and "delta Alt"

Altitude is the dominant feature of flying that affects all aspects of systems performance including engine, avionics, handling, cooling, and life support. External (ambient) pressure has an inverse relationship with altitude; over the range of typical military operations from sea level to ~50,000 ft, air pressure ranges from 760 mmHg down to 83 mmHg. As such, altitude requires adaptation to maintain operational integrity. From the perspective of the PBA study, there are two primary parameters that contribute to pilot health and safety related to altitude. The first is cabin pressure adaptation to external pressure and the relationship to breathing equipment including mask valves and regulator response. The second is rapid change in altitude that could induce barotrauma through delayed compensation of cabin pressure.

The "alt mean" parameter is defined as the arithmetic mean altitude in feet within each flight minute and the "delta alt" parameter is derived as the overall maximum change in altitude within each flight minute without regard to ascent or descent. Other variants of altitude changes including "within minute frequency" of changes and "within minute standard deviation" have been explored as derived from the 20 Hz data streams, but these were deemed less probative.

One caveat to the altitude parameters is that they are indirectly related to the pilot, primarily via cabin pressure. The F-15 and F-18 aircraft maintain cabin pressure on a schedule: from sea level to 8,000 ft, cabin pressure is the same as external pressure (760 to 564 mmHg); from 8,000 to 23,000 ft, cabin pressure is maintained at the 8,000 ft equivalent of 564 mmHg referred to as the isobaric region, and from 23,000 ft to the maximum altitude ~50,000 ft, cabin pressure is maintained at 5 psig above ambient pressure corresponding to 564 to 83 mmHg.

Cabin pressure is also explored directly in Section 5.1.5.4. As the altitude and cabin pressure are inversely correlated (with the exception of the isobaric range), the mixed-effects models in Section 5.2 require careful decisions when selecting one or the other for inclusion in the "full model".

The heat map visualization in Figures 5.16 and 5.17 shows mean altitude and delta altitude across all PBA flights included in the 1-min database, demonstrating excellent internal consistency within flight profiles. The profile B flights show the greatest amount of change in within minute altitude as expected because this profile contains the mid-altitude AeroBatics maneuvers.

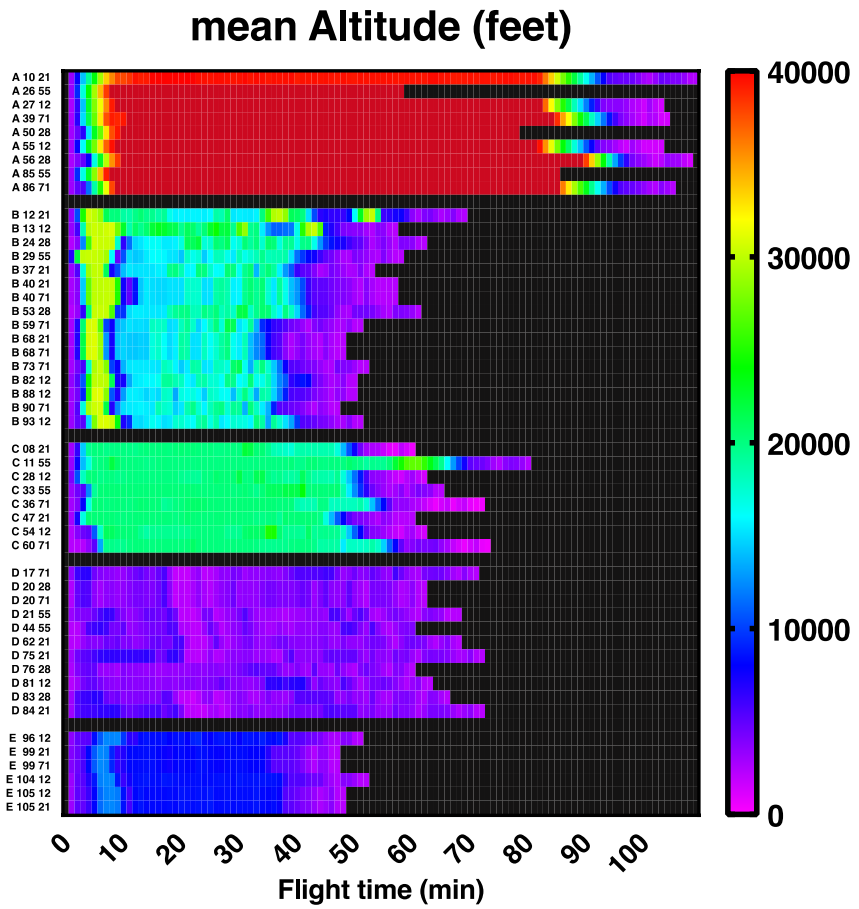

Figure 5.16. Heat Map Visualization of Aircraft Altitude (Alt mean) Averaged for Each Flight Minute (x-axis) and all PBA Flights (y-axis) by Profile, Flight#, Pilot#
All of the highest altitudes occur in Profile A and the lowest altitudes in Profile D, as expected. Visualization of the within-profile rows indicate excellent consistency making profile an important fixed effect.

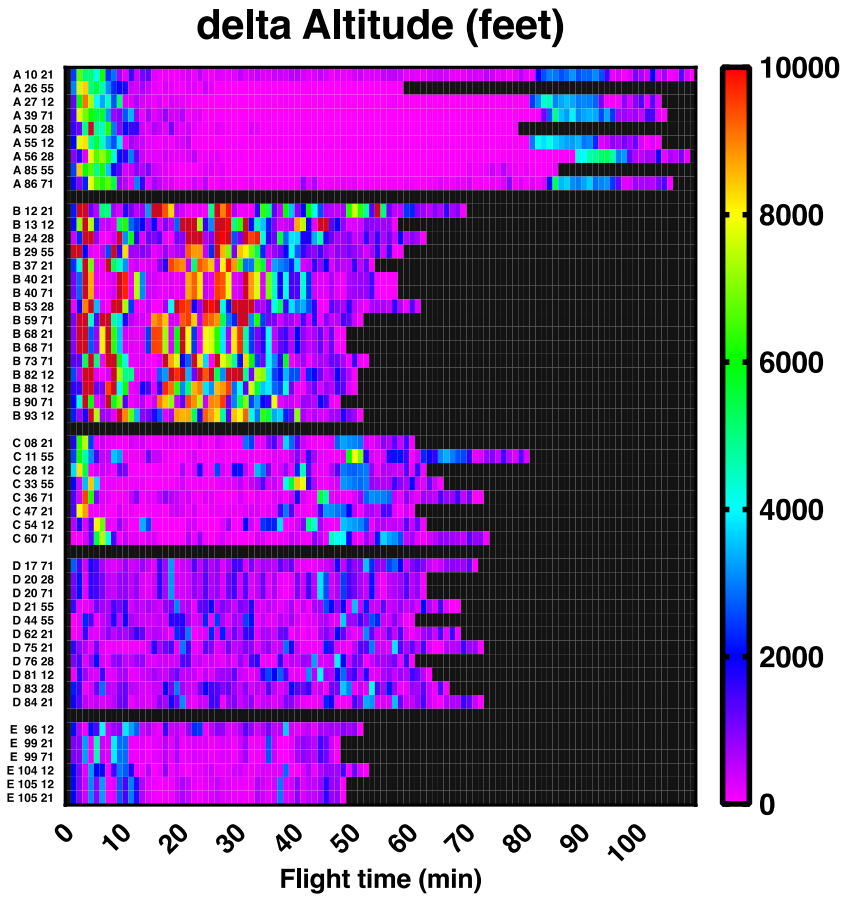

Figure 5.17. Heat Map Visualization of Change in Aircraft Altitude (delta Alt) for Each Flight Minute (x-axis) and all PBA Flights (y-axis) by Profile, Flight#, Pilot#
Within minute changes are found primarily in profile B as expected. Visualization of the within-profile rows indicate excellent consistency making profile an important fixed effect.

5.1.5.3 Independent (aircraft) Parameters – velocity

Linear aircraft velocity, like altitude, has only indirect influence on the pilot unless coupled with excess G-force. Certainly, velocity and altitude are correlated to some extent during flight maneuvers, but for the most part the pilot does not feel the absolute velocity, except perhaps when experiencing vibrations from turbulent air flow or changes in ambient conditions. There is a discontinuity when crossing the sound barrier, but this occurs only above ~1000 ft/sec (depending on altitude) and is considered to have negligible effect on the pilot.
The summary statistics indicate that the median velocity value for all PBA flights is 707 ft/sec (482 mph) and the 95th confidence range is 209 to 998 ft/sec (142 to 680 mph), with a 99th percentile of 1065 ft/sec (726 mph). As seen in Figure 5.18, profiles A, B, and C contain most of the highest velocities within flight minutes.

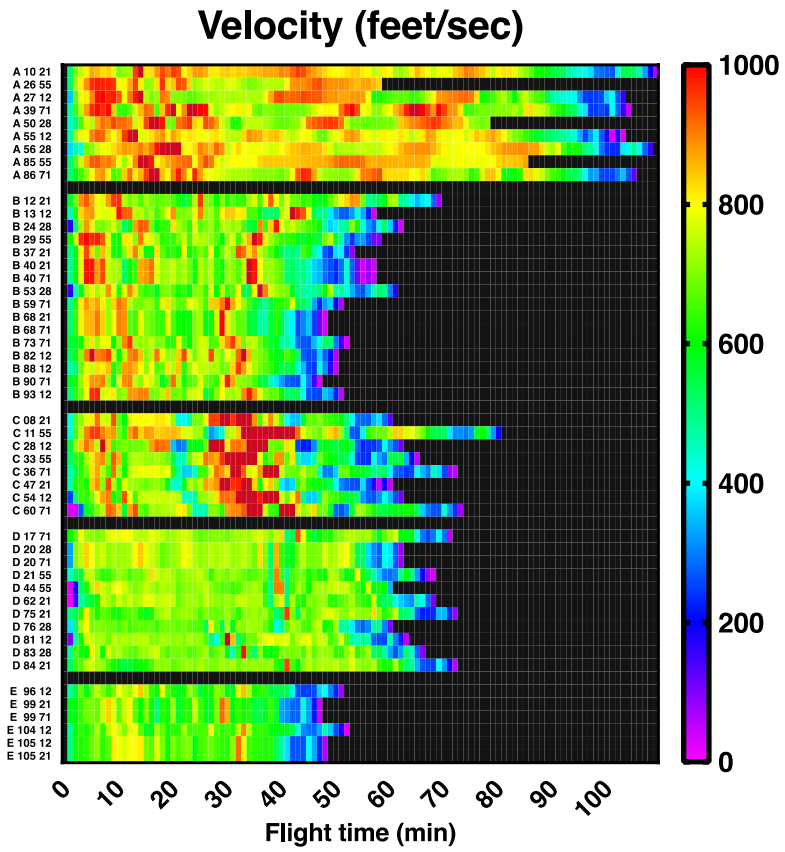

Figure 5.18. Heat Map Visualization of Aircraft Velocity (ft/sec) Averaged for Each Flight Minute (x-axis) and all PBA Flights (y-axis) by Profile, Flight#, Pilot#
The highest velocities occur in profiles A, B, and C; final descents show a reduction in speed as expected. Visualization of the within-profile rows indicate excellent consistency making profile an important fixed effect.

5.1.5.4 Independent (aircraft) Parameters – cabin pressure and delta pressure

The cabin pressure that the pilot experiences is maintained by a combination of valves and flows regulated by the aircraft's environmental control system (ECS). The aim is to achieve specific comfort and safety levels as the altitude (and external pressures) change. As described in more detail in Section 5.1.5.2, the designed values for cabin pressure are ambient pressure up to 8,000 ft altitude, held isobaric up to 23,000 ft, and then allowed to decrease with a 5-psi offset up to maximum altitude. As such, the isobaric region in the heat map in Figure 5.15 is 564 mmHg (equivalent to 8,000 ft altitude), denoted by the mid-green color. It is prominently displayed in profiles B and C, and to some extent in Profile E. The figure uses mmHg units as provided from the sensor system.

As the pilot breathes, the response of mask valves and regulators are referenced to the ambient cabin pressure. If the cabin pressure is stable in timeframes of breathing, presumably the breathing gear can respond appropriately. One conjecture is that within minute oscillations in cabin pressure from the ESC could compromise regulator/mask response and make breathing more difficult. Figure 5.19 explores the maximum within-minute changes in cabin pressure.

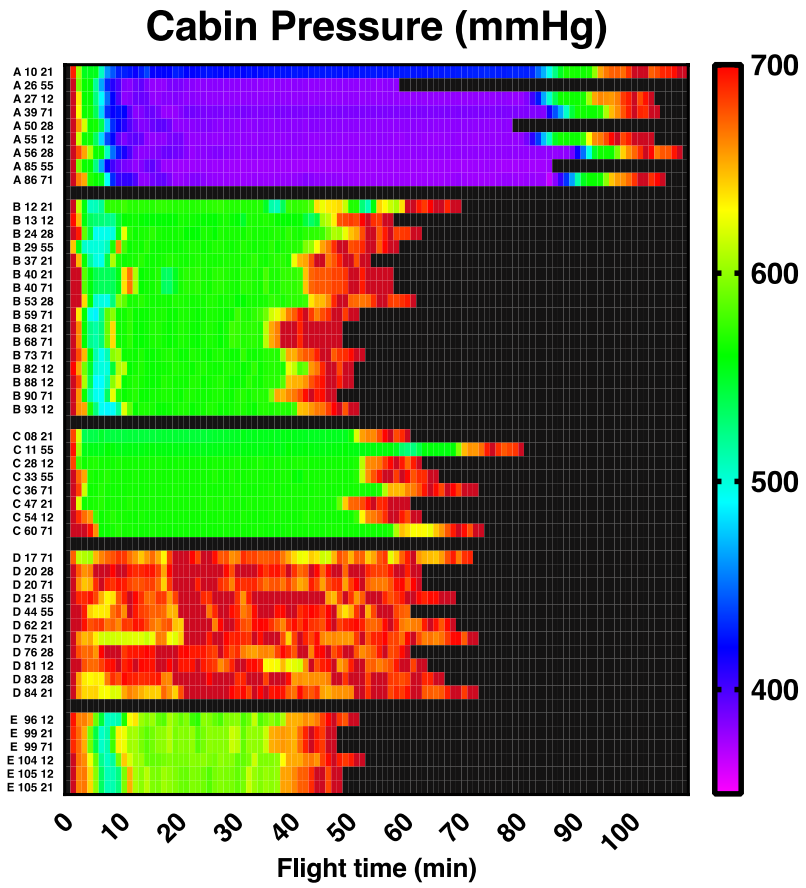

Figure 5.19. Heat Map Visualization of Aircraft Cabin Pressure (mmHg) Averaged for Each Flight Minute (x-axis) and all PBA Flights (y-axis) by Profile, Flight#, Pilot#
The lowest mean cabin pressures occur in Profile A above ~35,000 ft altitude; the purple color indicates about ½ atmospheres. The center sections of Profiles B, C, and E show that the aircraft is in the isobaric region at 8,000 ft equivalent pressure; the green color represents 550 mmHg which is equivalent to ~0.74 atmospheres. Red color indicates air pressures near 1 atmosphere (ground level). Visualization of the within-profile rows indicate excellent consistency making profile an important fixed effect.

As the pilot breathes, the response of mask valves and regulators are referenced to the ambient cabin pressure. If the cabin pressure is stable within breathing timeframes the AFE gear can respond appropriately. One concern is that within-minute oscillations in cabin pressure from the ESC could compromise regulator/mask response and make breathing more difficult. Figure 5.20 explores the maximum within-minute changes in cabin pressure.

The figure shows that Profiles A and C have relatively low within minute delta pressures and that the Profiles B, C, and E experience much more variability. In fact, the green to red range indicates within-minute pressure changes of 40 to 70 mmHg. These values are greater than the range of the differential mask pressure (DMP) parameter which tops out at ~20 mmHg, indicating that delta Cabin pressure may affect the pilot's ability to breathe easily.

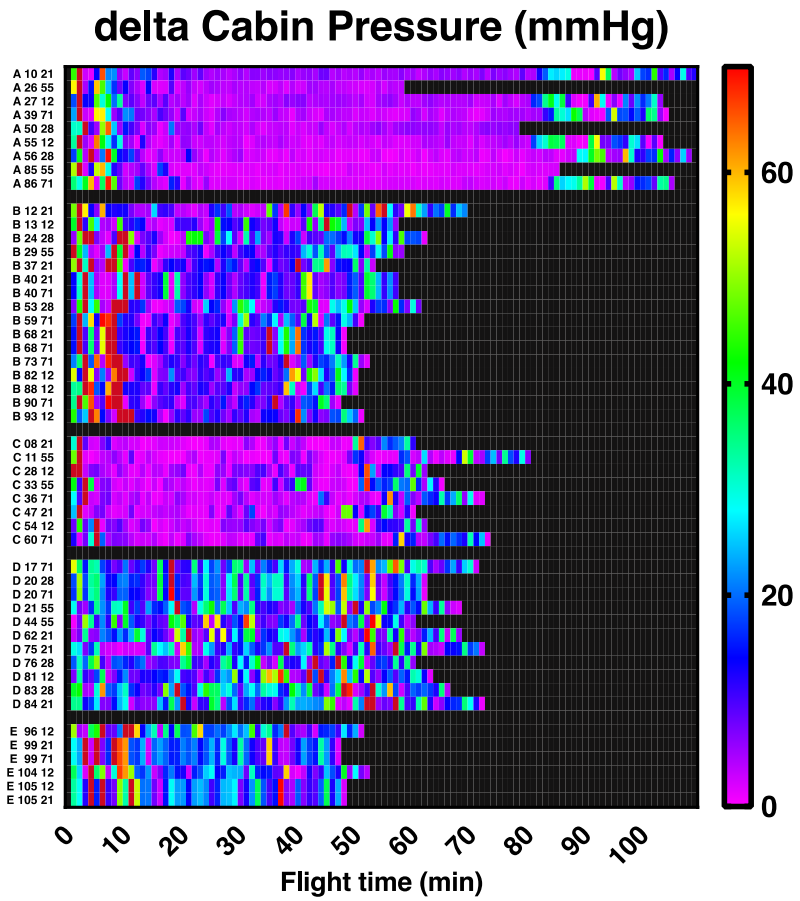

Figure 5.20. Heat Map Visualization of Change in Aircraft Cabin Pressure (mmHg) within Each Flight Minute (x-axis) and all PBA Flights (y-axis) by Profile, Flight#, Pilot# Profiles B, D and E show the most variability with the orange and red colors indicate fluctuations exceeding ~60 to 75 mmHg which are equivalent to about 7% to 10% of an atmosphere. The pressures developed by the pilot to activate mask/regulator flow are in the range up to 20 mmHg. In addition, flight profile B shows obvious "between flight" variability indicating potential disruptions in the normal behavior of the aircraft. Overall, this parameter demonstrates the most variability within profiles.

5.1.6 Summary of 1-Minute Data Statistics and Visualization

The analyses of the dependent and independent variables provide an overview of the general character and results from the PBA. The dependent (pilot) variables serve to quantify the levels of flow, and the instantaneous response from the breathing system that a pilot requires under a variety of actual military scenarios. These values provide specific targets for design and testing of masks, regulators, and breathing supplies. The QQ-plots indicate outliers and extreme values that warrant further investigation using higher resolution (20 Hz) data. Furthermore, the consistency of flights within profiles shown in the heat maps indicates that the VigilOX instrumentation is relatively robust in the face of combat maneuvers.

Specifically, some flights may require further detailed analyses of the dependent breathing variables as they standout visually in the heat maps. This does not mean there is anything wrong with the data; these data streams could reflect true pilot effects as they are all within physiological ranges. Flights are identified by Profile, flight#, pilot# as in the heat maps.

- BPM: Flights A,85,55 and C,54,12 – low values
- BPM: Flights B,24,28 and B,53,28 – high values
- Flow liters/min: Flight B,29,55 – some high values
- Max liters/min: Flights B,29,55 and B,68,21 – some high values
- Tidal liters/breath: Flight C,54,12 – some high values

The independent (aircraft) variables analyses serve primarily to document the range and variability of the pilot flight activities and stressors. For the most part, these data (velocity, altitude, G-force), are routinely monitored for all military flights. The notable exception is cabin pressure; this is the first time that an in-depth analysis of cabin pressure and variability has been statistically documented for real-world fighter pilot scenarios. For this section, the within-minute data was used to show that mean values are relatively stable, but that there is a great deal of cabin pressure change within flight minutes, especially in profiles incorporating aerobatics.

This Part 1 of the 1-min data analyses treats each parameter as an individual entity. Certainly, comparing heat maps could give some indication about how independent and dependent variables might be inter-related. For example, the high-altitude Profile A flights show a generally stable response in breathing rate and volumes, whereas the aerobatics in Profile B show a great deal of variance. However, such visual comparisons are only meant to be qualitative. In the following Part 2 of Technical Section 5, the focus is on the pilot-aircraft interaction using mixed-effects models to quantify how aircraft activity modifies pilot breathing responses quantitatively.

Part 1. Summary Statistics and Data Visualization

Findings:

F.5-1. Q-Q plots and heat maps are valuable visualization tools to quickly identify flight segments that contain breathing anomalies.

F.5-2. Higher breathing rates (BPM) are associated with aggressive aerobatic maneuvers.

F.5-3. The highest observed values of mean inspiratory flow rates in PBA pilots occurred in aerobatics profiles and some of the lowest observed values occurred in high altitude flights.

F.5-4. Highest values of peak inspiratory flow rate (maximum instantaneous flow) observed in PBA pilots under stress are below that of typical adult exertion stress tests observed in the laboratory. PBA profiles were limited to an aircraft maximum G-force of approximately 5.

F.5-5. Observations of PBA pilot tidal volume per flight minute are similar to those found in typical adults at low to moderate levels of aerobatic exercise.

F.5-6. PBA evaluated mask pressure variation to identify flight minutes with high oscillations and developed the Standard Deviation Mask Pressure (st. dev. MP) metric for use in the detection of potential breathing stress including those caused by mask valve dysfunction.

F.5-7. Heat maps of PBA flight minute data can be used to quickly identify outliers of the dependent breathing variables and flight segments recommended for further detailed analyses.

F.5-8. With the exception of breathing rate, flight minute pilot breathing data are lognormally distributed and must be treated as such in summary statistics and modeling evaluations.

Recommendations:

R.5-1. Quantitative measures of pilot breathing should be used in the creation of hardware and system specifications to meet pilot physiological needs and used to validate that individual integrated systems meet pilot physiological needs throughout all relevant flight envelopes." ***(F.5-1, F.5-7, F.5-8)***

R.5-2. Use of visualization tools: QQ-plots and Heat maps should be used to evaluate pilot – aircraft interactions, and implemented for integrated system testing/maintenance of jetfighters. ***(F.5-7, F.5-8)***

5.2 Mixed Effects Models: Evaluation of Aircraft – Pilot Interaction

Success of PBA is predicated on understanding the effects on pilot breathing from real-world flight activities using a controlled experimental design and curated dataset. The first step of the statistical analysis is developing clear hypotheses related to pilot breathing. The second step is then developing models to test those hypotheses. While the previous section (summary data across all flight minutes) provides the context for hypothesis testing, as well as some qualitative comparisons (e.g., heat map visualizations), more complex multivariable methods are required for a rigorous examination. Linear mixed-effects models allow the simultaneous evaluation of multiple independent variables (on the right side of the equation) with respect to their association with a single dependent (or "outcome") variable, in this case the pilot breathing parameter (on the left side of the equation).

5.2.1 Construction of Mixed-Effects Models for PBA

Mixed-effects models can be used to identify specific independent variables that are more or less likely to be associated with the dependent variable(s). As a simple example, if one assumes that higher respiration rate indicates more stress on the pilot, the resulting conjecture is that specific continuous variables (G-force, altitude, cabin pressure, etc.) are likely to modify this outcome. One may also hypothesize that other flight-specific variables (flight profile, mask configuration, etc.) can impact measurements of this outcome. Complex, multi-step procedures are used to examine all associations of interest, with results heavily influenced by the underlying data structure (including "balance") and the distribution of continuous variables.

The defining feature of the mixed-effects model is the ability to simultaneously evaluate fixed effects (experimental units explicitly defined for hypothesis testing) and random effects (experimental units drawn at random from a population of interest). The modeling approach used here is based on multivariable analysis using "restricted maximum likelihood" (REML) approximations that produce unbiased estimates of variance and co-variance. The underlying mathematics were first developed in 1937 by Bartlett (1937) and became a mainstream analytical tool implemented on mainframe computers for a variety of statistical applications (Harville 1977). The approach only became accessible for the general research community with the

advent of modern desktop computers with sufficient processing power and speed *circa* 1998. For this work, the "Mixed" Procedure of SAS statistical software (v. 9.4) was used (SAS Institute, Cary, NC).

5.2.1.1 Mixed-Effects Model Overview

The simplest form of the mixed effects model has a particular dependent variable on the left side and a linear multivariable function one the right side which is comprised of independent variables and coefficients that are ultimately calculated to minimize the error terms. For the PBA, the general form of the model considers one pilot parameter at a time as the dependent (y) variable, estimated as a function of all fixed and random effects. For example, a model considering 'breathing rate' as the dependent variable and 'configuration', 'altitude', 'G-force' could be written as:

$$Y_{h,i,j}\,(breathing\ rate) = \beta 0 + \beta 1(configuration)_{h,i} + \beta 2(altitude)_{h,i,k} + \beta 3(G\text{-}force)_{h,i,k} + \gamma_h + b_{hi} + \varepsilon_{hij} \quad \text{(eq. 5.1)}$$

Here, the investigator would be testing the hypothesis that the observed distribution of breathing rate would differ across specific 'configurations', and that measures would have a linear association (positive or negative) with 'altitude' and 'G-force'. The model subscripts *h*, *i*, and *j* refer to the h^{th} pilot, the i^{th} sortie, and the j^{th} flight segment, and the terms $\gamma_h + b_{hi} + \varepsilon_{hij}$ represent the random effects for 'pilot', 'sortie', and 'segment', respectively. Using these terms, the investigator can examine how variance observed in 'breathing rate' can be partitioned across randomly selected pilots, sorties, and flight 'segments'. The consideration of 'configuration' as a fixed effect and 'pilot' as a random effect can be used to communicate a key difference between fixed and random effects. For PBA, breathing measures are hypothesized to differ across specific 'configurations' (described in detail below). Thus, a limited number of explicit configurations are examined for their effects on breathing measures. These same breathing measures are also hypothesized to differ across 'pilots', but there is no hypothesis about specific pilots. As such, PBA pilots are a considered a random selection of all possible pilots, and 'pilot' number (along with 'sortie' and 'segment' number) is considered as a source of error (i.e., variation) in the breathing measures.

The β coefficients in the model are calculated best fit estimates that communicate the linear relationship (magnitude and direction) between independent variables and the dependent variable.

This (eq. 5.1) is only one example; ultimately, each model for a dependent variable can have different independent variables that explain the observed variance. The finalized model for each dependent variable, known as the "full" model, can be compared a "null" model (containing only a global intercept value [B0] and random effects) to estimate the amount of variability explained by model fixed effects. This procedure is shown in detail below.

5.2.1.2 Model Design Balance: Fixed Effects (categorical)

As described previously in Section 5.1, 50 total PBA flights were implemented for 1-min data evaluation across five flight profiles. The initial plan was to develop a balanced dataset across pilots, profiles, jets, and equipment. Upon triaging flights that met all criteria for these particular comparisons, the design balance became somewhat skewed. This is common in highly complex studies with finite resources. Table 5.7 shows the overall distribution of flights across the

designed profiles. (Note that FCP denotes front seat and RCP denotes backseat pilots.) The row totals are sufficiently balanced to allow statistical hypothesis testing across 'profiles'. The column totals for FCP vs. RCP, however, are quite unbalanced (45 vs. 5), and therefore likely to yield unreliable model results. Initial "full" model results for all dependent variables of interest showed no significant effects of 'seat' (FCP vs. RCP). Upon consideration of these preliminary results, and the lack of balance related to this variable, further testing of 'seat' was not performed in the final models.

Table 5.7. Design Balance – Flight 'Profiles' and Pilot Position (i.e., 'Seat')

Profile	Description	# FCP	# RCP	# Total
A	High Altitude	9	0	9
B	AeroBatics	14	2	16
C	Control	8	0	8
D	Down low	10	1	11
E	Isobaric G-Exercises	4	2	6
	Total	45	5	50

There are three basic configurations of breathing gear available for study within the 1-min datasets, as previously described in Technical Section 1. Again, the distribution of flights across these categories is somewhat skewed, but mixed modeling via REML estimation allows for evaluation despite minor imbalances. Table 5.8 shows the design balance for the respective gear configurations. Certainly, the USN and USAF configurations can be effectively compared (24 USN vs. 26 AF/AFRC flights), but the interaction between aircraft type (F-15 vs F-18) and AFE is more difficult to assess.

Table 5.8. Design Balance – Breathing Gear Configurations

Configuration	AFE	Regulator	O2 Connector	Plane	#
"F18_USN"	USN	--	CRU-103	F-18	24
"F18_AF"	AF/AFRC	CRU-73	EDOX	F-18	20
"F15_AF"	AF/AFRC	CRU-98	CRU-60	F-15	6

Throughout the PBA study, there were a series of repairs and updates to the VigilOX ISB modules resulting in six different configurations. This matrix (Table 5.9) is highly skewed making it difficult to reliably evaluate the effect of ISB model or revision within the full mixed models.

Table 5.9. Design Balance – VigilOX Systems

Configuration	Vigilox_ISB						#
	DEV003	DEV006	ISB001	ISB002	ISB003	ISB004	Total
F15_AF	3	3	0	0	0	0	6
F18_AF	2	0	7	1	5	5	20
F18_USN	1	0	4	5	14	0	24
Total	6	3	11	6	19	5	50

Configuration	Vigilox_ESB							
	EDEV04	EDEV05	EDEV08	ESB001	ESB002	ESB003	ESB004	Total
F15_AF	2	2	2	0	0	0	0	6
F18_AF	0	1	1	6	0	3	9	20
F18_USN	0	1	0	14	2	3	4	24
Total	2	4	3	20	2	6	13	50

The final interaction of interest is the pilot-profile analysis. Table 5.10 shows that pilots had two flights per profile on average, but that some of the profile/pilot boxes are under-represented. While a balanced dataset across pilots and profiles is highly desired, 'pilot' can still be examined as a random effect in the null and full mixed models, as each pilot flew a similar number of total flights. It should be noted that, in the full model, the random pilot effect is examined after adjusting for model fixed effects, including 'profile'.

Table 5.10. Design Balance – Pilot vs. Flight Profile: All Flights

Pilot	Profile Group					
	A	B	C	D	E	Total
12	2	4	2	1	3	12
21	1	4	2	3	2	12
28	2	2	0	3	0	7
55	2	1	2	2	0	7
71	2	5	2	2	1	12
Total	9	16	8	11	6	50

From this simple description, note that fixed effects for 'profile', 'configuration', and 'VigilOX' are worthy of examination, but that interaction terms can likely not be considered due to an overall lack of data across potential subcategories (e.g., 'profile×configuration'). Thus, any interaction effects would have to be considered as part of future efforts involving either more flights or a higher degree of experimental control (e.g., allowing variation in fewer experimental parameters).

The strength of mixed effects-models is that multiple variables can be analyzed at the same time and so the models gains strength overall. So, rather than assess each profile or each configuration in separate linear regression models, the "full" mixed models allow for simultaneous evaluation, while controlling for repeated observations (both within-flight and between-flights for a given pilot).

5.2.1.3 Variable Selection for Modeling: Independent (continuous) Variables

As discussed in Technical Section Part 1, there are many more variables that could be used for modeling than are listed in Table 5.5. The choices are based on which are easiest to understand from a practical perspective, and which are relatively independent of each other. For example,

altitude and cabin pressure are strongly correlated and so only one or the other should be chosen for the right side of the equation in any given model.

The first step for choosing which independent variables to include in the initial models is to prepare a correlation matrix. As these variables are not similarly distributed to each other, they were evaluated using non-parametric statistics (i.e., Spearman rank-order correlations). Table 5.11 shows the correlation coefficients; absolute values at 0.60 or above (highlighted in the table) were considered too correlated to allow both parameters to appear in the same model. Negative values indicate anti-correlation which has the same effect.

Table 5.11. Spearman Correlation Coefficients for Selected Independent Variables

	mean G3	max G3	mean Alt	delta Alt	mean Velocity	mean Cabin press	delta Cabin press
mean G3	1.00	0.88	-0.19	0.40	-0.01	0.24	0.39
max G3		1.00	-0.35	0.53	-0.04	0.39	0.52
mean Alt			1.00	-0.25	0.65	-0.96	-0.50
delta Alt				1.00	-0.11	0.26	0.65
mean Velocity					1.00	-0.60	-0.22
mean Cabin press						1.00	0.52
delta Cabin press							1.00

Not surprisingly, the mean G3 and max G are highly correlated, as are mean cabin pressure and mean altitude, and delta cabin pressure and delta altitude. The correlation between velocity and mean cabin pressure is unexpected. As such, the calculations can only incorporate one from each pair in the full model; the initial choices based on these observations were ‘mean_Velocity’, ‘delta_Cabin_press’, and ‘mean_G3’.

5.2.1.4 Variable Selection For Modeling: Dependent (breathing) Parameters

The selection of dependent (breathing) variables is not a statistical process but one of physiological interest. Each dependent variable is treated in a separate model; if they are correlated with each other, the results are expected to be similar, but no information is lost due to co-linearity. Initially, separate models were constructed for the parameters listed in Table 5.3. Other variants of breathing were also explored; for example, the standard deviation of mask pressure (‘s.d. Mask’) was assessed in addition to the differential mask pressure (‘DMP’) to assess finer structure in breathing variance. As expected, ‘DMP’ and ‘s.d. Mask’ are highly correlated. Table 5.12 shows the correlation coefficients among all dependent variables. Values at 0.60 or higher are highlighted indicating that results of their respective models are likely to be similar.

Table 5.12. Spearman Correlation Coefficients for Selected Dependent Variables

	breaths/min	mean Flow liters/min	max flow liters/min	mean liters/breath	DMP mmHg	s.d. Mask mmHg
breaths/min	1.00	0.52	0.04	-0.41	0.11	0.35
mean Flow liters/min		1.00	0.52	0.49	0.50	0.62
max flow liters/min			1.00	0.50	0.80	0.53
mean liters/breath				1.00	0.40	0.29
DMP mmHg					1.00	0.81
s.d. Mask mmHg						1.00

5.2.2 Developing Models of Increasing Complexity

The following discussion shows three model types to demonstrate how a mixed-effects model is developed and applied. Specifically, the methods for constructing the “Null Model” (including a global intercept and random effects), the “Full Model” (including all fixed and random effects),

and the "Reduced Model" (excluding one or more fixed effects from the full model) are described.

5.2.2.1 Developing the "Null Model"

The first step in mixed-effects modeling is developing a baseline against which to evaluate results of subsequent models that incorporate independent variables as fixed effects.

The basic null model begins with a description of the variance of a generic Y (dependent) variable based on only the global intercept and error terms:

$$Y\ (dependent\ Var)_{hij} = \beta 0 + \gamma_h + b_{hi} + \varepsilon_{hij} \quad \text{(eq. 5.2)}$$

where any given 1-minute estimate corresponds to the j^{th} flight 'segment' (i.e., 1 min), the i^{th} 'sortie', and the h^{th} 'pilot'. Given these designations, γ_h represents the random effect of the h^{th} pilot, b_{hi} represents the random effect of the i^{th} sortie for the h^{th} pilot, and ε_{hij} represents the random effect for the j^{th} 1-min segment of the i^{th} sortie for the h^{th} pilot. In this null model, the global intercept $\beta 0$ is used to estimate the average value of all Y's, with random effects then describing the magnitude of deviation for any Y_{hij} from this central value. Fittingly, residual error is maximized in the null model, and partitioned into that which is observed between pilots (corresponding to γ_h), between flights for a given pilot (corresponding to b_{hi}), and within flights (corresponding to ε_{hij}).

5.2.2.2 Developing the "Full Model"

The second step is to build the "Full Model" (eq. 5.3) which adds in the fixed effects that have been identified as potentially interesting in describing variance.

$$Y\ (dependent\ Var)_{hij} = \beta 0 + \beta 1\ (Config.)_{hi} + \beta 2\ (VigilOX)_{hi} + \beta 3\ (Profile)_{hi} + \beta 4\ (mean\_Velocity)_{hij} + \beta 5(mean\_G3)_{hij} + \beta 6(\ delta\_cabin\_pressure)_{hij} + \gamma_h + b_{hi} + \varepsilon_{hij} \quad \text{(eq. 5.3)}$$

This model considers the influence from some physical aircraft parameters, as well as that from within-flight changes based on flying conditions. The $\boldsymbol{\beta}$ coefficients are optimized by the calculations to reduce the $\gamma_h + b_{hi} + \varepsilon_{hij}$ error terms. Note that this is a generalized linear model (GLM) that includes mask configuration, VigilOX version, and flight profile of the i^{th} sortie for the h^{th} pilot, as well as the mean velocity, mean G3, and delta cabin pressure for j^{th} 1-min flight segment of the i^{th} sortie for the h^{th} pilot.

5.2.2.3 Developing the "Reduced Model"

The third step is to remove from the full models one or more specific fixed effects for the purpose of evaluating residual variance. This type of evaluation informs the amount of total variance explained by a specific fixed effect after adjusting for all other fixed effects. For PBA, one reduced model was considered, where 'VigilOX' was excluded as a fixed effect (eq. 5.4).

$$Y\ (dependent\ Var)_{hij} = \beta 0 + \beta 1\ (Config.)_{hi} + \beta 2\ (Profile)_{hi} + \beta 3\ (mean\_Velocity)_{hij} + \beta 4(mean\_G3)_{hij} + \beta 5(\ delta\_cabin\_pressure)_{hij} + \gamma_h + b_{hi} + \varepsilon_{hij} \quad \text{(eq. 5.4)}$$

5.2.3 Model Evaluation – Linkage to PEs

The most important feature of mixed-effects models is the ability to partition variance from a complex experiment with multiple input parameters. The big question to be answered is:

> ***How much of the change in breathing response is caused by differences among pilots, and how much is due to complex influences from the aircraft?***

The premise of PBA is that changes in breathing response are signs of pilot stress, and reducing these effects is likely to reduce the random appearance of PEs). As such, there are three possible paths that can lead to a PE outcome:

1. PEs can happen to any pilot at any time, because specific aircraft conditions and parameters conspire to overwhelm the pilot's physiology: airplane's "fault".
2. PEs occur only to certain pilots at random times, the aircraft systems are functioning nominally: pilot's "fault" or health state.
3. PEs occur at random due to interactions between a pilot's health state and the particular aircraft parameters at that time; confluence of events.

The first statement is the basis for root cause corrective action (RCCA) efforts implemented by the military. The second statement is generally the default assumption that there is an adverse event, but no overt equipment failure is found. The third statement, that there was an interaction effect, is probably closest to the truth.

PBA was designed to shed light on the interaction between aircraft and pilot. The "*h*" subscripts in the equations 5.2, 5.3, and 5.4 for the null, full, and reduced models (respectively) indicate the identity of the pilot for each parameter. Therefore, the mixed effects model allows the assessment of the amount of variability incurred due a difference in pilot # (*h*) only, as long as there are sufficient repeat measures; that is, different pilots flying the same profiles in the same airplanes using the same gear.

For example, Table 5.10, shows how many times each pilot flew each profile (average =2); as discussed before, this is not perfectly balanced, but the REML calculations can estimate the overall partition of variance with and without adjustment for the profile variable *"$\beta 3\ (Profile)_{hi}$*". The same calculations can be performed for other fixed effects variables, including mask configuration and VigilOX id. Again, these calculations incorporate information from all variables in the model; this feature of the mixed-effects model allows variance estimation and partitioning despite the imbalances shown in Tables 5.8, 5.9, and 5.10. The caution is that fewer repeat measures result in wider confidence limits of the estimates.

For the continuous independent variables like 'delta_cabin_pressure', 'mean_G3', and 'mean_velocity', there are strong statistics. For example, in the heat map for the mean altitude parameter in Figure 5.16, there are hundreds of individual measures of minute altitude ranging from ground-level to >40,000 ft, each tagged with that flight minute's values for all dependent (breathing) values. Although different profiles have more or fewer flight minutes for each aircraft continuous value, this is observed for all of the aircraft parameters regardless of profile #. The importance of knowing how much variance in breathing measures comes from the pilot vs. the aircraft is that this provides the template as to how to address the PE's problem. If variability in breathing response is mostly confined to differences among flight-related parameters, then the team leans towards path 1 above, and focuses deeper on understanding profiles, masks, etc. If

the variability in breathing response is mostly confined to differences among pilot #, then the focus should be more on pilot physiology, current health-state, mental stressors, etc. The one caveat here is the question of personal gear; for example, is the mask more of a pilot related parameter or an aircraft parameter? For the purposes of the mixed effects model, mask/regulator configuration was considered an independent variable.

These partitions could be different for different breathing parameters, which adds more power to the overall interpretation of results and gives direction for mitigation strategies. Recall that the initial hypotheses state that changes in physiological breathing parameters towards higher stress are linked with future probability of a PE occurrence.

5.2.4 Mixed-Effects Model Results

5.2.4.1 Variance Partitions

Each dependent variable was treated as the "$Y\ (dependent\ Var)_{hij}$" in the null, full, and reduced models. When statistically warranted, parameters were modeled after lognormal transformation to satisfy underlying assumptions. The generalized methods for estimating variance components from mixed model calculations are available in the literature (Pleil et al. 2018). Variance components estimates show that the pilot contribution to total variance is low for the most part; only the breathing rate (BPM) variable is more related to differences between pilots rather than influences from aircraft (independent) parameters with a 60% vs. 40% split. For convenience, results summaries for each dependent variable are listed below:

Breathing Rate Variance:

61% variance between pilots;
39% variance within pilots (17% between flights and 22% within flights)
Differences largely related to underlying pilot physiology

Inhalation Flow Variance (mean):

18% variance between pilots;
82% variance within pilots (57% between flights and 25% within flights)
Differences highly related to aircraft parameters: specific profiles and flight segments

Inhalation Flow Variance (max):

10% variance between pilots;
90% variance within pilots: 46% between flights and 44% within flights
Differences almost entirely related to aircraft parameters: specific profiles and flight segments

Breath Volume Variance:

19% variance between pilots;
81% variance within pilots: 49% between flights and 32% within flights
Differences highly related to aircraft parameters: specific profiles and flight segments

Differential Mask Pressure (DMP) Variance:

9% variance between pilots;
91% variance within pilots: 44% between flights and 47% within flights
Differences almost entirely highly related to aircraft parameters: specific profiles and flight segments

Standard Deviation Mask Pressure (s.d. MP) Variance:

17% variance between pilots;
83% variance within pilots: 59% between flights and 24% within flights
Differences highly related to aircraft parameters: specific profiles and flight segments

Figure 5.21 shows the relative distribution charts of the variance components graphically. The blue fields denote the variance attributed to the differences between pilots; the red and green fields partition the variance attributed to the aircraft parameters. Within-flight variability is an overall indicator of "typical" changes during a flight, and comprises activities common to all flights including take-off, landing, climbs, descents, etc. Between-flight variability is more of an indicator of the difficulty of the different profiles. This is illustrated in the independent variable heat maps in Sections 5.1.3.1 to 5.1.3.6.

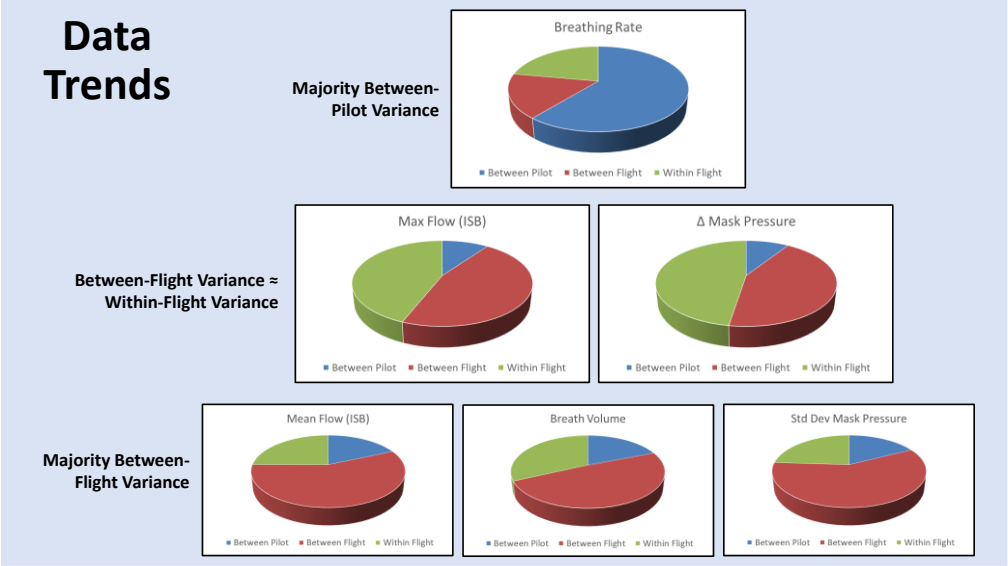

Figure 5.21. Graphical Representation of Variance Components
Only breathing rate shows a dominant between pilot effect; the remaining breathing variables are primarily driven by aircraft parameters.

5.2.4.2 β-parameter Estimates

The β-parameters in the various models are optimized values that provide the best fit between the independent variables and the particular dependent variable. These parameters cannot be compared directly as they are dependent on the units of the independent variables. However, they are important for making overall comparisons of value of fit between the null model and the improvement derived for estimating variance when adding more information to the right side of the equation. Each β-parameter has units of (dependent/independent) variable; for example, in the DMP model where DMP is in units of mmHg, the β-parameter for velocity has units of (mmHg)/(ft/sec), etc. The "p-value" associated with each β-parameter indicates the likelihood that the contribution to the model is statistically significant; the usual convention is to use $\alpha = 0.05$ as the discriminator level.

Tables 5.13 and 5.14 show the raw data output for each dependent (breathing) parameter; the "estimate" columns are the β-parameters and the Pr > |t| columns reflect the p-value with respect to the t-test statistic of significance at $\alpha = 0.05$. Values below 0.05 are considered significant for this work, and are shown in red. The intercept row represents the result for β_0 from the null

model from eq. 5.2. Table 5.13 results are based on dependent variables (breathing rate, mean flow, max flow, tidal volume) calculated from ISB and Table 5.14 results for dependent variable (DMP, st. dev. MP) are calculated from ESB. Note that the models use F-18 USN, VigilOX ISB004, and Profile Group C as the controls and are assigned "0" for the respective β-parameter; this is standard procedure in mixed effects modeling and serves to anchor the results within each group.

Table 5.13. Solutions for Effects of Dependent Variables Calculated from ISB Channels

Aircraft Effect		Breathing rate		flow volume (mean)		flow volume (max)		breath (tidal) volume	
		Estimate	Pr > |t|	Estimate	Pr > |t|	Estimate	Pr > |t|	Estimate	Pr > |t|
Intercept		16.1417	0.0022	3.0171	<.0001	3.9343	<.0001	0.3108	0.0455
Configuration	F15_AF	0.8345	0.6161	0.01476	0.8857	0.07755	0.4362	-0.01866	0.8726
Configuration	F18_AF	-1.158	0.1045	-0.142	0.0013	-0.0169	0.6923	-0.059	0.2361
Configuration	F18_USN	0	.	0	.	0	.	0	.
Vigilox_ISB	DEV003	-0.05461	0.9701	-0.02652	0.7682	0.4047	<.0001	-0.06074	0.552
Vigilox_ISB	DEV006	-2.7773	0.2095	-0.1275	0.3505	0.162	0.2221	0.01114	0.9427
Vigilox_ISB	ISB001	0.7274	0.5163	-0.2771	<.0001	0.03103	0.6433	-0.3295	<.0001
Vigilox_ISB	ISB002	0.9447	0.4924	0.05968	0.4814	0.1816	0.027	-0.01759	0.8543
Vigilox_ISB	ISB003	1.1507	0.3259	-0.1985	0.006	0.1724	0.0139	-0.2917	0.0004
Vigilox_ISB	ISB004	0	.	0	.	0	.	0	.
Profile_Group	A	-0.2344	0.8092	-0.1963	0.0011	-0.01493	0.7971	-0.2055	0.0025
Profile_Group	B	1.6057	0.0672	0.1117	0.0388	0.2468	<.0001	-0.00377	0.9509
Profile_Group	D	0.3456	0.7246	-0.03299	0.5854	0.02326	0.6924	-0.07043	0.3042
Profile_Group	E	0.6149	0.573	0.1072	0.1107	0.3593	<.0001	0.04723	0.5354
Profile_Group	C	0	.	0	.	0	.	0	.
mean_Velocity		0.00085	0.0001	0.000022	0.0689	0.000097	<.0001	-0.00002	0.0892
lndelta_cabin_press		0.1124	0.0057	0.01069	<.0001	0.0128	0.0003	-0.00073	0.7836
lnmean_G3		3.095	<.0001	0.2033	<.0001	0.141	<.0001	0.05617	<.0001

Table 5.14. Solutions for Effects of Dependent Variables Calculated from ESB Channels

Aircraft Effect		DMP		st.dev MP	
		Estimate	Pr > |t|	Estimate	Pr > |t|
Intercept		1.7772	<.0001	0.4505	0.0066
Configuration	F15_AF	0.1281	0.3706	-0.0333	0.7743
Configuration	F18_AF	0.09208	0.1234	0.01134	0.8153
Configuration	F18_USN	0	.	0	.
Vigilox_ESB	EDEV04	-0.08549	0.6598	-0.08933	0.5752
Vigilox_ESB	EDEV05	-0.08343	0.5107	-0.08758	0.4005
Vigilox_ESB	EDEV08	0.2345	0.1318	0.1148	0.3658
Vigilox_ESB	ESB001	-0.1906	0.0055	-0.1088	0.0605
Vigilox_ESB	ESB002	-0.07055	0.632	-0.1793	0.1411
Vigilox_ESB	ESB003	-0.01582	0.8596	-0.03203	0.6556
Vigilox_ESB	ESB004	0	.	0	.
Profile_Group	A	-0.01873	0.832	-0.04086	0.5678
Profile_Group	B	0.3618	<.0001	0.2706	<.0001
Profile_Group	D	0.2644	0.0062	0.1827	0.0236
Profile_Group	E	0.3372	0.0011	0.1053	0.2085
Profile_Group	C	0	.	0	.
mean_Velocity		-0.00008	0.0018	-0.00008	<.0001
lndelta_cabin_press		0.03418	<.0001	0.02379	<.0001
lnmean_G3		0.2195	<.0001	0.1436	<.0001

It is important to note that the individual input values for VigilOX descriptors are highly unbalanced (see Table 5.9) and therefore, should be treated with some skepticism. The configuration parameters are somewhat more balanced but the first row (F-15 AF) represents only 6/50 values and must also be treated carefully. The remaining parameters, Profile Group and the continuous variables (mean velocity, log delta cabin pressure, and log G3) are all well balanced and should be considered robust.

Based on the overall structure of the full model, the statistically significant results are summarized in Table 5.15. Here, the breathing rate is independent of profile and only influenced by flight velocity, cabin pressure and G-force, whereas max flow volume is only affected statistically by profiles B and E, but not by the fine-structure of the flights themselves. The remaining breathing parameters are scattered in their influences.

Table 5.15. Summary of Statistically Significant Aircraft Parameter Influences on Pilot Breathing Measurements

Pilot Breathing	Profile	Profile	Profile	Profile	mean_Velocity	delta_cabin_press	mean_G3
	A	B	D	E	feet/sec	mmHg	G
Breathing rate					X	X	X
flow volume (mean)	X	X				X	X
flow volume (max)		X		X			
breath (tidal) volume	X						X
DMP		X	X	X	X	X	X
st.dev MP		X	X		X	X	X

5.2.4.3 Interpretation of VigilOX Influence on Full Model

The midstream updates to VigilOX software and some minor technical modifications were not part of the PBA design, and so must be treated separately. As shown in Table 5.9, these differences are not balanced across the study and so their effect (if any) was treated as an aggregate phenomenon. The concept was to compare the full model (eq. 4) to the null model (eq. 2) both with and without inclusion of the VigilOX parameter. The difference should provide an estimate of the overall influence of this confounding effect.

Table 5.16 shows the relative explained variance components from full Model (eq. 5.3) and the reduced Model (eq. 5.4) wherein the VigilOX effect was removed. Overall, VigilOX model or revision had little influence over the totality of the PBA study. The greatest VigilOX influence was seen on the tidal volume (liters/breath) parameter. This issue arose in the QQ-plot of tidal volume measurements in Figure 5.8 wherein a number of values were found that were not physiologically possible. A modest VigilOX influence is seen for the max Flow parameter; as this measurement is dependent on instantaneous flow, it is surmised that software revisions may have affected detector response. The two effects are highlighted in the Table 5.16.

Table 5.16. Overall influence of VigilOX model/revision on pilot breathing parameters

Pilot Parameter	units	full Model	reduced Model
BPM	breaths/min	8%	10%
meanFlow	liters/min	25%	23%
maxFlow	liters/min	34%	24%
Tidal volume	liters/breath	24%	9%
DMP	mmHg	36%	30%
st. dev. MP	mmHg	40%	38%

Upon further investigation, the anomalous outcome for tidal volume appears to be heavily influenced by flight 54 and ISB004. The heat map shown in Figure 5.22 was rearranged by ISB model on the y-axis; the labels also indicate profile, flight#, and pilot#. Note that the ISB model data are mostly dependent on the flight profile and that the main outlier is the last row for flight 54. This appears quite influential as there are only five ISB004 flights overall. This particular flight is discussed in detail in Technical Section 6. DEV006 is slightly biased high, but this is

inconclusive as there are only three flights represented. Overall, the VigilOX influence on the global model appears minimal.

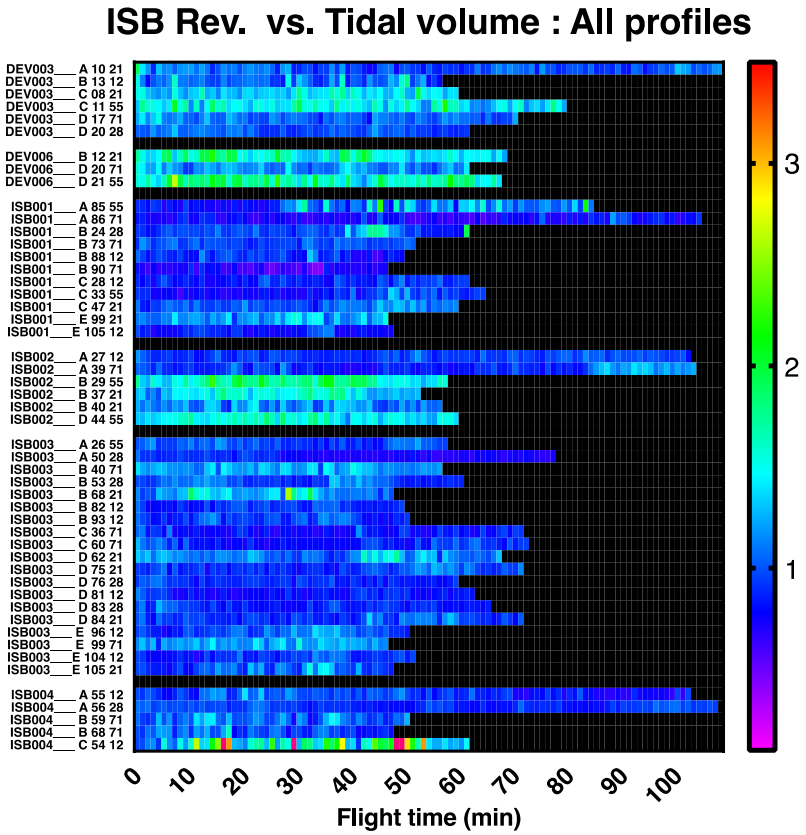

Figure 5.22. Heat Map Showing Outcome of VigilOX Variance Component Modeling and Influence on Tidal Volume
The overall differences within-VigilOX i.d. rows are dependent on aircraft parameters, and the between VigilOX patterns are relatively consistent. It is possible that DEV006 is biased slightly.

5.3 Conclusions from 1-min Data Analyses

The analyses of 1-minute data compilations provide a pragmatic window into the aircraft – pilot interaction. Prior to these evaluations, little had been documented about the actual physiological breathing needs of pilots in high performance aircraft in real-world scenarios. Three main outcomes from these analyses will help guide future activities and help reduce the incidence of adverse effects on pilots. This overall guidance is grouped by breathing supplies, aircraft flight segments, and future monitoring.

5.3.1 Guidance for Aircraft Breathing Supplies

Probably the most important outcome from Part 1 Technical Section of the 1-min data analyses is the determination of how much PBA pilots actually breathe during real-world scenarios. This is presented in Table 5.4 shows the statistical summary of median (central tendency) and extreme values. Of particular interest are the 97.5th and 99th percentile columns that set the lower limits as to what any breathing supply, OBOGS or LOX, needs to be capable at the particular percentile. For example, the median value of flow required by PBA pilots is about 17.8 liters/min, but 1% of the time, they needed 35 liters/min for a full minute. Of additional

interest is the maximum (instantaneous) flow requirement; overall, within any flight minute, the median value required is 74.4 liters/min of instantaneous flow, but 1% of the time, the breathing system needs to be able to respond to supply an instantaneous rate of 158 liters/min.

Similar guidance is derived from the BPM values. This parameter shows the response required for the mask/regulator part of the breathing supply. On average, the on/off frequency required is 18 times per minute; but at least 1% of the time, the pilot may require up to 31 on/off cycles per minute, possibly with 2 liters/breath each; the hysteresis in the mask/regulator system needs to accommodate this situation.

5.3.2 Guidance for Flight Activities

The mixed model discussion, which is the centerpiece of Part 2 of Technical Section 5, provides two main results. The first is partitioning the overall variance of response between effects driven by the aircraft parameter and effects driven by differences between pilots. This is important when deciding on training missions and other non-combat flying. Certainly, pilots need to practice all manner of aerobatics and aggressive flight segments, but the outcomes demonstrated in Figure 5.21 provide some guidance as to where mitigation could occur. There are three tiers of variance distribution. Breathing frequency (BPM) is primarily a between-pilot phenomenon, that is, some pilots breathe more frequently than others in response to the same aircraft stimuli. A mid-range occurs for max (instantaneous) inhalation flow (liters/min) and for delta mask pressure (DMP mmHg) wherein the between pilot differences are small and variance is coming mostly from the aircraft parameters being split evenly between- and within-flights. The third tier is comprised of mean inhalation flow (liters/min), breath tidal volume (liters/breath) and standard deviation of mask pressure (st.dev. MP mmHg) where there is also a small between-pilot variance component, but the between-flight variance is dominant.

The modeling results show that that the physiological make-up of the pilot primarily influences breathing frequency, but the remaining breathing parameters are influenced primarily by flying profile. Table 5.15 indicates that the important independent variables affecting breathing effort were found to be aircraft velocity, change in cabin pressure, and G-force.

5.3.3 Guidance for Future Monitoring

The direct measurement of pilot breathing parameters is as yet not a standard procedure in military jets. These analyses demonstrate the wealth of information that could be gleaned from physiological monitoring, show how to interpret the results with robust statistical analyses, and provide a baseline against which additional flights could be compared. Routinely deploying VigilOX or analogous monitoring systems would be a valuable surveillance tool for continuous monitoring of the pilot/aircraft interaction, and possibly assist in diagnosing adverse events, retrospectively.

Part 2. Mixed effects models

Findings

F.5-9. Mixed effects models of six dependent pilot physiological response metrics indicated that most variability was likely due to flight/equipment related factors, with the exception of breathing rate which was due to individual factors.

F.5-10. Breathing rate: 61% of total breathing rate variance is attributable to individual differences in PBA pilots indicating that breathing rate is more strongly dependent on individual pilot physiology than on external flight factors.

F.5-11. Inhalation Flow Variance (mean): Approximately 18% of total measurement variance is attributable to PBA individual pilot physiological differences indicating larger effect of flight/equipment on mean flow

F.5-12. Inhalation Flow Variance (max): Approximately 10% of measurement variance is attributable to PBA individual pilot physiological differences indicating larger effect of external stimuli on sudden rapid inhalations.

F.5-13. Breath Volume Variance: Approximately 19% of total breath volume variance is attributable to PBA individual pilot physiological differences indicating a larger effect of flight/equipment on breath volume.

F.5-14. Differential Mask Pressure (DMP) Variance: Approximately 9% of Differential Mask Pressure (DMP) variance is attributable to PBA individual pilot physiological differences. Factors affecting DMP variation are experienced similarly by all PBA pilots.

F.5-15. Standard Deviation of Mask Pressure Oscillations: Only 17% of Standard Deviation of Mask Pressure Oscillations variance is attributable to PBA individual pilot physiological differences indicating larger effects of flight/equipment.

F.5-16. Aircraft velocity, delta cabin pressure (max – min cabin pressure within a 1-min window), and G-force are significant predictors of Breathing Rate, Differential Mask Pressure, and Standard Deviation Mask Pressure.

F.5-17. Peak inspiratory flow is not strongly correlated with aircraft velocity, delta cabin pressure, or G-force, but rather with differences in flight profile.

F.5-18. G-force is a significant predictor for all six PBA pilot breathing response metrics.

F.5-19. A mixed-effects model analysis showed that VigilOX hardware and software updates throughout the PBA study were a significant predictor for 4 of the 6 dependent variables but did not affect the interpreted conclusions.

F.5-20. Mixed-effects model results indicate that the main sources of variability in PBA pilot breathing parameters are imposed by aircraft flight activities and breathing gear, rather than by individual PBA pilot physiology.

Recommendation:

R.5-3. Mixed-effects model results indicate that the main sources of variability in PBA pilot breathing parameters are imposed by aircraft flight activities and breathing gear, rather than by individual pilot susceptibilities. Mitigation of pilot stress is more likely achieved by modifying the aircraft and gear parameters. ***(F.5-9, F.5-11 to F.5-18)***

References

Bartlett MS. 1937. Properties of sufficiency and statistical tests. Proceedings of the Royal Society of London. Series A-Mathematical and Physical Sciences, 160(901):268-282.

Berndtsson G, 2004. Peak inhalation air flow and minute volumes measured in a bicycle ergometer test. Journal of the International Society for Respiratory Protection, 21(1-2):21-29.

Blackie SP, Fairbarn MS, McElvaney NG, Wilcox PG, Morrison NJ, Pardy RL. 1991. Normal values and ranges for ventilation and breathing pattern at maximal exercise. Chest 100(1):136-142.

Coyne K, Caretti D, Scott W, Johnson A, Koh F, 2006. Inspiratory flow rates during hard work when breathing through different respirator inhalation and exhalation resistances. Journal of Occupational and Environmental Hygiene, 3(9):490-500.

Evans JA, Whitelaw WA, 2009. The assessment of maximal respiratory mouth pressures in adults. Respiratory Care, 54(10):1348-1359.

Harville DA, 1977. Maximum likelihood approaches to variance component estimation and to related problems. Journal of the American Statistical Association, 72(358):320-338.

Lansing RW, IM BS, Thwing JI, Legedza AT, Banzett RB, 2000. The perception of respiratory work and effort can be independent of the perception of air hunger. American Journal of Respiratory and Critical Care Medicine, 162(5):1690-1696.

Lausted CG, Johnson AT, Scott WH, Johnson MM, Coyne KM, Coursey DC, 2006. Maximum static inspiratory and expiratory pressures with different lung volumes. Biomedical Engineering OnLine 5(1):29.

Nicolo A, Girardi M, Bazzucchi I, Felici F, Sacchetti M, 2018. Respiratory frequency and tidal volume during exercise: differential control and unbalanced interdependence. Physiological Reports, 6(21):e13908.

Pleil JD, 2016a. QQ-plots for assessing distributions of biomarker measurements and generating defensible summary statistics, Journal of Breath Research (Aug.) 10:035001.

Pleil JD, 2016b. Imputing defensible values for left-censored “below level of quantitation” (LoQ) biomarker measurements, Journal of Breath Research (Oct.) 10(4):045001

Pleil JD, 2015. Understanding new “exploratory” biomarker data: a first look at observed concentrations and associated detection limits, Biomarkers 20(2):168-169.

Pleil JD, Stiegel MA, Madden MC, and Sobus JR, 2011. “Heat Map Visualization of Complex Environmental and Biomarker Measurements”, Chemosphere 84:716-723.

Pleil JD, Sobus JR, Stiegel MA, Hu D, Oliver KD, Olenick C, Strynar MJ, Clark M, Madden MC, and Funk WE, 2014. Estimating common parameters of log-normally distributed environmental and biomonitoring data: harmonizing disparate statistics from publications, Journal of Toxicology and Environmental Health, Part B. Critical Reviews 17:341-368.

Pleil JD, Stiegel MA, Wallace MAG, and Funk WE, 2018. Human biomarker interpretation: the importance of intra-class correlation coefficients (ICC) and their calculations based on mixed models, ANOVA, and variance estimates. Journal of Toxicology and Environmental Health B, Critical Reviews 21(3):161-180.

Rennie CE, Gouder KA, Taylor DJ, Tolley NS, Schroter RC and Doorly DJ, 2011. Nasal inspiratory flow: at rest and sniffing. Int Forum Allergy Rhinol, 1(2):128–135.

Technical Section 6: Engineering Analysis of Pilot Breathing

This section is a comprehensive study of associations and interactions of various flight conditions, air crew equipment (hardware and control), and their effects on pilot breathing. It provides examples of breathing system anomalies, stressful flight conditions, and analytical tools to promote PE prevention, pilot safety and pilot health. It reflects the PBA's approach of focusing on the "human-in-the-loop" and treating the human-aircraft as a holistic, integrated system.

6.0 Introduction

This section develops the concept of using the high resolution 20-Hz data to discern specific events and anomalies that could trigger pilot breathing problems. As these data have already been aligned and curated in Technical Section 4, any perturbations are expected to be effects from the pilot, breathing gear, and aircraft interaction, not from data acquisition or sensor irregularities. This section is the most complex of the technical sections in that it deals with a basis set of measurement data from over 115 flights from about 30 data-channels, in aggregate representing about 200 million data points. This section is treated as a series of highly detailed investigations applying different statistical and graphical tools to explore various pilot – aircraft interactions, often within just a few consecutive breaths. Ultimately, the individual results are collected to present an overview of what happens at the short-time frame (50 ms) level of scrutiny serving as the philosophical contrast to the Technical Section 6 analyses that focused on the 1-minute reduced data.

This section also identifies specific issues regarding the pressure/flow interactions of pilot breathing gas that lead to discomfort and general breathing stress. These issues are driven by a number of different triggers; the most prominent triggers are mask valve response, regulator hysteresis, safety pressure, and cabin pressure fluctuations. Throughout the development of the analyses described, additional flights were conducted to focus on specific perturbations in the breathing system. This section provides completely novel insights into pilot breathing at breath-to-breath time resolution that have never been explored before.

The topics discussed in Technical Section 6 evolved over the two-year period of the PBA study. Overall, the PBA team derived implications of different regulator and mask configurations, and observed impacts of safety pressure, cabin pressure, and inlet flow and pressure disharmony. The following topics are each discussed in detail:

6.1 Comparison of USAF and USN Configuration with Positive Pressure
6.2 Cabin Pressurization and Effects on Pilot Breathing
6.3 Aircraft Pressure Study, With and Without Pressure Schedule Control, Priority 4 (E)
6.4 Priority 5 (H)
6.5 Summary of Profile H Mini-Study
6.6 Regulator Data Recorded through MadgeTech Instrumentation
6.7 Timing/Breathing Sequence Issues (including Phase Shift)
6.8 Pilot Breathing Assessment Results Analysis
6.9. Mini Studies
    6.9.1 Flight 29
    6.9.2 Flight 38
    6.9.3 Flight 95

6.1 Comparison of USAF and USN Configuration with Positive Pressure on F/A-18

There are two fundamental differences in air supply delivery implementation in the PBA, and they mimic USAF and USN mask/regulator configurations on F/A-18 LOX jets. USN uses the "safety pressure" mechanism; USAF does not. USN use a "100%" O_2 supply at all altitudes whereas USAF uses an O_2 schedule dependent on altitude controlled by a "diluter demand" function in the regulator. Both styles have benefits and challenges. Positive pressure could limit contamination from outside of the mask getting in but does increase the effort to crack open the exhalation valve in the mask during normal operation. Diluter demand schedules represent an effort to reduce oxidative stress at lower altitudes, but 100% O_2 simplifies the implementation of the regulator mechanics.

6.1.1 Introduction and Driving Differences

The USN configuration provides a small amount (~3 mmHg) of positive pressure, which could help overcome pressure drop through mask inlet passages if needed, assisting breathing. On the exhalation side, the pilot needs to push air past the positive pressure. Exhalation is a passive activity under regular breathing, which changes to a forced exhalation at times when positive pressure is present. PBA analytical tools (e.g., Hysteresis, Phase Shift tool) show that breathing under the USAF configuration without positive pressure on the F/A-18 is closer to natural open-air breathing. Figure 6.1 is a comparison of the same pilot's breathing with the Positive Pressure (CRU-103), and the Diluter Demand configuration on an F/A-18 legacy, LOX breathing system.

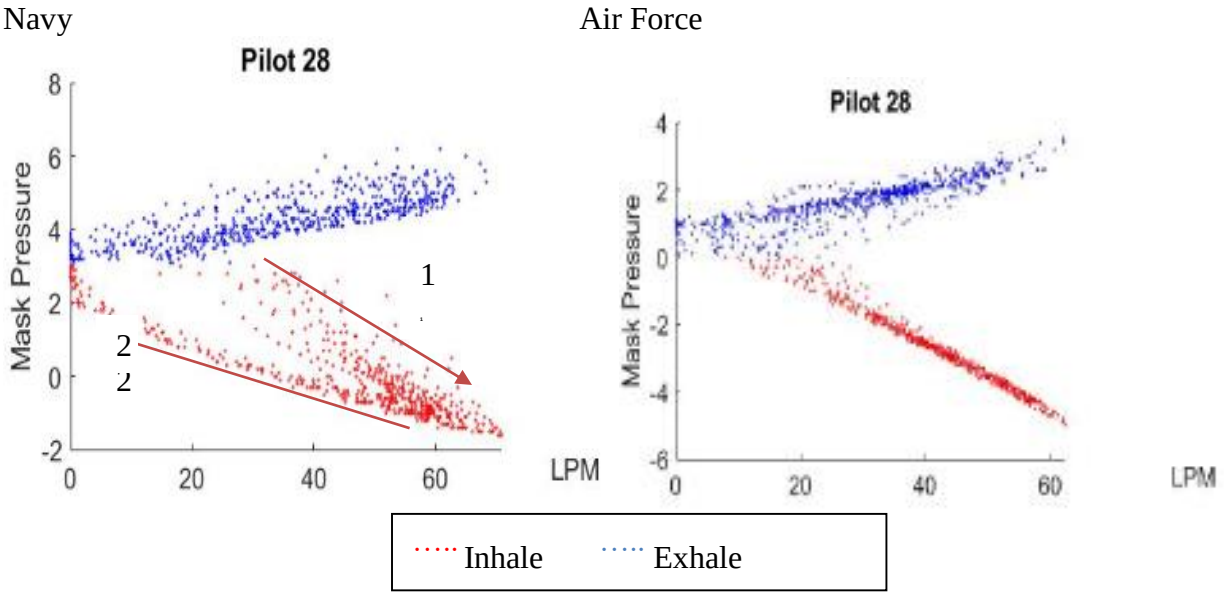

Figure 6.1. A Modified "Trumpet Curve" Relating Mask Pressure and Flow Rate Shown are 1200 co-timed data pairs from 20 Hz, 1-minute data. The USN-like configuration that provides, positive (safety) pressure (left panel) shows more flow rate during the 1st half of the inhalation, and less as the inhalation ramps down for the same amount of pressure representing a hysteresis effect. With the F/A-18 in USAF configuration with no safety pressure, it is a uniform flow response to pressure, both on the inhalation and exhalation sides.

6.1.2 O_2 Concentration in the USN and USAF F/A-18

In the USAF configuration, the oxygen concentration follows a schedule based on altitude, with typical values ranging from 30 to 50%. The USN supplies its pilots with what is referred to as

nominal 100% oxygen, although the concentration derived from VigilOX ppO_2 output is often 90% O_2. Note that this still significantly higher than open-air or USAF pilot breathing. Figure 6.2 represents the O_2 concentration differences during an aerobatic flight profile.

Navy Air Force

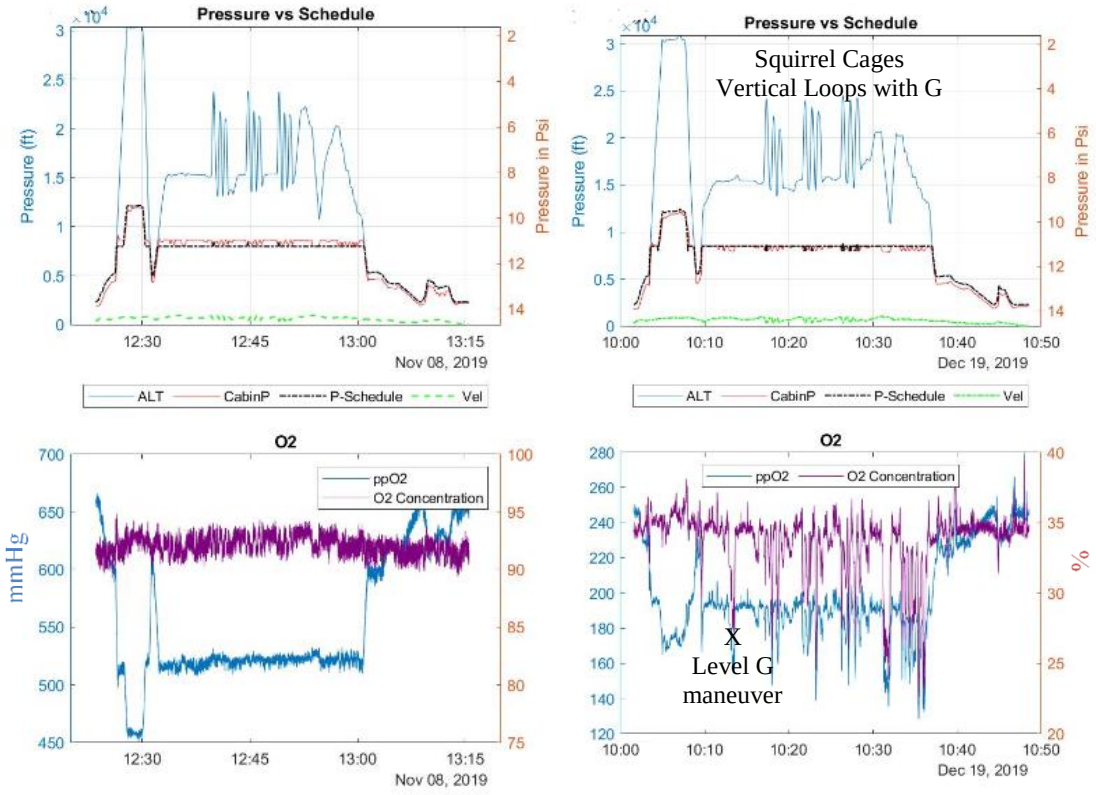

Figure 6.2. Under USN Schedule. O_2 Concentration Stays Between 90 and 95% Per the USAF schedule, O_2 may vary 10-15% not only with altitude change, but also during level G maneuvers which increase the dynamic (reference) pressure. These are Profile B flights.

The USAF O_2 concentrations were measured between 23% and 37% for altitudes up to 30,000 ft according to the O_2 schedule; at 45,000 ft the O_2 concentration increased to 45%, as documented in the high-altitude Profile A flights. In the case of the USN O_2 schedule, the partial pressure oxygen (ppO_2) constantly changes at a rate matching the ambient pressure, so the ratio of ppO_2/Line pressure stays at a near constant > 90%.

The effects of high O_2 concentration have been studied by Dr. Michael J. Decker, who lectured on The Impact of High Oxygen Levels on Cerebral Perfusion following his laboratory brain-MRI study (Damato E.G., Flak T.A., Mayes R.S., Strohl K.P., Ziganti A.M., Abdollahifar A., Flask C.A., LaManna J.C. Decker M.J. Neurovascular and Cortical Responses to Hyperoxia: Enhanced Cognition and Electroencephalographic Activity Despite Reduced Perfusion).

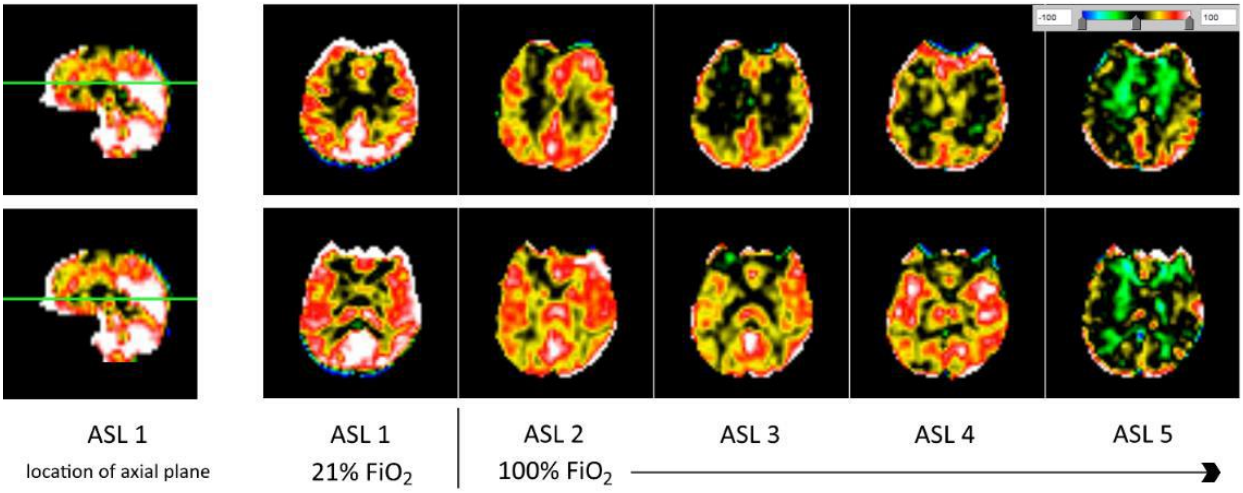

Figure 6.3. The Panels Show a Progression in Time of Brain Imaging
The baseline O_2 supplied is 21% (ASL 1), after which 100% O_2 is implemented for 28 minutes. Cerebral Perfusion with 100% O_2 shows marked reduction in Cerebral Blood Flow (CBF) in every study participant (30/30).

Legend: ASL = Arterial Spin Labeling (in this case taken at incremental time stamps of 7 minutes)
FiO_2 = Fraction of Inspired Oxygen

(Source: Damato E.G., Flak T.A., Mayes R.S., Strohl K.P., Ziganti A.M., Abdollahifar A., Flask C.A., LaManna J.C. Decker M.J. Neurovascular and Cortical Responses to Hyperoxia: Enhanced Cognition and Electroencephalographic Activity Despite Reduced Perfusion).

Cerebral blood flow (CBF) reduction is 63% of baseline at the final measurement (28-minute time point). However, while overall perfusion decreases, a segmented look reveals that certain very specific areas increase in blood flow. These areas are:

- Globus Pallidus (responsible for voluntary movement)
- Middle and Superior Occipital Gyri (Visual Processing)
- Angular Gyrus (Processing of visually perceived words, number processing and spatial cognition)

In other words, hyperoxia detected in the above areas is responsible for improved cognitive performance, task accuracy and response time, vision, and memory recall. In contrast, the area of the brain where perfusion is negatively affected (decreased blood flow) is the Frontal Lobe, controlling the Executive function. Other terms associated with this area are planning, working memory, inhibition, self-monitoring, and self-regulation.

6.1.3 Hysteresis Comparison for Safety Pressure/No Safety Pressure Configurations on LOX Equipped Aircraft

In Figure 6.4, the concept of breath-by-breath hysteresis of regulator response to the driving pressure is invoked. Ideal pilot breathing (through a mask and air supply), should strive to be similar to open-air breathing– a demand from the lung should result near-instantly in a proportional flow from the regulator, independent of when it occurs during the breath cycle.

In the positive pressure system (USN F/A-18), initial inhalation flow demand exceeds supply. Later within the breath, inhalation supply exceeds demand, as such, Pilot and Supply are ‘out of sync.’

Figures 6.4 (USAF) and 6.5 (USN) plot the Inhalation flow as a function of line-cabin differential pressure for a single inhalation breath per graph, with the hysteresis represented by the magnitude of the blue arrows.

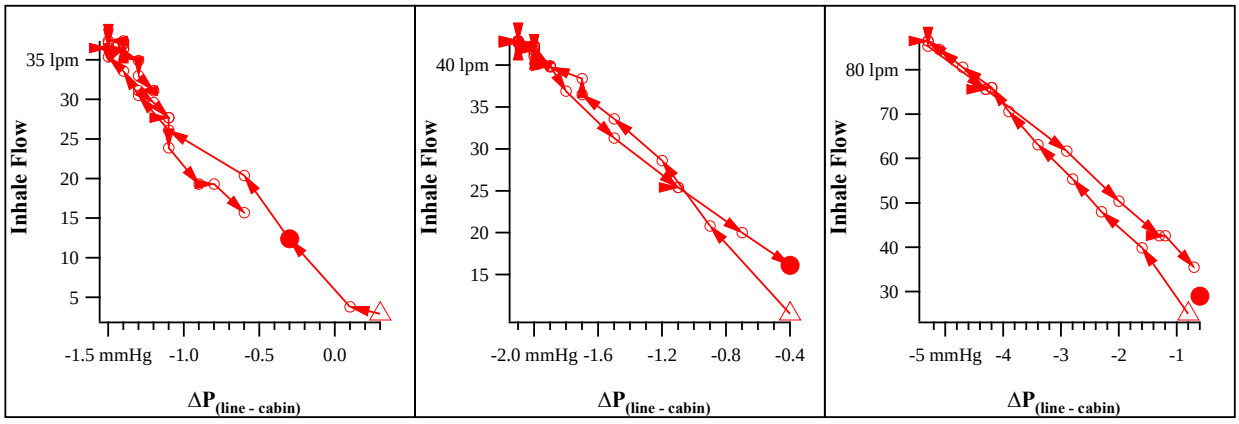

Figure 6.4. USAF, No Safety Pressure
Three consecutive breaths with almost no hysteresis (FLT-058)

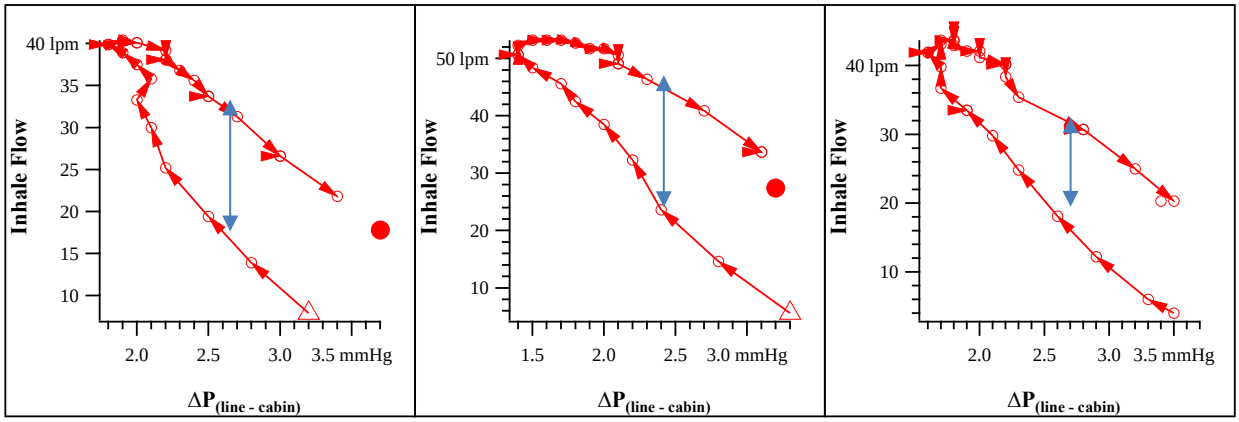

Figure 6.5. USN, with Positive Pressure Provided by Regulator
Three consecutive breaths with moderate hysteresis (FLT-045). The hysteresis is the difference in flow as indicated by the arrows are 0.25, 0.42 and 0.23 lps (converting from lpm to lps), respectively.

6.1.4 Effort of Breathing

The calculation of the breath effort is the work required to move gas in and out of the lungs. The PBA is limited to using mask pressure as a surrogate for lung pressure. During inhalation, lung pressure is always less than mask pressure, and during exhalation, pressure is always greater than mask pressure on exhalation. This means that with the PBA instrumentation, the associated effort is always slightly underestimated. The values reported are one component of the true 'work-of-breathing,' namely the effort required to move gas in and out of the lung.

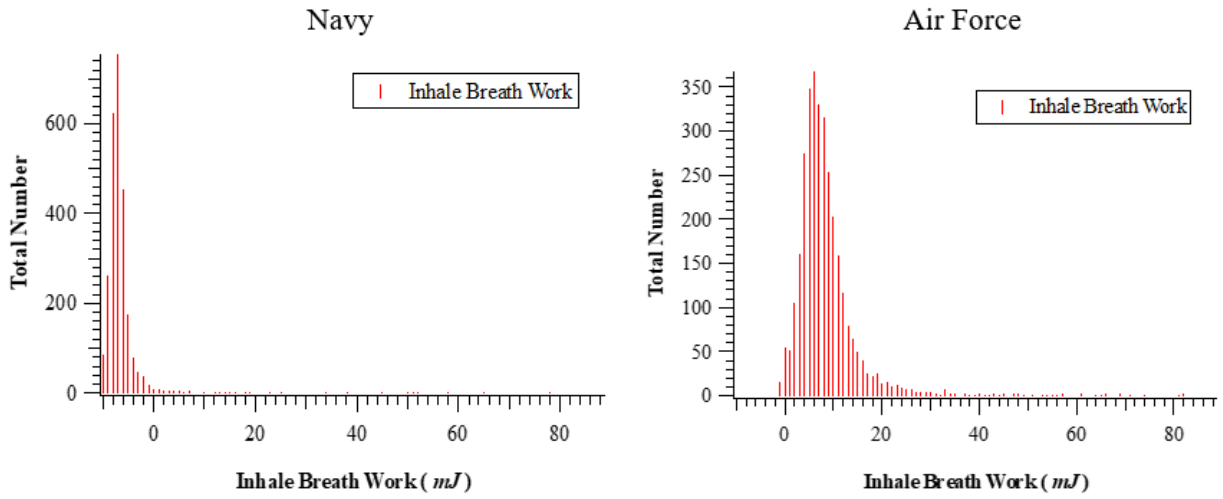

Figure 6.6. Partial Effort of Inhalation
Negative values in this example on the USN side are due to positive Mask Pressure (due to low draw from the supplied positive pressure) and a convention of the inhaled volume considered negative.

There are additional aspects of true work of breathing (WOB) that do not include actual breathing activity. These could be any isometric work where the pilot exerts pressure but due to no pressure change moves no volume; e.g., delta V (change in volume) is zero, but the pilot is exerting pressure. With these caveats, the results are useful for comparative effort calculation across configurations, pilots and profiles. Figure 6.7 shows the comparison of partial effort of exhalation from Flight 45, augmenting inhalation data shown previously in Figure 6.4. The front seat pilot (FCP) is in USN configuration, and the rear seat pilot (RCP) is in USAF configuration.

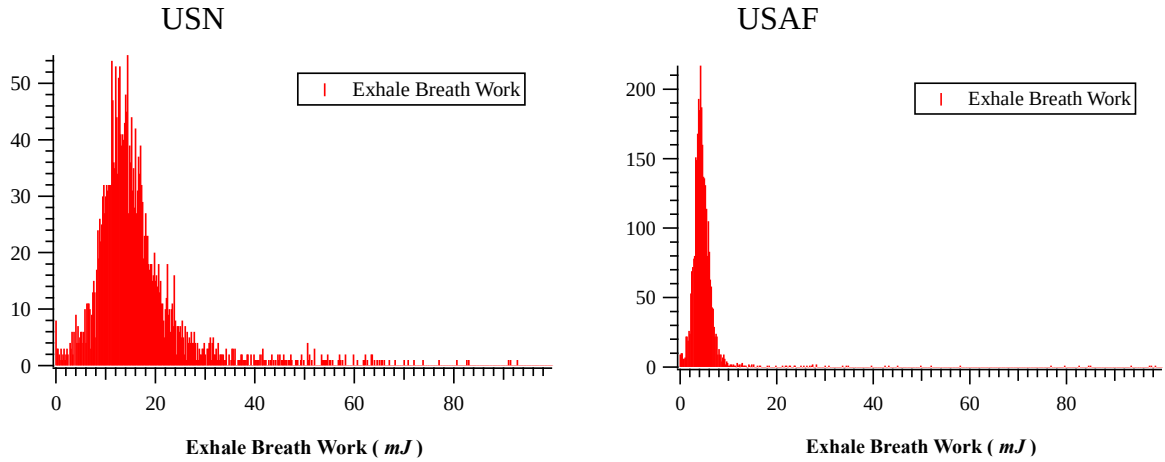

Figure 6.7. Flight 45, Dual Seat Instrumented with Different AFE
The Partial Effort of Exhalation is lower with the USAF regulator (RCP), than the USN (FCP) on an F/A-18.

Conclusion: while inhalation seems to be less "work" due to the positive pressure air supply, exhalation is more work. This finding coincides with pilot interviews.

6.1.5 Phase Shift

The PBA introduces the Phase Shift concept to measure driving pressure and resulting flow temporal disharmony for masked breathing. The use of Phase Shift is discussed further in Section 6.7.

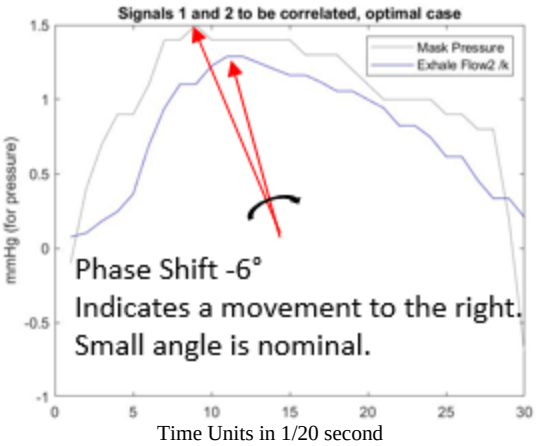

(a) Nominal Exhalation

Negative phase shifts (Figure 6.8a) are the result of pressure leading flow. A small delay/ shift is expected.

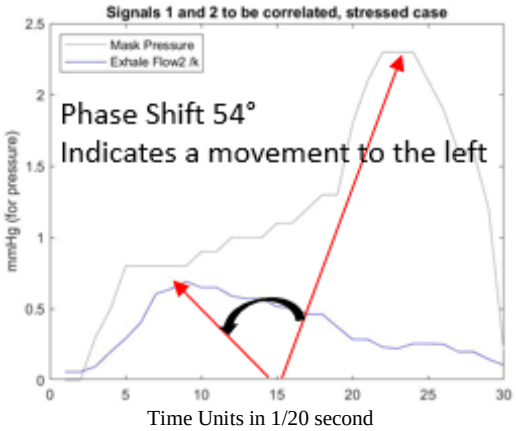

(b) A Pressure-Flow Mismatch

Positive phase shifts (Figure 6.8b), indicate a reverse order of flow peaking before the pressure peaks $T_{\text{Peak Pressure}} - T_{\text{Peak Flow}} > 0$

Figure 6.8. Nominal Exhalation and Pressure-Flow Mismatch

USN (CRU-103) and USAF (CRU-73) differences are characterized with this Phase Shift tool.

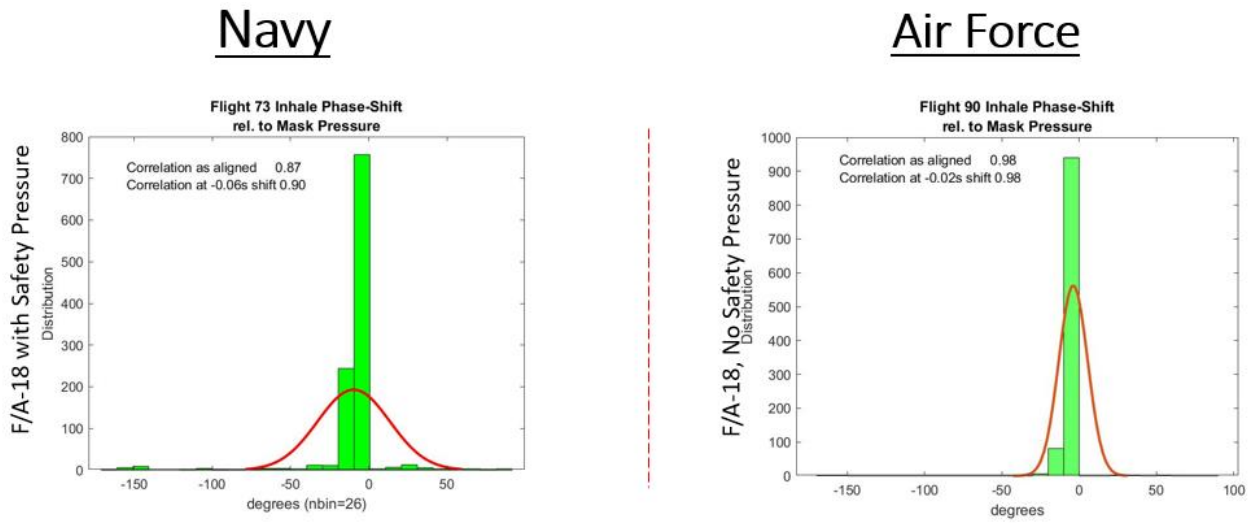

Figure 6.9. Inhalation Phase Shift

The F/A-18 USAF configuration w/o Safety Pressure (right) shows an unencumbered inhalation profile. Note the near-perfect 98% correlation achieved with no safety pressure (USAF). On the left, 30% of inhalations show phase lags of 10°-20° with the F/A-18 legacy USN configuration w/Safety Pressure. Same Pilot #71, both aerobatic Profile B.

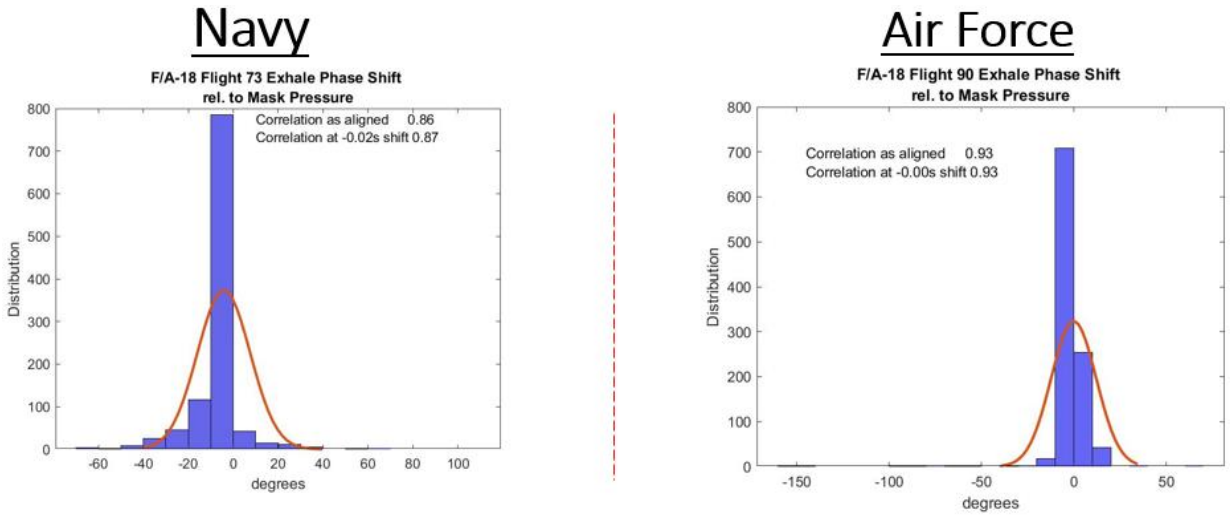

Figure 6.10. Exhalation Phase Shift
Comparison shows greater negative phase shifts (delayed response) during exhalation for the positive pressure setup (left), than the same F/A-18 flown with no positive pressure supply (right).

A final word on the Phase Shift tool, as compared with the legacy "trumpet curve," through which peak pressure and peak flow are related: the trumpet curve is agnostic to the time aspect of the peak flow delivery as related to peak pressure. In this sense, the Phase Shift adds a 3d dimension, Time, to the Pressure-Flow relationship. Further, the sign of the phase shift is an additional clue: a large negative shift means a slow response (e.g., sticky valve of the same function, or design choice when it comes to safety pressure); positive phase shift scenario includes an early closing valve leading to air volume being trapped and a pressure build-up, usually caused by the opposite function, e.g., positive pressure rushing *in*, clipping the *exhale*.

F.6-1*. *Phase shift analysis is a numerical tool to quantify disharmony between pilot breathing demand and the breathing system delivery. The test results are corroborated by independent pilot observations.*

R.6-1. For flights where both mask pressure and flow are availabl,e apply phase shift analysis for early detection of equipment issues or validation of pilot reports. Collapse flights or segments into bins or single numbers of Phase Shift Mean, +/- standard deviation, lag (time) and correlation coefficients. ***(F.6-1)***

There is virtually no "phase shift" in the no-safety pressure inhalation (Figure 6.4, USAF configuration on right). There are more lags in the USN configuration Exhalation with positive pressure (Figure 6.5 left). These results indicate that breathing from a LOX source on a diluter demand system, such as applied by the Air Force, is more natural (closer to open-air breathing).

6.1.6 Machine Learning Results Trained on Pressure – No Flow (PNF)

Data scientists (NASA Ames and WFF) set up semi-supervised learning and trained on identified PNF from two flights and applied the model to additional flights. From the flights tested, machine learning has found instances on the USN CRU-103 equipped flights. Especially instructional are side-by side comparisons of segments from the same flight (i.e., Flight 68), the front seater in USAF configuration, and the aft in USN configuration.

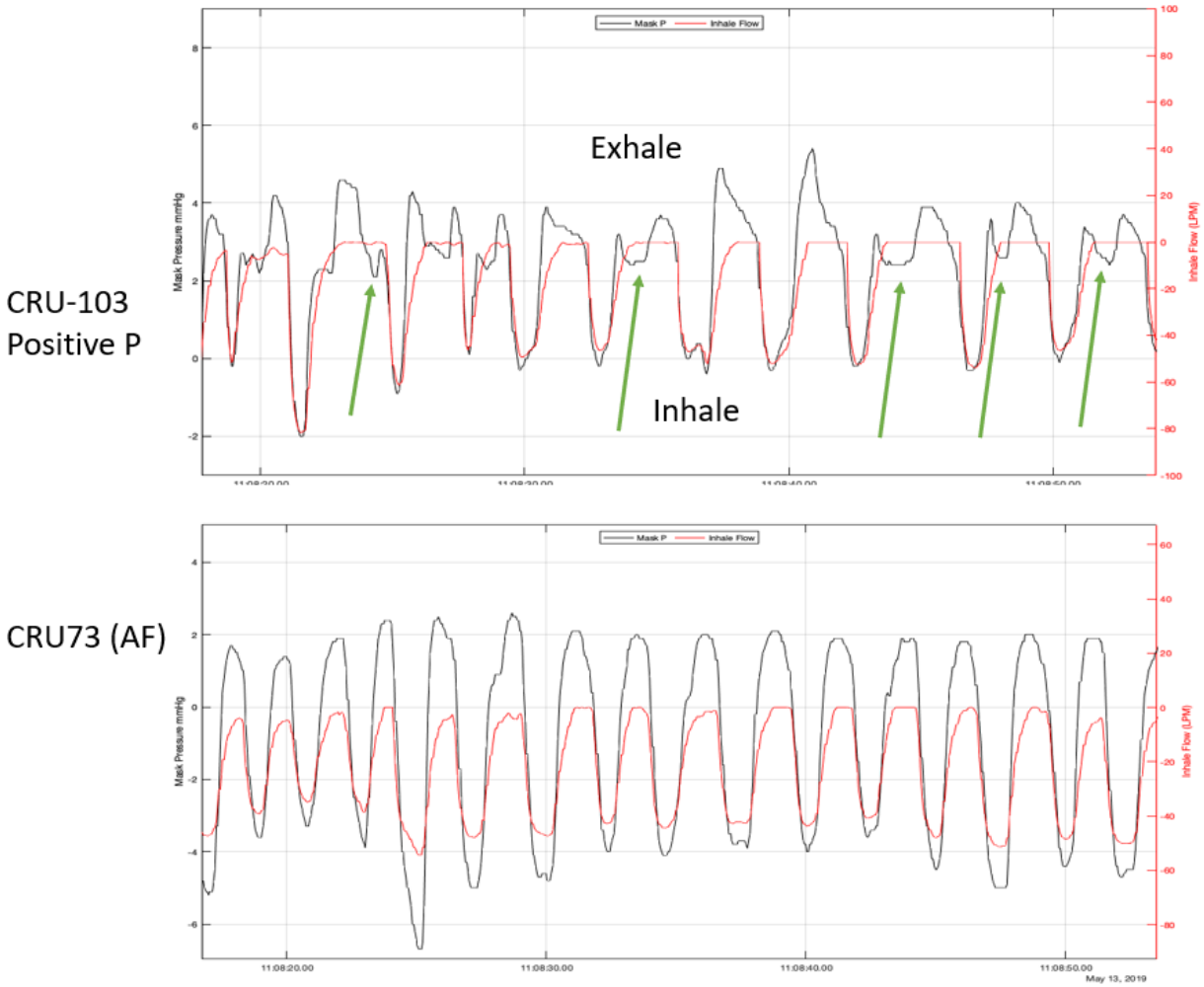

Figure 6.11. Max AB Climb Segment
The black line is Mask Pressure, and the red line is inhalation flow. The green arrows point to 'Pressure-no-flow' (PNF) examples, which is are breathing supply disharmony. These are on the USN configured seat, and not on the USAF.

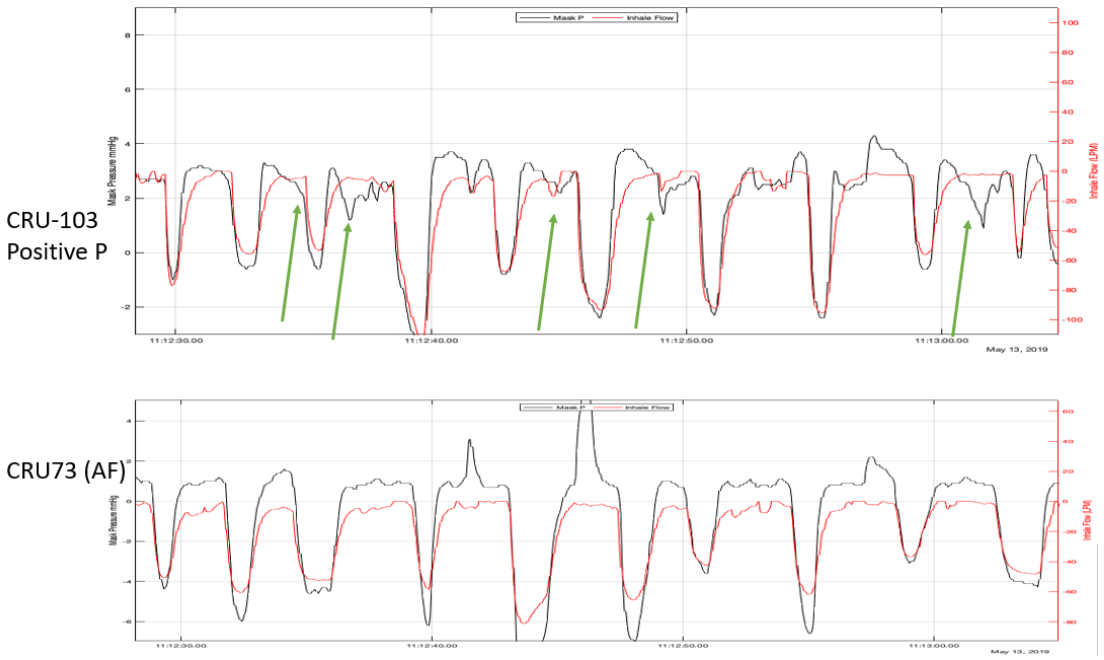

Figure 6.12. Combat Descent
The black line is Mask Pressure, and the red line is inhalation flow. The green arrows point to 'Pressure-no-flow' (PNF) examples, which are breathing supply disharmony. On this 2-seater flight, these are on the USN configured seat, and not on the USAF.

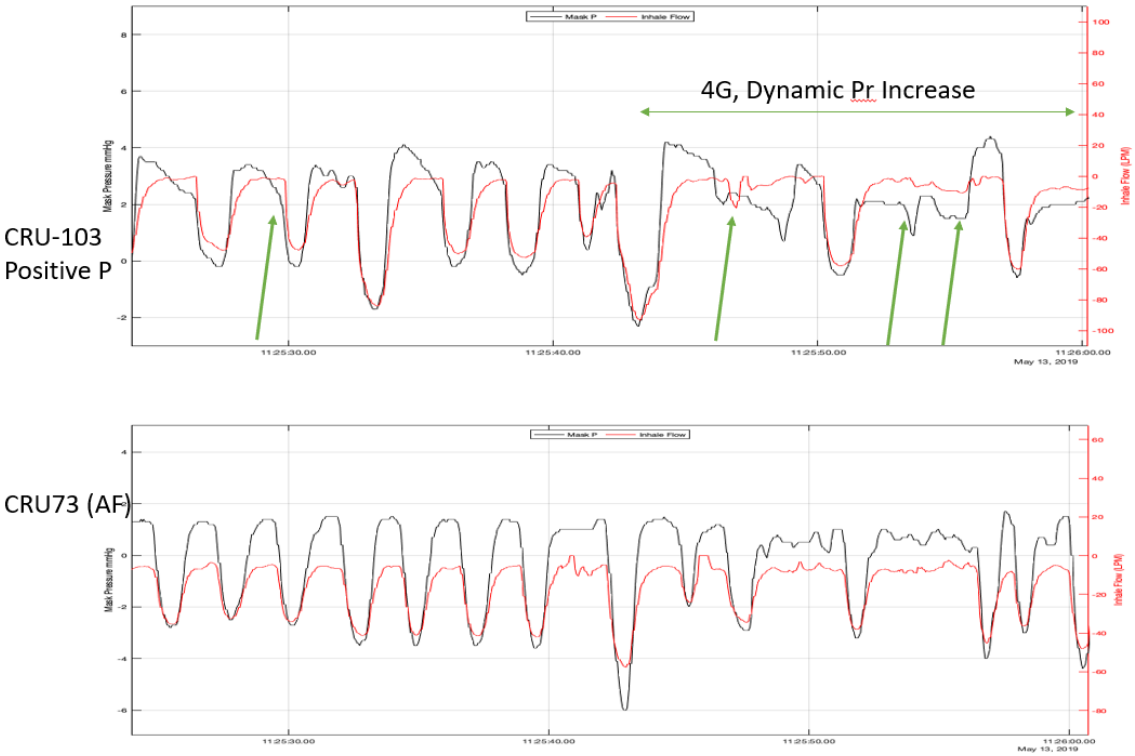

Figure 6.13. Squirrel Cage
The black line is Mask Pressure, and the red line is inhalation flow. The green arrows point to 'Pressure-no-flow' (PNF) examples, which are breathing supply disharmony. These are on the USN configured seat, and not on the USAF.

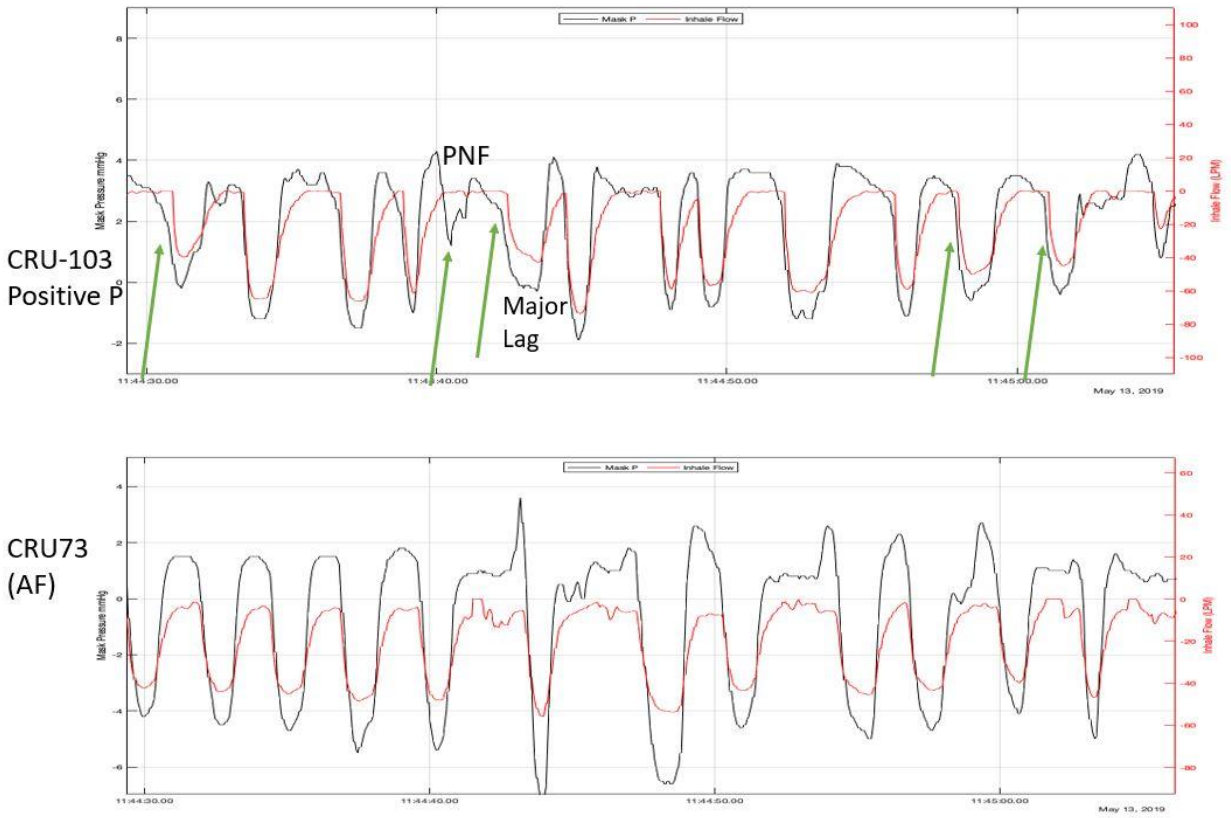

Figure 6.14. Tower Fly-By
The black line is Mask Pressure, and the red line is inhalation flow. The green arrows point to 'Pressure-no-flow' (PNF) examples, which are breathing supply disharmony. These manifest on the USN configured seat as major delays in the commencement of flow, post the pressure draw.

Conclusion from 2-seater, dual configuration flight: Overall, 12 segments were found, with multiple instances of PNF in each. Four have been selected above. Out of the 12, nine were from "dynamic" segments with static or dynamic pressure changes. Three however, such as the example in Figure 6.11, are from "benign" dynamic conditions. All PNF sections were found on the USN positive pressure side, and at matching, same time stamp windows from the USAF configuration (CRU-73, no positive pressure) inhalation flow was in harmony with the driving pressure. As a last step, the program counts the total number of breaths with PNF per flight. This test shows that breathing under the no safety pressure regime is more natural than under positive pressure.

F.6-2. PBA quantified aspects of flight that affect the human breathing system function and Air Crew Breathing System interactions

F.6-3*. *PBA found systematic disharmony between pilot breathing demand and breathing system delivery as indicated by magnitudes and timing of the pressure and flow data channels.*

F.6-4. A NASA machine learning Inductive Monitoring System can detect Mask Pressure-No-Flow (PNF) situations. In the sample ingested, 5x more positive IDs were found in the USN-like configurations with positive pressure and no diluter-demand. Even a short (less than 1s) PNF can correspond to a pilot perception of difficulty inhaling.

F.6-5*. *When PBA pilots reported subjective perceptions of difficulty breathing or experienced physiological symptoms, these were corroborated by in-flight objective measurements.*

R.6.2. Aircrew life support breathing system stakeholders should take actions to investigate, validate, and correct systems that lead to physiological symptoms and have corresponding anomalous pilot breathing patterns. ***(F.6-5)***

F.6-6. The pressure, flow, and timing response of the USAF configured diluter demand breathing system is consistent throughout the breath; for a given pressure there is a 1:1 relationship to the resulting flow.

6.1.6.1 Broader PNF Study: Dynamic Estimation of Safety Pressure Level

Examination of data from multiple PBA flights flown with the Navy life support configuration revealed that the supplied safety pressure, which was expected to be near 3.0 mmHg, varied considerably throughout the flights. Figure 6.15 shows the distribution of safety pressure deviations from 3.0 mmHg (zero point on the graph) for all 21 USN configured flights analyzed for the Pressure/No Flow (PNF) study. Ideally, all safety pressure measurements would fall on the zero deviation column, but the majority are well below that ideal, with most falling 2.3 mmHg below specification at 0.7 mmHg safety pressure. The spread of safety pressures both above and below the 3.0 mmHg specification is notable in that it shows significant variation of pressures applied to the inhalation line.

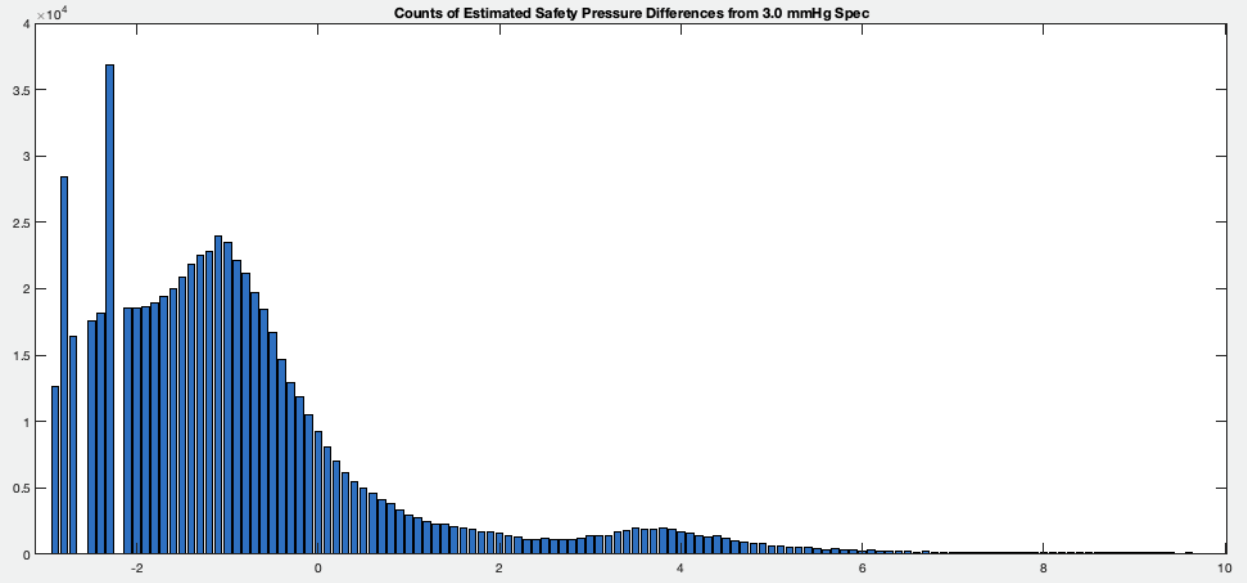

Figure 6.15. Distribution of Safety Pressure Shows Deviations (in mmHg) from 3.0 Safety Pressure Specification

These dynamic safety pressure estimates were calculated by subtracting the cabin pressure reading supplied by the ESB from the concurrent ISB line pressure during exhalation periods. Exhalation periods were defined as data samples with 8 lpm or greater exhalation flow, mask pressure at or above 1.5 mmHg, and ISB line pressure higher than ESB cabin pressure. Figure 6.15 shows counts of the raw values of ISB line pressure minus ESB cabin pressure for all qualifying exhalation samples in the 21 analyzed Navy flights, which amounted to 661,897 samples.

For the purpose of the Pressure/No-Flow (PNF) calculations, the pressures were mapped to a range of 1.5 to 3.5 mmHg, which smoothed the influence of the fluctuations in the raw safety pressure estimates. To accomplish this mapping, all safety pressure estimates below 1.5 mmHg were considered as 1.5 mmHg readings, and all estimated above 3.5 mmHg were considered as 3.5 mmHg readings. Readings in between 1.5 and 3.5 retained their original value.

The initial static pressure PNF analyses had expected at least 8 lpm inhalation flow with any mask pressure at or below 2.8 mmHg. This was based on the assumption of a relatively fixed safety pressure of 3.0 mmHg. The dynamic safety pressure PNF analysis estimated the near instantaneous safety pressure at the time of each inhalation by averaging the five most recent safety pressure estimates (0.25 seconds of data) from the immediately previous exhalation periods. With this scheme, inhalation flow of at least 8 lpm was expected when the mask pressure dropped 1.5 mmHg or more below the estimated dynamic safety pressure. Given the wide variation in actual safety pressure, this dynamic approach provided a more realistic analysis of PNF than using a fixed 3.0 mmHg safety pressure assumption.

Table 6.1 summarizes the statistical differences in the PNF phenomena after 36 flights analyzed, with 5x more events and greater standard deviation found in the USN configuration with positive pressure regulators.

Table 6.1. Shows 5x Greater Normalized Pressure-No-Flow Events in USN Configuration with Positive Pressure Regulator

	AF Event count	USN Event count	AF % events normalized on breaths per flight	USN % events normalized on breaths per flight
Average per 1hr flight	9.07	38.52	0.74	3.53
StdDev	11.67	37.28	0.94	3.48

F.6-7. Safety pressure, as defined by continuous pressure above ambient, and as used on USN aircraft, exacerbated or induced the vast majority of adverse breathing system interactions identified by PBA.

R.6-3. In light of unexplained PEs and data pointing to disharmony between pilot and air-system, re-evaluate the risk/benefit trade-off of the use of Safety-Pressure 100% of the time. Minimize safety pressure magnitude and duration of use where possible. ***(F.6-7)***

6.1.7 Statistics from 1-minute Data from the Aligned Dataset

Summary Statistics were calculated on 1-minute data segments on sensor provided channels and derived parameters and were tabulated for all approved flights. See Technical Section 5 for an in-depth discussion. Some heat maps relevant to USN – USAF differences are presented here (Figures 6.16 and 6.17).

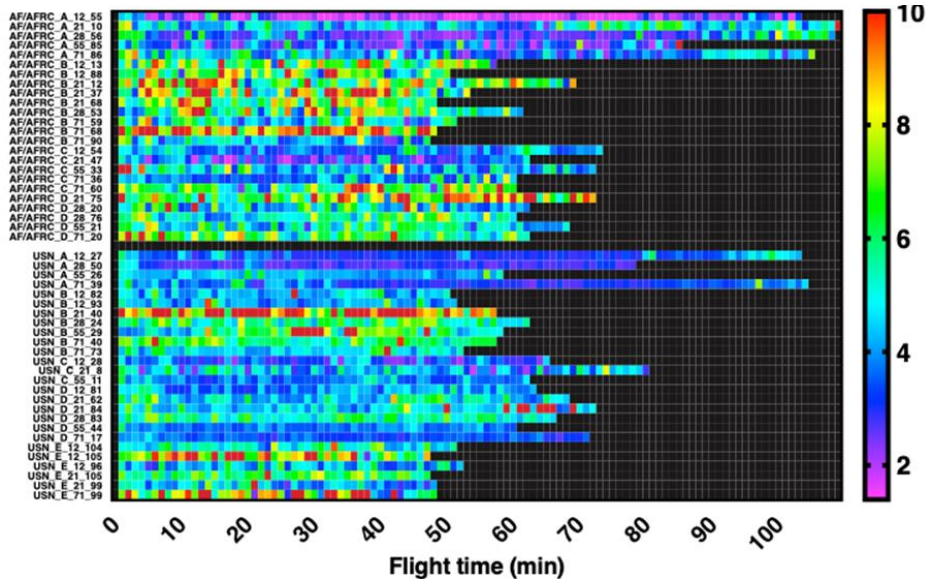

Figure 6.16. Inhalation Draw, Mask Pressure mmHg
During high altitude Profile A flights the inhalation draw is less in the USAF configuration, while in the aerobatic segment of Profile B, the inhalation draw is less in the USN configuration.

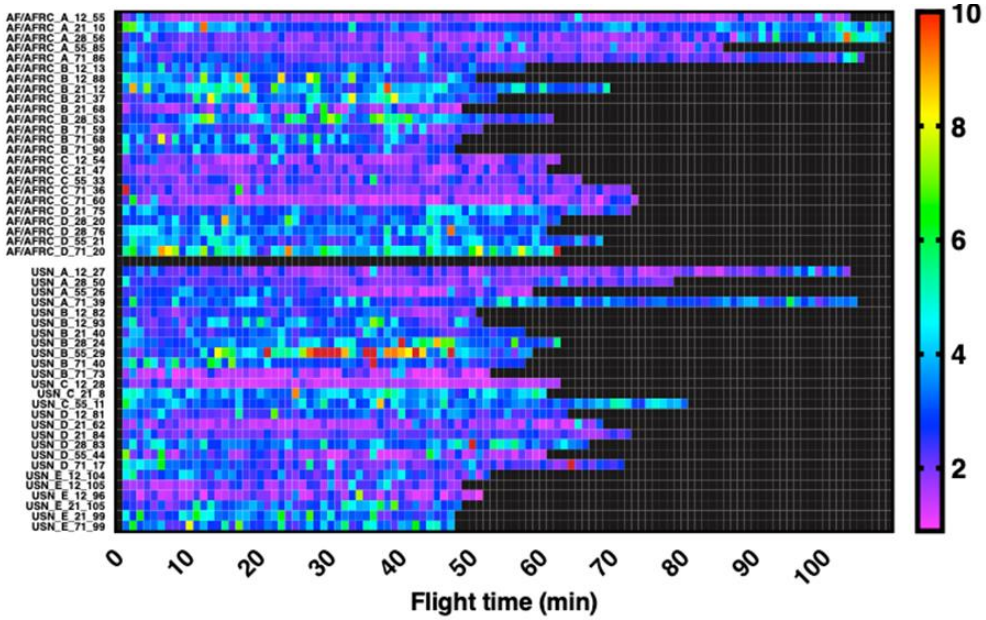

Figure 6.17. Exhalation Mask Pressure mmHg
The highest exhalation mask pressure (red) is found in a USN configuration flight, namely Flight 29, which coincided with the pilot account of "difficulty breathing".

The heat map comparisons confirm the detailed analysis presented in these analyses. Overall, mask draw during inhalation is somewhat greater in a USAF system, especially during the aerobatic profile B. However, the heat maps confirm the pilot accounts that the exhalation effort is easier overall in an USAF configuration.

6.2 Cabin Pressurization and Effects on Pilot Breathing

Cabin pressurization systems are reactive to a reference pressure sensor. By design, cabin pressure is to be maintained constant between 8,000 ft to 23,000 ft altitude (isobaric region). In

case of the F/A18, the reference pressure picks up not only external atmospheric pressure (altitude) but is also affected by dynamic pressure. As such, it is possible that rapid transitions through these threshold altitudes may engender response delays, possibly over- or under-shooting cabin pressure targets, or even result in rapid pressure oscillations. Because the pilot and breathing gear are directly affected by the ambient cabin pressure, these fluctuations can have an important effect on the pilot air supply.

6.2.1 Cabin Pressurization

Aircraft cabins are pressurized following a specific schedule to optimize human safety. The concept is that in stage 1, the lower altitude regions, no pressurization is necessary. There is a stage 2, called Isobaric, because the cockpit maintains the pressure from the lower bound of this region. This pressure cannot be sustained indefinitely with regards to altitude, thus there is a stage 3, in which the pressure resumes to decrease gradually with altitude, maintaining a differential (e.g., 5 PSI) to the outside ambient pressure (Figure 6.18).

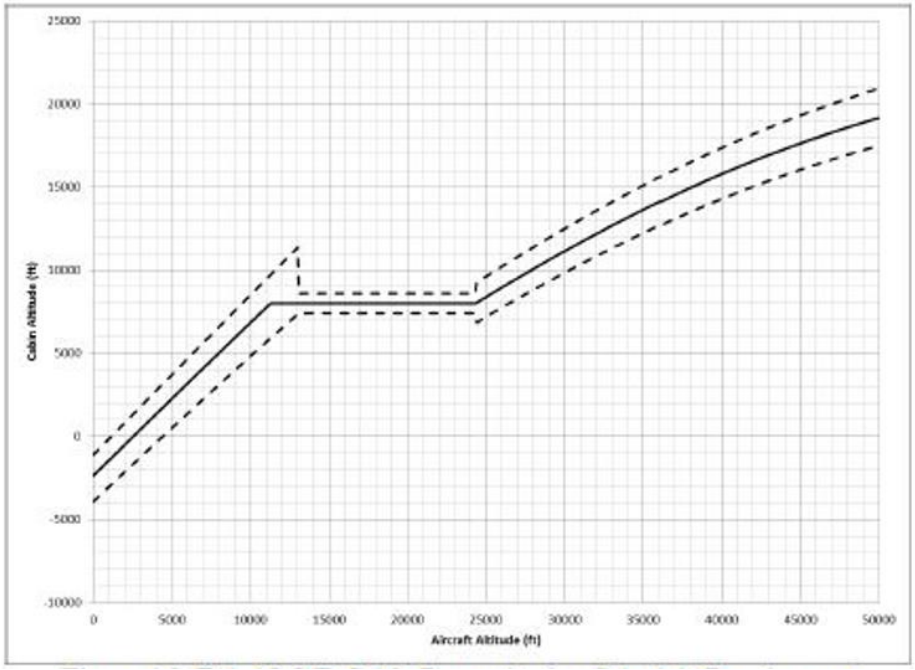

Figure 6.18. Cabin Pressurization Schedule for F/A-18 A/B

"Transition altitudes" are defined as the altitudes at which one pressure regime ends and the next one begins. The transition altitudes may be slightly different per different model aircraft, but the concept is the same. Per Figure 6.18, the transition altitudes for the F/A-18 legacy aircraft predominantly flown on the PBA are 8,000 ft. and 24,000 ft., with an allowed deviation of at least ±500 ft. in the Isobaric region, and ±1,000 ft. elsewhere.

As cabin pressure was supplied from the ISB block, ESB block, and on select flights the MadgeTech device, the PBA studied the excursions from the pressure schedules, as well as persistent pressure oscillations, and the effects of these on pilot breathing.

6.2.2 Cabin Pressure in Transition Bands

The PBA team found systematic pressure over- and under-shoots when crossing a transition band. Figures 6.19 and 6.20 are representative of this phenomenon.

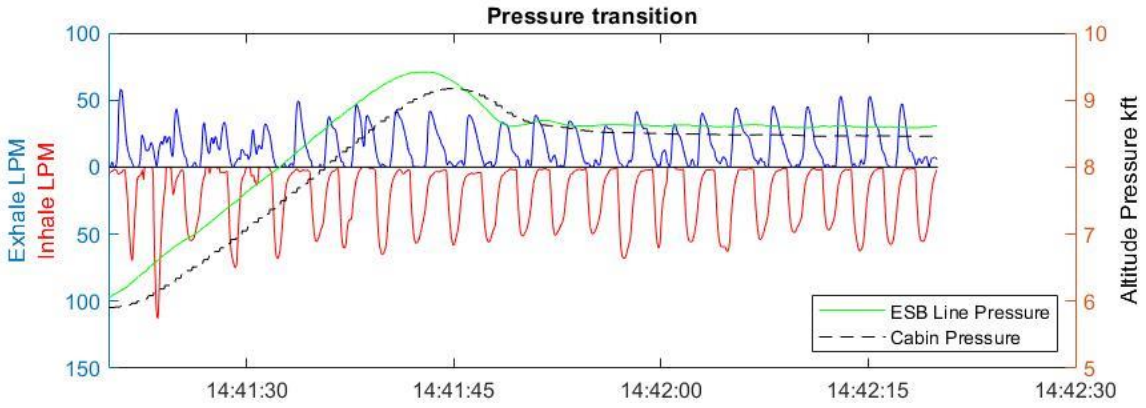

Figure 6.19. Phenomenon: Systematic Pressure Over- and Under-Shoots when Crossing a Transition Band

During Mil Power Climb, Altitude pressure overshoots (under-pressure) by about 1,000 ft, then balances out around 8,500 ft. (Flight 100, Tail #868)

The PBA team found this phenomenon across all PBA aircraft to varying extent. The Flight 100 example happens to be a flight with a CRU-103, and the Flight 87 example is with a CRU-73. This is a cabin pressure control issue, and not a regulator issue. In Figure 6.19 the pressure over/under-shoot is gradual, and does not seem to upset breathing, unlike in Figure 6.20.

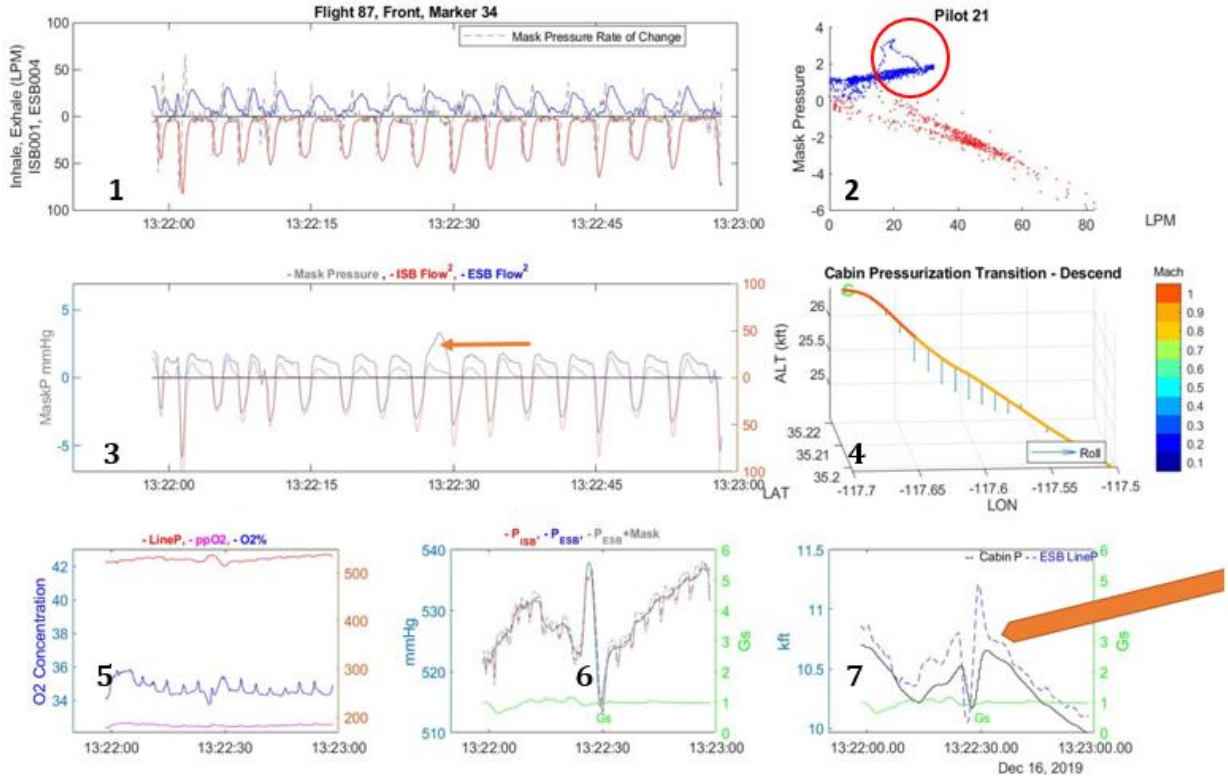

Figure 6.20. Phenomenon: Systematic Pressure Over- and Under-Shoots when Crossing a Transition Band

During a descent, around 24 kft is an example of an imperfect control, with two cycles Altitude pressure over/undershoots by about 1,000 ft. In this example, the instance of overshoot (Tile 7) affects the exhalation (Tiles 2 and 3). Also note the anomaly in the Trumpet curve on the exhalation side in Tile 2. The sample is from Flight 87, Tail #843

The pressure over/under-shoot in Figure 6.20 is not only felt in the cabin as ambient pressure change, but it also affects the exhalation. See the exhalation marked by the red arrow in tile 3: the exhalation mask pressure increases 2.5 times, while the resultant peak exhalation flow rate is one of the lowest in this 1-minute segment. The scenarios in Figures 6.19 and 6.20 are typical of crossing the transition altitudes, with a pronounced effect when the 1000' change happens within 2 seconds (Figure 6.20), as opposed to 5 seconds (Figure 6.19). Note that the two examples are from 2 different aircraft, which explains the different degrees of control, optimal on Tail #868, and sub-optimal on Tail #843. Looking at the signature of control response in the altitude transition band can provide a tell-tale sign regarding the state of cabin pressurization control.

F.6-8. The supply of the pilot breathing system can cause BSDs by 1) misalignments in time relative to demand, 2) excessive inspiratory and/or expiratory pressure impeding inhalation and/or exhalation, 3) flow restriction of inhalation and exhalation volumes especially under dynamic conditions

R.6-4. Cabin pressure fluctuations at a frequency that require pilot compensation should be monitored and mitigated to ensure smooth and predictable breathing gas delivery. ***(F.6-8)***

F.6-9. The frequency components of cabin pressure oscillations (situational or continuous) are close in frequency to pilot breathing, with a mode at 0.3 Hz. The cabin pressure oscillations and breathing frequency have a combined effect on pilot air supply and pilot breathing.

R.6-5. Perform Fast Fourier Transform analyses of unfiltered and un-smoothed cabin pressure (and pilot mask pressure, when possible). Use a prominent cabin pressure frequency as a trigger for maintenance check of systems that affect cabin pressure (e.g., control valve or exit valve). ***(F.6-9)***

6.2.3 Pressure Overshoots in Isobaric Regions, turns and descents

The example in Figure 6.21 is Flight 59, a dynamic Profile B. The pressure excursion marked "B" is a significant 2,500 ft. pressure equivalent. For context, the entire 1-hour flight profile is shown in the 2 left panels with altitudes up to 32,000 ft (left axis) and, for a detailed view, zoom in on the 1-minute of pressure disturbance on the right-hand side.

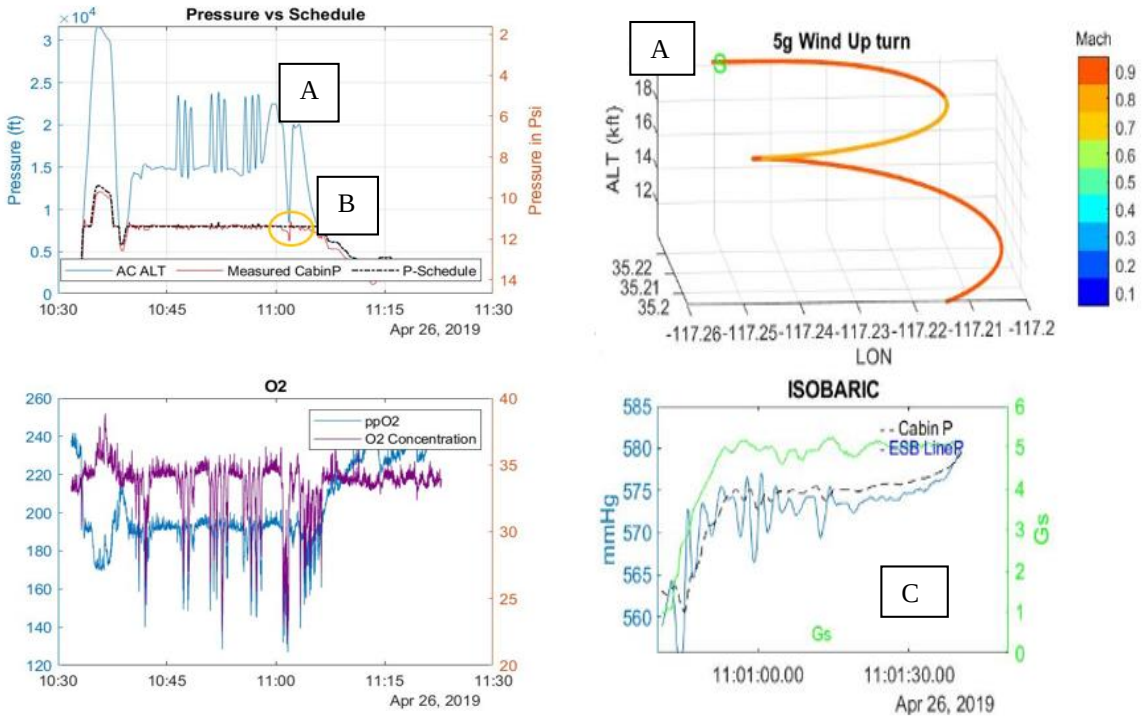

Figure 6.21. Flight 59, a Dynamic Profile B
"A" represents the segment of the 5 G's Wind-up turn followed by a 10,000 ft descent. The circled area "B" shows the 2,200 ft deviation of cabin pressure from the pressure schedule (red line dipping below black line). "C" shows a zoomed in view of the Dynamic Pressure oscillations (blue ESB line pressure) brought on by the 5 G's turn.

Note that during the dynamic portions, 4 G's 90-degree turn, three "Squirrel Cages", 5 G's wind-up turn, and even the Spiral descent, the ppO_2, and thus the O_2 concentration does drop to as low as 23% (Figure 6.21, lower left tile). Figure 6.2.5 is a zoom in on segment "A". The 5 G's wind-up turn starts after a 3,000-foot descent, which paired with Mach 0.9 already triggers a 10 mmHg, 0.3 Hz pressure oscillation, sustained by ramping up G's (Figure 6.21, marker "C").

Figure 6.22 shows how many times in a 5-minute segment around time segment "A" pilot breathing is changing and adapting. At the same time, these changes correlate with more cabin pressure deviations.

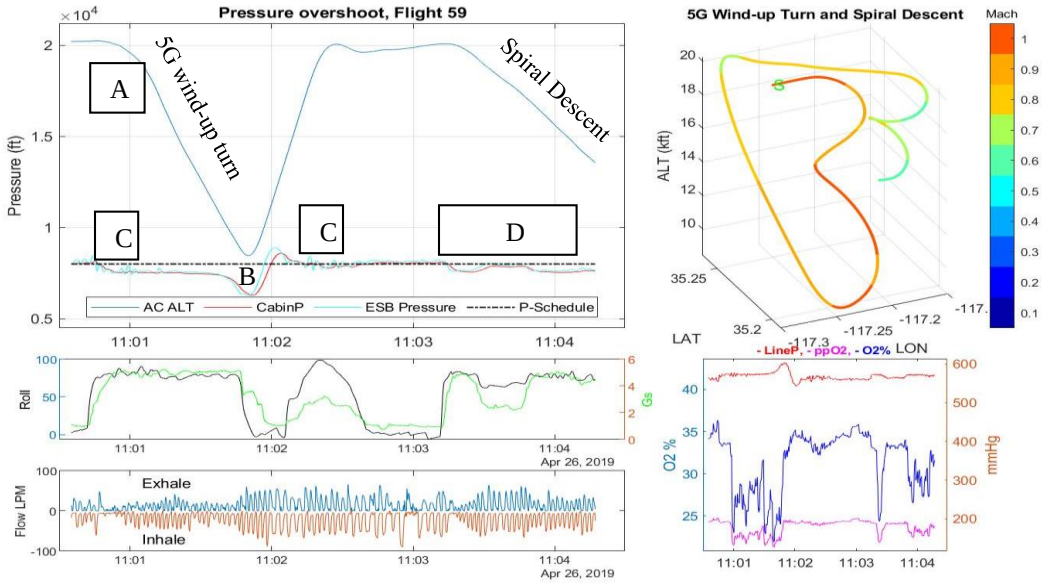

Figure 6.22. Illustrates Number of Times in 5-minute Segment Around Time Segment "A" Pilot Breathing Changes and Adapts
Zooms in on a 5 minute dynamic segment, including the 2,500 ft. cabin pressure swing, unexpected in the isobaric region (marked by "B"). It also shows the chaotic breathing and O_2 concentrations (in the lower left and right tiles respectively)

The segment in Figure 6.22 is from an isobaric region in which the cabin pressure is required to maintain a constant level (top left tile, black dashed line). This is contrasted with the pressure lines (red and cyan). The oscillations start before 11:01, and the cabin is slightly overpressure (due to dynamic factors). The overshoot is seen before 11:02, followed by an over-correction, and another set of oscillations at the end of the climb ("C"). At the spiral descent start, as the forces on the craft reach 4 G's due to the turns, the slight overpressure is seen again ("D"). During the same periods of high G, see the lower right tile of Figure 6.22, the O_2 concentration drops by 10% (purple line).

Regarding effects on pilot breathing, the flow is displayed in the bottom left tile of Figure 6.22. Breathing starts out shallow at Mach 1. In the 2nd 30 seconds of the 1 minute sustained high-G maneuver, as the strain builds, a diminished amplitude for inhalation/exhalation flow is observed. There is only time for a few long replenishing breaths, which occur after the pressure swing and G's. The peak flow rate repeatedly decreases at the start of each high G segment.

Continuing with this example, zoom in to the bottom of the 10,000 descent and show a 1-minute window so these dynamic effects on pilot breathing can be examined on a micro scale (Figure 6.23).

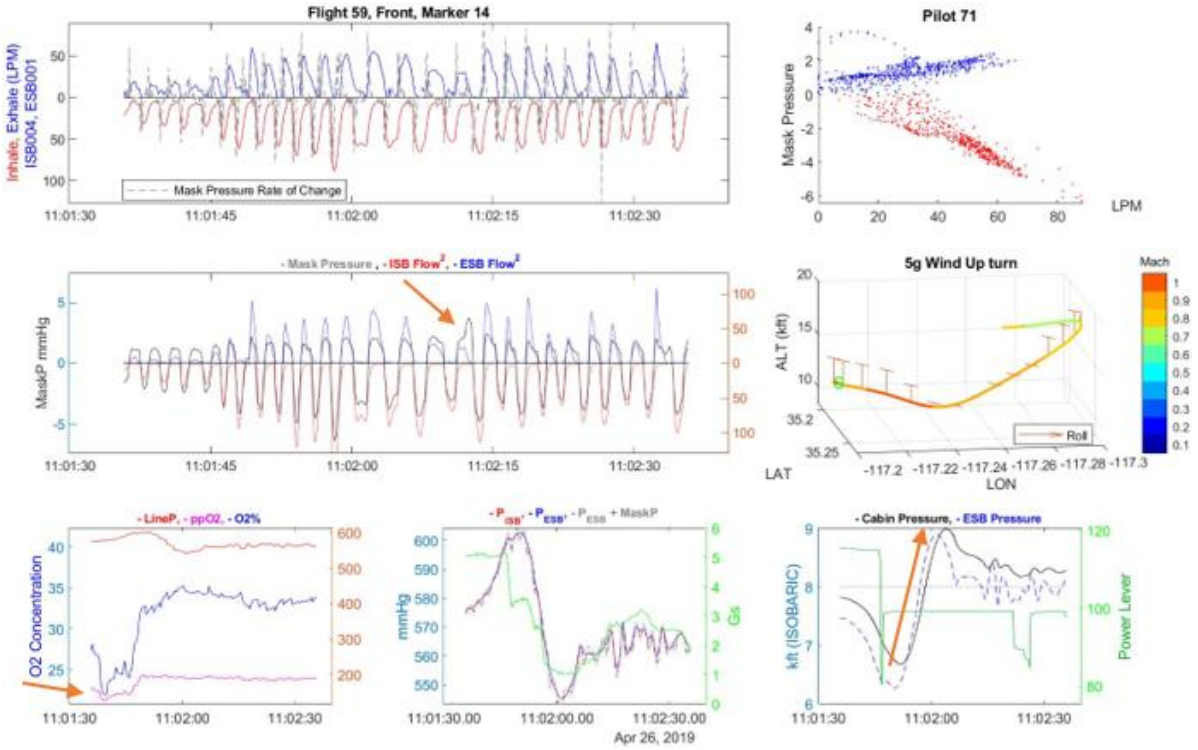

Figure 6.23. Zoom in on a 1-minute Segment Surrounding Minimum Altitude Point After Previous Turn and Descent
It includes the over/under-shoot (lower right) and also shows the chaotic breathing and O_2 concentrations (in the central and lower left tiles respectively)

This dynamic segment causes the O_2 concentration to drop to 22%, one of the lowest found in PBA data.

6.2.4 Pressure Fluctuations in Low Altitude Flights, While Straight and Level

Pressure fluctuations from static pressure altitude can also be studied in low altitude flights. In these, the effects of cabin pressurization are decoupled. The PBA created Profile D for this reason, and it is flown under 7,500 ft., below the Isobaric Region. Figure 6.24 illustrates a 1,500-ft deviation example. These examples are not random; they can be explained by dynamic pressure, and the reference pressure sensor of the F-A/18 aircraft, which is located in the Nose Wheel Well, and thus susceptible to higher pressures.

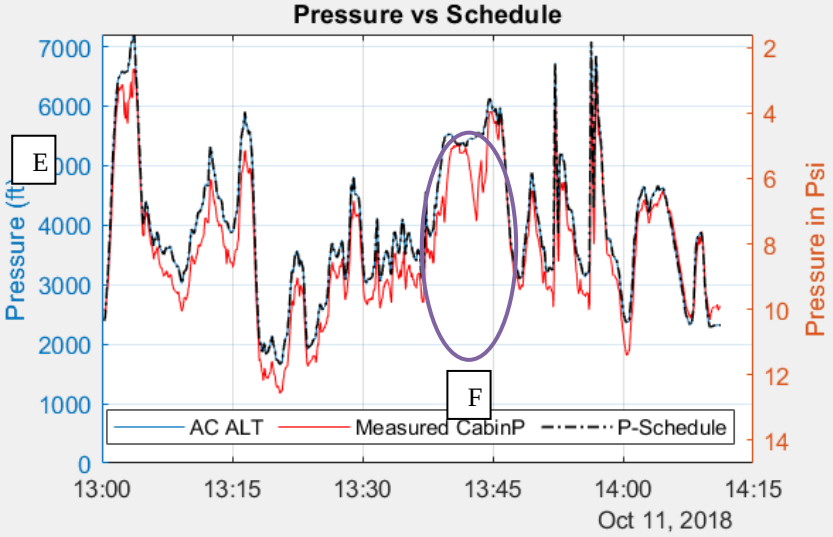

Figure 6.24. Cabin Pressure Deviates (E, F) by 1,000 to 1,500 ft from Altitude-Converted Pressure; Under 8,000 ft is same as Pressure Schedule

The example in Figure 6.24 is PBA flight 17. Below 8,000 ft the cabin pressure is designed to match the outside pressure, which calculate from the Altitude, thus the black and red lines are expected to overlap. There is a small offset overpressure present in the first half of the flight, usually brought on at canopy close, when the cabin pressure increases on average by a 300 ft. equivalent. This delta dissipates by the 2nd half of the flight. The overpressure episode "E" is caused by two 90-degree turns in succession, 4 G's and 5 G's, respectively. Both of these are level turns at 700-800 ftps, showing that a descent is not necessary to cause a pressure change; focus on the 3 highest over-pressures in "F" up to 1,500 ft. Figure 6.24 shows the entire flight; and Figure 6.25 zooms in on the pressure deviation segment.

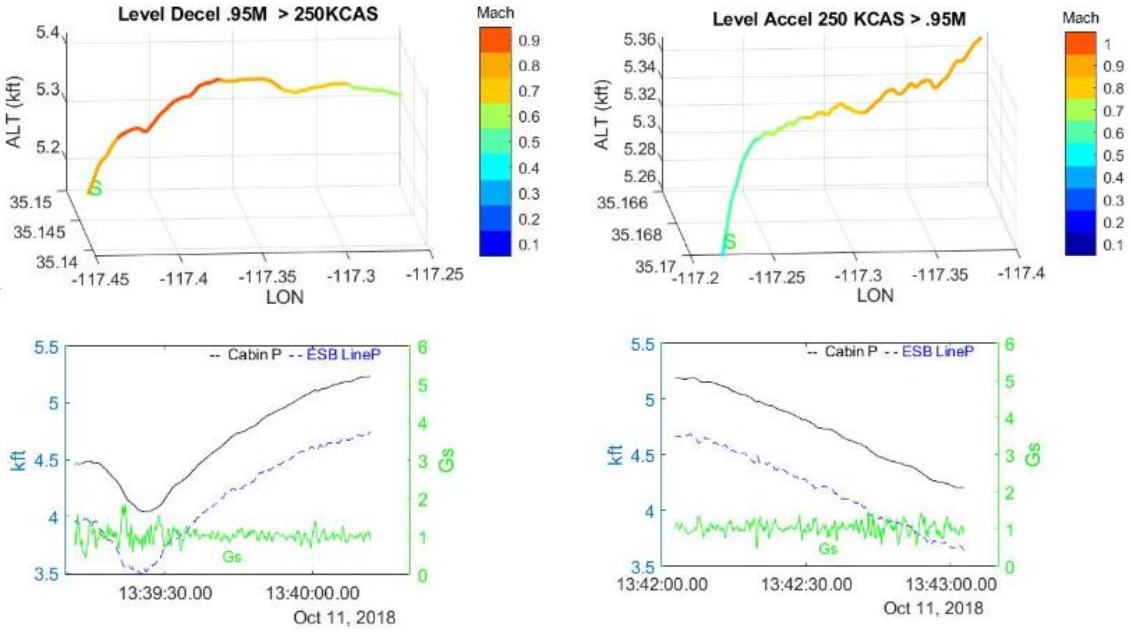

Figure 6.25. Zoom in on FLT-017, Section F from Figure 6.24; 2 Diverging Variations of Same Signal (top and bottom plots)

In Figure 6.25, left, correlating the Mach bar, shows that even a small acceleration/deceleration at 13:39:30 causes a "v" shape drop of 500 ft. As the deceleration continues beyond Mach 0.9, the original 100 ft distance closes, and by the end of the 1-minute window the altitude and cabin pressure match at 5.1 kft. On the right side, the altitude derived from the cabin pressure starts out at 13:42 at the same 5.26 kft as the altitude plotted in the 3D flight trajectory. At the end of the 1-minute, the disparity is 1,000 ft. Note that G's (3-axis) are not a factor in the increase of pressure. The factor adding to the dynamic pressure is the Velocity changing from 0.6 Mach to Mach 1.

Effects on breathing are shown in Figure 6.26, which is the last set from example 6.24. A level deceleration first results in lower pressure, followed by a Level 360° 5 G's turn that causes overpressure of perceived 500 ft, but overall a 900 ft difference from the true altitude.

After the 5th successive pressure change, in the first 20 seconds there are some high pressures at the start of exhalations and a double exhalation, indicating higher efforts. In the middle 20 seconds as the G's start, the baseline which used to be 3 mmHg positive pressure seems to downshift. It appears there is virtually no exhalation flow, but the pressure and flow track, which yield to the hypothesis of either the safety pressure decreasing during G's (when they are expected to increase, if anything), or inhalation valve not closing. In either case, both pressure and flow are diminished. In the last 20 seconds, there is diminished flow response to mask pressure on the inhalation, until 2 full recovery breaths are taken at the end.

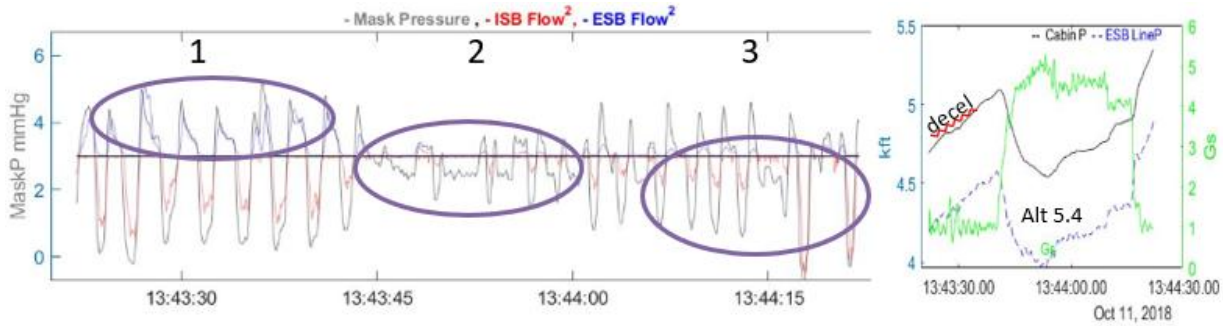

Figure 6.26. Shows Diminished Breathing Parameters in a Pressure and G Change Segment Circle 1 shows clipped exhalation; in Circle 2 the safety pressure level drops, and mask pressure and flow are much lower than in circle 1; in Circle 3 the red flow return relative to the mask pressure is diminished (the 2 lines are far from an overlap)

The example in Figure 6.2.6 shows that to provide a consistent pilot breathing experience, calling out absolute magnitudes as requirements or standards is not sufficient; rather, the complex in-flight system interactions should serve as guides for optimization.

Specifying absolute magnitudes of breathing parameters as requirements or standards is not sufficient; rather, the complex in-flight system interactions should serve as guides to provide an optimized pilot breathing experience.

6.2.5 Dynamic Pressure Model Applied

The static pressure alone, converted from altitude, does not capture the pressure experienced in the cockpit. Dynamic pressures come into play, and these two need to be combined. The section 6.2.4 example being under 8,000 ft is a good candidate to apply a formula based on what was

learned. Here are the 'before' picture (in mmHg), and the result 'after' applying the dynamic formula.

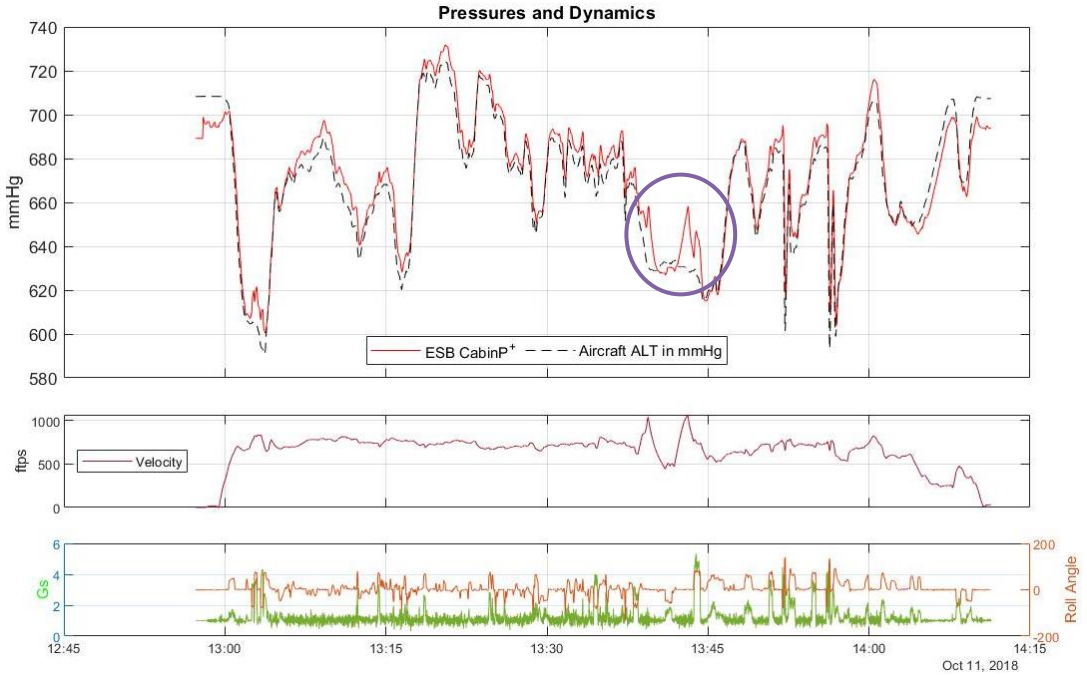

Figure 6.27. Under 8,000 ft, Cabin Pressure Should Match Pressure Altitude (top window)

The black line represents Static Pressure Altitude before applying a dynamic pressure model. The area circled in orange represents a pressure mismatch. This mismatch lines up with Velocity change and high G force (2nd and 3d window), giving an indication that the mismatch is caused by dynamic pressure.

Note the correlation with Velocity, G's and some angles, thus deriving Formula 6.1:

*Total Pressure = Static_P + Dynamic_P= Static_P + a*Velocity^x +b*G+max (k*roll, m*pitch)*

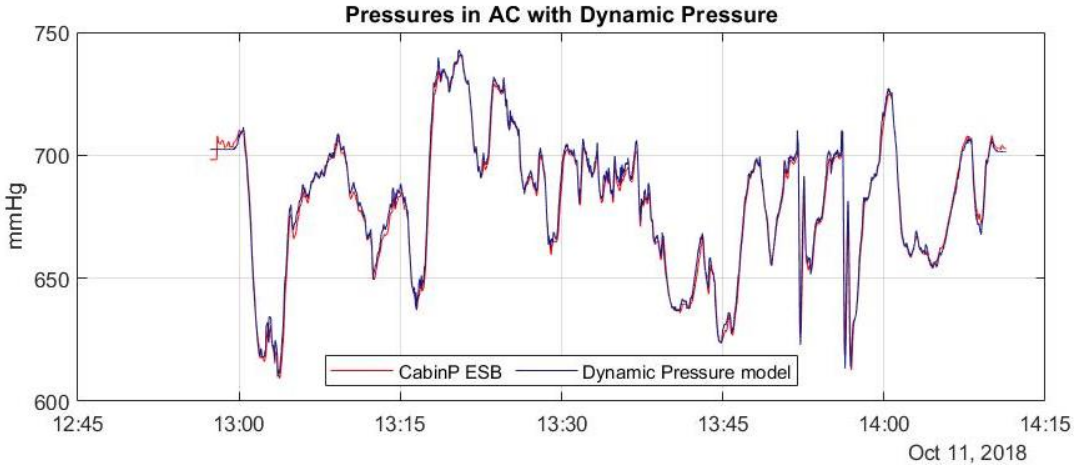

Figure 6.28. Flight 17, After Applying Total Pressure Formula, Including Dynamic Pressure

In Figure 6.28 there is no discrepancy problem as compared the Figure 6.27. At 13:42 for example, the cabin pressure and the model completely overlap, resolving the 1,000 ft delta from the altitude pressure equivalent (circled in Figure 6.27). Compared to early models of cabin pressure, the effects of dynamic maneuvers on cabin pressure and pilot breathing can now be better understood, considered, and anticipated. This means that while the PBA team knew that pilot breathing (rate, tidal volume) changes per segment of flight, there is a new pressure introduced which the human body needs to adapt to, with every dynamic maneuver. Thus, micro-adaptations occur significantly more in dynamic profile flights.

6.2.6 Pressure Oscillations at High Altitude, Above Isobaric Region

Pressure deviation also occurs in straight and level flight. To illustrate, zoom in on a high Mach segment of flight 39. The example in Figure 6.29 takes place at 45,000 ft, with a 100-ft alteration in altitude, thus it is considered "straight and level."

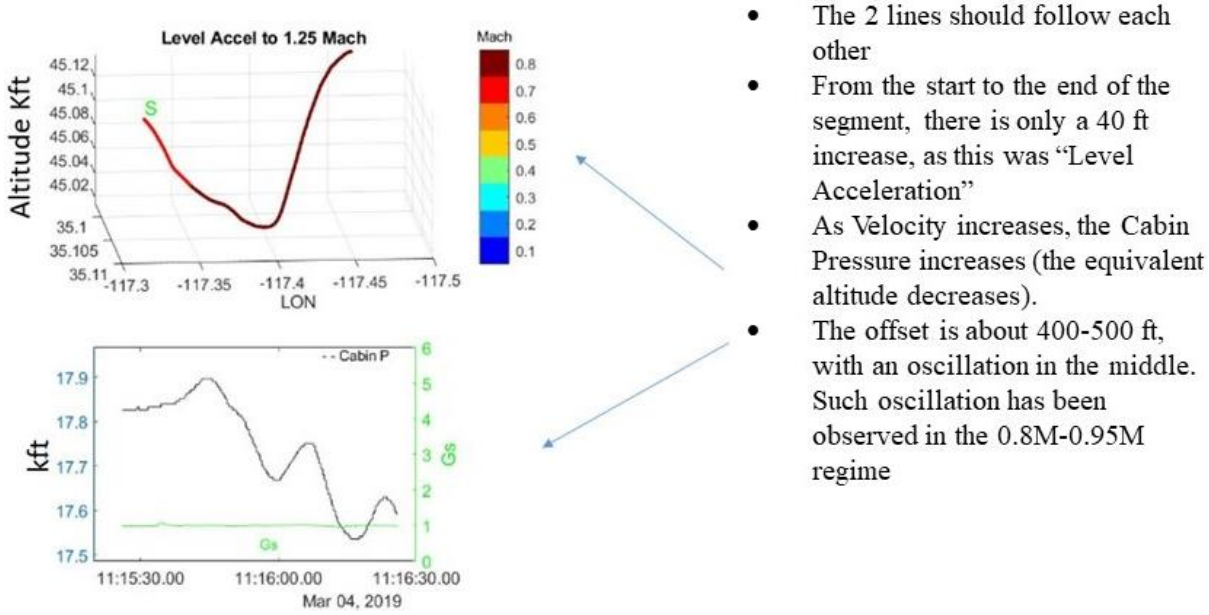

Figure 6.29. Flight 39, at Sustained Mach 0.8, Cabin Pressure Climbs Instead of Slightly Lowering per Differential Pressure Schedule

In summary, dynamic pressure is an important contributor to cabin reference pressure, thus cabin pressure itself. Cabin pressure control is designed to maintain the prescribed cabin pressure and breathing system regulators regulate to this pressure as a reference. This interaction is further studied in Section 6.3.

6.3. Aircraft Pressure Study, including Profile E without Pressure Schedule Control

PBA developed a subset of flights to "de-couple" the effects of the cabin pressure control to more completely understand the pressure effects experienced in the cabin by the pilot. As described, cabin pressure control engages at around 8,000 ft, maintaining isobaric conditions until about 23,000 ft. Above this altitude the pressure in the cabin starts to decrease as one would expect with the increase of altitude, maintaining a 5 PSI differential between the cabin and outside ambient pressure. A special category of flights (Profile E) was created for this investigation.

6.3.1 Cabin Pressure Study with Pressure Schedule Disabled (PBA Profile E)

To observe the cabin without pressure control, the PBA team engaged the "RAM DUMP" mode. The exit valve was continuously engaged, so pressurization above ambient was not achieved. The PBA team designed a profile and flight -cards with similar maneuvers as to the PBA profile B, for comparison. Four flights were flown in this modified configuration, following PBA Profile E (Flights 96, 99, 104 and 105). Altitude was limited to 13,000 ft for pilot safety.

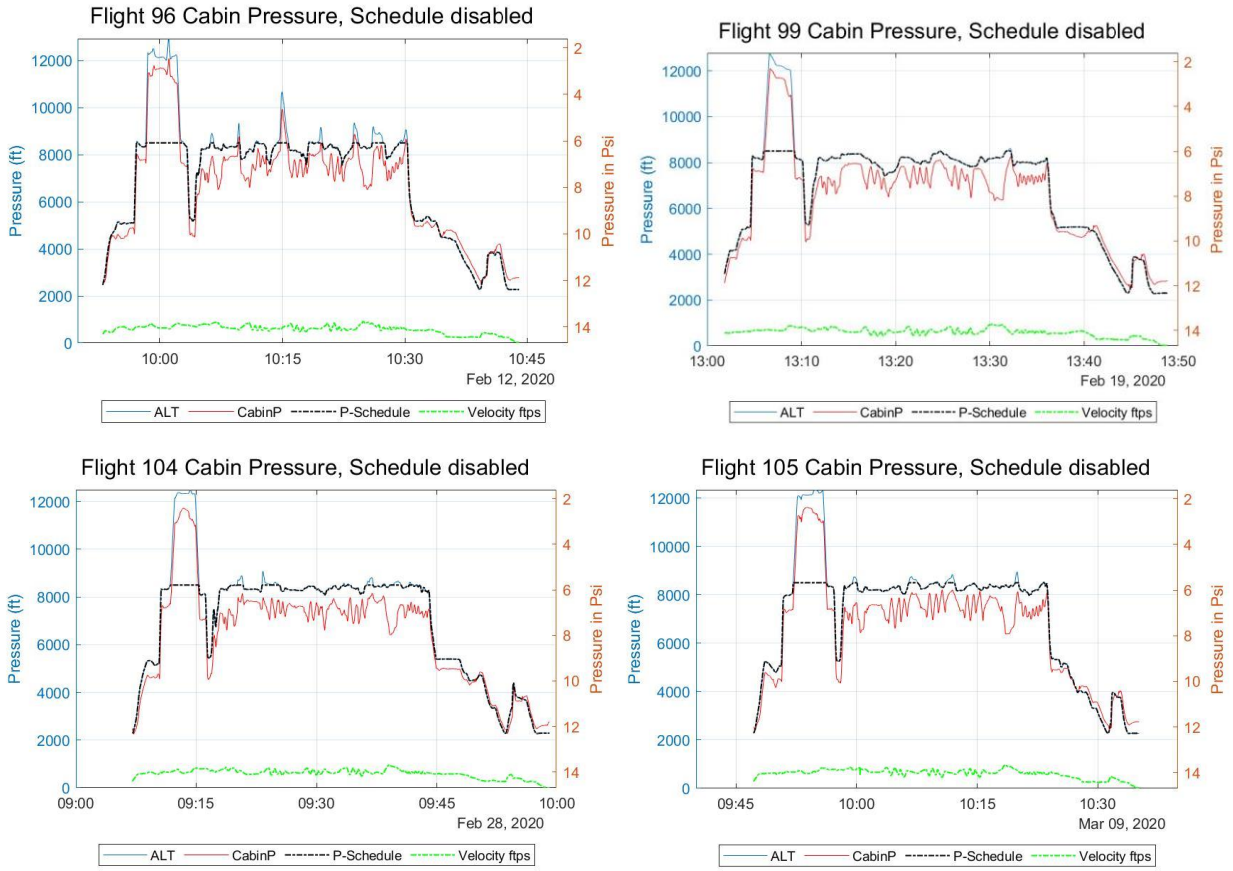

Figure 6.3.1. Unregulated Cabin Pressure Diverges from Pressure Altitude (the red line of cabin pressure does not overlap with the blue line representing altitude)

Figure 6.3.1 presents the cabin pressure (red line) relationship relative to the pressure altitude. The 'would-be' cabin pressure schedule coincides with the pressure altitude for the most part (black and blue lines overlap), except for the few minutes spent above 8,500 ft. The left and right y axis are aligned. The cabin pressure is higher in several segments than the pressure altitude. To show the cause, see the Profile E flown in Figures 6.3.2 and 6.3.3.

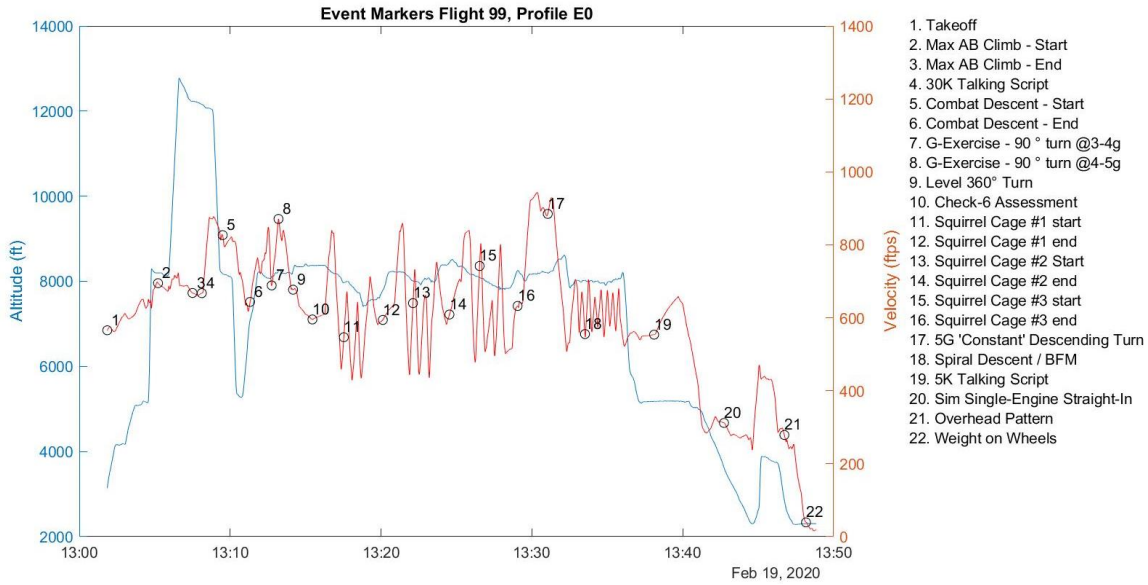

Figure 6.3.2. PBA Profile E Tested Effects of Dynamic Maneuvers Including G-turns (Markers 7-9), Vertical Loops (M11-M16), and Combined Turn and Descent (M18)

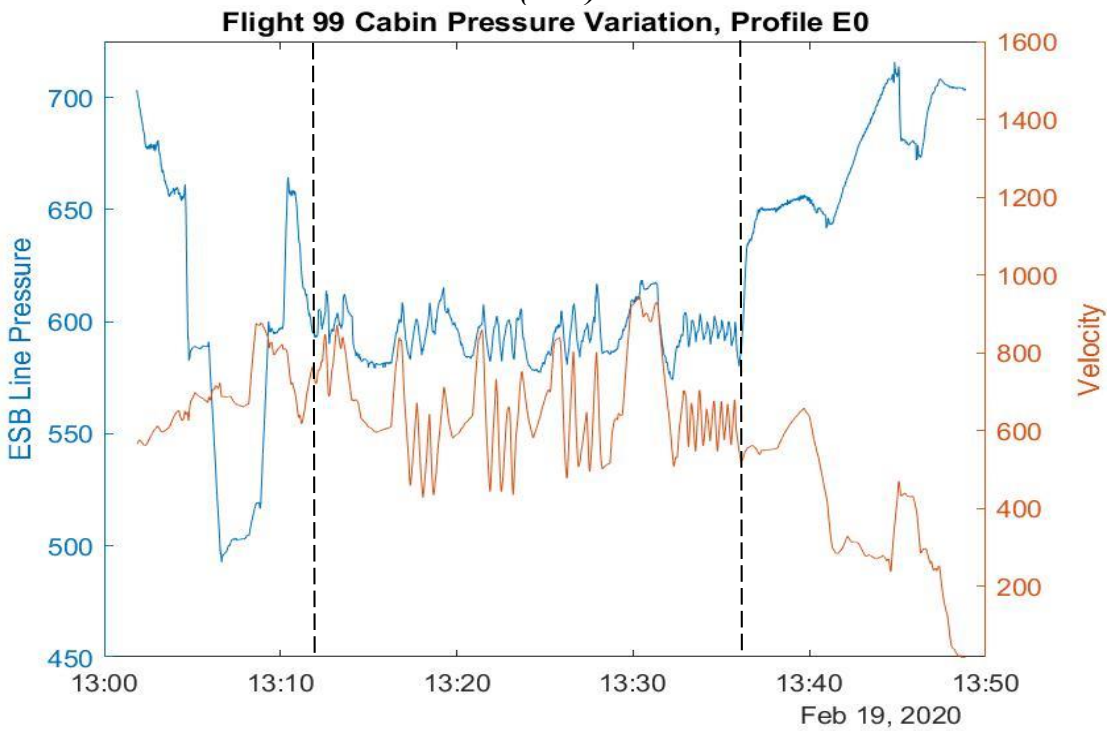

Figure 6.3.3. Correlation between Velocity (ftps) and Cabin Pressure (taken from the ESB line pressure in mmHg) Referring to the altitude line from Figure 6.3.2, it is known that in the middle section of the flight marked between the dashed lines, the altitude is closely maintained around 8,000 ft. The cabin pressure (blue line) however oscillates between 6,500 and 8,000 ft, and the pattern of change matches that of the velocity (red line).

The modified cabin experiment shows that the total pressure experienced is a combination of static pressure (a function of altitude) and dynamic pressure. This can be also understood as

changes in potential and kinetic energy, with the addition of external forces acted on by throttle change, which translates to velocity change. Dynamic pressure in the case of an aircraft is affected by velocity and angle-of-attack (AOA) change. PBA graphs show close correlation to G's as well, which is a derivative of velocity, coupled with angular velocity (Figure 6.3.4).

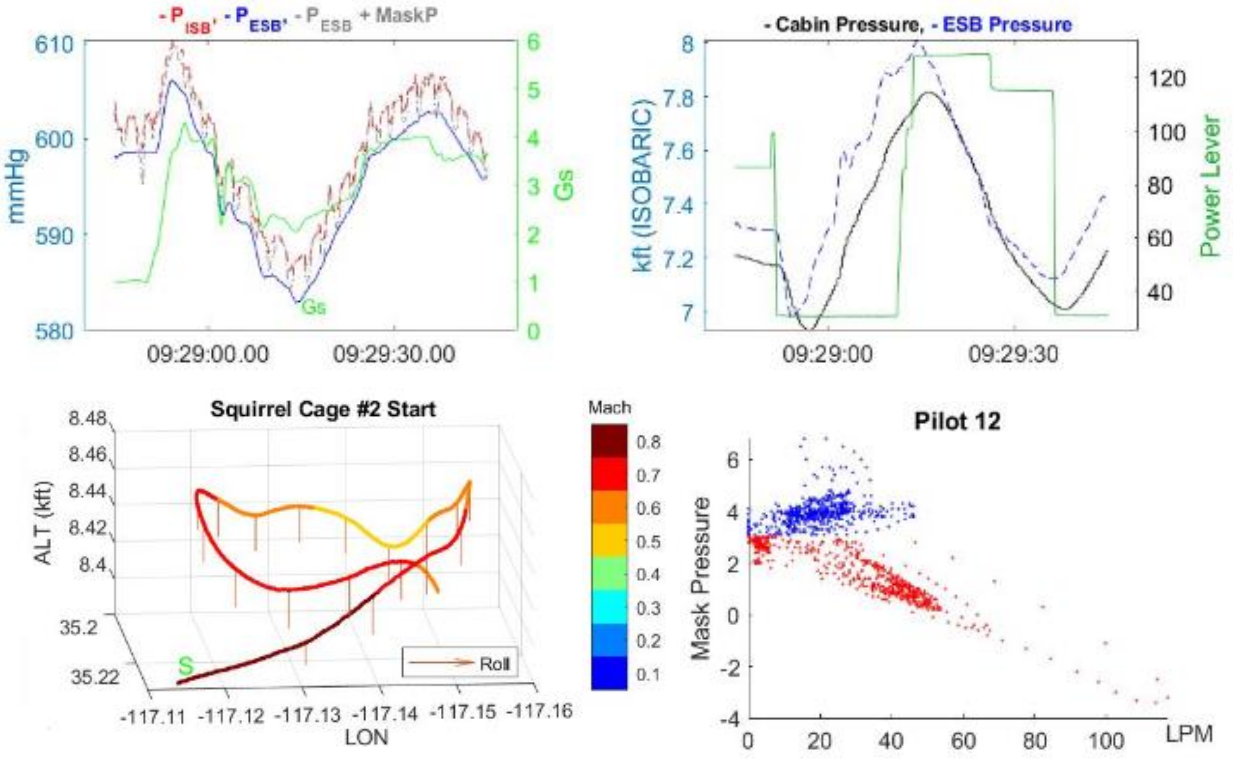

Figure 6.3.4. Flight 104
All inside pressures increase in unison with G's. The cabin pressure change is equivalent to 1000 ft altitude change, while the actual altitude change was only 50 ft. The G-forces and pressure change lead to an irregular trumpet curve of the pilot's air pressure-flow relationship.

In Figure 6.3.4 also note the irregular trumpet curve in this segment. In the lower right quadrant, the red dots for the inhalation pressure and flow have a high deviation, and the blue dots instead of being linear or a gentle arc, show an irregular pattern. At 6 mmHg mask pressure only 20 lpm flow rate was registered, a sign of extra effort being needed to exhale. The cabin pressure changes, due to dynamic pressure, the PBA team set out to decouple and study shown in this section are indifferent from the regulator. However, the changing cabin pressure means changes of the reference pressure for *any regulator*, which in case of Flight 104 was the CRU-103.

6.3.2 Cabin Pressure Control Example, Ideal

This example relies on flight 93, a Profile B aerobatic flight containing 10,000-ft span vertical loops (Squirrel Cages) similar to the G-loops in Profile E. Figure 6.3.5 shows how the pressure control system works, but note that 500-600 ft pressure changes remain within in the isobaric region even if the absolute pressure deviates slightly beyond the nominal barrier. In dynamic conditions, the craft's pressure sensor in the Nose Wheel Well is sensitive to the static and dynamic pressures. Converting to mmHg, the change is ~21 mmHg, which is four times as great as the range observed in a normal breath. This behavior was observed on every PBA flight. Pressure rises with dynamic pressure, and ideally resolves at the end of the causal maneuver.

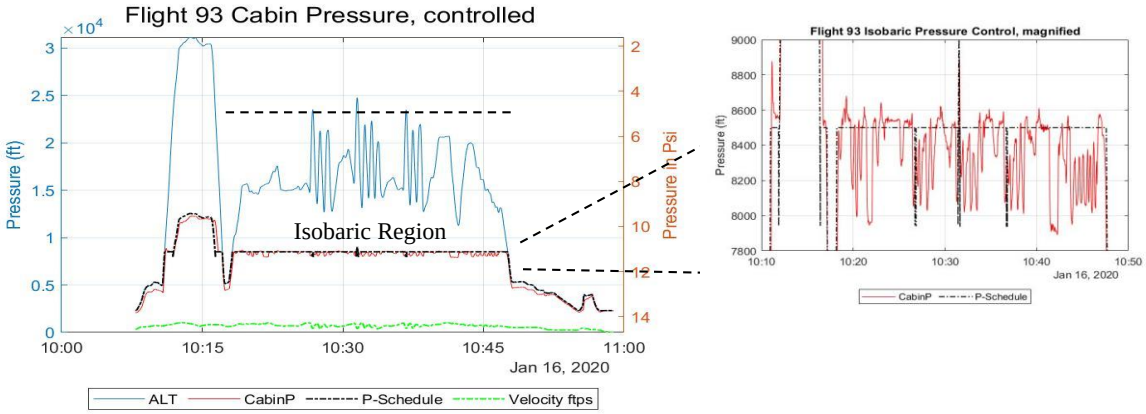

Figure 6.3.5. Flight 93 with Similar Maneuvers but with standard cabin pressure schedule, provides a contrast to Profile E. Some pressure changes remain due to dynamic pressure

The magnified section on the right side of Figure 6.3.5 shows that the Isobaric scheduling keeps pressure changes within 500 ft equivalent pressure change.

F.6-10. PBA routinely measured cabin pressure changes between 500-1000 ft equivalent pressure altitude due to dynamic pressure in all cabin pressure regimes. These pressure changes were documented even in isobaric regions where the aircraft should deliver constant cabin pressure.

6.3.3 Cabin Pressure Example of Uncontrolled Oscillations

Cabin pressure control is not always perfect. As air enters the cabin, and schedule needs to be maintained, an exit valve in the cabin lets out excess pressure. The PBA found that different aircraft have different response signatures to pressure perturbations. This is in line with the USN monitoring the canopy closure pressure response. At times, a set of circumstances of rapid pressure change can cause lasting imbalance. The example shown was consistently found an aircraft 843, post combat descent. Combat descent was characterized by a 45-degree descent, dropping 17 kft/minute. The combat descent flight parameters as flown on Profile F of the PBA are in Table 6.3.1.

Table 6.3.1. High Pitch Angle for Combat Descent, and a 69-degree Roll

Segment	mean Altitude delta kft	mean Max Velocity Knots	mean Min Velocity Knots	Mean Roll degrees	Max Roll degrees	Mean Pitch degrees	Peak Pitch degrees
Combat Descent	-24.66	529.79	436.72	3.91	69.14	-16.82	-44.35

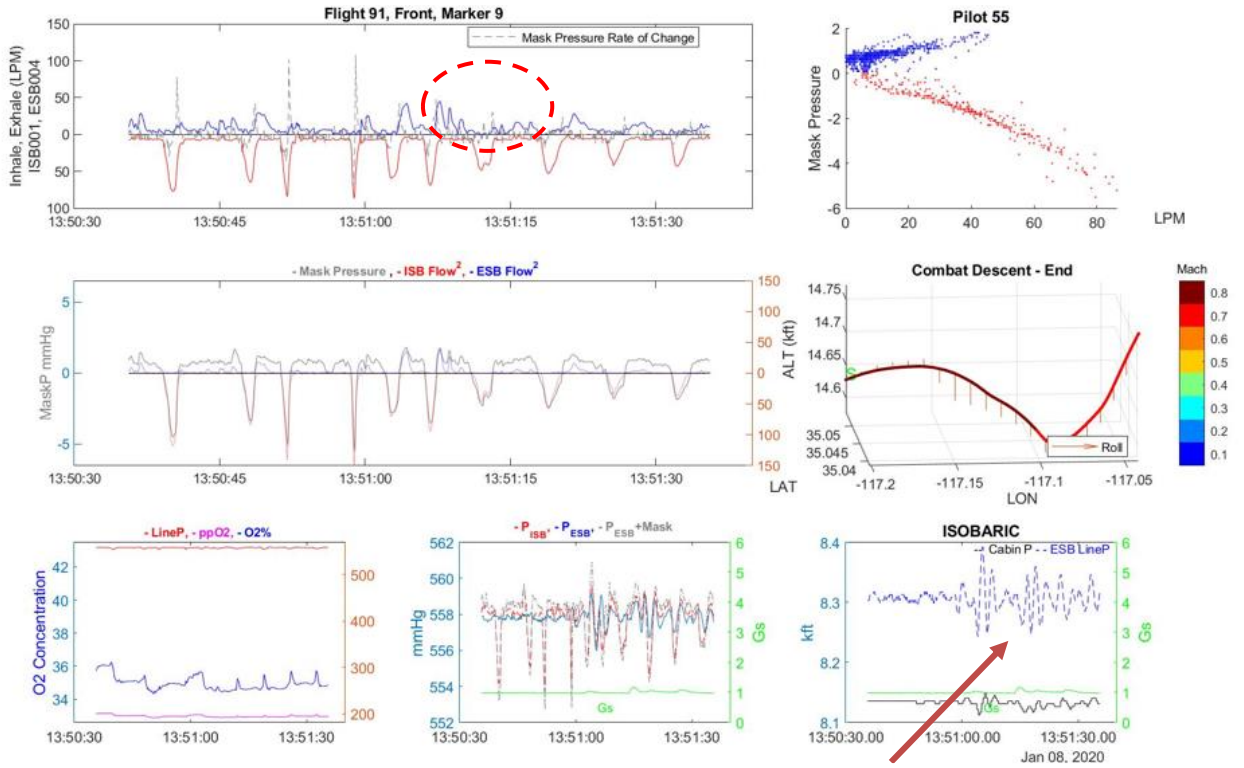

Figure 6.3.6. Flight 91
Cabin oscillations begin as the pitch angle changes at the bottom of a combat descent, and they last 1 minute. The breathing pattern also changes, as irregularities are observed in the triple and double exhalation.

6.3.4 Pressure Effects on Pilot Breathing

The PBA team integrated the flow rate for the same 1-minute period from Figure 6.3.6 and found the inhalation and exhalation volumes dropping in the second half of the window.

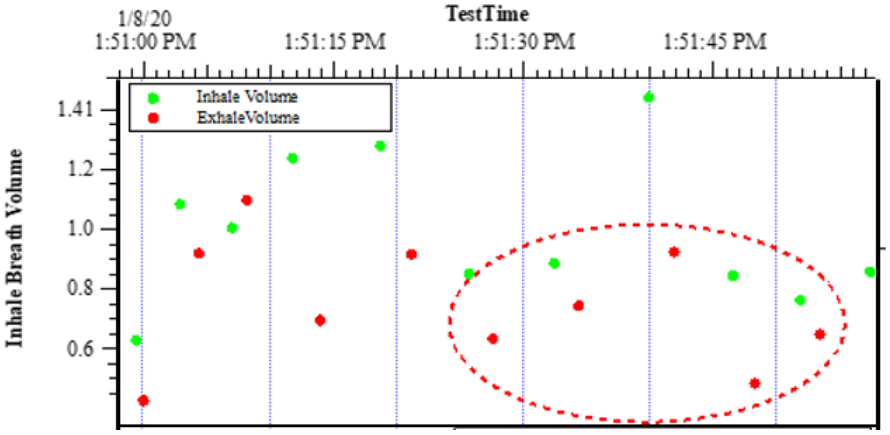

Figure 6.3.7. Breath Volume Decrease Occurs During Cabin Pressure Oscillations Depicted in Figure 6.3.6
Inhalation/exhalation flow reduces once the pressure oscillations begin, showing that low amplitude cabin pressure jitter does have a direct effect on pilot breathing

The hypothesis is that the rapidly and constantly varying cabin pressure changes the reference pressure for the breathing air regulators, and due to the unavoidable slight mechanical delay, the

pressure and resulting flow lags the pilot demand in these situations. This phenomenon also affects the successful completion of the exhale function. The hysteresis of the last five exhalations from the Figure 6.3.6 example is highly irregular, and the pressure-flow does not follow the expected near-linear relationship (Figure 6.3.8).

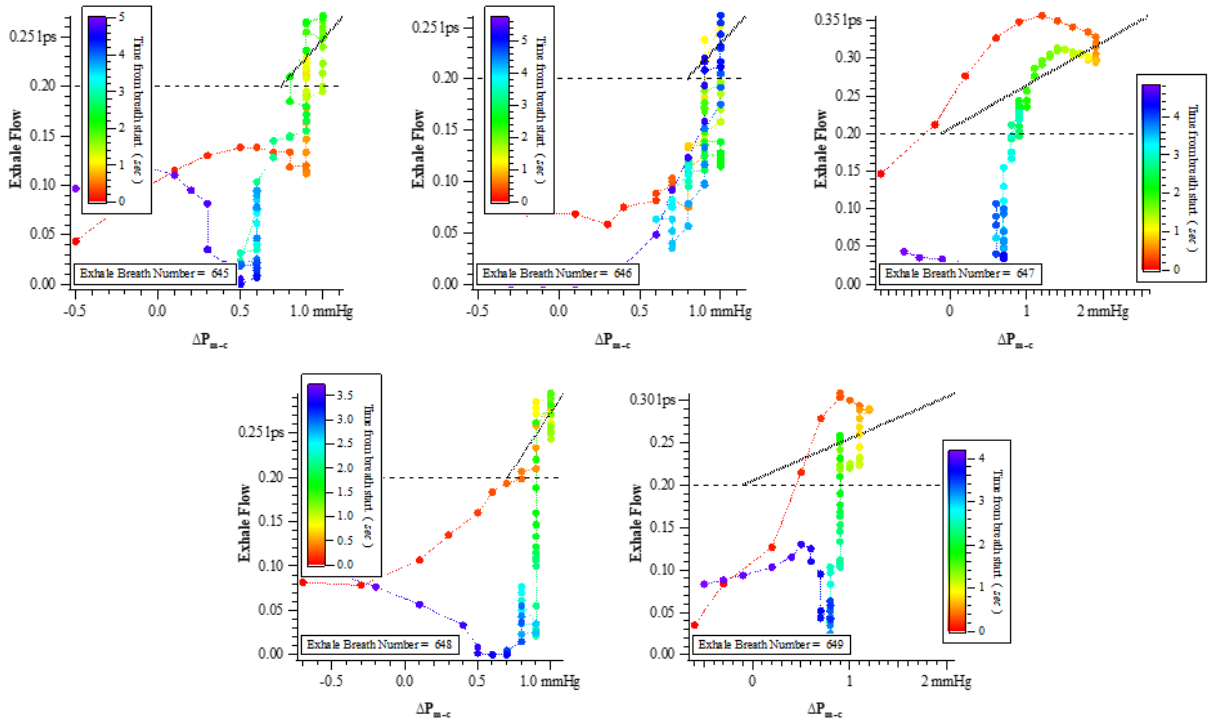

Figure 6.3.8. Irregular Exhalation Hysteresis in Period of Oscillations
Refer to Section 3.3.4 for ideal hysteresis plots for breathing with and without safety pressure. Irregular hysteresis is bad because the air was not expelled in accordance with the pressure exerted, which can indicate a labored or incomplete exhalation.

Fast Fourier Transform (FFT) frequency analysis are used to reveal the dominant frequency components of the oscillations, relative to breathing (Figure 6.3.9).

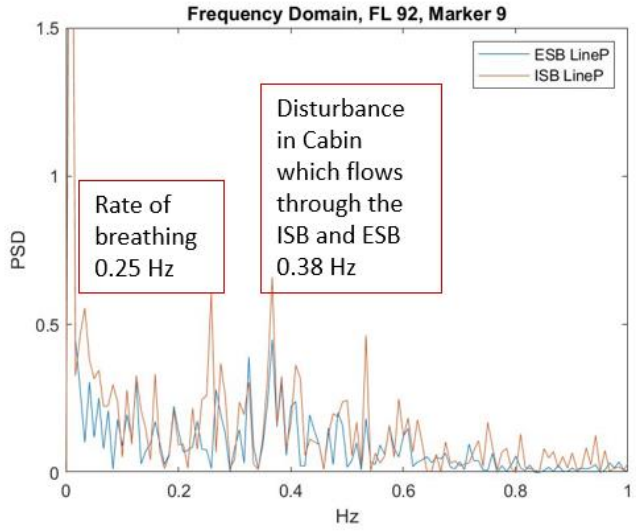

Figure 6.3.9. Oscillation on Aircraft 843 is Higher than Rate of Breathing

The oscillations were found consistently in post combat descents in flights 80 and 92 (USN configuration) and flights 87 and 91(USAF configuration) all using the same aircraft, F/A-18, Tail #843. The same oscillations were also found at the much slower airline descent segment as shown in Figure 6.3.10.

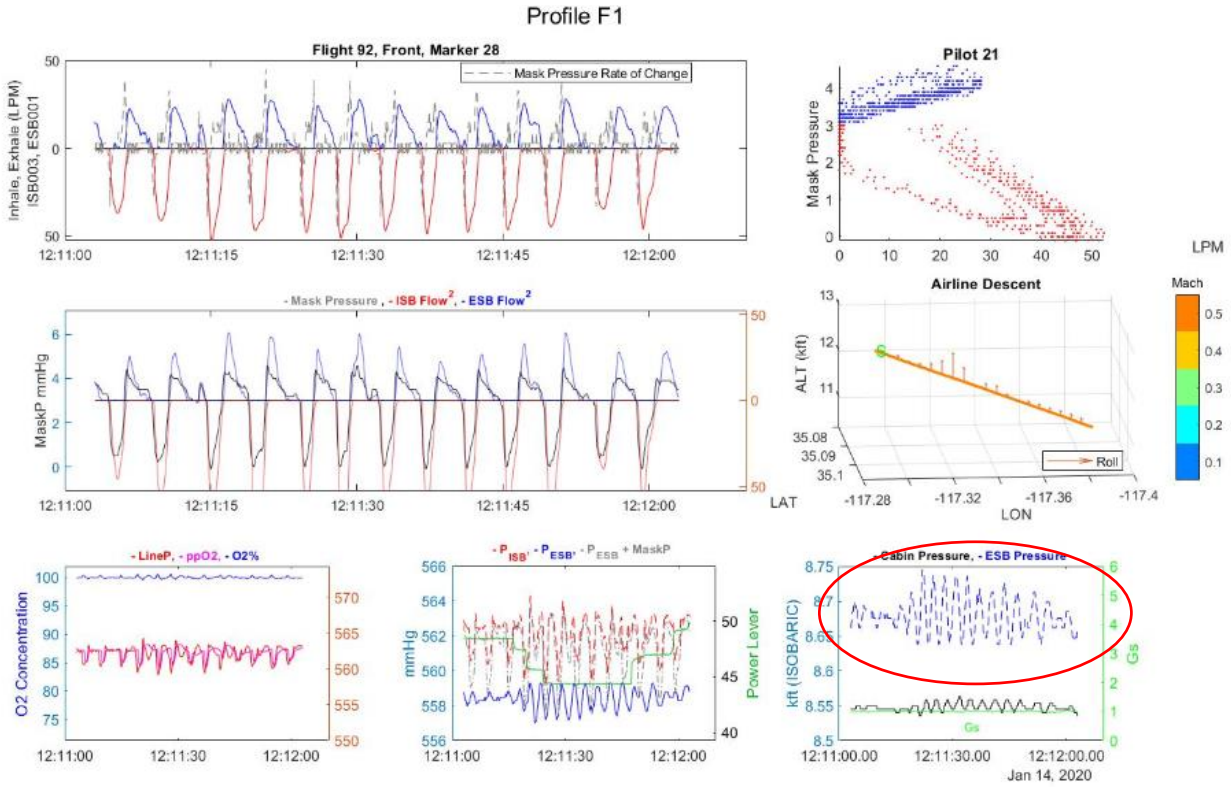

Figure 6.3.10. Cabin Pressure Oscillations Not Controlled
Cabin pressure oscillations are not controlled even at low velocity and 1 G, with only 1,000 ft altitude change in an isobaric region. Also notice the unsteady inhalations in the multiple rings of the red trumpet curve, and slanted exhalations.

Flight 98 represents a third aircraft, F/A-18, tail #868. The cabin pressure is also hard to control during level acceleration and deceleration, especially when velocity is accelerating or decelerating through Mach 1. Figure 6.3.11 shows the deceleration example.

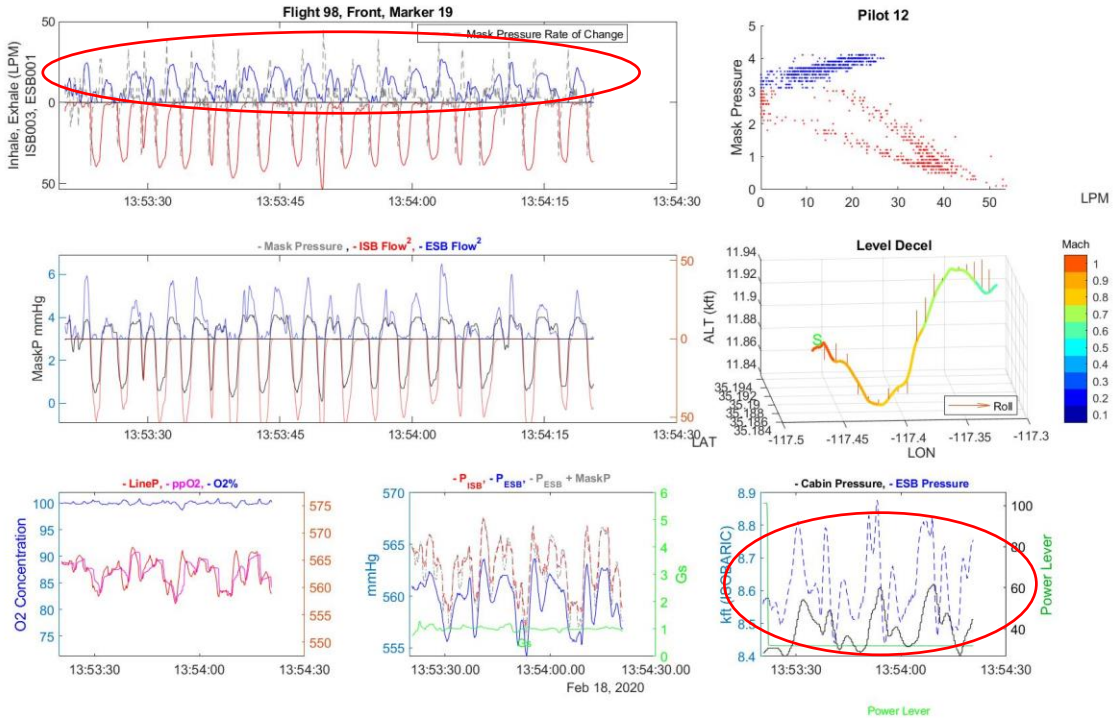

Figure 6.3.11. Cabin Oscillations Not Controlled
Cabin oscillations are not controlled even at through level deceleration in an Isobaric region. This pilot was supplied positive pressure; the difficulty is on the exhalation side with irregular and double exhalations.

The PBA found no such oscillations in the F/A-18 dual seat aircraft, Tail #846.

6.3.5 Cabin Pressure Control Summary

In summary, cabin pressure control is unpredictable, and appears dependent on the particular aircraft. Oscillations and perturbations in cabin pressure affect the breathing system response in providing airflow. In turn this affects the pilots' breathing response, especially with respect to ease of exhalation. As such, it is important to continually monitor the status of the pressure control system and mitigate any early signs of instability.

F.6-11. PBA identified cabin pressurization issues due to increase of dynamic pressure (affected by airspeed, G's, maneuvers, throttle position, and system settings). These changes also affect the entire breathing system.

6.4 Profile H Mini-Study

Profile H was designed as a prototype flight profile to test specific aspects of the aircraft breathing system and pilot/breathing system interactions. Profile H starts with a ground portion before take-off that consists of normal, relaxed breathing to achieve a baseline response, as well as some "maximal breathing" to 'push' the pilot's breathing response. Both instructions are repeated in flight for comparison. The profile also contains more challenging maneuvers to observe the breathing system response under more stressful aerobatics conditions. Finally, after landing there is another period of relaxed, normal breathing and maximum breaths.

This section presents the results of three PBA Profile H flights, all in USN flight gear. The detailed breathing data for these flights is supplemented by spirometry data as well as pulse oximetry data. These measurements were taken at four discrete times:

- In the 'ready room' before the pilot donned the flight gear,
- In the aircraft before take-off but before the pilot began breathing on the aircraft breathing system.
- In the aircraft after flight before the pilot disembarked the aircraft and was still in the flight gear.
- In the 'ready-room' after the pilot doffed the flight gear.

These biometric data allowed a first look into the effects of aircraft gear and activities on pilot breathing physiology. In addition, they provide a longitudinal control "within-pilots" by showing the potential effects from non-aircraft influences from day to day. This effect was first proposed in NASA's NESC Technical Assessment Report on F/A-18 and E/A-18 Fleet Physiological Episodes, to assess "pilot priming" as a predisposition to an adverse event.

6.4.1 Flight Profile GF/F

The list below provides the sequence of activities of the flight profile.

Mask Up
GB1- Normal Breathing - 3 min.
Mask Off - 2 min
Mask On
3 – Breaths: Maximal Inhalation, Normal Exhalation
3 – Breaths: Maximal Inhalation, Maximal Exhalation
Canopy Down
Taking Runway
Weight off Wheels
Mil Power Climb
15 kft - Normal Breathing - 3 min.
15 kft - 3 Breaths: Maximal Inhalation, Normal Exhalation
15 kft - 3 Breaths: Maximal Inhalation, Maximal Exhalation
15 kft - Remove Mask
15 kft - Mask Up
15 kft - Talking Script
Military Power Climb
OBOGS Descent - Start
OBOGS Descent - End
Military Power Climb
25 kft - Normal Breathing - 3 min
25 kft - 3 Breaths: Maximal Inhalation, Maximal Exhalation
25 kft - 3 Breaths: Maximal Inhalation, Maximal Exhalation
Combat Descent and Zoom Climb - Start
Normal Breathing - 1 min
Level Acceleration
Level Deceleration

End Deceleration
90° Turn @ 3 - 4g
90° Turn @ 4 - 5g
5 G's Constant" Descend Turn
Maximal Afterburner climb 7K
30 kft - Normal Breathing - 3 min
30 kft - 3 Breaths: Maximal Inhalation, Normal Exhalation
30 kft - 3 Breaths: Maximal Inhalation, Maximal Exhalation
Cruise Descent - Start
Cruise Descent - End
Spiral Descent
Normal Breathing - 3min
Weight On Wheels
Pull Clear
GBII- Norm Breathing - 3 min
3- Breaths - Max in & Norm Exhalation
3- Breaths - Max in & Max Exhalation
Canopy up
Mask Down

The pilot was provided instructions to follow this pattern closely to allow direct comparisons.

6.4.2 Flight Details

Table 6.4.1 shows the three Profile H flights, each with a different pilot, but using the same F-18 aircraft (Tail #868) and USN mask configuration with safety pressure.

Table 6.4.1. The aircraft, pilot and life support configuration for each flight of Profile H.

Flight #	Profile	FCP	FCP Gear	RCP	RCP Gear	Aircraft	Tail No.
98	H1	12	USN	n/a		F-18	868
100		28					
102		55					

Figure 6.4.1 shows a summary of the test flight profile with the aircraft altitude, acceleration, cabin pressure and the O_2 concentration of the breathing gas as a function of time. As expected, the graph confirms that the USN system provides the pilot with breathing gas at nearly 100% O_2. That was true for all three Profile H flights.

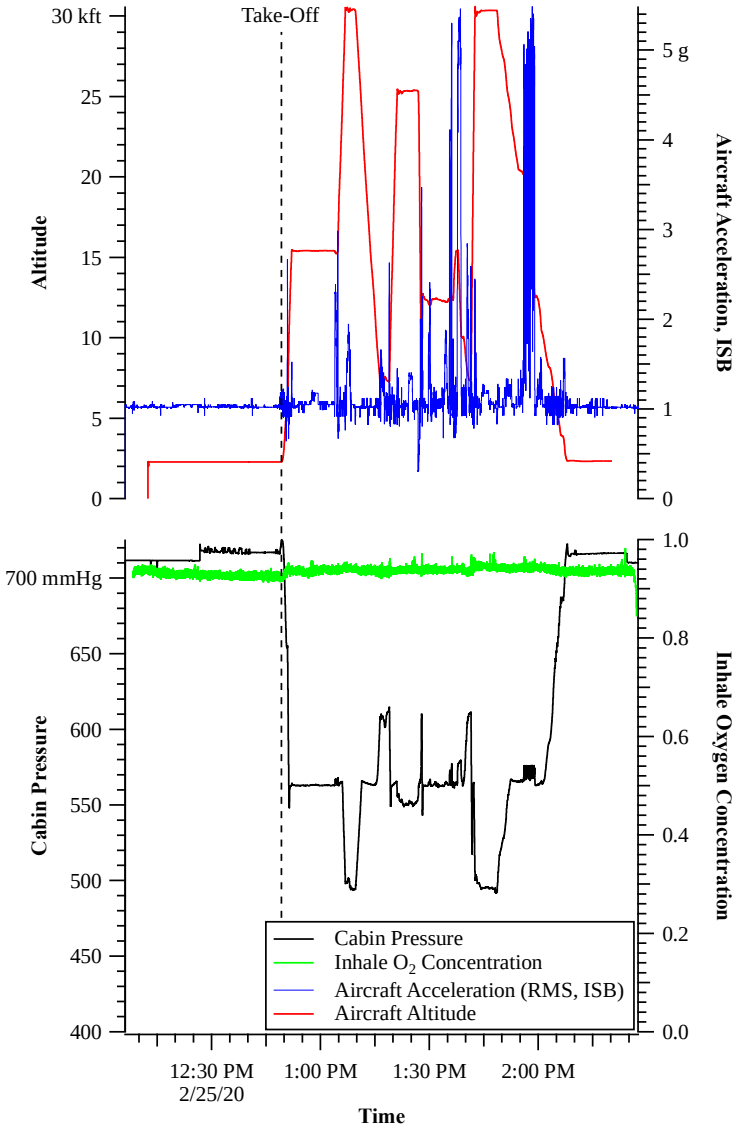

Figure 6.4.1. Cabin Pressure, Altitude, Aircraft Acceleration (RMS as measured by the ISB) and Supply O_2 Concentration as Function of Time for FLT-102
The other flights had nearly identical flight profiles.

6.4.3 Summary Data: Pilot Physiological Response

Figures 6.4.2 through 6.4.4 show the summary physiological data for FLT-098, FLT-100, and FLT-102, respectively. The plot shows the three-minute averaged data for tidal volume, respiration rate, minute ventilation and O_2 supply for the entire flight. The shading on the tidal volume represents plus or minus one standard deviation from the mean. The middle axes present the CO_2 as both partial pressure and as a mole fraction (expressed as a percentage). The upper axes are the aircraft altitude, cabin pressure and O_2 feed concentration (expressed as a percentage).

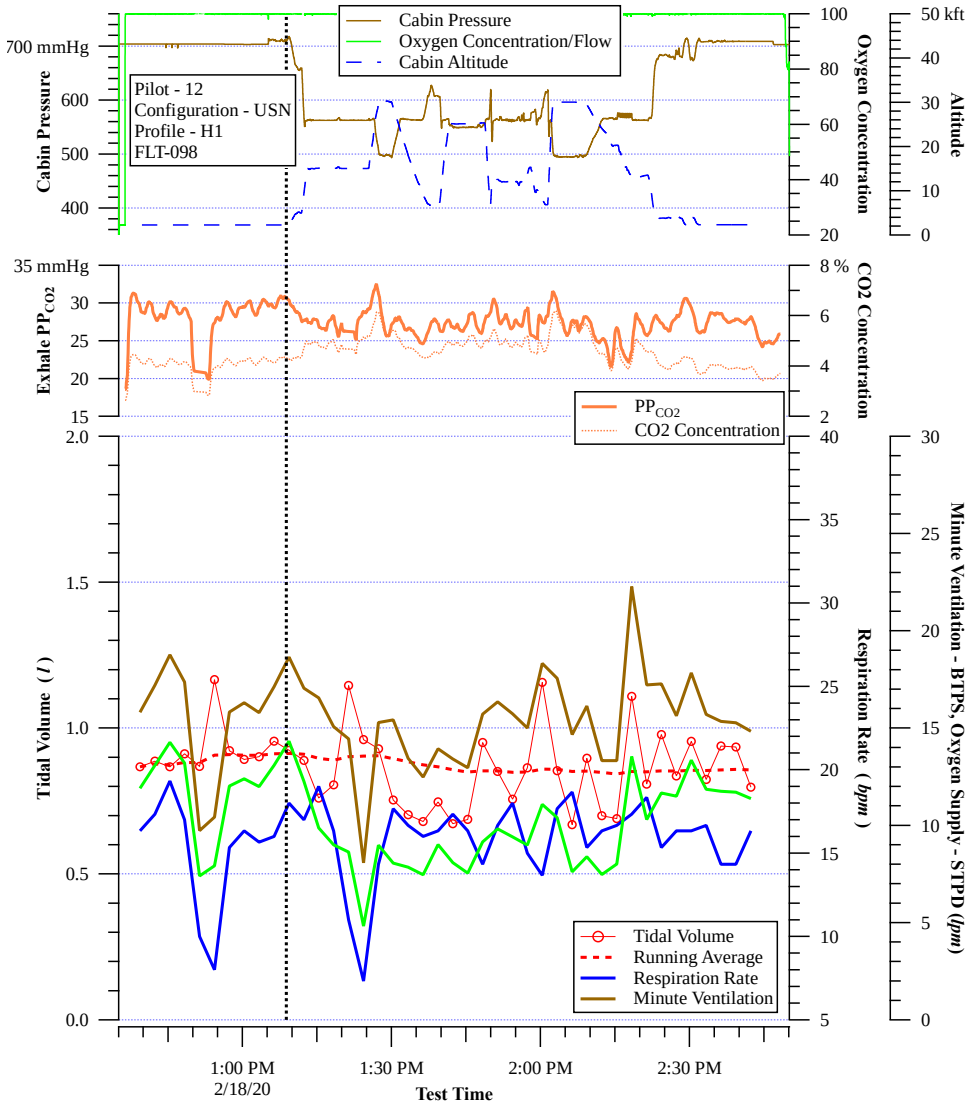

Figure 6.4.2. Summary Physiological Data for FLT-098
The plot shows the average tidal volume, respiration rate, minute and O_2 supply on the lower axes, CO_2 concentration (as partial pressure and percent) on the middle axes and aircraft information (cabin pressure, altitude and O_2 supply concentration) on the upper axes. The shading of the tidal volume data represents plus/minus one standard deviation of the 3-minute average.

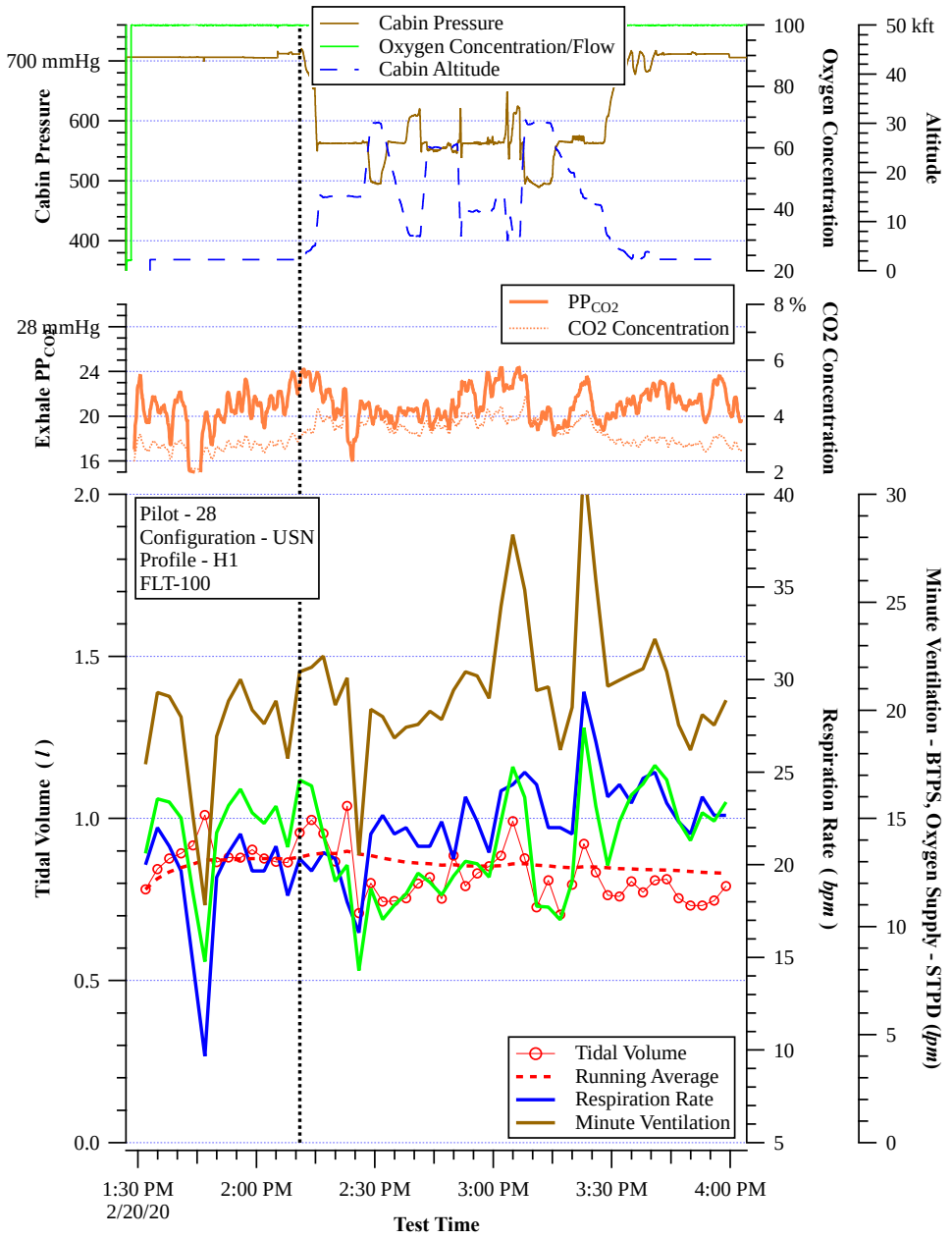

Figure 6.4.3. Summary Physiological Data for FLT-100
The plot shows the average tidal volume, respiration rate, minute and O_2 supply on the lower axes, CO_2 concentration (as partial pressure and percent) on the middle axes and aircraft information (cabin pressure, altitude and O_2 supply concentration) on the upper axes. The shading of the tidal volume data represents plus/minus one standard deviation of the 3-minute average.

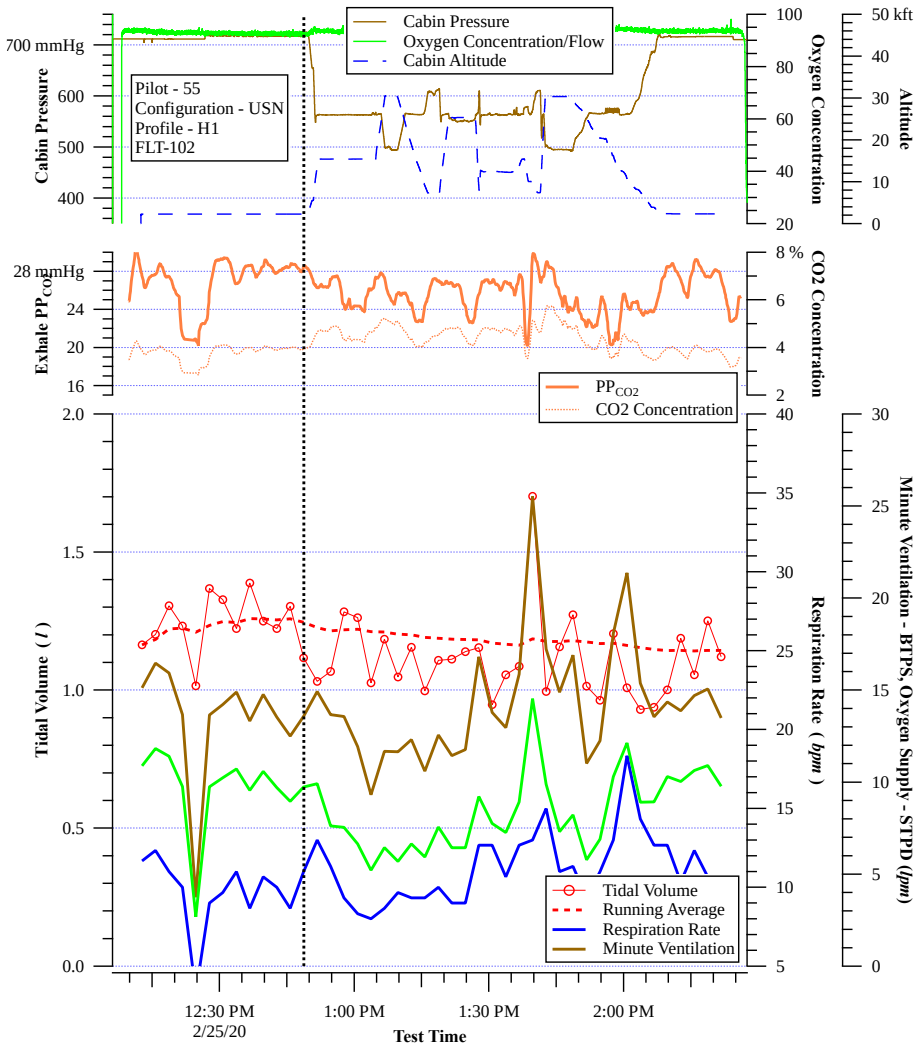

Figure 6.4.4. Summary Physiological Data for FLT-102
The plot shows the average tidal volume, respiration rate, minute and O_2 supply on the lower axes, CO_2 concentration (as partial pressure and percent) on the middle axes and aircraft information (cabin pressure, altitude and O_2 supply concentration) on the upper axes. The shading of the tidal volume data represents plus/minus one standard deviation of the 3-minute average.

6.4.4 Exhaled CO_2 Data

Figures 6.4.2 through 6.4.4 also show the exhaled CO_2 measurement from the VigilOX as both a partial pressure (in mmHg) and a percentage of the exhaled gas. The data for FLT-098 and FLT-100 show no discernible trend with time or for the different scripted breathing activities. FLT-102, however, does show distinct decreases in $PPCO_2$ in the max breathing activities as compared to the three minute averaged $PPCO_2$. For this pilot and flight, there is an approximately 4 mmHg drop in $PPCO_2$ during the max inhalation segments.

6.4.5 Event Specific Data

Section 6.4.1 shows that during the flight there are discrete, scripted events designed to test the interaction between the pilot and the breathing system at the limits of the pilot ability to inhale

and exhale. The physiological metrics during these scripted maximal breathing events are compared to segments of steady, relaxed breathing.

6.4.5.1 Steady Breathing Physiological Data

Figures 6.4.5 and 6.4.6 show the summary data for the analysis during the steady breathing segments and the maximal breathing segments immediately after the steady breathing portion of the designed flight. Figure 6.4.5 shows the three-minute averaged respiration rate and minute ventilation (based on ISB data) on the lower two axes (left and right) for each flight segment. The data show that the respiration rate is at or near its lowest value for the ground breathing before take-off for each pilot. The respiration rate for pilot 55 in FLT-102 is very low for the entire flight averaging a near-constant 10 bpm. The respiration rate for pilot 28 in FLT-100 increased about 20% after the first steady-breathing segment at 15 kft. The minute ventilation for pilots 12 and 55 were nearly equal while that for pilot 28 in FLT-100 was considerably higher.

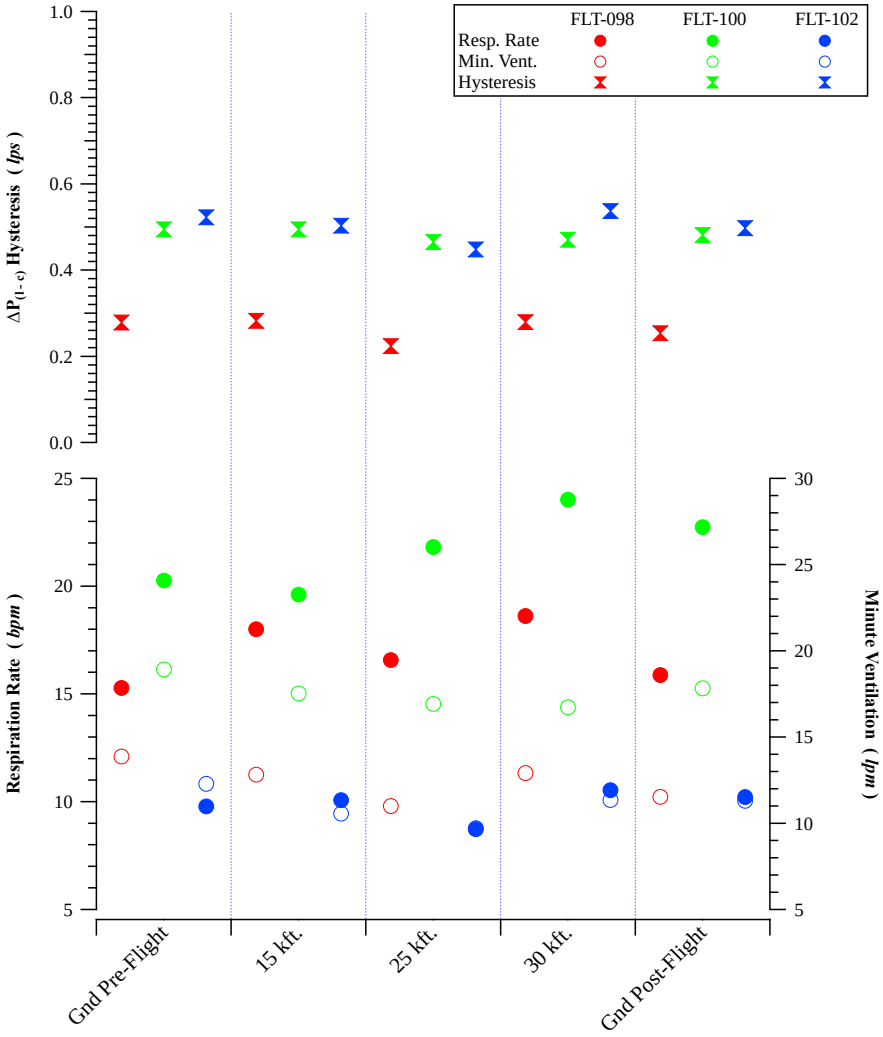

Figure 6.4.5. Respiration Rate, Minute Ventilation and Mean Hysteresis for Each Steady-Breathing Segment
The values in the graph represent the averages of the metrics over the 3-minute period referenced in Section 6.4.1.

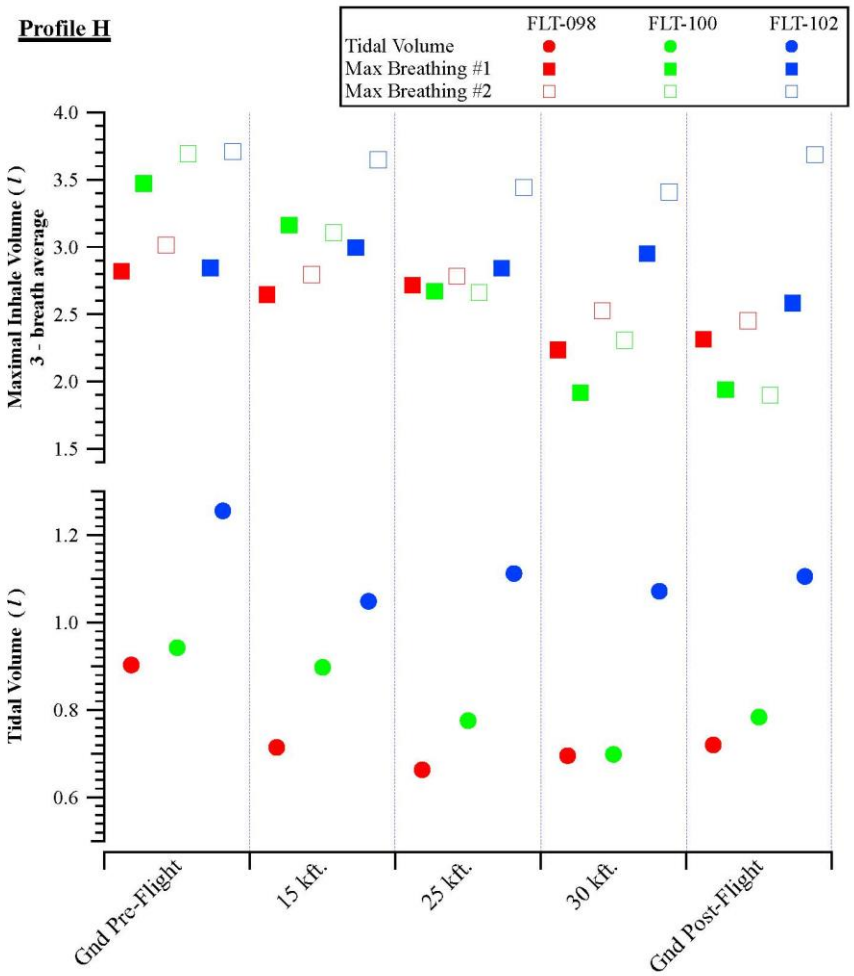

Figure 6.4.6. Mean Tidal Volume for Each Steady Breathing Segment (lower axis) and Average of 3-Breath Maximal Breathing Exercises (upper axes)
The first maximal breathing exercise (Max Breathing #1) is for a maximal inhale with a normal exhale. The second maximal breathing exercise (Max Breathing #2) is for a maximal inhale with a maximal exhale.

Figure 6.4.6 shows the mean tidal volume for the steady breathing segment and the mean inhalation volumes for the two maximum inhalation segments, one segment with normal exhalation and one with maximal exhalation. The data clearly show that for each flight the mean tidal volume decreased in flight as compared to the ground breathing baseline. There is some evidence of a little recovery to the pre-takeoff value during the post-flight ground breathing segment.

6.4.5.2 Steady-Breathing Pilot/Breathing System Interaction Data

Figure 6.4.5 also shows the hysteresis measured using the line-cabin pressure differential pressure for the three steady-breathing segments. The results clearly show the mean hysteresis is much lower for FLT-098 than for FLT-100 and FLT-102 for the three-minute steady breathing segments. For each flight, the hysteresis is nearly constant for each steady breathing period. Figure 6.4.7 shows the hysteresis (based on $\Delta P(l - c)$) histograms for the three flights and Table 6.4.2 shows the summary hysteresis statistics for the three flights.

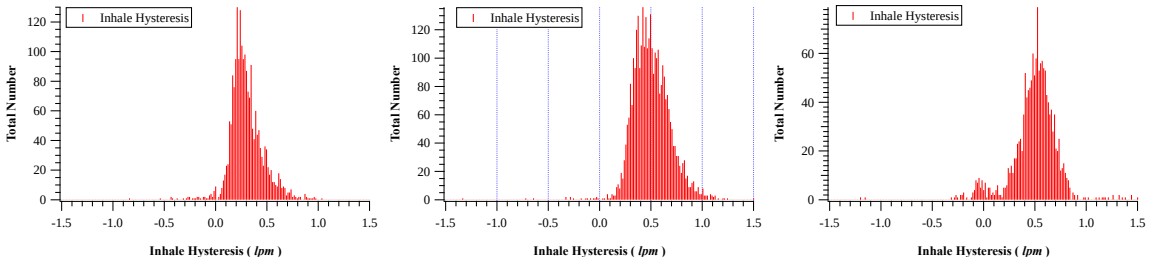

Figure 6.4.7. Inhalation Hysteresis Histograms (based on ΔP(l – c)) for, from left to right, FLT-098, FLT-100 and FLT-102.

Table 6.4.2 contains relevant statistics for the hysteresis histograms for the three flights in Figure 6.4.8. The data are for hysteresis measured using both ΔP(l – c) line – cabin, and ΔP(m – c). The data are for the distribution mean, standard deviation, and the fractions above 0.50, 0.71 and 1.0 lps, respectively.

Table 6.4.2. Relevant Statistics for Hysteresis Histograms for Three Flights in Figure 6.4.8

FLT-098	ΔP(l - c)	ΔP(m - c)
Mean Hysteresis (lps)	0.307	0.347
Standard Deviation (lps)	0.163	0.146
Fraction > 0.50 lps	0.111	0.099
Fraction > 0.75 lps	0.013	0.012
Fraction > 1.00 lps	0.000	0.000
FLT-100		
Mean Hysteresis (lps)	0.510	0.637
Standard Deviation (lps)	0.185	0.271
Fraction > 0.50 lps	0.489	0.648
Fraction > 0.75 lps	0.089	0.274
Fraction > 1.00 lps	0.011	0.108
FLT-102		
Mean Hysteresis (lps)	0.504	0.227
Standard Deviation (lps)	0.267	0.212
Fraction > 0.50 lps	0.565	0.026
Fraction > 0.75 lps	0.072	0.009
Fraction > 1.00 lps	0.017	0.005

The data show that the mean value of the hysteresis does not change significantly for each of the flight segments. The data also show that for FLT-098, the values of the hysteresis based on both (based on ΔP(l–c)) and (based on ΔP(m–c)) are low, especially for the USN configuration, and nearly equal.

The difference in hysteresis using these two differential pressures is interpreted as follows:

- The hysteresis values using ΔP(l–c) represent the regulator response to the demand signal since the pressure regulator regulates flow according to the outlet pressure relative to the cabin pressure.
- The hysteresis measured using ΔP(m–c) represents the regulator response to pilot demand.

In an ideal breathing system, there is little restriction to flow between the regulator and mask. In such a case, the values of the hysteresis should, in theory, be almost identical. When they are not equal it could be indicative of some kind of restriction between the mask and regulator outlet. For FLT-102, the hysteresis based on (based on ΔP(l – c)) is high, but the mean value (based on ΔP(l – c)) is relatively low.

F.6-12*. *Key physiological parameters of the breathing system are pressure, flow, volume and timing of supplied air. Systematic disharmony of the system can be measured by breathing hysteresis and breathing phase shift, which are new PBA methods of measuring BSDs. Instances of Pressure No Flow (PNF) was also an indicator of systematic disharmony of the system.*

R.6-6. Measure and track phase shift, hysteresis, and PNF (Pressure – No Flow) when evaluating aircraft system health – especially during times of peak breathing. (F.6-1, F.6-12)

R.6-7. Perform standardized flight test procedures to establish and evaluate an aircraft's pilot breathing system performance. ***(F.6-12)***

6.4.5.3 Maximal Inhalation Breathing

The data in Figure 6.4.6 also show that the maximal inhalation volumes also decrease in flight for each pilot, although to varying degrees. This is for both the normal and maximal inhalation segments. The combination of reduced tidal volume and maximal inhalation volumes suggest that there may be mild chronic hyperinflation occurring flight. This highlights the advantage of the specific profile in being able to determine these types of changes with the periods of steady and maximal breathing.

6.4.5.4 Ascent/Descents

The data visualizations and mixed effects models in Technical Section 5 have indicated that change in altitude is one of important factors affecting pilot response. More detailed analyses have confirmed that flight segments incorporating aggressive ascent and descent maneuvers are particularly relevant.

6.4.5.5 Nominal Breathing

Profile H incorporates a number of ascent/descent maneuvers that test the aircraft breathing system and pilot/breathing system interaction under conditions where the aircraft is undergoing rapid altitude changes. Tables 6.4.3 through 6.4.5 show the average tidal volume, respiration rate and minute ventilation (calculated from the ISB flow) for the different ascent/descent segments for the four Profile H flights.

Table 6.4.3. Average Tidal Volume (in l) During Each Ascent/Descent in Profile H
For reference the table also shows the value during the pre-flight steady-breathing period.

	Duration (s)	FLT-098	FLT-100	FLT-102	FLT-109aft
Pre-flight Steady Breathing	180	0.90	0.94	1.26	0.87
Mil Power Climb	70	0.78	1.01	0.95	0.72
Mil Power Climb	130	0.96	0.82	1.23	0.74
OBOGS Descent	420	0.70	0.74	1.07	0.75
Mil Power Climb	130	0.68	0.83	1.14	0.77
Combat Descent/Zoom Climb	70	0.85	0.86	0.87	0.75
Max AB Climb	70	0.84	0.84	0.88	0.70
Cruise Descent	340	0.67	0.76	1.00	0.62
Spiral Descent	180	1.07	0.92	1.16	0.81

Table 6.4.4. Respiration Rate (in bpm) During Each Ascent/Descent in Profile H
For reference the table also shows the value during the pre-flight steady-breathing period.

	Duration (s)	FLT-098	FLT-100	FLT-102	FLT-109aft
Pre-flight Steady Breathing	180	15.1	20.3	9.8	16.2
Mil Power Climb	70	20.2	20.9	12.9	18.7
Mil Power Climb	130	14.1	21.6	8.3	16.3
OBOGS Descent	420	16.3	22.4	9.5	15.0
Mil Power Climb	130	17.4	21.1	8.8	15.1
Combat Descent/Zoom Climb	70	17.1	24.6	13.5	16.1
Max AB Climb	70	17.6	27.3	16.5	18.0
Cruise Descent	340	17.1	22.0	10.0	15.2
Spiral Descent	180	18.9	29.9	18.7	18.4

Table 6.4.5. Minute Ventilation (in lpm) During Each Ascent/Descent in Profile H
For reference the table also shows the value during the pre-flight steady-breathing period.

	Duration (s)	FLT-098	FLT-100	FLT-102	FLT-109aft
Pre-flight Steady Breathing	180	15.1	20.3	9.8	16.2
Mil Power Climb	70	20.2	20.9	12.9	18.7
Mil Power Climb	130	14.1	21.6	8.3	16.3
OBOGS Descent	420	16.3	22.4	9.5	15.0
Mil Power Climb	130	17.4	21.1	8.8	15.1
Combat Descent/Zoom Climb	70	17.1	24.6	13.5	16.1
Max AB Climb	70	17.6	27.3	16.5	18.0
Cruise Descent	340	17.1	22.0	10.0	15.2
Spiral Descent	180	18.9	29.9	18.7	18.4

The tables also show the approximate duration of each maneuver. The durations range from slightly over one minute to approximately seven minutes. With the possible exception of the Mil Power and Max AB climbs, this duration should allow for a reasonable estimate of these time-averaged quantities. The order in the table is also the order in which they occurred in flight, so any changes that occur as a function of time at altitude are necessarily reflected in these values.

In general, the results in Table 6.4.3 show that the trends in tidal volume mostly mirror the tidal volume trends with time at altitude with the notable exception of the spiral descent. The tidal volumes, respiration rates and values of minute ventilation are at or near their maximum values for the spiral descent.

Tables 6.4.6 and 6.4.7 show the inhalation duration to total breath time ratio and exhalation peak pressure, respectively. The inhalation to breathe time ratio is near 0.50 for each pilot/flight except FLT-102 (Pilot 55) whose ratio was considerably lower. The ratio was relatively constant then for each ascent/descent except for the spiral descent where it tended to increase for each pilot.

The exhalation peak pressure showed no real trend with ascent/descent relative to the pre-flight breathing values. During the spiral descent that involved high G -levels, the pilot in FLT-100 did do some G -breathing. While the average value of the peak pressure for FLT-100 during the spiral descent is not much higher, the standard deviation of the peak exhalation pressure during this period is much higher. This is consistent with high peak exhalation pressures during the periods of G -breathing, but nominal peak exhalation pressures during normal breathing periods.

Table 6.4.6. Average Inhalation Time to Total Breath Time Ratio During Each Ascent/Descent in Profile H
For reference the table also shows the value during the pre-flight steady-breathing period.

	Duration (s)	FLT-098	FLT-100	FLT-102	FLT-109aft
Pre-flight Steady Breathing	180	0.47	0.46	0.33	0.46
Mil Power Climb	70	0.46	0.39	0.28	0.46
Mil Power Climb	130	0.50	0.39	0.25	0.44
OBOGS Descent	420	0.48	0.42	0.36	0.41
Mil Power Climb	130	0.45	0.41	0.24	0.41
Combat Descent/Zoom Climb	70	0.51	0.45	0.34	0.42
Max AB Climb	70	0.44	0.45	0.26	0.45
Cruise Descent	340	0.47	0.43	0.28	0.42
Spiral Descent	180	0.67	0.54	0.51	0.54

Table 6.4.7. The Average Exhalation Peak Pressure (mmHg) During Each Ascent/Descent in Profile H For reference the table also shows the value during the pre-flight steady-breathing period.

	Duration (s)	FLT-098	FLT-100	FLT-102	FLT-109aft
Pre-flight Steady Breathing	180	4.31	4.80	4.18	1.31
Mil Power Climb	70	4.31	4.80	4.18	1.31
Mil Power Climb	130	4.09	4.32	3.87	1.19
OBOGS Descent	420	4.02	4.27	3.65	1.20
Mil Power Climb	130	4.10	4.32	3.77	1.31
Combat Descent/Zoom Climb	70	3.99	4.29	3.64	1.45
Max AB Climb	70	4.53	4.77	4.16	1.73
Cruise Descent	340	3.96	4.22	3.62	1.02
Spiral Descent	180	3.95	4.92	3.87	1.64

6.4.5.6 Nominal Breathing

During an ascent or descent, the altitude and thus the pressure outside the cockpit change continuously. Depending on the altitude, the cabin pressure inside the cockpit will also change according to the cabin pressure schedule. The breathing system regulator controls flow during inhalation according to the line pressure at the outlet of the regulator, which in turn is referenced to the cabin pressure. The dynamic changes in pressure during an ascent or descent coupled with dynamic changes in G -level and engine thrust create an environment where the breathing system must compensate on a timescale on the order of a human breath.

With safety pressure systems, the inhalation line pressure acts to create a back-pressure on the exhalation valve. Therefore, during exhalation, when the inhalation valve is ideally closed, the inhalation line pressure (as referenced to the cabin) should create a constant, force on the exhalation valve.

The previous section suggests that the breathing system compensates for the dynamic flight conditions during the ascents and descents in Profile H. However, there are instances where dynamic changes in the environment overwhelm the breathing system compensation and result in disruptions to the normal breathing pattern. These disruptions were minor, and the pilots did not note any significant disruptions to their breathing. If these disturbances had been more prevalent and/or more severe, they could have engendered breathing difficulties and physiological changes.

Figure 6.4.8 shows a 1-minute time segment during the spiral descent in FLT-098 where the inhalation valve remains open during exhalation for one breath and several instances where the line pressure (referenced to the cabin or $\Delta P(l - c)$) drops below its nominal value and the safety pressure in the mask is lost.

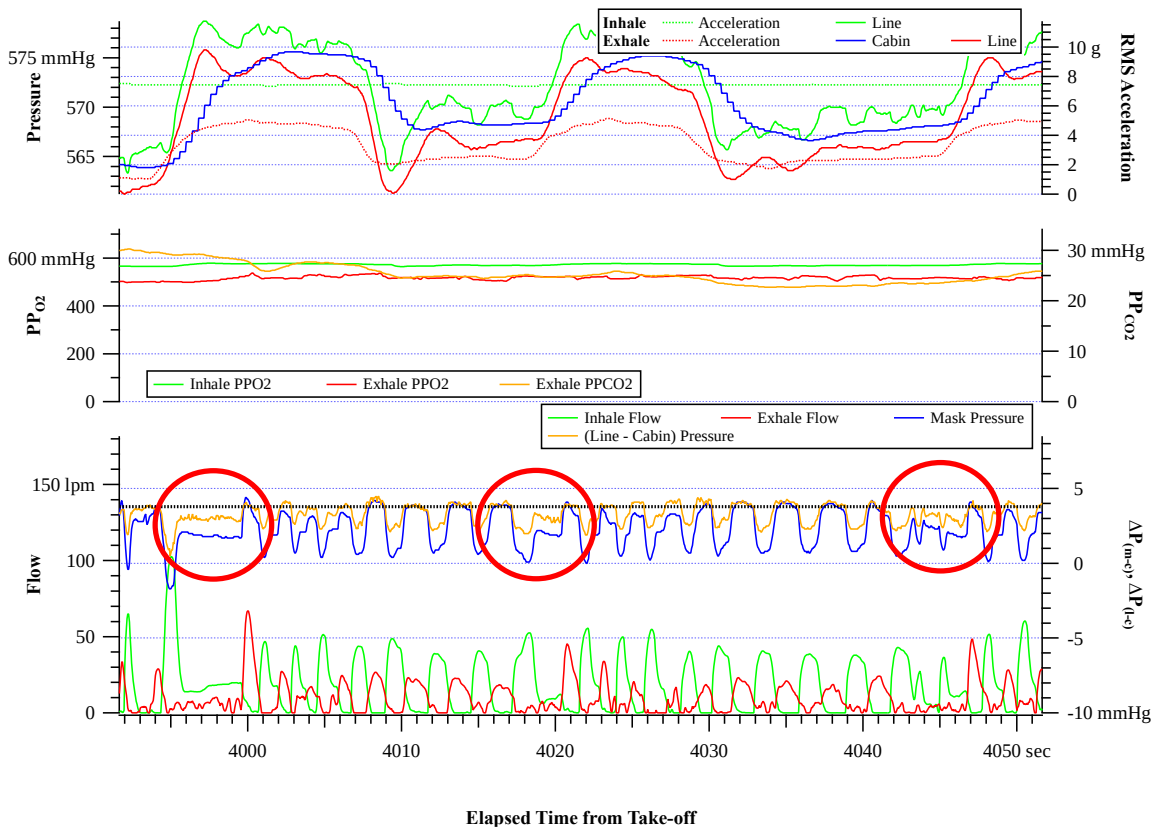

Figure 6.4.8. 1-minute Time Period During Spiral Descent in FLT-098
A 1-minute time period during the spiral descent in FLT-098 highlighting several instances (breaths, circled in red) where the inhalation line pressure (referenced to the cabin pressure) drops resulting in minor breathing rhythm disruptions. In the first instance there is evidence that the G-level might cause the inhalation valve to remain open during exhalation.

Figure 6.4.9 shows a time slice from FLT-109 (aft pilot) where there is a clear case where the breathing regulator is not compensating for the dynamic flight environment. Beginning just before 2440 sec after take-off the cabin pressure begins to decrease. The line-cabin differential pressure, however, increases (compared to mask pressure) as the regulator is not compensating properly for the changes in cabin pressure. The increasing line-cabin pressure then exerts an increasing force on the exhalation valve requiring the pilot to exert even more pressure to open the valve and exhalation. This causes a brief change in breathing rhythm until the system mostly recovers in approximately 20 seconds to restore nominal behavior.

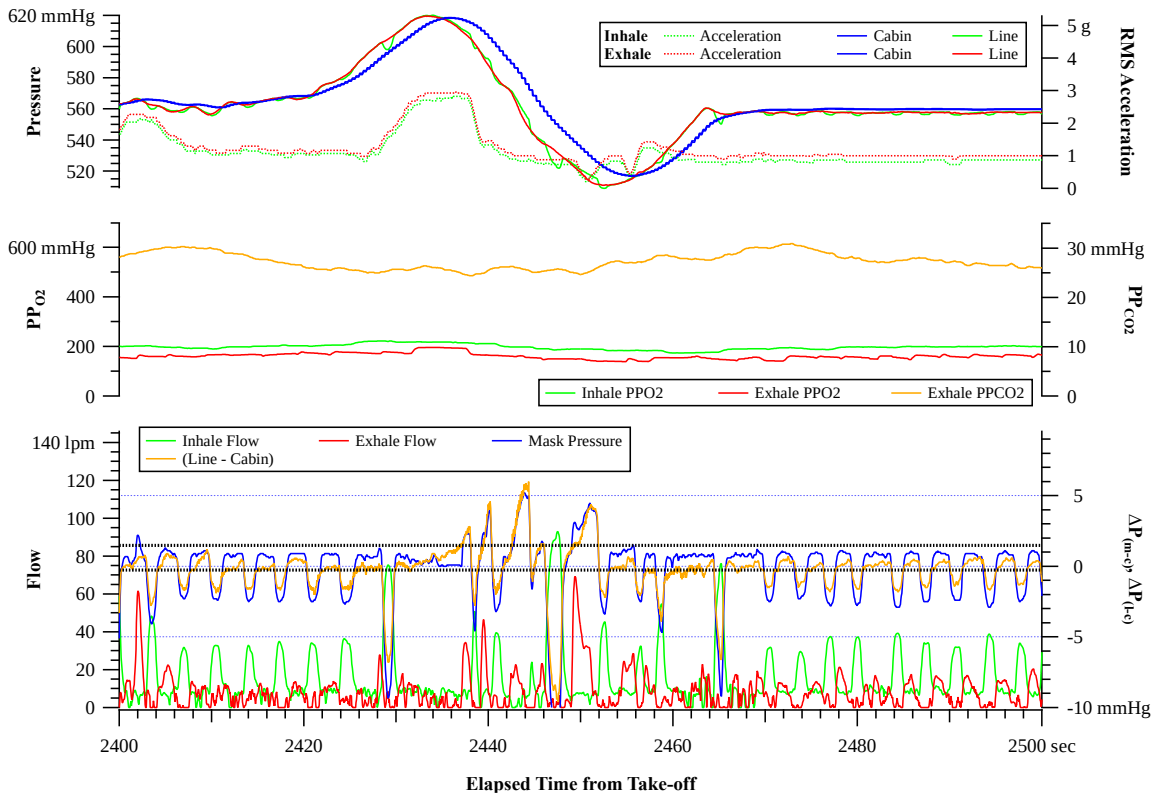

Figure 6.4.9. 100-second Time Period During FLT-109
A 100-second time period during FLT-109 (aft pilot) highlighting where the breathing regulator is not compensating for the dynamic changes in cabin pressure.

F.6-13. BSDs (deviations from normal linear pressure flow relationships) are not measured as part of acceptance testing or routine maintenance of aircrew breathing systems and no requirements exist to prevent excessive BSDs.

F.6-14. BSDs, as measured by breathing phase shift and hysteresis, can result in attenuated inhalation volume, delayed exhalation, reduced exhalation, and resistance in exhalation.

Summary of Profile H Mini-Study

Profile H is intended to be a standardized scripted profile which tests the aircraft, breathing system and the interaction between the pilot and breathing system. The profile consists of different scripted activities and periods of deliberate steady breathing. The results of the analysis of the three PBA flights with this profile show that a great deal of information about the breathing system and pilot/breathing system interaction can be discerned by comparing different flight segments within a flight and also between different flights.

6.5 Profile GF Mini-Study; Scripted Breathing Parameters

Certain specialty experiments were conducted to explore specific responses to scripted breathing maneuvers in conjunction with scripted aircraft environmental parameters. Some were conducted on the ground and then followed by a Profile F flight and given a “GF-profile” designator. Others were conducted as flight only experiments and given a “F-profile” designator. Some were inverted to result in a “FG-profile”. This is the only part of PBA wherein the pilot activities served as the independent variables. In all of the other PBA

experiments, pilot parameters were treated as a response. The various experiments are described in detail below.

6.5.1 Review of GF/F Profile Combinations

The Profile GF and F flights presented an opportunity to observe the effects of various human and aircraft inputs on pilot breathing. Both profiles follow a similar chain of events, with the pilot cycling through multiple cabin environmental and breathing system functions in addition to scripted alterations to the pilot's breathing pattern. The primary difference being that GF Profiles contain a segment where these events are also conducted in the cockpit on the ground prior to takeoff (hence the "G" for "ground"). Following the ground events, a typical Profile F flight is conducted. Likewise, the ground segment can be completed following the completion of a Profile F flight, resulting in the FG designation.

Typical Profile GF Ground Segment
Mask On, 2 minutes of relaxed breathing
10 normal breaths
3 breaths maximum inhalation, normal exhalation
3 breaths maximum inhalation, maximum exhalation
2 minutes of normal, relaxed breathing
Defog switch norm for 1 minute
Defog switch HOT for 1 minute
Defog switch COLD, cabin temperature knob full cold for 1 minute
Defog switch COLD, cabin temperature knob mid-range for 1 minutes
Defog switch NORM, cabin temperature now as required
Full COLD, full HOT, full COLD slowly over 1 minute
Oxygen Regulator ON/100%/NORM for 2 minutes
ON/NORM/NORM for 2 minutes
ON/NORM/EMERGENCY for 2 minutes
3 breaths maximum inhalation, normal exhalation
3 breaths maximum inhalation, maximum exhalation
ON/NORM/NORM for 2 minutes
ON/100% EMER for 2 minutes
ON/NORM/NORM for 1 minute
Talking script 1
Talking script 2
Open canopy, leave open for 1 minute, close canopy
Check six, left side 1 minute
Check six, right side 1 minute

Typical Profile F Script
Takeoff
Military power climb to 40,000 feet PA
Talking script 1
Talking script 2
10 normal breaths
3 breaths maximum inhalation, normal exhalation
3 breaths maximum inhalation, maximum exhalation
ON/NORM/EMER for 2 minutes

ON/NORM/NORM for 2 minutes
Defog lever HIGH for 2 minutes
Combat descent to 15,000 feet PA/idle power/speedbrakes/Mach 0.85 to 420 KCAS
Normal relaxed breathing for 2 minutes
3 breaths maximum inhalation, normal exhalation
3 breaths maximum inhalation, maximum exhalation
10 normal breaths
10 normal breaths
REMOVE MASK 10 normal breaths, replace mask
Cabin pressure dump, 2 minutes relaxed breathing
Cabin pressure ram dump, 2 minutes relaxed breathing
Cabin pressure normal
ON/100% NORM for 2 minutes
ON/NORM/NORM for 2 minutes
Maximum breathing for 10 seconds
Talking script 1
Talking script 2
Maximum afterburner climb to 45,000 feet PA, 350 KCAS to Mach 0.85
Climb at 350 KCAS at 2,000 ft/min from 22,000 to 26,000 feet
Descent at 350KCAS at 2,000 ft/min from 26,000 to 2,000 feet
Airline descent
Instrument approach
Closed pattern downwind abeam tower
Landing and shutdown

The GF and F profiles are scripted to deliberately vary multiple cockpit environmental settings, O_2 regulator settings, flight conditions, and breathing inputs that would otherwise only happen incidentally.

Varying the O_2 regulator output directly affects the amount of O_2 that is inhaled by the pilot. This represents a significant difference between the USAF configuration non-safety pressure masks and the USN configuration safety-pressure systems. Safety pressure regulators maintain 100% O_2 (or near 100% O_2, as will be discussed later), while non-safety pressure systems maintain a lower baseline (discussed below).

Varying flight conditions (altitude, velocity, G-force) can have a significant effect on the physiological response of the pilot. Variations in altitude, especially, like those produced by climbs and dives to and from over 40,000 ft, can lead to diminishing values of tidal volume. The influence of cockpit environmental settings on the aircraft breathing system is not necessarily intuitive, as changes in one could be reasoned to not affect the other. However, because the overall cabin environment is constantly changing, the environment in which the regulator, mask and pilot pulmonary system operate is also changing.

Pilot demand and aircraft response are coupled systems. This human-in-the-loop interface is not a simple one-way system, where pilot demand simply elicits a fixed response by the aircraft breathing system. There is feedback that occurs, where the response by the aircraft can cause the pilot to alter their demand to find an optimum equilibrium. As the pilot varies his demand, the performance of the responding system can be stressed in different ways. During maximum inhalation, pilot demand rapidly changes from stasis to maximum input, requiring a

corresponding response by the regulator. Maximum exhalation similarly requires the mask valves to respond rapidly to account for the sudden onset of large quantities of flow out of the pilot's lungs and into the mask.

6.5.2 Results from Profile GF/F flights

A total of eleven flights across profiles GF and F (six GF, four F, and one FG). One of these flights (FLT-031) took place in an F-15D, with the remainder being flown in the F/A-18 platform. Three flights (031, 041, and 045) occurred with a pilot in the rear seat, however, only flights 041 and 045 equipped the rear cockpit pilot with VigilOX. A summary of the flights is presented in Table 6.5.1.

Table 6.5.1. GF/F Flight Summary

Flight #	Profile	FCP	FCP Gear	RCP	RCP Gear	Aircraft	Tail No.
31	F	71	USAF	12	N/A	F-15	884
41	GF	28	USN	12	USAF	F/A-18	846
45	GF	12	USN	28	USAF		846
48	GF	55	USN	N/A			850
52	FG	71	USAF				850
57	GF	28	USAF				850
63	GF	71	USN				850
69	GF	21	USAF				850
80	F	55	USN				843
87	F	21	USAF				843
92	F	21	USN				843

All PBA F/A-18 USN configuration flights, mirroring USN current practices, maintained near-100% O_2, around 95% in the mask throughout the sortie. Some variations in Figure 6.5.1 could be due to O_2 % being a compound post-process calculation of ppO_2 and total line pressure, subject to compound error.

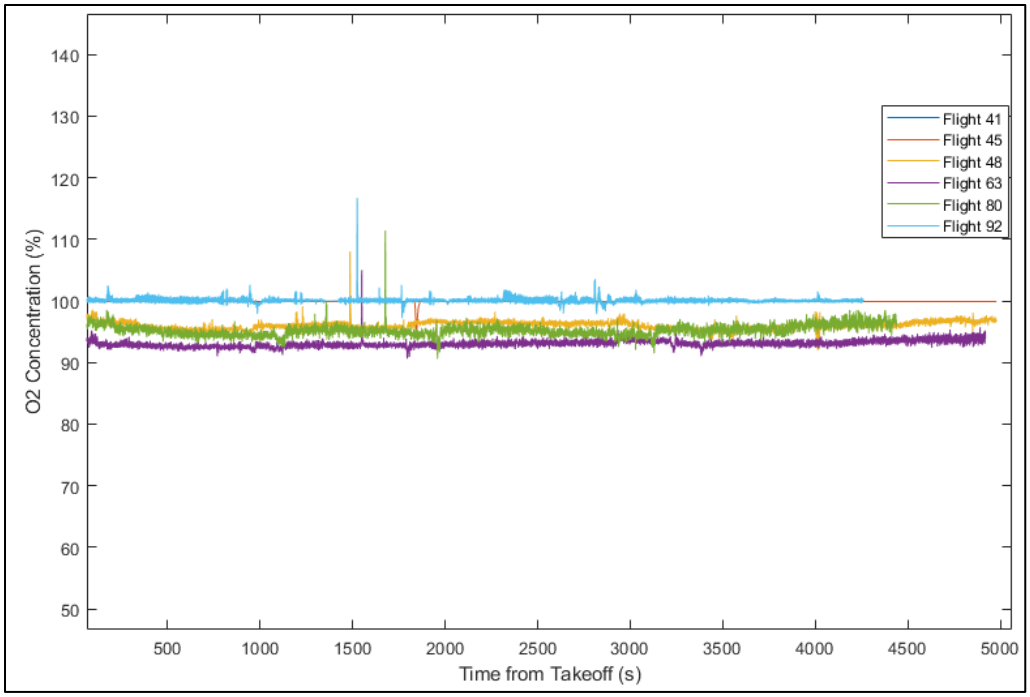

Figure 6.5.1. USN Regulator Equipped Breathing Air Supply O_2 Concentration Near 95% Instantaneous error of >100% O_2 is resulting from ppO_2/line pressure channels not updating at the same instance in a rapid-change environment.

F/A-18 aircraft configured with an USAF regulator are not designed to maintain 100% O_2 in the mask, and instead follow an altitude based O_2 schedule. O_2 baselines vary between flights, as can be seen in Figure 6.5.2. The six F/A-18 USAF configuration datasets exhibit baselines between 30% and 40%, centered around 35%. These flights utilize the CRU-73 regulator with an EDOX O_2 connector (Figure 6.5.2). Note that the PBA has flown Profile F in an F-15D airframe equipped with the CRU-98 regulator and CRU-60 O_2 connector (Flight 31, not shown), and noted a higher baseline of 48% O_2.

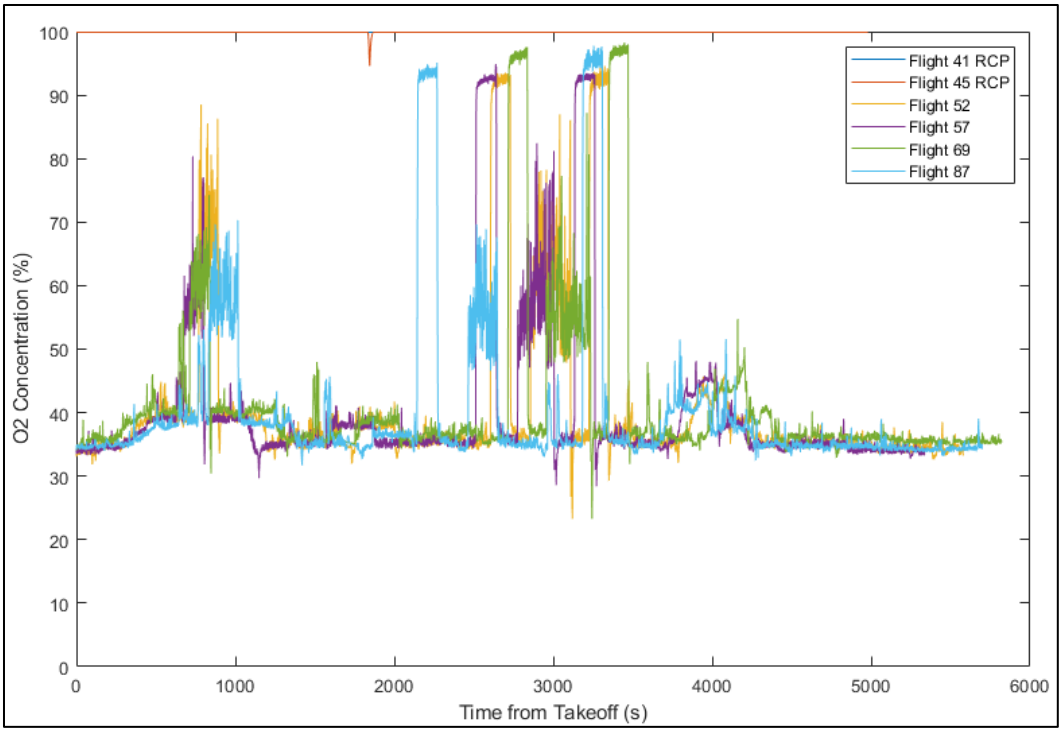

Figure 6.5.2. F/A-18 Non-Safety Pressure Sortie O_2 Concentrations Vary O_2 concentration increases with altitude as seen at 4,000 seconds: 45% O_2 corresponds to a climb to 40,000 ft. O_2 level near 100 % was resultant to exercising the "100% O_2" setting via a switch.

Figures 6.5.3 (a) and (b) show O_2 concentration and altitude vs time for flights 31 and 69 respectively. The CRU-98 regulator, used in Flight 31, compensates for flight at or above 40,000 ft by increasing the O_2 concentration in the mask to ~70%. The CRU-73 regulator, however, does not compensate to such a significant degree, increasing O_2 concentration to roughly 45%.

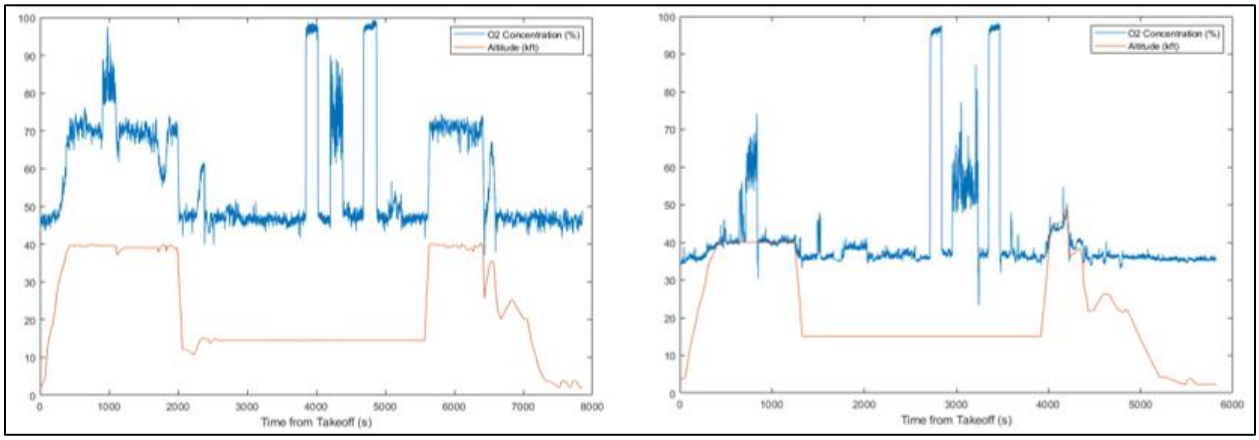

(a) F-15 ***(b) F/A-18***

Figure 6.5.3. O_2 Concentration and Altitude vs Time for (a) Flight 31 and (b) Flight 69

While the safety pressure sorties maintain O_2 concentrations near 100%, the non-safety pressure sorties follow the scripted cycling of regulator settings as described in the profile overview. There are multiple points in every GF/F/FG profile where the O_2 concentration supplied by the regulator is varied by pilot input. Pilots use 3 switches to set O_2 settings, invoke "Emergency" or

"100% O_2" modes. These events can be visualized in the spikes in O_2 concentration in Figure 6.5.4.

CRU-73 panel-mounted regulator

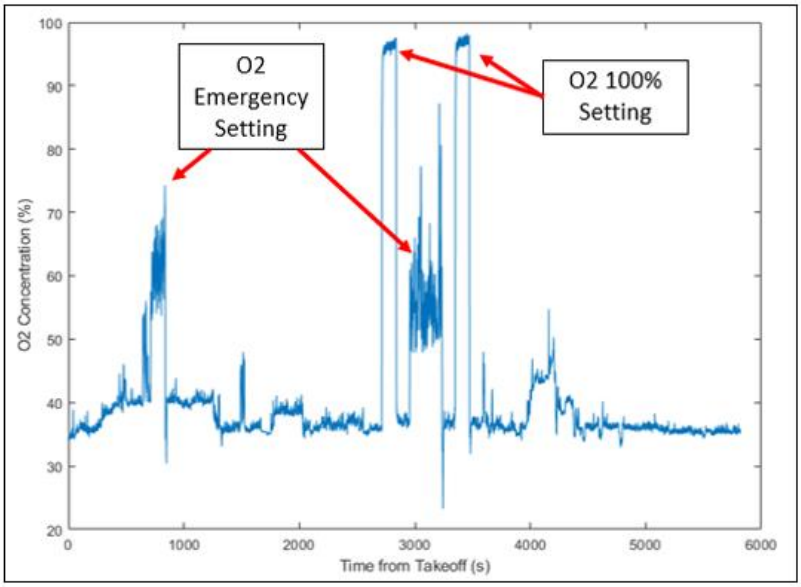

Figure 6.5.4. Flight 69 O_2 Concentration, as affected through the CRU-73 Regulator

Red is the Emergency lever: The NORMAL (or NORM) position provides normal operation with respect to pressure and dilution according to the position of the white lever. The EMERGENCY (or EMER) position provides 100% O_2 under increased pressure (safety pressure), regardless of the position of the white diluter lever.

White is the Diluter lever: NORM supplies a diluted mixture of 100% O_2 and cabin air, according to a schedule built into the regulator. "100%" supplies 100% O_2 all the time.

Green is the Supply lever: it has OFF and ON. In OFF there is no flow of air to the pilot.

Note that when the "Emergency" mode alone was engaged, during the short exercise the O_2 reached 50 to 70%

In Figure 6.5.4 that the "Emergency" (EMER) O_2 setting perturbs the regulator output with short-term oscillations. In both EMER events during Flight 69 (which is representative of all seven USAF configuration datasets), O_2 concentration increases but experiences a high degree of noise. The first instance of the EMER setting being selected results in a two-minute period in which the O_2 concentration varies between 53 and 75%, with constant noise over the duration of the event. The second instance sees O_2 levels vary between 47 and 87%, with even more noise than the first event.

The physiological effects of varying pilot and aircraft inputs were analyzed utilizing the methods described earlier in this report. The same variation noted across the PBA experiment, both between pilots and between flights flown by the same pilot, is present in the GF/F/FG profiles. A summary of mean values of key physiological parameters for each sortie is presented in Table 6.5.2. The 2-seater flights have a 2nd row with data from the Rear Cockpit Pilot (RCP).

Table 6.5.2. Flight Physiological Summary

Flight No.	Pilot No.	Mean Tidal Volume (L)	Mean Inhalation Effort (mJ)	Mean Exhalation Effort (mJ)	Mean Respiration Rate (bpm)
31 (AF)	71	0.776	1.869	0.682	17.556
41 (N)	28	0.970	-3.490	5.498	23.357
41 (AF) RCP	12	0.742	3.179	7.648	14.056
45 (N)	12	0.804	-5.492	3.765	18.245
45 (AF) RCP	28	0.732	2.549	11.904	21.236
52 (AF)	71	0.731	1.982	2.453	18.426
57 (AF)	28	0.865	3.453	11.531	20.782
63 (N)	71	0.874	-3.406	3.819	20.799
69 (AF)	21	1.054	6.816	11.791	17.346
80 (N)	55	1.081	-3.200	4.791	12.950
87 (AF)	21	0.980	6.152	9.289	19.022
92 (N)	21	0.886	-1.845	4.007	18.906

Table 6.5.2 contains a mix of USN and USAF configuration flights, with the USN Safety Pressure AFE having negative inhalation effort. Within each sortie, specific events produced significant deviations from the flight mean values. For each physiological parameter, the mean value over the duration of an event was calculated. In searching for off-nominal patterns in the data, events in which tidal volume varied by more than 10% or inhalation/exhalation effort varied by more than 50% were isolated. This consistently isolated two types of events; maximum breathing exercises and mask off exercises. Mask off events have been excluded from this analysis, leaving maximum breathing as the lone conditions identified by this simple filter.

Non- Safety Pressure flights, Profile F

The effects of maximum breathing can be clearly seen when contrasted with the mean breathing values across the sorties. Figure 6.5.5 displays tidal volumes for flights 31, 52, and 69. In multiple cases, maximum breathing produced tidal volumes more than double that of the sortie mean. Note the individual differences between the pilot of flights (31, 52), and that of a different pilot of flight 69.

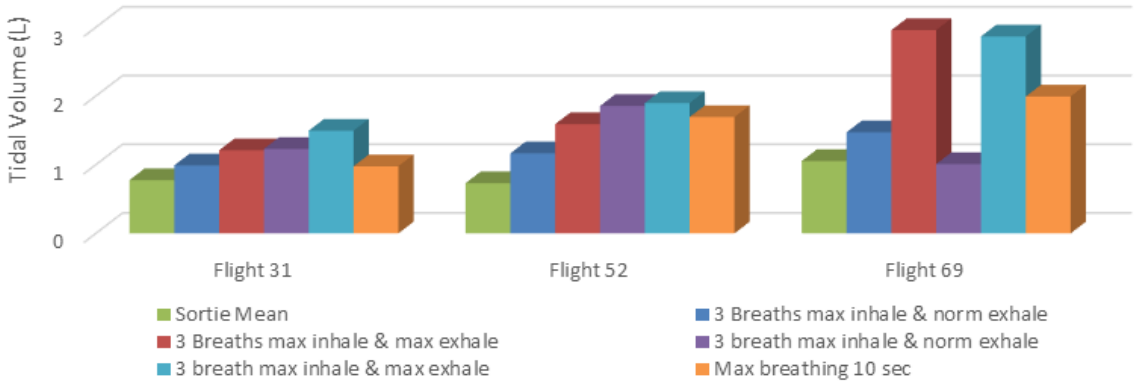

Figure 6.5.5. Tidal Volume for Maximum Breathing Events for Flights 31, 52 (same pilot), and 69 (different pilot) The flight conditions were all non-safety pressure, diluter demand regulator and varying O_2

Inhalation and Exhalation Effort

As would be expected with a more demanding inhalation cycle, inhalation effort almost uniformly increases for maximum breathing events, as shown in Figure 6.5.6. Flight 69 data represents a significant departure from the remainder of the observed data, due to the fact that it was flown by pilot 21, other than Flights 31 and 52, which were both piloted by the pilot 71. In three events the mean inhalation effort by pilot 21 (FLT-071) skyrockets to more than three times the maximum inhalation effort exerted by pilot 71 in Flight 52. The remaining two events display mean values that are less than the sortie mean, which is a significant departure from the observed trends.

Pilot 21 in flight 69 displays the same high-maximum behavior in exhalation effort (Figure 6.5.7). Of note is that during Flight 52 Event #37 (Heavy Breathing Exercise), mean exhalation effort is negative. This indicates continued flow through the mask during the inhalation cycle, a signature of regulator lag.

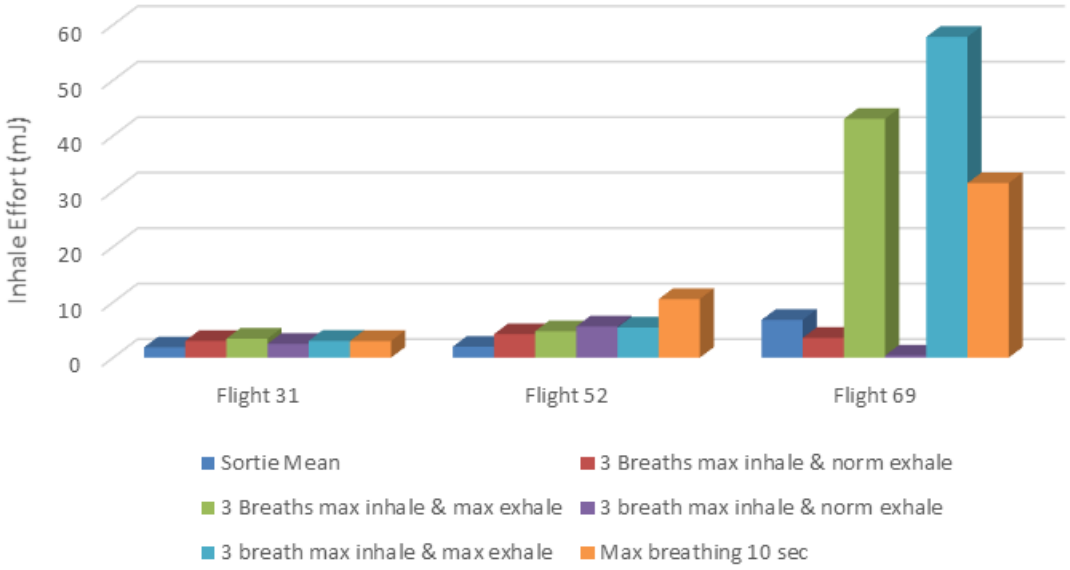

Figure 6.5.6. Inhalation Effort for Maximum Breathing Events for Flights 31, 52, and 69 (all non-safety pressure) with pilots 71, 71 and 21, respectively, shows wide scale individual differences

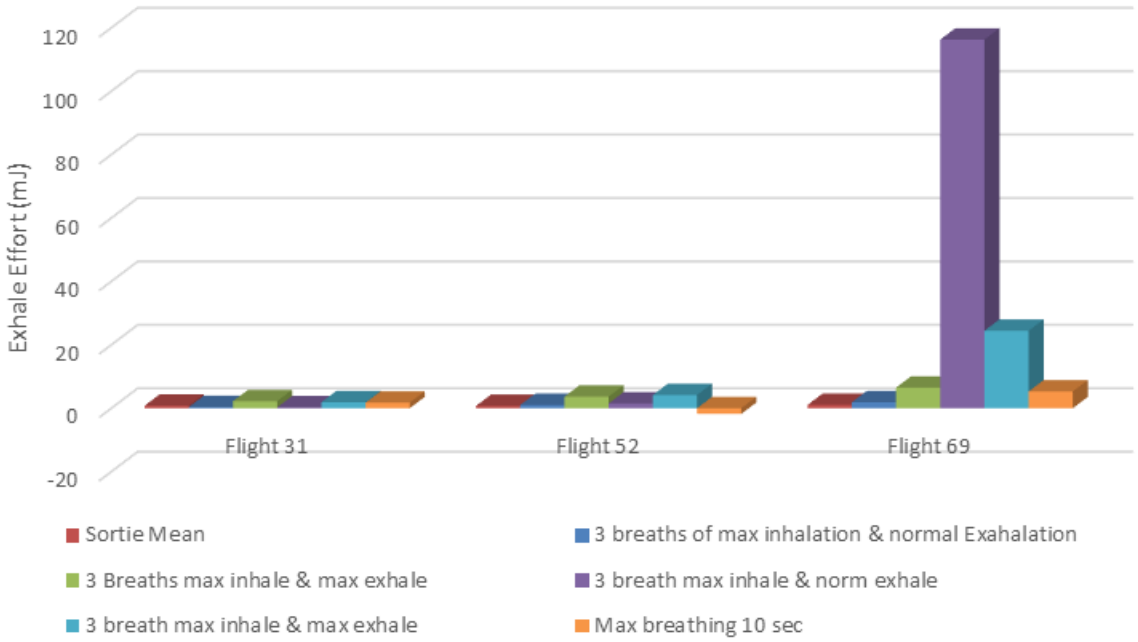

Figure 6.5.7. Exhalation Effort for Maximum Breathing Events for FLTs 31, 52, and 69 (all non-safety pressure) with pilots 71, 71 and 21, respectively, shows wide scale individual differences

Multiple parameters aimed at characterizing regulator response timing have been discussed so far in this report. As is discussed in Anti-G Straining Maneuver (AGSM) Characterization, integration of the flow rate over the mask pressure for an entire breath yields a parameter which can quickly identify flow disharmony between the pilot and aircraft. Integrated flow, measured in millijoules, yields positive values for an exhalation and negative values for an inhalation where there is little to no disharmony present. As regulator response degrades, these trends flip, with integration of the inhalation cycle yields positive values and integration of the exhalation cycle yields negative values. As can be seen in Table 6.5.3, the heavy breathing exercise (Event 37) during Flight 52 and all maximum breathing exercises (Events 7, 8, 15, 32, and 33) display off-nominal values of integrated flow.

Table 6.5.3. Mean Integrated Flow (over pressure) for Off-Nominal Flight Event Markers

Flight Event #	Mean Integrated Inhalation Flow (mJ)	Mean Exhalation Integrated Flow (mJ)
FLT-052 Event 37	-3.771	-2.910
FLT-069 Event 7	0.466	-0.049
FLT-069 Event 8	4.266	-1.441
FLT-069 Event 15	3.951	-0.963
FLT-069 Event 32	32.093	0.578
FLT-069 Event 33	3.617	-1.652

Positive values of inhalation integrated flow indicate significant amounts of flow into the mask while the pilot is attempting to exhale. This leads to high values of exhalation effort as the pilot must displace the gas flowing into the mask in addition to the volume contained in his lungs to exhale. This is the case in all five maximum breathing events for FLT-069. Positive inhalation integrated flow values indicate regulator lag, with the supply of gas into the mask continuing

beyond the point where pilot demand ceases. Negative values of exhalation/inhalation flow, conversely, indicate that exhalation flow is occurring at a high rate while the pilot is inhaling.

Safety pressure flights, Profile F

Safety pressure flights exhibit the same tidal volume behavior in FLT-0 31, FLT-052, and FLT-069. All maximum breathing events produce increases in tidal volume over the sortie mean, as seen in Figure 6.5.8.

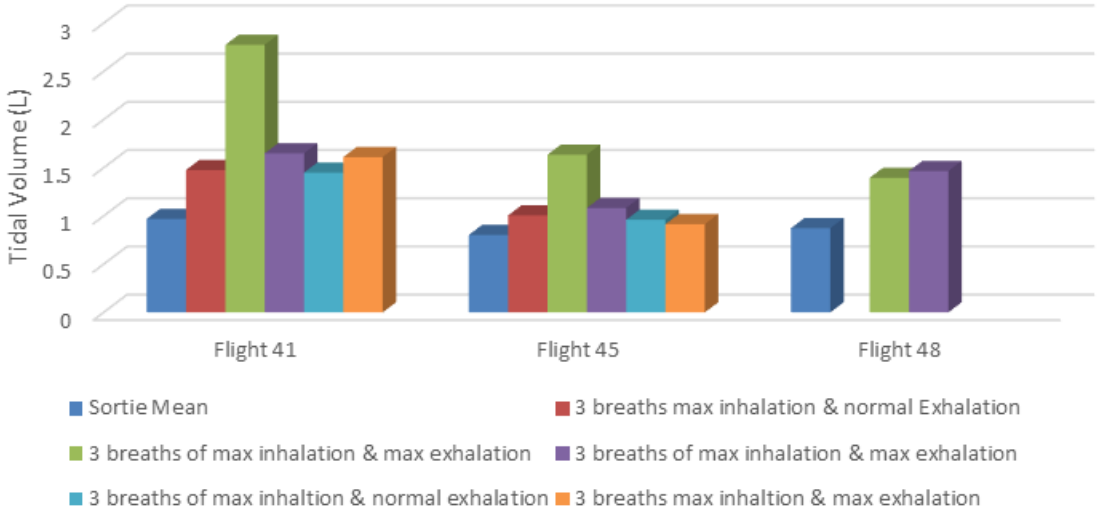

Figure 6.5.8. Tidal Volume for Maximum Breathing Events for Flights 41, 45, and 48 (all safety pressure) with pilots 28, 12 and 55 respectively highlight individual differences

Inhalation and Exhalation effort

Inhalation effort values reflect the behavior that has been previously identified with safety pressure flights. Inhalation effort values are commonly negative during safety pressure sorties, indicating that the aircraft is doing work on the pilot during the inhalation cycle. This is the case in all but four maximum breathing events (i.e., 9, 16, 17, and 29 during Flight 41).

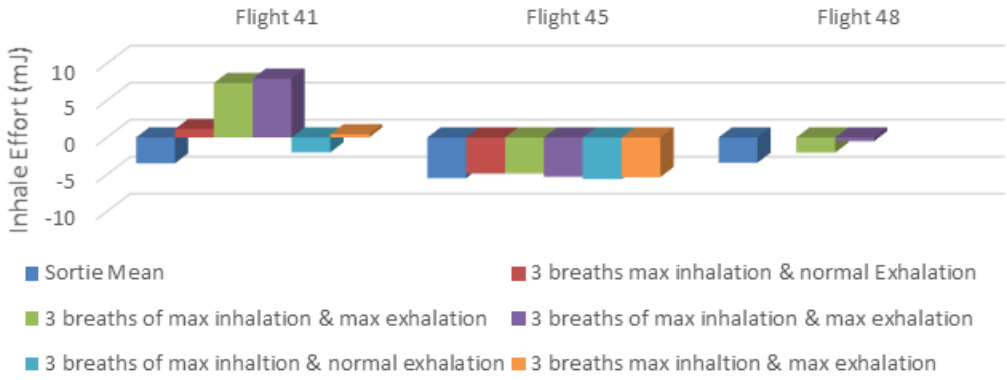

Figure 6.5.9. Inhalation Effort for Maximum Breathing Events for Flights 41, 45, and 48 (all safety pressure) with pilots 28, 12 and 55 respectively. Flights 41 and 45 were flown on a dual seater F/A-18, while FLT-048 on a single-seater.

Exhalation effort (Figure 6.5.10) shows consistent increases from the flight mean during any periods where the maximum breathing exercises are conducted.

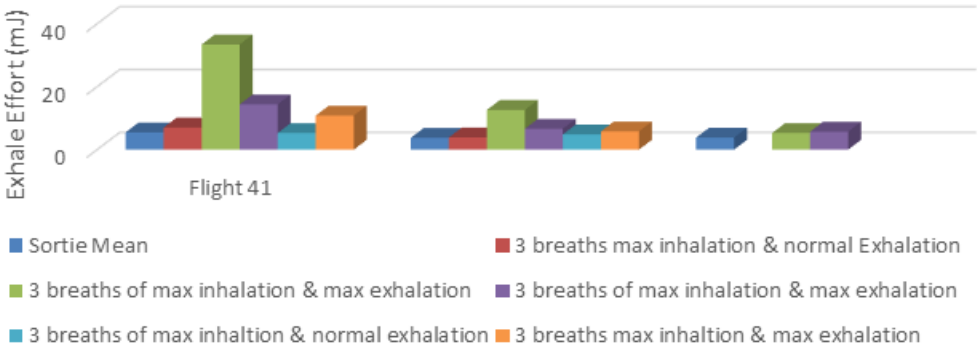

Figure 6.5.10. Exhalation Effort for Maximum Breathing Events for Flights 41, 45, and 48 (all safety pressure) with pilots 28, 12 and 55 respectively.

As seen with the non-safety pressure sorties, evidence of regulator lag is observed during maximum breathing exercises for USN configuration flights. Figure 6.5.11 shows integrated inhalation flow versus tidal volume for two non-safety pressure sorties (flights 69 and 87) and two safety pressure sorties (flights 80 and 92) maximum breathing events. This plot contains all maximum breathing pattern breaths for the four flights. Every maximum breathing breath exhibits positive values of integrated inhalation flow, indicating regulator lag. More significant lag events are those in which the integrated flow is greater than 10 mJ. This threshold is used to identify significant regulator lag and is further discussed in the Anti-G Straining Maneuver Characterization section. Figure 6.5.11 shows that the maximum breathing events produce significant quantities of regulator lag events, suggesting that the CRU-103 and CRU-73 regulators struggle to meet high pilot demand.

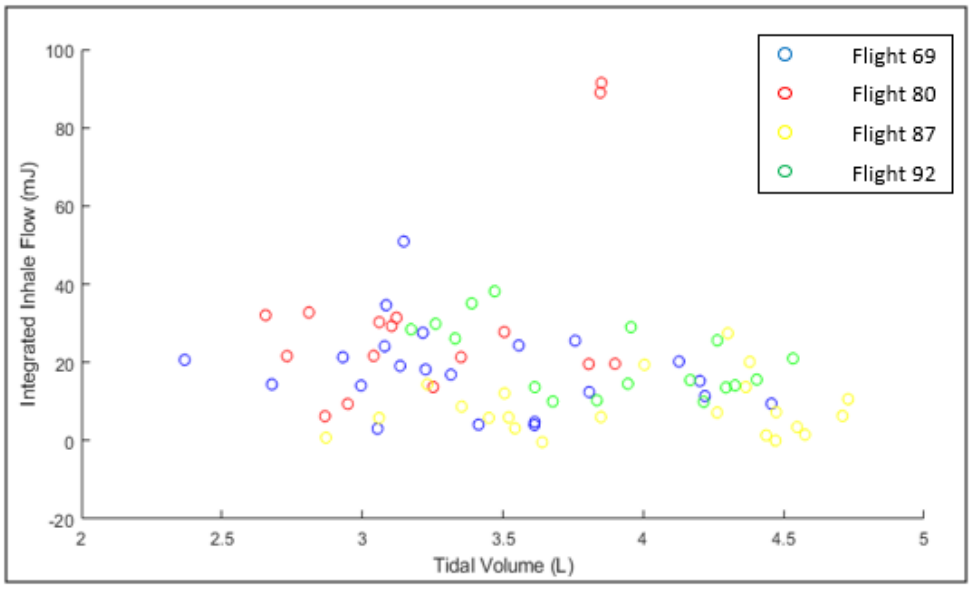

Figure 6.5.11. Tidal Volume vs Integrated Inhalation Flow for Maximum Breathing Most events are greater than 10 mJ Integrated Flow, indicating significant lag events

While events such as varying O_2 diluter and defog settings coupled with rapid altitude changes did not produce a consistent effect on physiological results, they did introduce a significant amount of noise into the data. This can be seen in Figure 6.5.12, which shows tidal volume, inhalation, and exhalation effort versus time for four events during Flight 69. When compared to

the normal breathing event, the three preceding events display a high degree of variation between breaths. This is especially visible when the defog is set to HIGH and when the aircraft undergoes a combat descent.

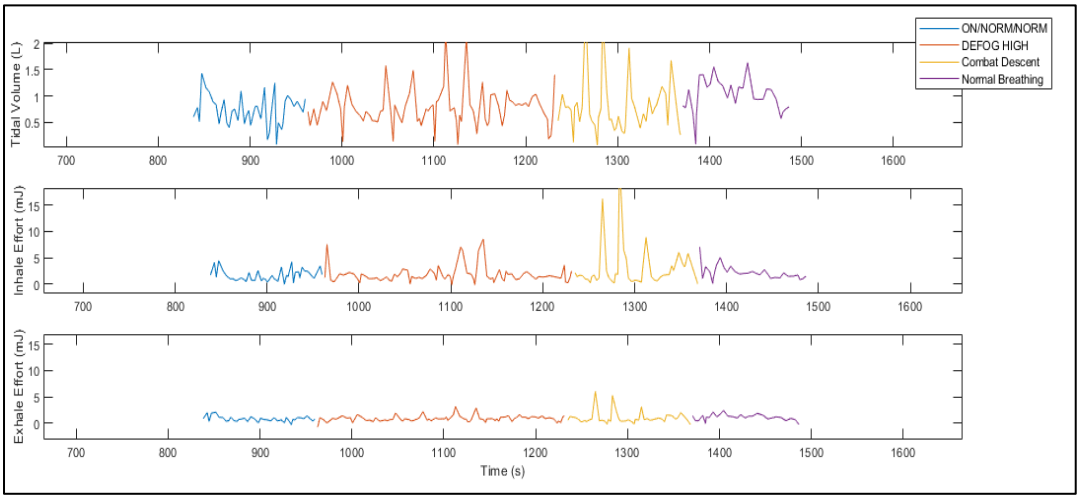

Figure 6.5.12. Flight 69 Tidal Volume, Inhalation Effort, and Exhalation Effort vs Time for Four Flight Events

Noise within the physiological data during these events could be due to multiple factors. During normal breathing events, pilots are focused on steady, even breathing. When completing other events, such as the combat descent, the pilot is instead focused on the maneuver itself. Breathing disruptions can be ignored to focus on flying, but if ignored long enough they may lead to symptoms. Instrument panels, yoke and throttle controls, visual cues from beyond the canopy, and myriad other details consume the pilot's attention. This leaves little to no bandwidth to think about breathing and the body reverts to autonomous breathing which could become erratic to compensate for the external factors. For example, a combat descent represents a stressful event where breathing could become highly varied, akin to riding a rollercoaster. In this elevated stress environment, natural breathing cadence could become interrupted. Additionally, a change in defog setting alters the cabin environment. The body will naturally react to a change in ambient conditions, one of which could be a change in the natural breathing cycle.

Figure 6.5.13 displays a decreasing trend in tidal volume over the duration of the normal breathing event. This is a common trend in the "10 Normal Breaths" events, although it does not occur uniformly for all occurrences of the event. Figure 6.5.13 shows tidal volume for three normal breathing events occurring during flights 48, 69, and 87 (one safety pressure and two non-safety pressure sorties). Figure 6.5.14 shows two consistent trends, an immediate spike in tidal volume followed by a steady decay. In all three flights the initial spike exceeds a tidal volume of 1.4L, while the decay drops below 0.9L. This behavior is consistent with the pilot recovering from an off-nominal breathing cycle. The initial spike akin to catching one's breath, with the subsequent decay representing a return to a natural breathing rhythm.

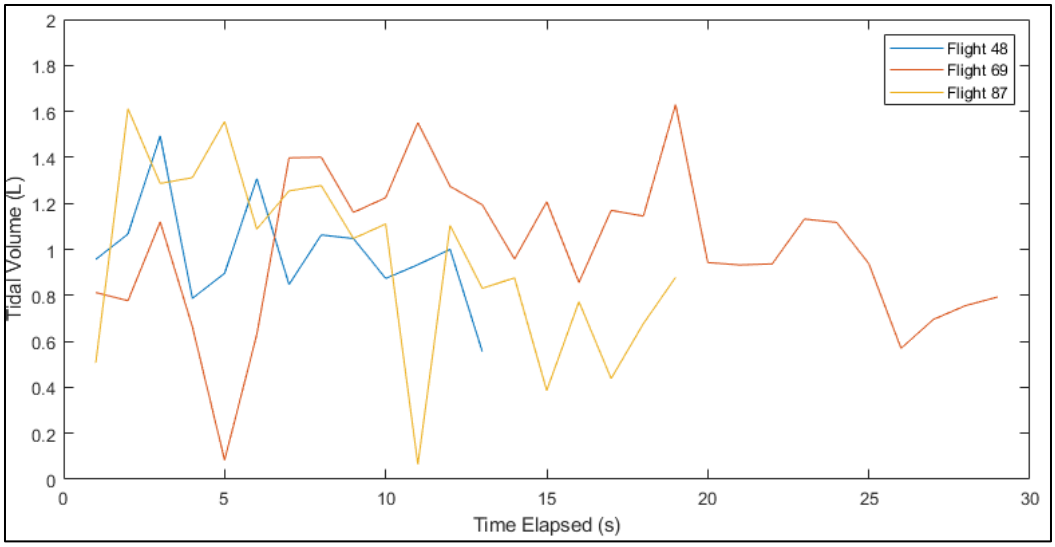

Figure 6.5.13. Decreasing Tidal Volumes During Normal Breathing for Flights 48, 69, and 87 Behavior Indicators

Inspection of trends in tidal volume with respect to inhalation and exhalation effort yields an interesting result. For non-safety pressure sorties utilizing the USAF configuration gear, inhalation effort proved to be a reliable indicator of tidal volume behavior. Inhalation effort trends tracked those of tidal volume, with spikes and drops in one being reflected in the other. For non-safety pressure flights, exhalation effort behavior reflected major events but largely remained independent of tidal volume.

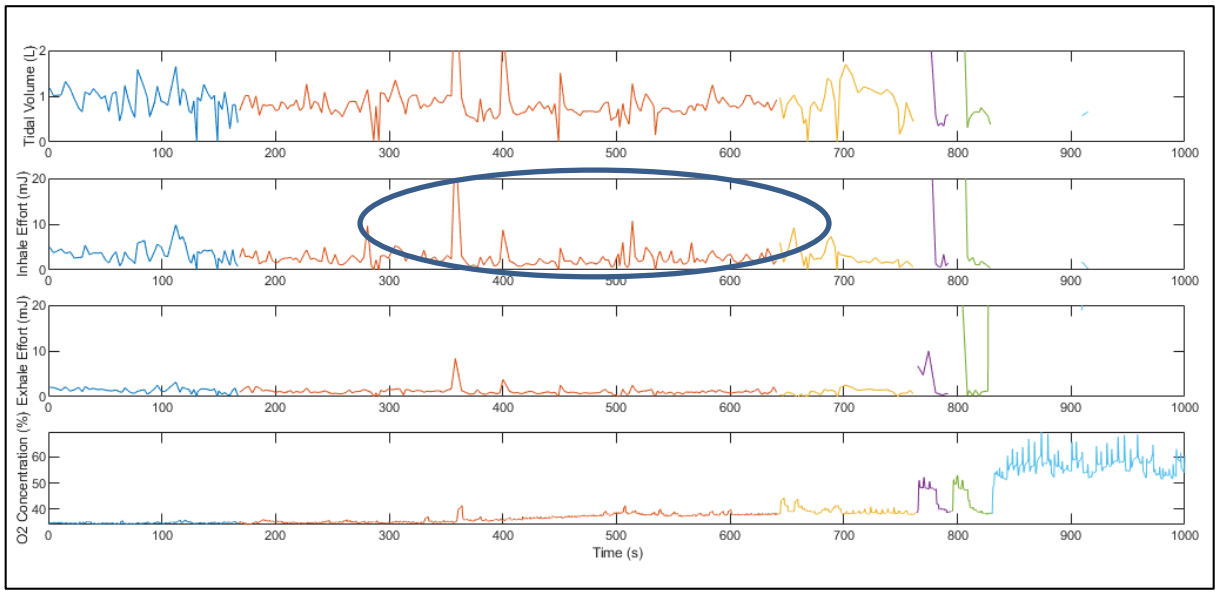

Figure 6.5.14. Tidal Volume, Inhalation Effort, Exhalation Effort, and O_2 Concentration vs Time for Flight 87, Non-Safety Pressure Flight
Inhale effort is indicator (over exhale effort).

This behavior is inverted for safety-pressure sorties. For flights using the USN configuration, exhalation effort trends track those of tidal volume far more accurately than inhalation effort, as evident in Figure 6.5.15.

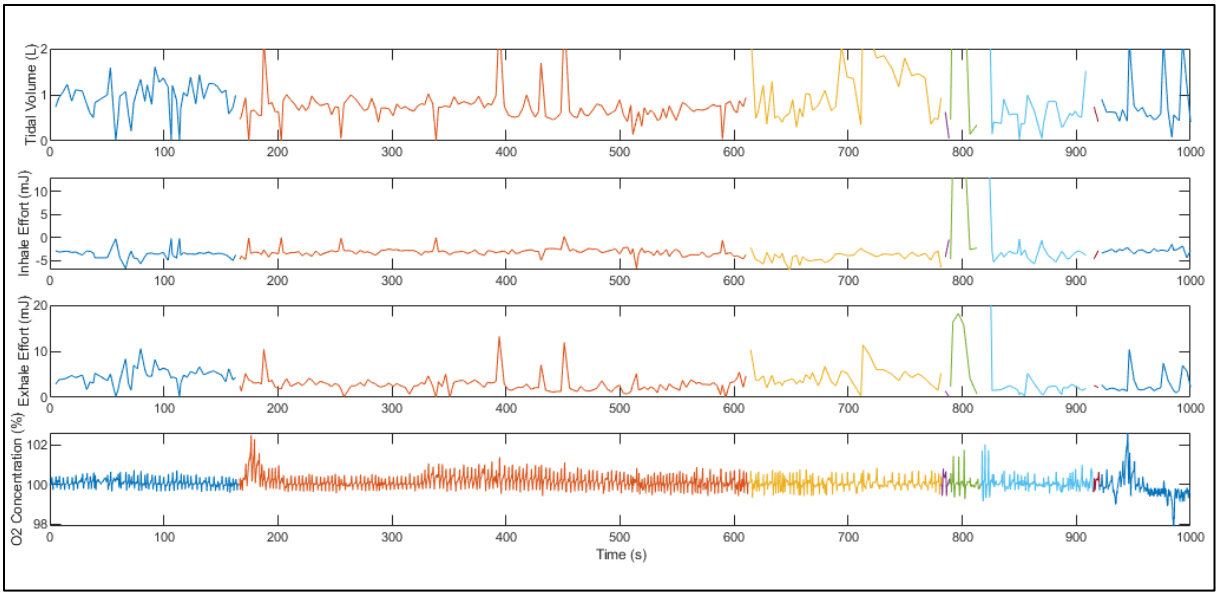

Figure 6.5.15. Tidal Volume, Inhalation Effort, Exhalation Effort, and O_2 Concentration vs Time for Flight 92, Safety Pressure Flight
Exhale effort is indicator (over inhale effort).

While inhalation effort behavior remains relatively consistent, save for major flight events, exhalation effort tracks the local maxima and minima of tidal volume behavior in safety-pressure flights. This is significant, as tidal volume should intuitively be a function of inhalation effort. Due to the presence of safety pressure inhalation effort is often negative, meaning that the aircraft is doing work on the pilot. The pilot works harder, however, to exhale. The pilot must exhale against a positive pressure in the mask, meaning that additional gas must be displaced to expend the contents of the lungs. This means that while the aircraft may supply inhalation flow at a relatively constant rate of work, the trends in tidal volume must be accounted for by the exhalation. An increase in tidal volume would then result in an increase in exhalation effort, as additional work must be done to expel the added volume of gas inspired. Likewise, a drop in tidal volume would result in a drop in exhalation effort.

6.6 Regulator Data Recorded through MadgeTech Instrumentation

6.6.1 Introduction

The PBA team used only LOX configuration aircraft. There was no question of the ECS producing sufficient pressure or volume breathing gas, sharing the bleed air source, as in the OBOGS equipped aircraft. Still, there were questions regarding variability of the air moving through the regulator, delivery of safety pressure, and timing.

The PBA team was able to instrument USN-like flights, equipped with the Cobham CRU-103 regulator providing positive pressure (also referred to as safety pressure), and near 100% O_2 levels, with MadgeTech devices coupled to the input of the regulator, and also downstream, resulting in effective cabin pressure. MadgeTech devices were used by the USN in conjunction with instrumented F/A-18 flights, and the unit used by the PBA team is on loan from the USN. The MadgeTech data is 0.5 Hz; therefore, it was up-sampled to match the 20-Hz VigilOX data. Due to this limitation, the PBA team looked at trends, correlations, minimums and maximums.

6.6.2 CRU-103 Regulator Description

The CRU-103 is a single stage regulator designed to show little difference in delivery pressure (droop) between zero flow and maximum flow capacity with varying flow rates, but a relatively large supply pressure effect. As such, a single-stage regulator is recommended in situations where inlet pressures do not vary greatly.

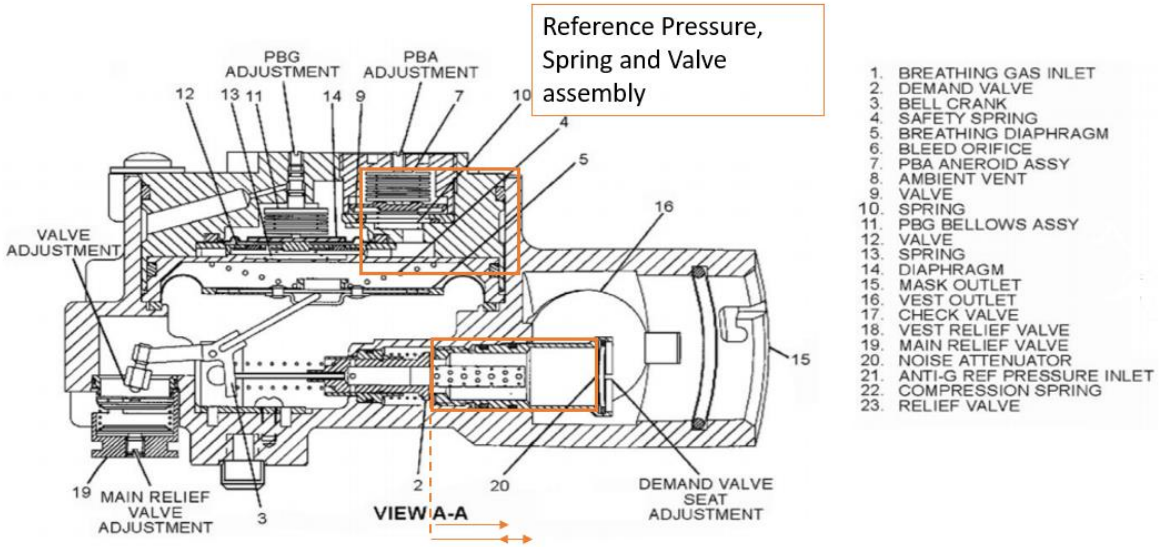

Figure 6.6.1. Regulator Regulates Down from ~80 to 12 to 14 PSI by Limiting Opening at Demand Valve, Item 2

The demand valve in conjunction with the "poppet and cable assembly" (Item 2 in Figure 6.6.1), control the flow of gas from the inlet side of the regulator to the outlet. MadgeTech measured the inlet supply pressure mostly between 80 to 100 PSI. The PBA had a chance to record inlet supply pressure during a Left Engine Flame-out and shut down (see Section 6.9.2, Mini Study on Flight 38), and concluded that the inlet pressure continued on at the high rates mentioned, with generous margins.

The CRU-103 Regulator inlet pressure has its own oscillation.

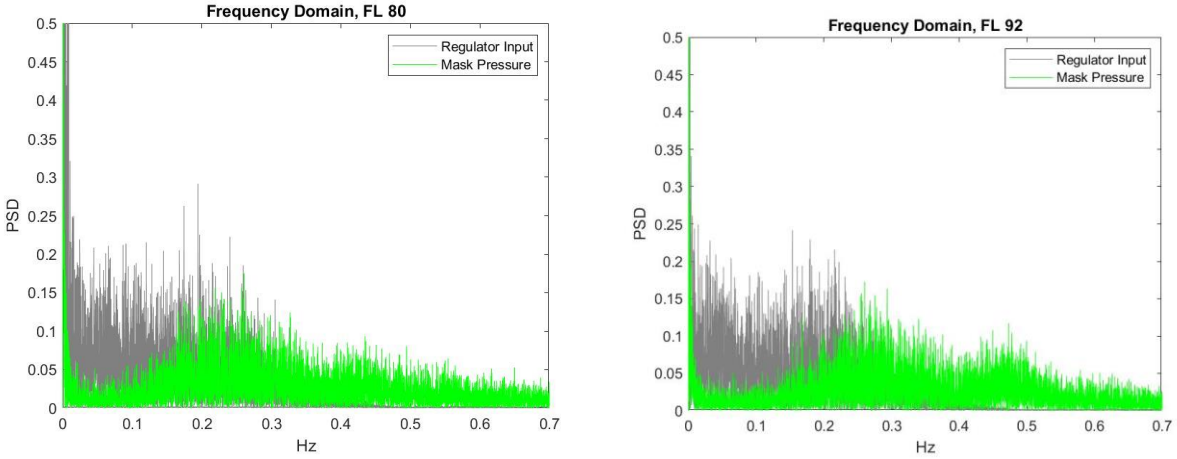

Figure 6.6.2. Oscillation of Regulator Inlet is at a Lower Frequency than that of Breathing as shown by the frequency domains calculated with fast Fourier transform (FFT) analysis

Some deep inhalations register as a 20 PSI dip on the inlet side. It is more typical to see the inlet pressure dip after the 2nd or 3rd maximum inhalation, as at 13:18:30. Others wash out, which explains the lower frequency domain of the inlet pressure; caveated as a reminder of the Madgetech signal being upsampled from 0.5 to 20 Hz.

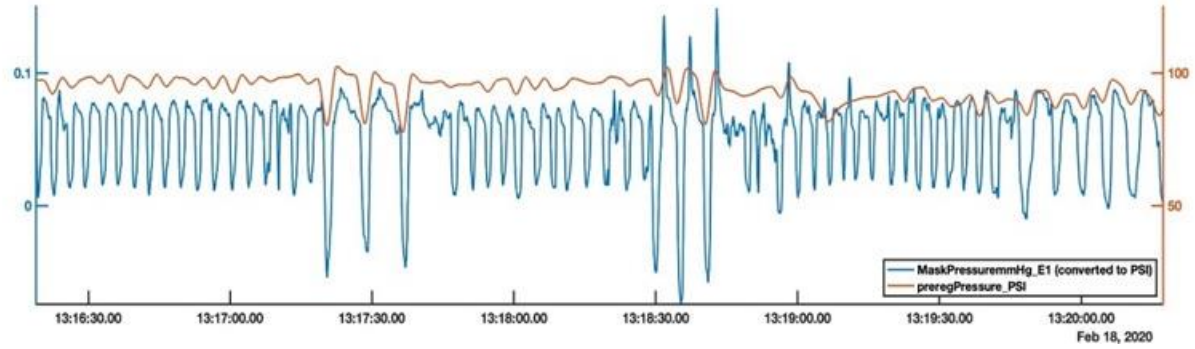

Figure 6.6.3. Flight 98
The prominent features are 3 Max Inhalations first with normal exhalations, then repeated with Max exhalations. The inlet pressure draws from 100 to 80 PSI, still plenty for the demand valve to work with.

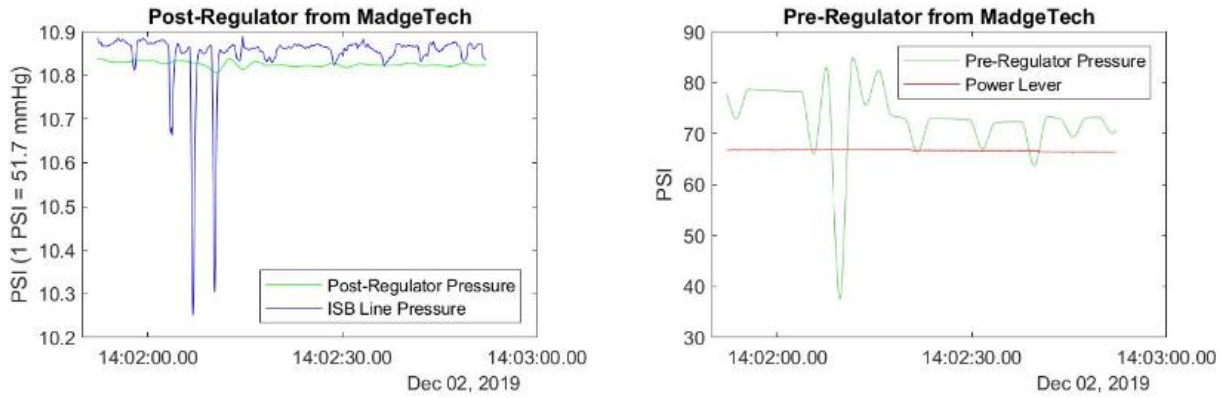

Figure 6.6.4. It is Possible to Draw Down Regulator Attached to LOX Supply to 37 PSI

It is possible to get the inlet pressure as low as 37 PSI.

The pressure decrease in the regulator is temporary, and it is caused by two, record depth 40 mmHg max inhalation draws. A hypothesis is that as the cooler liquid O_2 from the supply needs to flow through the warming area, the sudden large draws caused not enough conditioned supply air available to maintain the previous mean pressure at the outlet.

Under dynamic pressure increase, the amount of positive pressure in the mask decreases (see the blue dashed line in Figure 6.6.5).

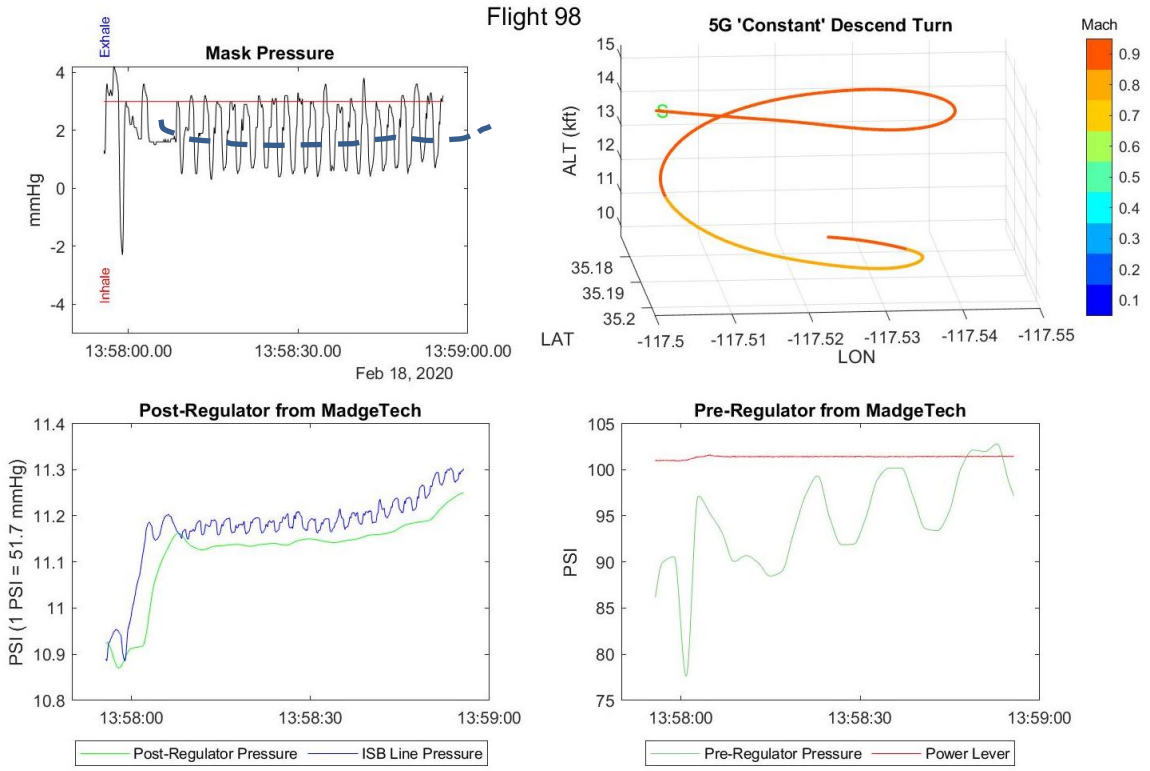

Figure 6.6.5. Under Dynamic Pressure Increase, Amount of Positive Pressure in Mask Decreases Top left tile. During a 5-G maneuver, the supplied positive pressure (blue dashed baseline mask pressure) rests at a lower 2 mmHg. The mode is 3 mmHg (red line).

Per Cobham, the manufacturer of the CRU-103 regulator, if the supply pressure increases, the pressure at the outlet decreases. In the first 30 seconds, the plane is level. The data in Figure 6.6.5 starts with a sharp inhalation seen in 3 tiles, followed by a cabin pressure increase equivalent to 15 mmHg still in the Isobaric region, due to no other reason but dynamic pressure. The regulator inlet pressure slowly increases from 75 PSI, all the while maintaining a slow oscillation.

During Mask-Off while on CRU-103, the inlet pressure should maintain at its high PSI as documented, but on occasion it could go to 0.

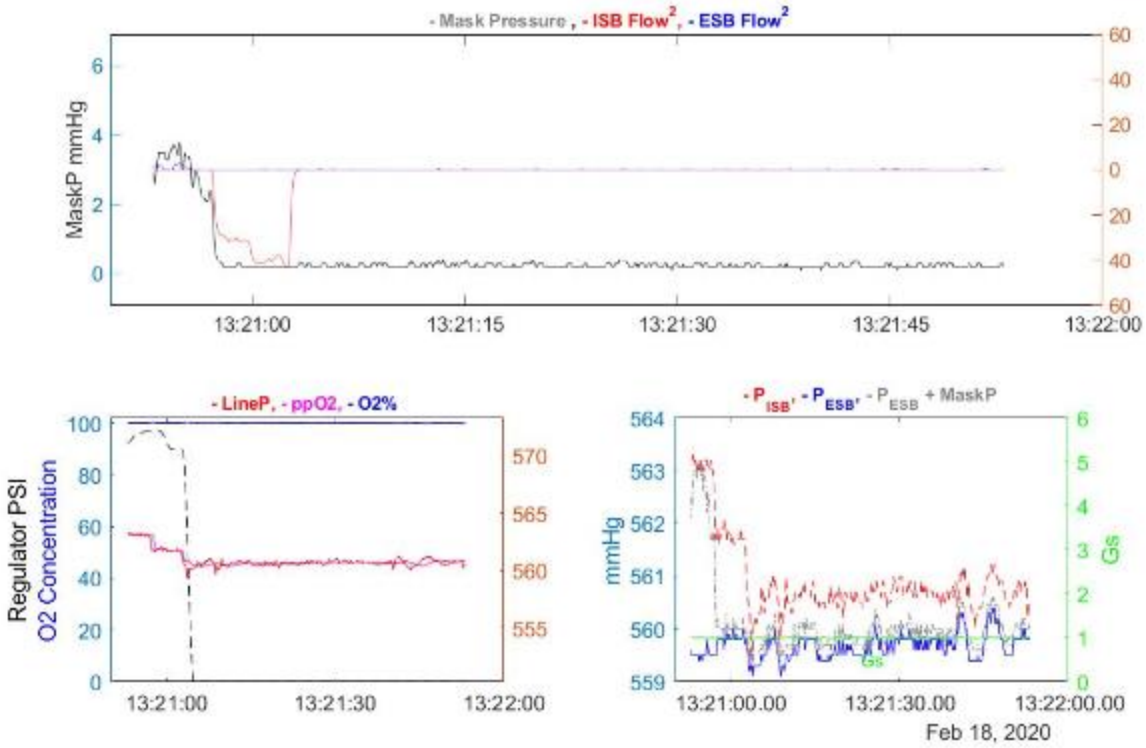

Figure 6.6.6. Mask Off During Flight 98 Starts Just Before 13:21
For 5 seconds there is free flow, and the regulator in the lower left tile maintains near 100 PSI inlet pressure. Just after 13:21 the Inlet pressure goes to 0, and consequently the flow stops.

According to Cobham, the demand valve failed closed in the Figure 6.6.6 example. The pressure and flow restarted when donning.

NASA PBA noted lags in air supply (Figures 6.6.7 and 6.6.8).

At times of fast, dynamic pressure change (descents, G's), the reference pressure in the regulator lags behind the dynamic pressure change instantly felt by the cabin. In sequence, the demand valve opens accordingly (or possibly partly or with offset in pressure), and the original demand does not accurately get translated to the line.

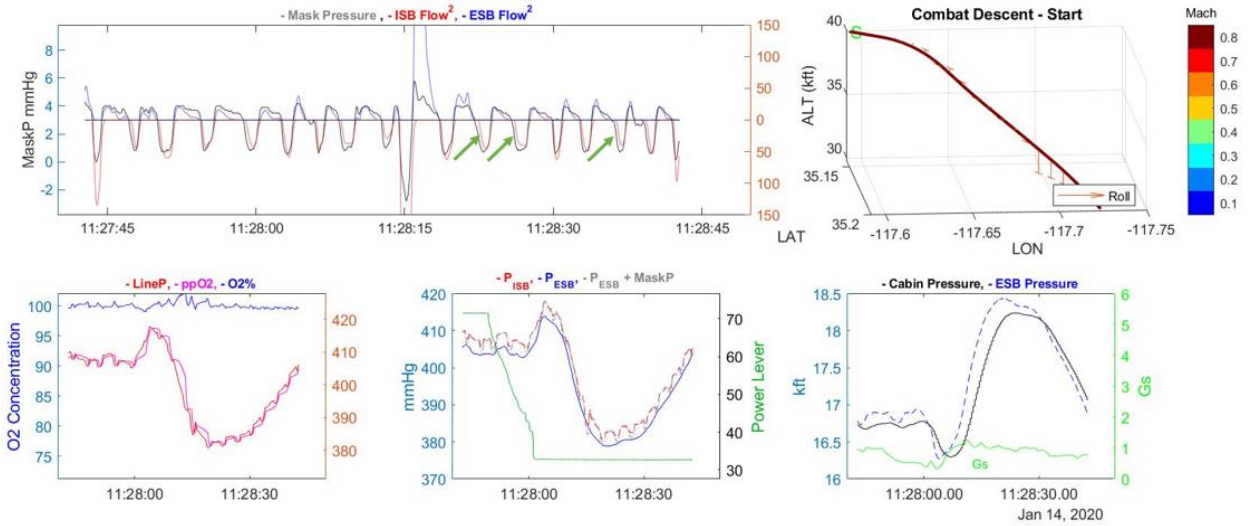

Figure 6.6.7. The Aircraft is Descending, thus, Cabin Pressure Should Increase At the same time, the Power Lever is pulled from 70 to 30, and the cabin pressure decreases by 2 kft before it climbs, note the inhalation flow lagging the mask pressure (green arrows).

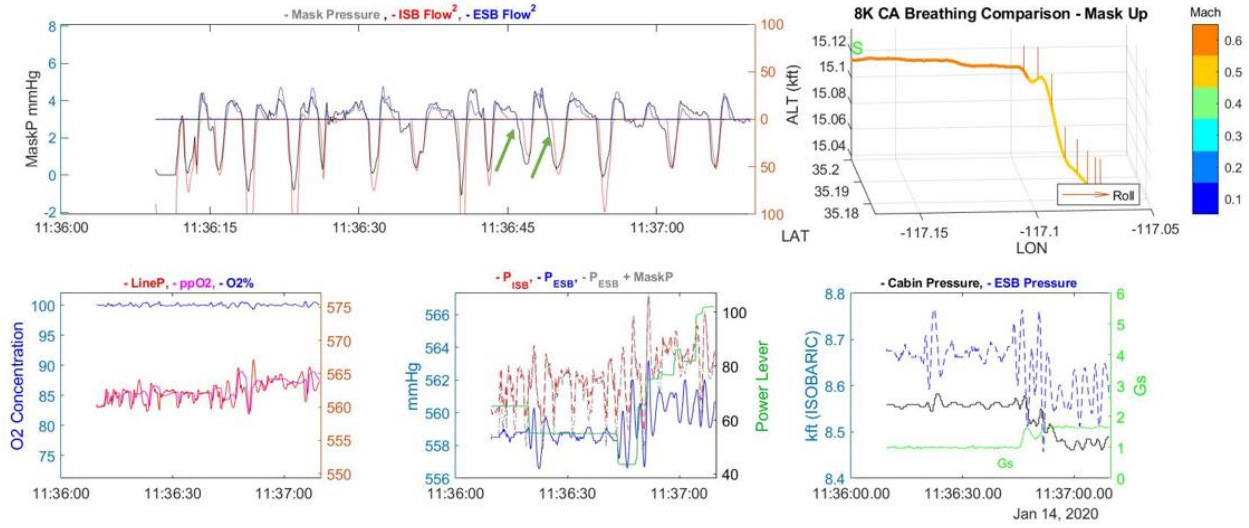

Figure 6.6.8. Flight 92; Just After Donning Mask After 40 Seconds of Free Flow developed a cabin and line pressure oscillation, observe the inhalation flow lag the mask pressure (green arrows).

In both Figures 6.6.7 and 6.6.8 the hypothesis is that the reference pressure at the regulator, the cabin pressure and mask pressure all changed, some quite dynamically, but not at the same rate or time, introducing a small lag. Though the lag is small, it can cause a sensation of inadequate flow response to the demand.

In summary, regulators are shown to have sufficient magnitude of pressure, but it is the timing that is critical, to translate the demand pressure for the matching amount of flow real-time under rapid changing dynamic conditions. A regulator which needs to provide a positive pressure adds one more component or failure point to the breathing air delivery system.

F.6-15. Despite using LOX breathing supply systems which are considered to be stable, PBA found regulator and mask performance anomalies.

F.6-16. PBA has determined that large regulator supply pressure variations are possible. The largest regulator supply pressure drop was 50 PSI (e.g., USN configuration, level flight, after 3 deep breaths). Frequent 20 PSI drops were observed (e.g., at the onset of 5 G turns.

R.6-8. Air delivery systems should be capable of delivering 5 lps for 3 seconds per pilot. ***(F.6-16)***

F.6-17. Breathing system performance can be evaluated by quantitative analysis of mask pressure changes. Ideal mask pressure changes are smooth and match the pressure changes of breathing in open air. Sharp, sudden, frequent pressure variations are not produced physiologically, therefore, these variations are the result of the breathing system or the environment and require pilot compensation

6.7 Timing/Breathing Sequence Issues

6.7.1 Introduction

The aircraft air breathing system's requirement should be to supply the pilot with the volume of air needed, when its needed. As of the writing of this report, pilot breathing metrics are focused on peak pressures compared to peak flow delivered (e.g., specified in MIL-STD 3050), without any regard to the characteristics of the timing of the pressure-flow delivery system.

PBA analysts created several methods to investigate timing disharmony in the "air supply-pilot" loop, as well as changes in inhale/exhale times relative to each other and relative effects on human physiology.

6.7.2 Time and Phase Shift

Driving Pressure and Resultant Flow:

Flow is created between connected points of a system at different pressures. The relationship between flow and pressure is defined as laminar (streamlined) or turbulent and is characterized by the Reynolds number (NR).

Table 6.7.1. Reynolds Numbers for Tracheo-Bronchial Tree showing high Reynolds numbers in the last 2 columns covering the flow rates measured in the PBA.

Location	Diameter mm	Velocity 6 L/min	Velocity 60 L/min	Velocity 200 L/min
Nasal canal	5	400	4,000	12,000
Pharynx	12	800	8,000	24,000
Glottis	8	1,600	16,000	48,000
Trachea	21	1,250	12,500	37,000
Bronchi	17	910	9,100	27,300
Bronchi	9	700	7,000	21,000
Bronchi	6	570	5,700	17,100
Bronchi	4	190	1,900	5,700
Bronchi	1	35	350	1,050

Physiological Reviews 41:314, 1961, journals.physiology.org

Turbulent flow occurs when NR > 2000. Reynold's number increases with the increase in linear velocity of gas (flow rate), density of gas, or tube radius. As an example, breathing in quickly (which occurs during G-breathing) creates more turbulent flow throughout the tracheobronchial tree and significantly increases the work of breathing. From Table 6.7.1, in the Nasal Canal, flow is turbulent at flow rates greater than 30 L/min. Pilot air supply flow rates measured with instruments such as VigilOX (at altitudes under 23 kft) are lower-bound at 40-50 lpm, with flow arriving via tubes with radius larger than in the human system, thus the supply flow is turbulent.

$$Q = k\sqrt{\frac{P_1 - P_2}{\rho}} \qquad \text{(Eq. 6.7.1)}$$

For pilot breathing, the supplied turbulent flow Q squared is proportional to the differential pressure ΔP (rearranging Equation 6.7.1), and this relationship is documented during the more than 100 flights analyzed by the PBA on specially instrumented F/A-18 LOX supplied aircraft.

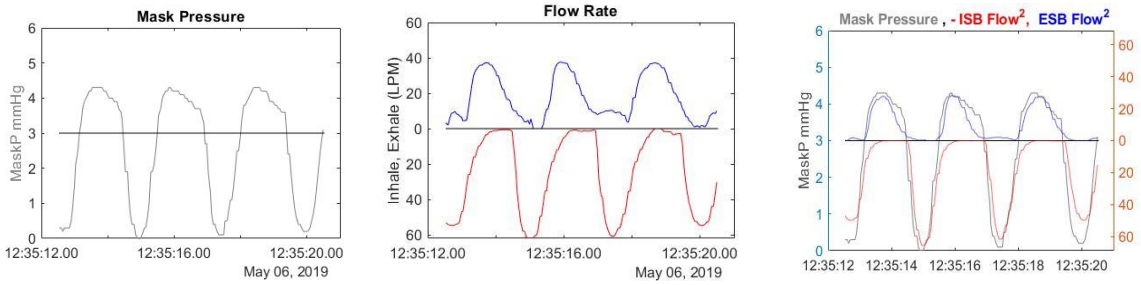

(a) ***(b)*** ***(c)***

Figure 6.7.1. Mask Pressure Delta Across Known Orifice (a) and Resulting Flow Rate (b), Yield Strong Correlation When Superimposed (c)

The rising edge of the flow is preceded by the mask pressure signal by 1 sample time (1/20th second).

Pressure Flow Disharmony is a mismatch between the pressure and flow profiles, including start/stop and time it takes to reach the peak (maximum). In the Figure 6.7.1a example, a mismatch between the Grey Mask Pressure and the Blue ESB (Exhalation) Flow2 is shown.

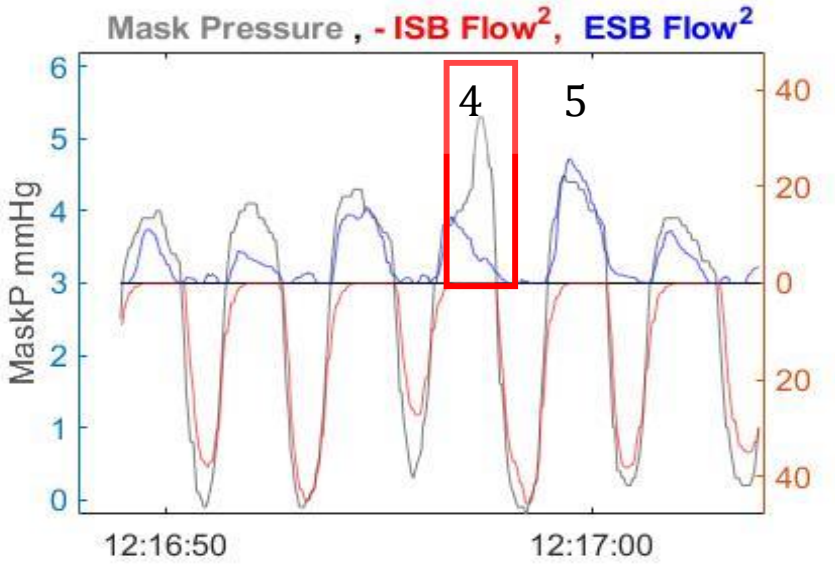

Figure 6.7.2. Exhalation #4 Flow Peaks at Start of Exhalation but it is cut short. As flow builds up without exiting, Mask pressure peaks at the end

Ideally, exhalation flow is an instantaneous response to a pressure signal. During exhalation through a mask, flow is expected to lag behind pressure due to exhalation valve cracking-pressure and finite valve resistance. For actual examples, exhalations #4 and #5 from Figure 6.7.2 are enlarged.

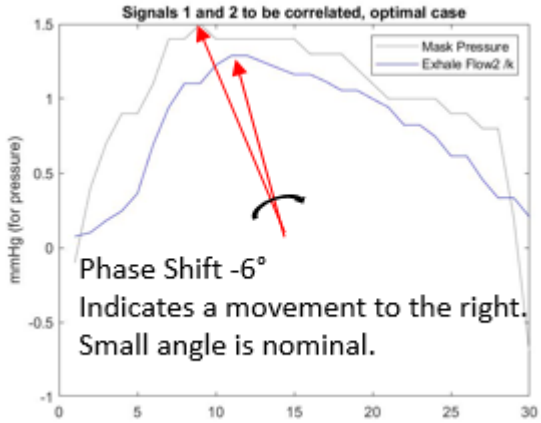

(a) Exhalation #5, Nominal Exhale

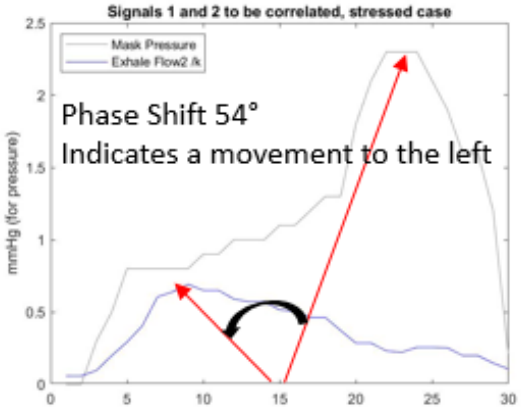

(b) Exhalation #4, Mismatch

Figure 6.7.3. Exhalations #4 and #5 from Figure 6.7.2 Enlarged

- Negative phase shifts (4b) indicate that pressure peaks before the flow peaks
- The smaller the lag, the more ideal the system (Small negative numbers are expected)
- The larger the lag, the more resistance in the system (e.g., when a valve that is sticky or "Slow to Open"), the pressure builds up, the valve opens with a delay, then flow peaks
- Positive phase shifts (4c), indicate that flow peaks before pressure peaks $T_{\text{Pressure Peak}} - T_{\text{Flow Peak}} > 0$
- This happens when the exhalation flow is pinched off. As a result, flow cannot exit, and pressure rises
- Imagine a valve that closes too early, pinching off flow (e.g., due to safety pressure in the compensation valve)

Both sensations of air lead and lag are experienced regularly in mask breathing, and pilots adjust to small phase shifts routinely.

Table 6.7.2. Metrics Calculated on the Exhalation Data from Figure 6.7.2

Breath Nr	Exhalation Starts	Exhalation Stops	Shift in Time * 1/20 s	Phase Shift Degree	Correlation Normalized
1	‘12:16:49.03’	‘12:16:50.33’	0	0.00	0.922
2	‘12:16:51.44’	‘12:16:52.63’	0	0.00	0.979
3	‘12:16:53.89’	‘12:16:55.33’	-1	-6.00	0.975
4	‘12:16:56.39’	‘12:16:57.74’	9	57.86	0.759
5	‘12:16:58.99’	‘12:17:00.33’	-1	-6.43	0.979
6	‘12:17:01.44’	‘12:17:02.89’	0	0.00	0.980

Quantitative Results Interpretation

Shift in Time. A Signal Processing algorithm performs a pair-wise comparison on each data point and determines the offset from the lowest error match within each inhalation or exhalation. This can be a + or - time lag. The VigilOX instrument used in this experiment is limited to 1/20 second output, thus given the physics and the instrument, a “0” or (-1) in this category is good mark, as a mask pressure change should “lead” flow. Time Shift from the 6.7.2 example amounts to a half a second, but with the entire exhalation being 1.5 seconds, this means that instead of ramping up at the onset when it is needed, the pressure peaks as the breath function is “winding down,” ready to transition.

Phase Shift in degrees. This builds on the Shift in Time, and it takes in consideration the length of the exhalation. For example, exhalations with a lag of -1 can correspond to a -6° to -10° phase shift for a shorter exhalation. A “0” or (-6) in this column is a good mark.

Normalized Correlation (R). Compares paired points of the signals. This characterizes how the shape of the pressure and flow of the entire exhalation (not just the timing) compare. The output is [0, 1]. A 0.9+ is really good (green table entry); a 0.75 (red) is weak for the F/A-18 aircraft equipped with safety pressure.

The time/phase shift of an entire flight can be visualized by plotting the binned distribution. Dozens of PBA flights were characterized regarding phase shift. Flights 89 and 90 are typical “good” flights and are characteristic of the USN/USAF configurations on a legacy F/A-18. Inhalation was analyzed in the same manner as exhalation, and distribution plots prepared for comparison (Figure 6.7.4).

Inhalation results of Phase-Shift Analysis

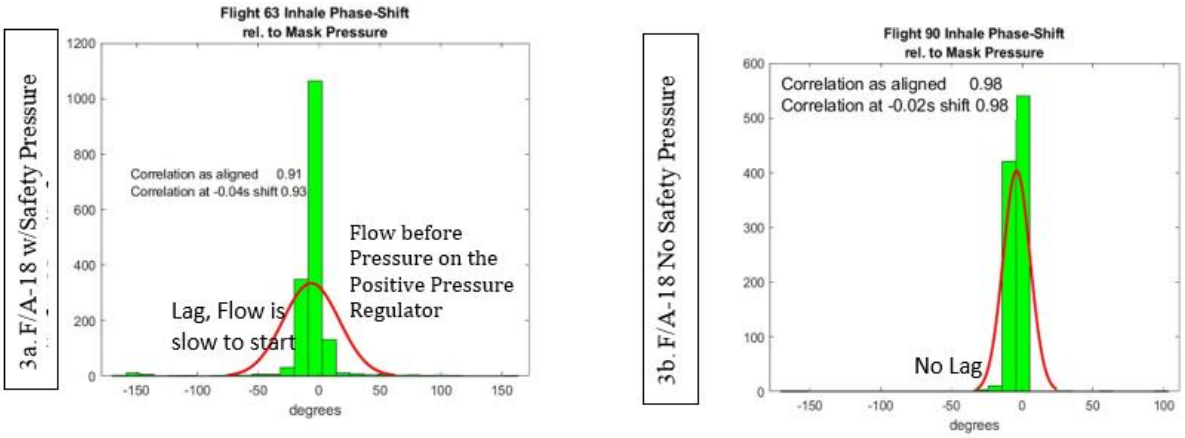

Figure 6.7.4. Inhalation Distribution Plots
The F/A-18 USAF configuration w/o Safety Pressure shows an unencumbered inhalation profile, while the F/A-18 legacy USN configuration w/Safety Pressure has some 20 to 30 degree lag. Correlation numbers are near-perfect 98% for the Diluter Demand no positive pressure system, contrasted with 91% for the Positive-Pressure system

Exhalation results of Phase-Shift Analysis

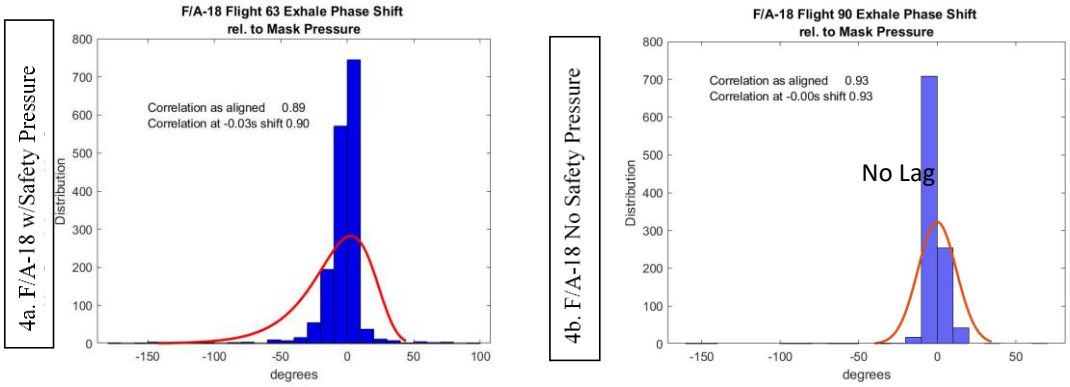

Figure 6.7.5. Exhalation Distribution Plots
Shows greater counts of negative phase shifts (delays) for the USN configuration (left), as compared to the USAF configuration (right) with virtually no lag. Pressure-Flow Correlation is a little higher (by 4%) on the USAF flight

In some flights, signs of stress of breathing can be easily spotted with the Time-Shift/Phase-Shift technique. The pilot after flying PBA flight 29 (USN configuration), reported "difficulty exhaling," which in the long duration (over 1 minute) cases lead to the feeling of "oxygen starvation." This was reported in about 5 minutes of a 60-minute flight, so the number of large phase shifts are in line with the pilot's experience (Figure 6.7.6).

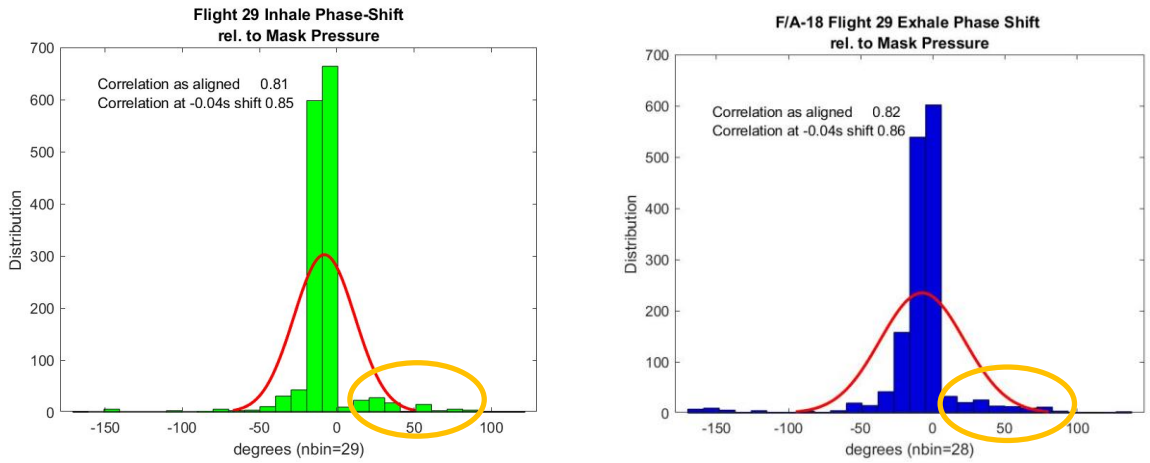

Figure 6.7.6. Flight 29 Inhale and Exhale Phase Shifts Relative to Mask Pressure Flight 29 shows having positive phase shifts. On the exhalation side this is indicative of late pressure build-up and truncated flow that is not fully expelled, backing up the pilot's statement of difficulty exhaling

F.6-1.* *Phase shift analysis is a numerical tool to quantify disharmony between pilot breathing demand and the breathing system delivery. The test results are corroborated by independent pilot observations.*

R.6-1. For flights where both mask pressure and flow are available, apply phase shift analysis for early detection of equipment issues or validation of pilot reports. Collapse flights or segments into bins or single numbers of Phase Shift Mean, +/- standard deviation, lag (time) and correlation coefficients. ***(F.6-1)***

R.6-6. Measure and track phase shift, hysteresis, and PNF (Pressure – No Flow) when evaluating aircraft system health – especially during times of peak breathing. ***(F.6-1, F.6-12)***

6.7.3 Breath Timing Start and Hand-off Slip Example

Figure 6.7.7 shows a 1-minute segment with an example of pressure draw down (red arrow) and a visible delay in the commencing flow (green arrow). This segment also has very high inhale hysteresis seen in the trumpet curve (top right tile).

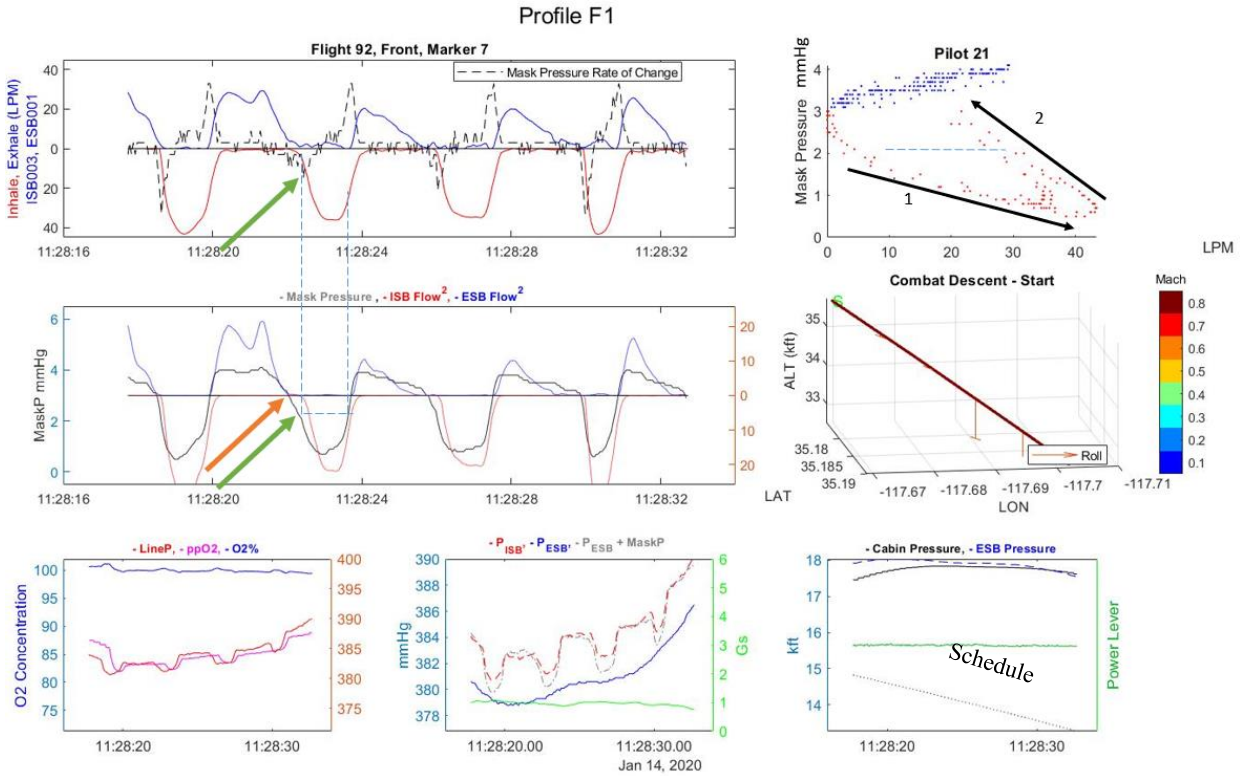

Figure 6.7.7. 1-minute Segment with Example of Pressure Draw Down and Visible Delay in Commencing Flow
The orange and green arrows point to a half second delay between mask pressure draw and meaningful flow. There is also a great difference of flow rate for the same amount of pressure (black arrows 1 and 2). For 2 mmHg of Mask pressure, there is 3 lpm flow at the start of inhalation, and 29 lpm during the ramp-down phase.

There is an inflection point (marked by the green arrows in Figure 6.7.7), before which there is no meaningful air flow. One difference shown between the marked breath and the others is that in the top tile, the mask pressure rate of change is significantly lower (black dashed line). The flow does not start until the rate of change is 10 Liters per Minute per Second. Another possibility is that the CRU-103 provided safety pressure in that instant dropped from 3 to 2 mmHg (the PBA has seen examples of unsteady positive pressure level during G's, even though the G-sensor is not connected). In this 15 second example the G's are steady at 1 G. Consider if the pilot continues breathing with the same "acceleration" as before, and contracts his diaphragm the amount his system is conditioned to (e.g., 2 mmHg), but the positive pressure that was a given dropped 1 mmHg; as a result, the mask pressure change is not enough to start the breath. At the end of the inhalation, there is not a crisp handoff of inhalation flow stopping before exhalation flow starts (the red inhalation trumpet curve does not go back to the origin). Tile 1 shows that just before 11:28:23 there is still a 29 lpm inhalation flow as the mask pressure goes above safety pressure and exhalation flow starts. Note that this was part of "Combat Descent," 30 seconds after the start, and the aircraft descended 2,000 ft in 15 seconds. The velocity and power lever are steady. Cabin pressure was on a downward slope, but at breath #2 it is increasing slightly (just 1 mmHg), then as the craft rolls, pressure continues to increase, while the schedule decreases.

F.6-18. Pressure compensated masks, like the MBU-20/P, in combination with the CRU-103 regulator, can suffer adverse system interactions under certain dynamic breathing conditions.

R.6-9. Investigate pressure compensated mask/regulator system interactions, their effects on pilots, and correct as necessary. ***(F.6-18)***

F.6-19. PBA documented a delay of flow at the start of inhalation due to the regulator's (i.e., CRU-103) inability to maintain the prescribed safety pressure. This timing delay between pilot demand and regulator supply presents as a BSD.

Summary of Breathing Gear Anomalies and Stressful Flight Conditions

The PBA's goal is to study complex interactions between the pilot, aircraft in motion, and the air supply. It was widely accepted that OBOGS air delivery systems are more complex, and jets with LOX tanks should be "easy breathers." Yet PEs occur on LOX aircraft as well, and de-coupling the possible PE causes from the OBOGS, the PBA has shown the myriad ways pilot breathing can become sub-optimal, even compromised.

6.8 Pilot Breathing Assessment Results Analysis

This section reflects the PBA philosophy and devised analytical tools. It introduces the concept of cabin pressure micro-oscillations, which when combined with breathing demand pressure of the same scale, affect the air flow delivery, resulting in a mismatch and pilot breathing "fighting the machine." Flight 29 data is used to demonstrate.

The section concludes with remarks on PBA flight and pilot breathing analysis, findings and recommendations.

Introduction

On very rare occasions, over the course of thousands of flights, USN F-18 pilots reported breathing difficulties while executing flight operations. Breathing difficulties sometimes reduced mental capacity during certain phases of the flight. The USN asked NASA to help determine the cause of F-18 pilot breathing difficulties. The NESC Review Board supported a program, called the PBA, to develop a standard method to evaluate pilot breathing in F-18 jets.

Through the course of the PBA, 110 sorties were conducted. Most of the data in this report are obtained from three sorties – flight 28 (FLT-028), flight 29 (FLT-029), and flight 106 (FLT-106). The data primarily represents the performance of one breathing mask regulator (Cobham CRU-103, serial number (S/N) 20294) and one plane (Tail #850). Selected data from other flights and breathing apparatuses are also presented for comparison. Environmental parameters measured inside the cabin and pilot breathing apparatus show that pilot breathing patterns are significantly affected during specific flight conditions.

Assessment Description

One primary goal of the PBA was to directly relate pilot breathing behavior to different flight profiles. One of five different flight profiles were implemented in all PBA sorties to make data comparison across different flights easier and more informative. The five flight profiles are designated as follows:

Profile A: High altitude
Profile B: High dynamics

Profile C: Standard profile
Profile D: Low altitude
Profile E: Special flight profile

Data from over 1000 breaths were obtained during each sortie. Breathing measurements were made with a VigilOX instrument package, which measured the pressure in the mask inlet and outlet lines. From these measurements, air flow rates were calculated. In addition, the cabin pressure was measured indirectly via a pressure transducer located near the mask outlet line opening into the cabin. All parameters were recorded as a function of time, longitude, latitude, and altitude to enable time- and maneuver-based assessment.

Two selected datasets obtained during FLT-028 are shown in Figure 6.8.1. FLT-028 was conducted as a Profile C sortie. The plots show the following parameters recorded by the VigilOX:

PISB = inhalation line pressure
PESB = cabin pressure (sensor located in exhalation line)
PESB + MaskP = sum of cabin pressure and mask pressure

PISB is measured downstream of the regulator in the mask inlet line and PESB is measured downstream of the mask in the mask outlet line. Because of the sensor's location, PESB provides an indication of cabin pressure. It should be noted that pressure oscillations induced by pilot exhale cycles are overwhelmed by the contributions from cabin pressure oscillations. A flat PESB line generally denotes a constant plane altitude. The power level correlates with engine throttle adjustments performed by the pilot.

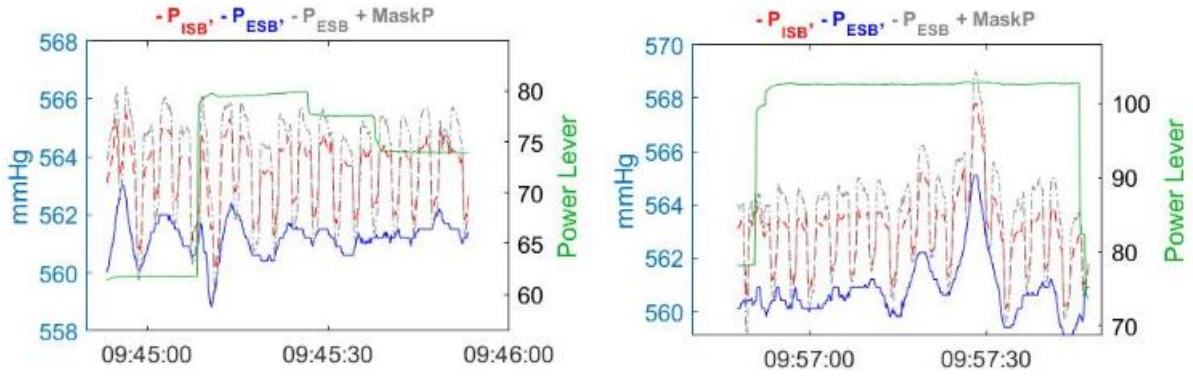

Figure 6.8.1. Two Selected Datasets Obtained During FLT-028
Pressure measured within the mask inlet line (P_{ISB}), cabin (P_{ESB}), and mask (MaskP) over selected time intervals during FLT-028 using a VigilOX. The plots also include the power level set by the pilot. Note the oscillation present of the ESB line pressure, indicative of unsteady cabin pressure on aircraft Tail #850.

To characterize pilot breathing performance, the PBA analyzed and processed the recorded data to enable specific analytical approaches, which included:

- Mask inlet line, mask, and cabin pressures were used to assess regulator response to cabin pressure changes over a wide range of flight profiles
- Differences between mask and mask inlet line pressures during dynamic maneuvers were used to evaluate the breathing system response performance to pilot breathing needs

- Discrepancies between inhale and exhale flow rates were used to examine breathing system synchrony – exemplifying the presence of breathing system hysteresis, a key metric in assessing pilot breathing
- FFT analysis was used on PESB and PISB measurements to determine if there were remarkable relationships among oscillating cabin and mask pressures during dynamic flights
- Comparative measurements of pressure and flow were used to contrast the performance of different pilot breathing systems during identical flight conditions

Breathing Apparatus Anatomy and Function

In the USN F-18, the pilot wears a positive pressure breathing mask sealed around the mouth and nose, which is fed by a Cobham CRU-103 pressure demand O_2 gas regulator. Figure 6.8.2 shows the cross-section of the regulator assembly. A demand valve (item 2 in Figure 6.8.2) consists of a poppet system that operates by referencing cabin pressure and responding to pilot breathing demands. Nominally, it regulates mask pressure (also known as the safety pressure) at approximately 3 mmHg above cabin pressure. Under normal conditions, the regulator responds quickly to pilot demand (lower pressure created by the pilot's respiratory system) by increasing the gas flow rate into the mask. At the end of the inhalation process, the inlet flow ceases, the mask pressure rises, the demand valve closes, and the pilot's exhalation breath subsequently exits the mask through a separate flow path.

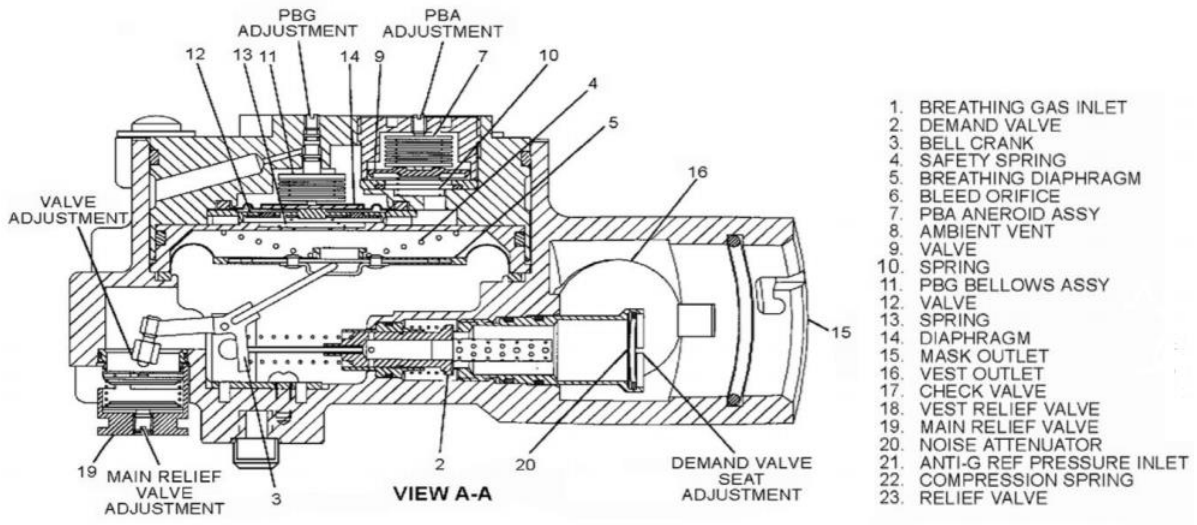

Figure 6.8.2. Cross-section View of Cobham's CRU103 Positive Pressure Oxygen Regulator Key parts are labelled numerically and denoted in the list at right.

Focal Points of the PBA

In practice, the regulator response to pilot breathing demand is slightly delayed, which reduces the air volume delivered to pilot below the demand. This is caused by the purely mechanical operation of the regulator assembly. The characteristic difference in demand volume versus delivered volume was examined by the PBA.

To support pilot breathing needs, the regulator references cabin pressure, and facilitates a variable gas flow through the regulator and into the mask to maintain the 3 mm Hg positive pressure under varying cabin conditions. The pilot may experience breathing difficulties if the

regulator does not quickly change the flow rate according to environmental changes. The PBA also examined positive pressure regulator performance and its effects on pilot breathing, under a variety of cabin pressure conditions.

The USN periodically performs health checks on each CRU-103 regulator throughout the operational life. Prior to delivery, CRU-103 regulators are subjected to bench top tests under steady-state conditions. In general, CRU-103 regulators that crack easily, and flow quickly are considered nominally operational. The same bench top tests are applied to units that are removed for maintenance, overhaul, or repair. The CRU-103 regulator function is never evaluated under flight-like conditions, which could lead to erroneous conclusions on regulator health for use in dynamic flight conditions. A secondary regulator used by the USAF (CRU-73), which operates differently from the CRU-103, was investigated for comparison by the PBA.

Pre-flight activities can provide clues to aircraft systems health. While the aircraft is on the ground with the canopy open, the mask pressure of 3 mm Hg above cabin pressure is noted in Figure 6.8.3. However, the cabin pressure rapidly increases to ~20 mmHg during canopy close. In response to the PESB spike, the mask regulator responds to maintain a positive pressure in the mask. However, the PESB unexpectedly oscillates for a significant time period after canopy closure. The effects of PESB oscillations in response to cabin pressure fluctuations on pilot breathing were examined by the PBA.

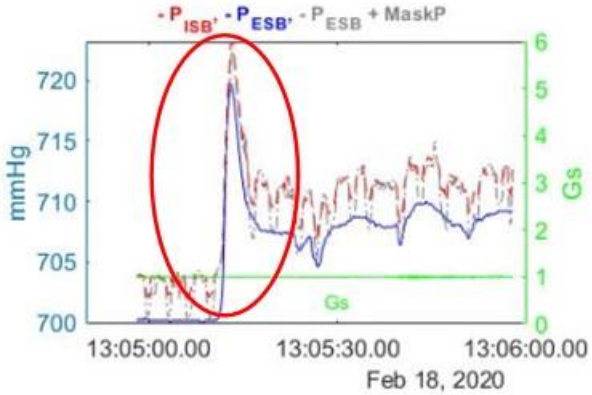

Figure 6.8.3. Mask Pressure
Pressure measured within the mask inlet line (PISB), cabin (PESB), mask (MaskP) and G -force during ground-based health check of the F-18 aircraft cockpit canopy pressure breathing system. The pressure spike measured during canopy closure is circled in red.

Results and Discussion

A. Flight Profile B and Pilot Breathing Issues

After each PBA flight, pilots were interviewed to evaluate their experience and were matched to key variables including the aircraft tail number, regulator model, regulator S/N, and flight profile. Post-flight interviews revealed pilot breathing difficulties were associated with the most dynamic and aerobatic flights (typically profile B). Figure 6.8.4 shows the aircraft altitude recorded during a brief period of FLT-029– designated as profile B0. Markers are shown on the plot, which correspond to individual aerobatic maneuvers that are denoted in the legend at the right of the figure. Instances of pilot breathing issues are highlighted in red in Figure 6.8.4. During FLT-029, the pilot performed rapid descents, high-G 90° turns, squirrel cages, a high-G wind-up turn, and a high-G spiral descent.

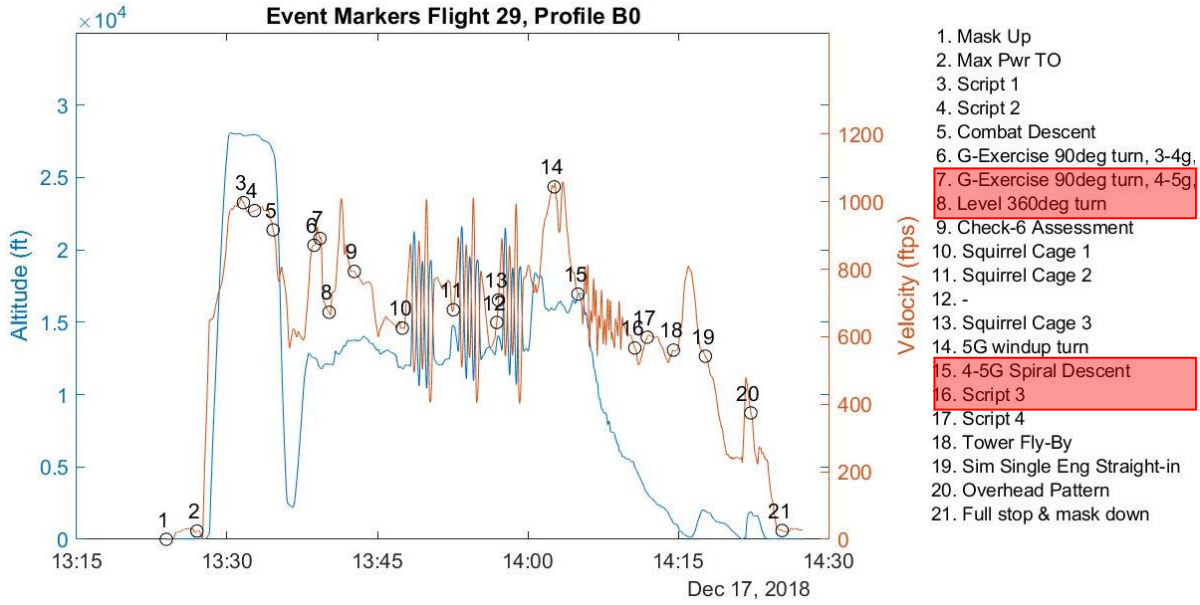

Figure 6.8.4. Altitude Measured as Function of Time During FLT-029
Key events occurring throughout the flight are numbered on the plot and described in the list at right. Events during which the pilot experienced breathing difficulties are highlighted in red.

The following excerpts are transcribed directly from the pilot interview after FLT-029 and are denoted according to corresponding event markers shown in Figure 6.8.4:

M7: Couldn't exhale completely. It was more difficult than normal to exhale quickly through the mask. Felt as if exhaling against a partially closed valve or having to exhale against positive pressure.

M8: Difficult to exhale completely in a quick fashion. Very hard to take a "quick breath" due to extra time required to exhale breath completely. Under G -force, this resulted in a partial exhalation and ensuing partial inhalation therefore an "incomplete breath." This resulted in several partial breaths and eventual oxygen starvation. Quick, full breaths under G were not possible.

M13: Couldn't exhale completely in a short period of time (as if the exhale path was partially blocked).

M14: Ran out of oxygen due to partial breaths due to trouble exhaling quickly. I could not have continued this maneuver much longer than 1-minute due to inability to get a full breath.

M15: After 4 minutes, was out of breath and could not complete further.

During FLT-029, breathing became so difficult that the pilot had to cut maneuver 15 short. After the pilot complained of breathing difficulties during FLT-029, the corresponding regulator was sent to JSC where it was subjected to a steady state flow test. The regulator performed nominally. The regulator was also sent to the manufacturer (Cobham) for testing and similar results were obtained. The offline testing did not indicate any specific issue with the regulator.

The pilot reports difficulty exhaling during aerobatic maneuvers. (See section 6.9.1 for additional plots from FLT-029). According to the pilot's account, breathing is easy when maneuvers are gentle. In general, less dynamic flight profiles did not cause pilot breathing difficulties. This

claim is supported by flight data and discussion included later in the report. Figure 6.8.5 shows data recorded during squirrel cage maneuvers of FLT-029. The PISB and PESB fluctuate up to 20 mmHg. Such large fluctuations are generally observed during rapid cabin pressure changes. This observation led the PBA team to believe the pilot breathing difficulties arise due to changes in cabin pressure concurrent with high dynamic flight maneuvers.

Interestingly, pilots did not report breathing difficulties during any other flight profile, even across different flight profiles in which the same aircraft, regulator, and pilot were used. The evidence presented in this section highlights the correspondence between dynamic flight maneuvers and pilot breathing difficulties. Additional correlations will be discussed in detail in later sections.

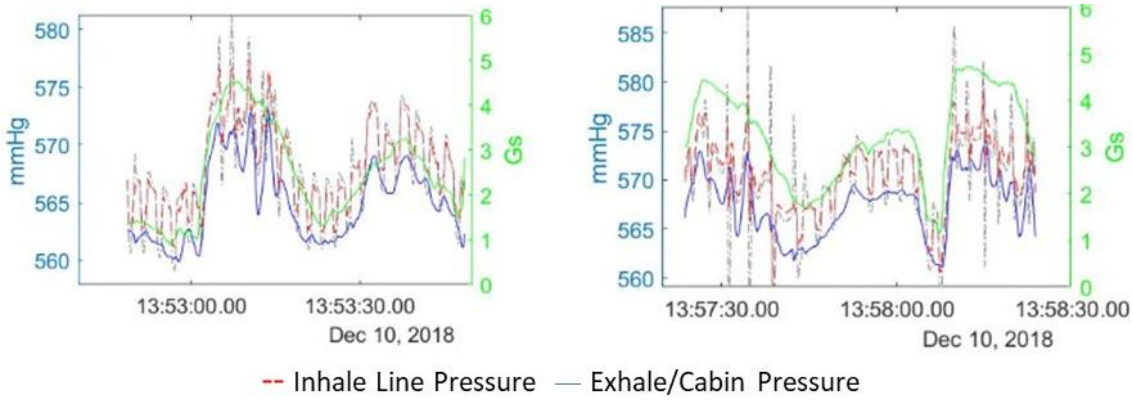

Figure 6.8.5. Data Recorded During Squirrel Cage Maneuvers of FLT-029
Plots of mask inhale line pressure (P_{ISB}), cabin pressure (P_{ESB}), which were measured by VigilOX, and the measured g-forces (G's) during select highly dynamic timeframes of FLT-029.

B. Flight Tests with a Modified CRU-103 Regulator

FLT-106 was designed to examine the contribution of the regulator cabin pressure compensation feature to pilot breathing difficulties. To do so, the test flight implemented a modified mask regulator wherein the spring that serves to regulate mask pressure was removed (item 4 in Figure 6.8.2) and its corresponding diaphragm (item 5 in Figure 6.8.2) was replaced with a custom part, which did not include a hole through which air could leak as the conventional hardware does. Figure 6.8.6 shows selected VigilOX data obtained during FLT-106. Despite the benign flight Profile F, the pilot reported difficulty breathing throughout the entire sortie. Significant PESB oscillations were measured during the flight and PISB fluctuated over an unexpectedly large range. When an unmodified CRU-103 is used, PISB fluctuations with a magnitude of 3 to 4 mmHg occurred. During FLT-106, 6 to 9 mmHg fluctuations were measured. Furthermore, the regulator was unable to maintain a positive pressure in the mask – a critical function in maintaining proper pilot breathing performance. (In retrospect, this is not unexpected; it shows the importance of every detail in the regulator, down to the fine-tuned spring). The modifications prevented the regulator from responding adequately to cabin pressure oscillations. The flight data highlighted the importance of the bleed hole included in the unmodified CRU-103 diaphragm to provide flow compensation for a given hole size and flow path. Regulator compensation response lags can manifest differently depending on the internal configuration and flow path sizes. Consequently, FLT-106 informed the PBA team of the cabin pressure compensation mechanism time lag.

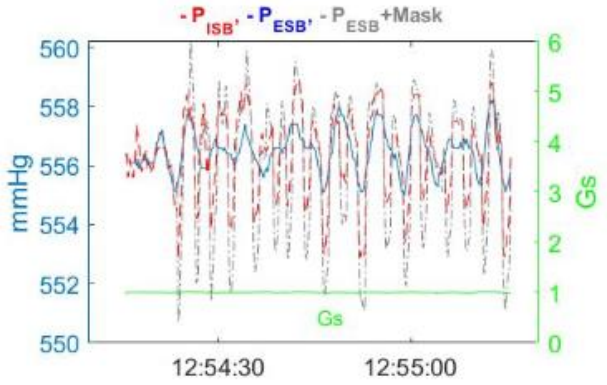

Figure 6.8.6. Pressures Measured by VigilOX During Selected Timeframe of FLT-106
Mask inhale line pressure (P_{ISB}), cabin pressure (P_{ESB}), and mask pressure (MaskP) measured by VigilOX during a selected timeframe of FLT-106. The g-forces (G's) exerted on the aircraft during the flight are also shown.

C. Breathing Hysteresis

An unresponsive CRU-103 regulator implies the pilot breathing demand is not adequately met by the positive pressure regulator. When the pressure differential between the mask and ISB line (Figure 6.8.7a) and between the ISB line and the cabin (Figure 6.8.7b) are measured throughout FLT-029 and plotted in histograms, two peaks are evident in each plot. The peak centered at 0.0 represents times when the pressure differential between the mask and the ISB line or between the ISB line and the cabin is near zero, which indicates the pilot air demand is met. The peak centered around 0.7-0.8 represents times during FLT-029 when the pressure differential between the mask and the ISB line or between the ISB line and the cabin is significant, which indicates the pilot air demand is not met. This data reveals hysteresis between the pilot and the breathing system during periods of high air demand and is denoted as breathing hysteresis by the PBA. The breathing hysteresis measures the asynchrony between the demand signal received by the regulator and the regulator supply. The mask hysteresis represents the asynchrony between the pilot demand and the regulator supply. Ideally, the hysteresis is negligible and the line and mask hysteresis are equal, which would indicate the pilot breathing needs are immediately translated to the ISB line or ESB line and the system supplies the desired volume of air to the pilot accordingly. However, many breathing hysteresis events were measured during FLT-029. It is the highest mean breathing hysteresis value for a Profile B flight flown throughout the PBA (see Table 6.8.1). The fraction of breaths with very high values of hysteresis (greater than 0.75 lps) is high for both the line and mask values, but particularly for the hysteresis measured by the mask pressure. In addition, the standard deviation of the distribution is more than a factor of two higher than that for a typical Profile B flight.

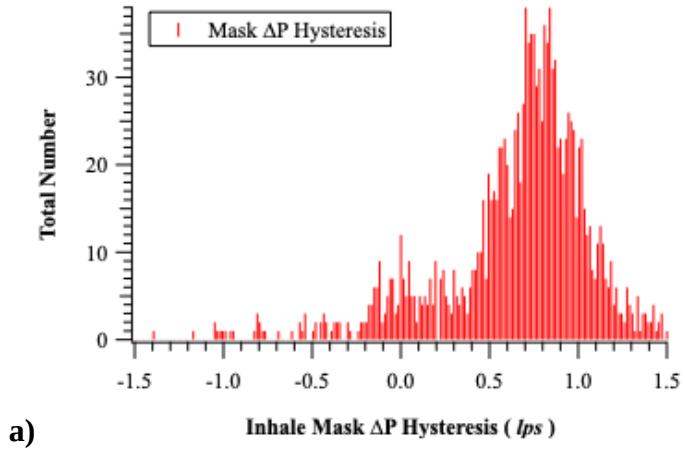

a)

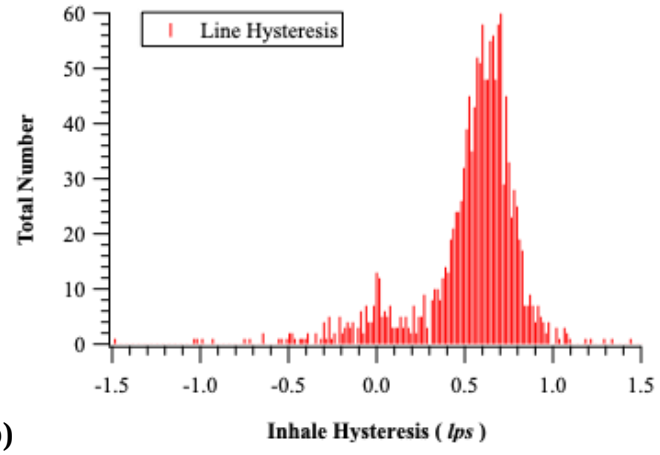

b)

Figure 6.8.7. Histograms Displaying Breathing Hysteresis Phenomenon Observed In a) mask pressure and b) the line-cabin differential pressure measured during FLT-029.

Two conclusions can be drawn by comparing the two histograms in Figure 6.8.7:

1. Pilot demand does not get transmitted to the regulator in time.
2. When the demand does get transmitted, it is not at the rate demanded.

The PBA team hypothesized early in the study that at times of fast, dynamic pressure change, the reference pressure of the regulator lags the dynamic pressure change in the cabin. The demand valve opens accordingly, and the original demand is not accurately translated to the line. This hypothesis will be substantiated, and the physical impacts of breathing hysteresis will be elucidated by the additional data and discussion presented below.

Table 6.8.1. Inhale Hysteresis
Inhale hysteresis based on the line-cabin pressure differential pressure measured during the PBA profile B flights, during which the CRU-103 regulator was used.
The highlighted rows correspond with flights flown by Pilot 55.

Flight	Mean Hysteresis (lps)	Standard Deviation (lps)
FL93	0.38	0.14
FL89	0.36	0.13
FL82	0.35	0.11
FL78	0.49	0.12
FL73	0.35	0.10
FL71	0.34	0.11
FL67	0.42	0.12
FL65	0.34	0.11
FL51	0.32	0.11
FL46	0.39	0.18
FL40	0.43	0.12
FL38	0.47	0.15
FL29	0.52	0.30

D. Relating Breathing Frequency and Cabin Pressure Oscillation Frequency

The lag between mask pressure and air flow (i.e., breathing hysteresis) measured during multiple flights throughout the PBA indicates the pressure inside the mask is affected by, and therefore related to the pressure in the cabin. F-18 cabin and regulator pressure measurements performed during a number of dynamic flights indicates the breathing frequency exhibited by the pilot is higher than the frequency of cabin pressure oscillations during high-G maneuvers (Figure 6.8.1). The PESB fluctuated, but the PISB envelope closely followed the PESB fluctuations and the pilot did not report breathing difficulties. A flat PESB line generally denotes a constant plane altitude.

In FLT-028, Profile C was flown and a CRU-103 (S/N 20294) regulator was employed. The pilot did not report any difficulties breathing throughout the duration of FLT-028. However, breathing hysteresis and cabin pressure oscillations were observed during the flight. In Figure 6.8.1, the PISB and PESB and oscillate at different frequencies from each other, as expected. The envelope of the PISB data does not directly match the PESB curve, which indicates the cabin pressure oscillations directly affect the pressure in the inlet line of the pilot's mask. Furthermore, the significant (up to 10 mmHg) PESB oscillations measured during FLT-028 indicate the aircraft environmental control system cannot adequately accommodate the pressure fluctuations induced by altitude changes throughout FLT-028. The cabin pressure oscillations experienced during the most dynamic flights (profile B) are significantly greater in magnitude than those measured in Profile C flown in FLT-028. This observation led the PBA team to focus on pilot breathing during the most dynamic flights.

The CRU-103 regulator (S/N20294) was also employed in FLT-024 and FLT-029, which involved the highly dynamic flight profile B. During FLT-024 and FLT-029, the pilots reported intolerable breathing difficulties, which could be explained by the dynamic profile flown. The PESB oscillates by up to 20 mmHg during certain dynamic maneuvers of flight Profile B

(FLT-029, Figure 6.8.8a). In addition, higher frequency oscillations are superimposed over lower frequency oscillations in PESB, which are associated with low-G maneuvers. The envelope of the PISB data obtained during FLT-029 (Figure 6.8.8a) shows the PISB lags behind the PESB fluctuations, which clearly shows the cabin pressure fluctuations affect the ISB flow into the mask and therefore the regulator ability to adequately respond to the pilots breathing needs.

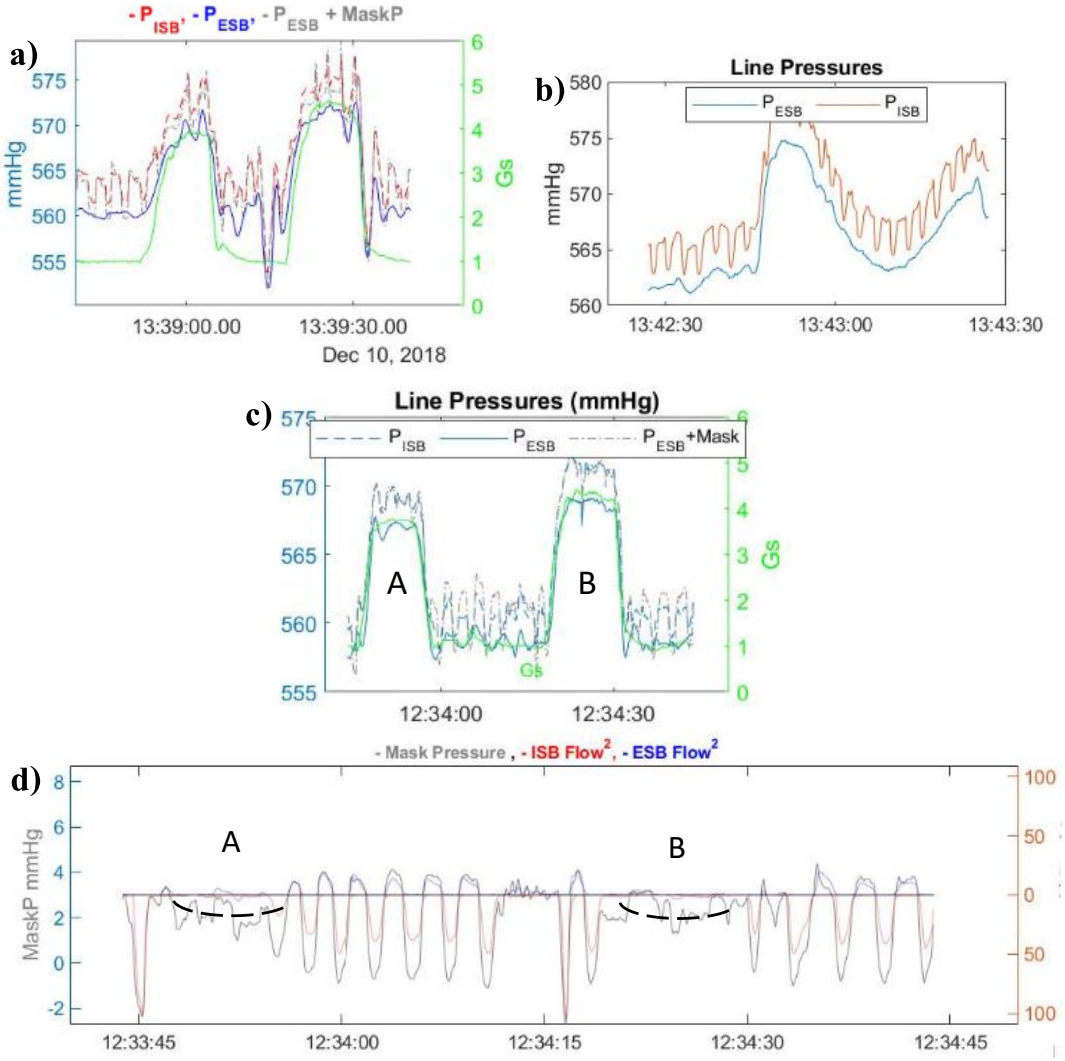

Figure 6.8.8. Pressure Measured During a Select Time Frame
a) Pressure measured in the mask inlet line (P_{ISB}), cabin (P_{ESB}), and mask (MaskP) during a select time frame of FLT-029 and c, d) FL73. b) P_{ISB} and P_{ESB} measured during a select timeframe of FLT-040.

High-frequency oscillations are absent from the PISB and PESB (Figure 6.8.8b) obtained during a squirrel cage maneuver of a different profile B flight (FLT-040) using a CRU-103 regulator (S/N 20292). The FLT-040 data contrasts the FLT-029 data despite the flights only differing by regulator serial number and aircraft tail number (FLT-040: Tail #846, FLT-029: Tail #850). This suggests the environmental control system function has a significant effect on the pilot breathing system ability to adequately respond to the pilot's breathing needs during dynamic maneuvers. The absence of high frequency PESB oscillations in the FLT-040 data also indicate that Tail #846 is a balanced aircraft, while Tail #850 is not. Therefore, pilot breathing difficulty is

occurring in a specific aircraft Tail #850 when equipped with a specific mask regulator (S/N 20294) while flying a highly dynamic flight profile. A balanced aircraft is defined here as one that includes a defect-free, seamless seal at the canopy interface, which minimizes dynamic maneuver-induced cabin pressure perturbations, and an environmental control system that can adequately respond to cabin pressure fluctuations with significant and rapid changes in altitude.

Figure 6.8.8c and 6.8.8d show the PESB, PISB, MaskP, and the flow rates through the mask inlet (ISB Flow) and outlet (ESB Flow) lines measured during two dynamic maneuvers of FL73 (Profile B, Tail #846). The PISB and PESB respond to the significant fluctuations in G -forces exerted on the plane during the two maneuvers, which agrees with similar measurements obtained during other dynamic flights. The ISB Flow and ESB Flow shown in Figure 6.8.8d exhibit a regular oscillatory pattern centered around ~3 mmHg as expected when using a CRU-103 regulator. However, the data shown in Figure 6.8.8d also shows the regular ISB Flow and ESB Flow oscillations are disrupted during the two dynamic maneuvers, as evidenced by the erratic ISB Flow and ESB Flow data beginning at ~12:33:48 and ~12:34:20. In addition, the dynamic maneuvers also cause a decrease in ISB Flow and ESB Flow, which indicates that as the cabin pressure increases, the regulator outlet pressure decreases and falls below 3 mmHg. This phenomenon is also observed during dynamic maneuvers performed in FL98 (see Figure 6.8.10 and corresponding discussion below) and represents an additional contribution to the overall disharmony of the pilot breathing and environmental control systems. It is therefore critical to enable adequate cabin pressure control by maintaining the aircraft health.

The discrepancies between the PISB and PESB data obtained during FLT-029 (Figure 6.8.8a) clearly show the positive pressure CRU-103 regulator cannot adjust quickly enough to accommodate the cabin pressure oscillations. The regulator lag cabin pressure oscillations are not always perceived by the pilot, which would explain the limited number of reports of breathing difficulties from pilots, but almost always affect ease of breathing. Therefore, overcoming positive pressure regulator dysfunction during dynamic flights is critical to pilot breathing performance.

E. Fighting the Machine

The mask pressure lag can only be qualitatively assessed from the raw PESB, PISB, and PISB+MaskP data. To quantitively assess the relationship between cabin pressure and PISB oscillation frequency, magnitude, and regularity, the mask pressure and cabin pressure measured during FL73 and FLT-029 were subjected to a fast FFT to extract statistical information. FLT-029 and FL73 both involved flight profile B and positive pressure CRU-103 regulator. However, a balanced aircraft was employed in FL73 (Tail #846), while an unbalanced aircraft was employed for FLT-029 (Tail #850). Additionally, different CRU-103 regulator S/Ns were used in each flight. The FFT data from FL73 and FLT-029 are shown in Figure 6.8.9. The ‘control’ data obtained from FL73 shows an absence of characteristic oscillatory frequencies in cabin pressure and a characteristic frequency peak in breathing oscillations at 0.33 Hz, which indicates the pilot typically breathes about 20 times per minute. The frequency peak in pilot breathing exhibits a relatively narrow full width at half maximum (FWHM), which indicates the pilot breathing rate remains relatively consistent throughout the flight. In contrast, a characteristic peak at 0.17 Hz appears in the FLT-029 cabin pressure FFT spectrum, while a peak at 0.33 Hz appears in the FLT-029 breathing FFT spectrum. In contrast to the FL73 data, the FWHM of the peak in the FLT-029 breathing FFT spectrum is much higher than in FL73.

During FLT-029, the pilot compensates for breathing difficulties by increasing their breathing rate, which leads to higher counts at higher frequencies.

When the FFT is performed on a small dataset from FLT-029, the peaks in the cabin pressure and breathing frequency spectra are more apparent (Figure 6.8.9c). If two sinusoidal waves with frequencies of 0.17 Hz and 0.33 Hz are added together (Figure 6.8.9d), the envelope function of the sum curve oscillates at a much smaller frequency compared to the two contributing waves. This indicates the destructive interference between the two waves periodically generates minima in the envelope function. Interestingly, a cyclic and repeating pattern of incrementally decreasing peak inhale pressure over the course of three breaths and subsequent increase in peak inhale pressure is measured throughout FLT-029. This cyclic and repeating pattern is shown for a small dataset obtained during FLT-029 in Figure 6.8.9e, where each cycle of diminishing peak inhale pressure is denoted by an arrow. This cyclic and repeating pattern is measured throughout the flight according to additional datasets presented elsewhere.

The phrase ‘Fighting the Machine’ was coined in the PBA to describe the cyclic decreasing maximum inhale pressure caused by the periodic destructive interference between the cabin pressure oscillations and pilot breathing oscillations. Additional data obtained from other maneuvers performed during separate flights also show the ‘Fighting the Machine’ phenomenon in the inhale pressure data, which indicates this phenomenon is widespread. Critically, the Fighting the Machine phenomenon could cause the breathing difficulties reported by pilots during dynamic flights.

When mask pressure and cabin pressure destructively interfere, either the cabin pressure is at a maximum and the mask pressure is at a minimum or cabin pressure is at a minimum and the mask pressure is at a maximum. When the cabin pressure is at a maximum and the mask pressure is at a minimum, the pilot’s ability to exhale is compromised most. In this case, the unidirectional flow valve at the ESB line connection is more difficult to crack open, which is caused by the combination of high cabin pressure outside the mask and low pressure inside the mask. When the cabin pressure is at a minimum and the mask pressure is at a maximum, the pilot’s ability to inhale is compromised most. In this case, the unidirectional flow valve at the ISB line connection is more difficult to crack open, which is caused by the high pressure inside the mask and the low regulator delivery pressure. Theoretically, if the pilot alters his or her breathing frequency or inhalation/exhalation volume, the Fighting the Machine phenomenon can be overcome. The pilot can increase breathing frequency or increase his/her maximum inhale pressure using a nominal breathing rate to interrupt the destructive interference cycle between the mask pressure and cabin pressure.

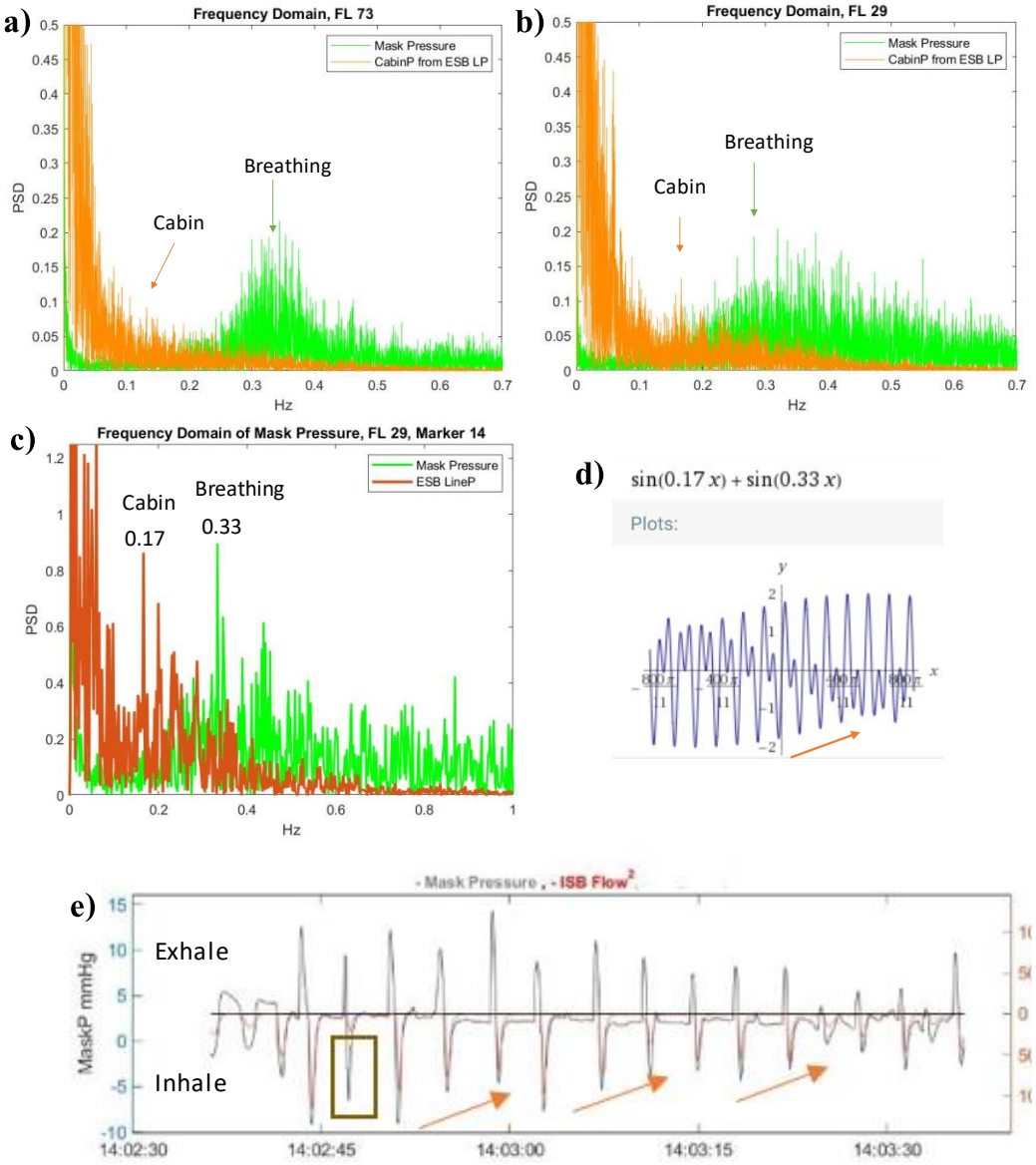

Figure 6.8.9. Mask Pressure Data

Mask pressure data that was obtained during a) FL73 and b,c) FLT-029 after transforming the data via a fast Fourier transform (FFT). The dataset displayed in c) is a small selection of data from the complete FLT-029 dataset displayed in b). d) Graphical display of a function including contributions from two sine waves with frequencies of 0.17 and 0.33, where the arrow denotes the periodic effect of destructive interference on the magnitude of the envelope function. e) Mask pressure and PISB measured during FLT-029 displaying the 'Fighting the Machine' phenomenon, where each arrow highlights a grouping of three consecutive MaskP minima with incrementally decreasing magnitude thereby highlighting the physical manifestation of the 'Fighting the Machine' phenomenon theoretically shown in d).

F. Effects of Cabin Pressure Fluctuations on Inhale Characteristics

The PBA program sought to substantiate the response lag between the regulator and cabin pressure. All pressure measurements discussed thus far were obtained using a VigilOX detector. The VigilOX samples data at a rate of 20 Hz. To augment the data obtained via VigilOX, a

0.5-Hz MadgeTech pressure transducer was included between the regulator and the mask in starting Flight 73. The PBA received this instrument on loan from NAWCAD, and its use was compatible with USN AFE. Figure 6.8.10 shows data obtained from FL98 using MadgeTech pressure sensors. The flight trajectory in terms of longitude, latitude, and altitude coordinates for a 90° turn performed during FL98 is shown in Figure 6.8.10a. The pressure measured upstream and downstream of the regulator throughout the 90° turn are shown in Figures 6.8.10b and 6.8.10c. Significant differences between the pre-regulator and post-regulator pressure measurements are evident. Furthermore, the pressure measured between the mask and the regulator lags the PISB measured on the cockpit side of the regulator in the mask inlet line. This confirms the mask pressure does not adequately respond to cabin pressure oscillations and supports the VigilOX data discussed in earlier sections. The abrupt and significant increase in PISB during the 90° turn is also accompanied by the onset of erratic and low amplitude mask pressure oscillations (Figure 6.8.10d), which corroborates the irregular breathing detected during dynamic maneuvers performed in FL73 (Figures 6.8.10d and 6.8.10e).

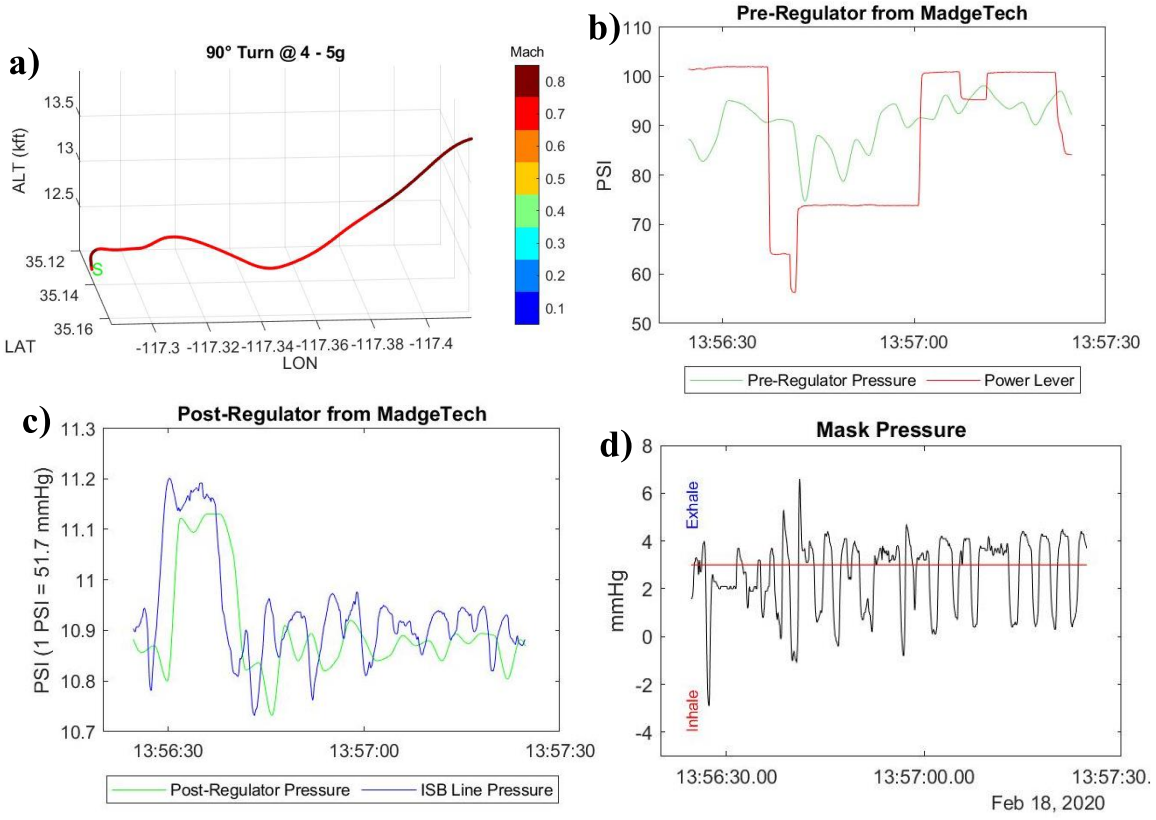

Figure 6.8.10. Data Obtained from FL98 using MadgeTech Pressure Sensors a) Longitude, latitude, and altitude coordinates measured during a 90° turn of FL98. b) Pressure measured in the mask inlet line upstream of the regulator by a MadgeTech sensor during the 90° turn of FL98. c) Pressure measured between the mask and the regulator (post-regulator) and within the ISB line (ISB Line Pressure) during the 90° turn of FL98. d) Mask pressure measured during the 90° turn of FL98.

If the CRU-103 regulator responds quickly to changes in its reference pressure, then it should be able to respond to pilot breathing needs. When there are delays in this response, the air demands of the pilot cannot be accurately translated to the mask inlet line. Figure 6.8.11 shows the derivative of MaskP and PISB measured during a profile B flight, which correspond with the true

pilot air demand and the air demand translated to the mask inlet line, respectively. Local minima correspond with maximum pressure changes during inhalation events, while local maxima correspond with maximum pressure change during exhalation events. The change in MaskP (DMP) peaks at much higher values than the change in PISB (DLP), which shows the pilot air demand is not adequately translated to the mask inlet line during dynamic maneuvers. This data corroborates the breathing hysteresis phenomenon.

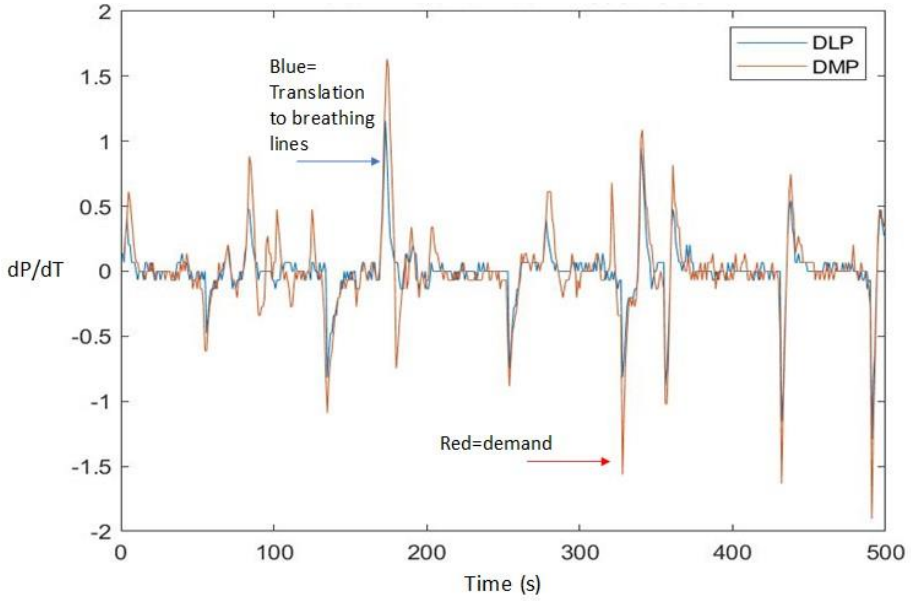

Figure 6.8.11. Derivative of MaskP and PISB Measured During Profile B Flight
Time derivatives of the inlet line pressure (DLP) and mask pressure (DMP), which were measured during FLT-029.

G. Determining the Role of Mask Function on Pilot Breathing

Mask function, in addition to the aircraft health, is critical to meeting the pilot breathing needs during dynamic flights. Different physical mechanisms are implemented across different pilot breathing systems, including the USN positive pressure regulator (CRU-103) and the USAF diluter demand regulator (CRU-73). Like the CRU-103, the CRU-73 provides O_2 to the pilot as needed during inhalation and stops the flow when the demand ceases during exhalation. However, the CRU-73 does not supply a positive pressure to the mask. The CRU-73 mask pressure oscillates about a net zero pressure and dilutes incoming O_2 with cabin air during instances of particularly high demand (i.e., during a dynamic maneuver). The diluter demand regulator may supply O_2 deficient cabin air to the pilot during parts of the flight where the cabin pressure oscillations are rapid and significant but does not put the pilot at risk of hypoxia because the O_2-deficient air is only supplied for a few seconds at a time. To directly compare the effect of regulator function on pilot breathing and exclude the effects of cabin pressure oscillations on regulator function, the PBA flew two pilots on the same aircraft during FLT-068, a profile B flight. One of the pilots was outfitted with a CRU-103 regulator, while the other was outfitted with a CRU-73 regulator. The effects of cabin pressure oscillations on regulator function were excluded by using a healthy aircraft in FLT-068 (Tail #846).

Figure 6.8.12a shows the trajectory of the dynamic climb in terms of latitude, longitude, and altitude coordinates. Figure 6.8.12b shows the change in cabin pressure, PESB, and G -force

exerted on the plane over the course of the maneuver depicted in Figure 6.8.12a. The cabin pressure decreases linearly throughout the climb and levels out once the climb is completed as expected. Cabin pressure oscillations are not detected throughout the climb.

Despite the nominal and linear cabin pressure change measured during the FLT-068 climb, the MaskP measured from the pilot using the CRU-103 regulator is highly erratic compared to the breathing demand of the pilot (Figure 6.8.12c). Therefore, the CRU-103 regulator function is impeding the pilot's ability to breathe. Furthermore, cabin pressure oscillations are not the only phenomenon affecting pilot breathing. Figure 6.8.12c shows the MaskP and the flow rate through the mask inlet line (Fin) measured from the CRU-103 regulator and Figure 6.8.12d shows the MaskP and Fin measured from the CRU-73 regulator. The Fin decreases to a local minimum at the maximum flow rate during each inhale and increases to zero flow rate during each exhale. When a CRU-103 regulator is used, the Fin is zero for multiple seconds at a time, which indicates multiple seconds pass between each inhale cycle. This is not a typical or sustainable breathing pattern for the pilot. Theoretically, the MaskP should match the uniform oscillatory behavior of the Fin and exhibit inflection points at 3 mmHg due to the positive pressure supplied by the mask if the regulator accurately responds to the pilot's breathing needs. However, the MaskP measured from the CRU-103 regulator includes numerous departures from the Fin curve. The MaskP follows the Fin closely most of the time when the pilot inhales. However, near the end of most inhale cycles where the Fin approaches zero, the MaskP decreases abruptly and typically remains constant or continues to decrease slightly at the end of the inhale cycle (see arrows). In addition, the MaskP does not increase above 3 mmHg, which indicates exhalation difficulty. This MaskP departure from the Fin curve indicates instances when the pilot cannot exhale because the cabin pressure fluctuations prevent the regulator from translating the pilot's breathing needs. In stark contrast, the Fin curve obtained from the CRU-73 regulator exhibits a higher frequency of inhale cycles and therefore less time between breaths. Critically, the MaskP measured from the CRU-73 regulator exhibits the same frequency and qualitative shape as the corresponding Fin, which indicates the CRU-73 accurately translates the pilot's breathing needs to the system. Furthermore, the CRU-73 supports a sufficient breathing rate and magnitude during dynamic maneuvers. Therefore, a CRU-73 regulator eliminates the pilot breathing difficulties reported when the CRU-103 regulator is used (excluding differences in pilot physiology).

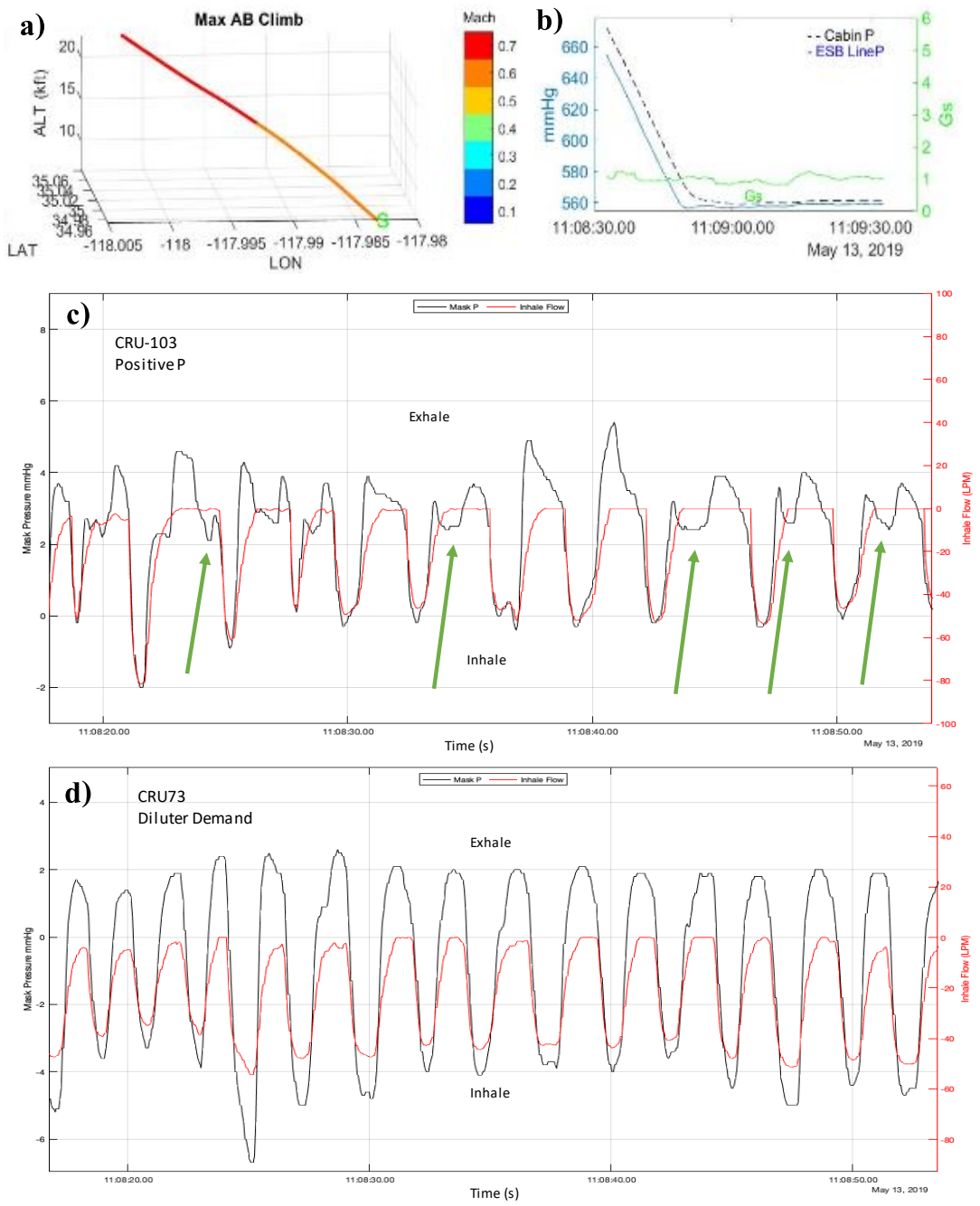

Figure 6.8.12. Measurements Taken During a Rapid Climb of FLT-068 a) Longitude, latitude, and altitude coordinates, and b) cabin pressure (CabinP), exhale line pressure (ESB lineP), and G -forces (G's) measured during a rapid climb of FLT-068. Inhale flow (red) and mask pressure (black) measured from two pilots flying on FLT-068, one wearing a c) CRU-103 regulator and the other wearing a d) CRU-73 regulator.

The peaks in MaskP were measured for each pilot throughout FLT-068 and plotted versus the corresponding maximum flow rate (F). Each MaskP-F data pair is plotted in two modified trumpet curves in Figure 6.8.13 according to the regulator used. The blue data points correspond with exhalation events and the red data points correspond with inhalation events. When the CRU-73 was used, a certain amount of MaskP induced a relatively repeatable F, as expected of a

nominally performing regulator that adequately accommodates the pilot's breathing needs. The F increases more with increased MaskP during an exhale than during an inhale when the CRU-73 is used. In contrast, significant scatter manifests in the data obtained from the pilot using the CRU-103. The inhale data is grouped into two distinct linear regions, one of which corresponds with the positive inflection portion of the MaskP measured during an inhale and the other corresponds with the negative inflection portion of the MaskP measured during an inhale. The difference between these two groupings represents the breathing hysteresis magnitude. Therefore, the breathing hysteresis exhibited by a CRU-103 is far more severe than that exhibited by a CRU-73. Furthermore, the breathing hysteresis is also measured while exhaling, which indicates the F varies throughout the flight for identical MaskP.

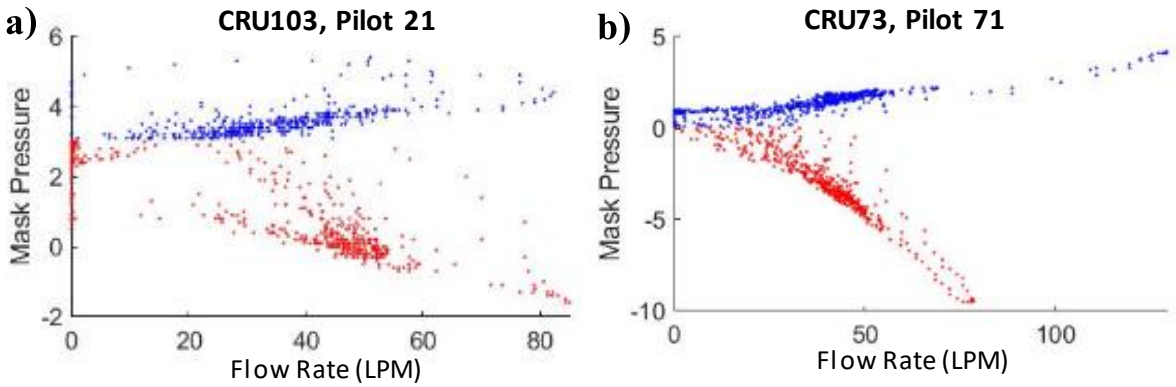

Figure 6.8.13. Modified Trumpet Curves
Modified trumpet curves showing the mask pressure measured during exhalation events (blue) and inhalation events (red) from the two pilots that flew FLT-068, where one pilot wore a a) CRU-103 regulator and the other wore a b) CRU-73 regulator.

H. Diagnosing Off-Nominal Aircraft 'Health'

The data discussed thus far show cabin pressure oscillations (Figures 6.8.8 through 6.8.11) and the CRU-103 regulator function (Figures 6.8.12 and 6.8.13) negatively affect pilot breathing. In this document, aircraft health refers to the cabin pressure stability during flight. When an aircraft is denoted as healthy, high frequency cabin pressure oscillations are nearly or completely absent from cabin pressure measurements during dynamic maneuvers. The health of F-18 aircraft is commonly characterized by measuring the cabin pressure during and immediately after canopy close to evaluate the performance of the environmental control system and evaluating the amount of time it takes for the system to dampen out initial cabin pressure oscillations (Figure 6.8.3). The PESB oscillates for a significant amount of time after canopy close, which indicates less than optimal health and necessitates aircraft maintenance.

Ideally, aircraft health can be maintained to prevent cabin pressure oscillations and support nominal pilot breathing performance. The effect of aircraft health on pilot breathing has been directly observed by considering the DMP throughout each PBA flight (Figure 6.8.14). Each row in Figure 6.8.14 represents a single flight, where the letter denotes the flight profile, the first two-digit number denotes the flight number, and the second two-digit number denotes the pilot. The color scale at the right of Figure 6.8.14 represents the range of relative breathing difficulty according to the DMP, where greater breathing difficulties are expected to coincide with a higher number. The DMP measured during Profile B flights FLT-012-FLT-0-68 indicate the pilot

experienced significant breathing challenges according to the high density of green, yellow, and red data points. Tail #850 was flown for all Profile B flights from FLT-012 to FLT-068 except for FLT-013 and FLT-040, which were flown using Tail #846. After FLTR-068, routine maintenance was performed on Tail #850 and was not used in subsequent PBA flights. Coincidentally, the DMP data obtained during FLT-073-FLT-093 indicates the pilot should not have experienced any breathing issues according to the significant decrease in green, yellow, and red data points. The dramatic improvement in ease of pilot breathing after switching from Tail #850, an unhealthy aircraft, to a different healthy aircraft according to the corresponding DMP data indicates the aircraft health has a direct effect on regulator function and pilot breathing. Aircraft health monitoring could be improved to more accurately identify when aircraft maintenance is necessary and therefore minimize pilot breathing difficulties during dynamic flights.

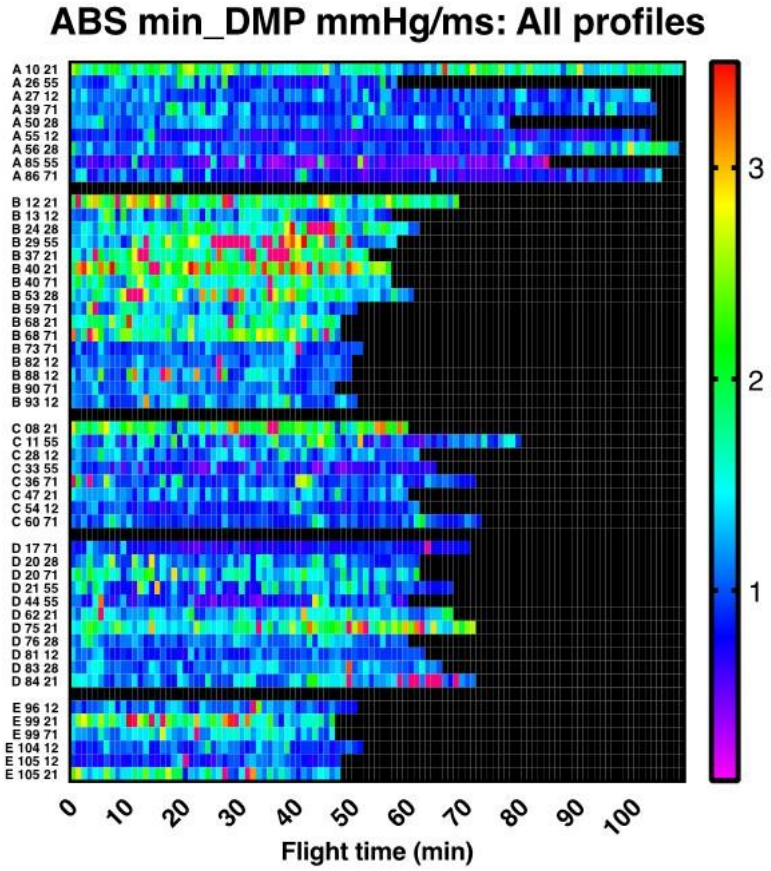

Figure 6.8.14. 'Monet' Plot Showing Derivative of Mask Pressure Measured Throughout an Assortment of PBA Flights
Each row corresponds with the flight profile, number, and pilot denoted along the y-axis. Each colored rectangle represents one minute of data from the corresponding flight. The scale at right is displayed to correlate colors used in the plot with a relative number from 0-3.5, where a larger number indicates greater breathing difficulty.

The data presented thus far has shown CRU-103 regulator function is directly affected by cabin pressure oscillations, which are directly affected by aircraft health. It would be useful to study CRU-103 regulator performance without external perturbations caused by cabin pressure oscillations and/or the aircraft environmental control system. For information on CRU-103

performance during low altitude flights while the cockpit is vented and/or the cabin pressure regulation system is turned off, see Section 6.3.1.

Conclusions

Throughout this report, characteristics of pilot breathing difficulties and aircraft health in mask pressure, cabin pressure, mask inlet line pressure, rate of mask pressure change, rate of inlet line pressure change, and flow rate are presented in various forms, which were measured during numerous PBA flights. The datasets presented show the CRU-103 positive pressure regulator cannot adequately support pilot breathing needs during dynamic flights when the mask pressure does not respond to cabin pressure changes. The mask pressure lag is exacerbated during highly dynamic maneuvers, which is likely caused by the more rapid and significant cabin pressure oscillations that also manifest during dynamic maneuvers. Breathing difficulties manifest during some dynamic flights when a positive pressure regulator is used, but do not manifest when a diluter demand regulator is used. At times of fast, dynamic flight profiles (e.g., ascents, descents, high-G maneuvers), the regulator response lags the dynamic pressure change in the cabin. The demand valve opens accordingly, and the original demand is not accurately translated to the mask inlet line. The discrepancy between pilot breathing demand and system supply has been denoted ‘breathing hysteresis’ in this work and can be used as a metric to evaluate the magnitude of pilot breathing characteristics and positive pressure regulator function. Both the positive pressure regulator function and the aircraft health play critical roles in breathing system performance. Breathing hysteresis can be overcome if the pilot increases breathing frequency beyond 0.4 Hz. The aircraft health is typically monitored by gauging the damping efficiency of the environmental control system during the minutes after canopy close and could be used as a diagnostic tool to assess aircraft ‘health’ and drive maintenance critical to maintain a healthy pressure regulator system.

F.6-20. PBA found subjective breathing difficulty reported in flight correlated to objective measurements of breathing system performance.

R.6-10. Subjective reports of breathing difficulty from pilots should be trusted as a significant indication of breathing system performance and followed up in a methodical manner including assessment with objective data. (F.6-20, F.8-1)

F.6-21. Even small amplitude cabin pressure oscillations (e.g., a few mmHg) will impact the regulator reference pressure and response. The severity of the combined effect determines the impact to pilot breathing.

F.6-22. When an aircraft cannot maintain steady cabin pressure, the regulator has a harder time adjusting. This lag is especially pronounced in a dynamic profile (rapid altitude changes, G’s at 4 G’s or higher).

R.6-11. Regulators should be bench tested with pressure and flow rate changes commensurate with an operational flight environment. ***(F.6-20)***

F.6-24. PBA discovered that aircraft cabin pressure fluctuates in a manner which can have both a primary impact to the pilot’s physiology, and a secondary impact through oscillatory fluctuation in reference pressure for the pilot’s breathing regulator, resulting in complex impacts to pilot breathing.

R.6-12. Develop and deploy a cabin pressure sensor that can measure the absolute magnitude of the cabin pressure and is also capable of measuring sub-mmHg pressure oscillations about the absolute pressure in the 0.01 to 10 Hz range. ***(F.6-24)***

6.9 Mini-Studies

This section contains mini studies of specific flights the PBA found important to highlight. These are meant to be stand-alone studies, thus some repetition might occur relative to the main Section 6.

6.9.1 Mini Study on Flight 29. This was the one PBA flight after which the pilot reported significant breathing difficulties. PBA investigates possible causes

6.9.2 Mini Study on Flight 38. This flight is significant because "smoke in the cabin" caused an early return to base. The PBA explores the minutes leading up to the smoke, including not well controlled, larger than normal cabin pressure oscillations

6.9.3 Mini Study on Flight 95. This was a Profile H proficiency flight, which experienced a momentary flame-out of one engine, followed by emergency landing. In all cases the PBA studies the significant hardware event in conjunction with its effects on pilot breathing

6.9.1 Mini Study on Flight 29

Flight 29 is significant because post flight the pilot reported breathing difficulties while on a USN-like configuration with safety pressure, on an aerobatic flight, Profile B. The flight profile and instructions from the flight card are shown in Figure 6.9.1.

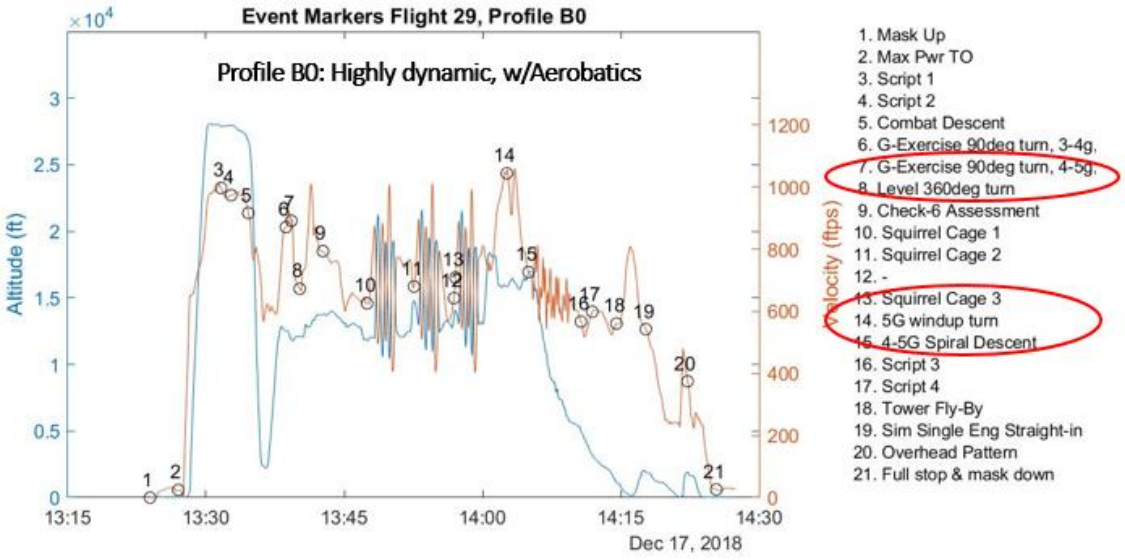

Figure 6.9.1. Flight Profile and Instructions from Flight Card
Pilot was having difficulty breathing, most notably during maneuver 7, 8, 13, 14 and 15. The graph shows Altitude and Velocity vs Time, with flight segments referenced to the left-side panel.

The pilot provides a vivid personal account at the highlighted event markers (M).

- M7 (5 G 90-degree turn): "Couldn't exhale completely. It was more difficult than normal to exhale quickly through the mask. Felt as if exhaling against a partially closed valve or having to exhale against positive pressure."
- M8 (Level 360 turn): "Difficult to exhale completely in a quick fashion. Very hard to take a "quick breath" due to extra time required to exhale breath completely. Under g-force, this resulted in a partial exhalation and ensuing partial inhalation therefore an "incomplete breath." This resulted in several partial breaths and eventual oxygen starvation. Quick, full breaths under G were not possible."
- M13 (Squirrel Cage #3): "Couldn't exhale completely in a short period of time (as if the exhalation path was partially blocked)."
- M14 (5 G Wind-up turn): "Ran out of oxygen due to partial breaths due to trouble exhaling quickly. I could not have continued this maneuver much longer than 1-minute due to inability to get a full breath."
- M15 (Spiral Descent): "After 4 minutes, was out of breath and could not complete further."

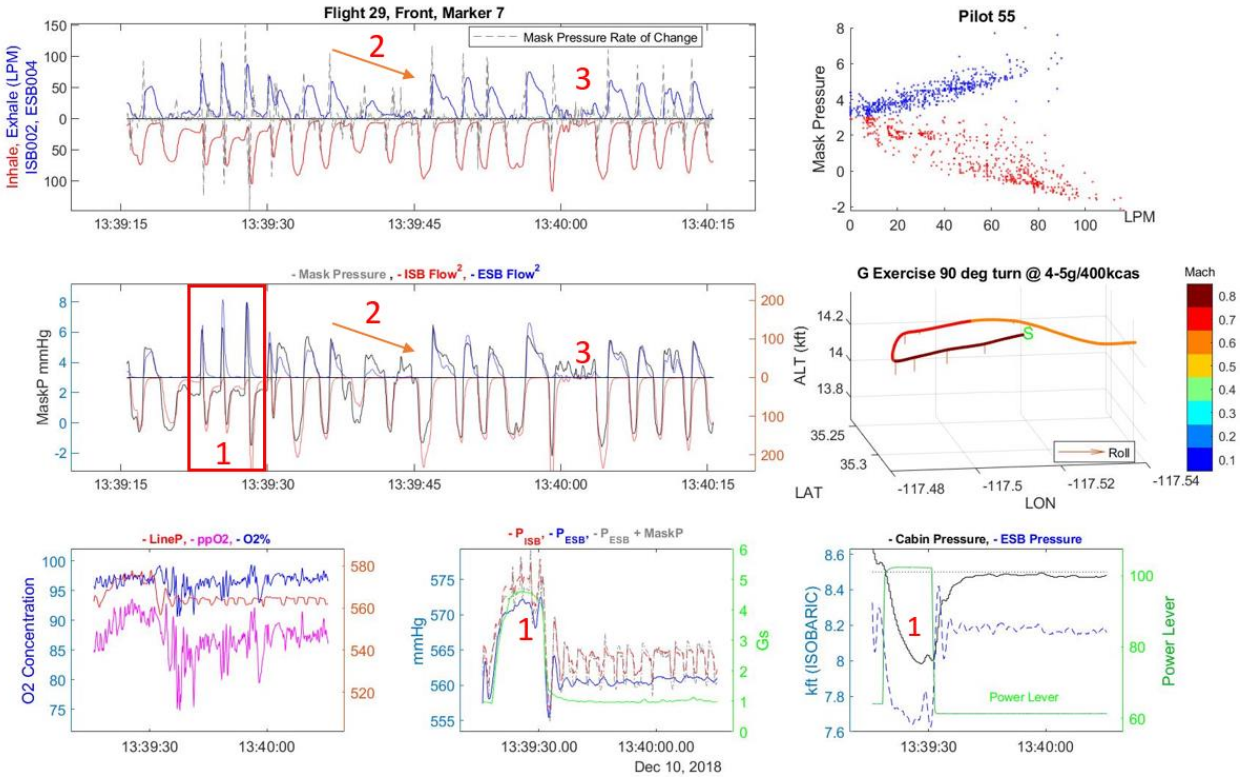

Figure 6.9.2. Marker 7.
The pilot "couldn't exhale completely." There was (1) G-breathing during a high-G portion with increased dynamic and cabin pressure; (2) diminishing exhalation flow followed by (3) no flow expelled.

In Section 1 of Figure 6.9.2, cabin pressure climbs 12 mmHg due to dynamic pressure from the G forces, in an Isobaric region. This is equivalent to 500-800 ft. equivalent pressure change, as converted from the lower-sampled cabin pressure and the ESB line pressure respectively. At the same time, under the G forces the pilot applied the characteristic G breathing with a sharp, short-

timed exhalation. Unlike regular breathing in which the exhalation has time to finish in a gentle down-slope, under G-breathing even before the peak of the exhalation, a large downward mask pressure change is initiated, and the inhalation flow is observed, while simultaneously the exhalation valve still slowly closing. This is a narrow-width inhalation with low volume, followed by a pause and repeat.

Section 2 of Figure 6.9.2 shows the diminishing values of the exhalation flow rate, to the point where during the last breath in the grouping there is actually no exhalation flow response to the mask pressure elevation. There is another area with no exhalation flow under mark "3," all of which backup the fact that the pilot "couldn't exhale completely."

Physiologically Section 2 of Figure 6.9.2 shows diminishing flow and is impacting inhaled and exhaled tidal volumes. One can see a decrease in exhaled volume and secondarily a decrease in inhaled volume. In essence, the alveoli are trapping air and increasing dead space or non-gas exchanged air. This would result in limiting the volume available for inhalation. In this particular segment, the mask pressures indicate increased effort with line pressures still fairly high and there should be concomitant flow with this effort. The flow should match this effort fairly well, but this is indicating decreasing tidal volumes. So intuitively the effort or "work" of breathing is increased but, not matched with flow. With the pressures being fairly high in relationship to natural air way pressures, there is likely some airway collapse. This coupled with the tidal volume decreases would result in limiting total alveolar volume. This would be symptomatically perceived as lack of flow.

The Phase Shift was introduced as an analysis tool in Section 3, measuring temporal and correlative disharmony between the driving pressure and response flow. This is applied to the 1-minute section of the 5 G turn (Figure 6.9.3).

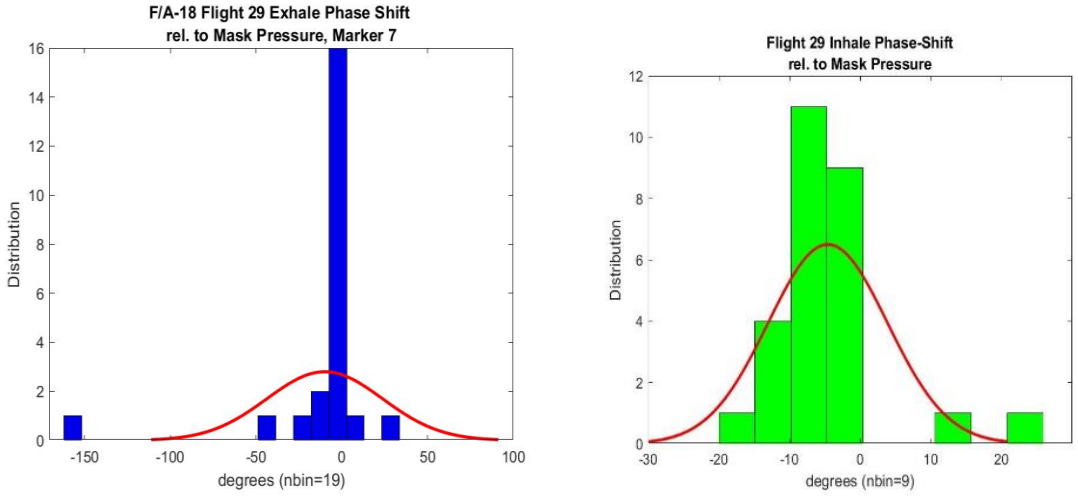

Figure 6.9.3. 1-minute Section of 5-G Turn
Phase Shift confirms pressure-flow disharmony prevalent during exhalation (left) with high phase shifts (50 and 150 degrees, compared to the ideal 6-10 degrees). The inhalation side (right) is not affected by large phase shifts, just constant small lags, characteristic of positive pressure systems.

The next maneuver, a level 360-degree turn, lasted 45 seconds, during which time nearly 5 G's were sustained (Figure 6.9.4), the cabin pressure increased with G's, and the characteristic G breathing is observed. During the first 30 seconds of G breathing, in the top tile, the dashed grey line shows the rate-of-change of mask pressure. Basically, how hard the pilot has to contract his

diaphragm, increase, while getting the same flow in return. This continues to a point where it cannot be increased any further. After 13:40:30, the inhalation effort diminishes. Inhalation flow does not return to 0, and there is very little variation, meaning very little actual flow consumed. At the same time, over a series of shallow breaths, the exhalation flow diminishes to 0 (both trends signified by the orange arrow). The conclusion is that under the conditions present in that aircraft the day of this flight, G breathing past 30 seconds was not sustainable under a load of 5 G's. Normal breathing resumes as G's subside.

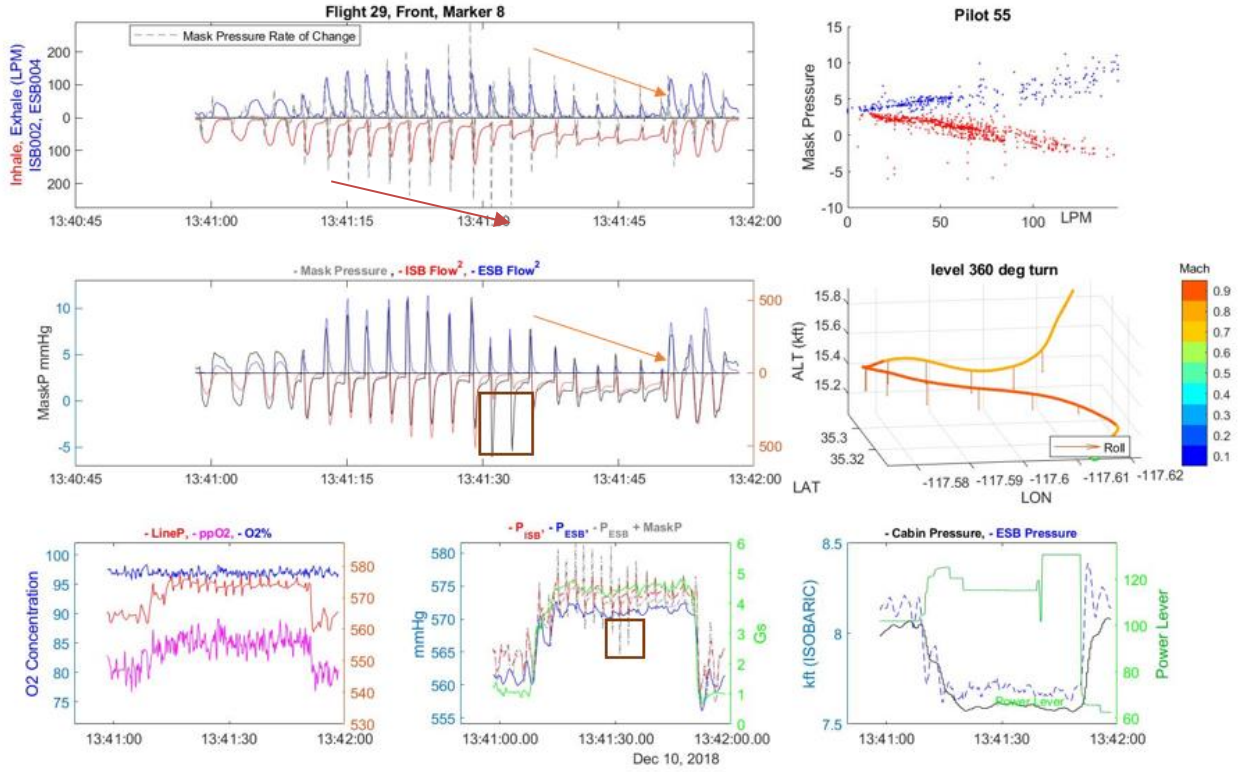

Figure 6.9.4. Marker 8; "Quick, Full Breaths Under G Were Not Possible"

Physiologically the marker 8 segment in Figure 6.9.4 shows again diminishing flow and is first impacting inhaled and then exhaled tidal volumes. There are also significant large pressure peaks, which should vastly increase the flow relative to the effort. These are well above normal airway pressures of 3-5 mmHg. The increasing pressures should have a flow continuously with the pressures generated. In this case, the tidal volumes are consistent and lower. They should be increasing with the pressure increases, but instead fairly even and indicating restricted flow. The decreased inhalational tidal volumes do not fill the alveoli adequately and as evidenced here, result in diminished exhaled volume. This indicates that the remaining alveolar volume is physiological dead space. In this case, the pilot perceives inability to exhale completely, as expressed in the post-flight report.

The maneuver the pilots dub "Squirrel Cage" is 3 consecutive loops. Figure 6.9.5 shows 1.5 loops performed in 1 minute, which was the 3rd execution of this maneuver.

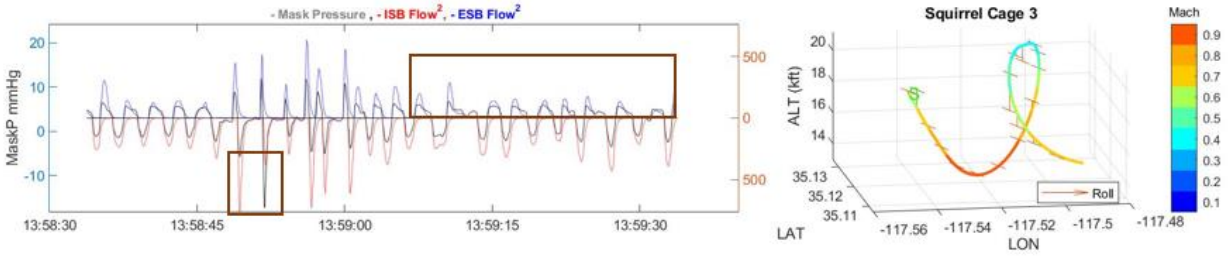

Figure 6.9.5. Marker 13; Pilot's Remark "Couldn't exhale completely" is evidenced by the low exhale flow rate and irregular shape in the maroon block * (13:59 to 13:59:30).

In Figure 6.9.5, the high velocity and G forces are periodic instead of sustained, and the pilot has not commented until the 3d repetition of this exercise. The PBA pilots have flown this Profile B before, but this was the 1st time with a positive pressure regulator. Regardless, the data regarding system responses speak for themselves. At 13:58:50, notice a large flow-rate (red) and no proportional driving pressure; the 2nd inhalation in the highlighted window is a draw from 3 to -14 mmHg, a 17 mmHg delta, with half the expected flow rate. From this timestamp until 13:59 the pilot was performing G-breathing. However, in the window highlighting the last 30 seconds, there is disharmony between the exhalation side of the mask pressure, and the resulting flow. This disharmony can be quantified and displayed in Figure 6.9.6.

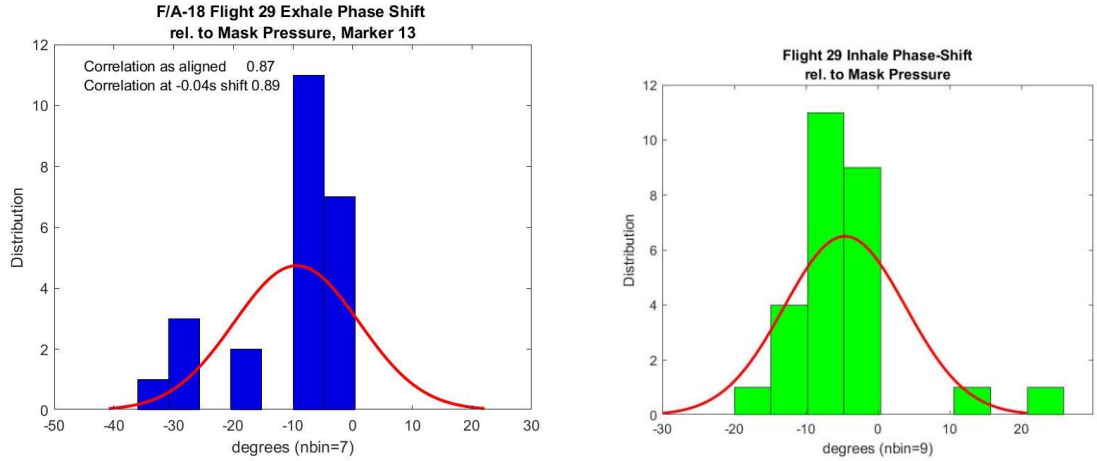

Figure 6.9.6. Disharmony Between Exhalation Side of Mask Pressure and Resulting Flow The phase shift tool shows 7 breaths (out of 23) with a lag of -20 to -40 degrees. Ideally all data should be in a bin to the left of 0 if volume were to instantly and proportionally follow pressure.

Interpreting the lag in Figure 6.9.6, lag on the inhale side is bad because flow is not delivered instantaneously. Lag on the exhale side means that there is pressure build-up before the flow is expelled (results in difficulty exhaling).

In Figure 6.9.5 at marker 13, again the pressures in excess of airway pressures and then decreasing pressures are observed. This may well represent respiratory fatigue in fighting to get adequate exhaled volume expelled.

Breathing deficiency and fighting the machine continue during the next 5 G exercise (Figure 6.9.7).

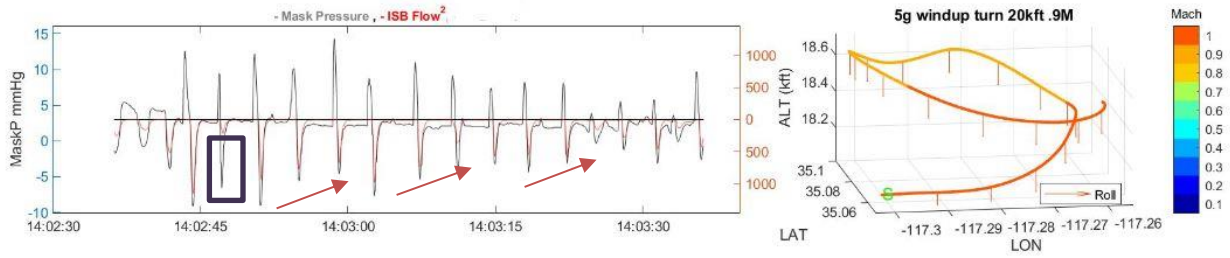

Figure 6.9.7. Marker 14; Breathing Deficiency and Fighting Machine During Next 5 G Exercise "Ran out of O_2 due to partial breaths due to trouble exhaling quickly. I could not have continued this maneuver much longer than 1-minute due to inability to get a full breath." Showing inhalation #4 having almost no flow response to a 10 mm mask pressure delta. Peak mask pressure and peak flow rate diminish with time.

To investigate the "ran out of oxygen" comment, the Minute Ventilation from segment 14 is compared with the other segments (Figure 6.9.8).

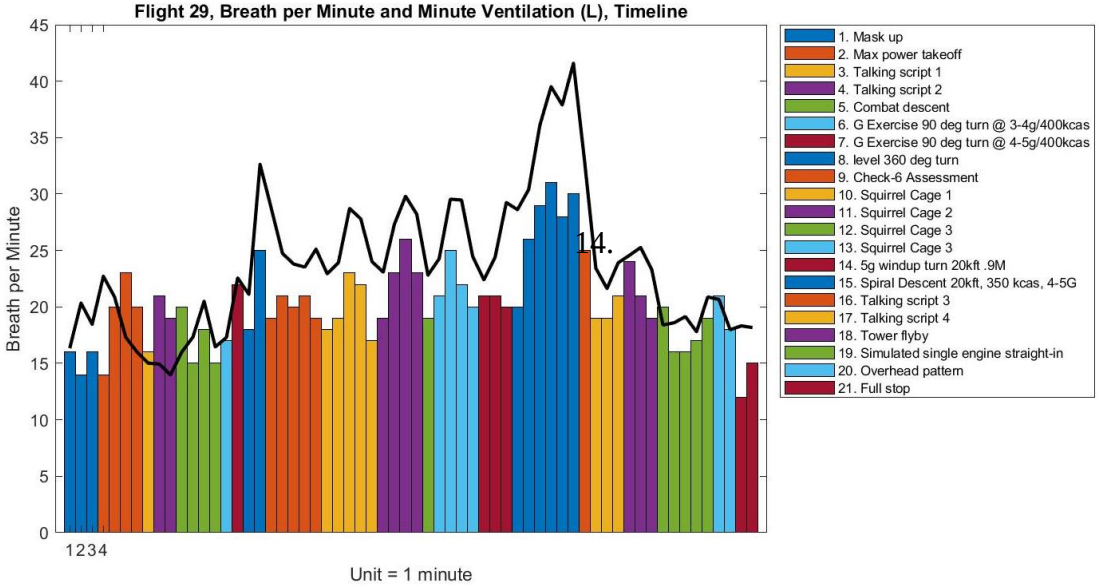

Figure 6.9.8. Minute Ventilation from Segment 14 Compared with Other Segments Each new color represents the start of a new instruction. Minute ventilation (L, STPD) is trending over the BPM bars. Wider color blocks comprise of the maneuver first, then a higher ventilation recovery. At Marker 14, minute ventilation is 19L

To put the pilot experience during segment 14 in perspective, the mask pressure was also evaluated (Figure 6.9.9). The green segment at 14:04 shows that during the 5 G's (sustained) Turn, the mask pressure ranges from -9 to +14 mmHg. Given this flight being in USN-like configuration with the CRU-103 regulator providing an approximately 3 mmHg safety pressure (higher than the reference ambient pressure), means that during inhalation, the pilot drew down from 3 to -9 mmHg (12 mm delta) resulting in 200 PLM peak flow rate, and to exhale, the pilot was pushing past 3 to 14 (11 mm delta). This is the segment in which the pilot works the hardest continuously for almost a minute, pulling and pushing air through 23 mmHg, for a return that is one of the lowest liters per minute ventilation.

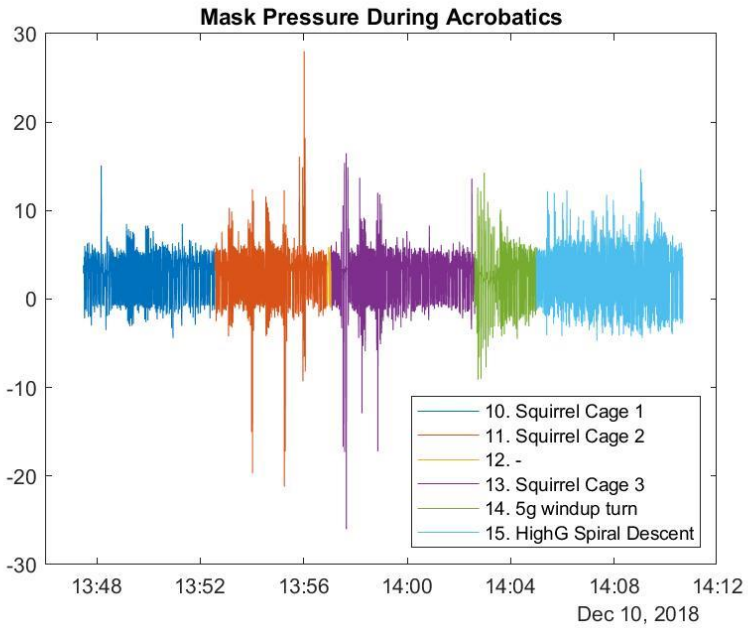

Figure 6.9.9. Marker 14; Mask Pressure Elevated
Mask pressure is elevated in portions of the dynamic high-G maneuvers listed in the legend. There are breaks between high-G and high mask pressure exertion, except for the Spiral Descent in which there is a 5 G short segment every 20 seconds, thus mask pressure oscillates as pilot breathing adapts

Physiologically Figure 6.9.7 shows diminishing expiratory and inspiratory pressures. This is occurring in sequential segments; this is indicating a pilot struggling to get more volume with more pressure. This indicates decreases in exhaled and inhaled volumes. Again, this indicates alveoli are increasing in dead space or non-gas exchanged air. This would result in limiting the volume available for inhalation. Thus, the pilot tries to take a deep breath to make up the volume and pressures decreasing again as the inhaled volume was not adequate. In this particular segment, the mask pressures indicate increased effort with line pressures still fairly high and there should be concomitant flow with this effort. This pattern of breathing is indicative of impending respiratory failure.

F.6.25. Minute ventilation is greatest during the post-G recovery segment.

Forty minutes into the flight, part of the descent was a spiral descent (Figure 6.9.10).

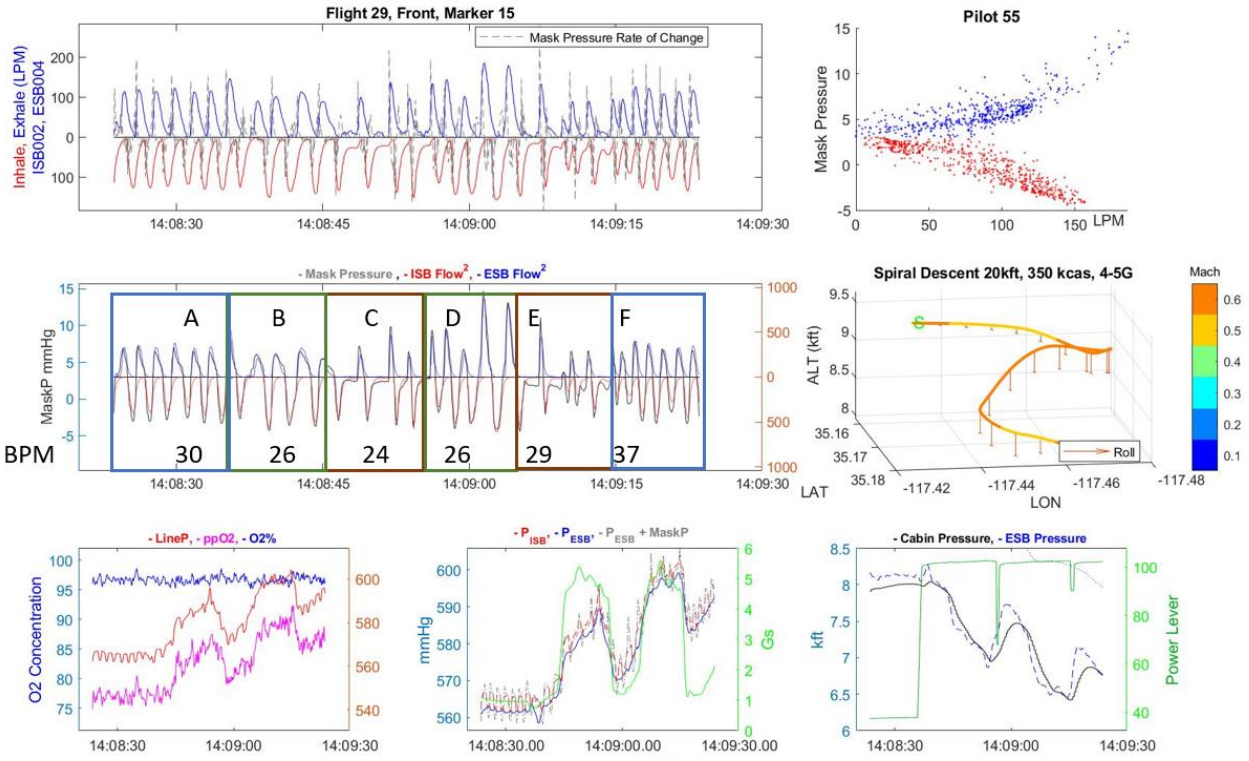

Figure 6.9.10. Marker 15; "After 4 Minutes, Was Out of Breath and Could Not Complete Further"

In the 4th minute of Spiral Descent, it is clear how demanding this maneuver is. Within 1 minute, the pilot's breathing changed 6 times, marked A-F in Figure 6.9.10. Since the pilot remarked on minute 4, this is the segment shown. The pilot started the maneuver at 20,000 ft, and by 14:08:30 already performed 6 half-spiral turns. In each turn the G's go up to 5, then return to 1-G, and repeat. Section A is recovery breathing after the previous spiral, at 3 BPM. Section B is still recovery, but with wider inhalations, equivalent to 26 BPM. Sections C and E are G-breathing, with the inhalation in E very minimal, perhaps a sign of physical stress, backing up the pilot's remark of feeling "out of breath and could not complete any further." D and F are recoveries with 26 and 37 BPM respectively. Note the really high 15 mmHg exhalation mask pressures in section D, as if there were additional lung capacity that could not get released before. This section also lit up in summary statistics (Figure 6.9.11).

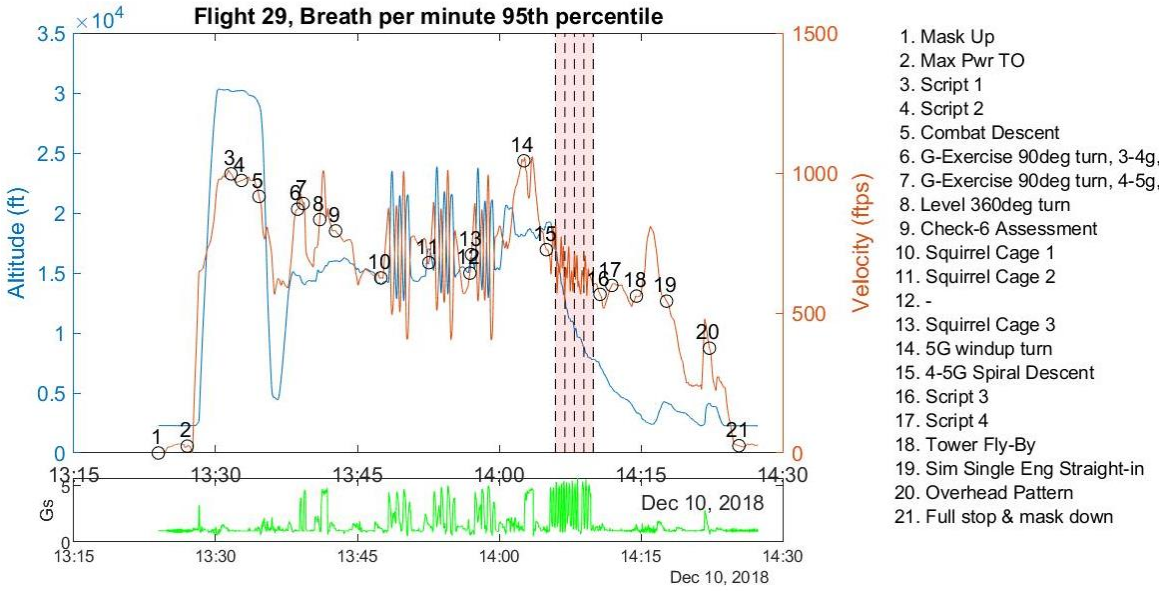

Figure 6.9.11. Spiral Descent BPM is in 95th Percentile of 27 Flights' Data

By applying the phase shift tool, the pressure-flow health of the entire flight can be evaluated (Figure 6.9.12).

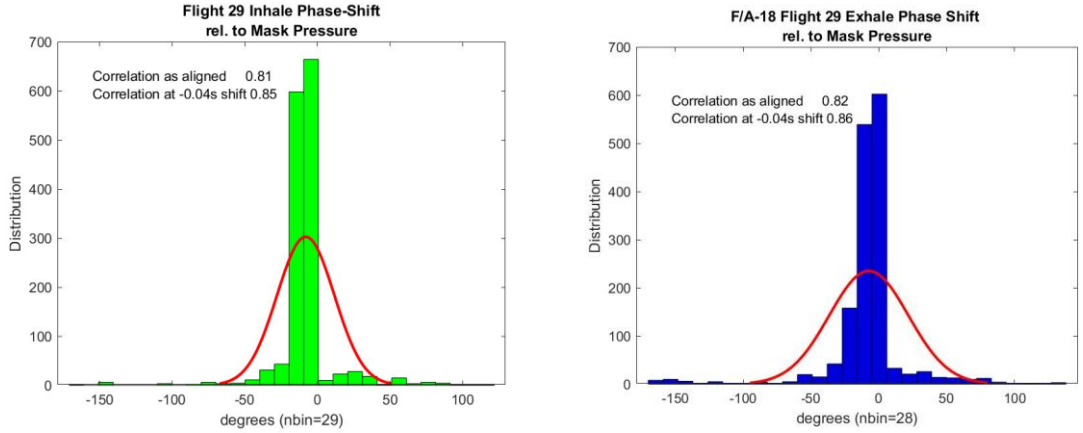

Figure 6.9.12. Flight 29 Exhibits Low Mask Pressure-Flow Correlation (relative to 95-98% achievable). Both the inhalation side (left), and exhalation side (right) show some lagging flow, (negative phase shift), and pressure peaking late (positive phase shift). The exhalation distribution shows more stress (180 exhalations with -25-degree phase shift).

The PBA has applied summary statistics to compare not just flights, but flight minutes, thus allowing to draw conclusions on specific segments (Figures 6.9.13 through 6.9.16).

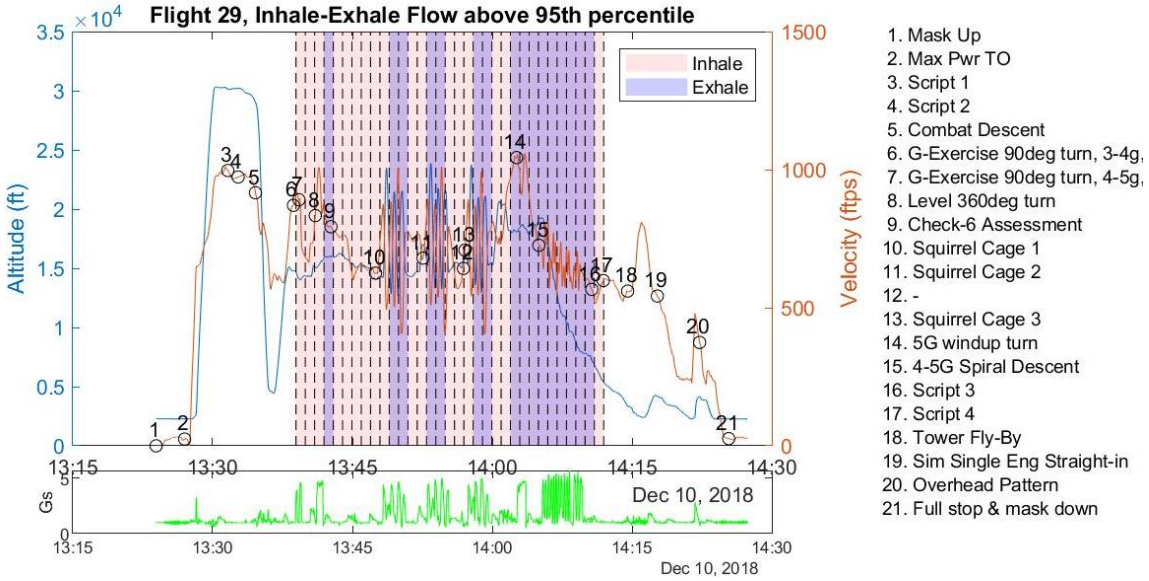

Figure 6.9.13. Flight 29 Flow During High G is in 95th Percentile in Mixed Population of USN and USAF Configuration Flights

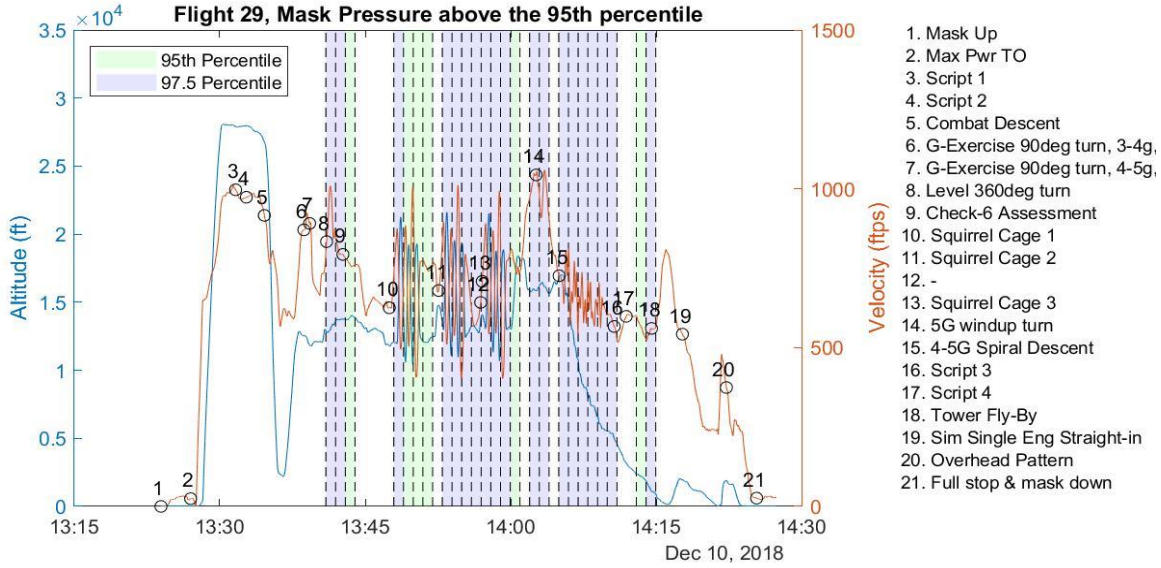

Figure 6.9.14. Mask Pressure Values in Flight 29 are in 95th Percentile in all Areas Pilot Highlighted Difficulty Breathing

Note that for example, inhalation or exhalation valve problems both would manifest in higher positive mask pressure, corresponding to the exhalation segment.

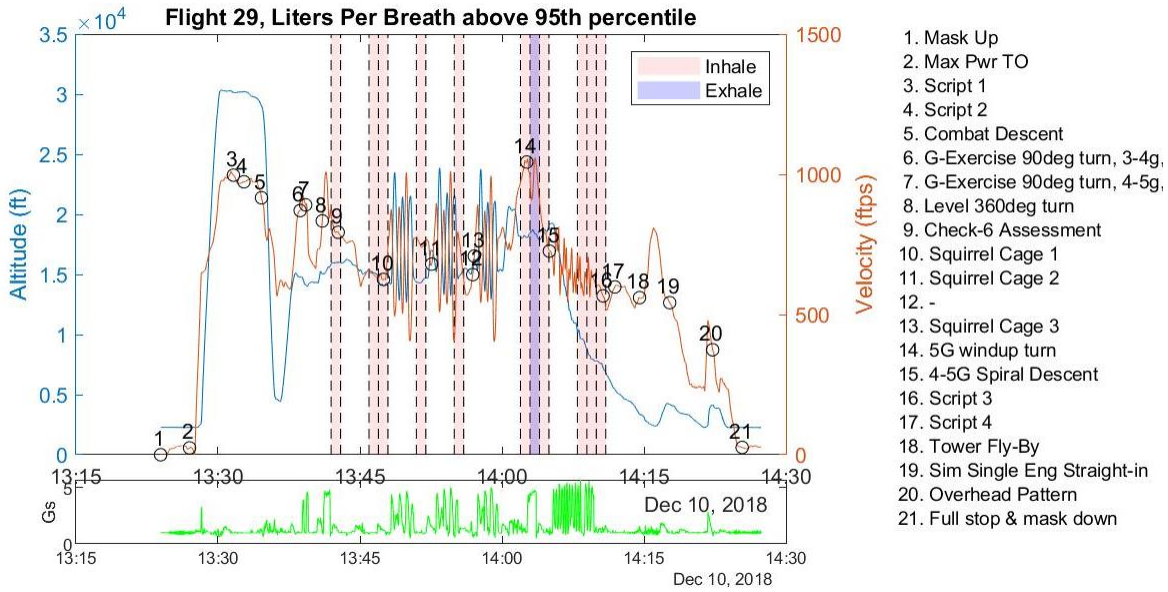

Figure 6.9.15. Liters per Breath Lights Up Not During G Breathing, but In-Between, During Recovery

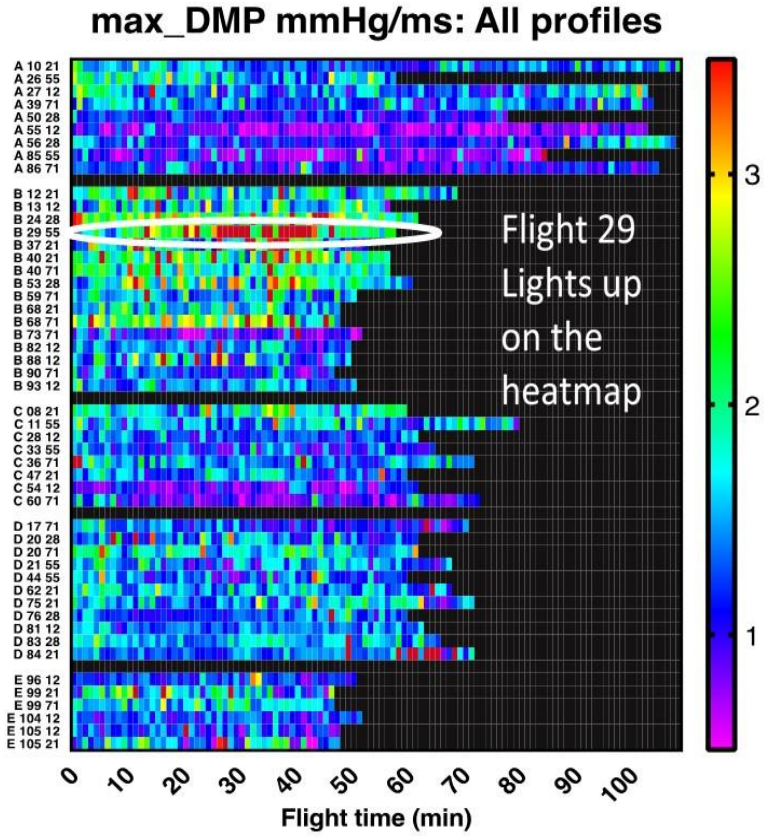

Figure 6.9.16. Flight 29 has Highest "Delta Mask Pressures" Defined as Mask Pressure Rate of Change
The max positive values are a form of the effort at the onset of the exhalation

Physiological Analysis and Hysteresis

Flight Summary

In addition to phase shift, hysteresis is also a measure of the 'synchrony' between the pilot and the breathing system. The line hysteresis measures the asynchrony between the demand signal received by the regulator and the regulator supply. The mask hysteresis represents the asynchrony between the pilot demand and the regulator supply. Ideally the hysteresis is low, and the mask and line hysteresis are equal meaning that the pilot demand, regulator demand signal and regulator supply are in good harmony. This was not the case for FLT-029.

Figure 6.9.17 shows the mask and line hysteresis, respectively for the entire sortie. The data show that the line hysteresis is quite high, the highest mean value for a Profile B in the USN configuration for all of the PBA flights. In addition, the standard deviation of the distribution is more than a factor of two higher than the value for a typical PBA Profile B flight (the most physiologically demanding) flight in USN configuration (Table 6.9.1).

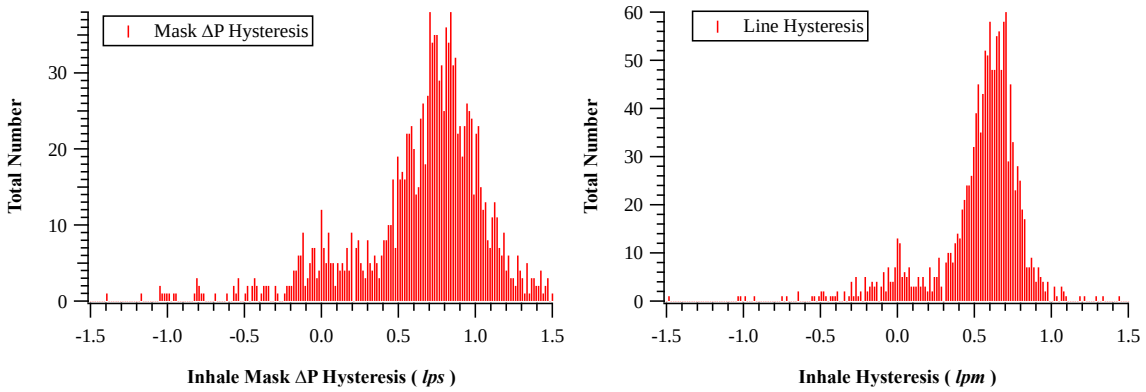

Figure 6.9.17. Histograms for Hysteresis Based on Mask Pressure (left), and Line-Cabin Differential Pressure (right) for FLT-029

Comparing the two histograms in Figure 6.9.17, concluded:

1. Pilot demand does not get transmitted to the regulator in time, and

2. When it does, it is not at the rate demanded.

A hypothesis is that at times of fast, dynamic pressure change (ascents, descents, G's), the reference pressure in the PBA aneroid of the regulator, lags behind the dynamic pressure change instantly felt by the cabin; the demand valve opens accordingly, and the original demand does not accurately get translated to the line.

Table 6.9.1. Inhalation Hysteresis based on Line-Cabin Pressure Differential Pressure for PBA Profile B flights in USN Configuration
The highlighted rows are those with Pilot 55.

Flight	Mean Hysteresis (lps)	Standard Deviation (lps)
FLT-093	0.38	0.14
FLT-089	0.36	0.13
FLT-082	0.35	0.11
FLT-078	0.49	0.12
FLT-073	0.35	0.10
FLT-071	0.34	0.11
FLT-067	0.42	0.12
FLT-065	0.34	0.11
FLT-051	0.32	0.11
FLT-046	0.39	0.18
FLT-040	0.43	0.12
FLT-038	0.47	0.15
FLT-029	0.52	0.3

Examining the hysteresis for FLT-029 (Table 6.9.2) in more detail shows that the values for the mask and line hysteresis are considerably different, indicating that the pilot demand is not being adequately transmitted to the line and when the demand does reach the regulator, the regulator response is not good. The fraction of breaths with very high values of hysteresis (greater than 0.75 lps) is high for both the line and mask values, but particularly for the hysteresis measured by the mask pressure.

Table 6.9.2. Hysteresis summary for FLT-029 including the line and mask hysteresis means and standard deviations and the fraction of breaths with hysteresis greater than 0.5, 0.75 and 1.0 lps.

	Line Hysteresis	Mask Hysteresis
Mean Hysteresis (lps)	0.54	0.68
Standard Deviation (lps)	0.30	0.43
Fraction > 0.50 lps	0.72	0.77
Fraction > 0.75 lps	0.16	0.50
Fraction > 1.00 lps	0.01	0.17

Specific Event Breakouts

Event Marker 7

Figure 6.9.18 shows a raw VigilOX data slice (the same time as Figure 6.9.4) and then the inhalation flow versus line-cabin and mask pressures. These highlight the breathing dysfunction in this time slice. Ideally the flow response to the line and mask pressures is equal. While the regulator response to the line-cabin differential pressure is reasonable, the mask pressure decreases to very low values before the regulator responds. The end result of this is that for this particular breath the peak flow is half what mil spec for that peak mask pressure indicates.

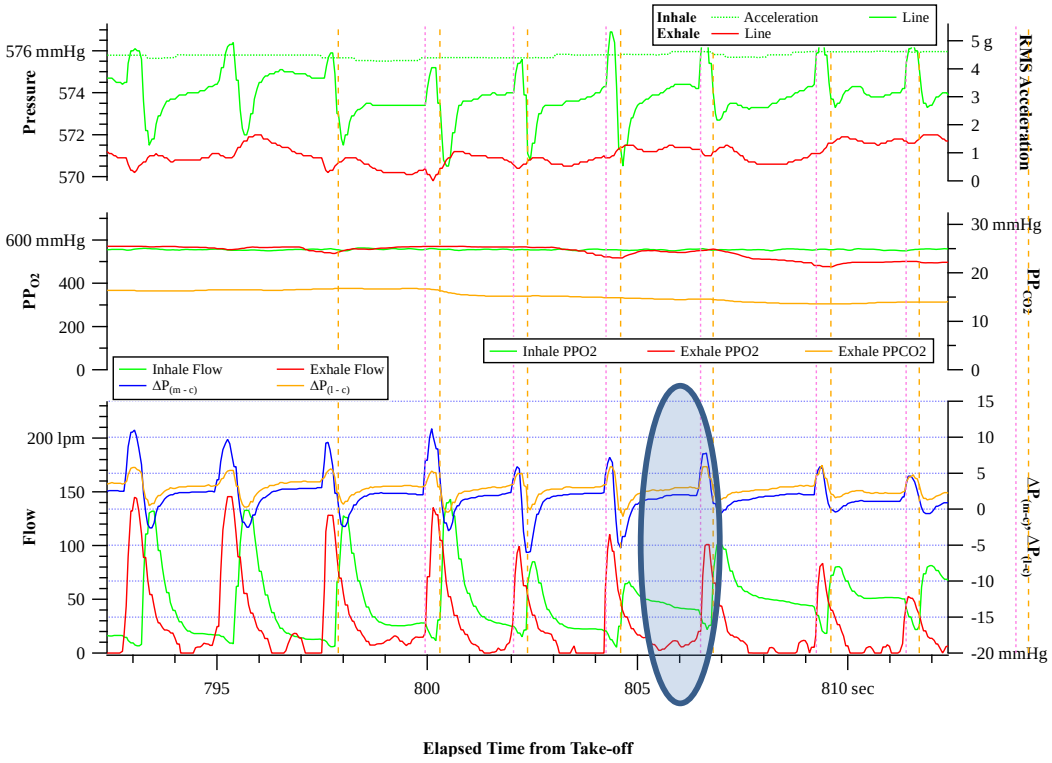

Figure 6.9.18. Raw VigilOX Data from Same Time Slice as in Figure 6.9.4

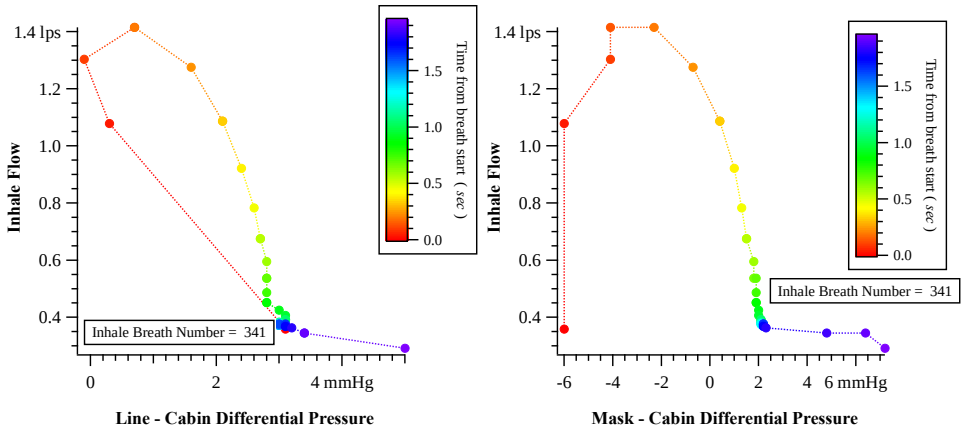

Figure 6.9.19. Inhalation Flow versus Line-Cabin Differential Pressure and Mask Pressure for Inhalation Highlighted by Oval in Figure 6.9.18.

Figure 6.9.20 shows the line and mask hysteresis values for the time segment of Figure 6.9.5, the squirrel cage maneuver. During this period the ESB flow sensor seemed to be providing reliable values and the inhalation and exhalation breath values were nearly equal. The data show that during this period the peak exhalation flow was approximately one half the mil spec for the peak mask pressure for that breath. Again, the hysteresis shows values that vary from very high to very low, a trend that is indicative of breathing dysfunction.

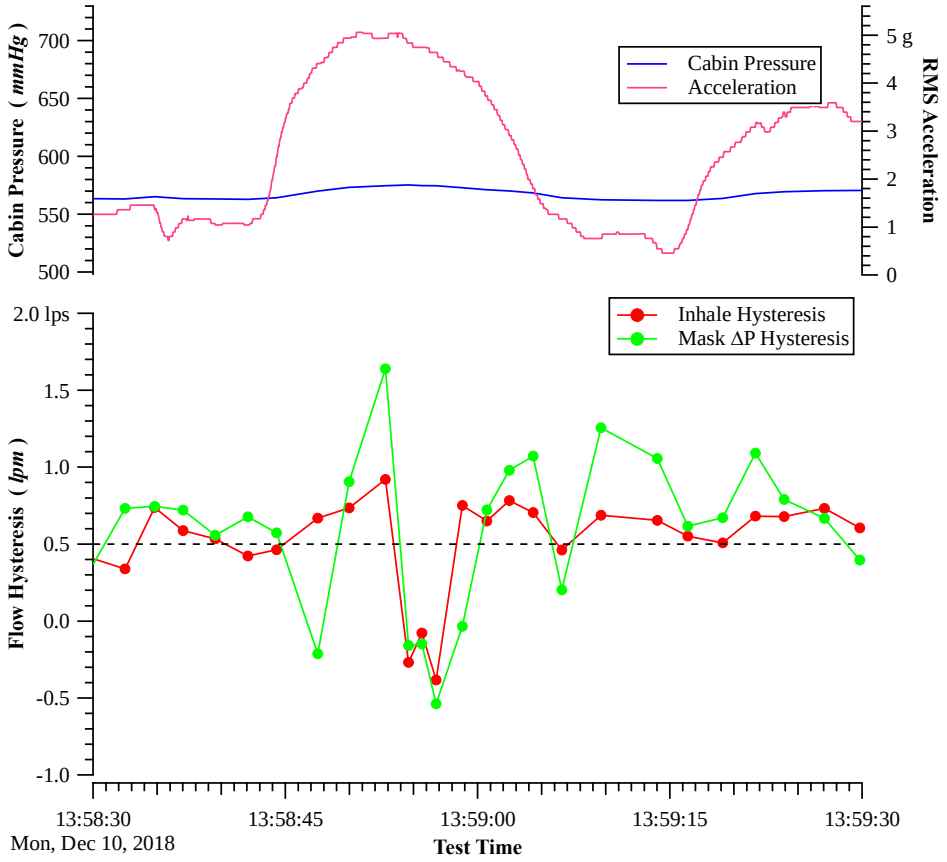

Figure 6.9.20. Line and Mask Hysteresis for Same Time Segment as Figure 6.9.5

Figure 6.9.21 shows the line and mask hysteresis for the 1-minute segment of Figure 6.9.7 – Event Marker 14. The graph shows that values of both the line and mask hysteresis oscillate from excessively high to very low, sometimes in phase with each other and sometimes out of phase. The result is that the peak flows during this time is as low as half of the mil spec for the peak mask pressure. These results reinforce the results of the breathing asynchrony during this time.

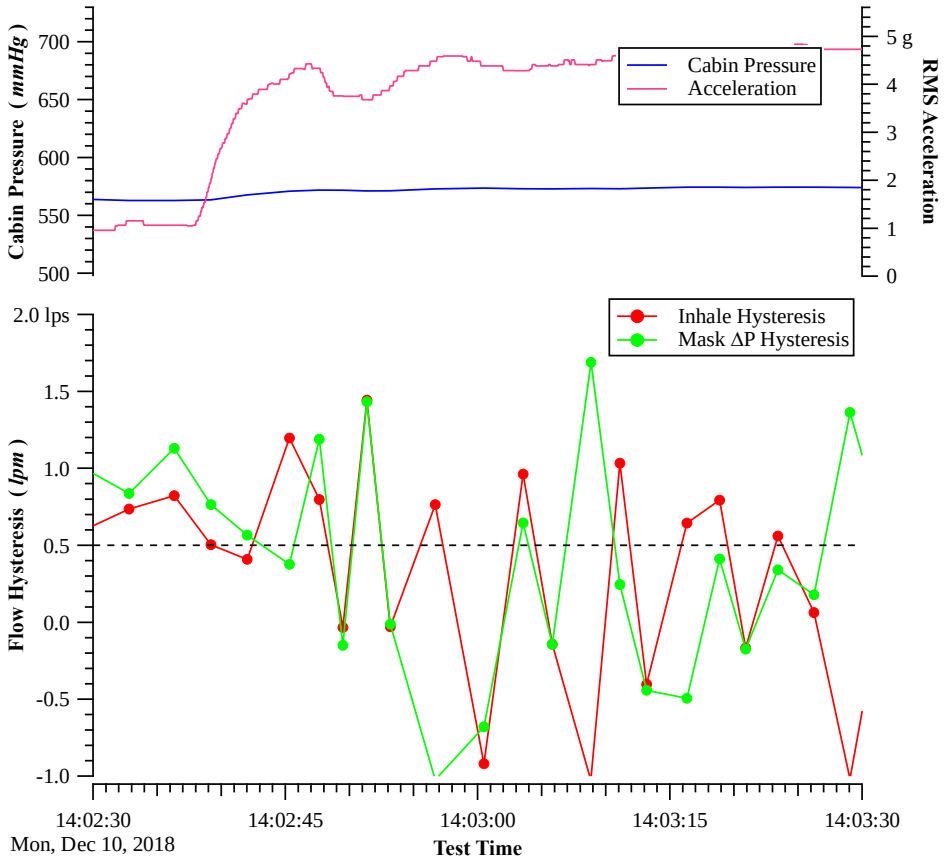

Figure 6.9.21. Line and Mask Hysteresis for 1-minute Time Slice from Around Event Marker 14; Same Time as in Figure 6.9.7

Figure 6.9.22 shows the values of the line and mask hysteresis for the spiral descent (Event Marker 15). This is a relatively long maneuver and the data show the value of the mask hysteresis fluctuates between very high and negative values; the fluctuations at the same frequency as the values of the acceleration. The values of the line hysteresis also fluctuate, but the values are different that the values of the mask hysteresis.

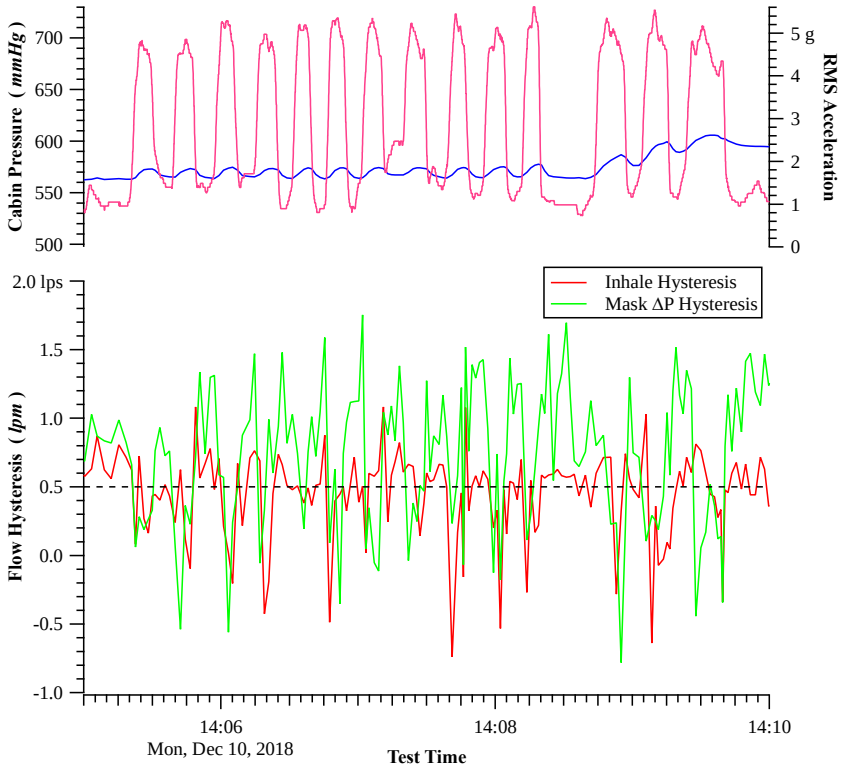

Figure 6.9.22. Line and Mask Hysteresis Values are High for Spiral Descent Featured in Figure 6.9.10.

Mask hysteresis is a good tool to indicate the disharmony between the pilot demand and regulator supply.

6.9.2 Mini Study on Flight 38

Flight 38 was a Profile B aerobatic flight, during which the pilot(s) noticed the smell of oil, followed by smoke in the cockpit. At this point, they initiated Return to Base (RTB) procedures. They also noticed large cabin pressure transients leading up to the event, but the deciding factor was the smoke in the cabin. Listed in Figure 6.9.2.1 are the elements of the Flight Cards the pilots executed. Events 7 and 8 are considered “high G-force events.”

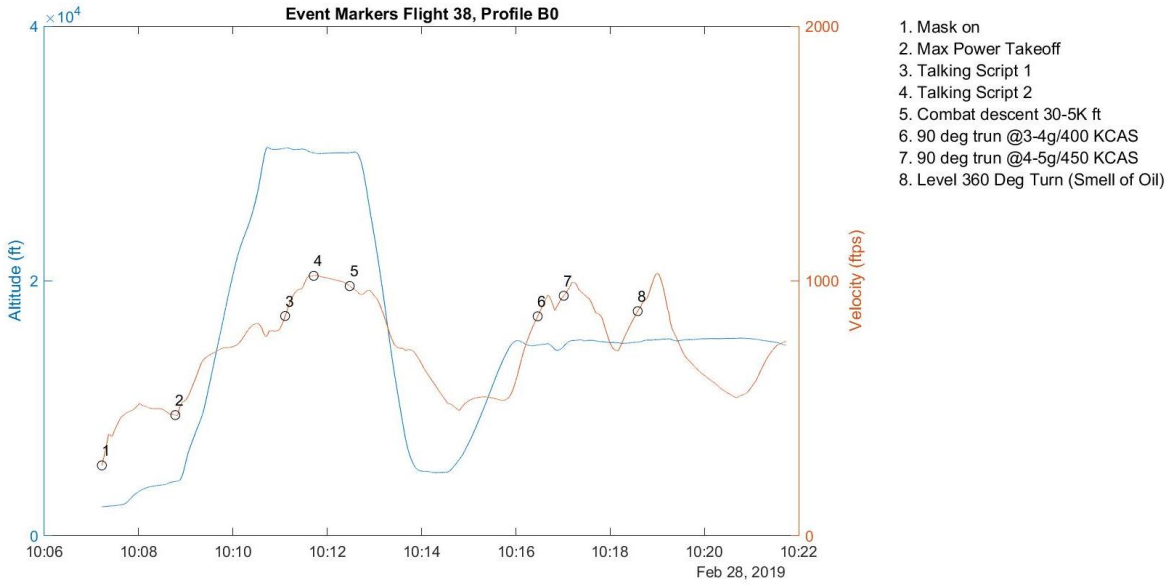

Figure 6.9.2.1. Elements of Flight Cards
Shows that only 15 minutes of the planned 1-hr flight was executed

The PBA performed a pressure check to see if the flight was off the pressure schedule prescribed by Boeing (Figure 6.9.2.2).

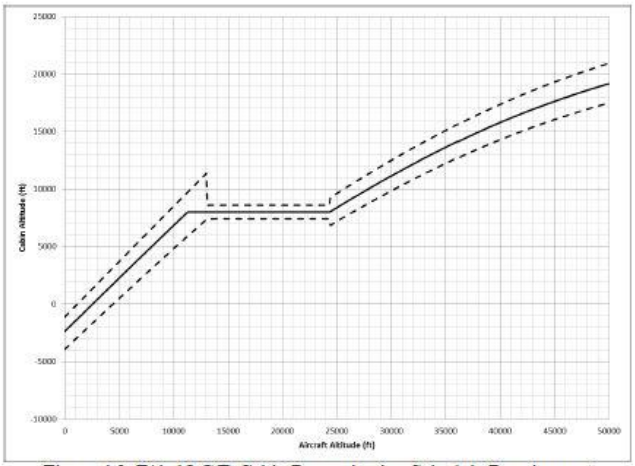
Figure 4.3: F/A-18 C/D Cabin Pressurization Schedule Requirement

Figure 6.9.2.2. Pressure Check Performed by PBA
Shows the cabin pressure reducing with altitude, then enters an isobaric region, followed by maintaining a differential pressure (5 Psi) relative to ambient

The Cabin Subsystem schedule is managed by the Cabin Air Pressure Regulator (CAPR) in all ranges of the envelope, and this valve is backed up by the Cabin Safety Valve (CSV) in case the CAPR fails closed (Interim Phase 1 Report, USN PMA-265/Boeing). Figure 6.9.2.3 shows the aircraft having some difficulty with cabin pressure control in the Isobaric region.

Note that preceding the incident, between 10:16 and 10:20, there were indeed cabin pressure oscillations. Starting at 10:18, after some of the oscillations, the temperature in the cabin started increasing, rising 4 degrees C in 4 minutes. Then, the pressure fluctuations were zoomed in.

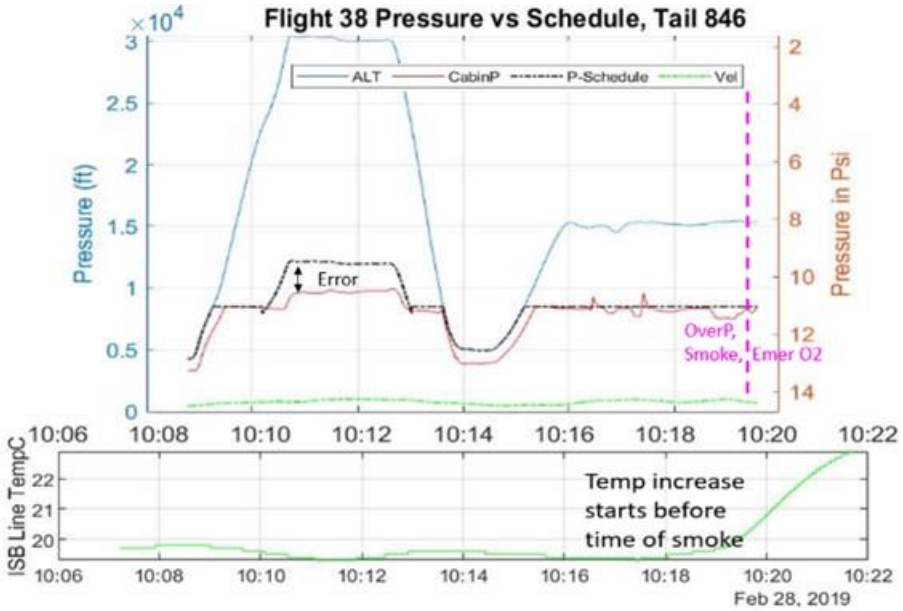

Figure 6.9.2.3. Shows Flight Profile Until Over-Pressure and Ensuing Smoke at which point the Emergency O_2 was engaged and the aircraft returned to base. Note the peaks of deviation between pressure schedule (black dashed line) and cabin pressure (red) between 11:16 and 11:20.

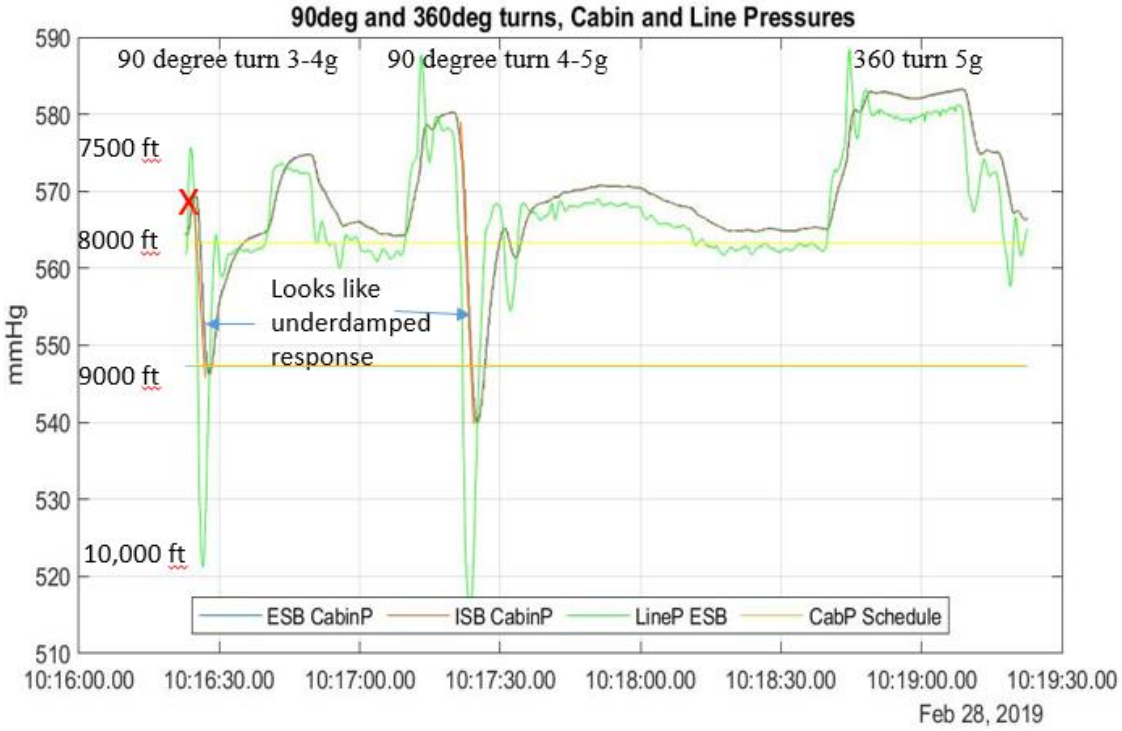

Figure 6.9.2.4. Shows 2 Cabin Pressure Dips the prominent one being a nearly 2,000 ft pressure excursion, and registering over then under the 8,000 ft prescribed isobaric pressure

From Figure 6.9.2.4, it is concluded that the cabin pressure oscillations are co-timed with dynamic, 3-5g maneuvers. An increase of dynamic pressure affects the pressure sensor of the

craft in the Nose Wheel Well, and through several repeatable observations through the PBA study, the team confirms that with change of acceleration (G's), roll and pitch angles, the cabin pressure goes off schedule, and it equalizes after a few oscillations. These pressure changes are usually an equivalent of 500 ft pressure change, but in this flight are 1,500-2,000 ft equivalents. This is captured in the pilot report as well:

Card 4A: 15K PA (8K Cabin) 90 degree 3-4 G 400KCAS (M7 10:16:27). Note at the mark just before we performed the maneuver there was a loud noise with a whoosh of air in the cockpit. Pilot's ears popped noting a pressure change. Backseat pilot looked at the Cabin Altitude and noticed it had dropped to roughly 6K and was climbing back to normal 8K.

Card 4B: Level 360 degree turn 450 KCAS - 5g (M9 10:18:34). As we rolled out of the 360-degree turn backseat pilot noticed a greyish/blue smoke/haze in the cockpit and smelled smoke. Backseat pilot "gang loaded" the regulator ON-100% O_2- EMERG pressure. Front seat Pilot was already on 100% O_2 with pressure since wearing USN gear. Smoke cleared quickly (within 10-15sec). Pilots decided to RTB.

Figure 6.9.2.5 further analyzes the cause and effect of the pressure imbalance, and imperfect control response.

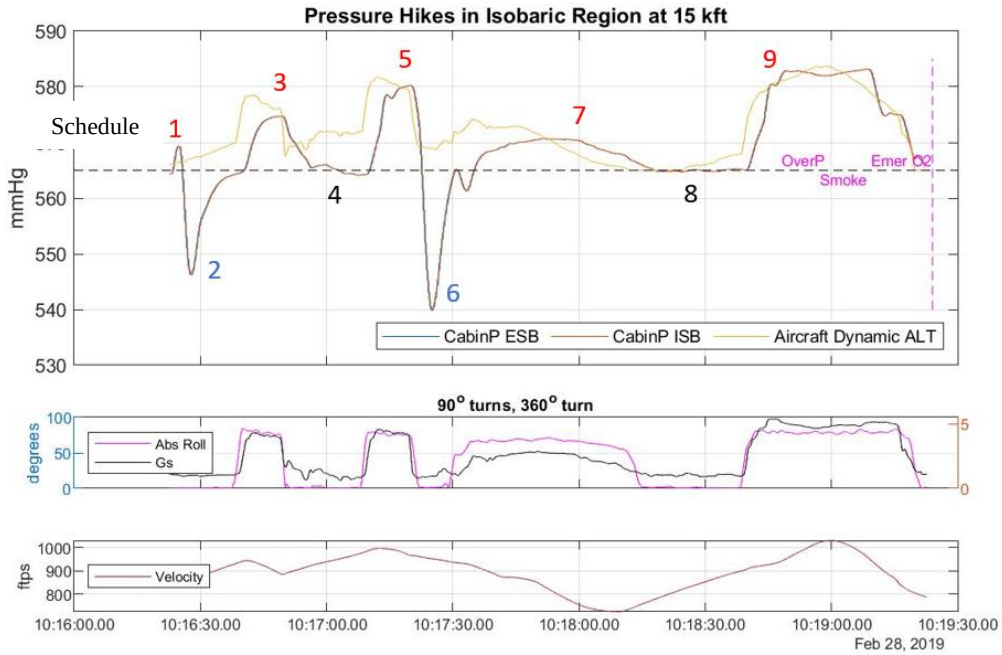

Figure 6.9.2.5. Shows NASA-Modified Cabin Pressure Model, Incorporating Dynamic Pressure

The yellow line in the top figure is the result of a modified cabin pressure model with inputs of Velocity and G's. As the Cobham and the PBA team noted, the VigilOX cabin pressure is sampled at a lower rate than line pressures, and the signal is averaged, thus it manifests a delay and lack of peaks/transients. With that in mind, the team's model closely predicts what cabin pressure would feel like, without pressurization control (odd segments). As these events occurred at 15 kft in the Isobaric pressure control region, the aircraft control was trying to maintain pressure. It over-dampened the oscillations in segments 2 and 4, and the team's data recording stopped after the 360 degree turn, during which the last over-pressure, and consequently the

smoke occurred. Emergency Oxygen and RAM DUMP were activated. Figures 6.9.2.6 and 6.9.2.7 deal with the pressure issue's effect on breathing.

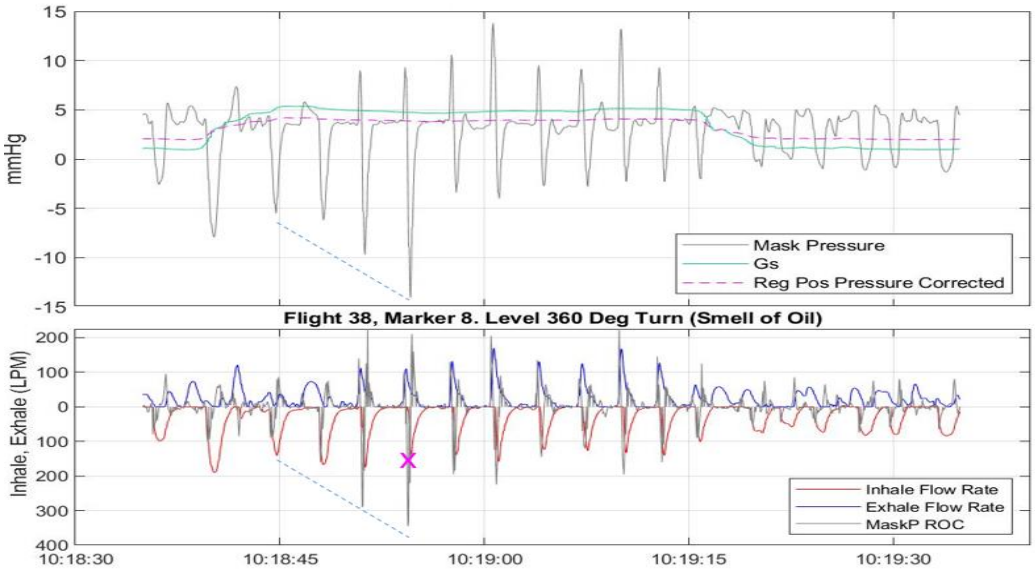

Figure 6.9.2.6. Captured G-breathing During 5-G Turn, and Diminished Volumetric Return for Increasing Mask Pressure

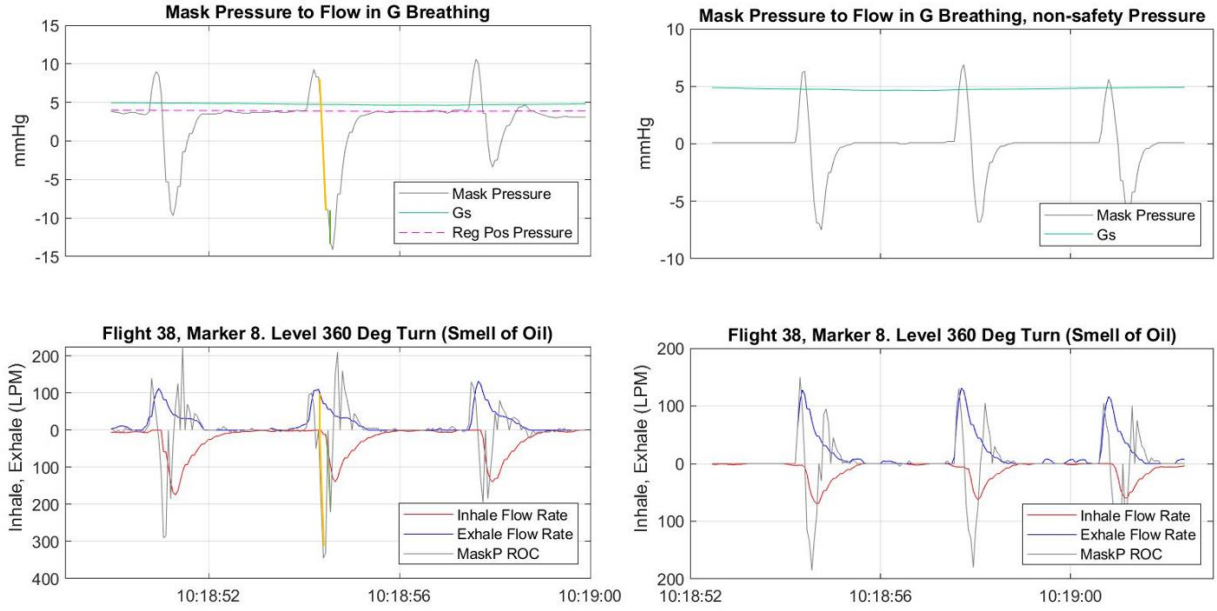

Figure 6.9.2.7. Rate of Change (ROC) of Mask Pressure More Inefficient with Positive Pressure (left) than without (right)

The PBA team compared G-breathing and mask pressure rate of change between the front seater pilot breathing under a positive pressure system, and the aft seater with no positive pressure. Notice the "double-tap" nature of the ROC of Mask Pressure, picking up velocity – returning to zero. In Figure 6.9.2.7, by the nature of G-breathing, the inhale expansion is initiated at the top of the exhalation, the short exhalation period not giving enough time for the exhalation valve to close, before the inhalation valve opens. The exhalation flow continues significantly after the beginning of inhalation flow.

Regarding the incident on Flight 38, while the PBA data shows increased cabin pressure with dynamic movement, these changes are usually in the positive direction. Not having accurate control and over-dampening, doubled the range of the cabin pressure oscillation, and may be a sign or predecessor of the aircraft not working properly, as it resulted in smoke in the cockpit.

6.9.3 Mini Study Flight 95

Flight 95 was a Profile H flight, which experienced a momentary flame-out of one engine, followed by emergency landing. This was a dynamic proficiency flight for pilot breathing characterization under various conditions. It includes breathing exercises, as well as different types of ascent/descent maneuvers. Amongst these, combat descent has been identified by the PBA as one type of maneuver, which has a longer rebound or recovery period for the cabin pressure to equalize. Event 17 in Figure 6.9.3.1 was such a Combat Descent, which was scripted to be followed by an immediate 30 degree zoom climb. However, due to a momentary left engine flame out, the exercise sequence was terminated. Failure of the left engine to restart, prompted the crew to declare emergency landing.

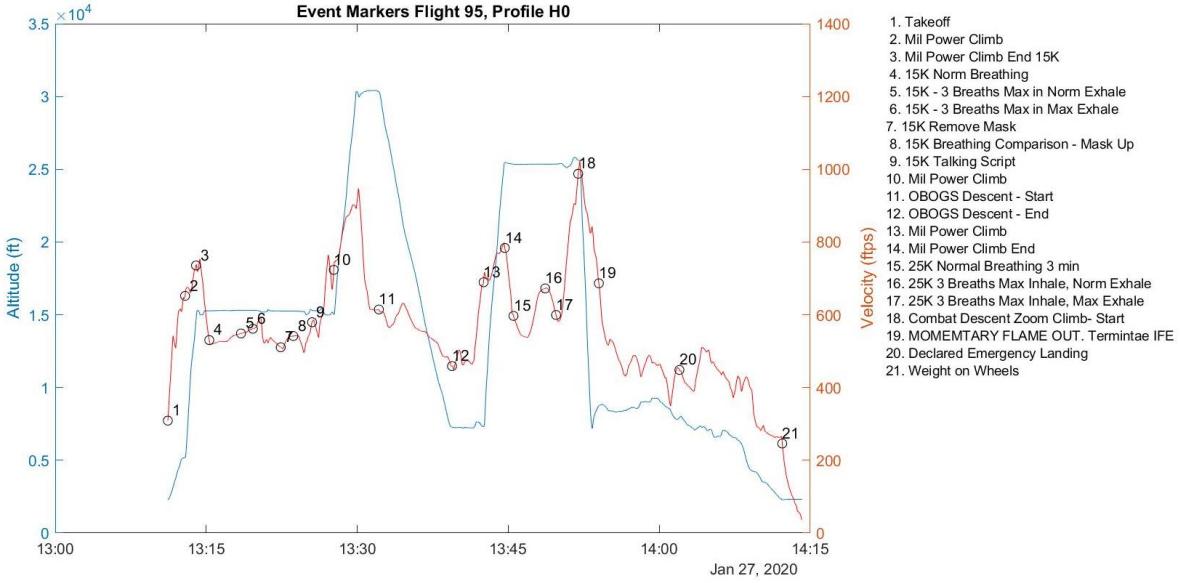

Figure 6.9.3.1. Captures Momentary Engine Flame Out During Combat Descent at Marker 19

Figure 6.9.3.2 shows a check on the cabin pressure deviations from schedule.

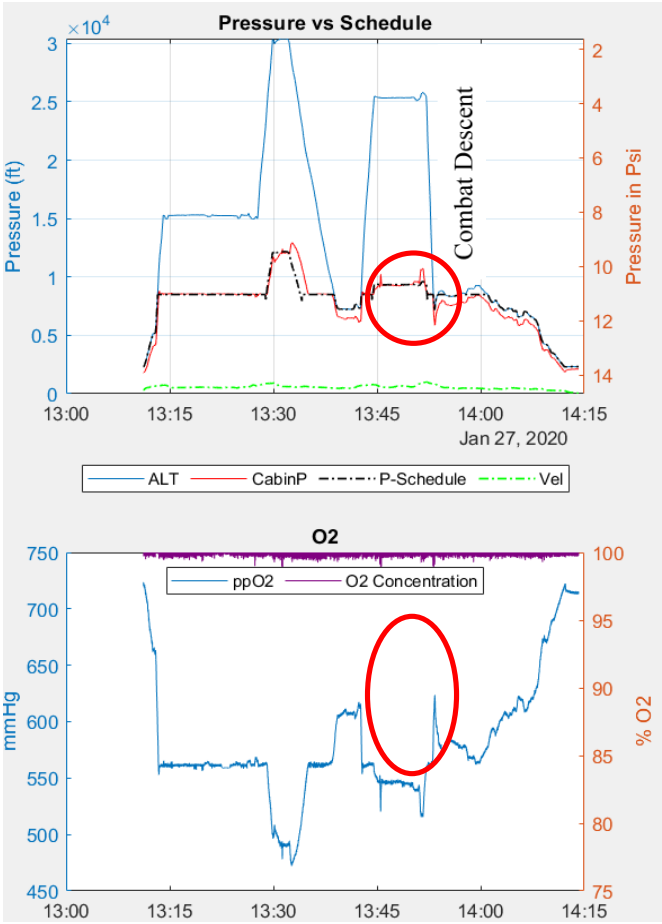

In Figure 6.9.3.2, the pressure check reveals through and post the OBOGS-like descent a slight under-pressure, then over-pressure between 13:30 and 13:43. At 13:45 there is a spike of under-pressure, followed by another under-pressure and over-pressure, just before and after the combat descent. As this flight was a "Navy-like configuration" and the CRU-103 maintains 100% O_2, as cabin pressure changes, the ppO_2 changes with it, thus these pressure excursions are clearly visible in the ppO_2 signal as well..

Zoomed in on the 1st pressure swing reported by the pilots:

> "Card 9
> -At 13:45:31
> Power was adjusted near this point and there was a noticeable cabin 'bump'."

Figure 6.9.3.2. Shows Pressure Deviations Around Combat Descent (top), and Corresponding O_2% Dips from 100% (bottom)

Figure 6.9.3.3 shows the zoom in at the end of Combat Descent.

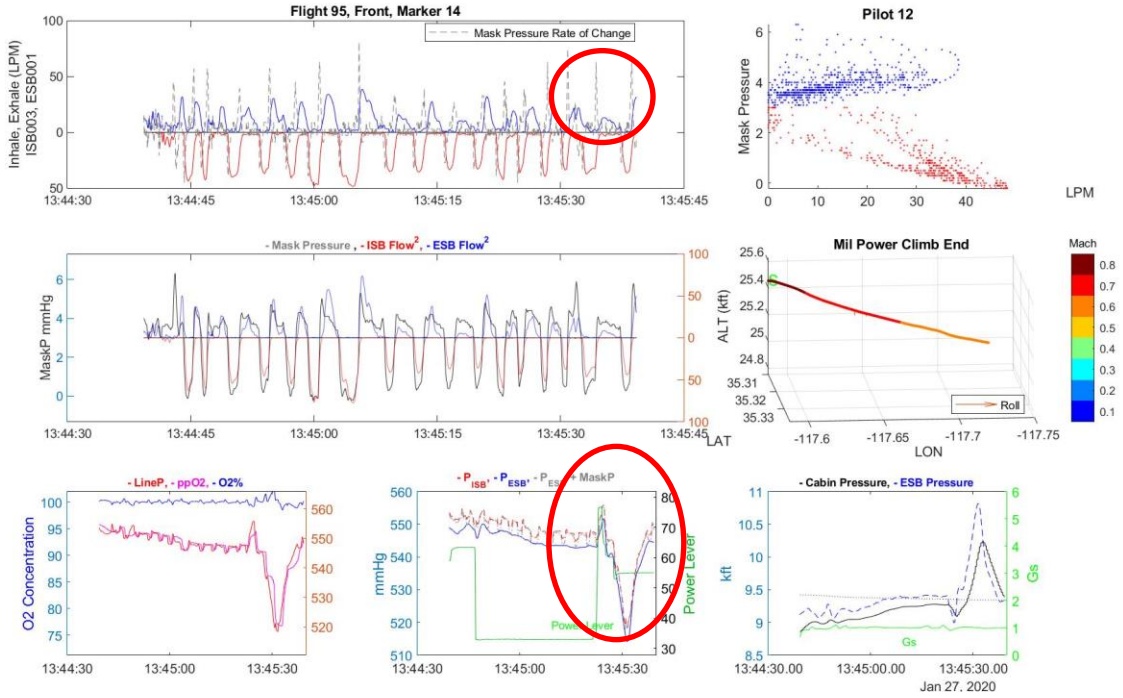

Figure 6.9.3.3. Row 3 Shows Pressure Transient Felt and Heard by Pilots

Tiles 5 and 6 capture the deep "V" shape of the pressure drop of 35 mmHg, picked up by the line pressures and ppO_2 channels. The pressures first change with the Power Level (Tile 6), but then the cabin continues to lose pressure sharply before it recovers. To put the 35-mmHg change in perspective, in Tile 7 plots the more dynamic ESB line pressure and the bit sluggish and smoothed cabin pressure, and the line pressure reports an 1800-ft. equivalent change (the filtered cabin pressure shows 1200 ft.). The episode lasts 15 seconds. If the time into the Inhale/Exhale plots are traced, a double exhalation and a low volume exhalation (blue line) is noted in this period. Tile 4 shows that the pilot was 45 seconds after leveling off from a Mil Power Climb, decelerating, but otherwise flying straight and level. G's were also not a factor (Tile 7).
There was some pressure disturbance early on as well, at a lesser extent, at the end of the first Mil Power Climb (Figure 6.9.3.4). The downshift is more gradual, and the disturbance here is just 250 ft. equivalent.

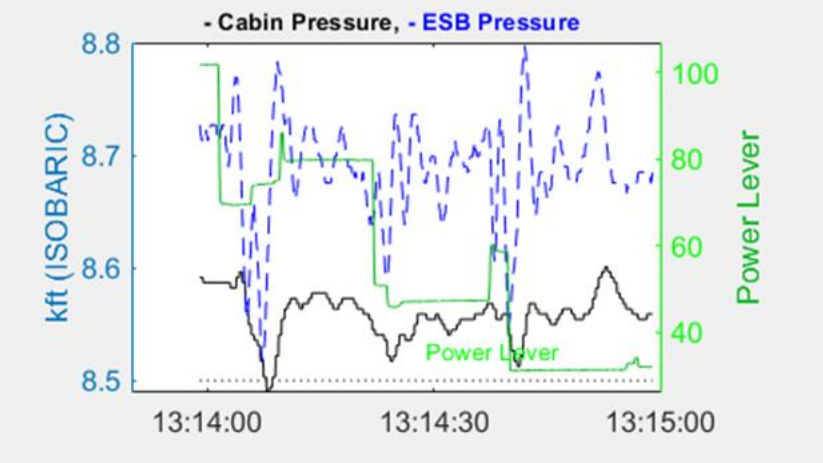

Figure 6.9.3.4. Pressure Oscillation Post Mil Power Climb

Returning to the 25 kft altitude, a Combat Descent was performed (Marker 18) with no problems. At the end of the dive, the left engine flamed out. As it failed to restart, the Left Engine Power Lever switched from 30 to 1 (Figure 6.9.3.5).

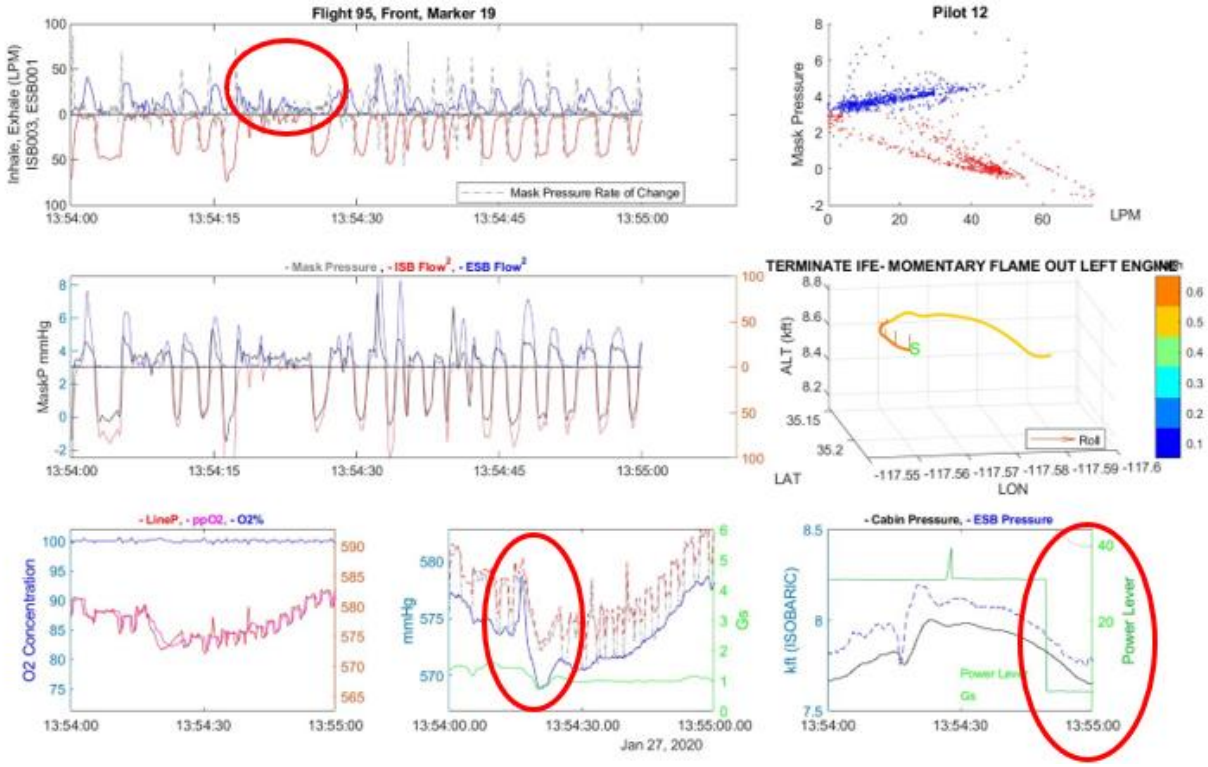

Figure 6.9.3.5. Post Combat Descent, Left Engine Flame-out

There was one more pressure blip (+5/-10 mmHg, 500 ft equivalent) in the window of the engine flame-out, paired with low exhalations, before the left engine powers down at 13:54:50. The power lever remained at the lowest setting from this point until landing; the regulator input power remained unphased, as designed and expected (Figure 6.9.3.6).

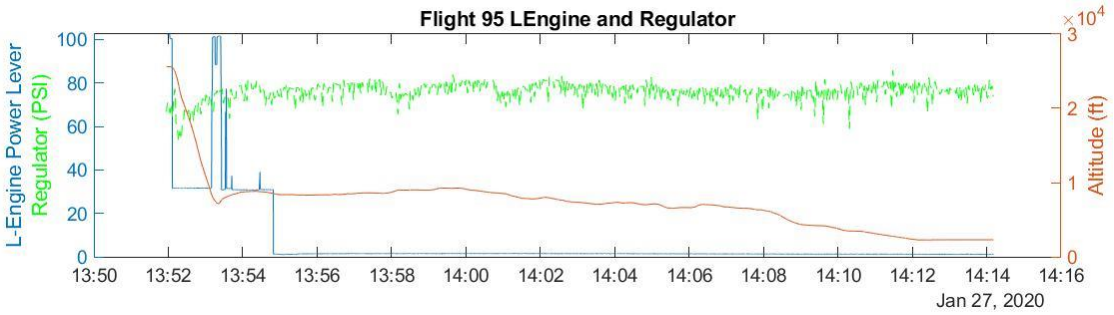

Figure 6.9.3.6. Shows Regulator Unaffected After Switching to Single Engine

The PBA ties together adverse hardware events with their effects on pilot breathing.

Technical Section 7: Pilot Physiology and Medical Outcomes

7.0 Introduction

A pervasive problem that has emerged with modern generations of fighter aircraft mechanized with OBOGS and demand regulators is the phenomenon of Physiological Incidents or Physiological Events (PEs). These physiological incidents have grounded entire aircraft fleets for months at a time and have manifested in different ways on the same type of aircraft. The F-22 Raptor was the first aircraft to have notable Physiological Incidents. The USN's Hornet, Growler, and Super Hornet fleet had experienced a major spike in physiological incidents over the better part of a decade. Then the USN/Marine T-45 and USAF T-6 fleets found itself with incidents of high-profile Physiological Incidents. Lastly, the joint F-35 program has sustained numerous difficulties with "Unexplained Physiologic Events" (UPEs). These PEs were described as "hypoxia like" as the symptoms were the ones that manifest themselves as O_2 starvation to the tissues. It was first though that something wrong with OBOGS installed on these aircraft could be identified but has proved to be only one of numerous causes to the PE problem. Pilots have become more aware of how to better recognize the onset of their personal hypoxia-like symptoms. These can be insidious by their very nature, and difficult to place an exact time or cause to these PEs. Correcting some of the OBOGS shortcomings has proven to help, but this did little to solve the root causes of the PE problems. The search for root causes was primarily focused on the mechanical systems of the aircraft. What was needed was a look into the physiological interactions with the aircrew breathing system in flight. This study was dedicated to the task of measuring the mask interactions that have effects on physiological parameters in the flight environment. The laboratory studies may have been indicative of problems but were unrevealing as to the root causes.

The engineering design consideration of any breathing gas system of a high-performance aircraft is simple in concept: provide sufficient O_2 to prevent hypoxia. In practice, the dynamic range and response characteristics of those systems may be insufficient to sustain optimal physiologic function during high-performance flight. Hypoxia is inextricably linked to not only the supply of O_2, but also to the organs, structures and function that allow breathes by taking in O_2 and expelling CO_2. To match the highly adaptable and variable human physiology to the machine is a highly complex process which, is deceptively difficult and may inadvertently evoke unforeseen technical issues capable of compromising intended function of any breathing systems. Any of the current breathing systems can impose an excessive burden on the requisite physiological adaptation on the pilot, resulting in adverse and undesirable physiological changes. If they do not tax the limits of human physiological adaptation and reserves these burdens often will go unnoticed or barely perceived. The body will attempt to respond within the confines of the system, but at the limits of available physiological compensation mechanisms, the response may be inadequate. Poor breathing and lung function affect all aspects of physiology. As the USAF Chief of Pulmonary Medicine said, "Fit pilots are poor perceivers of decline in lung function hence need objective measures (in flight)". It is difficult to mitigate imperceptible, perceptible but unaddressed, and unrecognized declines in physiological function. Accordingly, it is critically important for stakeholders to have a thorough understanding of respiratory physiology.

7.1 Basic Physiology

To forge a more thorough understanding of the implications of pilot symptoms of hypoxia, it is crucial to develop a foundational model of normal human respiratory physiology and how this

physiology reacts when exposed to the cockpit environment: high altitude, varying high O_2 tension, and high forces of acceleration. The effects that any one of these in-flight conditions has on compromising respiratory function cannot be understated. It may be best to think of human respiration, particularly in-flight, as a dynamically dynamic system; it can tolerate and adapt to certain deviations to a limit. The body will respond to changes to restore homeostasis through a multitude of mechanisms to be discussed, but the body to compensate is finite. The goal of a breathing system is to stay safely away from the boundaries of these finite limits. However, any breathing system built around ground-tested, best case breathing parameters will always fail to account for the omnipresent effects that any in-flight perturbations away from 'normal' can have. In more severe perturbations, these respiratory challenges to normal function will result in reduced performance or incapacitation – incompatible with safety of flight.

Breathing, or more precisely, ventilation, is an automatic, rhythmic, and neutrally regulated mechanical process. The contraction and relaxation of the skeletal muscles of the diaphragm, abdomen, and rib cage cause gas to move into and out of the alveoli of the lung. The human respiratory cycle is tightly controlled by central and peripheral nervous system chemoreceptors which respond to local concentrations of carbon dioxide (pCO_2), oxygen (pO_2) and acidity (pH). At rest, an averaged sized male will consume 0.34 L (STPD)/min of O_2. Through chemo regulatory control, this will increase to 1.00 L (STPD)/min of O_2 consumption during strenuous tasks such as air combat maneuvering. To provide this drastic increase in O_2 requirement and to offload all the resultant CO_2 produced, the body will alter volumes and rates to achieve desired ventilation, or movement of air.

Inspiration is the active phase of breathing and is initiated by neural influences from the respiratory control centers in the brainstem. During inspiration, the diaphragm along with the intercostal muscles contract which, in turn, cause the thoracic cavity to expand. As the thoracic cavity expands, the distensible lungs passively expand. The surface of the lung is coupled to the thoracic cavity by a thin layer of liquid. The liquid coupling allows the lung to "move" during breathing and to adapt to the shape of the thorax.

As the thoracic cavity expands, the pressure in the terminal air spaces (alveolar ducts and alveoli) decreases. Once the pressure in the thorax decreases to a subatmospheric level, the pressure differential results in the flow of fresh air down the branching airways and into the terminal air spaces. As the pressure in the airways equalizes with the atmospheric pressure, inspiration ends.

The inspiratory muscles work against resistance: the elasticity of the lungs, the airway resistance, and the resistance of the chest wall. All of these are altered in the cockpit environment; the shape of the lungs adapts to the same shape as that of the thoracic cavity. If thoracic size is temporarily reduced, (e.g., cockpit posture, flight gear, harness, etc.) lung size is also reduced. This will alter the natural breathing rhythm or cadence and increase the work of breathing and can lead to a variety of symptoms such dyspnea or breathlessness. Impedance to inspiration will increase the negative pressure inside the lung and result in under-ventilation.

Expiration is generally more passive compared to the active muscle recruitment during inspiration. During expiration, the elastic recoil properties of the lung and decreasing size of the thoracic cavity cause pleural and alveolar pressures to rise to greater than atmospheric level. Consequently, gas flows out of the lung and continues to do so until the pressure in the alveoli equilibrates with atmospheric pressure. Expiration is relatively passive at rest, but at higher levels of ventilation some expiratory muscles are engaged and contribute to the expiratory

process. When breathing against positive pressure, inspiration becomes passive and exhalation is then the active process. This requires recruitment of muscles that are incorporated in the opposite manner and thus increases the workload until adapted for that function.

Muscle groups enabling ventilation: The combined efforts of muscles of the chest wall, principally the diaphragm, expand the volume within the thoracic cavity, leading to inspiration. Of these, the diaphragm is the primary muscle of ventilation.

The diaphragm (Figures 7.1.1 and 7.1.2) is a dome-shaped muscle that separates the thoracic from the abdominal cavity. It is a thin, sheet-like muscle that originates on the lower rib cage (costal diaphragm) and lumbocostal spine (crural diaphragm) and inserts on the central tendon.

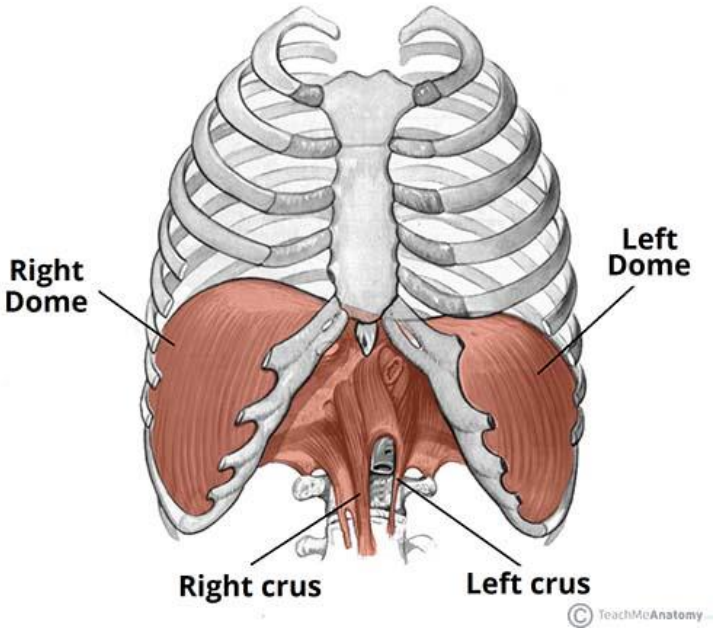

Figure 7.1.1. Diaphragm Anatomy from Front

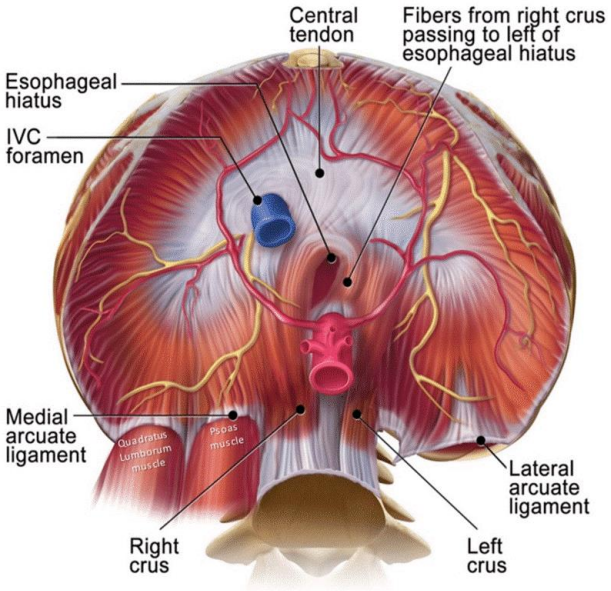

Figure 7.1.2. Diaphragm Anatomy from Below

The diaphragm can be considered as a cylinder capped by a dome (Figures 7.1.1 and 7.1.2). During inspiration the muscle fibers of the diaphragm shorten, but the dome of the diaphragm does not change shape.

Movement of diaphragm acts to increase thoracic volume by several mechanisms. During contraction, the diaphragm is directed downwards with a piston like action. As the diaphragm descends down from the thoracic cavity and into the abdominal cavity thoracic volume concomitantly increases. Due to its insertion on the lower ribs, the diaphragm imposes a cranially directed force on the lower rib cage, lifting the ribs and rotating them laterally.

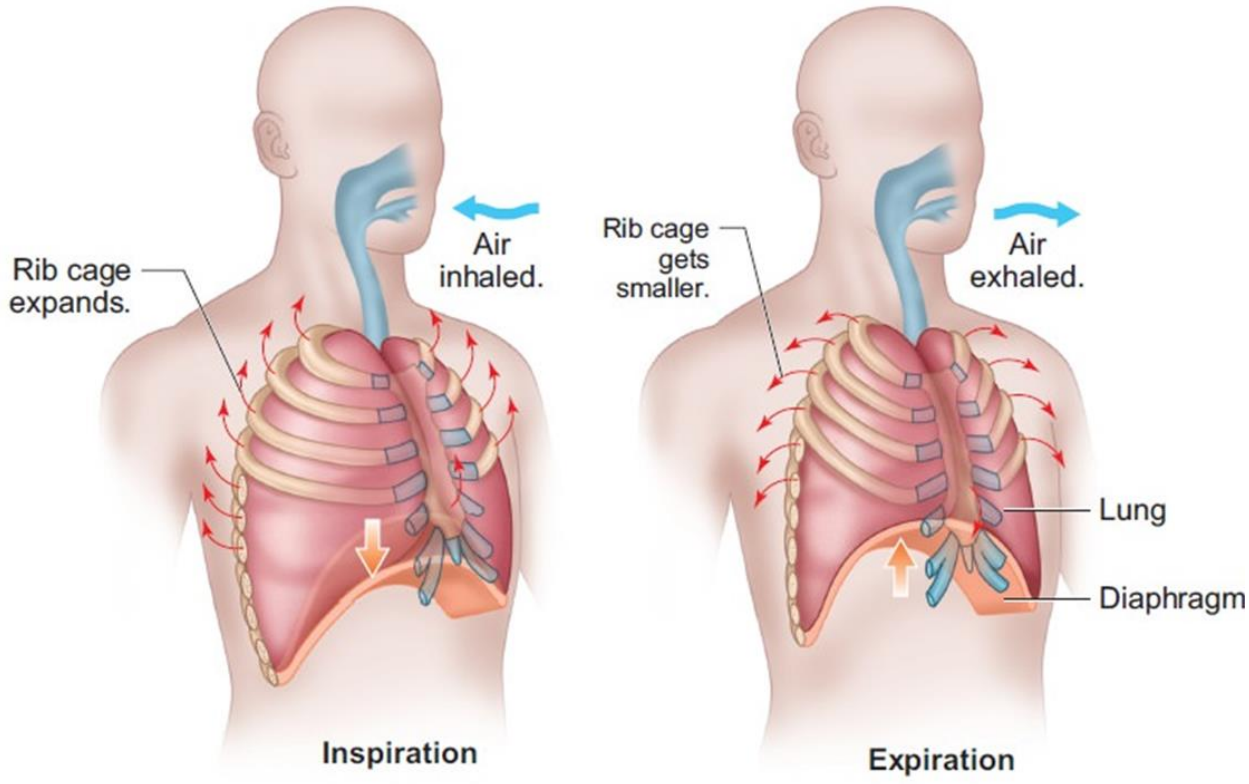

Figure 7.1.3. Inspiration and Expiration Muscular Mechanics (https://www.brainkart.com/article/Mechanism-of-breathing_33205/)

In addition to the diaphragm, the intercostal muscle group contributes to inspiratory portion of ventilation. The intercostal muscles can be divided into three groups: the parasternal intercostals, and the external and internal intercostals.

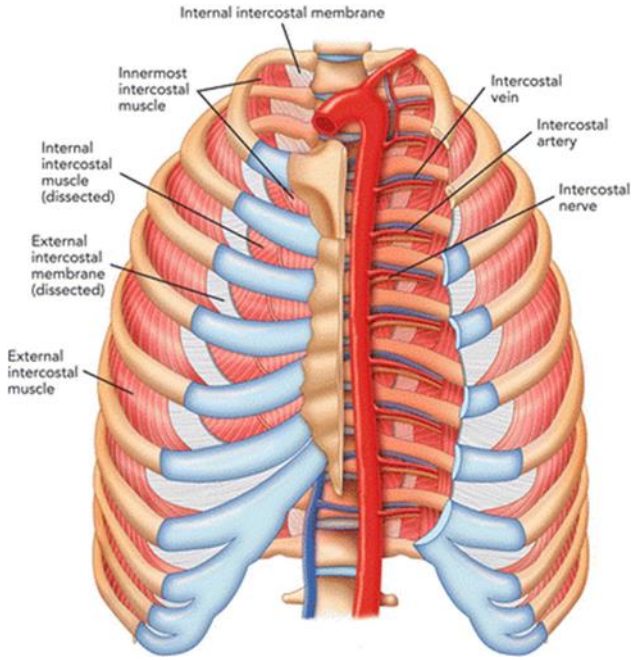

Figure 7.1.4. Intercostal Muscles

The parasternal intercostals originate on the lower rib, adjacent to the sternum, and then insert onto both the sternum and the rib directly above. The parasternal intercostals have an inspiratory mechanical action. The external and internal intercostals are located more laterally between the ribs. Due to their fiber orientation and pattern of activation during breathing, the external intercostals also tend to produce an inspiratory action. In addition to the intercostal muscles, several muscles in the neck (scaleness, sternocleidomastoid) elevate the sternum and upper two ribs during deep inspiration, aiding in the inspiratory action on the thorax. During inspiration, enlargement of the upper rib cage is due to actions of the neck and intercostal muscles, but enlargement of the lower rib cage is due to the actions of the diaphragm and intercostal muscles.

While the parasternal and external intercostals are concerned with inspiration, the internal intercostals tend to produce an expiratory action on the rib cage during quiet breathing (Figure 7.1.5). An additional rib cage muscle, the triangularis sterni, originates on the inner aspect of the sternum and inserts on the ribs adjacent to the sternum and also has an expiratory action on the rib cage.

Additionally, four expiratory muscles are located in the anterolateral abdominal wall: the transversus abdominis, internal and external obliques, and rectus abdominis. These muscles reduce thoracic size by increasing abdominal pressure which moves the diaphragm back into the thorax cavity. Those movements, in conjunction with their action of pulling down on the rib cage, decrease thoracic volume to facilitate exhalation.

The diaphragm, parasternal intercostal, and external intercostal muscles are the most consistently active during resting breathing in humans. Consequently, these are considered to be the primary ventilatory muscles while the others can be considered as accessory ventilatory muscles. Their activation occurs when ventilatory demands increase, for example, with exercise. Respiratory muscle fatigue and reductions in ventilation are reported during use of inspiratory and expiratory positive pressure.

These breathing muscles enable ventilation through the conducting airways (the nose, mouth, pharynx, larynx, trachea, bronchi, and bronchioles) before entering the alveoli.

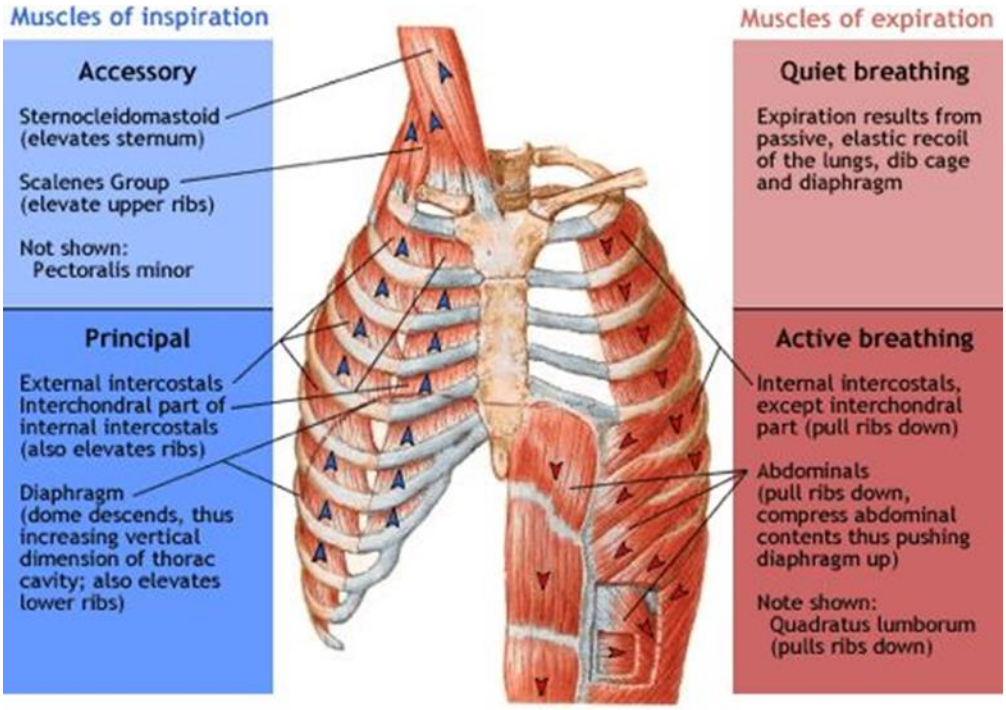

Figure 7.1.5. Actions of the Muscles in Breathing

Lung anatomy

Simplified the respiratory system is the organ system that conducts gas exchange of O_2, to be used by the metabolism, and CO_2, which is the waste gas from metabolic use. There are two distinct parts. The first is the conducting airways that transmit the gases into and out of the lungs. This is made up by the nose and the nasal cavity, sinuses, mouth, throat (pharynx and larynx [voicebox]), and trachea (windpipe) with its subsequent branches to and into the lung (bronchial tubes and bronchioles (tubes from the bronchi to the alveoli [air sacs]). The lung contains portions of the bronchial tubes, the bronchioles and the alveoli.

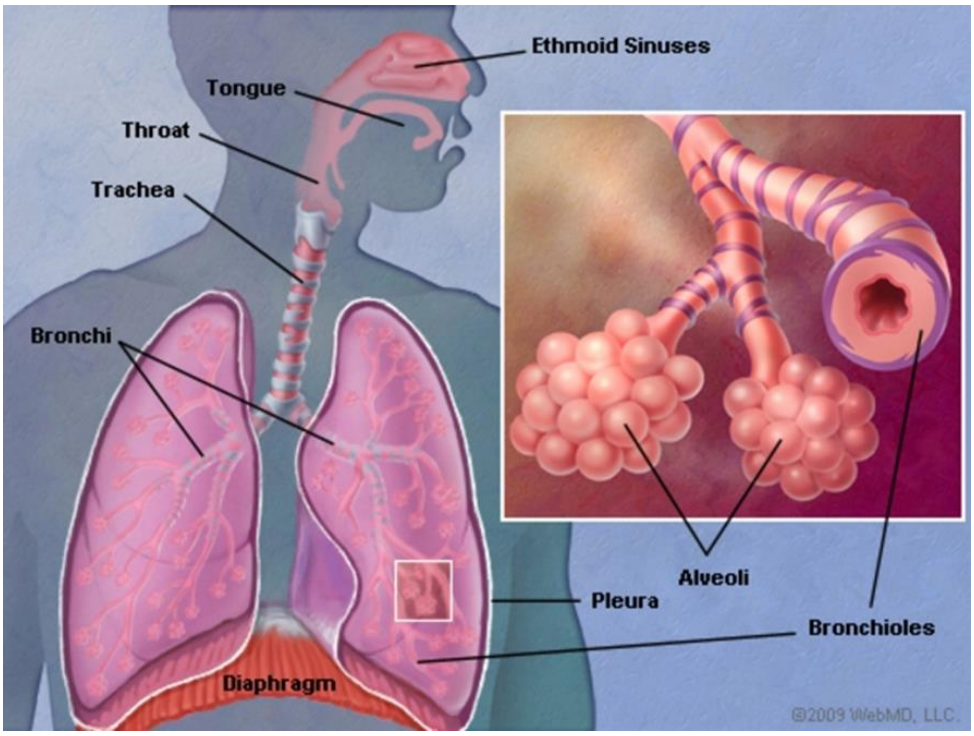

Figure 7.1.6. Pulmonary (Lung) Anatomy

The alveoli are the clusters of air sacs at the end of the bronchioles that conduct the rapid gas exchange. Capillaries that conduct gasses to and from the circulatory system encompass the membrane surrounding the alveoli. These capillaries are the connection to the circulatory system.

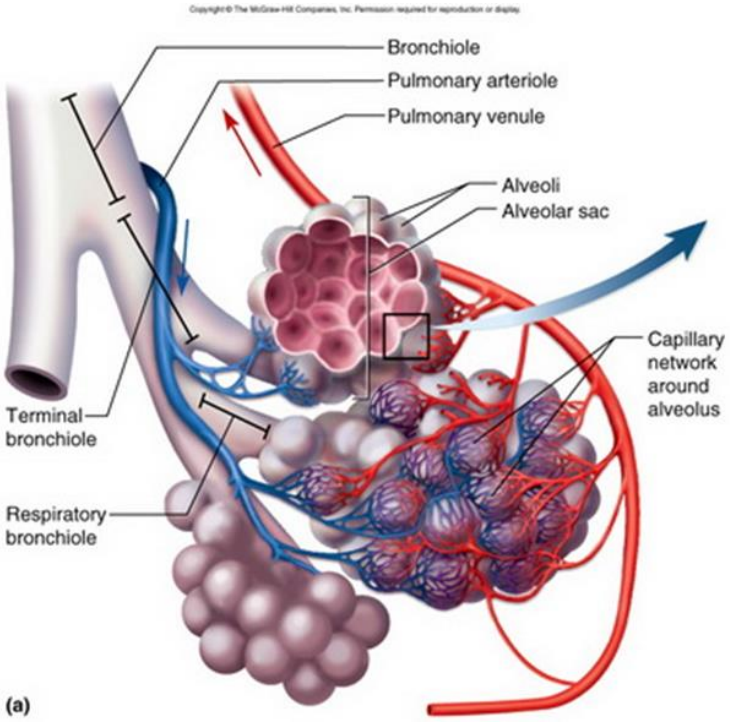

Figure 7.1.7. Alveolar anatomy
mrsbioblog.blogspot.com

Pulmonary Volumes are the volume of air present in the lungs and airways at different phases of the respiratory cycle.

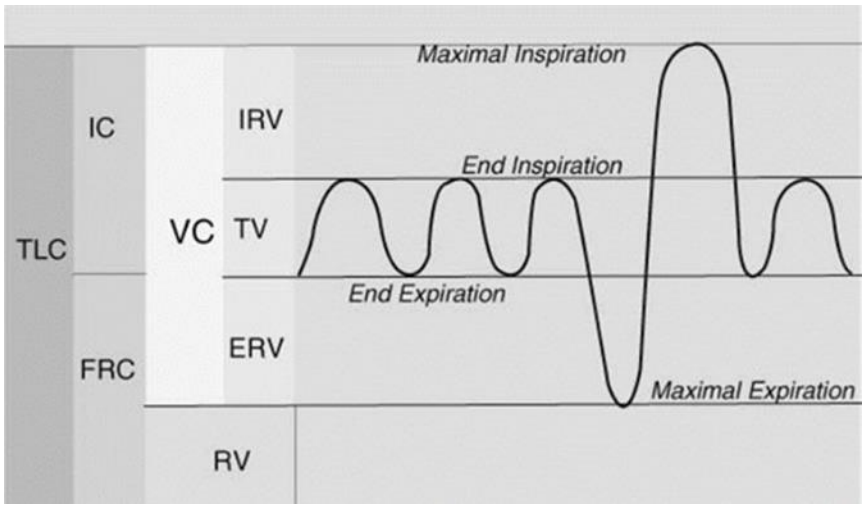

Figure 7.1.8. Pulmonary Volumes

The volume of air that is moved with each breath is defined as the Tidal Volume (TV). At rest TV is approximately 0.5L or 500 mL, which can increase greatly with exertion. Resting lung volumes are defined by the relationship between the inward elastic pull of the lung tissue and the outward expansile force of the chest wall. When relaxed, the lung has a volume of air within defined as Functional Residual Capacity (FRC). This is made up of the Expiratory Residual Volume (ERV) and Residual Volume. The expiratory reserve volume (ERV) is the additional air that can be forcibly exhaled after the expiration of a normal TV. The residual volume (RV) is made up of physiological dead space (air that does not undergo gas exchange – see following section). This residual volume is typically fixed for an individual in the range of 1.2 L (1200 mL). Active inhalation will expand the lungs to a volume greater than FRC, and passive exhalation will return lungs to FRC.

Vital capacity (VC) is the maximum volume of air that can be moved in the lungs – a maximum effort inhalation followed by a maximum effort exhalation. Typically, VC is on the order of 5L (5000mL). Total lung capacity (TLC) is the sum of VC and RV. Inspiratory capacity (IC) is the maximum volume of inhale from FRC. Inspiratory reserve (IRV) and expiratory reserve (ERV) represent the volumes of air that can be moved at end inspiration and end exhalation, respectively.

Numerous features of the breathing gas system and aircrew equipment can serve, often synergistically, to adversely affect resting lung volumes. If expansion of the chest wall is limited, as is the case when strapped into the aircraft, this will limit lung volumes including VC. By decreasing the natural outward pull of the chest, or outright resisting chest expansion, more inspiratory force is required for breathing. If lung elasticity is also increased, as is the case with unequal ventilation due to atelectasis or collapse of alveoli or segments of alveoli, this will further increase the effort of breathing. Chest wall restriction also limits the body's natural defense mechanisms against atelectasis. An increase in the aircrew breathing system or mask pressure will result in resistance to exhalation and hyperinflation. These instances of overpressure will be discussed further in detail in subsequent sections.

Dead Space: Air that does not undergo gas exchange is referred to as physiologic dead space. The total dead space volume is made up of alveolar and anatomical dead space. Alveolar dead space is the gas that remains in the individual air sacs or alveoli to keep the alveoli open (Residual Volume). Anatomic dead space refers to air in the conducting passageways of the respiratory system, including the nose, mouth, pharynx, larynx, trachea and airways up to the terminal bronchioles. O_2 and CO_2 do not significantly exchange between gas and blood while in the conducting airways. This physiologic dead space, or residual volume, is typically approximately 150 mL in an average adult.

Dead space will increase with use of aircrew equipment, the largest contribution coming from the mask. Mechanical dead space (e.g., in a mask) can become rebreathed air that increases in CO_2 if not completely replaced with each breath volume delivered to the mask. This will increase the content of CO_2 to the lungs. Mechanical dead space can also become additional retained (unexhaled) air with excessive expiratory pressure. This dead space does not participate in gas exchange and can lead to increased alveolar CO_2. Increased physiologic dead space (e.g., atelectasis or retained air) limits gas exchange and can contribute to hyperinflation. Furthermore, following a rapid decompression event, dead space volume will cause an immediate reduction in available inspired O_2, potentially leading to hypoxia. As a principle, added dead space volume by aircrew equipment should be no more than 150 mL.

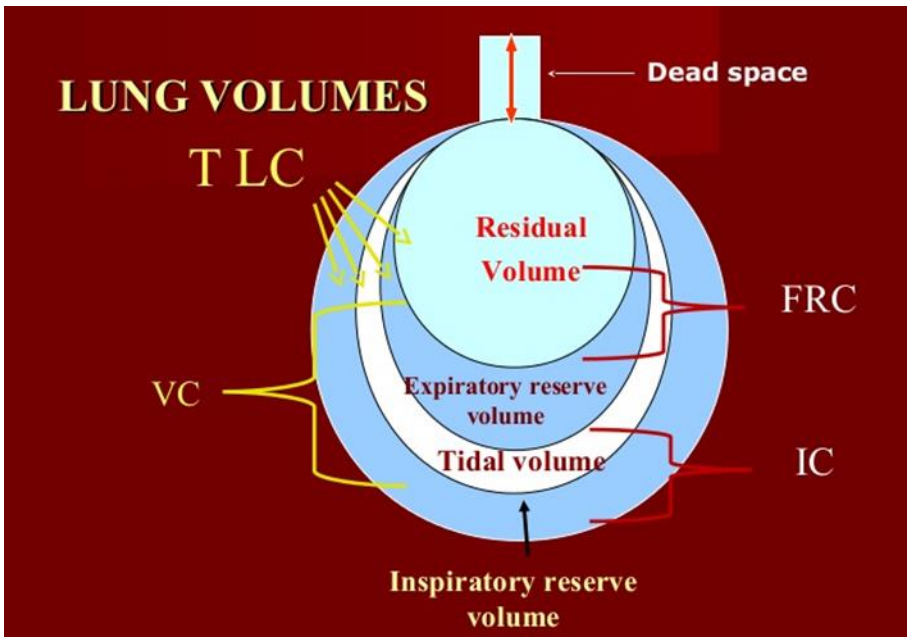

Figure 7.1.9. Illustration of the lung and alveolar volumes
TLC = Total Lung Capacity
VC = Vital Capacity
FRC = Functional Residual Capacity
IC = Inspiratory capacity

Ventilation Rates: Pulmonary ventilation is the volume of gas per unit time entering the lungs, often defined as MV in units of L/min. Alveolar ventilation is the volume of gas per unit time that functions in for gas exchange, accounting for dead space. The alveolar ventilation rate (AVR) is the expression of this functional exchange of air, defined below:

AVR	=	frequency	X	(TV – dead space)
(ml/min)		(breaths/min)		(ml/breath)

The normal respiratory rate at rest is variable between individuals and within a given individual. Normal rates for the pilots range from 12 to 18 BPM. The breath structure at rest characteristically has an inspiration to exhalation time ratio of 1:2 to 1:3, with more time spent in exhalation – a passive process. This will increase toward 1:1 inhalation/exhalation under exertion. Safety pressure also changes the I/E ratio closer to 1:1 due to higher pressures causing exhalation to become more active instead of passive. During anti-G straining maneuvers, breath structure is radically different, notable for rapid, maximum exhalation and inhalation efforts in a very short period of time. Flow limitations, pressure variations and desynchrony in demand/supply will alter the breath structure forcing the pilot to attempt to adapt. This will be explained in detail.

Flow of gas across the capillary wall into the blood stream within individual alveoli is influence by the partial pressures of gasses in the alveoli. An effective breathing gas system would be tailored to maintain the O_2 content within the alveoli at physiological levels (about 104 mmHg) while minimizing the toxicity associated with high inspired O_2.[1-8] The general alveolar gas equation describes the partial pressure of O_2 within the alveoli as a function of the inspired O_2 concentration:

$P_AO_2 = P_IO_2 – P_ACO_2 * (F_IO_2 + [1 – F_IO_2]/R)$
P_AO_2 = partial pressure of oxygen in the alveoli, normally 100 mmHg
P_ACO_2 = partial pressure of carbon dioxide
F_IO_2 = fractional inspired oxygen content
R = respiratory quotient, approximately 0.8 in the healthy aviator

Alveolar ventilation rate is negatively influenced by decreased TV and increased dead space. The body has many mechanisms to alter ventilation in response to fluctuations in gas exchange and composition in the blood stream. In response to increased PCO_2, the body will increase ventilation in a linear fashion. For every 1 mmHg increase in PCO_2 above normal (range 35 to 45 mmHg), ventilation will increase by 2 to 3 L/min. Ventilation will increase first elevating the TV and then by raising the respiratory rate. In an otherwise healthy adult, this drive will increase to a point past which central respiration fails, usually in the arterial range of 60 to 80 mmHg PCO_2. The ventilatory response to high PCO_2 is increased in the presence of hypoxia. The ventilatory response to hypoxia is based on Hemoglobin saturation and the provision of adequate blood flow to the lungs. Compensation to hypoxia occurs when the O_2 saturation is below about 95-96% or a drop in arterial O_2 contraction of 10-20 mmHg. This is done by various combinations of increased lung volume and respiratory rate. Maximal compensation is reached at an arterial O_2 pressure of 50 to 60 mmHg.

Gas exchange at the alveoli is connected to capillaries and is influenced by and has impacts on the cardiovascular system. This ratio of ventilation (V) of the lung to perfusion with blood (Q) is referred to as ventilation-perfusion ratio or V/Q. It is normal for the upright lung under the force of gravity to have more blood flow to the lower regions of the lung, and lesser blood flow near the apices. These regional differences are physiologic. Conditions which alter local ventilation or perfusion will adversely impact the function of the lung and the efficiency of respiration.

Airway resistance: Airway resistance limits the flow rates of gas into or out of the lung, is generated by aerodynamic forces of air movement within the lung. It is principally a function of airway diameter. Airway resistance is optimized at normal, resting FRC. Under conditions of increased airway resistance, the body will slow respiratory rates to provide more efficient respiration. It will be increased by changes in lung volumes and numerous additional conditions present in the breathing gas system of the F-35, including high O_2 concentrations and the atelectasis that will ensue. Any increased airway resistance is undesirable. Impedance to expiration will reduce average and peak flow rates, prolong exhalation and, over time, lead to lung hyperinflation.

Cardiac Output: Breath dynamics, lung volumes, and ventilation pressures are intrinsically linked with cardiac output and vascular function. This is particularly of consequence in the demand regulator breathing gas system at work in the F-35 where pressure oscillations are similar in magnitude as pulmonary circulation. In normal, resting physiology, active inhalation occurs with a decrease in intrathoracic pressure, which helps draw low pressure venous blood into the right heart, increasing right heart output and filling the pulmonary arteries and capillaries. This leads to an intra-breath increase in blood volume in the pulmonary circulation, facilitating gas exchange. During exhalation, intrathoracic pressure will increase, helping to push oxygenated blood back through the left heart and into systemic circulation. Output is limited by net blood flow from the right side of the heart through the pulmonary circulation, which may be reduced with excessive airway pressures. For reference, the right atrial pressure normally is approximately 2 – 6 mmHg and normal right pulmonary artery pressure during contraction (systole) is 15 – 25 mmHg. Positive airway pressures which exceed the low pressure venous and pulmonary circulatory systems will impact cardiac output.

Basic Anatomy and Physiology – (Reference Sections Ref Sec I 1-8 and XIV 344-345).

7.2 Flight Related Pathophysiology

7.2.1 Hypoxia

The effects of hypoxia vary in different organ systems. In healthy individuals, the heart and lungs are tolerant of moderate deficiencies of O_2, whereas the brain is tolerant of very little decrements in O_2. Moreover, the amount of O_2 consumed by the body depends primarily upon the degree of physical and mental activity of the individual. Hypoxia, therefore, tends to be a progressive condition, rather than a single discrete event. In this condition, the respiratory system compensates first by increasing respiratory rate (the number of BPM), then by increasing tidal volume (the amount of air breathed in and out with each breath). The cardiovascular system compensates by increasing the heart rate. These changes allow the body to adjust to mild hypoxic conditions by increasing O_2 delivery. The brain is less tolerant of even small decreases in O_2 and becomes more dysfunctional as hypoxia progresses. In fact, the brain is the first organ system to display symptoms of O_2 deficiency, and this is due in part to the high metabolic demand of the Central Nervous System (CNS). Notably, the onset of hypoxia may be insidious and unrecognized because the onset of signs and symptoms usually do not cause discomfort or pain. Likewise, the nature and timing of these effects will vary from crewmember to crewmember. Thus, from the physiologic standpoint, the concept of hypoxia can be rather complicated, even when dealing with a simple "hypoxic hypoxia," as will be delineated in the following sections.

Types of Hypoxia: There are four types of hypoxia, each with a different underlying mechanism. The first, *hypoxic hypoxia*, is the well-known phenomenon of not having sufficient

O_2 in the breathing air to adequately meet the demand of the body's tissues. A second type of hypoxia is known as *stagnant hypoxia*, in which there is not adequate blood flow of oxygenated blood to the tissues. Stagnant hypoxia is one element of the phenomenon of "pulling G's" (see the Acceleration Atelectasis section); similarly, the concept of "ischemic hypoxia" (also discussed later) is another example of stagnant hypoxia (though combined to some degree with hypoxic hypoxia). The stagnant (regional) hypoxia associated with hyperoxia may be more adequately described as a perfusion hypoxia. The constriction of blood vessels to regions of the brain with hyperoxia should probably be thought of as a subtype of stagnant hypoxia or possibly as a standalone type. A third type of hypoxia is known as *hypemic hypoxia*, sometimes called "anemic hypoxia," and it occurs when there is an inadequate amount of functioning red blood cells or, more specifically, when there is an inadequate amount of normally functioning hemoglobin with the red blood cells to bind the O_2 for delivery to the tissues. Carbon monoxide poisoning would be one such example of hypemic hypoxia. The fourth type of hypoxia is *histotoxic hypoxia*, in which the mitochondria of the cells, where the O_2 is utilized, is disrupted. Cyanide poisoning is an example of histotoxic hypoxia. The principle type of hypoxia highlighted in the PBA assessment is hypoxic hypoxia. Primarily the interaction of the mechanical system is not providing adequate volume or concentration of O_2 to the alveolar gas exchange system.

Hypoxic Hypoxia: Time of Useful Consciousness: In the atmosphere, the percentage of O_2 at any given altitude remains constant, at approximately 21% of the corresponding atmospheric pressure. Atmospheric pressure, however, varies geometrically with altitude as shown in the following table:

Table 7.2.1. Altitude-Gas Pressures

Altitude (Feet)	Atmospheric Pressure (mmHg)	Partial Pressure of Oxygen (mmHg)	Arterial Pressure of Oxygen (mmHg)
(Sea Level) 0	760	160	103
10,000	523	110	61
18,000	380	80	38
20,000	350	74	34
22,000	321	67	33
23,000	308	64	32
24,000	295	62	31

(Derived from Davis et al, 2008, Fundamentals of Aviation Medicine, 4th Ed., LWW, Ch2, p30-31)

Once inhaled into the lung, atmospheric O_2 is mixed with water vapor from the body as well as the expired CO_2 in the lung. It must, likewise, cross the alveolar wall and the arterial endothelium. Therefore, the *arterial* pressure of O_2 to which the hemoglobin molecules within the red blood cells are exposed will always be less than the corresponding partial pressure of O_2 in the atmosphere, as shown in the last column of Table 7.2.1.

Altitude and the rate of altitude change make a difference in the severity and rate of onset of hypoxia. At lower altitudes, the onset of hypoxia is slower and less pronounced. At higher altitudes, all symptoms may occur quite rapidly. Flying at altitudes of 8,000 to 10,000 ft for more than 4 hours without supplemental O_2 leads to symptoms such as slowed reaction, diminished motor coordination, and deficiencies in concentrating or solving problems. Flying above 10,000

ft can lead to definite impacts on short-term memory and complex task integration start to be displayed.

This leads to the important concept of Time of Useful Consciousness (TUC). Simply put, the TUC is the duration during which a healthy individual exposed to hypoxia can be expected to maintain normal neurologic function (i.e., correctly perceive incoming information, process that information appropriately, and execute appropriate responses based on that information). The TUC does not necessarily involve a complete loss of consciousness; rather, it reflects the extent to which an individual's decision-making ability is significantly impaired due to the lack of O_2. Most normal, healthy people have an unlimited TUC at approximately 10,000 ft or below. However, at a (cockpit) altitude of 40,000 ft, which might be experienced in a rapid decompression, the time of useful consciousness is only 15-20 seconds; this amount of time is inadequate to respond to an emergency at that altitude. (Thus, the critical factor in *sudden* exposure to hypoxia in the flying environment is getting to a lower altitude, preferably a cockpit altitude of 10,000 ft or lower, as quickly as possible.) Standard textbooks of Aerospace Medicine give the following, generally accepted values of TUC times for healthy individuals:

Table 7.2.2. Times of Useful Consciousness (TUC)

ALTITUDE (Cabin) in Feet	TUC (Approximate) in Minutes (Unless Otherwise Noted)
50,000	6-9 seconds
43,000	9-15 seconds
40,000	15-20 seconds
35,000	½-1
30,000	1-3
28,000	2.5 - 3
25,000	3-5
23,500	7-8
22,000	10-12
20,000	17-18
18,000	20-30
10,000	>60

(Dehart, R. L.; J. R. Davis (2002). Fundamentals Of Aerospace Medicine: Translating Research Into Clinical Applications, 3rd Rev Ed. United States: Lippincott Williams And Wilkins. p. 720)

Prevention of Hypoxic Hypoxia: To prevent hypoxia, modern aircraft are designed to maintain a minimum alveolar O_2 pressure (PAO_2) of 103 mmHg. (Note that, as previously mentioned, the alveolar partial pressure is different—and always just a bit higher—than the arterial partial pressure of O_2, i.e., the pressure of O_2 in the arterial blood itself). The required alveolar partial pressure is easily maintained without the need for supplemental O_2 up to a cockpit altitude of 10,000 ft. When the pilot climbs further in altitude, several compensation mechanisms are employed. First, there is the process of increasing the pressure of the cockpit. Secondly, for fighter aircraft, the cockpit pressurization is supplemented with an increased partial pressure of O_2 in the breathing supply. For example, while breathing 100% O_2 at 39,000 ft, the alveolar O_2 pressure is approximately equivalent to a 10,000-ft altitude without supplemental O_2, which is perfectly acceptable. However, this increased percentage of O_2 has its limits. For example, at

45,000 ft on 100% O_2, the alveolar O_2 pressure is only 34 mmHg, and is roughly equivalent to 20,000 ft without supplemental O_2, which is not acceptable. Thus, at extreme altitudes, the pressure of the inspired O_2 itself is actually increased, so as to be able to maintain an adequate partial pressure of O_2 at the alveolus. However, even this positive pressure breathing (PPB) itself has its limits since above 50,000 ft there is not enough total pressure to maintain an adequate partial pressure of O_2 in the alveolus, even with positive pressure breathing. Therefore, the conventional wisdom is that above 50,000 ft, a pressure suit—either partial or full—is required to maintain sufficient O_2 levels in the alveolus. The F-22 AFE, including the UPG, is in fact designed to act as such a partial pressure suit in the event of cockpit decompression above 50,000 ft.

Hypoxia Sections – (Ref Secs IX-X 290-309)

Atelectasis is the term applied to describe collapse of alveoli, the functional end-units of the lung. The alveoli of the lung are the end of the airways progressing through many generations of division, ultimately originating from the nose and mouth. That is, the airways divide into the left and right lungs, then divide again within the different parts of the lung and continue to do so for many divisions until the microscopic, terminal alveoli result. The bronchial airways, just prior to the alveoli, are very small and have no "reinforcing" support structure that hold them open. The alveoli themselves are dependent on an adequate amount of gas (primarily Nitrogen) to remain open. Collapsed alveoli will cease to participate in gas exchange until reopened, perhaps by coughing or deep breathing. However, even after being reopened by such a maneuver, these alveoli will be unstable and more likely to collapse again. Atelectasis is a lung decrease in ventilation that also affects circulation. The blood flowing past these collapsed alveoli is not absorbing O_2, and the result of such blood flow is called "shunt." In the case of a normal lung, the combined weight of the blood, the lung tissue itself and the chest wall together cause the small airways at the very base of the lung to collapse; i.e., atelectasis. At the same time as the weight of the lung causes lung collapse at the bases, the alveoli at the very top part of the lung have plenty of air ventilated through them, but they have limited blood flow. This area of limited blood flow is termed "dead-space ventilation." In normal circumstances, both shunt and dead-space ventilation affects only a very small part of the overall volume of lung tissue. There are a multitude of medical causes of atelectasis, but to the healthy aviator, the etiologies of high prevalence and concern are acceleration and absorption atelectasis. Atelectasis of any kind will result in reduced lung function and can cause symptoms of chest pain, irritation, or cough.

Absorption Atelectasis: One of the disadvantages to excessive O_2 is absorption atelectasis. Normally, the pressure of nitrogen within the alveolus will maintain patency through the breath cycle. If the small airways are closed off, O_2 trapped in the alveoli can be absorbed by the blood, thus effectively absorbing most (if not all) of the gas in the alveoli if there is no significant off-gassing of nitrogen from the blood into the alveolus. With little or no gas pressure to keep the alveolus open, it will collapse. If nitrogen is removed from the alveolus, as is the case when breathing concentrated O_2, the body will rapidly absorb available O_2 within the alveolus. This will decrease the pressure of gas within the alveolus and lead to alveolar collapse. There is a critical point at which inspired oxygenated gas entering the alveolus is balanced by O_2 uptake by the bloodstream, with atelectasis becoming increasingly likely with inhaled gasses composed of 60% or more of concentrated O_2. Referred to as Denitrogenation Absorption Atelectasis (DAA), this can cause significant and cumulative changes in lung ventilation and perfusion over time.

The concept of absorptive atelectasis is real, and certainly deserves particular attention with regard to the special circumstances of the fighter environment. In the medical literature, it has been shown that shunt resulting from absorptive atelectasis is minor in younger patients, but can rise to as high as 11% in older (>55 years old), otherwise healthy volunteers breathing 100% O_2 for 30 minutes; this may even worsen with continued breathing of high concentrations of O_2. Further review of the medical literature reveals absorptive atelectasis to be more likely in the following circumstances:

1) A low regional ventilation-perfusion ratio, which limits replenishment of alveolar O_2. In general, some amount of airway closure is required for this mechanism to be important, as in people who have low tidal volumes (the very fit), as well as in the context of high G's. Breathing dynamics, e.g., low tidal volume, will be discussed in further detail later.
2) Qualitative or quantitative alterations of surfactant, which promotes alveolar collapse; this will further reduce the ventilation-perfusion ratio. (Surfactant is produced in the alveolus to reduce the surface tension of fluid in the lungs. This helps make the alveoli more stable, keeps them from collapsing when an individual exhales). Surfactant abnormalities are admittedly not likely to normally be a major factor in the fighter community. If, however, segments of lung have significant atelectasis, this will result in unequal distribution of surfactant in the alveolus. This can contribute to worsening atelectasis.
3) An impaired pattern of respiration that fails to correct atelectasis (e.g., ventilation at low tidal volumes and/or without intermittent sighs). This condition is seen to be prevalent in the Air Crew Breathing experiments. Furthermore, decrements in vital capacity (usable lung volume) of up to 20% have been noted after hyperoxic exposure in numerous publications. This is presumably due to a combination of absorptive atelectasis and the shallow breathing due to pleuritic pain associated with tracheobronchitis. Once established, absorptive atelectasis is not rapidly reversed by a reduction of the concentration of inspired O_2. Of note, in the Aerospace Medicine literature, it has been noted that symptoms of acceleration atelectasis may be lessened by an adequate concentration of nitrogen at the alveolus, and/or positive pressure breathing that helps keep the alveoli open.

Acceleration Atelectasis: Under vertical acceleration forces, + G, there will be regional changes in blood flow in the lungs which will lead to the formation of acceleration atelectasis. When a fighter pilot makes very tight turns while flying an aircraft, the resulting centrifugal force tends to push the blood from the top part of his or her head down into the lower parts of the trunk and the legs. This is known as "pulling G's," and in most modern fighter aircraft, the amount of G's pulled can be up to nine times the force of gravity (i.e., "9 G's"). In some cases, too much blood can be pushed down from the brain, and this can result in the loss of consciousness (i.e., G-induced loss of consciousness or "G-LOC"). In the lung, the effect of pulling G's is to "push" the blood and upper lung segments down on the lower parts of the lung. As a result, there will be a larger amount of collapsed airways due to the increased effective "weight" on the lower lung under G forces. At + 5 G_z and greater, the upper half of the lung will effectively be non-perfused. This non-perfused lung is effectively ventilated dead space. Because the lower regions of the lung have increased blood flow and collapsed, will result in no ventilation but high perfusion. This can result in shunting of deoxygenated blood to mix with oxygenated blood in circulation, lowering the O_2 content in arterial circulation. The overall result is that acceleration

atelectasis of the lower portions of the lung portions limits pulmonary volumes which normally play a more significant role in ventilation due to higher perfusion.

Acceleration atelectasis will begin to occur by + 3 G_z and be prominent from + 5 to + 9 G_z. That is why various anti-G protection measures have been developed over the years, such as the Anti-G Straining Maneuver (AGSM), the Advanced Tactical Anti-G Suit ("ATAGS"), and positive pressure breathing (PPB) (i.e., forcing air into the lungs at higher G's to counteract the tendency of blood in the head to flow down into the chest). To a large extent, positive pressure breathing will counter the tendency toward acceleration-induced atelectasis, but this counteracting effect does not completely eliminate the phenomenon. Use of anti-G suits may exacerbate acceleration atelectasis by restriction of the diaphragm and fall in FRC if not counteracted by an AGSM. Sustained, this can result in a shunt of deoxygenated blood on the order of 20 to 25% of total blood flow. Acceleration atelectasis will be exacerbated with inspiration of high O_2 concentrations. Atelectasis will reduce the functional capacity of the lung, limiting and whenever feasible measures should be taken to minimize the causal forces. (This use of positive pressure breathing "for G" is in distinction to the use of PPB "for altitude" (i.e., to provide enough O_2 to the alveolus). Of note, the two uses of PPB are not mutually exclusive (i.e., one can be using PPB for both G effect and for altitude simultaneously, if needed).

Atelectasis Sections – Ref Secs I, X 1-8, 301-309, and Appendix 4 References 1-47.

Hyperoxia: Inspiration of higher O_2 concentration, necessary with increases in altitude with less O_2, has a multitude of undesirable adverse effects as concentrations increase. An aircraft designer might be tempted to think that too much O_2 in healthy individuals is never a bad thing. For instance, if an engineer had to design an O_2 delivery system for an aircraft, it would be better to err on the side of providing too much O_2, rather than not enough. A potential benefit of breathing 100% O_2 tends to wash out nitrogen from the body's tissues and could thereby serve as a useful risk mitigator against decompression sickness. This is a valid strategy if the pilot is exposed to ambient pressure at high altitudes. In application the second reason may be warranted for high altitude reconnaissance, the first assumption is not valid.

Problems resulting from high concentrations of O_2 have long been demonstrated in the clinical and aerospace literature. Simply breathing 100% O_2 itself for prolonged periods of time can cause substernal discomfort due to its irritant effect and can even damage airways and pulmonary tissue. O_2-enriched air can lead to the production of reactive O_2 species which can directly cause inflammation, alveolar damage, and respiratory distress, concurrent with and in addition to absorption atelectasis, as previously discussed. Inflammation of large airways can be observed by bronchoscopy in most medical patients treated with 90% O_2. This is thought to reflect as hyperoxic bronchitis and is sometimes referred to as "tracheobronchitis." In fact, the general term "oxygen toxicity" refers to the tracheobronchial and pulmonary tissue damage resulting from breathing high levels of O_2 for prolonged periods of time. Unfortunately, there is no single upper limit of O_2 concentration at sea level for the prevention of O_2 toxicity, and the relative importance of the duration and magnitude of hyperoxic exposure is also not clearly understood. Factors that are difficult to quantify, such as the adequacy of a given patient's antioxidant defenses, probably also play a role in determining individual susceptibility. Nonetheless, elevated levels of O_2 may lead to particular problems in the fighter community, due to the effects of high O_2 levels on the lung.

Since the partial pressures of gasses decrease in ascent to altitude, the denitrogenation occurs faster. The effects on vital capacity were demonstrated by the RAAF in document #D18123622 submitted to the USN RCCA Aerospace Medicine and Physiology Team. Vital capacity was reduced by a further 15% after flight, to an average of 28% below baseline (but as much as 35% in some cases). In aviation it is known that hyperoxia has resulted in complaints of cough, dyspnea, and chest pain in aviator's flying at altitudes between 14-20,000 Ft for 5 hours or longer. Dussault et al. revealed that when breathing 100% O_2, high-grade atelectasis was present by CT and was manifested by cough and chest pain. After inhaling only 44.5% O_2 only a small grade atelectasis was visualized and not manifested by frank symptoms. Dassault also found that acceleration and absorption atelectasis are independent of one another.

Hyperoxia has been shown to produce significant negative cerebral and cardiovascular effects. Prominent are atelectasis, increased systemic vascular resistance index (SVRI), reduced Heart Rate, Cardiac Index (CI), and stroke index (SI). Hyperoxia has resulted in decreased cerebral blood flow and metabolic rates. This has led to the supposition that high concentrations of O_2 may be causal in the physiological incidents in various aviation platforms. Multiple studies have found that arterial hyperoxia induced various amounts of vasoconstriction peripherally. The magnitude of the constriction was proportional to the level of inhaled O_2 and prominent in vessels ~ 15–25 μm in diameter. Pronounced constriction was seen in muscle vasculature, while constriction was seen in the skin and intestines has not been shown to be as prominent. Studies have showed that in healthy humans, hyperoxia lowered the efferent sympathetic nerve activity to skeletal muscle under resting conditions. By reduction of the sympathetic system, there is a limitation in the response to physiological stress. Hyperoxia has resulted in cerebral blood flow decreases and metabolic rates. This is of significant concern in the dynamic environment of the fighter and military training aircraft.

A primary consideration is that hyperoxia sets up a physiologically vulnerable state that further alterations in vascular O_2 or intravascular pressure may produce a "relative hypoxia" or perfusion hypoxia in tissues. The hyperoxia is the precursor and major contributor to alterations in respiratory or cardiovascular alterations in conjunction with the dynamic aviation environment. The dynamic environment of tactical aviation may well play a contributory role as well as intra-individual variability. Articles in anesthesia, critical care medicine, emergency medicine, and wound care have shown the disadvantageous effects of inhaling high O_2 concentrations.

Hyperoxia Ref – See Appendix 4 and Appendix 4 References 1-47

Oxygen induced changes in neurovascular tone: A topic of ongoing interest, the inhalation of high concentrations of O_2 has been found to cause regional blood flow changes in the brain and changes in brain function. Damato et. al demonstrated reduced blood flow by MRI, with some preservation of cognitive function. Although memory may not be affected, some areas of reasoning and judgement may be affected. These vascular changes are under investigation and may prove insightful in delineating the pathophysiology of Hyperoxic cerebrovascular changes and cognition.

Hyperoxia Ref – See Appendix 4 and Appendix 4 References 1-47

Rapidly Oscillating Hyperoxic Concentrations: During the T-6 Safety Investigation Board for unexplained PEs, it was determined that fluctuating O_2 can cause hypoxic like symptomology. While there are currently no formal studies on humans or pilots to reference, the medical

literature on animals does support this. Boehme et al demonstrated that oscillating O_2 induced release of proinflammatory cytokines in the lung, followed by onset of inflammation.

Ref – Boehme S, Hartmann EK, Tripp T, Thai SC, Matthias D, Abraham D, Baumgardner JE, Markstaller K, Klein KU, PO_2 oscillations induce lung injury and inflammation, Critical Care (2019) 23:102, pp1-12

Oscillation Pressure Effect on Surfactant: Surfactant is the coating that helps to prevent alveolar collapse. Pressure oscillations facilitate atelectasis formation by displacing surfactant. In combination with decreased nitrogen and/or acceleration, this further increases the amount of atelectasis in the lungs. Higher pressure oscillations can also cause barotrauma to the airways and alveoli. High pressure oscillations potentiate lung damage through a variety of mechanisms. High pressure oscillations cause mechanical stress and strain within the lungs, as the mechanical force applied to the pulmonary epithelium lining the airway and the alveoli initiates a resultant inflammatory response within the lungs. An inflammatory response can spread to other organs causing secondary barotrauma.

Asynchrony: A pervasive problem in mechanical ventilation of critical patients, but it also is a contributing factor in aircrew breathing systems. One form of asynchrony (dysynchrony) involves timing of mechanical triggering of the system to the pilot's individual breaths. Asynchrony is defined as the triggering or cycling of a breath that either leads or lags the pilot's inspiratory effort. Regarding the size of a breath, asynchrony means the inspiratory flow or TV does not match the patient's demand (too much/little, too early/late). Asynchrony will lead to increased work of breathing, excessive fatigue of respiratory muscles, and non-specific respiratory discomfort. Volume and flow mismatches can cause micro-trauma in the form of barotrauma due to alveolar over distention even if the pressures are not excessive in the traditional sense of high PIP/PEEP. Asynchrony is a subtle problem for which patients have no way to perceive or communicate its presence directly.

Ref Sec VII 171-235

Inspiratory Resistance: O_2 delivery equipment (e.g., O_2 supply, hose, mask, etc.) imposes resistance to flow for the pilot. Numerous studies on inspiratory flow have been conducted, and the effects have been shown to vary greatly, though most of the studies have been conducted with the very short intervals of 10-30 minutes. In general, resistance to flow through O_2 delivery equipment has been shown to cause the following:

1) A change in respiratory minute volume. Moderate resistance produces slowing and deepening of breaths, while high resistances cause rapid and shallow breathing,
2) A decrease in lung ventilation. The reduction in ventilation is greatest when the systems resistance is in inspiration and expiration
3) Alveolar ventilation reduction. Over a prolonged period of time, this can gradually increase the alveolar CO_2 level, with increased expiration of CO_2.
4) Increase in the functional residual capacity. Recall from the physiology section, this is an increase in the volume of air that is left over at the end of passive expiration. In laymen's terms, the lung does not empty fully. This occurs when the resistance is in expiration.
5) A decrease in the maximum ventilatory capacity. This is a reduction in the maximal volume that can be breathed in one minute. In essence you have reduced your Vital Capacity (VC).

6) Increases in the total respiratory work per minute. This increases fatigue and worsens respiratory effort over time. The diaphragm is particularly susceptible in this regard.
7) Subjective breathing difficulties. This is an increased conscious appreciation of breathing resistance, ranging from mild to the sensation of impending asphyxia.

Individuals vary in their responses to O_2 delivery system resistances, and the same individual may vary his own responses. Susceptible individuals may actually, at times, hyperventilate and exhibit symptoms of hypocarbia (low CO_2 levels).

Ref Sec IV 27-47

Airway pressures: A high amount of airway pressures weather inspiratory and/or expiratory have been shown to cause barotrauma. Pulmonary barotrauma with aircrew equipment results from excessive positive mechanical pressure ventilation. Excessive positive pressure can lead to elevation of the trans-alveolar pressure or the difference in pressure between the pressure in the alveolus and the pressure in the interstitial space surrounding the alveolus. Elevation in the trans-alveolar pressure may lead overdistention and the increased pressures in the alveoli units lead to inflammatory changes. This can eventually lead to alveolar rupture, which results in leakage of air into the extra-alveolar tissue. There is no specific airway pressure guaranteed to exclude risk of barotrauma. In fact, the main determinant of alveolar overdistension is end-inspiratory volume rather than pressure. However, the latter is easier to measure. Plateau pressure (the pressure at the end of inspiration) probably a better estimate of peak alveolar pressure than peak airway pressure. Based on animal studies and the knowledge that human lungs are maximally distended at a respiratory system recoil pressure of 35 cm H_2O. Thus, maintaining a plateau pressure < 35 recommended. (16-26)

Ref Sec III 16-26

Inspiratory Over Pressure: Inspiratory flow is determined by tidal volume/inspiratory time. High flow rates will result in higher peak airway pressures. Excessive inspiratory pressures will in turn result in increased intrathoracic pressure and lead to potential hemodynamic consequences (particularly decreased venous return, leading to decreased cardiac output and at worst, hypotension (low blood pressure). High airway pressures may result in inadequate ventilation if peak inspiratory pressure is too high, the excess pressure can cause overdistention of the alveoli to the point that they lose structural integrity and collapse. Pilots will feel uncomfortable and feel bloated or over expanded with an abrupt bolus of gas (high volume in a relatively short period of time). Peak inspiratory pressure (P_{IP}) is the highest level of pressure applied to the lungs during inhalation. In normal breathing, it may sometimes be referred to as the maximal inspiratory pressure (M_{IPO}), which is a negative value. Peak inspiratory pressure increases with any airway resistance or with excessive mask pressures. (27-47)

In the results presented in this dedicated PBA trial, it will be shown that the safety pressure regulator response is not proportional to the demand from the pilot. This effect varies at the beginning, middle and end of the response to the pilot input. An insufficient response at the beginning of the breath, and an overaggressive safety pressure response at the end of the breath is very different physiologically from a proportional or nearly linear response for which the body is accustomed. High safety pressure in combination with sudden and unexpected inhalation flow towards the end of inhalation can lead to inspiratory overpressure.

Ref Sec IV 27-47

Excessive expiratory pressure: Hyperinflation: Inappropriate and excessive exhalation pressures will lead to dynamic hyperinflation. Hyperinflation is the increase in lung volume (over inflation) that occurs whenever insufficient exhalation time prevents the respiratory system from returning to its normal resting end-expiratory equilibrium volume between breath cycles. This results in trapped air, inability of the pilot to initiate a breath, and an increased work of breathing. Hyperinflation also results in limited inhalation volumes, as the excessive exhalation volume is not displaced. Limiting inspired volumes results in increasing the physiologic dead space. In the case of dynamic expiratory hyperinflation, volumes of both inspiration and exhalation are decreased, TV is diminished and a state of hypoventilation results. Persistent breathing dysfunction (oscillations, lung over-inflation, and forceful exhalation) can cause long term changes to pulmonary function.

Ref Sec V 48-134

Excessive expiratory pressure: **Decreased Cardiac Output**: High exhalation pressures have pulmonary pathophysiological consequences but can cause cardiovascular perfusion problems as well. Normal respiratory dynamics function as a negative pressure system during inhalation. As described previously, the diaphragm descends and produces a negative pressure in the airways that draws air for gas exchange in. This same negative intrathoracic pressure decreases the right atrial pressure and draws blood from the inferior vena cava and increases venous return to the heart. The increased airway exhalation pressure is reflected in the airways and alveoli. This in turn is transmitted to the thoracic cavity and decreases the negative pressures from the diaphragm (creating a positive pressure). This increases right atrial pressure, decreasing venous return. This affects the pulmonary flow and decreases overall heart volume. This has a doubling effect of decreasing cardiac output as well as less effective cardiac function. This can result in overall drop in mean arterial pressure, which in a fighter aircraft can result in brain hypoxia.

Ref Sec V 48-134

Barotrauma: If peak inspiratory pressure is too high, the compensatory reaction is to limit TV so as to prevent excessive pressure on the airways and alveolus. Barotrauma is the principal complication of high-pressure ventilation. It is caused by overdistention of alveoli by inappropriately high inspiratory pressures, high continuous expiratory pressures, or excessive tidal volumes. Any one of these in excess or combination of these can cause barotrauma. (158-170) An excess pressure in inspiration or expiration, can cause over distention of the alveoli to the point that they lose structural integrity and collapse. High alveolar pressures can be due to excessive TV, gas trapping, excessively high expiratory pressures or low compliance ("stiff lungs" or lung tissue that has limited elasticity). Even pressures as low as 15-20 cmH2O can result in barotrauma. This may result in hypoventilation of the patient and hypoxia. Chronically high airway pressure may cause micro-barotrauma to the alveoli that accumulates over time.

Ref Sec VI 135-170

Chest Wall Restriction: Upper Pressure Garment (UPG): Specialized studies in the human centrifuge and altitude chambers at the Brooks City-Base revealed that the F-22 UPG filled and retained the BRAG safety pressure at ALL times, rather than only as originally scheduled. In fact, the UPG pressure was often above the pilot's O_2 mask pressure, and pilots were actually *increasing* the UPG pressure with each inspiration. This altered pattern of breathing is not

unexpected, since chest wall restriction significantly reduces the peak and inspiratory flows. As demonstrated in the following chart, the differential pressure in the UPG vest and the mask result in a difficult inhalation.

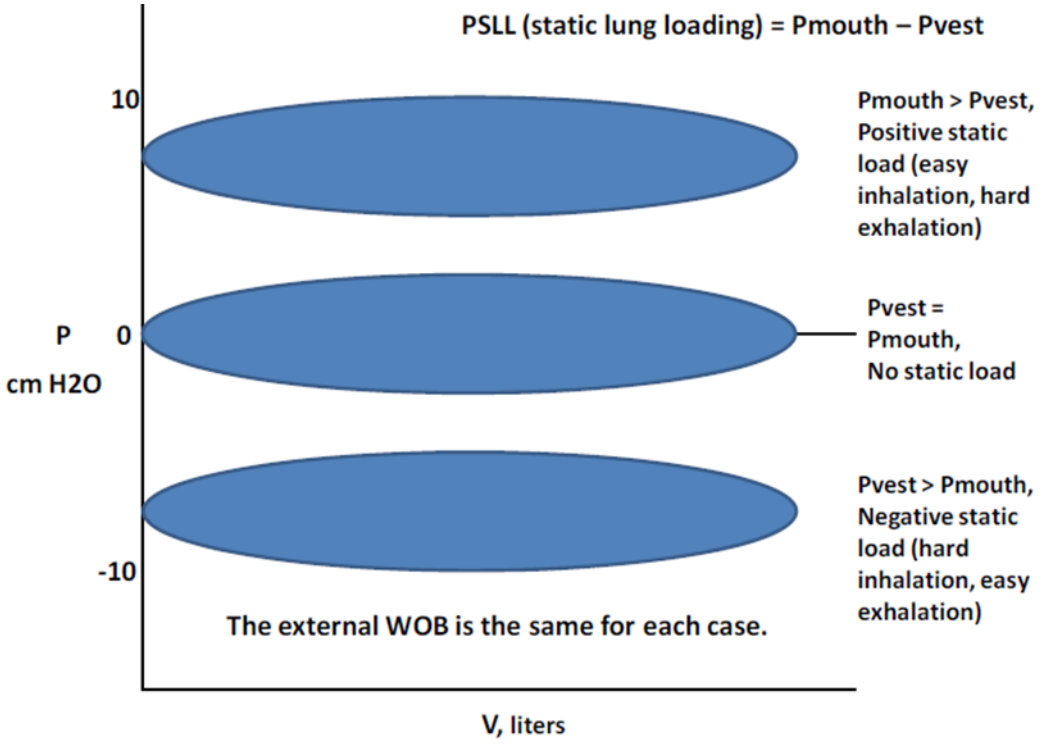

Figure 7.2.1. Static Lung Loading from NESC F-22 Report

As shown Figure 7.2.1, the effects of static lung loading (SLL) cannot be detected by measures of external WoB. However, it does have a big effect on *internal* elastic WoB of the rib cage. Negative SLLs shrink the rib cage, making it harder to inhale, and positive SLL expands the rib cage, making it harder to exhale. When inspiratory O_2 flow is already limited, due to external flow resistance, the addition of negative static lung loading worsens the situation. In short, the UPG is inflating inappropriately due to a "cracking pressure" on the UPG valve that is not quite correct at lower G's. The result is that the inflated UPG restricts the pilot's chest wall movement, and thereby keeps him or her from being able to take in a full deep breath. Likewise, without being able to take deep breaths, it is more difficult to cough adequately. Therefore, the chest wall restriction resulting from inappropriate UPG inflation inhibits effective reversal (clearance) of the atelectasis.

Ref Sec VIII 236-289

Chest Wall Restriction – Pulmonary: Chest wall restriction has numerous consequences on the lung and ultimately breathing functions. Studies have shown that restrictions in chest wall expansion have reductions in VC (vital capacity), resulting in an altered breathing pattern, and also reduced cardiac output.[236-289] Specifically this has been shown to decrease the tidal volumes, decreased compliance (i.e., increased stiffness) of the chest wall, and a reduction in exercise capacity. Prominently the forced expiratory vital capacity (FVC) and forced expiratory volumes in 1 second (FEV1) have been shown in studies to be significantly reduced in exercise. Forced expiratory volume (FEV) measures how much air a person can exhale during a forced

breath. The amount of air exhaled may be measured during the first (FEV1), second (FEV2), and/or third seconds (FEV3) of the forced breath. Forced vital capacity (FVC) is the total amount of air exhaled during the FEV test. In studies of normal subjects, chest wall restrictions show reduced total lung capacity (TLC) by a mean of 34% (range, 28–43%), vital capacity (VC) by 41% (range, 30–50%), and FRC by 31% (range, 22–38%). Residual volumes (RVs) decreased by 15% (range, 6–24%). The expiratory reserve volumes (ERV) consistently showed the greatest decrease, averaging 51% (range, 36–60%). In three studies reporting on closing volume it was uniformly reduced by CWS, on average 18% (range, 14–20%). Also, excessive chest wall restriction over time will limit the maximal amount of inhalation, thus reducing Inspiratory Capacity. These lung volume decreases result in hyperpnea (Subjects trying to increase the lung volumes by either increasing the time of inspiration, or volumes of inhalation). Gonzalez et al. also showed there was a "significant and quantifiable increase in the O_2 cost associated with external chest wall restriction which is directly related to the level of chest wall restriction." Thus, work of breathing and muscle fatigue are noticeably increased.

Ref Sec VIII 236-289

Chest Wall Restriction -Cardiac Output: Another possible outcome of chest wall restriction is a decrease in the amount of blood pumped by the heart over a given period of time, an amount known as the cardiac output (CO). Review of the medical literature reveals the fact that severe chest wall restriction can reduce cardiac output. Miller *et al* showed that a 38-40% reduction in static, resting forced vital capacity the cardiac output by about 10-12%. This decrease is caused by a decrease in chest volume, thereby reducing the amount of venous return into the chest (and the heart), resulting in a reduced amount of blood pumped by each beat. Yet, pure chest wall restriction is unlikely to be strong enough to cause a significant reduction in cardiac output in healthy adults. A significant reduction more than likely results from a combination of many factors. That is, high-G flight, atelectasis, mismatched AFE, positive pressure ventilation, and/or decreased venous return can, in various combinations, impinge on the cardiac output. It is also helpful to keep in mind that pulling G's in a fighter aircraft is very demanding physically, so the pilots are in effect experiencing such factors while exercising (i.e., pulling G's), and while attempting to recover from exercise. (362-371)

Ref Sec VIII 236-289 and 362-371

Chest Wall Restriction -Aircrew Flight Equipment: One of the best ways of clearing areas of atelectasis in the lung is by taking in deep breaths (sighing) and by coughing. In the F-22 investigation for example, numerous observations were shown that the clearing of atelectasis was inhibited in the pilot due to chest wall restriction associated with use of the Combat Edge vest in an overinflated or asynchronous state. From the work on the F-22, a concern about the use of the parachute harness was explored.

Ref Sec VIII 236-289

Chest Wall Restriction - Work of Breathing (WOB)

In addition to the effects on cardiac output, chest wall restriction can significantly alter the WoB. The method of calculating WOB was popularized by E. J. M. Campbell, in which plots of pleural pressure against lung volume reveal the passive characteristics of the lungs and chest wall, and show the pressures generated (and work performed) by the respiratory muscles during breathing.

The framework can serve as a brief guide to develop an understanding of some of the vulnerabilities of the respiratory system. Many of the physiological properties of the lung will vary between breaths or within an individual breath to maintain the proper balance of O_2 and CO_2 within the blood. This highly tuned, highly responsive system will respond consciously and subconsciously to external forces. The body will make efforts, consciously or subconsciously, to attempt to restore alveolar ventilation. If there are external forces at work limiting the pilot's physiological response, the emanation will be undesirable symptoms of dyspnea, nausea, cough, or worse. If the human's physiologic reserve is depleted rapidly, or insidiously, the pilot may acutely become incapacitated. Within the violently dynamic nature of high-performance aircraft, the magnitude of small, consistent perturbations can have cumulative and devastating effects, even if the breathing gas systems are functioning within current design specifications. The dynamically dynamic human system is constantly responsive to pressure, volume and time, and so any fluctuation will result in changes that affect the function of the entire system.

Ref Sec VIII and XIII 236-289, 336-343

7.3 Pulmonary Consequences

Pulmonary consequences: Progressive loss of minute ventilation has been revealed to occur as a result of complex interactions between the breathing gas system and pilot physiology. Loss of minute ventilation is reflective of inability of the pilot to adequately adapt to the breathing environment. Many of the patterns revealed in the data, including dyssynchrony, increased impedance to airflow, and undesired dynamic pulmonary changes, are interacting synergistically to reduce minute ventilation.

Dyssynchrony is the product of mismatch between pilot demand and regulator supply flow. The data demonstrates that pilot demand and airflow supply are disjointed. Early in the breath demand exceeds supply, whereas later at the end of the breath by supply exceeds demand. When supply exceeds demand at the end of a breath, this will result in an excess volume of air being forcibly delivered to the pilot, with a number of concerning effects. The data has demonstrated metrics of hysteresis and phase shift. Increasing time to 50% inhalational volume will physiologically result in reduction in tidal volumes, consistent with trends observed. Dyssynchrony will also facilitate dynamic hyperinflation of the lungs in conjunction with increased impedance to airflow.

Alveolar overdistension: Overdistention is a consequence of pressure demand/flow mismatches. The data demonstrates that pilot demand and airflow supply can become disjointed. Early in the breath demand exceeds supply, whereas later at the end of the breath by supply exceeds demand. When supply exceeds demand at the end of a breath, this will result in an excess volume of air being almost forcibly delivered to the pilot, with a number of concerning effects. This undesired and excess airflow will be directed to more patent and highly ventilated regions of the lung. The possible end result of regional alveolar over distention if forcible exhalation is initiated during peak regulator flow will further increase transpulmonary pressures and stress on the alveoli. On the microscopic level, the alveolar over distension will lead to inflammation, disrupted blood flow, collapse and loss of function. Alveoli that have been over distended may be subsequently stretched open on successive breaths; they will be unstable and prone to collapse again. The cyclical atelectasis that results will lead to further injury and the shear forces will be transmitted locally, causing neighboring alveoli to also collapse. The end result is somewhat of a 'micro-

tear' in lung tissue, with cumulative progressive injury, inflammation and loss of tissue function, which will continue as long as the pressure demand and flow mismatches continue.

The pathological effects of breathing gas system hysteresis or desynchrony will be most pronounced during periods of high metabolic demand with large lung volumes and rapid breath rates but can also impact function during quiet breathing due to the disproportionately large magnitude of the desynchrony compared to the small pressures used at rest. The body may attempt to compensate for this process with slowed respiration with feedback from lung stretch receptors via the Hering-Breuer reflex, but this will pose yet another risk for hypoventilation.

Ref Sec III 16-26

Circulatory consequences: Pulmonary circulation is affected by the demand regulator safety pressure system, with downstream changes in cardiac output and systemic vascular function. These changes can be classified by their principle etiology: effects of safety pressure, pressure and flow hysteresis, and pressure oscillations. Safety pressure increases pressure within alveoli, reducing capillary perfusion pressure. The effects of low safety pressure (3 mmHg) alone are small but are additive with other increases or fluctuations in inspired gas pressures. Higher positive airway pressures will increase pulmonary artery pressure and right heart loading, decreasing right heart output and exacerbating any underlying shunting or V/Q mismatch.

Pressure oscillations alter pulmonary blood flow. These oscillations can be transmitted to alveoli, and the resultant physiological effects depend on a host of factors. These factors include the frequency and magnitude of the oscillations, the time during breath when the oscillations occur, and the current physiologic state of the lung (lung volumes, atelectasis, etc.). If the magnitude of the oscillations is large, they may be additive with safety pressure to cause pathological reductions in pulmonary capillary perfusion, increase right heart strain and worsening any existing V/Q mismatch. If the oscillations occur in the presence of regulator hysteresis, the effects may be magnified, with significant changes in regional blood flow.

Airway and thoracic pressures above venous or right heart pressures will be transmitted to the systemic venous system and cerebral veins, limiting flow and reducing perfusion. As shown in the previous sections, there could be a concomitant reduction in ventilation and reduced cardiac output with chest wall restriction. High thoracic pressures will can trigger the baroreceptors in the aortic arch with reflexive slowing of heart rate and reducing cardiac output even further. Reduced cardiac output, in conjunction with reduced cerebral perfusion pressures and coexisting reflexive hypoventilation are a recipe primed for hypoxic insult.

Ref Sec III, IV, and V 16-134

Mask Pressure Swings: Low mask pressures and lower swings in mask pressure are usually thought to denote a system that is performing well, but that is not necessarily true when a flow restriction is present. Conversely, elevated mask pressures and larger mask pressure swings are traditionally considered to denote a poorly performing system, but pilots do not perceive that those pressures as large or objectionable when the flow adequately responds in synchrony with large demands. In either of the previous cases, pilot perception of breathing performance may not correlate well with the magnitude of mask pressure. Rather, pilot perception of breathing dynamics appears to depend more upon receiving a flow commensurate with demand and without delay. Excessively high inspiratory and/expiratory pressures will cause a commensurate decrease in TVs. The higher the peak pressures, the more the TVs will be restricted to prevent

barotrauma. However, fast oscillations as seen in the data can cause barotrauma before reflexes can protect against excessive pressures. At higher metabolic demands the protective restriction on TV will result in hypoxia over time.

It is likely that breath dynamics demonstrated that are significantly disrupted are a precedence to increased ventilatory effort and lower demand mask pressures. Subconscious physiological adaptive measures to flow restriction are being exacerbated by the inefficient pulmonary dynamics of lower respiratory volumes. Expressly, with significant pressure and timing mismatches, pilot will be fighting the machine to maintain normal homeostatic breathing, but if significant compromise of these compensatory mechanisms is overcome, the pilot loses the fight.

Oscillating Pressure consequences:

Aircrew, under most circumstances, would be unaware of the effects of increased resistance in the breathing gas system, highlighting the insidious nature of some of these issues. High flow resistances would be expected to cause slower, deeper breathing, which does not here appear to be the case. However, with any degree of flow or inhale resistance, the body will adapt to preserve minute volume (MV).

Conventional thinking equates large drops in mask pressure as deleterious as a result of increased work of breathing associated with large mask pressures. Traditionally, when a flow restriction was present, there was a corresponding increase in large negative pressures, which intuitively makes sense when breathing against an insufficient flow, such as a pinched off mask or straw. Dr. J Camperman identified similar findings in his MBU 20/P mask engineering studies/research and noted these in the T-45 memo to T45 Integrated Project Team (IPT) Lead (7 Jul 18) and the T-6 memo to JPATS T-6 Program Office (15 Oct ‘19).

This combination of airflow restriction without a corresponding drop in mask pressure would be less prominent in a diluter demand breathing system, wherein flow response is proportional to the mask pressure demand and limited principally by regulator function. However, in an electronic safety pressure demand regulator, the flow response may not be in synchrony with the demand from the pilot. Rather, the supplied air can vary at the beginning, middle and end of the inhalation demand. This hysteresis or desynchrony between the pilot and regulator can cause significant changes in respiratory dynamics, akin to trying to drink water from a faulty faucet that is unpredictably varying its output from a dribble to high pressure stream. Air can be adequately provided at the beginning of the breath, and too much is being delivered after demand ceases at the end of the breath. This is very different physiologically from a proportional or nearly linear response of demand in normal breathing.

Physiologically, demand regulators with safety pressure create numerous issues and alter normal breathing dynamics. As previously discussed, at rest, inhalation is active and effort-driven, while exhalation is passive. With even small amounts of safety pressure, inhalation will become more passive while exhalation alternatively now becomes an active process. This inhalation/exhalation reversal will change chest wall and lung dynamics, usually resulting in expansion of the lung and increase in FRC. Exhalation now becomes prolonged, and indicative of increased effort needed to breathe out against pressure. The work of breathing will increase, and even the small safety pressures utilized in modern demand regulator systems will have the repercussion of hyperinflation and fatigue over time. Higher levels of positive pressure, particularly above the intrapleural pressure of -4 mmHg, have adverse consequences. Trained individuals can tolerate pressure breathing up to 30 mmHg for very short periods, to compensate

with a high-altitude cabin pressure decompression. In the high G_z regime, combined with G-straining maneuvers, a pressure of 60-90 mmHg can be tolerated in short durations. If left unabated it will eventually and invariably lead to hyperinflation, hypoventilation, fatigue, and respiratory failure.

Ref Sec III, IV, VI and VII 16-47, 135-235

Hyperinflation: The following depictions are designed to illustrate the influences of over-pressurization leading to hyperinflation (i.e., continued increases in FRC). Pilot reported instances of hyperinflation and increased FRC correspond to the higher exhale pressures, decreased exhale flows, longer exhale times, saw tooth exhale pressure oscillations, and lower tidal volumes. Together these suggest the pathology of increased FRC occurs regularly with significant potential to cause harm.

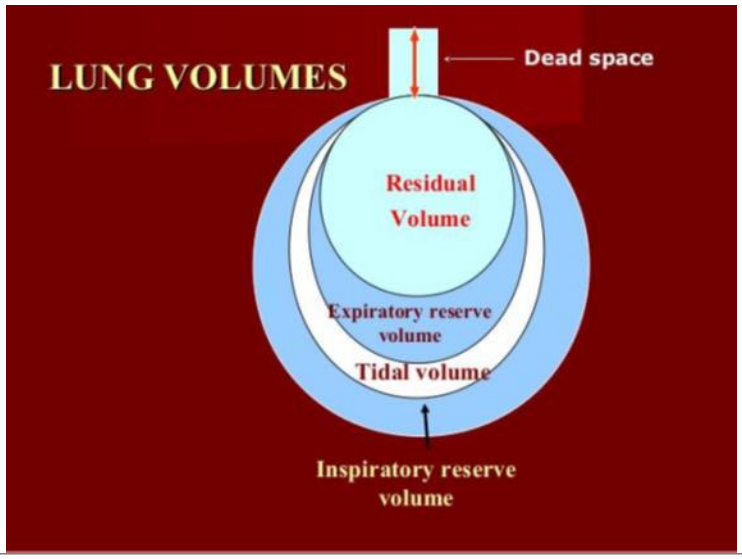

Tidal Volume (TV) – Air that moves into and out of the lungs with each breath (approximately 500 ml)

Inspiratory Reserve Volume (IRV) – Air that can be inspired beyond the tidal volume (2100–3200 ml)

Expiratory Reserve Volume (ERV) – Air that can be evacuated from the lungs after a tidal expiration (1000–1200 ml)

Residual Volume (RV) – Air left in the lungs after strenuous expiration (1200 ml); keeps alveoli inflated

Figure 7.3.1. Normal Relaxed Breathing

Figure 7.3.1 shows a normal alveolar volume distribution with labeled and defined respiratory volumes. The individual alveolus is used to help visualize what happens to the lung volumes as a whole as residual volume increases (regional differences occur in the lungs, but the principle concept is the same).

There is a progression of effects in the face of excessive inhalation or exhalation pressures. During inspiratory overpressure, the natural compensation mechanism is decreased tidal volumes to prevent barotrauma (this compensation is not depicted). Decreased tidal volume increases the airway and alveolar dead space by the amount of decreased tidal volume. A complete reduction in tidal volume to zero (breath hold) results in no barotrauma, but also no air exchange, as the entire lung becomes dead space.

In expiratory hyperinflation, the residual volume expands as depicted in Figure 7.3.2. Normal residual volumes (left) become larger through a combination of higher inhale pressure (i.e., larger breath due to being stuffed with air) and higher exhale pressure (i.e., incomplete exhale due to reduced exhale flow or time). Passive exhale is no longer sufficient to return the lungs to their starting residual volume, and the residual volume gradually expands (middle). A complete expansion of the residual volume (right-like blowing up a balloon and tying off the end) results in no air exchange, as the entire alveolus becomes dead space. Natural compensation is for exhale to become active (requiring the use of muscles not normally engaged) with a significant increase in the work of exhaled breathing. The higher lung volumes associated with increased residual volume result in muscles having to work from a position of mechanical disadvantage, as they are already stretched out.

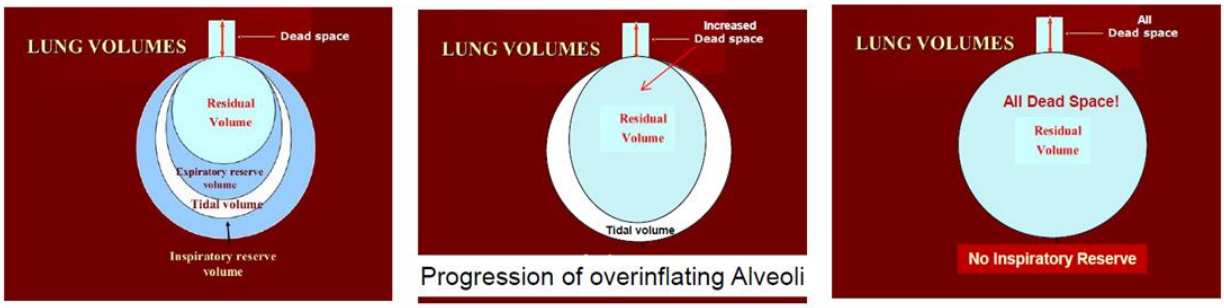

Figure 7.3.2. Normal Relaxed Breathing and Progressive Hyperinflation

Persistent breathing dysfunction from BSDs (e.g., oscillations, restricted exhalation, and attenuated inhalation) can lead to decreased Inspiratory Capacity. Medical literature, multiple pilot reports, and data indicate lower TVs all infer pilots experience lung over-inflation and increased Functional Residual Volumes.

Demand regulators also inherently introduce desynchrony into the breathing system. As a general principle, demand regulators can be tuned for responsiveness or maximum flow. As previously discussed, however, breathing patterns in flight are highly variable and will simultaneously require instantaneous response and high flow rates, as is the case with anti-G straining maneuver breathing. Current regulations, based on pressure and flow rate specifications, do not account for the synchrony with human respiration or the hysteresis that they inherently produce.

Oxygen concentrations varied by 20 to 40% over 1-minute intervals in several occurrences. Large breaths produced a precipitous drop in breathing gas O_2 concentration. These wide swings, within the current standards which require only O_2 concentration to meet a certain minimum depending on altitude, have a potential host of concerning effects. As mentioned previously, too much O_2 can restrict blood flow and produce toxins (reactive O_2 species (ROS), including superoxide) that are especially injurious to the brain. The body has natural mechanism to alter blood flow to limit the development of inflammation or reactive O_2 species in highly metabolic tissues including the central nervous system. These mechanisms generally involve a restriction in blood flow on the order of 10 to 40% depending on the study. Furthermore, this vasoconstriction generally will persist for a period of time after removal of the hyperoxic gas, usually on the order of several minutes up to days in severe cases. This can create a vulnerable period, if the body is adapted to hyperoxic gas and the hyperoxic gas is removed or oscillates in concentration, and results in increased risk to more metabolically active tissues. This is critical in

the extremely metabolically active Central Nervous System (CNS). This vulnerable period also appears to include increased inflammation and cellular lung damage when oscillations in hyperoxic concentrations exceed the ability of the homeostasis mechanisms to compensate and keep pace with the continuous changes. Decreases of $\geq$ 20% O_2 concentration also increase absorption atelectasis. If this occurs sequentially and rapidly in less than 5 minutes, the atelectasis is worsened with each swing, due to lack insufficient time to re-inflate with nitrogen.

The O_2 swings shown not comprehensive, nor representative of the total range of airborne performance. The O_2 variability of many airframes has been well documented and validated independently by the many USAF and USN investigations. These data reinforce the importance of understanding and mitigating the physiological impact of high and rapidly varying O_2 concentrations in pilot breathing gas. They also reinforce the importance of end to end systems testing as the data show variations due to systems interactions and aircraft differences.

7.4 Pilot Breathing Assessment - Physiological measurements

Pulmonary function tests are measurements of breathing and lung function. One specific PFT is Spirometry, which measures airflow and derives lung volumes. In a spirometry test, while you are sitting, you breathe into a mouthpiece and the spirometer records the amount and the rate of air that you breathe in and out over a period of time. When standing, some numbers might be slightly different. Spirometry assesses the integrated mechanical function of the lung, chest wall, respiratory muscles, and airways. This is done by measuring the total volume of air exhaled from a full lung (total lung capacity [TLC]) to maximal expiration (residual volume [RV]). This volume, the forced vital capacity (FVC) and the forced expiratory volume in the first second of the forceful exhalation (FEV_1). These values are useful clinical in assisting in determining disease processes. FEV_1 reduction is a reflected reduction in the maximum inflation of the lungs (TLC); obstruction of the airways; respiratory muscle weakness. Airway obstruction is the most common cause of reduction in FEV_1. Airway obstruction in pathological conditions may be secondary to bronchospasm, airway inflammation, loss of lung elastic recoil, increased secretions in the airway, or any combination of these causes. In a normal healthy pilot this is likely due to the mechanical system. Direct Lung volume measurement can be done in two ways:

1) The most accurate way to determine lung volumes is called body plethysmography. You sit in a clear airtight box that looks like a phone booth and changes in pressure inside the box help determine the lung volume. This allows an assessment of Functional Residual Capacity and specific airway resistance. By incorporating maximal inhalation and exhalation inside the box, total lung capacity and residual volumes can be determined.
2) Lung volume can also be measured when you breathe nitrogen or helium gas through a tube for a certain period of time. The concentration of the gas in a chamber attached to the tube is measured to estimate the lung volume.

In the PBA, the spirometry was done to establish a baseline pulmonary function for the study. This primarily emphasis was to examine tidal volume (the volume of normal quiet breathing) and vital capacity (the volume of a maximum inhalation through to a maximum exhalation, in a slow controlled manner-vital capacity combining the inspiratory capacity and expiratory reserve volumes). In the RAAF Institute of Aviation Medicine study (Characterisation of the Impact of the Super Hornet and Growler Flight Environment on Lung Function) there were significant changes in pulmonary functions. The Vital capacity was 15% lower than baseline due to the parachute harness system. This was prominent in Super Hornet torso harness than the Classic

Hornet harness. This likely reflects that the parachute restraint is integrated into the Super Hornet torso harness. Vital capacity in Super Hornet aircrew as measured within 10 minutes of landing was 28% lower than baseline. The maximal amount of Vital Capacity loss was up to 35% lower. The Super Hornet pilots had a reduction of vital capacity to 70% (but as low as 60% in some participants) of the population matched predicted vital capacity. This is a Super Hornet-unique characteristic; it was not seen in the Classic Hornet cohort. Also, of note, was that the Super Hornet and Growler breathing gas system supplies O_2 concentrations close to 94% throughout flight. The report did also note that Super Hornet aircrews complained of dyspnea (a sensation of being unable to take a deep breath) while airborne. This subjective finding was reported by only 1 (of 8) Classic Hornet aircrew members. A similar situation exists in the NESC study between the USN Super Hornet torso harness and the USAF parachute rig which is secured via the seat restraints.

Originally the pilots were to have body plethysmography to have a baseline of all lug volumes, but due to COVID-19 restrictions, this was substituted by ground spirometry.

Pulse Oximetry

Pulse Oximetry is a noninvasive method of measuring the O_2 level in the peripheral blood. This is more specifically by measuring the percentage of oxy O_2 that the hemoglobin is carrying. This peripheral hemoglobin saturation (SpO_2) is not always identical to the Arterial Oxygen Saturation (SaO_2), but the two are very closely correlated such that the SpO_2 is used as valuable clinical tool. There are several situations in dynamic aircraft operations that present challenges to the use of pulse oximetry in flight. Erroneous SpO_2 readings can be caused by motion or exposure to ambient sunlight or excessive light. Factors such as hypoperfusion (decrease in circulation) of the extremities can also lead to errors. This is prominent with the higher G_z maneuvers that a fighter or advanced trainer must perform. Another factor that must be considered is that SpO_2 readings in distal extremities may be delayed. Comparing measurements from the central circulation, finger measurements were delayed by around 30 seconds and toe measurements were delayed by up to 90 seconds. The use of reflectance probes has been attempted with "Under the helmet" sensor packages, but these suffer from venous pooling due to the increased relative weight in the high G_z regime. Thus far no acceptable method to date has been seen to measure pulse oximetry in the dynamic flight regime, but systems are in development to try and glean that information. The Air Crew Breathing study utilized the Rad 97 on the ground avoiding the complications of the high G inflight regime.

The RAAF Institute of Aviation Medicine study found O_2 saturation immediately after flight demonstrated a small-but-significant decrement in Super Hornet pilot SpO_2 compared to the pre-flight condition. This reduction was not seen in the pulse Oximetry results for the Classic Hornet aircrew. Although a pre-flight 3-point reduction to 95% (but as low as 88% in one individual the RAAF study) would be unlikely to cause hypoxia-like symptoms alone, it could pose a significant pre-condition that would erode the physiological reserve and lower the threshold for developing a physiological event in the presence of concurrent physiological stressors. If a significant physiological drop had occurred post flight, then a significant ventilation/perfusion mismatch was indicated. Thus, the Rad 97 pulse oximeter was employed to see if there was a significant decrease that would indicate that hemoglobin had a physiologically significant amount of desaturation. Specifically, a pulmonary (lung) ventilation perfusion mismatch is a mismatch in ventilation and perfusion (lung circulation). Alveolar gas exchange depends on the air movement to the alveoli, but also the flow of blood to the alveolar capillaries surrounding the

alveoli. In essence it required adequate O_2 in the alveoli, *and* adequate blood flow past alveoli to pick up O_2. If either ventilation to the lungs or blood flow are compromised, then a ventilation perfusion mismatch has occurred. This ventilation/perfusion ratio is abbreviated V/Q and a mismatch is labeled as a V/Q mismatch. There are two types of mismatches: dead space and shunt. Dead space mismatches result from inadequate tidal volumes are not incorporated into gas exchange. There are three types of dead space as previously elucidated. These are Anatomic (the airways), Physiologic (Alveolar Residual Volume), and Mechanical (Aircrew breathing hardware). A principle contributor of dead space being examined in these studies is the airway equipment used to provide breathing air to the pilot. Anatomic or airway dead space is fairly fixed, but the physiological dead space and circulation can change minute to minute with alterations in air supply to the lungs, cardiac output, and the pulmonary blood flow. One contributor to ventilation perfusion mismatches are shunts which are the results of O_2 not entering the pulmonary circulation. This can be a lack of perfusion/circulation to the alveoli or fluid in the lungs. Pathological shunting occurs in pneumonia, pulmonary edema, or plugging of the airways. As observed, contributors in pilots to shunting are atelectasis, and to a lesser extent decreased cardiac output. Predominant ABS findings here of chest wall restriction (decreased Tidal Volumes [TV]), asynchrony, and alveolar over pressurization are leading to increased dead space.

7.4.1 PBA Pulmonary Study

The PBA (Pilot Breathing Assessment) examined the inflight mask and system interactions with emphasis on physiological measurements using scripted flights in LOX system NASA F-15 and F/A-18 aircraft.

Study Design

This study had distinct components:

1) Physiological profiles conducted with spirometry and pulse oximetry preflight for baselines then with fight associated groupings.
2) Study
    a. A Baseline was conducted preflight to establish baselines wearing light suit only and seated.
    b. Conducted after AFE (which included parachute assembly in USAF or USN standard configurations and the VigilOX assembly) donning. AFE is otherwise known as Aircrew Life Support Equipment in other countries. The pilot or back seater were sitting in the cockpit, strapped into the ejection seat, with restraints and AFE adjusted as required for flight.
    c. Conducted post flight after taxi and flight. The post-flight cockpit configuration was crewmember sitting in the cockpit strapped in the ejection seat. The test was performed as soon as practicable after landing. Restraint and AFE remain as worn during flight; mask removal delayed until immediately prior to powering down the aircraft and opening the canopy, to minimize the time breathing air before the spirometry testing. Given the manner in which the spirometry was measured, the timings of post-flight spirometry in the cockpit were slightly longer for the rear seat (4-5 minutes) than the pilot in the front seat (2-3 minutes).
    d. Post egress from aircraft and doffing AFE and only in flight suit. Measured while seated.

3) The test plan comprised conducting similar testing on two NASA platforms – the F-15 Eagle and the F/A-18 Classic Hornet.
4) The study comprised datasets:
    a. A pilot (or rear seat) on F-15 Eagle
    b. A pilot (or rear seat) on F/A-18 Classic Hornet.
    c. A pilot (or rear seat) in USAF Flight Crew Parachute Assembly
    d. A pilot (or rear seat) in USN Flight Crew Parachute Assembly
5) The Flight Profile was comprised of dedicated repeatable sorties or aerobatic patterns.
6) The Aircraft profiles for the F-15 and F/A-18 Classic Hornet are in the following table. Both ACES and NACES ejection seats have the same mounting angels and maintain the same posture. Use of the two jet types as far as cockpit arrangements is not thought to be a significant confounder for the physiological effects of flying fast-jets.

F-15B/D				
Tail No.	Model (MDS)	Date Acquired	Serial No.	Production Year
N836NA*	F-15B	24 Jan 1993	74-0141	1974
N884NA	F-15D	21 Sep 2010	78-0564	1978
N897NA	F-15D	21 Sep 2010	79-0007	1979
* N836NA is primarily a Research platform occasionally used for mission support				

F/A-18A/B					
Tail No.	Model	Date Acquired	BUNO	Production #	Year /Lot / Block
N843NA [1]	F/A-18A [2]	8 Feb 1991	161519	A-027	1982 / Lot IV / Block 6
N850NA [1]	F/A-18A	24 Feb 1993	161703	A-038	1982 / Lot V / Block 8
N846NA	TF/A-18 [2,3]	1 Mar 2000	161355	B-006	1981 / Lot IV / Block 5
N867NA	F/A-18B	30 Oct 2018	161947	B-024	1985 / Lot VI / Block 12
N868NA	F/A-18B	30 Oct 2018	161938	B-022	1983 / Lot VI / Block 11

[1] Aircraft retired [2] Previous Blue Angel aircraft [3] Lot IV upgraded to Lot V (TF/A-18 to F/A-18B), Block 5

Life Support Training.

The LSS team were also technically trained to play an essential role in gathering pulmonary function testing of the pilots 1 hour prior to flight, at the jet-side both before and after flight, and 1 hour after flight. NASA JSC and AFRC flight surgeons developed clinical protocols and provided approximately 80 hours of training to the LSS team so they could administer these protocols to pilots throughout the flight program. In addition, field training was provided on-site by vendors, both with medical doctors, researchers, LSSs and pilots. Two trips to Armstrong Research center and were dedicated training sessions on the equipment by the Physician and technical members of the PBA study. Another trip was made to the pulmonary function and pulse ox manufactures for orientation and training on the devices. The LSS team supported each of the flights, from outfitting the pilots prior to each flight, to mastering the use of Spiro/Rad97, conducting pulmonary testing, creating LSS reports to rigorously document LSS metadata, and uploading all the data set from each of the data systems.

Protocol

Spirometry and Pulse Oximetry were tested in several distinct segments. Spirometry testing for in-flight baselines by was done with the laptop running the SpiroDoc in oscilloscope mode. This is followed by the resting Tidal Volume (TV), Expiratory Reserve Volume (ERV), and Inspiratory Slow Vital Capacity (IVC) obtained together in sequence. The Forced Vital Capacity (FVC) will be done separately after the IVC testing.

The first test in the sequence run with the SpiroDoc connected to a laptop computer. The laptop computer then operated the SpiroDoc in oscilloscope mode using the .exe file provided by the manufacturer. During this test the test subject was to be wearing a nose-clip and be seated comfortably and breathe in a relaxed, normal manner for 3 minutes. Talking was to be minimized and preferably eliminated.

The total test time was about 3 minutes during which the test subject is doing relaxed, normal breathing. The test session will consist of 7 test points with each test point containing a sequence of 4 spirometry tests:

a) A baseline was conducted preflight to establish baselines wearing light suit only and seated.

b) Conducted after Aircrew Life Support Ensemble (AFE – which included parachute assembly in USAF or USN standard configurations and the VigilOX assembly) donning. The pilot or back seater were sitting in the cockpit, strapped into the ejection seat, with restraints and AFE adjusted as required for flight.

c) Conducted post flight after taxi and flight. The post-flight cockpit configuration was crewmember sitting in the cockpit strapped in the ejection seat. The test was performed as soon as practicable after landing. Restraint and AFE remain as worn during flight; mask removal delayed until immediately prior to powering down the aircraft and opening the canopy, to minimize the time breathing air before the spirometry testing. Given the manner in which the spirometry was measured, the timings of post-flight spirometry in the cockpit were slightly longer for the rear seat (4-5 minutes) than the pilot in the front seat (2-3 minutes).

d) Post egress from aircraft and doffing AFE and only in flight suit. Measured while seated.

The test plan comprised conducting similar testing on two platforms – the F-15 Eagle and the being the F/A-18 Classic Hornet.

1. The study comprised of these datasets:
    a. A pilot (or rear seat) on F-15 Eagle
    b. A pilot (or rear seat) on F/A-18 Classic Hornet.
    c. A pilot (or rear seat) in USAF Flight Crew Parachute Assembly
    d. A pilot (or rear seat) in USN Flight Crew Parachute Assembly
2. The Flight Profile was comprised of a dedicated repeatable sortie or aerobatic pattern
3. Aircraft profiles the F-15 was X years older than F/A-18 Classic Hornet. Both ACES and NACES ejection seats have the same mounting angels and maintain the same posture. Use of the two jet types is not thought to be a significant confounder for the physiological effects of flying fast-jets.

Spirometry Testing with Extended Resting Tidal Volume: The spirometry test was done with the laptop running the SpiroDoc in oscilloscope mode. This is followed by the resting Tidal Volume (TV), Expiratory Reserve Volume (ERV), and Inspiratory Slow Vital Capacity (IVC) obtained together in sequence. The Forced Vital Capacity (FVC) will be done separately after the IVC testing.

The first test in the sequence run with the SpiroDoc connected to a laptop computer. The laptop computer then operated the SpiroDoc in oscilloscope mode using the .exe file provided by the manufacturer. During this test the test subject was to be wearing a nose-clip and be seated comfortably and breathe in a relaxed, normal manner for 3 minutes. Talking was to be minimized and preferably eliminated.

The total test time was about 3 minutes during which the test subject is doing relaxed, normal breathing. The test session will consist of 7 test points with each test point containing a sequence of 5 spirometry tests:

The 7 test points will be in this order:

1. Flight suit, in ready room
2. USAF flight gear, in ready room
3. USAF flight gear, in hanger, in front seat of F-18, strapped in
4. Flight suit, in ready room
5. USN flight gear, in ready room
6. USN flight gear, in hanger, in front seat of F-18, strapped in
7. Flight suit, in ready room

Spirometry Tests to be done per test point in this order:

The Extended Test Additional Procedure

1. Resting Tidal Volume and respiratory patterns (3-minute test with relaxed normal breathing)

Normal Test Procedure

2. Resting Tidal Volume
3. Expiratory Reserve Volume (ERV)
4. Inspiratory Slow Vital Capacity (IVC)
5. Forced Vital Capacity with Flow-volume loop

It was emphasized that the participant must be seated upright in a static chair with backrest and must not lean forward during the test. Also, when doing the when doing pre and post flight testing in the aircraft the test subject must not lean forward during the test. The test subjects were reminded of the test procedure, including desired endpoints and common pitfalls. For each of the tests, the subjects head should still be in the same position with the chin slightly elevated. For tests 2 thru 5 in the sequence, switch the SpiroDoc on and set to Doctor Mode following procedure in the Spirodoc User's Manual, Rev 2.4

7.4.2 Pulmonary Function Testing and Peripheral Hemoglobin Saturation - Data Analysis

Spirometry – FVC

Spirometry was performed serially using a SpiroDoc automated spirometer (MIR Technology, Rome Italy) and a disposable turbine. The device was calibrated in accordance with OEM instructions. The SpiroDoc can recorded the following respiratory measures.

a. Tidal Volume (TV). TV is the volume of air displaced from the lungs during quiet, resting breathing.

b. Expiratory Reserve Volume (ERV). ERV is the volume of air that can be forcibly exhaled at the end of a normal, resting exhalation.

c. Inspiratory Capacity (IC). Inspiratory Capacity is the volume of air that can be breathed into the lungs from the end of a normal, resting exhalation.

d. Vital Capacity (VC). VC (measured as Expiratory Vital Capacity, EVC) is the maximum volume of air that can be expelled from the lungs after a maximal inspiration. It is the difference between a full breath in and a full breath out. VC is the sum of IC and ERV.

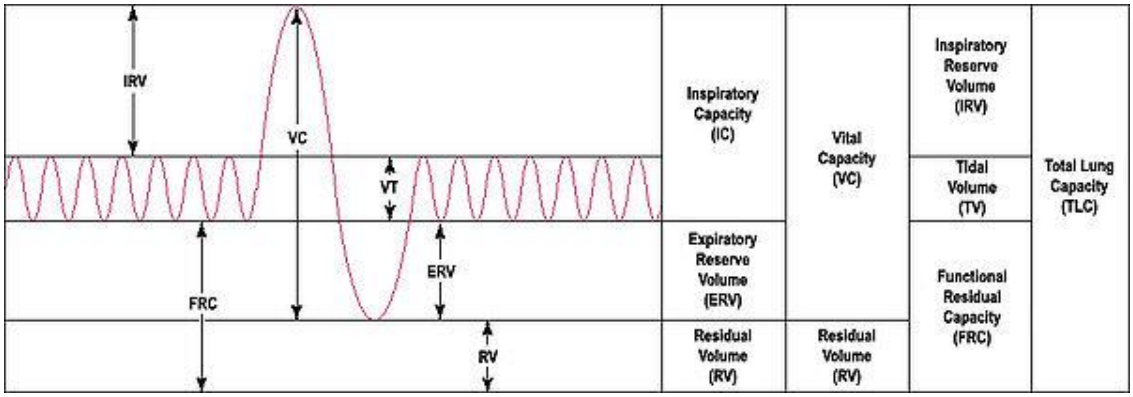

Figure 7.4.1. Measurements of Pulmonary Function Tests

(https://www.criticalcarepractitioner.co.uk/human-physiology/respiratory-system-physiology/)

All of the Spirometry was conducted in accordance with guidelines published jointly by the American Thoracic Society and European Respiratory Society and American Thoracic Society. (Miller MR, Hankinson J, Brusasco V, Burgos F, Casaburi R, Coates A, et al. Standardisation of spirometry. European Respiratory Journal. 2005;26:319-38: Graham BL, Steenbruggen I, Miler MR, Barjaktarevic IZ, Cooper BG, Hall, GL, Hallstrand TS, Kaminsky DA, McCarthy K, McCormack MC, Oropez CE, Rosenfeld M, Stanojevic S, Swanner MP, Thompson BR, Standardization of Spirometry 2019 Update. An Official American Thoracic Society and European Respiratory Society Technical Statement, October 15 2019, Am Jour of Resp and Crit Care Med Volume 200, Number 8. Pp e70-88).

The primary parameter examined here is the Forced Vital Capacity (FVC) or the total amount of air exhaled during the Forced Expiratory Volume (FEV) test. The FEV measures how much air a person can exhale during a forced breath. In examining the other parameters, the IC, and TV had data correlation and processing issues that could not be resolved prior to publication, and thus not included. Overall, they showed the same patterns as the FVC. The testing was divided up into segments of baseline, pre-flight, post-flight and post egress as previously described. The

following figures and tables show the FVC over the ABS test sequence. Table 7.4.1 uses a box-plot to describe the grouped data at each of the test sequences and Table 7.4.2 is a summary of the results. The pattern reveals that a significant decrease in FVC occurs with donning AFE and seated in the aircraft. The following shows the overall results.

Table 7.4.1. FVC across observations: Flight Profiles A to D

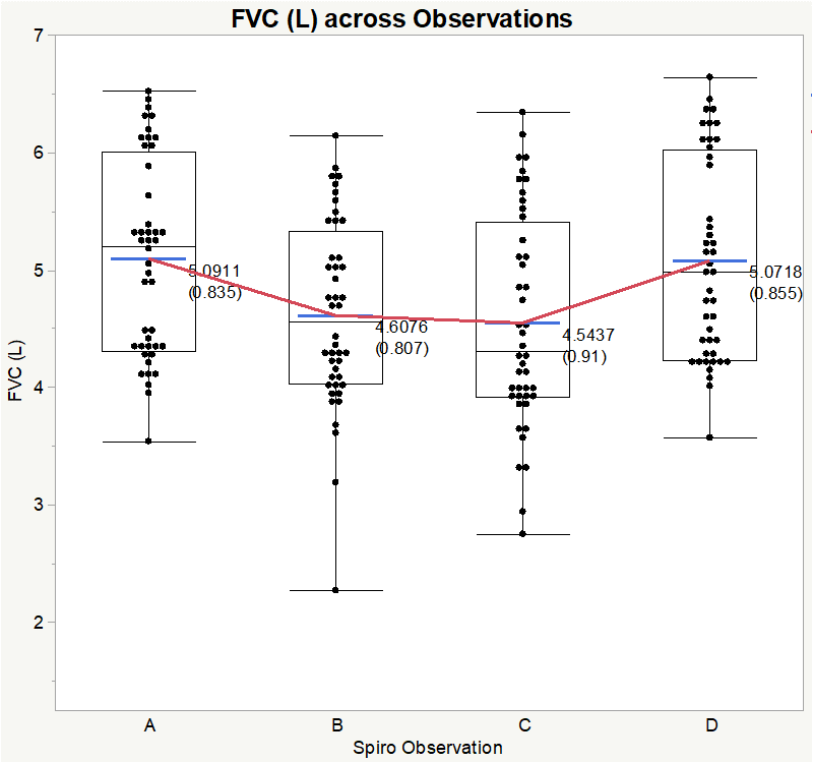

Table 7.4.2. FVC for Flight Profiles A-D

FVC (L) N = 44

Spiro Test	Mean	Std Dev	Min	Max	Range
All	**4.83**	**0.88**	**2.27**	**6.64**	**4.37**
A	5.09	0.83	3.54	6.52	2.98
B	4.61	0.81	2.27	6.14	3.87
C	4.54	0.91	2.75	6.34	3.59
D	5.07	0.86	3.57	6.64	3.07

The FVC shows a definite decrease in mean FVC with donning AFE and seated in the aircraft. Similar values but slightly diminished were obtained post flight with aircrew AFE in place and seated in the aircraft. FVC had essentially returned to baseline post doffing AFE, in the seated position, and in flight suit only.

FVC delta from baseline. This demonstrates the drop from baseline by using the mean of all individuals as the starting baseline as the zero point and using the mean drops in FVC to demonstrate the decreases from baseline. Seen side by side the overall FVC distribution and the delta from baselines are demonstrated by the following block diagrams and summary tables. The following tables illustrate the FVC expressed as a volume change from the baseline condition for the PBA Evaluation sequence. The data is summarized in following tables.

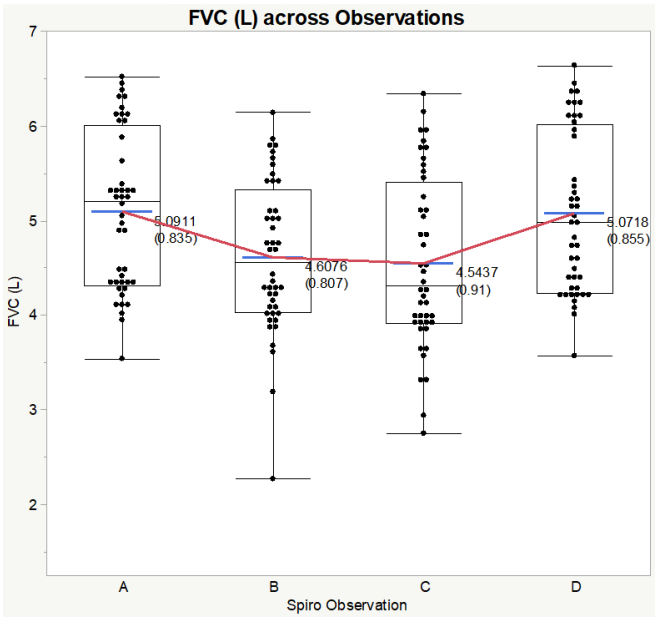

Figure 7.4.2. FVC Volume Changes from Baseline Condition Overall (Table 7.4.3) and Delta from Baseline (Table 7.4.4)
A = In flight suit
B = In flight suit in the gear
C = In flight suit in the gear, in the aircraft
D = In flight suit

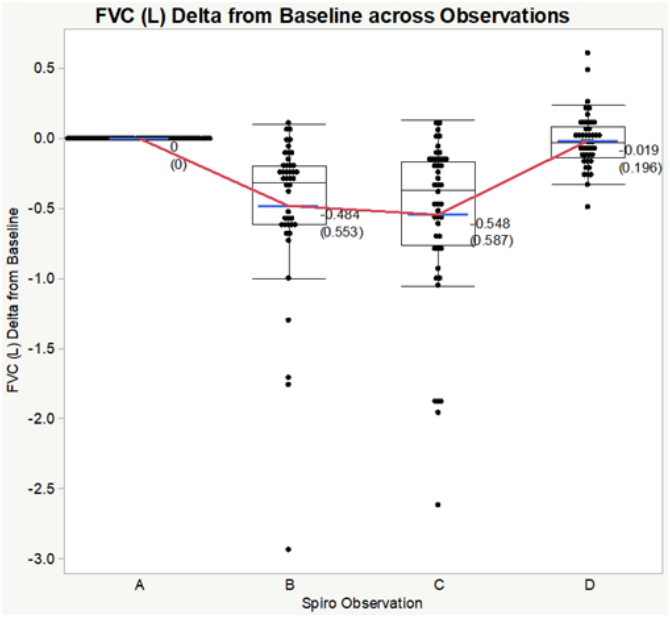

Figure 7.4.3. FVC Volume Changes from Baseline Condition Overall (Table 7.4.3) and Delta from Baseline (Table 7.4.4)
A = In flight suit
B = In flight suit in the gear
C = In flight suit in the gear, in the aircraft
D = In flight suit

Table 7.4.3. FVC Overall
Sequences A to D

FVC Overall

FVC (L) N = 44

Spiro Test	Mean	Std Dev	Min	Max	Range
All	**4.83**	**0.88**	**2.27**	**6.64**	**4.37**
A	5.09	0.83	3.54	6.52	2.98
B	4.61	0.81	2.27	6.14	3.87
C	4.54	0.91	2.75	6.34	3.59
D	5.07	0.86	3.57	6.64	3.07

Table 7.4.4. Delta from Baseline

FVC Delta from Baseline

FVC (L) N = 44

Spiro Test	Mean	Std Dev	Min	Max	Range
All	**-0.26**	**0.48**	**-2.94**	**0.61**	**3.55**
A	0	0	0	0	0
B	-0.48	0.55	-2.94	0.1	3.04
C	-0.55	0.59	-2.62	0.13	2.75
D	-0.02	0.2	-0.49	0.61	1.1

FVC Summary

Overall, the pattern of changes seen in the PBA demonstrated an impact related to donning AFE and strapping into the ejection seat. The data shows that, relative to baseline that the FVC in the baseline condition is higher than all other conditions. There is a significant difference in FRC wearing AFE compared to other conditions, except for the baseline condition. The FVC was diminished by 480 ml or 9.4%. FRC after flight was decreased in relation to the pre-flight condition. This is 550 ml, or 10.8 % from baseline, and 1.4% below the pre-flight FVC. The FVC after flight was increased after egressing the aircraft and after removing AFE.

The tables illustrates the fact that FVC expressed as a volume change from the baseline condition for the PBA Evaluation sequence a significant diminished pulmonary (lung) capacity existed prior to flight with just donning AFE and seated in the aircraft. This is further worsened after flight. The data shows that, relative to baseline FVC exhibits a reversal when egressing the cockpit and after removing AFE to essentially baseline. This shows a complete or near recovery to baseline pulmonary volumes.

Pulse Oximetry – SpO_2

Spirometry was performed serially using a Masimo Rad-97. This model provides noninvasive and continuous monitoring pulse oximetry and upgradeable rainbow SET™ technologies, including total hemoglobin (SpHb®) and acoustic respiration rate (RRa®). Parameters utilized were SpO_2, pulse rate, Perfusion Index, and PVi. The perfusion index indicates the strength of blood flow peripherally and serves to indicate the adequacy of the sensor to pick up the peripheral O. The PVi provides a continuous noninvasive measure of the relative variability during respiratory cycles. This is prominent as a dynamic indicator of fluid responsiveness in ICU patients of mechanically ventilated adult patients.

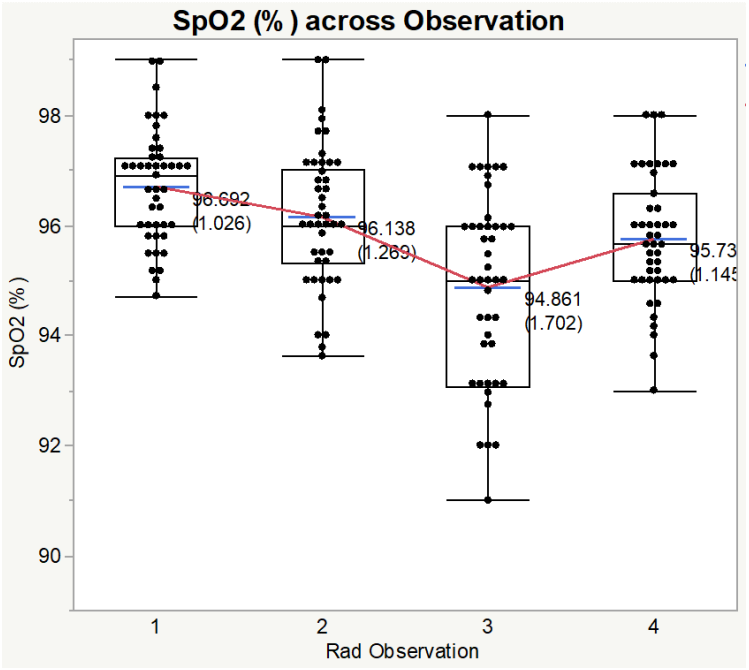

Figure 7.4.4. SpO_2 Across Measurement Sequence
A = In flight suit
B = In flight suit in the gear
C = In flight suit in the gear, in the aircraft
D = In flight suit

Table 7.4.5. Peripheral O_2 Saturation

SpO2% N = 43

Rad Test	Mean	Std Dev	Min	Max	Range
All	**95.86**	**1.46**	**91**	**99**	**8**
1	96.69	1.03	94.71	99	4.29
2	96.14	1.27	93.62	99	5.38
3	94.86	1.7	91	98	7
4	95.74	1.14	93	98	5

Sequences labeled at 1 to 4 in difference to FVC
1 = In flight suit
2 = In flight suit in the gear
3 = In flight suit in the gear, in the aircraft
4 = In flight suit

The overall SpO_2 shows a decrease with AFE donning and seated in the aircraft, but a physiologically significant drop post flight.

SpO_2 delta from baseline. This demonstrates the drop from baseline by using the mean at baseline as the zero point and using the mean drops in SpO_2 to demonstrate the decreases from baseline. Seen side by side, the delta from baselines are demonstrated by the following block diagrams and summary tables.

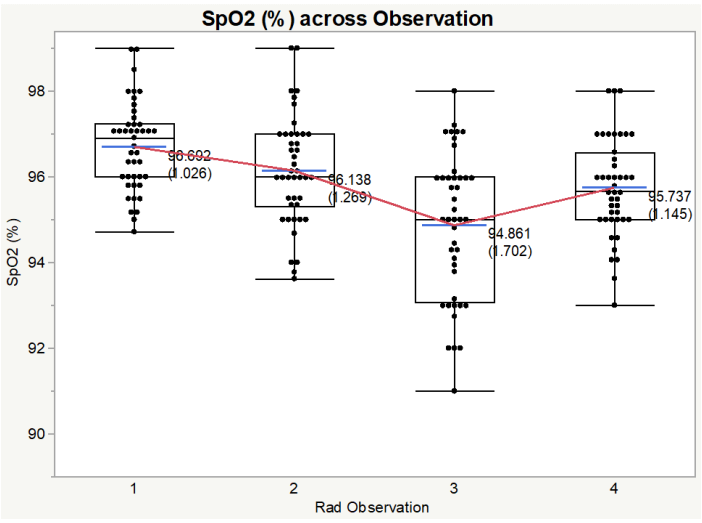

Figure 7.4.5. Peripheral O_2 Saturation Overall: Sequences labeled at 1 to 4

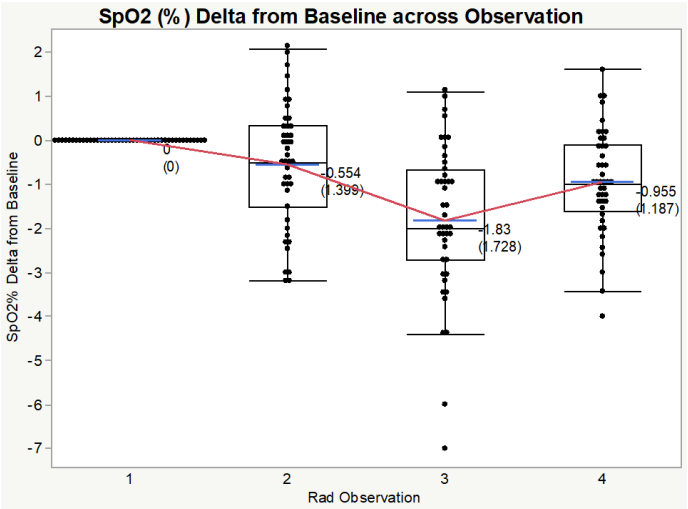

Figure 7.4.6. Peripheral O_2 Saturation Delta from Baseline: Sequences labeled at 1 to 4

Table 7.4.6. Peripheral O_2 Saturation Overall: Sequences labeled at 1 to 4

SpO2% Overall

SpO2% N = 43

Rad Test	Mean	Std Dev	Min	Max	Range
All	**95.86**	**1.46**	**91**	**99**	**8**
1	96.69	1.03	94.71	99	4.29
2	96.14	1.27	93.62	99	5.38
3	94.86	1.7	91	98	7
4	95.74	1.14	93	98	5

Table 7.4.7. Peripheral O_2 Saturation Delta from Baseline: Sequences labeled at 1 to 4

SpO2% Delta from Baseline

SpO2% N = 43

Rad Test	Mean	Std Dev	Min	Max	Range
All	**-1.11**	**1.54**	**-7**	**2.09**	**9.09**
2	-0.55	1.4	-3.19	2.09	5.28
3	-1.83	1.73	-7	1.09	8.09
4	-0.96	1.19	-4	1.61	5.61

Oximetry/SpO_2 deltas

Overall, the pattern of changes seen in the PBA evaluation of peripheral hemoglobin saturation demonstrated an impact related to donning AFE and strapping into the ejection seat. The data shows that, relative to baseline that the SpO_2 in the baseline condition is significantly higher than all other conditions. There is a significant difference in SpO_2 wearing AFE compared to other conditions, except for the baseline condition. The SpO_2 was diminished in relation to the pre-flight condition in all subsequent measurements. Oximetry at baseline had a median value of 96.69% and a range of 94.71% to 99%. Oximetry wearing AFE and strapped into the ejection seat was lower than the baseline condition. Oximetry measured after flight (mean 94.86%, range of 91-98%) was lower than baseline and the pre-flight measurements (mean 96.14%, range 93.62-99%). Oximetry increased but did not return to baseline (mean 95.74%) after egressing the cockpit and removing AFE. The post doffing values in fact were 0.96% lower with a range of 93-98%. The post flight and post doffing values < 93.5% represent significant physiological impacts and ventilation perfusion mismatches.

The lowest SpO_2 values and the lowest 10% SpO_2 were examined. These were divided by pilot and profile. The following tables and figures were generated.

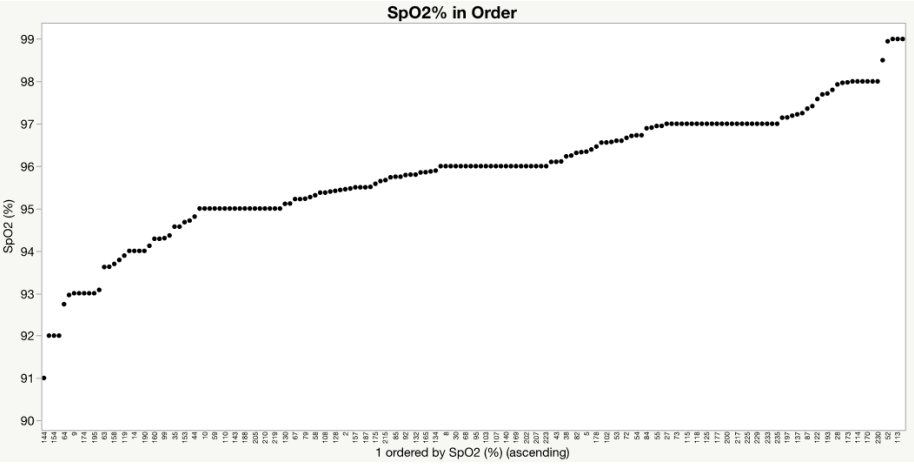

Figure 7.4.7. Lowest 10% SpO_2

Table 7.4.8. Lowest 10% SpO_2

SpO2% Lowest 10%		SpO2 (%)				
		N	Mean	Std Dev	Min	Max
	All	17	92.91	0.77	91	93.89
Pilot	12	7	93.28	0.46	92.74	93.89
	28	9	92.82	0.67	92	93.69
	71	1	91	.	91	91
Profile	B	5	93.41	0.51	92.74	93.89
	D	2	92.5	0.71	92	93
	E	5	92.53	1.05	91	93.69
	F	3	93.03	0.05	93	93.08
	H	2	92.81	1.15	92	93.63
Configuration	USAF	4	92.95	0.73	92	93.79
	USN	13	92.89	0.81	91	93.89

The vast majority of the lowest SpO_2 readings are in the USN configuration. These represent a mean of 92.89% peripheral hemoglobin saturation. Healthy individuals at sea level usually exhibit O_2 saturation values between 96% and 99%. On 100% O_2, the saturation or SpO_2 should be 99-100%. The mean saturation was 92.89%. This represents a pulmonary (lung) ventilation perfusion mismatch, which is a mismatch in ventilation and perfusion (lung circulation). As previously discussed. Alveolar gas exchange depends on the air movement to the alveoli, but also the flow of blood to the alveolar capillaries surrounding the alveoli. The O_2 saturation level below 93.5% seen in USN aircrew after flight is disconcerting. It was taken after the aircrew had been breathing air for an estimated time of less than 5 minutes after landing. This may have been more pronounced if measured during flight. Although this degree of hypoxia would not, if circulation was normal, by itself produce hypoxia-like symptoms. These values represent a significant physiological decrement that would degrade the physiological reserve and lower the threshold for developing hypoxia in flight. This lowers the threshold for developing a physiological event in the presence of concomitant reduction in physiological reserves.

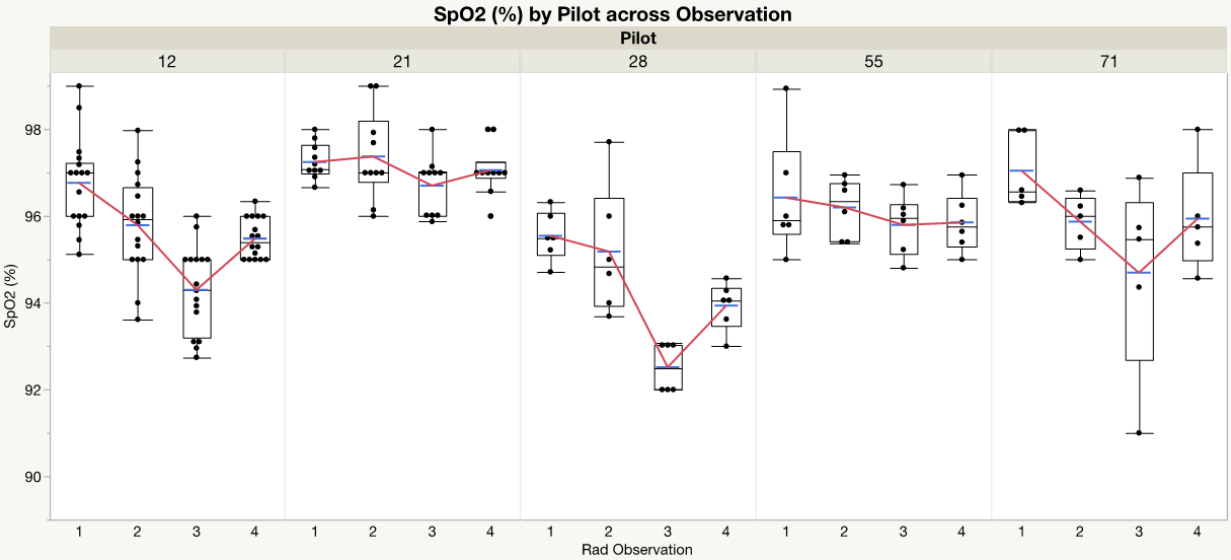

Figure 7.4.8. SpO_2 by Observation in Sequence

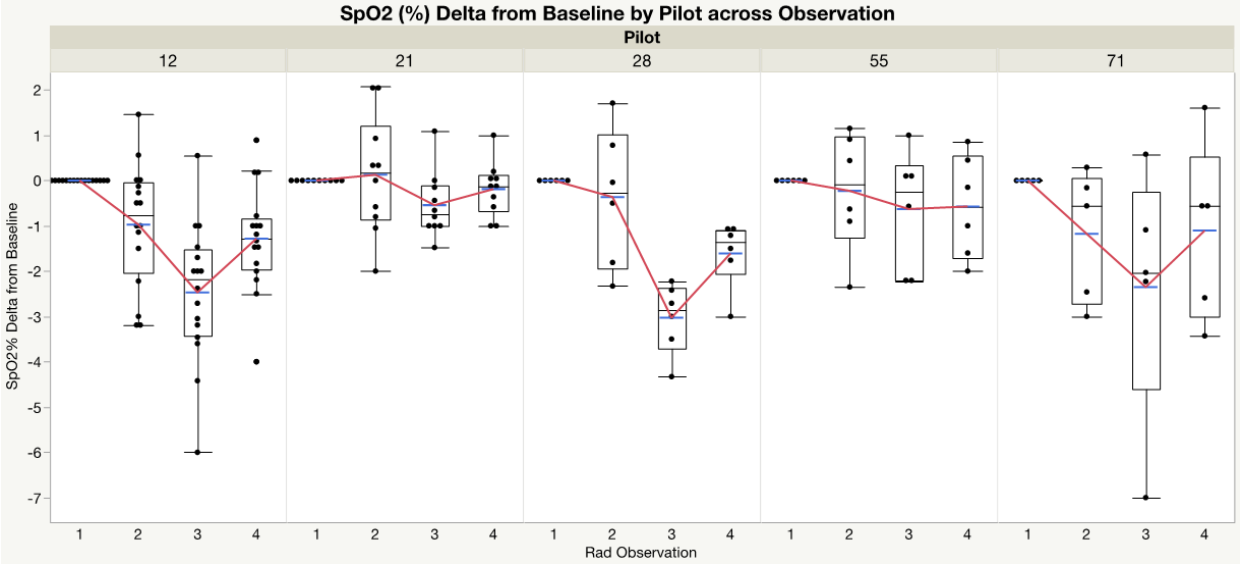

Figure 7.4.9. SpO_2 by delta from Baseline in Sequence

Oximetry Summary

Overall, the data indicates that aircrew experience a reduction in oximetry after flight that persists after egressing the aircraft and doffing the AFE. This is physiological significant in the USN configuration as the USN utilizes hyperoxic ranges of O_2 concentration in flight.

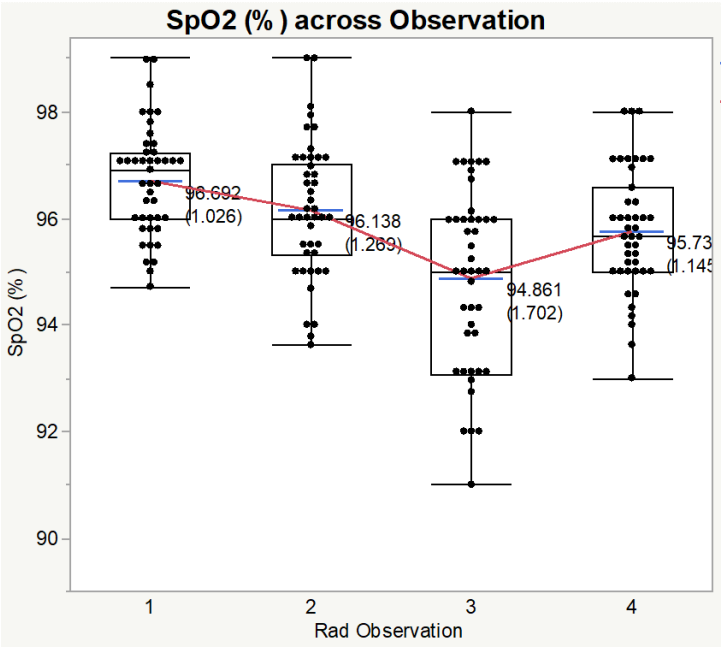

Figure 7.4.10. SpO_2 Across Observations in Sequence

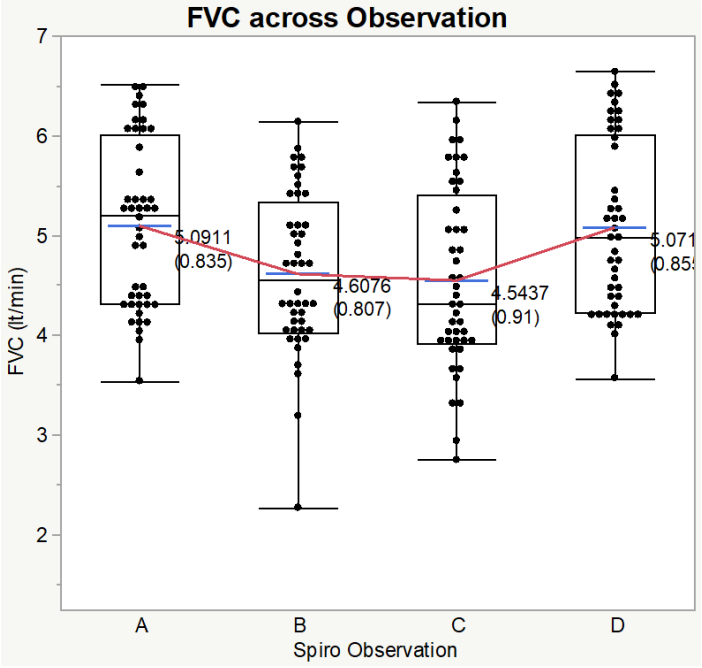

Figure 7.4.11. FVC Across Observations in Sequence

Table 7.4.9. SpO_2 Across Observations in Sequence

SpO2% N = 43

Rad Test	Mean	Std Dev	Min	Max	Range
All	**95.86**	**1.46**	**91**	**99**	**8**
1	96.69	1.03	94.71	99	4.29
2	96.14	1.27	93.62	99	5.38
3	94.86	1.7	91	98	7
4	95.74	1.14	93	98	5

Table 7.4.10. FVC Across Observations in Sequence

FVC (L) N = 44

Spiro Test	Mean	Std Dev	Min	Max	Range
All	**4.83**	**0.88**	**2.27**	**6.64**	**4.37**
A	5.09	0.83	3.54	6.52	2.98
B	4.61	0.81	2.27	6.14	3.87
C	4.54	0.91	2.75	6.34	3.59
D	5.07	0.86	3.57	6.64	3.07

There is significant inter-pilot variability that should be noted.

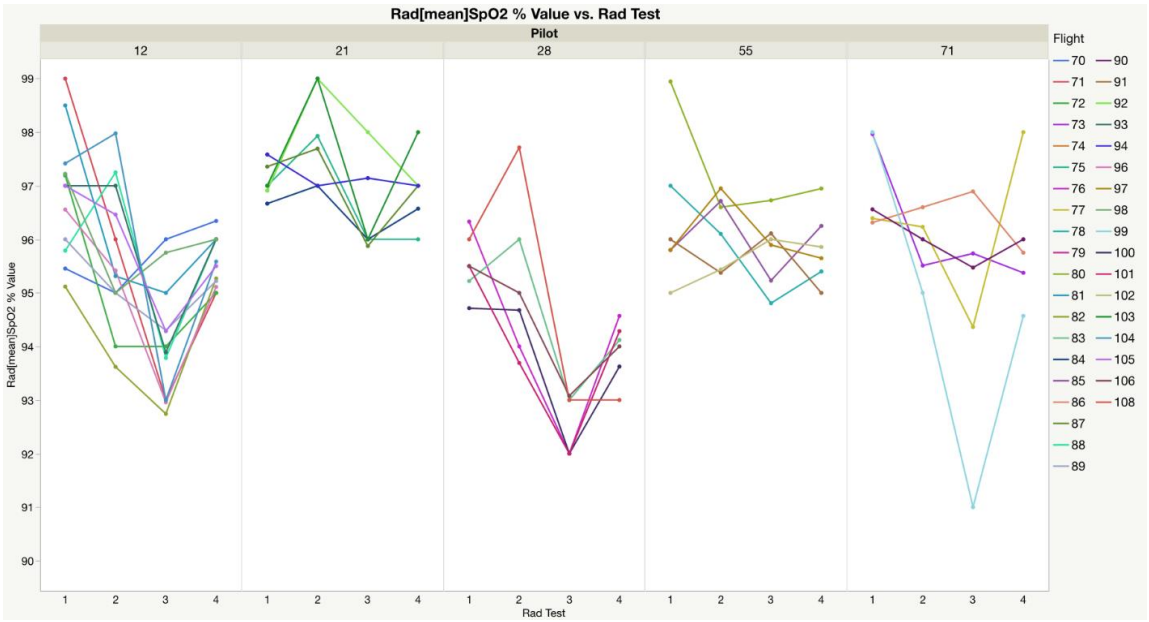

Figure 7.4.12. SpO_2 Inter-Pilot Variability

Overall, pilots 21 and 55 have generally very narrow ranges of effect by observation. The other pilots have significant post flight decrements in SpO_2.

Extended Spirometry

It was recognized that there were limitations in making comparisons between USAF and USN AFE configurations. Thus, a dedicated study on the two different configurations from baseline in flight suit only to pre-flight with AFE donned. The pilot or back seater were sitting in the cockpit, strapped into the ejection seat, with restraints and AFE adjusted as required for flight. The results from the extended spirometry are as follows.

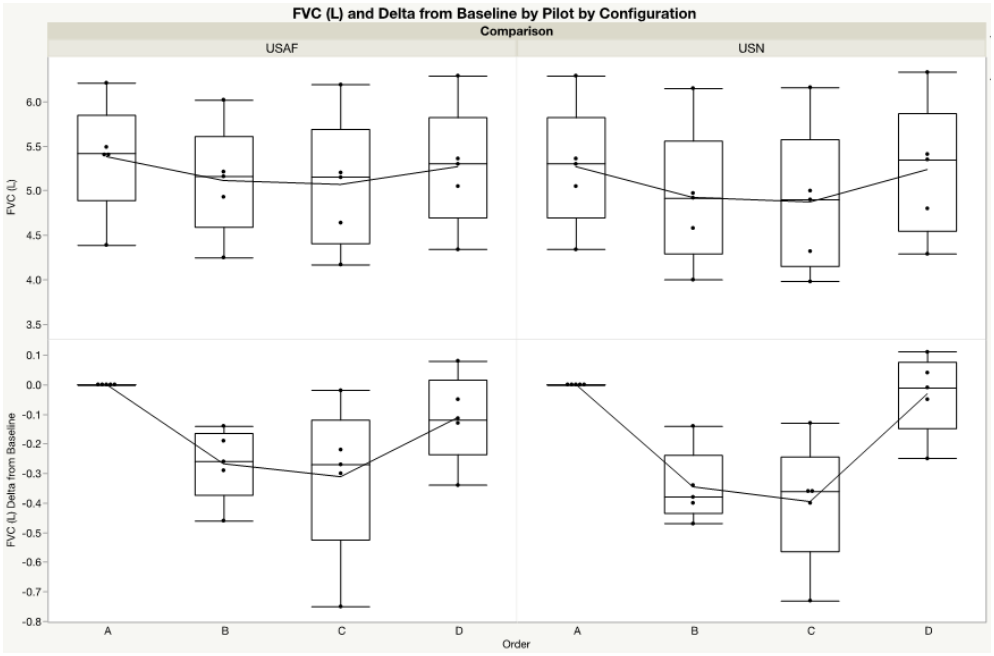

Figure 7.4.13. FVC observed and Delta from Baseline in Sequence and AFE Comparison

There were individual responses that can hide differences on cursory examination of the numbers.

Table 7.4.11. Delta FVC from Baseline in Sequence and AFE Compared

FVC (L)	A		B		C		D	
Pilot	**USAF**	**USN**	**USAF**	**USN**	**USAF**	**USN**	**USAF**	**USN**
All	5.38	5.27	5.11	4.92	5.07	4.87	5.27	5.24
12	4.39	4.34	4.25	4.00	4.17	3.98	4.34	4.29
21	6.21	6.29	6.02	6.15	6.19	6.16	6.29	6.33
28	5.39	5.05	4.93	4.58	4.64	4.32	5.05	4.80
55	5.49	5.36	5.20	4.96	5.19	5.00	5.36	5.35
71	5.42	5.30	5.16	4.92	5.15	4.90	5.30	5.41

- A = In flight suit
- B = In flight suit in the gear
- C = In flight suit in the gear, in the aircraft
- D = In flight suit

But a closer examination of the deltas from baseline, reveals a definite difference in USAF and USN configurations of AFE and being seated in the aircraft.

Figure 7.4.14. Delta FVC from Baseline in Sequence and AFE Compared

Again, the graphic demonstration in Figure 7.4.14 is the FVC by pilot number, the line graphs are the AFE configuration and the sequence is denoted by

- A = In flight suit
- B = In flight suit in the gear
- C = In flight suit in the gear, in the aircraft
- D = In flight suit

Table 7.4.12. Delta FVC from baseline in sequence and AFE configurations compared

Delta from Baseline	A		B		C		D	
Pilot	**USAF**	**USN**	**USAF**	**USN**	**USAF**	**USN**	**USAF**	**USN**
All	0	0	-0.27	-0.35	-0.31	-0.40	-0.11	-0.03
12	0	0	-0.14	-0.34	-0.22	-0.36	-0.05	-0.05
21	0	0	-0.19	-0.14	-0.02	-0.13	0.08	0.04
28	0	0	-0.46	-0.47	-0.75	-0.73	-0.34	-0.25
55	0	0	-0.29	-0.40	-0.30	-0.36	-0.13	-0.01
71	0	0	-0.26	-0.38	-0.27	-0.40	-0.12	0.11

The delta FVC were then compared by percentages.

Table 7.4.13. Percent Delta FVC from Baseline in Sequence and AFE Configurations Compared

FVC (L) % Change	Delta 1-2		Delta 1-3		Delta 1-4		Delta 2-3		Delta 3-4	
Pilot	**USAF**	**USN**	**USAF**	**USN**	**USAF**	**USN**	**USAF**	**USN**	**USAF**	**USN**
All	-5.28%	-7.36%	-6.56%	-8.68%	3.93%	7.18%	-1.16%	-1.19%	3.93%	7.18%
12	-3.29%	-8.50%	-5.28%	-9.05%	3.92%	7.23%	-1.92%	-0.50%	3.92%	7.23%
21	-3.16%	-2.28%	-0.32%	-2.11%	1.59%	2.69%	2.75%	0.16%	1.59%	2.69%
28	-9.33%	-10.26%	-16.16%	-16.90%	8.12%	10.00%	-6.25%	-6.02%	8.12%	10.00%
55	-5.58%	-8.06%	-5.78%	-7.20%	3.17%	6.54%	-0.19%	0.80%	3.17%	6.54%
71	-5.04%	-7.72%	-5.24%	-8.16%	2.83%	9.43%	-0.19%	-0.41%	2.83%	9.43%

Delta 1-2 compares individual baseline to post donning AFE. Here the USN is 2.08% lower than the USAF configuration.

Delta 1-3 compares individual baseline to being seated and strapped into the aircraft with AFE. Here the USN is 2.12% lower than the USAF configuration.

Delta 1-4 compares individual baseline to post doffing and egressed from the aircraft. Both USAF and USN still have not returned to baseline. Here the USN is 2.12% lower than the USAF configuration.

Delta 2-3 compares post donning AFE to being strapped into the aircraft with AFE.

The pattern of changes for the USN configured aircrew versus USAF configured aircrew cohort indicate that the USN AFE cohort experience a greater reduction in FVC when donning their torso harness, followed by a lesser reduction when strapping into the ejection seat. The USAF AFE cohort also experience a reduction when donning their AFE, followed by a smaller reduction when strapping into the ejection seat. This is consistent with the relative importance of tightening the torso harness with its more upper body restriction for USN AFE vs USAF AFE when connecting to the parachute harness. Notwithstanding differences previously outlined, the combined effect of donning AFE and strapping into the ejection seat results in similar reduction of FVC in both cohorts. The reduction of FVC seen after doffing and egressing the aircraft is returning to but has not returned to baseline. FVC wearing properly fitted AFE is lower than baseline, although the USN AFE configuration was definitely more pronounced. The USN configuration chest expansion is affected more by the torso harness than the seat restraint used in

the USAF configured aircrew. This likely reflects that the parachute restraint is integrated into the USN torso harness, then the USAF pelvis centric restraint system.

Inflight Analysis

Asynchrony: is a pervasive problem in in management of critical care patients, but it also as demonstrated in PBA as a contributing factor in aircrew breathing systems. Asynchrony has been previously discussed. The primary form delineated in PBA is the asynchrony (dyssynchrony) that involves timing of mechanical triggering of the system to the pilot's individual breaths. One type of asynchrony is defined as the triggering or cycling of a breath that either leads or lags the pilot's inspiratory effort. Regarding the size of a breath, asynchrony means the inspiratory flow or TV does not match the patient's demand (too much/little, too early/late). Asynchrony will lead to increased work of breathing, excessive fatigue of respiratory muscles, and non-specific respiratory discomfort. Volume and flow mismatches can cause micro-trauma in the form of barotrauma due to alveolar over distention even if the pressures are not excessive in the traditional sense of high PIP/PEEP. Asynchrony is a subtle problem for which patients have no way to perceive or communicate its presence directly.

As introduced previously, the Phase Shift as an analysis tool, measuring temporal and correlative disharmony between the driving pressure and response flow. Pressure-Flow Disharmony is the mismatch between the pressure profile and the flow profile, including start/stop times and the time it takes to reach the peak (maximum). Phase Shift in degrees builds on finding the optimal time-shift between 2 signals and takes in consideration the length of the exhale. Since breath time varies with every breath, analysis can normalize each breath by its length such that the breath phase length totals 180 degrees. Negative phase shifts indicate that mask pressure peaks before the flow peaks. Positive phase shifts indicate that flow peaks before mask pressure peaks. The phase shift is detailed fully in the section on the metrics to characterize Pressure-Flow disharmony. In addition to phase shift, hysteresis is also a measure of the 'synchrony' between the pilot and the breathing system. The line hysteresis measures the asynchrony between the demand signal received by the regulator and the regulator supply. The mask hysteresis represents the asynchrony between the pilot demand and the regulator supply. Ideally the hysteresis is low, and the mask and line hysteresis are equal, signifying that the pilot demand, regulator demand signal and regulator supply are in good harmony. This was not the case for flights 19 and 29 (FLT-017, FLT-029).

Hysteresis is measured in liters per second (lps). The PBA team established that breath hysteresis should be $\leq$ 0.30 lps before significant asynchrony occurs and tidal volumes were demonstrably reduced. The USAF configurations averaged 0.10 lps with few breaths over 0.30 lps. USN is typically values of 0.40 lps with few values over 0.60 lps. Flight 17 (FLT-017) had an average of 0.70 lps and a large number of breaths over 1.0 lps.

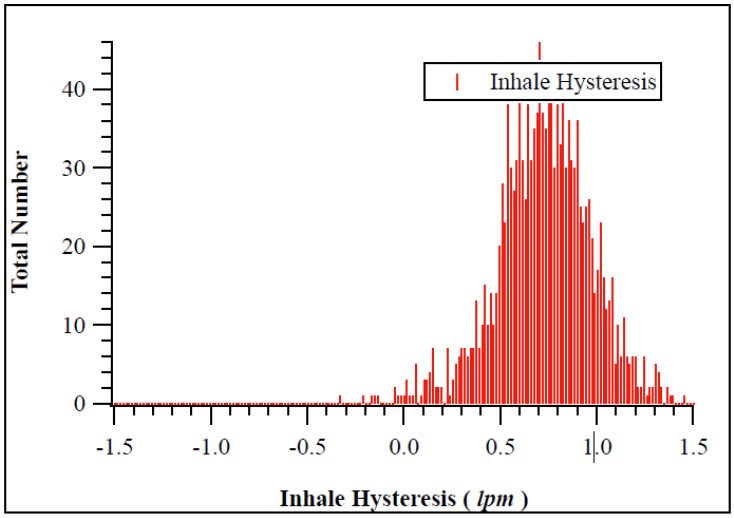

Figure 7.4.15. Inhale Hysteresis FLT-017

In data summary you can see the chaotic nature of the hysteresis, as well as Line Mask Differential Pressures, and Breath Mid-pressures for FLT-017.

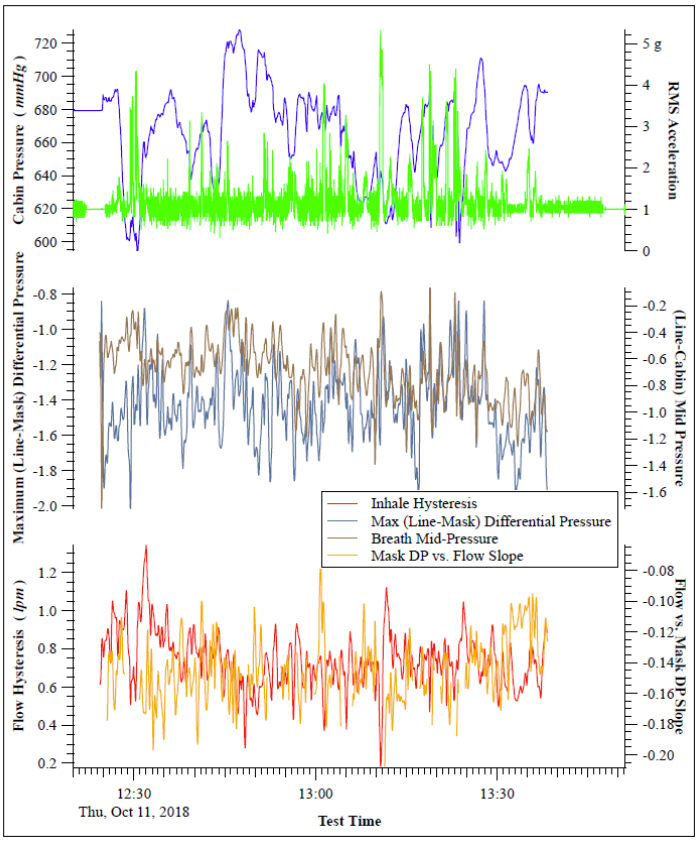

Figure 7.4.16. Breathing summary FLT-017

This is a clear demonstration of the often chaotic breathing patterns inflight as compared to the baseline ground breathing or the regular sinusoidal breathing pattern historically simulated for testing.

Examination of Flight 29 (FLT-029) revealed a significant of breathing asynchrony or hysteresis.

	Cabin	Mask
Mean Hysteresis (lps)	0.541	0.678
Standard Deviation (lps)	0.297	0.434
Fraction > 0.50 lps	0.720	0.770
Fraction > 0.75 lps	0.156	0.499
Fraction > 1.00 lps	0.013	0.170

Again, notice respiratory rates and minute volumes increasing significantly in response to a stressor.

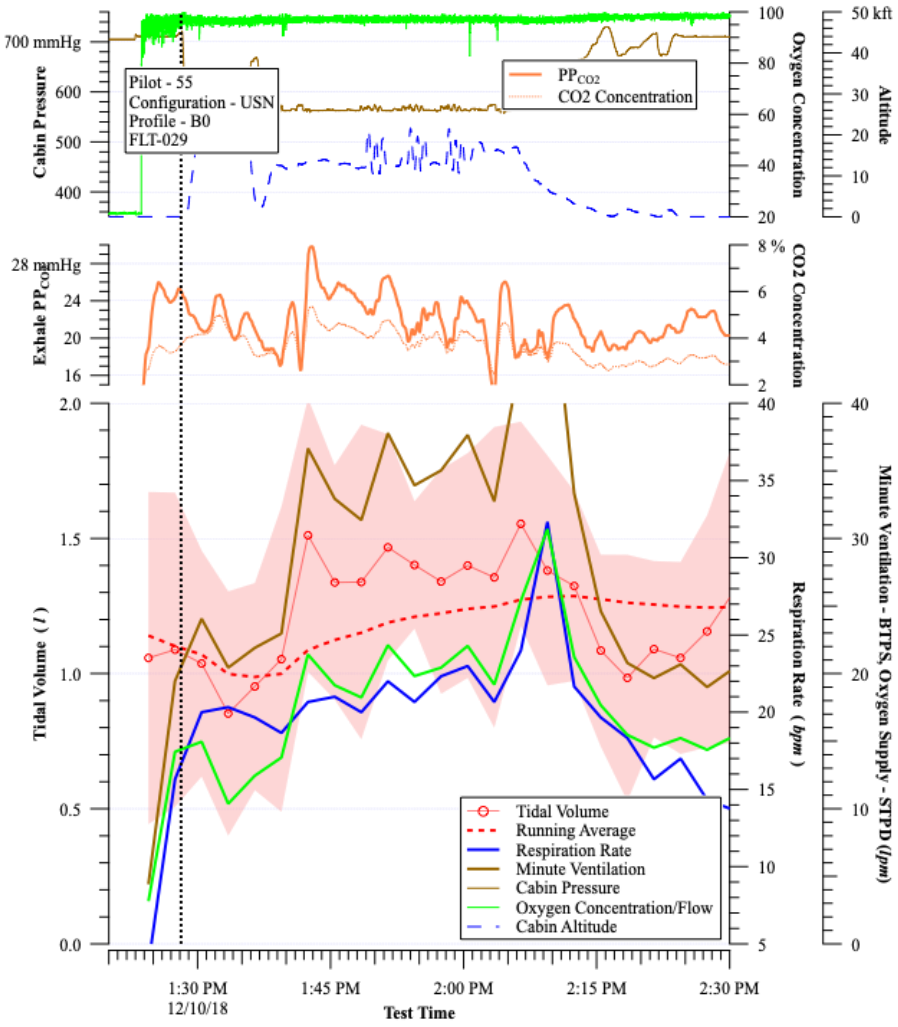

Figure 7.4.17. Breathing Summary T, PCO_2 and Cabin P: FLT-029

One should note the O_2 flow also followed the minute ventilation. Note the rapid drop off of tidal volume right before the increase in minute ventilation. Hysteresis showed parameters outside of the normal values.

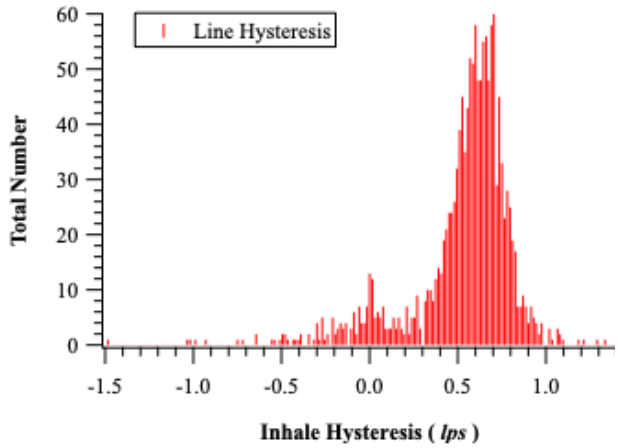

Figure 7.4.18. Inhale Hysteresis FLT-029

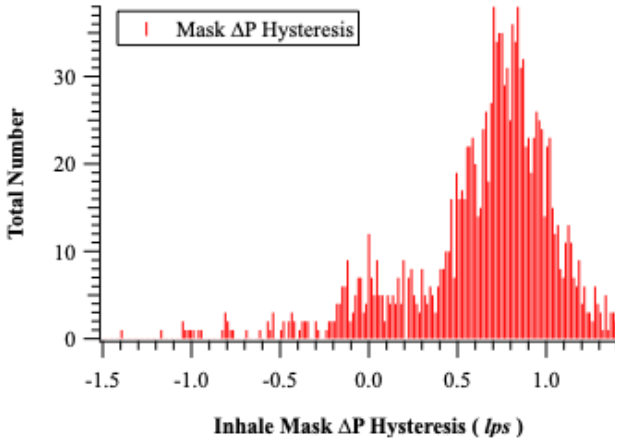

Figure 7.4.19. Mask ΔP Hysteresis FLT-029

Flight 29 has an in-depth analysis elsewhere in this report. An overview of findings elucidated significant impacts to tidal volume. Despite the drive to increase minute volumes, it was shown that diminishing flow impacted inhaled and exhaled tidal volumes. There was a decrease in exhaled volume and secondarily a decrease in inhaled volume. In essence, the alveoli were trapping air and increasing dead space or non-gas exchanged air. This results in limiting the volume available for inhalation. In this particular segment, the mask pressures indicated increased effort with line pressures still fairly high and there should have been concomitant flow with this effort. The flow should match this effort fairly well, but this is indicating decreasing tidal volumes. So intuitively the effort or "work" of breathing is increased, but not matched with flow. With the pressures being fairly high in relationship to natural air way pressures, there is likely some airway collapse. This coupled with the tidal volume decreases would result in limiting total alveolar volume. This would be symptomatically perceived as lack of flow. There were also significant large pressure peaks, which should vastly increase the flow relative to the effort. These are well above normal airway pressures of 3-5 mmHg. The increasing pressures should have had a flow continuously with the pressures generated. Instead the tidal volumes were consistent and lower. There should have been increased tidal volumes with the pressure increases, but instead they were fairly even and indicated restricted flow. The decreased inhalational tidal volumes do not fill the alveoli adequately and thus resulted in diminished exhaled volume. This indicates that the remaining alveolar volume is physiological dead space. Thus, the pilot's perception of cannot exhale completely, due to inadequate volume in the alveoli and airways to adequately exhale. Unfortunately, flights 17 and 29 were in the technical evaluation phase of VigilOX, and detailed Ground physiology measures were not in place due to delayed equipment acquisition. While the preflight measurement of physiological reserve decreases was not compared to the inflight measurements, the Inflight measurements gave great insight into pressure and flow disturbances and the reduction in tidal volumes. One aspect that may prove insightful is the hysteresis divided by peak flow. This should be investigated in future publications.

Tidal volumes in flight.

The sensor package also gives insight into physiological responses to reductions in tidal volumes. For flight analysis, the baseline was established as the 3-minutes of steady breathing before take-off. The convention was to utilize a portion before take-off of a breathing a section

of a 3 minute “clean (no talking, mask off) window”. This gave a good starting condition of breathing tidal volumes. As has been demonstrated the preflight pilot condition has a reduction of FVC (Forced Vital Capacity) and O_2 saturations observed in aircrew strapped into the ejection seat. This represents a generic effect of the physical constraints and should be taken into account for analysis.

The following quite clearly shows the increases in respiratory rate to improve minute volume in response to tidal volume reductions. In the following chart you can see reductions in tidal volumes, ventilation rates, and O_2 supplied rates. Again, this is FLT-017.

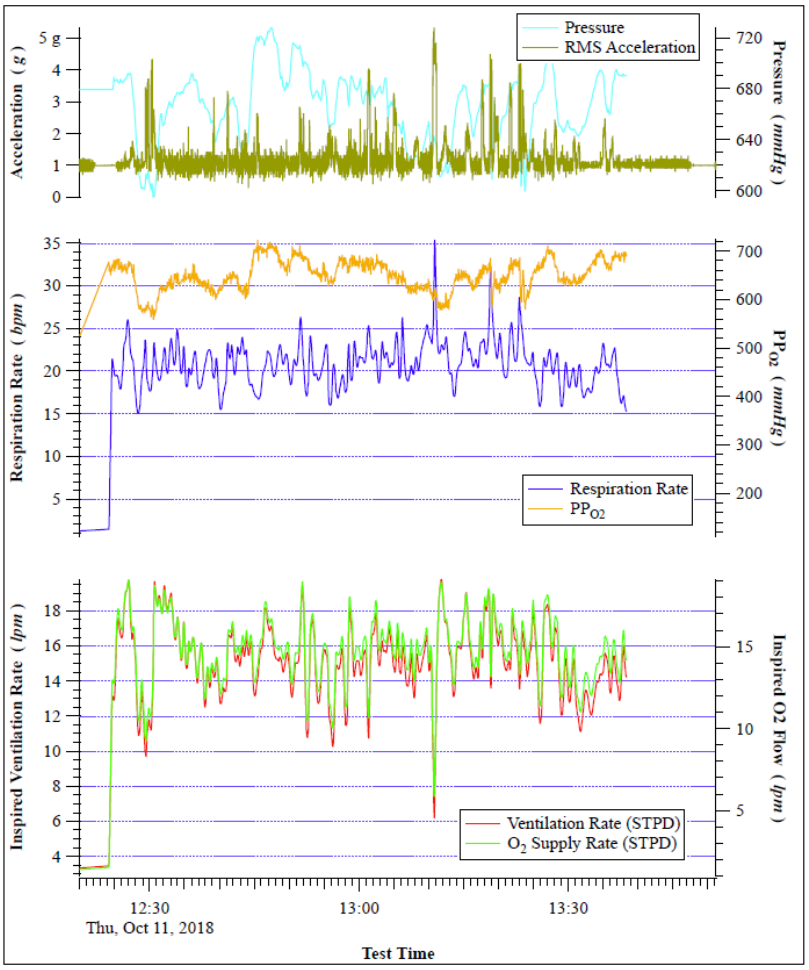

Figure 7.4.20. Ventilation Rate, Respiratory Rate and G Load Comparison in FLT-017

The following clearly shows the increases in respiratory rate to improve minute volume in response to tidal volume reductions.

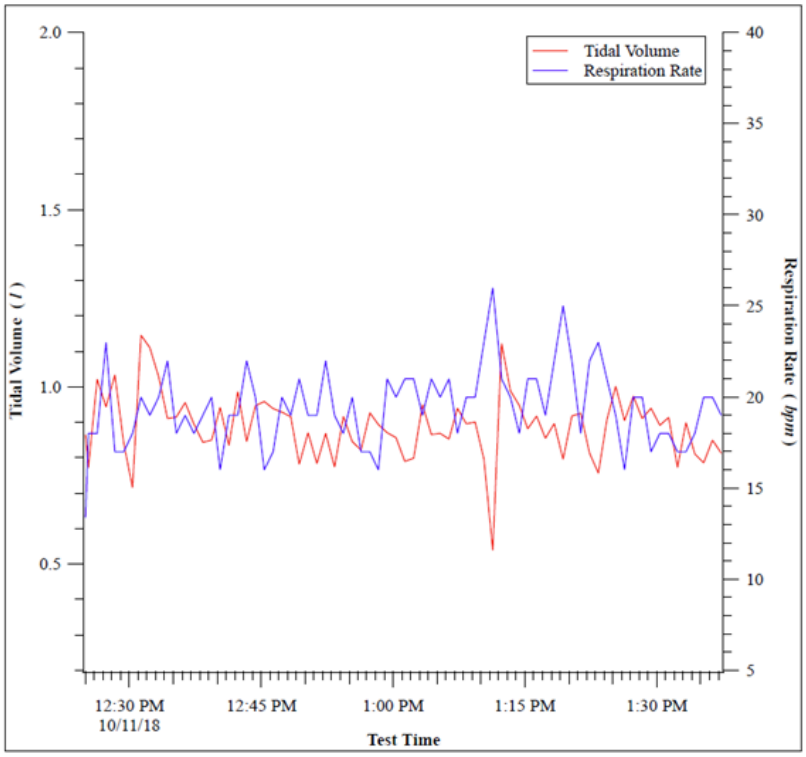

Figure 7.4.21. Respiratory Rate and Tidal Volume in FLT-017

This demonstrates a clear pilot physiological response to increase the minute volume but met with a reduction in supplied volume. With responding to a higher G_z Load, the rate and/or the depth of breathing increases to meet the demand. Under 4-5 G's the rate and depth of breathing are increased to meet the demand imposed. This is breathing for G's as opposed to G straining at higher (>5-6 G_z) and can be in association with increased constant feed pressure (Pressure Breathing for G's – PBG). Here you can see the increase in respiratory rate for the G's < 5, but the corresponding increases in tidal volume are not increasing. In response to aircraft maneuvering and increased acceleration, there should be an increase in minute volume to compensate for physiological stressors. This is not occurring and implicates a lack of system response. At higher G's (>5-6) the title volume can decrease due to the increased chest wall pressure and the abdominal bladder of the anti-G suit inflates which prevented the diaphragm from fully moving downward. Noted after the G maneuvers there is an increased demand in tidal volumes for metabolic recovery from elevated G_z. This is an implication of lack of system response to increased demands, and an investigation of causality of the tidal volume reversals should be undertaken.

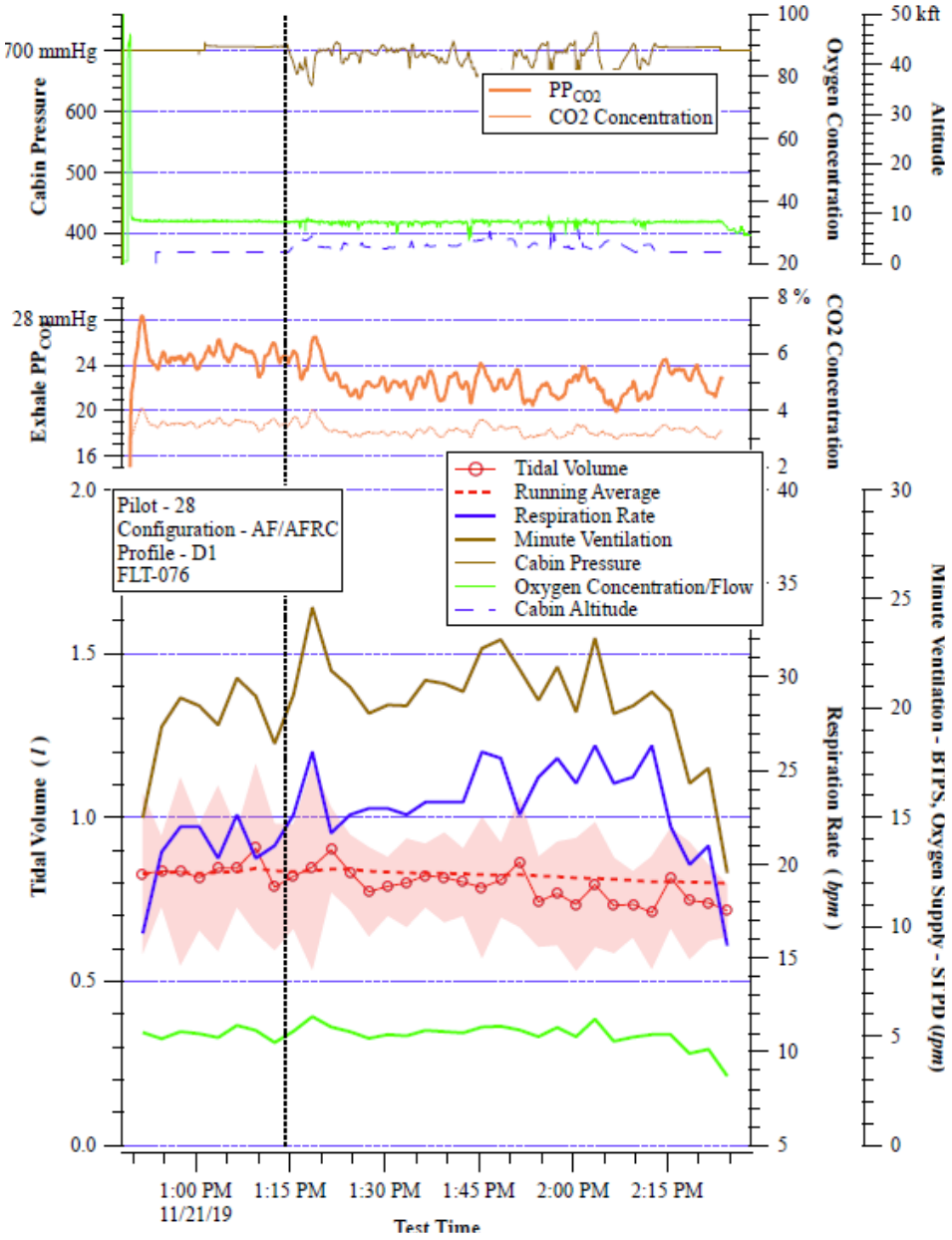
700 mmHg
600
500
400
Cabin Pressure
100
80
60
40
20
Oxygen Concentration
50 kft
40
30
20
10
0
Altitude
PPCO2
CO2 Concentration
28 mmHg
24
20
16
Exhale PPCO2
8 %
6
4
2
CO2 Concentration
Tidal Volume
Running Average
Respiration Rate
Minute Ventilation
Cabin Pressure
Oxygen Concentration/Flow
Cabin Altitude
Pilot - 28
Configuration - AF/AFRC
Profile - D1
FLT-076
2.0
1.5
1.0
0.5
0.0
Tidal Volume (l)
40
35
30
25
20
15
10
5
Respiration Rate (bpm)
30
25
20
15
10
5
0
Minute Ventilation - BTPS, Oxygen Supply - STPD (lpm)
1:00 PM
11/21/19
1:15 PM
1:30 PM
1:45 PM
2:00 PM
2:15 PM
Test Time

(a)

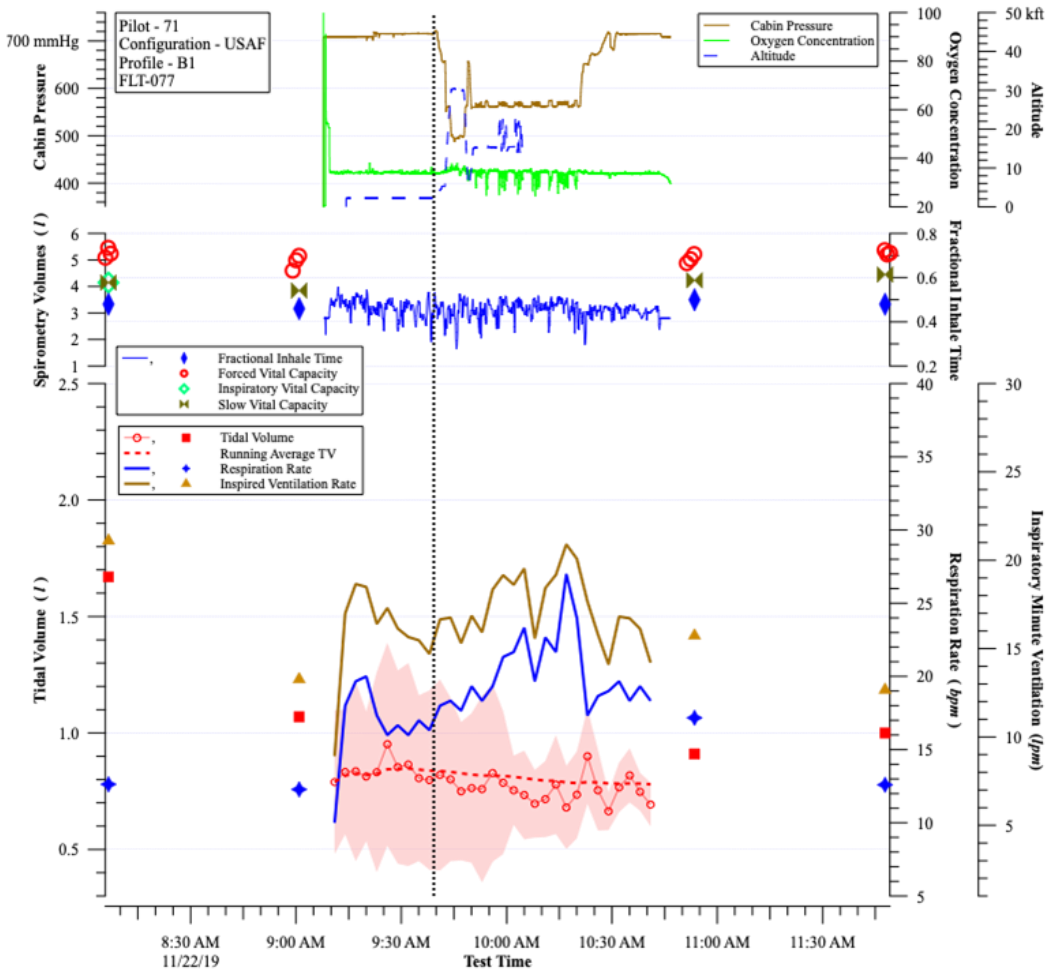

(b)

Figure 7.4.22. a) FLT-079 and b) FLT-077

These figures demonstrate a clear pilot physiological response to a reduction in supplied volume. The respiratory rate and minute ventilation are increasing with a gradually decreasing tidal volume. This is an indication of some type of respiratory asymmetry occurring. The rate and minute volume of the pilot are increasing to maintain the tidal volume from the system. This can be restricted flow, or hysteresis in the system. Note that the FLT-079 is a D profile with very little G_z and clearly shows the physiological response with a decreasing tidal volume with no G effect.

Low tidal volumes require the pilot to make up and maintain Vital Capacity, and thus leads to a higher respiratory rate. This physiologic strategy is used to preserve oxygenation and prevent the gradual increase in CO_2 and excessive hypercarbia (abnormally high level of CO_2 in the circulating blood). Blood carbon dioxide ($PaCO_2$) levels generally vary inversely with minute volume. A typical healthy adult will alter minute volume in an attempt to maintain physiologic homeostasis. A normal minute volume while resting is about 5–8 liters per minute in humans. Minute volume generally decreases when at rest and increases with exercise. For example, during light activities minute volume may be around 12 liters. Riding a bicycle increases minute ventilation by a factor of 2 to 4 depending on the level of exercise involved. Moderate exercise

can generate between 40 and 60 liters per minute. PBA has shown instantaneous flow up to 218 L/min in the aerobatics flight regime up to +5 G_z.

Initial examination of the relationship of tidal volumes to flight profiles, Profile A had the worst reductions. This was up to 40.5% decrease in TV maximum.

Table 7.4.14. Relationship of Tidal Volumes to Flight Profiles

FLT-xxx	*50*	*55*	*56*	*61*	*70*	*86*
Pilot	*28*	*12*	*28*	*21*	*12*	*71*
Configuration	*USN*	*USAF*	*USAF*	*USN*	*USAF*	*USAF*
Pre-Flight TV (l)	0.829	0.876	0.884	1.063	0.908	0.822
Mid-Flight TV (l)	0.628	0.575	0.584	0.716	0.540	0.616

Profile B had typically constant or increasing TV owing to the increased metabolic demand of the higher G_z profile. PBA has revealed that by delivering an unpredictable amount of flow at the beginning, middle, and end of each breath and that it changed from breath-to-breath. Such rapid changes in the breath-to-breath supply forces the pilot to continually compensate by adjusting breathing rate, volume, and exhale/inhale force. A detailed examination of the tidal volumes in flight is another open item unable to be fully accomplished due to the time restriction on production of the PBA report.

Limitations

The spirometric and oximetry measurements have been described in terms of their mean or median values, describing the central tendency of a population. Central tendency is defined as a statistical measure that identifies a single value as representative of an entire distribution. It aims to provide an accurate description of the entire data. Standard deviation describes the distribution of measures around the mean. However, central tendencies and distribution may not accurately describe the extent to which lung function is affected in some individuals. PEs are noted to be infrequent events affecting individuals in isolated events. This is in contrast to whole populations of pilots on the majority of sorties. Thus, it is likely that the critical focus should be on the physiological response of some individuals to dynamic flight as opposed to the group effects. This was also noted in the RAAF IAM study, *Characterisation of the Impact of the Super Hornet and Growler Flight Environment on Lung Function*. "The observation that *most aircrew* do not experience an adverse response to the flying environment does not provide any reassurance that physiologically-significant changes may be present in *some individuals*; measuring trends in the 25th percentile (or other agreed measure) promotes focus on non-central responses." Direct quartile separation of the individuals was not able to be performed due to the time limitations imposed to publish the report. This should be performed in a subsequent peer reviewed article.

Ref Sec XII 332-335

A brief look at the SpO_2 and focusing on some of the individual results, some dramatic drops in oximetry data for 3 of the pilots. Pilots 12 and 71 had dramatic drops of 6% and 7% saturations.

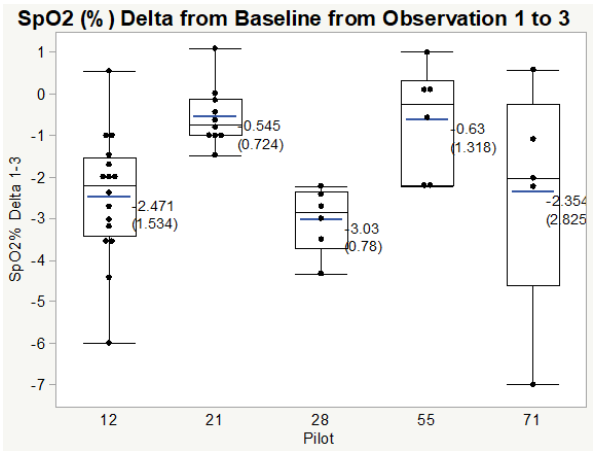

Figure 7.4.23. Pilot SpO_2 Deltas from baseline

Table 7.4.15. Pilot SpO_2 Deltas from baseline

		SpO2% Delta 1-2				SpO2% Delta 1-3				SpO2% Delta 2-3				SpO2% Delta 1-4				SpO2% Delta 3-4			
Pilot	N	Mean	Std Dev	Min	Max	Mean	Std Dev	Min	Max	Mean	Std Dev	Min	Max	Mean	Std Dev	Min	Max	Mean	Std Dev	Min	Max
All	43	-0.55	1.4	-3.19	2.09	-1.83	1.73	-7	1.09	-1.28	1.54	-4.98	1	-0.96	1.19	-4	1.61	0.88	1.17	-1.14	3.64
12	16	-0.98	1.36	-3.19	1.46	-2.47	1.53	-6	0.55	-1.49	1.62	-4.98	1	-1.28	1.16	-4	0.89	1.19	0.95	0	2.58
21	10	0.13	1.31	-2	2.09	-0.55	0.72	-1.48	1.09	-0.67	1.31	-3	1	-0.19	0.59	-1	1	0.36	0.84	-1	2
28	6	-0.37	1.53	-2.33	1.71	-3.03	0.78	-4.33	-2.22	-2.67	1.12	-4.71	-1.69	-1.61	0.73	-3	-1.09	1.42	0.95	0	2.57
55	6	-0.23	1.32	-2.35	1.15	-0.63	1.32	-2.22	1	-0.4	0.99	-1.48	0.74	-0.57	1.14	-2	0.86	0.06	0.74	-1.11	1.02
71	5	-1.18	1.46	-3	0.29	-2.35	2.82	-7	0.58	-1.18	1.8	-4	0.29	-1.11	1.97	-3.43	1.61	1.25	2.23	-1.14	3.64

An in-depth analysis of the tidal volumes, hysteresis, and FVC changes in relationship to flight profiles and ALS configuration needs to be undertaken. Again, this was unable to be accomplished due to urgency of report completion and should be the subject of a subsequent technical or scientific peer reviewed paper.

When strategies are developed to prevent, control, or reverse the conditions that can contribute to PEs, the rationale needs to encompass the entire range or individuals. Thus, these interventions must include the ones at the extreme range (the outliers) as well as the impacts to all aircrew. The measures of central tendency may be adequate to describe a population as a whole and can serve as a baseline for observations. Caution must be maintained to consider factors that may place certain aircrew at risk are operationally significant at the boundaries of human endurance. This paradigm is essential, and the aeromedical communities must examine all relevant data and develop a consensus to abate PE risk factors. This must be performed in a manner that retains focus on sub-elements of the aircrews.

The study is unable to quantify the effects seen in the USN cohort that are attributable to the torso configuration, breathing near-100% O_2, or the compounding effect of high-G exposure. This analysis also does not examine the effects of oscillating O_2 pressures such as seen in the F-35 or T-6. This investigation is unable to quantify the effects seen in the USAF cohort that are attributable to the AFE, or the compounding effect of high-G exposure. These need to be examined in centrifuge and comparative in flight studies. As designed the pilots were to have body plethysmography to have a baseline of all lung volumes, but due to COVID-19 restrictions, this was substituted by ground spirometry. Spirometry provided the measure of pulmonary (lung) volume baseline and was a consistent technique to reference for all changes seen. Standardized methods were used and repeatable. The body plethysmography would have given an insight into the total lung volumes and physiological boundaries of the study pilots and should be considered in further explorations of the ABS techniques.

Inadequate sortie numbers

The study did not have enough sorties to examine in detail the differences in profile or configuration in flight. It was recognized early that the amount of sorties would not delineate configuration differences of the AFE. Thus, the extended spirometry ground profile was developed. The graphic representations in Figure 7.2.24 reveals the sparse data and empty cells that indicate that each pilot did not perform all the sorties, did not have comparative flights of USN and USAF configurations. This resulted in an imbalanced study. Unfortunately, finances limited number of flights that would have taken to perform a completely balanced study.

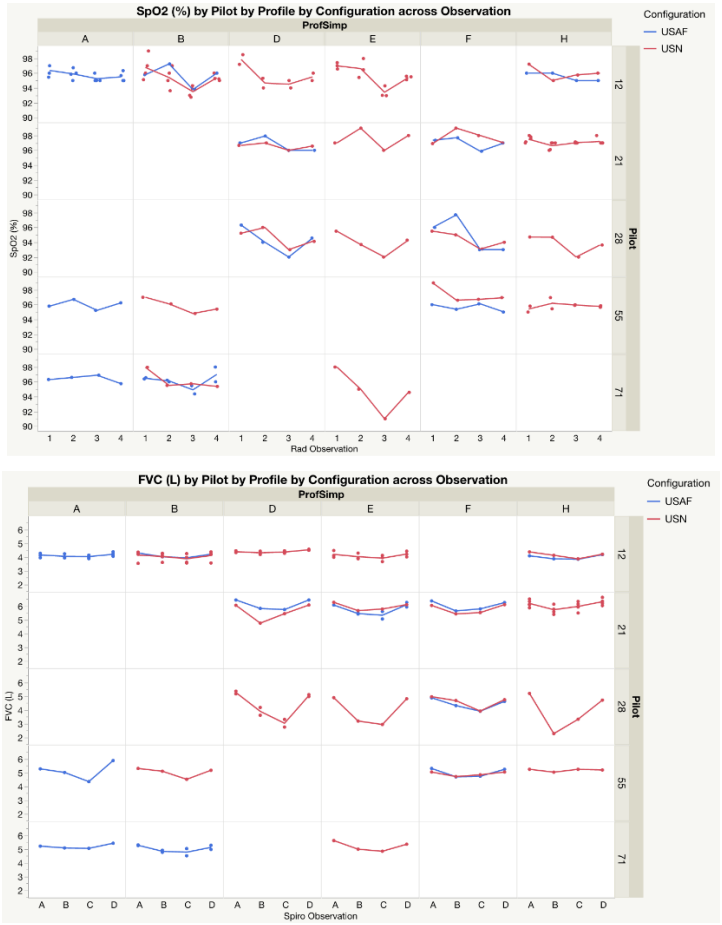

Figure 7.4.24. Study Gap Analysis

The lack of data results in the inability to for an assessment of flight profiles or configurations. The differences in AFE and cockpit configuration were arranged and examined in detail as each pilot was assessed for FVC. Gaps in the data were elucidated. These deficiencies were determined early enough that a ground study could be conducted and supplement the inflight data. The USN and USAF preflight differences were subsequently examined in detail with the extended spirometry.

Originally the pilots were to have body plethysmography to have a baseline of all lung volumes, but due to COVID-19 restrictions, this was substituted by ground spirometry. The plethysmography would serve as an accurate check of the SpiroDoc measurements and also give the TLC (total lung capacity [TLC]), and an accurate the forced vital capacity (FVC). The FVC

is the total volume of air exhaled from a full lung (total lung capacity [TLC]) to maximal expiration (residual volume [RV]). This would also have given insight into the full physiological reserve of each individual.

The primary parameter examined with spirometry was the Forced Vital Capacity (FVC) or the total amount of air exhaled during the FEV test. The Forced expiratory volume (FEV) measures how much air a person can exhale during a forced breath. In examining the other parameters, the IC, and TV had data correlation and processing issues that could not be resolved prior to publication, and thus not included. These need to be processed and examined in detail and again, the time constraint to publish did not allow for adequate analysis.

Exhalation line CO_2 was acquired in flight and will be examined elsewhere. There were initially some sensor issues and accuracy discrepancies. When the sensor package was adjusted later, there seemed to be a stable reading. The indications are that normal and slightly elevated CO_2 levels were acquired compared to normative ranges of end tidal CO_2. These values may represent exhalation line retention, mask retention, and include human increased production and/or retention. A mask sensor developed by JPL is in work and will with adequate resolution help to resolve these questions. Initial trials in flight have been performed and further analysis is forthcoming.

Flight Profile Limitations

The PBA study was done to evaluate the Breathing systems and an exploration of monitoring inflight of key physiological parameters. No integrated study had been done to quantify the interactions in flight of multiple parameters that has been seen. The aerobatics profiles were limited to up to 5 G_z. The full priority was to establish a method of evaluating physiological parameters and ABS interactions that can serve as a baseline to evaluate systems in the future. This will augment validation of ABS systems and can also serve to aid in PE investigation post flight. Many other centrifuge studies and limited in-flight evaluations have been performed which failed to reveal the complex human machine interactions. A caveat that must be stated, is that this study did not explore the far corners of the G_z boundaries, the human interactions required to compensate for those higher stresses, and the ABS system interactions. These flights should not be equated to BFM (Basic Fighter Maneuvering) or ACM (Air Combat Maneuvering) regimes. BFM, more commonly known as dogfighting, are actions that a fighter aircraft makes during air combat maneuvering. These consist of many varying tactical turns, rolls, and other actions to gain a tactical advantage over an enemy aircraft. These use the three-dimensional space of air combat, where maneuvers are not limited by simple two-dimensional turns and not in a set pattern. These also are not restrained to just 5 G_z. The maneuvers involved in tactical execution of BFM and ACM can reach up to 9+ Gz. The ability to sustain this acceleration is highly dependent upon the airframe involved. However, in all fighter airframes, these flight regimes involve several minutes of aggressive, physiologically demanding flying at the limits of the acceleration envelope of the involved aircraft. These physiological means and deltas of the PBA do not apply to the BFM and ACM arena. This is an open area of exploration that will require further study. This examination of Aircrew Breathing systems will help to elucidate the non-demanding portions of the flight envelope in which PEs have occurred.

Pulmonary Function Testing and Peripheral Hemoglobin Saturation Conclusions

On the basis of the data collected during the study, the NESC has formed the view that:

The reduction of FVC and SpO_2 observed in aircrew strapped into the ejection seat may represent a generic effect of the physical constraints associated with strapping into an ejection seat and wearing AFE. This effect is present in both the USAF and USN configurations.

Overall, the pattern of changes seen with FVC in the ABS cohort indicate that FVC is reduced after AFE is donned and crew seated in the ejection seat. The flight crew appear to have a greater effect post flight in SpO_2 with torso harness and strapped into the ejection seat (USN configuration). The reduction seen in pilots is not totally reversed by egressing from the cockpit, and removal of the AFE. The USN configuration was shown to have a more significant reduction in FVC and SpO_2 in the data that included the extended Spirometry. This is consistent with differences in the harness configuration used in the two cohorts. The torso harness used by USN aircrew serves as the parachute restraint harness in the event of an ejection; the torso harness is adjusted firmly to ensure adequate restraint under canopy, and the torso harness itself is clipped into the parachute rig when strapping into the ejection seat. On the other hand, the USAF aircrew are secured to the parachute rig via the seat restraints; the torso harness is not required to be secured as tightly, but rather the seat harness is adjusted firmly to ensure adequate restraint under canopy. This difference when wearing AFE is significant. Although it would be possible to loosen the USN torso harness somewhat in the hope of further alleviating chest restriction, this must be approached in a manner that does not undermine the primary objective of the torso harness, which is to secure the aircrew to the parachute harness when they are strapped in the ejection seat.

The reduction in FVC and oximetry observed after flight is consistent with a significant ventilation/perfusion mismatches. Simply put, there is not enough O_2 by concentration or volume getting to the lungs. This is probably due to a number of factors. A principle cause of ventilation perfusion mismatches is atelectasis, a known effect of aircrew breathing near 100% O_2. These effects have not been seen in studies where the O_2 concentration is limited to below or equal to 65%. The presence of prolonged reduction of FVC and oximetry in the findings is consistent with ventilation reduction in capacity. Predominantly this has been shown to be a result of non-obstructive atelectasis. Non-obstructive atelectasis can be caused by loss of contact between the parietal and visceral pleurae, compression, loss of surfactant, and replacement of parenchymal tissue by scarring or infiltrative disease. The specific causes as delineated in the PBA study are principally the loss of tidal volume. In the high maneuvering and Gz regime the decreases in tidal volume are due to hyperoxia, chest wall restriction, acceleration, breathing system asynchrony, and singularly or combined inspiratory expiratory overpressure. All lead to non-obstructive atelectasis and the loss of effective alveolar volume. The reduction in FVC measured in the cockpit before flight in aircrew show a trend of reversal back to baseline after egressing the cockpit.

The O_2 saturation level of less than 98% seen in USN configuration after flight is alarming. It was taken after the aircrew had been breathing air for approximately 5 minutes after landing, removal of the facemask, and may have been more pronounced if measured during flight. This is in the paradigm of > 95% supplied O_2. Although this degree of hemoglobin desaturation would not by itself produce hypoxia-like symptoms, it represents a prominent physiological erosion.

This is a finding that indicates degraded physiological reserve and lowers the threshold for developing hypoxia in flight.

The sensation of difficulty taking a deep inspiration or expiration during and after flying has been reported by pilots that have reported PEs. The sensation of restricted breathing during and after flight is consistent with a reduction in tidal volumes and atelectasis, and this is reinforced by the studies here. The pattern seen in the results, including both the progressive degradation and recovery of FVC and oximetry during the test sequences, the sensation of respiratory insufficiency, are all consistent with restricted tidal volumes, loss of Vital Capacity, and the development of atelectasis.

7.4.3 Discussion

Hypoxia and Oxygen Saturation: The O_2 saturation in USN configuration below 98% is a disconcerting finding. As a review O_2 saturation which is referred to as O sats, refers to the extent to which hemoglobin is saturated with O_2. O_2 transport by blood is also influenced by the O_2 affinity of hemoglobin, as defined by the shape and position of the O_2-hemoglobin dissociation curve.

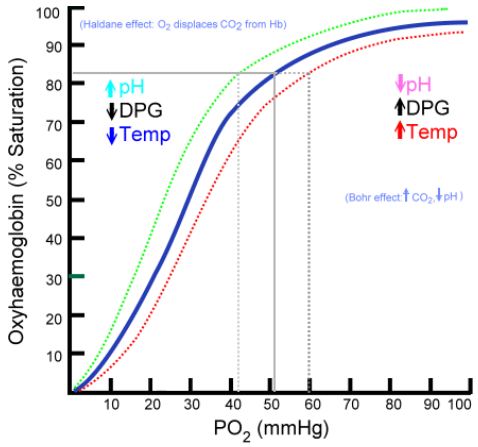

Figure 7.4.25. USN Configuration
(Jacquez, John (1979). Respiratory Physiology. McGraw-Hill. pp. 156–175
https://en.wikipedia.org/wiki/Oxygen%E2%80%93hemoglobin_dissociation_curve#/media/File:Oxyhaemoglobin_dissociation_curve.png)

An important feature of the O_2-hemoglobin relationship is the manner in which the dissociation curve steepens as arterial P_aO_2 falls below 60 mm Hg. As a result, with ascent to high altitude, arterial P_aO_2 falls into a range in which the O_2 content of hemoglobin drops precipitously with only small decreases in Po_2.

SpO_2 (%)	P_aO_2 (mmHg)
97	95
92	60
89	50
75	40
50	27

Normal arterial O_2 is approximately 75 to 100 millimeters of mercury (mm Hg). Values under 60 mm Hg usually indicate the need for supplemental O_2. This results in an O_2 saturation under ideal conditions normally 95–100% with a range of +/- 2%. The pulse oximeter will read 100% for an arterial blood level of $\geq$ 90 mmHg. A peripheral hemoglobin O_2 saturation reading can be 100% when PaO_2 (Arterial Blood Gas measurement) is 90 mmHg or 300 mmHg. At a high FIO_2 (inspired O_2 level) of supplemental or external O_2, the saturation readings cannot distinguish a PaO_2 above 90 mmHg. The normal PaO_2 on FIO_2 100% should be >500 mmHg and on an FIO_2 of 50% it should be >250 mmHg (a linear relationship). O_2 saturation drop is delayed in response. O_2 delivered externally maintains oxygenation without desaturation for minutes despite apnea (respiration or breathing stops). The timing of post flight oximetry readings should reflect the conditions seen at the end of flight due to the delay in desaturation. It is known that CO_2, however increases with apnea and respiratory acidosis (a hazardous build-up of CO_2) develops. A measurement of expired CO_2 or End-Tidal CO_2 is a better monitor of respiratory status. This reflects decreased respirations or apnea minutes before O_2 saturation drops.

Healthy individuals at sea level usually exhibit O_2 saturation values between 96% and 99% and should be above 95%. At 5000 Ft altitude or 1,500 meters (about one mile high) O_2 saturation should be above 92%. A SpO_2 value below 90% causes symptomatic hypoxia. As shown in the results, all the pilots were at or above 95% prior to flight. Two pilots maintained saturations above 95%. The results in other pilots showed a decrement to below 95% and thus a significant loss of hemoglobin saturation. Maintaining above 95% would be expected with an adequately responsive ABS that did not reduce the physiological reserves.

Medical definitions of hypoxia are based upon pathological considerations. Defined it is the inadequate supply of O_2 to the tissues. Hypoxia may be classified as either generalized, affecting the whole body, or local, affecting a region of the body. Hypoxemia (low arterial O_2) is a marker that the supply of O_2 to the tissues is deficient and thus results in hypoxia (low tissue O_2).

Healthy Adult - Sea Level, Room Air, A-a O_2 = 4 mmHg, PAO2 = 101

	PaO_2 (mmHg)	SaO_2 (%)
Normal values (on air)	> 80	> 95
Mild hypoxemia	60-79	90-94
Moderate hypoxemia	40-59	75-89
Severe hypoxemia	< 40	< 75

(Pgimer, ABG and spirometry, RML Hospital CME, slide share at https://www.slideshare.net/ShivashankarS1/understanding-abgs-and-spirometry)

Mild hypoxia usually in healthy individuals will be asymptomatic (no symptoms). Most causes of mild hypoxia are compensated with altering minute volume or pulmonary vascular redistribution. Hypoxia symptoms are produced when the tissue is unable to extract adequate O_2 to function fully. In mild hypoxia in healthy individuals, there is enough O_2 supplied to the tissues to not result in overt symptoms, but physiological indicators of compensation. Hypoxia can be recognized from both objective (perceived by an observer or measured) and subjective (perceived by the pilot only) symptoms. Objective signs include increased rate and depth of breathing, tachycardia (rapid heartbeat), mental confusion, cognitive slowing, euphoria, poor judgment, loss of muscle coordination with loss of posture, cyanosis (blue colored lips and nails) and eventually loss of consciousness. Behavioral changes may be noted by the affected

individual, as well as by an observer. The subjective symptoms include fatigue, tingling, and numbness, blurred vision, hot and cold flashes, tunnel vision, apprehension, breathlessness, headache, dizziness, nausea, hot and cold flashes. In aviation medicine hypoxia is further classified into four stages based on altitude, the associated performance decrements, and physiological symptoms.

Indifferent Stage, 0 - 1,500 m (0 - 5,000 ft) -No physiological responses or performance decrements related to hypoxia are typically observed between these altitudes for a person in good health.

Complete Compensatory Stage, 1,500 - 3,500 m (5,000 - 11,400 ft)- Visual sensitivity at night is decreased by 10% at 1,500 m (5,000 ft) and by 30% at 3,000 m (10,000 ft). Performance of new tasks may be impaired due to memory issues. The nervous system, however, is able to maintain its primary functions and performance, for the most part, is unaffected. Other classification systems combine the Complete Stage into the Indifferent Stage and use 0-10,000 ft to encompass all variability and ease of standardization.

Partial Compensatory Stage, 3,500 - 6,000 m (11,400 - 20,000 ft) - Between these altitudes, a drastic increase in breathing is needed to maintain proper cardiovascular function. Nervous system functioning begins to degrade, but there can also be great individual variability in the symptoms for a given altitude. This is otherwise known as the Disturbance Stage as normal cardio-pulmonary systems are failing to provide adequate tissue O_2. This traditionally uses 10,000 – 20,000 ft again to encompass all individual variability and ease of standardization.

Cognitive disturbances are typical at these altitudes. They are characterized by two main components:

1. Loss of self-monitoring and cognitive feedback
2. Difficulty in thinking

In the absence of self-monitoring, it is impossible for an individual to recognize whether actions are hazardous. This, combined with slow thinking, can be extremely dangerous. Many times fixation occurs and a tendency to repeat an action without the realization that the action was just completed. Judgment degrades and physical movement becomes uncoordinated.

Critical Stage, above 5,500 m (18,000 ft) - Above this altitude, complete incapacitation can occur with little or no warning. All senses fail, and a pilot will become unconscious within a very short period of time. No stimuli such as the radio will be able to help a pilot suffering from hypoxia, especially fulminant hypoxia, above 5,500 meters (18,000 ft).

Combining altitude with O_2 saturations and effects yields the following chart.

Stage of Hypoxia	Cabin Altitude		PaO_2(mmHg) and percentage saturation of Hemoglobin
	Breathing Air	Breathing 100 O_2	
Indifferent	0-3,30m 0-10,000 ft	10,300-12,000m 33,000-40,000 ft	60-104 mmHg 90-97%
Compensatory	3,030-4,500m 10,000-15,000 ft	12,000-13,000m 40,000-42,500 ft	42-60 mmHg 80-90%
Disturbance	4,500-6,000m 15,000-20,000 ft	13,000-13,500m 42,500-45,000 ft	42-35 mmHg 70-80%
Critical	6,000-7,000m 20,000-23,000 ft	13,500-13,800m 45,000-46,000 ft	35-30 mmHg 60-70%

(From https://www.cfinotebook.net/notebook/aeromedical-and-human-factors/hypoxia)

As delineated in the PBA Evaluation these are associated with the following:

Reduced Oxygen Tension

High altitude. The total partial pressure of oxygen (or percentage of Oxygen) is reduced.

Hypoventilation

Airway obstruction which can be proximal as in laryngeal edema or foreign body inhalation, or distal as in bronchial asthma thus the restriction against reactant asthma in fighter pilots

Restricted movement of chest wall as with a restricting AFE. This is demonstrated in the reduced FVC.

Ventilation-perfusion Mismatch (V/Q Mismatch)

Decreased V/Q ratio: (Impaired ventilation) or high perfusion, e.g., chronic bronchitis, obstructive airway disease, mucus plugs, pulmonary edema all impair the ventilation and therefore decrease the ratio of ventilation to perfusion. A low V/Q ratio produces hypoxemia by decreasing the alveolar O_2 level (PAO_2) and subsequently arterial O_2 level (P_aO_2). Atelectasis and reduction of Vital Capacity (Tidal Volumes) are the principle causes of V/Q mismatching implicated in findings.

Modern combat aircraft impose significant insults on the lungs, which under certain conditions can lead to collapse of alveoli as previously described. The primary regions for Atelectasis are the basal alveoli (the ones at the lung bases). G-forces indirectly produce weight, thus G -force is often described as a "weight per unit mass". Thus, segments at lung bases are subjected to increased weight and collapse as a result. One of the principle types of atelectasis in high G_z fighter aircraft is acceleration atelectasis, which describes the circumstances when this occurs as a result of the higher G's. Any dynamic flight environment with exposure to > +3 Gz will incrementally worsen with increasing centrifugal forces of Gz. The conditions known to worsen the development of acceleration atelectasis are

1) Breathing more than 60% O_2 (Absorption Atelectasis)
2) Wearing an anti-G suit with an abdominal bladder

The USN breathing gas system supplies $\geq$ 94% O_2 under typical operating conditions. Breathing near-100% O_2 alone can lead to collapse of the basal alveoli, even in the absence of high-G

exposure. This effect is magnified if lung expansion is restricted, as fast-jet aircrew would experience with prolonged sitting, hunched posture, and harness restraints that limit chest expansion. Recent studies have shown that absorption atelectasis is seen in most subjects breathing 75% O_2, in many subjects breathing 60% O_2, and in some individuals breathing 45% O_2. Acceleration atelectasis is accentuated by absorption atelectasis after as few as two 5-Gz exposures separated by a 30-s interval when breathing 95% O_2. This combined effect can be seen in as few as four 5-Gz cycles when breathing 60% O_2. This results in physiologically significant hypoventilation and shunt of pulmonary circulation, resulting in a reduction of hypoxia tolerance. These effects have an incremental manifestation some people report significant effects, whilst others report more mild effects. Atelectasis is known to occur in fast-jet aircrew breathing high concentrations of O_2 for as little as 15 minutes (1). Atelectasis can lead to a reduction in Vital Capacity by up to 60% and reduce the arterial O_2 to an equivalent of breathing air at 8 000 ft (1). This degree of mild hypoxia erodes the physiological reserve and increases susceptibility to hypoxia-related physiological events. Atelectasis is minimized when breathing air with at least 40% nitrogen (1). This cannot be achieved with the most OBOGS breathing gas systems if its design does not incorporate a dilution-demand regulator.

Hypoxia and Saturation Discussion Ref Sec IX- X 290-309

A form of Non-obstructive atelectasis is Compression Atelectasis occurs from any compression of the lung that forces air out of or restricts the number of available alveoli. In this case it is a result of Chest wall restriction. This has been discussed previously and noted to have numerous consequences on the lung and ultimately breathing functions. Studies have shown that restrictions in chest wall expansion have reductions in VC (vital capacity), resulting in an altered breathing pattern, and also reduced cardiac output. The principle offender for the entirety of the flight is the AFE. A transient increase in chest wall compression or restriction is the increase pressure exerted by increasing levels of Gz. This subset of Compression Atelectasis is classified as Acceleration Atelectasis. Thus, work of breathing and muscle fatigue are noticeably increased in highly dynamic flight.

The reduction in FVC and oximetry taken together are an indicator of significant V/Q mismatches. As pointed out the A principle cause of these mismatches is atelectasis. The presence of prolonged reduction of FVC and oximetry in the findings is consistent with ventilation reduction in capacity that has occurred prior to flight and compounded by the flight. The specific causes as delineated in the PBA study are principally ventilatory with the loss of tidal volume. In the high maneuvering and Gz regime the decrease in tidal volume are chest wall restriction, acceleration, breathing system asynchrony, and singularly or combined inspiratory expiratory overpressure. Hyperoxia is a clear concern in the USN configuration. All lead to non-obstructive atelectasis and the loss of effective alveolar volume. The reduction in FVC measured in the cockpit before flight in aircrew are reversed toward baseline after egressing the cockpit and indicate trending toward recovery to a normal physiological baseline.

The reduction in FVC was as little as 100 ccs up to 3 liters. These again are monumental drops in Vital capacity. They indicate a significant restriction of FVC and prominent atelectasis. When creating a rapid expansile or contacting chest force to move air, there must be adequate lung volume to generate that force. Whitley found in a centrifuge study up to 8 G_z, a mean peak inhalation flow of 125.5 L/min-1 (n = 135, SD = 42.1) with a maximum of 274 L/min-1. The study showed a mean peak exhalation flow was 154.4 L/min-1 (n = 135, SD = 49.6) and up to a maximum value of 308 L/min-1. The maximum reduced FVC seen would have resulted in

inadequate flow generation. The consequence to that would be near or complete incapacitation at those demands.

Overall physiological evaluation of the PBA has shown that from individual breaths to the entire sequences of minute ventilations, there is a consistent pattern of significantly lower tidal volumes occurring. Essentially the pilot now is forced to oxygenate with residual volume and decreased tidal volume. This results in an increased alveolar dead space. A result of that is the system has effectively increased the airway resistance. Chest wall restriction and decreased tidal volumes result in decreased lung compliance. Atelectasis from a combination of factors reduces the amount of alveolar surface area. Pressure oscillations of the breathing system facilitate atelectasis formation by surfactant not covering adequately the alveolar surface. O_2 delivery is not only impacted by the O_2 swings in concentration, but by the inadequate volume of O_2 in restricted tidal volumes.

Excessive pressure in relation to Safety Pressure.: High Inspiratory flow rates result in higher peak airway pressures. Excessive inspiratory pressures will in turn result in increased intrathoracic pressure and lead to potential hemodynamic consequences (particularly decreased venous return, leading to decreased cardiac output and at worst, hypotension (low blood pressure). High airway pressures may result in inadequate ventilation if peak inspiratory pressure is too high, the excess pressure can cause overdistention of the alveoli to the point that they lose structural integrity and collapse. Inappropriate and excessive exhalation pressures will lead to dynamic hyperinflation. Hyperinflation is the increase in lung volume (over inflation) that occurs whenever insufficient exhalation time prevents the respiratory system from returning to its normal resting end-expiratory equilibrium volume between breath cycles. This results in trapped air, inability of the pilot to initiate a breath, and an increased work of breathing. Hyperinflation also results in limited inhalation volumes, as the excessive exhalation volume is not displaced. Limiting inspired volumes results in increasing the physiologic dead space. In the case of safety pressure, this is more akin to CPAP (continuous positive airway pressure) unlike PEEP which is only delivered at the end of an "expiration," or breath normally humans can tolerate. Positive pressures of 4-10 cm H_2O can be well tolerated, but requires a constant, uninterrupted flow and have no oscillations. Higher pressures to 20 cm H_2O are also tolerated but do result in higher rates of drying the mucous membranes and nose bleeds. In a system with increased peak pressures or flow, the addition of continuous airway pressures serves to worsen hyperinflation. Also, in a hyper-inflated state, higher exhalation pressures serve to worsen exhalation dynamic hyperinflation. Hyperinflation due to asynchrony results in insufficient exhalation time preventing the respiratory system from returning to its normal resting end-expiratory equilibrium volume between breath cycles. So, in using safety pressure, it must use in the light of normal inspiratory flow rates, peak pressures, a synchronized breathing system, and normal tidal volumes. None of those preconditions exist in the breathing systems tested. Thus, safety pressure results in an additional restriction physiologically as well as mechanically, being a contributor to dyssynchrony.

Ref Section XI 310-331

Work of Breathing: Special mention needs to be made concerning work of breathing. This has often been equated to the cause of a physiological episode. This is not a cause, but an indicator or result of system dysfunction. Work of breathing is defined as the energy used to inhale and exhale gas through a person's lungs. It is the product of pressure and volume for each breath. The components include the effort needed to overcome elastic recoil of the lung, energy to

overcome airway resistance and lung viscosity, overcoming airway resistance and lung viscosity and the displacement of the chest wall and abdomen. It can increase considerably due to illness or, ambient pressure, or breathing gas composition. In the aircraft, it increases with gas flow restriction imposed by the aircraft breathing apparatus. Increasing work of breathing observed by PBA are disturbances in exhalation and or inhalation volumes, which can be variable; increased exertional pressure; and prolonged exhalation episodes, that all result in decreased volume inhaled. Specific instances were found that increase the work of breathing were regulator asynchrony events, delaying the volume supplied to the pilot. This resulted in the diaphragmatic contracting with no volume change, causing increased negative pressure until a tidal volume was supplied. This exertional muscle contraction is present despite not flow with a valve restriction and the reversed with excessive pressure by the delayed response. In the F-22, it was found that excessive chest wall restriction led to decreased tidal volumes. This resulted in increased work of breathing due to physiological compensation attempting to counteract the decreased Vital Capacity. This was in combination with the atelectasis induced ventilation mismatches and resulted in uncompensated hypoxia. Essentially the "hypoxia like symptoms" were due to hypoxia!

The PBA has delineated findings indicative of breathing system dysfunction. There were instances of pilots having symptoms of breathing dysfunction. There were

1) Trouble Inhaling
2) Trouble Exhaling
3) Compensated Breathing (slower/longer breaths, increased minute ventilation by increased rate and/or depth of breathing)
4) Shortness of breath
5) Elevated respiratory rate, (tachypnea)
6) Air hunger
7) Sore Lungs for days/weeks (Due to increased work of breathing)

These signs and symptoms can overlap those of hypoxia, but with the PBA work, they are directly linked to a human-system breathing dysfunction. These were predecessors to symptoms of frank or uncompensated hypoxia. These include:

1) Confusion, lethargy, and/or compromised judgment
2) Headaches
3) Rapid heart rate (tachycardia)
4) Euphoria and a false sense of well-being
5) Tingling, warm sensations
6) Elevated blood pressure (hypertension)
7) Nausea
8) Cough intra or post flight
9) Lack of coordination
10) Dizziness or fainting [syncope]
11) Visual changes, such as tunnel vision
12) A late and inconsistent finding of a bluish tinge to the lips and extremities [cyanosis].

Ref Sec XIII 336-343

Myths Busted: Prevalent in USN and USAF investigations was the moniker of "Hypoxia Like Symptoms". In the Previous NESC F-22 and F/-18 reports, the primary culprit was whole body or regional (brain) hypoxia. Here in the PBA, further root causes to hypoxia are revealed. The reduction in FVC and oximetry taken together are an indicator of significant V/Q mismatches. As pointed out the A principle cause of these mismatches is atelectasis. The specific causes as delineated in the PBA Study are principally ventilatory with the loss of tidal volume. In the high maneuvering and Gz regime the decrease in tidal volumes are chest wall restriction, acceleration, breathing system asynchrony, and singularly or combined inspiratory expiratory overpressure. Hyperoxia is a clear concern in the USN configuration. All lead to non-obstructive atelectasis and the loss of effective alveolar volume. In the F-22, it was found that excessive chest wall restriction led to decreased tidal volumes. This resulted in increased work of breathing due to physiological compensation attempting to counteract the decreased Vital Capacity. This was in combination with the atelectasis induced ventilation mismatches and resulted in uncompensated hypoxia. Anytime you rise in altitude, your partial pressure of O_2 decreases. Thus, the increased risk of hypoxic hypoxia. Aircraft that have hyperoxia conditions occur (F/A-18, F-35 and T-6) also raise the risk of hypoxic hypoxia.

There is a common notion that Hypoxia symptoms have overlap with several other conditions. Although true, there is a distinct difference in the setting, sequence of symptoms onset, intensity of symptoms, and duration of symptoms. Hypoxia typically is subtle and insidious, cognitive function has early decrements, and breathing signs and symptoms are a hallmark early. CO_2 is more overt, headaches and irritability are early, and cognition is preserved until late with the onset of unconsciousness and lethargy. Another condition that arises in discussions is hyperventilation. Some facts that are drivers are the supposition that high-altitude environment can increase CO_2 loss. The compensation for altitude involves increasing minute volume and dead space. Essentially the end tidal CO_2 goes down. But in studies mimicking the flight environment, the blood pHs have been in the normal range with arterial CO_2 only slightly decreased. This raises the question of having a diagnosis of hyperventilation with no alkalization (respiratory alkalosis)! In the setting of the dynamic aircraft regime, hypoxia is a primary cause of hypoxia symptoms until proven otherwise. Essentially the "hypoxia like symptoms" were due to hypoxia! There are multifactorial aspects of PEs involved that result in hypoxia. For example, the hornet community it is likely that the pilots have physiological impediments due to their flight gear imposing a restrictive pathology, in conjunction with hyperoxia. The F-22 Raptor encountered a thoracic restriction, coupled with a higher G envelope and greater propensity for acceleration atelectasis. The F-35 encounters its issues due to erratic O_2 output in concentration and pressure, as well as an excessive expiratory pressure resulting in the decreased TV, and decreased FRC already elaborated.

Ref Section X 346-361 and Appendix 4

Another myth is that the maximum instantaneous tidal volumes are only 90 L/min. The 200 lpm peak flow requirement of MIL-D-85520 was deemed adequate for high-G aerobatics and air combat maneuvering. Technical memo AD-A271 811 (20 September 1993) showed that peak flows had exceed the 200 lpm peak flow recommended by MIL-D-85520. In fact, flows were recorded up to 294 L/min in a simulated air combat maneuvering in F/A-18, F-14, A-6, A-7, and S-3 aircraft. In fact, in a USN publication, NAVAIRWARCENACDIV Warminster's Dynamic Flight Simulator indicated that a peak flow of 288 L/min ATPD was required to perform the *L-1*

anti-G straining maneuver (a “coached” L-1 maneuver in a flight simulator). Mask studies by Coyne et.al. discovered peak and instantaneous flow rates of up to 374 L/min in one test and another with peak flow rate approximately 424 L/min. Whitley found that up to 8 G_z in the Naval Air Warfare Center Dynamic Flight Simulator produced a mean peak inhalatory flow of 125.5 L.min-1 (n = 135, SD = 42.1) up to a maximum value of 274 L.min-1. The mean peak exhalatory flow was recorded at 154.4 L.min-1 (n = 135, SD = 49.6) and a maximum value of 308 L.min-1. These were above the mask cavity pressures dictated by the Air Standardization and Coordination Committee (ASCC) limit of +/- 14 mmHg. These ASCC limits for Minimum Physiological Design Requirements were 3.3 L/s -1 (200 L. min -1). Previous studies by Harding and White et.al. found maximums of 350 L/min and 480 L- min -1 cited clinically. Coyne’s et.al. article even discerned that the main contributor to exhalation is the mask valve. This begs the question why were these flows not incorporated into standards and why was not the mask valves more thoroughly investigated. The PBA reinforces these findings and recommends that the current standards need to be rewritten.

Ref Sec X 346-361

7.5 PBA Conclusions

Documented NESC interviews of pilots reporting having experienced mild physiological symptoms at some point in their F-22, F-35, F-16 with OBOGS, A-10s with OBOGS and T-6 flying. Many pilots disclosed experiencing them on a regular basis.

The synergistic combination of BSDs (constantly changing pressure, flow, and synchrony) and inconsistent O_2 concentrations leads to pervasive respiratory dynamics changes. Continuous breathing disharmony and pressure/flow asynchrony are consistent with pulmonary Micro-trauma of the alveoli, airways, and chest wall remodeling. The effects of these many disparate physiological responses, in aggregate, can predispose to pathological hypoxia. These factors are all present on aircraft not equipped with diluter demand to OBOGS (non- MSOGs) or LOX supplies. All of these cofactors can rise to levels capable of causing harm. This has been referenced in previous NESC reports and now numerous findings are demonstrated inflight with this study. Of interest, the physiological changes in response to fluctuations in inspired O_2 concentrations on the order of 40% are not well understood, but highly concerning for contributing to individual PEs or long-term cumulative damage. The destructive synergy of these factors is consistent with the documented permanent damage to lung physiology responsible for the medical retirement of at least one F-35 pilot, consistent with pilot complaints over the last 8 years, and consistent with interview accounts of symptoms experienced by pilots.

The human is described as a pressure differential generator, and controls breathing with pressures. This is in stark contrast to the breathing system which is not responding to a pilot’s pressure signals with appropriate flows. The pilot is being forced to adapt physiologically to an unpredictable and/or highly oscillatory flow. The result is pilot compensation but is met by the inadequate aircraft breathing system deleterious performance. This results in the form of lower MV, lower TV, increased functional reserve capacity, and high likelihood of atelectasis, increased dead space, micro-trauma, hyperinflation, and an increased predisposition to or mild hypoxia. At take-off and in flight the pilot is sitting precariously on a hypoxic cliff staring into a Physiological Episode Canyon. The pilot is faced with multiple factors on every flight. Combinations of insults and the right set of circumstances, the pilot’s capability to compensate is exceeded and pushed “over the edge”.

Vir in Machina Dissociation

The overall description of the breathing dissociation/asynchrony between the pilot and the Air Crew Breathing System is a "Man in the Machine (loop) Dissociation" or "Vir in Machina Dissociation". The data collected and presented in this brief as well as previous NESC reports, provide evidence of significant systems interactions in aircraft changing breathing dynamics decreasing ventilation reserves and oxygenation. These include:

1. Pressure Oscillations, valve interactions, and over aggressive regulator pressures can result in disharmony and dysfunction during both inhalation and exhalation.
2. Pilots may begin to have insufficient ability to draw air into their lungs or insufficient ability to exhale air out, but not directly recognize the deficit. This causes altered respiration to compensate.
3. In addition, there are times when the O_2 concentration or volume drops quickly and significantly during increased respiratory demand on the system.
4. Hyperinflation or Atelectasis can lead to large increases in alveolar dead space.
5. Slower responding inhalation flows can lead to lower volumes and longer times.
6. Higher mask pressure during exhalation lead to longer exhalation times.
7. Reduction of FVC and Oximetry indicates impaired ventilation and Ventilation-perfusion Mismatches (V/Q Mismatch).
8. Together these combine to result in significant observed decreases in minute ventilation.
9. Evidence of mild compensatory hypoxia.
10. Evidence suggests these factors can cause or contribute to PEs.

Different aircraft have different roots of negative respiratory breathing impacts.

1. For the F-22: Chest Wall restriction and hyperoxia lead to atelectasis and the resultant increased work of breathing. The aircraft breathing system (machine) imposed an increased level of ventilatory drive due to Ventilation-perfusion Mismatches and the malfunction of the combat edge system worsened the degradation of the physiological reserves. Brain circulation reduction in circulatory reserve and the result is the pilot is vulnerable to circulation and oxygenation decreases by hyperoxia.
2. For the F/A-18: Initial physiological reserves are diminished due to restrictive flight ensemble. Then a demanded increasing level of ventilatory drive in the human is associated with a reduced capacity of the mechanical system to develop adequate flow or pressure to meet the demand. This is dependent on the particular failure mode. The pilot places a demand, but the machine fails to respond adequately. Brain circulation reduction in circulatory reserve and is rendered vulnerable to circulation and oxygenation decreases by hyperoxia.
3. For the F-35: The machine is driving an increased level of ventilatory drive and compensation (bad). The human responds to preserve Alveolar Ventilation (good). The machine is limiting the amount of compensatory volume and effectively restricting flow and volume (ugly). The machine is placing a demand on the pilot and then limits the response.

7.5.1 Summary Pulmonary Insults

Pilots flying fast dynamic fighters and trainers are subjected to various alterations in the breathing dynamics that can cause distinct respiratory system pathophysiology.

1) Hyperoxia
    a. Absorption atelectasis resulting in decreased lung volumes and altered lung circulation
    b. Cerebrovascular constriction in specific brain regions placing these regions at risk for regional hypoxia
2) Acceleration atelectasis
    a. Decreased tidal volumes, diminished cardiac volume with higher G_z, and chest wall increased work of breathing
3) Rapid Oscillating Hyperoxic concentrations
    a. Accelerated cerebrovascular constriction in specific brain regions resulting in regional hypoxia
4) Breathing System Asynchrony
    a. Asynchronous timing – mechanical triggering of breath lags or leads the pilots breathing cycles. Lagging a breath diminishes tidal volumes delivered to the pilot. Leading a breath (oversupply) induces restricted volumes physiologically to prevent hyperinflation.
    b. Asynchronous volumes or flow – The inspiration flow or volume does not match the pilot's inspiratory effort. Too much volume causes a physiological reaction to limit the volume to prevent hyperinflation or to little reduces TVs
    c. Asynchrony leads to increased work of breathing, excessive fatigue of respiratory muscles, and non-specific respiratory discomfort. Excessive flow or pressure will result in alveolar micro-trauma
5) Inspiratory overpressure
    a. Results in an increase in dead space volume over time
    b. Chest wall muscular remodeling with chronic exposure
6) Expiratory overpressure
    a. Results in dynamic hyperinflation, air trapping (increased dead space), and decreased inspired TV
    b. Decreased venous return to the heart causing deceased cardiac output and reduced circulatory pressure and volume (decreased blood pressure)
7) Inspiratory and expiratory overpressure combined
    a. Results in increased dead space volume more rapidly than just inspiratory or expiratory overpressure
        i. Expiratory dynamic hyperinflation results in worsened air trapping (increased dead space) by additional decreased inspiratory TV.
        ii. Higher likelihood of larger areas of micro-trauma and barotrauma
    b. Chest wall muscular remodeling
    c. Combined effect further worsens the individual decreases in venous return to the heart. Substantial reduction in cardiac output and reduces circulatory pressure and volume (decreased blood pressure)
8) The above breathing dynamics insults singularly or in combination can result in
        a. Cerebral (brain) hypoxia and cognitive dissociation

b. Increased work of breathing, excessive fatigue of respiratory muscles, and non-specific respiratory discomfort
c. Excessive flow or pressure will result in alveolar micro-trauma
d. Accumulated micro-trauma (acutely or chronically over time) induce permanent alveolar and airway barotrauma leading to altered pulmonary function and quantified by testing
e. Symptoms of hypoxia

On the basis of the data collected, the physiological analysis has shown that significant physiological decrements are occurring that would degrade the physiological reserve and lower the threshold for developing hypoxia in flight. Preflight results delineated a reduction of FVC and O_2 saturations observed in aircrew strapped into the ejection seat. These findings represent a generic effect of the physical constraints associated with strapping into an ejection seat and wearing AFE. This effect is present in both the USAF and USN configurations, but more prominent in the USN torso harness system. The post flight doffing values data represent significant physiological impacts and ventilation perfusion mismatches. Specific results post flight revealed that O_2 saturation drops < 95%, representing mild hypoxia. PBA revealed significant breathing system anomalies including breathing system asynchrony, and also inspiratory and expiratory over-pressurization. The synergistic combination of BSDs (constantly changing pressure, flow, and synchrony) and inconsistent O_2 delivery leads to pervasive respiratory dynamics changes.

Implications: The PBA team, in developing a system to evaluate an ABS, has elucidated a significant amount of physiological impacts to pilot's respiratory reserves. Previous to the PBA, inflight breathing machine human relationships were inferred from limited flight data and laboratory inferences. The PBA now has a system to aid in breathing system evaluation and in mask direct human breathing insight. Previously all hypoxia or physiological incident caution and warnings had been relying on the pilot's symptoms. No dedicated physiological respiratory warning system has been in use. Inflight systems in development currently concentrate on O_2 and CO_2 detection in the peripheral blood system. These are all lagging indicators and do not examine the breathing system disruptions that ***Lead*** to hypoxia. The work here can aid in the development of in mask sensor suits to be preventative to a breathing PE, rather than reactive. Simply put, a system can be developed to indicate a breathing system has failed before the human fails and undertake remediation. The study should further emphasize that Pilots continue to be trained to recognize a hypoxic event. The PBA has now developed tools to evaluate a breathing system to validate a design or modifications to a design. The data could also be used to drive development of a superior breathing system that is better optimized for normal human physiology, develop tightened specifications on OBOGS and regulator systems and refinements to new aircraft specifications. These tools can now also inform and investigate a system after a PE, by analyzing a breathing system that by technical ground testing seems within specifications.

7.6 Findings

F.7-1. As designed, current mechanical regulators cannot effectively respond to the full dynamic range of all breathing profile conditions during in-flight operation.

F.7-2*. *PBA spirometry found that the Aircrew Flight Equipment (AFE) and being harnessed to the seat reduced measured available lung volume prior to flight. Functional Vital*

Capacity (FVC) measurements taken from PBA pilots just prior to take off revealed a large decrease in FVC mean from baseline.

F.7-3*. *PBA spirometry found further decreased Functional Vital Capacity (FVC) in PBA pilots immediately after landing as compared to the respective immediate pre-flight measurements.*

F.7-4. PBA found Oxygen Saturation (SpO_2) measurements were lower than baseline (seated in flight suit, not in aircraft) in all subsequent observations, including recovery.

F.7-5*. *PBA found Oxygen Saturation (SpO_2) did not return to baseline by the time of the recovery measurement taken at approximately one hour post-flight.*

F.7-6*. *Numerous instances of mild hypoxia (SpO_2 < 95%) were indicated in both the post flight and post doffing observations as measured by pilot Oxygen Saturation.*

F.7-7*. *PBA found pilot Oxygen Saturation (SpO_2) measurements taken immediately after flight were below the < 93.5% cutoff indicating critical physiological impacts due to hypoxia. Especially problematic is that the vast majority of the lowest SpO_2 readings are found in the 100% supplied oxygen configuration (CRU-103) throughout the flight. There were no pilot subjective reports of hypoxia symptoms.*

F.7-8. FVC and Oximetry post-flight measurements of the PBA pilots indicated the presence of impaired in-flight lung gas exchange indicative of lung and circulation mismatches (Ventilation-perfusion Mismatches - V/Q Mismatch).

F.7-9. PBA pilots reported a concern that high temperature exposure was enough to induce adverse physiological responses with some mission impact.

R.7-1. Prior interviews with PBA, F-35, and F/A-18 fleet pilots indicate heat exposure is a common hazard. Appropriate mitigations for heat-stress should be identified and deployed. ***(F.7-9)***

References

I. Main references applied to all sections.

1. Critical Care Medicine (Third Edition), Principles of Diagnosis and Management in the Adult, 2008 Elsevier Inc, 1806 pages
2. Ismail C, Smith JR, Dellinger RP, Chapter 9 - General Principles of Mechanical Ventilation, Critical Care Medicine (Third Edition), Principles of Diagnosis and Management in the Adult, 2008, Pages 153-175
3. Pilamanis, AA, Sears, WJ, Raising The Operational Ceiling: A Workshop on the Life Support and Physiological Issues of Flight at 60,000 Feet and Above, AL/CF-SR-1995-0021, Armstrong Labs, Brooks Air Force Base, 13-15 June 1995
4. Gradwell DP, Rainford D, Ernsting's Aviation and Space Medicine, 5th Edition, CRC Press, Jan 2016,
5. Ward J, Chapter 3, Respiratory Physiology
6. Gradwell DP, Chapter 4, Hypoxia and Hyperventilation
7. Gradwell, Chapter 5, Prevention of Hypoxia
8. Gradwell DP, Macmillan AJF, Oxygen Systems, Pressure Cabin and Clothing

II. Airway and Alveolar pressures.

9. Albert, R.K. For every thing (turn...turn...turn....). Am.J.Respir.Crit.Care Med 155:393-394, 1997.
10. Antonelli, M., Conti, G., Rocco, M., Bufi, M., De Blasi, R.A., Vivino, G., Gasparetto, A., and Meduri, G.U. A comparison of noninvasive positive-pressure ventilation and conventional mechanical ventilation in patients with acute respiratory failure. N.Engl.J.Med 339(7):429-435, 1998.
11. Esteban, A. and Ala, I. Clinical management of weaning from mechanical ventilation. Intens.Care Med. 24:999-1008, 1998.
12. Hilbert G et al. Noninvasive ventilation in immunosuppressed patients with pulmonary infiltrates, fever, and acute respiratory failure. N.Engl.J.Med 344 (7):481-487, 2001.
13. MacIntyre N. Improving patient/ventilator interactions. In Vincent J-L. (ed) Yearbook of Intensive Care and Emergency Medicine 1999. Springer-Verlag, Berlin, 1999; pp234-243
14. Pinsky, M.R. The hemodynamic consequences of mechanical ventilation: an evolving story. Intens.Care Med. 23:493-503, 1997.
15. Slutsky AS. Consensus conference on mechanical ventilation - January 28-30, 1993 at Northbrook, Illinois, USA. Part 2. Intensive Care Med 1994; 20:150-162

III. Overpressure

16. Dreyfuss D, Soler P, Basset G et al (1988) High inflation pressure pulmonary edema. Respective effects of high airway pressure, high tidal volume, and positive end-expiratory pressure. Am Rev Respir Dis 137:1159–1164
17. Romand J, Shi W, Pinsky MR (1995) Cardiopulmonary effects of positive-pressure ventilation during acute lung injury. Chest 108:1041–1048
18. Dreyfuss D, Soler P, Saumon G (1992) Spontaneous resolution of pulmonary edema caused by short periods of cyclic overinflation. J Appl Physiol 72:2081–2089
19. Fu Z, Costello ML, Tsukimoto K et al (1992) High lung volume increases stress failure in pulmonary capillaries. J Appl Physiol 73:123–133
20. Omlor G, Niehaus GD, Maron MB (1993) Effect of peak inspiratory pressure on the filtration coefficient in the isolated perfused rat lung. J Appl Physiol 74:3068–3072
21. Kolobow T, Moretti MP, Fumagalli R et al (1987) Severe impairment in lung function induced by high peak airway pressure during mechanical ventilation. An experimental study. Am Rev Respir Dis 135:312–315
22. Gattinoni L, Pesenti A, Caspani ML et al (1984) The role of total static lung compliance in the management of severe ARDS unresponsive to conventional ventilation. Intensive Care Med 10:121–126
23. Maunder RJ, Shuman WP, McHugh JW et al (1986) Preservation of normal lung region in the adult respiratory distress syndrome. Analysis by computed tomography. JAMA 255: 2463–2465
24. Gattinoni L, Pesenti A, Avalli L et al (1987) Pressure-volume curve of total respiratory system in acute respiratory failure. Am Rev Respir Dis 136:730–736
25. Loick HM, Wendt M, Rötker J et al (1993) Ventilation with positive end-expiratory airway pressure causes leukocyte retention in human lung. J Appl Physiol 75:301–306
26. Zapol WA (1992) Volutrauma and the intravenous oxygenator in patients with adult respiratory distress syndrome (editorial). Anesthesiology 77:847–849

IV. High Pressures - High Peak Inspiratory Pressures

27. Acute Respiratory Distress Syndrome Network: Ventilation with lower tidal volumes as compared with traditional tidal volumes for acute lung injury and the acute respiratory distress syndrome. N Engl J Med 2000; 342:1301–8
28. Hickling KG, Henderson SJ, Jackson R: Low mortality associated with low volume pressure limited ventilation with permissive hypercapnia in severe adult respiratory distress syndrome. Intensive Care Med 1990; 16:372–7
29. Hickling KG, Walsh J, Henderson S, Jackson R: Low mortality rate in adult respiratory distress syndrome using low-volume, pressure-limited ventilation with permissive hypercapnia: A prospective study. Crit Care Med 1994; 22: 1568–78 4. Amato MB, Barbas CS, Medeiros DM, Magaldi RB, Schettino GP, LorenziFilho G, Kairalla RA, Deheinzelin D, Munoz C, Oliveira R, Takagaki TY, Carvalho CR: Effect of a protective-ventilation strategy on mortality in the acute respiratory distress syndrome. N Engl J Med 1998; 338:347–54
30. Mead J, Takishima T, Leith D: Stress distribution in lungs: A model of pulmonary elasticity. J Appl Physiol 1970; 28:596–608
31. Zakynthinos SG, Vassilakopoulos T, Daniil Z, Zakynthinos E, Koutsoukos E, Katsouyianni K, Roussos C: Pressure support ventilation in adult respiratory distress syndrome: Short-term effects of a servocontrolled mode. J Crit Care 1997; 12:161–7
32. Rich PB, Reickert CA, Sawada S, Awad SS, Lynch WR, Johnson KJ, Hirschl RB: Effect of rate and inspiratory flow on ventilator-induced lung injury. J Trauma 2000; 49:903–11
33. Smith R, Venus B: Cardiopulmonary effect of various inspiratory flow profiles during controlled mechanical ventilation in a porcine lung model. Crit Care Med 1988; 16:769–72
34. Imanaka H, Shimaoka M, Matsuura N, Nishimura M, Ohta N, Kiyono H: Ventilator-induced lung injury is associated with neutrophil infiltration, macrophage activation, and TGF- 1 mRNA upregulation in rat lungs. Anesth Analg 2001; 92:428–36
35. Modell HI, Cheney FW: Effects of inspiratory flow pattern on gas exchange in normal and abnormal lungs. J Appl Physiol 1979; 46:1103–7
36. Al-Saady N, Bennett ED: Decelerating inspiratory flow waveform improves lung mechanics and gas exchange in patients on intermittent positive-pressure ventilation. Intensive Care Med 1985; 11:68–75
37. Peevy KJ, Hernandez LA, Moise AA, Parker JC: Barotrauma and microvascular injury in lungs of nonadult rabbits: Effect of ventilation pattern. Crit Care Med 1990; 18:634–7
38. Dreyfuss D, Soler P, Basset G, Saumon G: High inflation pressure pulmonary edema: respective effects of high airway pressure, high tidal volume, and positive end-expiratory pressure. Am Rev Respir Dis 1988; 137:1159–64
39. Halter JM, Steinberg JM, Schiller HJ, DaSilva M, Gatto LA, Landas S, Nieman GF: Positive end-expiratory pressure after a recruitment maneuver prevents both alveolar collapse and recruitment/derecruitment. Am J Respir Crit Care Med 2003; 167:1620–6
40. Gattinoni L, Pesenti A, Avalli L, Rossi F, Bombino M: Pressure–volume curve of total respiratory system in acute respiratory failure: Computed tomographic scan study. Am Rev Respir Dis 1987; 136:730–6 EFFECTS OF PEAK INSPIRATORY FLOW ON LUNG INJURY 727 Anesthesiology, V 101, No 3, Sep 2004 Downloaded from anesthesiology.pubs.asahq.org by guest on 05/09/2020
41. Hickling KG: The pressure–volume curve is greatly modified by recruitment: A mathematical model of ARDS lungs. Am J Respir Crit Care Med 1998; 159:1172–8

42. Hernandez LA, Peevy KJ, Moise AA, Parker JC: Chest wall restriction limits high airway pressure induced lung injury in young rabbits. J Appl Physiol 1989; 66:2364–8
43. Dreyfuss D, Basset G, Soler P, Saumon G: Intermittent positive-pressure hyperventilation with high inflation pressures produces pulmonary microvascular injury in rats. Am Rev Respir Dis 1985; 132:403–8
44. Nishimura M, Honda O, Tomiyama N, Johkoh T, Kagawa K, Nishida T: Body position did not influence the location of ventilator-induced lung injury. Intensive Care Med 2000; 26:1664–9
45. Duggan M, McCaul CL, McNamara PJ, Engelberts D, Ackerley C, Kavanagh BP: Atelectasis causes vascular leak and lethal right ventricular failure in uninjured rat lungs. Am J Respir Crit Care Med 2003; 167:1633–40
46. Wilson MR, Choudhury S, Goddard ME, O'Dea KP, Nicholson AG, Takata M: High tidal volume ventilation upregulates intrapulmonary cytokines in an in vivo mouse model of ventilator-induced lung injury. J Appl Physiol 2003; 95: 1385–93
47. Frank JA, Matthay MA: Science review: Mechanisms of ventilator-induced injury. Crit Care 2003; 7:233–41 23. Dreyfuss D, Ricard J-D, Saumon G: On the physiologic and clinical relevance of lung-borne cytokines during ventilator-induced lung injury. Am J Respir Crit Care Med 2003; 167:1467–71

V. Dynamic Hyperinflation - Exhalation

48. Marcy TW, Marini JJ. Modes of mechanical ventilation. In: Simmons DH, Tierney DF, editors. Current pulmonology. St Louis:Mosby Year Book; 1992:43–90.
49. Derenne JP, Fleury B, Pariente R. Acute respiratory failure of chronic obstructive pulmonary disease. Am Rev Respir Dis 1988;138(4): 1006–1033.
50. Gottfried SB, Rossi A, Milic-Emili J. Dynamic hyperinflation, intrinsic PEEP, and the mechanically ventilated patient. Intensive Crit Care Digest 1986;5:30–33.
51. Tobin MJ, Lodato RF. PEEP, auto-PEEP, and waterfalls (comment). Chest 1989;96(3):449–451. 5. Hall JB, Wood LDH. Liberation of the patient from mechanical ventilation. JAMA 1987;257(12):1621–1628.
52. Schmidt GA, Hall JB. Acute or chronic respiratory failure: assessment and management of patients with COPD in the emergency setting. JAMA 1989;261(23):3444–3453.
53. Kondili E, Alexopoulou C, Prinianakis G, Xirouchaki N, Georgopoulos D. Pattern of lung emptying and expiratory resistance in mechanically ventilated patients with chronic obstructive pulmonary disease. Intensive Care Med 2004;30(7):1311–1318.
54. Fleury B, Murciano D, Talamo C, Aubier M, Pariente R, Milic-Emili J. Work of breathing in patients with chronic obstructive pulmonary disease in acute respiratory failure. Am Rev Respir Dis 1985;131(6): 822–827.
55. Pepe PE, Marini JJ. Occult positive end-expiratory pressure in mechanically ventilated patients with airflow obstruction: the auto-PEEP effect. Am Rev Respir Dis 1982;126(1):166–170.
56. Bergman NA. Intrapulmonary gas trapping during mechanical ventilation at rapid frequencies. Anesthesiology 1972;37(6):626–633.
57. Jonson B, Nordstro¨m L, Olsson SG, Akerback D. Monitoring of ventilation and lung mechanics during automatic ventilation: a new device. Bull Physiopathol Respir (Nancy) 1975;11(5):729–743.
58. Marini JJ. Should PEEP be used in airflow obstruction? (editorial) Am Rev Respir Dis 1989;140(1):1–3.

59. Iotti GA, Olivei MC, Palo A, Galbusera C, Veronesi R, Comelli A, et al. Unfavorable mechanical effects of heat and moisture exchangers in ventilated patients. Intensive Care Med 1997;23(4):399–405.
60. Campbell RS, Davis K Jr, Johannigman JA, Branson RD. The effects of passive humidifier dead space on respiratory variables in paralyzed and spontaneously breathing patients. Respir Care 2000;45(3): 306–312.
61. Scott LR, Benson MS, Pierson DJ. Effect of inspiratory flowrate and circuit compressible volume on auto-PEEP during mechanical ventilation. Respir Care 1986;31(11):1075–1079.
62. Smith TC, Marini JJ. Impact of PEEP on lung mechanics and work of breathing in severe airflow obstruction. J Appl Physiol 1988; 65(4):1488–1499.
63. Gottfried SB. The role of PEEP in the mechanically ventilated COPD patient. In: Marini JJ, Roussos C, editors. Ventilatory failure. Berlin: Springer-Verlag; 1991:392–418.
64. Blanch L, Fernandez R, Saura P, Baigorri F, Artigas A. Relationship between expired capnogram and respiratory system resistance in critically ill patients during total ventilatory support. Chest 1994; 105(1):219–223.
65. Ranieri VM, Giuliani R, Cinnella G, Pesce C, Brienza N, Ippolito EL, et al. Physiologic effects of positive end-expiratory pressure in patients with chronic obstructive pulmonary disease during acute ventilatory failure and controlled mechanical ventilation. Am Rev Respir Dis 1993;147(1):5–13.
66. Pride NB, Macklem PT. Lung mechanics in disease. In: Fishman AP, editor. Handbook of physiology. The respiratory system. Mechanics of breathing, vol. 3, part 2. Bethesda: American Physiological Society 1986:659–692.
67. Hall JB, Wood LDH. Management of the critically ill asthmatic patient. Med Clin North Am 1990;74(3):779–796.
68. McFadden ER Jr. Acute severe asthma. Am J Respir Crit Care Med 2003;168(7):740–759.
69. Rogers PL, Schlichtig R, Miro´ A, Pinsky M. Auto-PEEP during CPR: an “occult” cause of electromechanical dissociation? Chest 1991;99(2):492–493.
70. Iotti GA, Braschi A. Measurements of respiratory mechanics during mechanical ventilation. Rhazurns, Switzerland: Hamilton Medical Scientific Library; 1999.
71. Rossi A, Polese G, Brandi G, Conti G. Intrinsic positive end-expiratory pressure (PEEPi). Intensive Care Med 1995;21(6):522–536.
72. Brochard L. Intrinsic (or auto-) PEEP during controlled mechanical ventilation. Intensive Care Med 2002;28(10):1376–1378.
73. Younes M. Dynamic intrinsic PEEP (PEEPi ,dyn). Is it worth saving? (editorial) Am J Respir Crit Care Med 2000;162(5):1608–1609.
74. Hernandez P, Navalesi P, Maltais F, Gursahaney A, Gottfried SB. Comparison of static and dynamic measurements of intrinsic PEEP in anesthetized cats. J Appl Physiol 1994;76(6):2437–2442.
75. Zakynthinos SG, Vassilakopoulos T, Zakynthinos E, Roussos C. Accurate measurement of intrinsic positive end-expiratory pressure: how to detect and correct for expiratory muscle activity. Eur Respir J 1997;10(3):522–529.
76. Gottfried SB, Reissman H, Ranieri VM. A simple method for the measurement of intrinsic positive end-expiratory pressure during controlled and assisted modes of mechanical ventilation. Crit Care Med 1992;20(5):621–629.

77. Broseghini C, Brandolese R, Poggi R, Bernasconi M, Manzin E, Rossi A. Respiratory resistance and intrinsic positive end-expiratory pressure (PEEPi) in patients with the adult respiratory distress syndrome (ARDS). Eur Respir J 1988;1(8):726–731.
78. Iotti GA, Braschi A, Brunner JX, Smits T, Olivei M, Palo A, Veronesi R. Respiratory mechanics by least squares fitting in mechanically ventilated patients: applications during paralysis and during pressure support ventilation. Intensive Care Med 1995;21(5):406–413.
79. Brochard L. Intrinsic (or auto-) positive end-expiratory pressure during spontaneous or assisted ventilation. Intensive Care Med 2002; 28(11):1552–1554.
80. Fabry B, Guttmann J, Eberhard L, Bauer T, Haberthur C, Wolff G. An analysis of desynchronization between the spontaneously breathing patient and ventilator during inspiratory pressure support. Chest 1995;107(5):1387–1394.
81. Rossi A, Appendini L. Wasted efforts and dyssynchrony: is the patient-ventilator battle back? (editorial) Intensive Care Med 1995; 21(11):867–870.
82. Tobin MJ, Jubran A, Laghi F. Patient-ventilator interaction. Am J Respir Crit Care Med 2001;163(5):1059–1063.
83. Kondili E, Prinianakis G, Georgopoulos D. Patient-ventilator interaction. Br J Anaesth 2003;91(1):106–119. AIR TRAPPING, AUTO-PEEP, AND DYNAMIC HYPERINFLATION RESPIRATORY CARE • JANUARY 2005 VOL 50 NO 1 121
84. Haluszka J, Chartrand DA, Grassino AE, Milic-Emili J. Intrinsic PEEP and arterial PCO2 in stable patients with chronic obstructive pulmonary disease. Am Rev Respir Dis 1990;141(5 Pt 1):1194– 1197.
85. Ninane V, Yernault JC, de Troyer A. Intrinsic PEEP in patients with chronic obstructive pulmonary disease: role of expiratory muscles. Am Rev Respir Dis 1993;148(4 Pt 1):1037–1042.
86. Lessard MR, Lofaso F, Brochard L. Expiratory muscle activity increases intrinsic positive end-expiratory pressure independently of dynamic hyperinflation in mechanically ventilated patients. Am J Respir Crit Care Med 1995;151(2 Pt 1):562–569.
87. Fernandez R, Benito S, Blanch L, Net A. Intrinsic PEEP: a cause of inspiratory muscle ineffectivity. Intensive Care Med 1988;15(1):51– 52.
88. Tuxen DV. Permissive hypercapnic ventilation. Am J Respir Crit Care Med 1994;150(3):870–874.
89. Hubmayr RD, Abel MD, Rehder K. Physiologic approach to mechanical ventilation. Crit Care Med 1990;18(1):103–113.
90. Tuxen DV, Lane S. The effects of ventilatory pattern on hyperinflation, airway pressures, and circulation in mechanical ventilation of patients with severe air-flow obstruction. Am Rev Respir Dis 1987; 136(4):872–879.
91. Georgopoulos D,Mitrouska I,Markopoulou K, Patakas D, Anthonisen NR. Effects of breathing patterns on mechanically ventilated patients with chronic obstructive pulmonary disease and dynamic hyperinflation. Intensive Care Med 1995;21(11):880–886.
92. Leatherman JW, McArthur C, Shapiro RS. Effect of prolongation of expiratory time on dynamic hyperinflation in mechanically ventilated patients with severe asthma. Crit Care Med 2004;32(7):1542– 1545.
93. Leatherman JW, Ravenscraft SA. Low measured auto-positive endexpiratory pressure during mechanical ventilation of patients with severe asthma: hidden auto-positive end-expiratory pressure. Crit Care Med 1996;24(3):541–546.

94. Perret C, Feihl F. Respiratory failure in asthma: management of the mechanically ventilated patient. In: Vincent JL, editor. Yearbook on intensive care and emergency medicine. Berlin: Springer-Verlag; 1992:364–371.
95. Darioli R, Perret C. Mechanical controlled hypoventilation in status asthmaticus. Am Rev Respir Dis 1984;129(3):385–387.
96. Georgopoulos D, Kondili E, Prinianakis G. How to set the ventilator in asthma. Monaldi Arch Chest Dis 2000;55(1):74–83.
97. Corbridge TC, Hall JB. The assessment and management of adults with status asthmaticus. Am J Respir Crit Care Med 1995;151(5): 1296–1316.
98. Papiris S, Kotanidou A, Malagari K, Roussos C. Clinical review: severe asthma. Crit Care 2002;6(1):30–44.
99. Koutsoukou A, Armaganidis A, Stavrakaki-Kallergi C, Vassilakopoulos T, Lymberis A, Roussos C, Milic-Emili J. Expiratory flow limitation and intrinsic positive end-expiratory pressure at zero positive end-expiratory pressure in patients with adult respiratory distress syndrome. Am J Respir Crit Care Med 2000;161(5):1590– 1596.
100. Gattinoni L, Bombino M, Pelosi P, Lissoni A, Pesenti A, Fumagalli R, Tagliabue M. Lung structure and function in different stages of severe adult respiratory distress syndrome. JAMA 1994;271(22): 1772–1779.
101. Puybasset L, Cluzel P, Chao N, Slutsky AS, Coriat P, Rouby JJ. A computed tomography scan assessment of regional lung volume in acute lung injury. The CT Scan ARDS Study Group. Am J Respir Crit Care Med 1998;158(5 Pt 1):1644–1655.
102. Armaganidis A, Stavrakaki-Kallergi K, Koutsoukou A, Lymberis A, Milic-Emili J, Roussos C. Intrinsic positive end-expiratory pressure in mechanically ventilated patients with and without tidal expiratory flow limitation. Crit Care Med 2000;28(12):3837–3842.
103. Koutsoukou A, Bekos B, Sotiropoulou C, Koulouris NG, Roussos C, Milic-Emili J. Effects of positive end-expiratory pressure on gas exchange and expiratory flow limitation in adult respiratory distress syndrome. Crit Care Med 2002;30(9):1941–1949.
104. The Acute Respiratory Distress Syndrome Network. Ventilation with lower tidal volumes as compared with traditional tidal volumes for acute lung injury and the acute respiratory distress syndrome. N Engl J Med 2000;342(18):1301–1308.
105. de Durante G, del Turco M, Rustichini L, Cosimini P, Giunta F, Hudson LD, et al. ARDSNet lower tidal volume ventilatory strategy may generate intrinsic positive end-expiratory pressure in patients with acute respiratory distress suyndrome. Am J Respir Crit Care Med 2002;165(9):1271–1274.
106. Vieillard-Baron A, Prin S, Augarde R, Desfonds P, Page B, Beauchet A, Jardin F. Increasing respiratory rate to improve CO2 clearance during mechanical ventilation is not a panacea in acute respiratory failure. Crit Care Med 2002;30(7):1407–1412.
107. Richard JC, Brochard L, Breton L, Aboab J, Vandelet P, Tamion F, et al. Influence of respiratory rate on gas trapping during low volume ventilation of patients with acute lung injury. Intensive Care Med 2002;28(8):1078–1083.
108. Branson RD, Davis K Jr, Campbell RS. Monitoring graphic displays of pressure, volume and flow: the usefulness of ventilator waveforms. World Federation of Critical Care 2004; February:8–12.
109. Marini JJ. Patient-ventilator interaction: rational strategies for acute ventilatory management. Respir Care 1993;38(5):482–493.

110. Petrof BJ, Legare M, Goldberg P, Milic-Emili J, Gottfried SB. Continuous positive airway pressure reduces work of breathing and dyspnea during weaning from mechanical ventilation in severe chronic obstructive pulmonary disease. Am Rev Respir Dis 1990;141(2): 281–289. 6
111. Baigorri F, de Monte A, Blanch L, Ferna´ndez R, Valle`s J, Mestre J, et al. Hemodynamic responses to external counterbalancing of autopositive end-expiratory pressure in mechanically ventilated patients with chronic obstructive pulmonary disease. Crit Care Med 1994; 22(11):1782–1791.
112. Tuxen DV. Detrimental effects of positive end-expiratory pressure during controlled mechanical ventilation of patients with severe airflow obstruction. Am Rev Respir Dis 1989;140(1):5–9.
113. Martin JG, Shore S, Engel LA. Effect of continuous positive airway pressure on respiratory mechanics and pattern of breathing in induced asthma. Am Rev Respir Dis 1982;126(5):812–817.
114. Ferna´ndez MM, Villagra´ A, Blanch L, Ferna´ndez R. Non-invasive mechanical ventilation in status asthmaticus. Intensive Care Med 2001;27(3):486–492.
115. Hess DR, Kacmarek RM. Essentials of mechanical ventilation. New York: McGraw-Hill; 2002.
116. Rossi A, Polese G, Milic-Emili J. Monitoring respiratory mechanics in ventilator-dependent patients. In: Tobin MJ, editor. Principles and practice of intensive care monitoring. New York: McGraw-Hill; 1998: 553–596.
117. Marini JJ. Monitoring during mechanical ventilation. Clin Chest Med 1988;9(1):73–100. Erratum in: Clin Chest Med 1988 Jun;9(2):following x.
118. Truwit JD, Marini JJ. Evaluation of thoracic mechanics in the ventilated patient. Part II: Applied mechanics. J Crit Care 1988;3(3): 199–213.
119. Marini JJ, Rodriguez RM, Lamb V. The inspiratory workload of patient-initiated mechanical ventilation. Am Rev Respir Dis 1986; 134(5):902–909. AIR TRAPPING, AUTO-PEEP, AND DYNAMIC HYPERINFLATION 122 RESPIRATORY CARE • JANUARY 2005 VOL 50 NO 1
120. Mancebo J, Albaladejo P, Touchard D, Bak E, Subirana M, Lemaire F, et al. Airway occlusion pressure to titrate positive end-expiratory pressure in patients with dynamic hyperinflation. Anesthesiology 2000;93(1):81–90.
121. Sinderby C, Navalesi P, Beck J, Skrobic Y, Comtois N, Friberg S, et al. Neural control of mechanical ventilation in respiratory failure. Nat Med 1999;5(12):1433–1436.
122. Sassoon CS, Foster GT. Patient-ventilator asynchrony. Curr Opin Crit Care 2001;7(1):28–33.
123. Leung P, Jubran A, Tobin MJ. Comparison of assisted ventilator modes on triggering, patient effort, and dyspnea. Am J Respir Crit Care Med 1997;155(6):1940–1948.
124. Tobin MJ. Advances in mechanical ventilation. N Engl J Med 2001; 344(26):1986–1996.
125. Fernandez R, Mendez M, Younes M. Effect of ventilator flow rate on respiratory timing in normal humans. Am J Respir Crit Care Med 1999;159(3):710–719.
126. Lagui F, Karamchandani K, Tobin MJ. Influence of ventilator settings in determining respiratory frequency during mechanical ventilation. Am J Respir Crit Care Med 1999;160(5 Pt 1):1766–1770.
127. Yamada Y, Du HL. Analysis of the mechanisms of expiratory asynchrony in pressure support ventilation: a mathematical approach. J Appl Physiol 2000;88(6):2143–2150.

128. Mancebo J. Triggering and cycling off during pressure support ventilation: simplicity or sophistication? (editorial) Intensive Care Med 2003;29(11):1871–1872.
129. Marini JJ. Weaning from mechanical ventilation (editorial). N Engl J Med 1991;324(21):1496–1498.
130. Vassilakopoulos T, Zakynthinos S, Roussos Ch. Respiratory muscles and weaning failure. Eur Respir J 1996;9(11):2383–2400.
131. Jubran A, Tobin MJ. Pathophysiologic basis of acute respiratory distress in patients who fail a trial of weaning from mechanical ventilation. Am J Respir Crit Care Med 1997;155(3):906–915.
132. Pelosi P, Solca M, Ravagnan I, Tubiolo D, Ferrario L, Gattinoni L. Effects of heat and moisture exchangers on minute ventilation, ventilatory drive, and work of breathing during pressure-support ventilation in acute respiratory failure. Crit Care Med 1996;24(7):1184–1188.
133. Le Bourdelles G, Mier L, Fiquet B, Djedaini K, Saumon G, Coste F, Dreyfuss D. Comparison of the effects of heat and moisture exchangers and heated humidifiers on ventilation and gas exchange during weaning trials from mechanical ventilation. Chest 1996;110(5):1294– 1298.
134. Epstein SK, Ciubotaru RL. Influence of gender and endotracheal tube size on preextubation breathing pattern. Am J Respir Crit Care Med 1996;154(6 Pt 1):1647–1652. Erratum in: Am J Respir Crit Care Med 1997 Jun;155(6):2115.

VI. Barotrauma

135. Ioannidis G, Lazaridis G, Baka S, Mpoukovinas I, Karavasilis V, Lampaki S, Kioumis I, Pitsiou G, Papaiwannou A, Karavergou A, Katsikogiannis N, Sarika E, Tsakiridis K, Korantzis I, Zarogoulidis K, Zarogoulidis P. Barotrauma and pneumothorax. J Thorac Dis. 2015 Feb;7(Suppl 1):S38-43.
136. Gattinoni L, Bombino M, Pelosi P, Lissoni A, Pesenti A, Fumagalli R, Tagliabue M. Lung structure and function in different stages of severe adult respiratory distress syndrome. JAMA. 1994 Jun 08;271(22):1772-9.
137. Boussarsar M, Thierry G, Jaber S, Roudot-Thoraval F, Lemaire F, Brochard L. Relationship between ventilatory settings and barotrauma in the acute respiratory distress syndrome. Intensive Care Med. 2002 Apr;28(4):406-13.
138. Eisner MD, Thompson BT, Schoenfeld D, Anzueto A, Matthay MA., Acute Respiratory Distress Syndrome Network. Airway pressures and early barotrauma in patients with acute lung injury and acute respiratory distress syndrome. Am. J. Respir. Crit. Care Med. 2002 Apr 01;165(7):978-82.
139. Carron M, Freo U, BaHammam AS, Dellweg D, Guarracino F, Cosentini R, Feltracco P, Vianello A, Ori C, Esquinas A. Complications of non-invasive ventilation techniques: a comprehensive qualitative review of randomized trials. Br J Anaesth. 2013 Jun;110(6):896-914.
140. Anzueto A, Frutos-Vivar F, Esteban A, Alía I, Brochard L, Stewart T, Benito S, Tobin MJ, Elizalde J, Palizas F, David CM, Pimentel J, González M, Soto L, D'Empaire G, Pelosi P. Incidence, risk factors and outcome of barotrauma in mechanically ventilated patients. Intensive Care Med. 2004 Apr;30(4):612-9.
141. Thorevska NY, Manthous CA. Determinants of dynamic hyperinflation in a bench model. Respir Care. 2004 Nov;49(11):1326-34.

142. Mughal MM, Culver DA, Minai OA, Arroliga AC. Auto-positive end-expiratory pressure: mechanisms and treatment. Cleve Clin J Med. 2005 Sep;72(9):801-9.
143. Esteban A, Anzueto A, Frutos F, Alía I, Brochard L, Stewart TE, Benito S, Epstein SK, Apezteguía C, Nightingale P, Arroliga AC, Tobin MJ., Mechanical Ventilation International Study Group. Characteristics and outcomes in adult patients receiving mechanical ventilation: a 28-day international study. JAMA. 2002 Jan 16;287(3):345-55.
144. International consensus conferences in intensive care medicine: Ventilator-associated Lung Injury in ARDS. This official conference report was cosponsored by the American Thoracic Society, The European Society of Intensive Care Medicine, and The Societé de Réanimation de Langue Française, and was approved by the ATS Board of Directors, July 1999. Am. J. Respir. Crit. Care Med. 1999 Dec;160(6):2118-24.
145. Tuxen DV, Lane S. The effects of ventilatory pattern on hyperinflation, airway pressures, and circulation in mechanical ventilation of patients with severe air-flow obstruction. Am. Rev. Respir. Dis. 1987 Oct;136(4):872-9.
146. Brower RG, Lanken PN, MacIntyre N, Matthay MA, Morris A, Ancukiewicz M, Schoenfeld D, Thompson BT., National Heart, Lung, and Blood Institute ARDS Clinical Trials Network. Higher versus lower positive end-expiratory pressures in patients with the acute respiratory distress syndrome. N. Engl. J. Med. 2004 Jul 22;351(4):327-36.
147. Gattinoni L, Pesenti A, Avalli L, Rossi F, Bombino M. Pressure-volume curve of total respiratory system in acute respiratory failure. Computed tomographic scan study. Am. Rev. Respir. Dis. 1987 Sep;136(3):730-6.
148. Tsuno K, Prato P, Kolobow T. Acute lung injury from mechanical ventilation at moderately high airway pressures. J. Appl. Physiol. 1990 Sep;69(3):956-61.
149. Chiumello D, Pristine G, Slutsky AS. Mechanical ventilation affects local and systemic cytokines in an animal model of acute respiratory distress syndrome. Am. J. Respir. Crit. Care Med. 1999 Jul;160(1):109-16.
150. Acute Respiratory Distress Syndrome Network. Brower RG, Matthay MA, Morris A, Schoenfeld D, Thompson BT, Wheeler A. Ventilation with lower tidal volumes as compared with traditional tidal volumes for acute lung injury and the acute respiratory distress syndrome. N. Engl. J. Med. 2000 May 04;342(18):1301-8.
151. Amato MB, Meade MO, Slutsky AS, Brochard L, Costa EL, Schoenfeld DA, Stewart TE, Briel M, Talmor D, Mercat A, Richard JC, Carvalho CR, Brower RG. Driving pressure and survival in the acute respiratory distress syndrome. N. Engl. J. Med. 2015 Feb 19;372(8):747-55.
152. Lu Q, Rouby JJ. Measurement of pressure-volume curves in patients on mechanical ventilation: methods and significance. Crit Care. 2000;4(2):91-100.
153. Sun XM, Chen GQ, Chen K, Wang YM, He X, Huang HW, Luo XY, Wang CM, Shi ZH, Xu M, Chen L, Fan E, Zhou JX. Stress Index Can Be Accurately and Reliably Assessed by Visually Inspecting Ventilator Waveforms. Respir Care. 2018 Sep;63(9):1094-1101.
154. Lin YC, Tu CY, Liang SJ, Chen HJ, Chen W, Hsia TC, Shih CM, Hsu WH. Pigtail catheter for the management of pneumothorax in mechanically ventilated patients. Am J Emerg Med. 2010 May;28(4):466-71.
155. Currie GP, Alluri R, Christie GL, Legge JS. Pneumothorax: an update. Postgrad Med J. 2007 Jul;83(981):461-5.
156. Clancy DJ, Lane AS, Flynn PW, Seppelt IM. Tension pneumomediastinum: A literal form of chest tightness. J Intensive Care Soc. 2017 Feb;18(1):52-56.

157. Reed R, D'Alessio F, Yarmus L, Feller-Kopman D. Abdominal compartment syndrome due to subcutaneous emphysema. BMJ Case Rep. 2012 Feb 25;2012
158. Ahmed K, Amine EG, Abdelbaki A, Jihene A, Khaoula M, Yamina H, Mohamed B. Airway management: induced tension pneumoperitoneum. Pan Afr Med J. 2016;25:125.
159. Marini JJ. Tidal volume, PEEP, and barotrauma. An open and shut case? Chest 1996 Feb;109(2):302-4
160. Hudson LD, Protective ventilation for patients with acute respiratory distress syndrome. N Engl J Med 1998 Feb 5;338(6):385-7
161. Schnapp LM, Chin DP, Szaflarski N, Matthay MA, Frequency and importance of barotrauma in 100 patients with acute lung injury. Crit Care Med 1995 Feb;23(2):272-8.
162. Gattinoni L, Bombino M, Pelosi P, Lissoni A, Pesenti A, Fumagalli R, Tagliabue M, Lung structure and function in different stages of severe adult respiratory distress syndrome. JAMA 1994 Jun 8;271(22):1772-9
163. Weg JG, Anzueto A, Balk RA, Wiedemann HP, Pattishall EN, Schork MA, Wagner LAThe relation of pneumothorax and other air leaks to mortality in the acute respiratory distress syndrome. N Engl J Med 1998 Feb 5;338(6):341-6.
164. Pepe PE, Hudson LD, Carrico CJ, Early application of positive end-expiratory pressure in patients at risk for the adult respiratory-distress syndrome. N Engl J Med 1984 Aug 2;311(5):281-6
165. Gammon RB, Shin MS, Groves RH, Hardin JM, Hsu C, Buchalter SEClinical risk factors for pulmonary barotrauma: a multivariate analysis. Am J Respir Crit Care Med 1995 Oct;152(4 Pt 1):1235-40.
166. ARDS Network. Ventilation with lower tidal volumes as compared with traditional tidal volumes for acute lung injury and the acute respiratory distress syndrome. N Engl J Med 2000;342:1301–1308
167. Brochard L, Roudot-Thoraval F, Roupie E, Delclaux C, Chastre J, Fernandez-Mondejar E, Clementi E, Mancebo J, Factor P, Matamis D, et al., Tidal volume reduction for prevention of ventilator-induced lung injury in acute respiratory distress syndrome: the Multicenter Trial Group on tidal volume reduction in ARDS. Am J Respir Crit Care Med 1998 Dec;158(6):1831-8
168. Stewart TE, Meade MO, Cook DJ, Granton JT, Hodder RV, Lapinsky SE, Mazer CD, McLean RF, Rogovein TS, Schouten BD, et al., Evaluation of a ventilation strategy to prevent barotrauma in patients at high risk for acute respiratory distress syndrome: Pressure- and Volume-Limited Ventilation Strategy Group. N Engl J Med 1998 Feb 5;338(6):355-61
169. Gattinoni L, Pelosi P, Suter PM, Pedoto A, Vercesi P, Lissoni A, Acute respiratory distress syndrome caused by pulmonary and extrapulmonary disease: different syndromes? Am J Respir Crit Care Med 1998 Jul;158(1):3-11
170. Amato MB, Barbas CS, Medeiros DM, Magaldi RB, Schettino GP, Lorenzi-Filho G, Kairalla RA, Deheinzelin D, Munoz C, Oliveira R, et al.Effect of a protective-ventilation strategy on mortality in the acute respiratory distress syndrome. N Engl J Med 1998 Feb 5;338(6):347-54

VII. Dyssynchrony

171. Online reference: https://www.ncsrc.org/wp-content/uploads/2014/08/Patient-Ventilator-Dysynchrony-in-CMV-Volume-Kriner1.pdf

172. Petrof BJ, Jaber S, Matecki S. Ventilator-induced diaphragmatic dysfunction. Curr Opin Crit Care 2010;16:19-25.
173. Levine S, Nguyen T, Taylor N, Friscia ME, Budak MT, Rothenberg P, et al. Rapid disuse atrophy of diaphragm fibers in mechanically ventilated humans. N Engl J Med 2008;358:1327-35.
174. Kress JP, Pohlman AS, O'Connor MF, Hall JB. Daily interruption of sedative infusions in critically ill patients undergoing mechanical ventilation. N Engl J Med 2000;342:1471-7.
175. Schweickert WD, Gehlbach BK, Pohlman AS, Hall JB, Kress JP. Daily interruption of sedative infusions and complications of critical illness in mechanically ventilated patients. Crit Care Med 2004;32:1272-6.
176. Garnacho-Montero J, Madrazo-Osuna J, GarcíaGarmendia JL, Ortiz-Leyba C, Jiménez-Jiménez FJ, Barrero-Almodóvar A, et al. Critical illness polyneuropathy: risk factors and clinical consequences. A cohort study in septic patients. Intensive Care Med 2001;27:1288-96.
177. Putensen C, Zech S, Wrigge H, Zinserling J, Stüber F, Von Spiegel T, et al. Long-term effects of spontaneous breathing during ventilatory support in patients with acute lung injury. Am J Respir Crit Care Med 2001;164:43-9.
178. de Wit M, Miller KB, Green DA, Ostman HE, Gennings C, Epstein SK. Ineffective triggering predicts increased duration of mechanical ventilation. Crit Care Med 2009;37:2740-5.
179. Thille AW, Rodriguez P, Cabello B, Lellouche F, Brochard L. Patient-ventilator asynchrony during assisted mechanical ventilation. Intensive Care Med 2006;32:1515-22.
180. Blanch L, Villagra A, Sales B, Montanya J, Lucangelo U, Luján M, et al. Asynchronies during mechanical ventilation are associated with mortality. Intensive Care Med 2015;41:633-41.
181. Bosma K, Ferreyra G, Ambrogio C, Pasero D, Mirabella L, Braghiroli A, et al. Patient-ventilator interaction and sleep in mechanically ventilated patients: pressure support versus proportional assist ventilation. Crit Care Med 2007;35:1048-54.
182. Georgopoulos D, Prinianakis G, Kondili E. Bedside waveforms interpretation as a tool to identify patient-ventilator asynchronies. Intensive Care Med 2006;32:34-47.
183. Sassoon CS, Gruer SE. Characteristics of the ventilator pressure- and flow-trigger variables. Intensive Care Med 1995;21:159-68.
184. Aslanian P, El Atrous S, Isabey D, Valente E, Corsi D, Harf A, et al. Effects of flow triggering on breathing effort during partial ventilatory support. Am J Respir Crit Care Med 1998;157:135-43.
185. Goulet R, Hess D, Kacmarek RM. Pressure vs flow triggering during pressure support ventilation. Chest 1997;111:1649-53.
186. Prinianakis G, Kondili E, Georgopoulos D. Effects of the flow waveform method of triggering and cycling on patient-ventilator interaction during pressure support. Intensive Care Med 2003;29:1950-9.
187. Racca F, Squadrone V, Ranieri VM. Patient-ventilator interaction during the triggering phase. Respir Care Clin N Am 2005;11:225-45.
188. Slutsky AS. Mechanical ventilation: American College of Chest Physicians' Consensus Conference. Chest 1993;104:1833-59.
189. Prinianakis G, Kondili E, Georgopoulos D. Patientventilator interaction: an overview. Respir Care Clin N Am 2005;11:201-24.

190. Tobin MJ, Jubran A, Laghi F. Patient-ventilator interaction. Am J Respir Crit Care Med 2001;163:1059-63.
191. Sharshar T, Desmarais G, Louis B, Macadou G, Porcher R, Harf A, et al. Transdiaphragmatic pressure control of airway pressure support in healthy subjects. Am J Respir Crit Care Med 2003;168:760-9.
192. Sinderby C, Navalesi P, Beck J, Skrobik Y, Comtois N, Friberg S, et al. Neural control of mechanical ventila- https://doi.org/10.4266/kjccm.2017.00535 Elvira-Markela Antonogiannaki, et al. Mechanisms and Bedside Recognition 321 tion in respiratory failure. Nat Med 1999;5:1433-6.
193. Kondili E, Xirouchaki N, Georgopoulos D. Modulation and treatment of patient-ventilator dyssynchrony. Curr Opin Crit Care 2007;13:84-9.
194. Georgopoulos DB, Anastasaki M, Katsanoulas K. Effects of mechanical ventilation on control of breathing. Monaldi Arch Chest Dis 1997;52:253-62.
195. Brander L, Leong-Poi H, Beck J, Brunet F, Hutchison SJ, Slutsky AS, et al. Titration and implementation of neurally adjusted ventilatory assist in critically ill patients. Chest 2009;135:695-703.
196. Bonmarchand G, Chevron V, Chopin C, Jusserand D, Girault C, Moritz F, et al. Increased initial flow rate reduces inspiratory work of breathing during pressure support ventilation in patients with exacerbation of chronic obstructive pulmonary disease. Intensive Care Med 1996;22:1147-54.
197. Bonmarchand G, Chevron V, Ménard JF, Girault C, Moritz-Berthelot F, Pasquis P, et al. Effects of pressure ramp slope values on the work of breathing during pressure support ventilation in restrictive patients. Crit Care Med 1999;27:715-22.
198. Chiumello D, Pelosi P, Taccone P, Slutsky A, Gattinoni L. Effect of different inspiratory rise time and cycling off criteria during pressure support ventilation in patients recovering from acute lung injury. Crit Care Med 2003;31:2604-10.
199. Chiumello D, Pelosi P, Calvi E, Bigatello LM, Gattinoni L. Different modes of assisted ventilation in patients with acute respiratory failure. Eur Respir J 2002;20:925-33.
200. Thille AW, Cabello B, Galia F, Lyazidi A, Brochard L. Reduction of patient-ventilator asynchrony by reducing tidal volume during pressure-support ventilation. Intensive Care Med 2008;34:1477-86.
201. Leung P, Jubran A, Tobin MJ. Comparison of assisted ventilator modes on triggering, patient effort, and dyspnea. Am J Respir Crit Care Med 1997;155:1940- 8.
202. Younes M, Kun J, Webster K, Roberts D. Response of ventilator-dependent patients to delayed opening of exhalation valve. Am J Respir Crit Care Med 2002;166:21-30.
203. Vaporidi K, Babalis D, Chytas A, Lilitsis E, Kondili E, Amargianitakis V, et al. Clusters of ineffective efforts during mechanical ventilation: impact on outcome. Intensive Care Med 2017;43:184-91.
204. Vitacca M, Bianchi L, Zanotti E, Vianello A, Barbano L, Porta R, et al. Assessment of physiologic variables and subjective comfort under different levels of pressure support ventilation. Chest 2004;126:851-9.
205. Nava S, Bruschi C, Rubini F, Palo A, Iotti G, Braschi A. Respiratory response and inspiratory effort during pressure support ventilation in COPD patients. Intensive Care Med 1995;21:871-9.
206. Rossi A, Polese G, Brandi G, Conti G. Intrinsic positive end-expiratory pressure (PEEPi). Intensive Care Med 1995;21:522-36.

207. Fabry B, Guttmann J, Eberhard L, Bauer T, Haberthür C, Wolff G. An analysis of desynchronization between the spontaneously breathing patient and ventilator during inspiratory pressure support. Chest 1995;107:1387-94.
208. Imanaka H, Nishimura M, Takeuchi M, Kimball WR, Yahagi N, Kumon K. Autotriggering caused by cardiogenic oscillation during flow-triggered mechanical ventilation. Crit Care Med 2000;28:402-7.
209. Hill LL, Pearl RG. Flow triggering, pressure triggering, and autotriggering during mechanical ventilation. Crit Care Med 2000;28:579-81.
210. Carteaux G, Lyazidi A, Cordoba-Izquierdo A, Vignaux L, Jolliet P, Thille AW, et al. Patient-ventilator asynchrony during noninvasive ventilation: a bench and clinical study. Chest 2012;142:367-76.
211. Sassoon CS, Zhu E, Caiozzo VJ. Assist-control mechanical ventilation attenuates ventilator-induced diaphragmatic dysfunction. Am J Respir Crit Care Med 2004;170:626-32.
212. Du HL, Yamada Y. Expiratory asynchrony. Respir Care Clin N Am 2005;11:265-80.
213. Prinianakis G, Plataki M, Kondili E, Klimathianaki M, Vaporidi K, Georgopoulos D. Effects of relaxation 322 The Korean Journal of Critical Care Medicine: Vol. 32, No. 4, November 2017 https://doi.org/10.4266/kjccm.2017.00535 of inspiratory muscles on ventilator pressure during pressure support. Intensive Care Med 2008;34:70-4.
214. Kondili E, Prinianakis G, Georgopoulos D. Patientventilator interaction. Br J Anaesth 2003;91:106-19.
215. Yamada Y, Du HL. Analysis of the mechanisms of expiratory asynchrony in pressure support ventilation: a mathematical approach. J Appl Physiol (1985) 2000;88:2143-50.
216. Akoumianaki E, Lyazidi A, Rey N, Matamis D, PerezMartinez N, Giraud R, et al. Mechanical ventilation induced reverse-triggered breaths: a frequently unrecognized form of neuromechanical coupling. Chest 2013;143:927-38.
217. Simon PM, Habel AM, Daubenspeck JA, Leiter JC. Vagal feedback in the entrainment of respiration to mechanical ventilation in sleeping humans. J Appl Physiol (1985) 2000;89:760-9.
218. Simon PM, Zurob AS, Wies WM, Leiter JC, Hubmayr RD. Entrainment of respiration in humans by periodic lung inflations: effect of state and CO(2). Am J Respir Crit Care Med 1999;160:950-60.
219. Meza S, Mendez M, Ostrowski M, Younes M. Susceptibility to periodic breathing with assisted ventilation during sleep in normal subjects. J Appl Physiol (1985) 1998;85:1929-40.
220. Tobin MJ. Monitoring of pressure, flow, and volume during mechanical ventilation. Respir Care 1992;37:1081-96.
221. Jubran A, Van de Graaff WB, Tobin MJ. Variability of patient-ventilator interaction with pressure support ventilation in patients with chronic obstructive pulmonary disease. Am J Respir Crit Care Med 1995;152:129-36.
222. Terzi N, Pelieu I, Guittet L, Ramakers M, Seguin A, Daubin C, et al. Neurally adjusted ventilatory assist in patients recovering spontaneous breathing after acute respiratory distress syndrome: physiological evaluation. Crit Care Med 2010;38:1830-7.
223. Spahija J, de Marchie M, Albert M, Bellemare P, Delisle S, Beck J, et al. Patient-ventilator interaction during pressure support ventilation and neurally adjusted ventilatory assist. Crit Care Med 2010;38:518-26.

224. Xirouchaki N, Kondili E, Vaporidi K, Xirouchakis G, Klimathianaki M, Gavriilidis G, et al. Proportional assist ventilation with load-adjustable gain factors in critically ill patients: comparison with pressure support. Intensive Care Med 2008;34:2026-34.
225. Piquilloud L, Vignaux L, Bialais E, Roeseler J, Sottiaux T, Laterre PF, et al. Neurally adjusted ventilatory assist improves patient-ventilator interaction. Intensive Care Med 2011;37:263-71.
226. Kondili E, Prinianakis G, Alexopoulou C, Vakouti E, Klimathianaki M, Georgopoulos D. Respiratory load compensation during mechanical ventilation: proportional assist ventilation with load-adjustable gain factors versus pressure support. Intensive Care Med 2006;32:692-9.
227. Lecomte F, Brander L, Jalde F, Beck J, Qui H, Elie C, et al. Physiological response to increasing levels of neurally adjusted ventilatory assist (NAVA). Respir Physiol Neurobiol 2009;166:117-24.
228. Sassoon CS, Foster GT. Patient-ventilator asynchrony. Curr Opin Crit Care. 2001; 7(1):28–33.
229. Racca F, Squadrone V, Ranieri VM. Patient-ventilator interaction during the triggering phase. Respir Care Clin. 2005; 11(2):225–245.
230. Dick CR, Sassoon CS. Patient-ventilator interactions. Clin Chest Med. 1996; 17(3):423–438.
231. Tobin, MJ.; Fahey, PJ. Management of the patient who is "fighting the ventilator. In: Tobin, MJ.; Fahey, PJ., editors. Principles and Practice of Mechanical Ventilation. New York: NY: McGraw Hill; 1994.
232. Nilsestuen JO, Hargett KD. Using ventilator graphics to identify patient-ventilator asynchrony. Respir Care. 2005; 50(2):202–234.
233. Kirby RR. Improving ventilator-patient interaction: reduction of flow dyssynchrony [editorial]. Crit Care Med. 1997; 25(10):1630.
234. Mellott, KG.; Grap, MJ.; Sessler, CN.; Wetzel, P. Manifestations of patient ventilator dyssynchrony in critically ill patients. Paper presented at: 19th annual conference of the Southern Nursing Research Society; February 3, 2005; Atlanta, Georgia;
235. Kallet RH, Luce JM. Detection of patient-ventilator asynchrony during low tidal volume ventilation, using ventilator waveform graphics. Respir Care. 2002; 47(2):183–185.

VIII. Chest Wall Restriction

236. Gonzalez J, Coast JR, Lawler JM, Welch HG. A chest wall restrictor to study effects on pulmonary function and exercise. 2. The energetics of restrictive breathing. Respiration. 1999;66(2):188-94. doi:
237. Coast JR, Cline CC. The effect of chest wall restriction on exercise capacity. Respirology. 2004 Jun;9(2):197-203. doi:
238. Cline CC, Coast JR, Arnall DA, A chest wall restrictor to study effects on pulmonary function and exercise. 1. Development and validation, Respiration 1999;66(2):182-7
239. Bradley CA, Anthonisen NR. Rib cage and abdominal restrictions have different effects on lung mechanics. J Appl Physiol 1980;49: 946–952.
240. 2 Butler J, Caro CG, Alcala R, Dubois AB. Physiological factors affecting airway resistance in normal subjects and in patients with obstructive respiratory disease. J Clin Invest 1960;39:584–591.
241. Caro CG, Butler J, Dubois AB. Some effects of restriction of chest cage expansion on pulmonary function in man: an experimental study. J Clin Invest 1960;39:573–583.

242. Douglas NJ, Drummond GB, Sudlow MF. Breathing at low lung volumes and chest strapping: a comparison of lung mechanics. J Appl Physiol 1981;50:650–657.
243. Klineberg PL, Rehder K, Hyatt RE. Pulmonary mechanics and gas exchange in seated normal men with chest restriction. J Appl Physiol 1981;51:26–32.
244. O'Donnell DE, Hong HH, Webb KA. Respiratory sensation during chest wall restriction and dead space loading in exercising men. J Appl Physiol (1985) 2000;88:1859–1869.
245. Scheidt M, Hyatt RE, Rehder K. Effects of rib cage or abdominal restriction on lung mechanics. J Appl Physiol 1981;51: 1115–1121.
246. Stubbs SE, Hyatt RE. Effect of increased lung recoil pressure on maximal expiratory flow in normal subjects. J Appl Physiol 1972;32: 325–331.
247. Sybrecht GW, Garrett L, Anthonisen NR. Effect of chest strapping on regional lung function. J Appl Physiol 1975;39:707–713.
248. van Noord JA, Demedts M, Cle´ment J, Cauberghs M, Van de Woestijne KP. Effect of rib cage and abdominal restriction on total respiratory resistance and reactance. J Appl Physiol (1985) 1986;61: 1736–1740.
249. Pride NB, Permutt S, Riley RL, Bromberger-Barnea B. Determinants of maximal expiratory flow from the lungs. J Appl Physiol 1967;23: 646–662.
250. Nakamura M, Sasaki H, Takishima T. Effect of lung surface tension on bronchial collapsibility in excised dog lungs. J Appl Physiol 1979;47: 692–700.
251. Bachofen H, Schu¨ rch S, Urbinelli M, Weibel ER. Relations among alveolar surface tension, surface area, volume, and recoil pressure. J Appl Physiol (1985) 1987;62:1878–1887.
252. Young SL, Tierney DF, Clements JA. Mechanism of compliance change in excised rat lungs at low transpulmonary pressure. J Appl Physiol 1970;29:780–785.
253. Faridy EE, Permutt S, Riley RL. Effect of ventilation on surface forces in excised dogs' lungs. J Appl Physiol 1966;21:1453–1462.
254. Estenne M, Gevenois PA, Kinnear W, Soudon P, Heilporn A, De Troyer A. Lung volume restriction in patients with chronic respiratory muscle weakness: the role of microatelectasis. Thorax 1993;48: 698–701.
255. Littleton SW. Impact of obesity on respiratory function. Respirology 2012;17:43–49.
256. O'Donnell DE, Ciavaglia CE, Neder JA. When obesity and chronic obstructive pulmonary disease collide. Physiological and clinical consequences. Ann Am Thorac Soc 2014;11:635–644.
257. Salome CM, King GG, Berend N. Physiology of obesity and effects on lung function. J Appl Physiol (1985) 2010;108:206–211.
258. Jones RL, Nzekwu MM. The effects of body mass index on lung volumes. Chest 2006;130:827–833.
259. Ray CS, Sue DY, Bray G, Hansen JE, Wasserman K. Effects of obesity on respiratory function. Am Rev Respir Dis 1983;128:501–506.
260. Behazin N, Jones SB, Cohen RI, Loring SH. Respiratory restriction and elevated pleural and esophageal pressures in morbid obesity. J Appl Physiol (1985) 2010;108:212–218.
261. Hedenstierna G, Santesson J. Breathing mechanics, dead space and gas exchange in the extremely obese, breathing spontaneously and during anaesthesia with intermittent positive pressure ventilation. Acta Anaesthesiol Scand 1976;20:248–254.
262. Naimark A, Cherniack RM. Compliance of the respiratory system and its components in health and obesity. J Appl Physiol 1960;15: 377–382.

263. Pelosi P, Croci M, Ravagnan I, Tredici S, Pedoto A, Lissoni A, Gattinoni L. The effects of body mass on lung volumes, respiratory mechanics, and gas exchange during general anesthesia. Anesth Analg 1998;87: 654–660.
264. Pelosi P, Croci M, Ravagnan I, Vicardi P, Gattinoni L. Total respiratory system, lung, and chest wall mechanics in sedated-paralyzed postoperative morbidly obese patients. Chest 1996;109:144–151.
265. Sharp JT, Henry JP, Sweany SK, Meadows WR, Pietras RJ. The total work of breathing in normal and obese men. J Clin Invest 1964;43: 728–739.
266. Sharp JT, Henry JP, Sweany SK, Meadows WR, Pietras RJ. Effects of mass loading the respiratory system in man. J Appl Physiol 1964;19: 959–966.
267. Douglas FG, Chong PY. Influence of obesity on peripheral airways patency. J Appl Physiol 1972;33:559–563.
268. Collins LC, Hoberty PD, Walker JF, Fletcher EC, Peiris AN. The effect of body fat distribution on pulmonary function tests. Chest 1995;107: 1298–1302.
269. Lazarus R, Sparrow D, Weiss ST. Effects of obesity and fat distribution on ventilatory function: the normative aging study. Chest 1997;111: 891–898.
270. Pellegrino RG, Gobbi A, Antonelli A, Torchio R, Gulotta C, Pellegrino GM, Dellaca` R, Hyatt RE, Brusasco V. Ventilation heterogeneity in obesity. J Appl Physiol (1985) 2014;116:1175–1181.
271. Leith DE, Mead J. Mechanisms determining residual volume of the lungs in normal subjects. J Appl Physiol 1967;23:221–227.
272. McDonough JE, Yuan R, Suzuki M, Seyednejad N, Elliott WM, Sanchez PG, Wright AC, Gefter WB, Litzky L, Coxson HO, et al. Small-airway obstruction and emphysema in chronic obstructive pulmonary disease. N Engl J Med 2011;365:1567–1575.
273. O'Donnell DE, Deesomchok A, Lam YM, Guenette JA, Amornputtisathaporn N, Forkert L, Webb KA. Effects of BMI on static lung volumes in patients with airway obstruction. Chest 2011;140: 461–468.
274. Ora J, Laveneziana P, Wadell K, Preston M, Webb KA, O'Donnell DE. Effect of obesity on respiratory mechanics during rest and exercise in COPD. J Appl Physiol (1985) 2011;111:10–19.
275. Barr RG, Ahmed FS, Carr JJ, Hoffman EA, Jiang R, Kawut SM, Watson K. Subclinical atherosclerosis, airflow obstruction and emphysema: the MESA Lung Study. Eur Respir J 2012;39:846–854.
276. Cao C, Wang R, Wang J, Bunjhoo H, Xu Y, Xiong W. Body mass index and mortality in chronic obstructive pulmonary disease: a metaanalysis. PLoS ONE 2012;7:e43892.
277. Guenette JA, Jensen D, O'Donnell DE. Respiratory function and the obesity paradox. Curr Opin Clin Nutr Metab Care 2010;13: 618–624.
278. Verleden SE, Vasilescu DM, Willems S, Ruttens D, Vos R, Vandermeulen E, Hostens J, McDonough JE, Verbeken EK, Verschakelen J, et al. The site and nature of airway obstruction after lung transplantation. Am J Respir Crit Care Med 2014;189: 292–300.
279. Eberlein M, Diehl E, Bolukbas S, Merlo CA, Reed RM. An oversized allograft is associated with improved survival after lung transplantation for idiopathic pulmonary arterial hypertension. J Heart Lung Transplant 2013;32:1172–1178.
280. Yalcin HC, Perry SF, Ghadiali SN. Influence of airway diameter and cell confluence on epithelial cell injury in an in vitro model of airway reopening. J Appl Physiol (1985) 2007;103:1796–1807.

281. Dixon DL, De Pasquale CG, De Smet HR, Klebe S, Orgeig S, Bersten AD. Reduced surface tension normalizes static lung mechanics in a rodent chronic heart failure model. Am J Respir Crit Care Med 2009;180:181–187.
282. Haber PS, Colebatch HJ, Ng CK, Greaves IA. Alveolar size as a determinant of pulmonary distensibility in mammalian lungs. J Appl Physiol 1983;54:837–845.
283. Alexander HLKW. Symptomatic relief of emphysema by an abdominal belt. Am J Med Sci 1934;187:687–692.
284. Dodd DS, Brancatisano TP, Engel LA. Effect of abdominal strapping on chest wall mechanics during exercise in patients with severe chronic air-flow obstruction. Am Rev Respir Dis 1985;131: 816–821.
285. Torchio R, Gulotta C, Ciacco C, Perboni A, Guglielmo M, Crosa F, Zerbini M, Brusasco V, Hyatt RE, Pellegrino R. Effects of chest wall strapping on mechanical response to methacholine in humans. J Appl Physiol (1985) 2006;101:430–438.
286. Harty HR, Corfield DR, Schwartzstein RM, Adams L. External thoracic restriction, respiratory sensation, and ventilation during exercise in men. J Appl Physiol (1985) 1999;86:1142–1150.
287. Brack T, Jubran A, Tobin MJ. Effect of elastic loading on variational activity of breathing. Am J Respir Crit Care Med 1997;155: 1341–1348.
288. van der Kaaij NP, Kluin J, Haitsma JJ, den Bakker MA, Lambrecht BN, Lachmann B, de Bruin RW, Bogers AJ. Surfactant pretreatment decreases long-term damage after ischemia-reperfusion injury of the lung. Eur J Cardiothorac Surg 2009;35:304–312, discussion 312.
289. Waldhausen JA, Giammona ST, Kilman JW, Daly WJ. Effect of transplantation of canine lung on pulmonary compliance and surfactant. JAMA 1965;191:1002–1005.

IX. Oxygen Saturation.

290. Hafen BB, Sharma S. Oxygen Saturation. [Updated 2020 Aug 12]. In: StatPearls [Internet]. Treasure Island (FL): StatPearls Publishing; 2020 Jan-.
291. Kaufman DP, Kandle PF, Murray I, Dhamoon AS. StatPearls [Internet]. StatPearls Publishing; Treasure Island (FL): Jul 26, 2020. Physiology, Oxyhemoglobin Dissociation Curve.
292. Clause D, Detry B, Rodenstein D, Liistro G. Stability of oxyhemoglobin affinity in patients with obstructive sleep apnea-hypopnea syndrome without daytime hypoxemia. J. Appl. Physiol. 2008 Dec;105(6):1809-12.
293. Hanning CD, Alexander-Williams JM. Pulse oximetry: a practical review. BMJ. 1995 Aug 05;311(7001):367-70.
294. Bongard F, Sue D. Pulse oximetry and capnography in intensive and transitional care units. West. J. Med. 1992 Jan;156(1):57-64.
295. Hinkelbein J, Koehler H, Genzwuerker HV, Fiedler F. Artificial acrylic finger nails may alter pulse oximetry measurement. Resuscitation. 2007 Jul;74(1):75-82.
296. Grace RF. Pulse oximetry. Gold standard or false sense of security? Med. J. Aust. 1994 May 16;160(10):638-44.
297. Pu LJ, Shen Y, Lu L, Zhang RY, Zhang Q, Shen WF. Increased blood glycohemoglobin A1c levels lead to overestimation of arterial oxygen saturation by pulse oximetry in patients with type 2 diabetes. Cardiovasc Diabetol. 2012 Sep 17;11:110.
298. Sarikonda KV, Ribeiro RS, Herrick JL, Hoyer JD. Hemoglobin lansing: a novel hemoglobin variant causing falsely decreased oxygen saturation by pulse oximetry. Am. J. Hematol. 2009 Aug;84(8):541.

299. Lee WW, Mayberry K, Crapo R, Jensen RL. The accuracy of pulse oximetry in the emergency department. Am J Emerg Med. 2000 Jul;18(4):427-31
300. American Thoracic Society; American College of Chest Physicians. ATS/ACCP Statement on cardiopulmonary exercise testing. Am. J. Respir. Crit. Care Med. 2003 Jan 15;167(2):211-77

X. Aviation, Gz, and Hypoxia - AIN

301. Green NDC. Long duration acceleration. In: Gradwell DP, Rainford DJ, editors. Ernsting's Aviation and Space Medicine. 5th ed. Boca Raton: CRC Press; 2016.
302. Pollock RD, Tank H, Edwards F, Stevenson AT. Cummulative +Gz exposure and its effects on acceleration atelectasis. 89th Annual Scientific Meeting Aerospace Medicine Association; 6-10th May 2018; Dallas TX 2018.
303. Smith AM. Health status review of F/A-18F Super Hornet aircrew. IAM Report 2015-006-CR. . Adelaide: RAAF Institute of Avition Medicine.; 2015.
304. Fong KL, Fan SW. An overview of the physiological effects of sustained high +Gz forces on human being. Annals of the Academy of Medicine, Singapore. 1997;26(1):94-103.
305. Frerichs I, Dudykevych T, Hinz J, Bodenstein M, Hahn G, Hellige G. Gravity effects on regional lung ventilation determined by functional EIT during parabolic flights. Journal of applied physiology (Bethesda, Md : 1985). 2001;91(1):39-50.
306. Green ND. Lung volumes during +Gz acceleration and the effects of positive pressure breathing and chest counter-pressure. Journal of gravitational physiology : a journal of the International Society for Gravitational Physiology. 1994;1(1):P41-4.
307. Haswell MS, Tacker WA, Jr., Balldin UI, Burton RR. Influence of inspired oxygen concentration on acceleration atelectasis. Aviation, space, and environmental medicine. 1986;57(5):432-7.
308. Tacker WA, Jr., Balldin UI, Burton RR, Glaister DH, Gillingham KK, Mercer JR. Induction and prevention of acceleration atelectasis. Aviation, space, and environmental medicine. 1987;58(1):69-75.
309. Air and Space Interoperability Council (ASIC). Minimum physiological requirements for aircrew demand breathnig systems. Air Standard 61/101/6A. Washington DC: Air and Space Interoperability Council (ASIC); 2000.

XI. Safety Pressure.

310. Gupta S, Donn SM, Continuous positive airway pressure: Physiology and comparison of devices. Seminars in fetal & neonatal medicine, 2016 Jun
311. Gupta S,Donn SM Continuous Positive Airway Pressure: To Bubble or Not to Bubble?, Gupta S,Donn SM,, Clinics in perinatology, 2016 Dec
312. Polin RA,Sahni R, Newer experience with CPAP.Seminars in neonatology : SN, 2002 Oct
313. Brown LK,Javaheri S, Positive Airway Pressure Device Technology Past and Present: What's in the "Black Box"?, Brown LK,Javaheri S,, Sleep medicine clinics, 2017 Dec
314. Schwab RJ,Badr SM,Epstein LJ,Gay PC,Gozal D,Kohler M,Lévy P,Malhotra A,Phillips BA,Rosen IM,Strohl KP,Strollo PJ,Weaver EM,Weaver TE, An official American Thoracic Society statement: continuous positive airway pressure adherence tracking systems. The optimal monitoring strategies and outcome measures in adults. American journal of respiratory and critical care medicine, 2013 Sep 1

315. Tingting X,Danming Y,Xin C, Non-surgical treatment of obstructive sleep apnea syndrome., Tingting X,Danming Y,Xin C,, European archives of oto-rhino-laryngology : official journal of the European Federation of Oto-Rhino-Laryngological Societies (EUFOS) : affiliated with the German Society for Oto-Rhino-Laryngology - Head and Neck Surgery, 2017 Nov 24
316. Johnson BP,Shipper AG,Westlake KP, Systematic Review Investigating the Effects of Nonpharmacological Interventions During Sleep to Enhance Physical Rehabilitation Outcomes in People With Neurological Diagnoses. Neurorehabilitation and neural repair. 2019 Apr 2;
317. C.A. Kushida, A.D. Chediak, R.B. Berry, et al.Clinical guidelines for the manual titration of positive airway pressure in patients with obstructive sleep apneaJ. Clin. Sleep Med., 4 (2008), pp. 157-171
318. H.C.C. Huang, D.R. Hillman, N. McArdleControl of OSA during automatic positive airway pressure titration in a clinical case series: predictors and accuracy of device download data, Sleep, 35 (9) (2012), pp. 1277-1283
319. O. Marrone, A. Salvaggio, S. Romano, G. InsalacoAutomatic titration and calculation by predictive equations for the determination of therapeutic continuous positive airway pressure for obstructive sleep apnea, Chest, 133 (3) (2008), pp. 670-676
320. K.B. Hertegonne, J. Volna, S. Portier, R. De Pauw, G. Van Maele, D.A. PevernagieTitration procedures for nasal CPAP: automatic CPAP or prediction formula? Sleep Med., 9 (7) (2008), pp. 732-738
321. M.W. JohnsA new method for measuring daytime sleepiness: the Epworth Sleepiness Scale, Sleep, 14 (1991), pp. 540-545
322. C.A. Kushida, M.R. Littner, T. Morgenthaler, et al.Practice parameters for the indications for polysomnography and related procedures: an update for 2005, Sleep, 28 (4) (2005), pp. 499-521
323. C. IBer, S. Ancoli-Israel, A.L. Chesson, S.F. Quan, American Academy of Sleep Medicine, Westchester IL, The AASM manual for the scoring of sleep and associated events, Rules, terminology, and technical specifications, 2007.
324. R.B. Berry, R. Budhiraja, D.J. Gottlieb, D. Gozal, C. Iber, V.K. Kapur, C.L. Marcus, R. Mehra, S. Parthasarathy, S.F. Quan, S. Redline, K.P. Strohl, S.L.D. Ward, M.M. TangrediRules for scoring respiratory events in sleep: update of the 2007 AASM manual for the scoring of sleep and associated events, J. Clin. Sleep Med., 8 (5) (2012), pp. 597-619
325. V. Hoffstein, S. Mateika, Predicting nasal continuous positive airway pressure, Am. J. Respir. Crit. Care Med., 150 (2) (1994), pp. 486-488
326. J.S. Loredo, C. Berry, R.A. Nelesen, J.E. Dimsdale, Prediction of continuous positive airway pressure in obstructive sleep apnea, Sleep Breath., 11 (1) (2007 Mar), pp. 45-51
327. J.R. Stradling, M. Hardinge, J. Paxton, D.M. SmithRelative accuracy of algorithm-based prescription of nasal CPAP in OSA, Respir. Med., 98 (1994), pp. 152-154
328. G.-H. Lee, M.J. Kim, E.M. Lee, C.S. Kim, S.A. Lee, Prediction of optimal CPAP pressure and validation of an equation for Asian patients with Obstructive Sleep Apnea, Respir. Care, 58 (5) (2013), pp. 810-815
329. M. Knauert, S. Naik, M.B. Gillespie, M. KrygerClinical consequences and economic costs of untreated obstructive sleep apnea syndrome, World J. Otorhinolaryngol., 1 (1) (2015), pp. 17-27

330. A. Qaseem, J.E. Holty, D.K. Owens, P. Dallas, M. Starkey, P. Shekelle, Clinical Guidelines Committee of the American College of Physicians, Management of obstructive sleep apnea in adults: a clinical practice guideline from the American College of Physicians, Ann. Intern. Med., 159 (7) (2013), pp. 471-483
331. T.E. Weaver, A.M. SawyerAdherence to continuous positive airway pressure treatment for obstructive sleep apnea: implications for future interventions, Indian J. Med. Res., 131 (2010), pp. 245-258

XII. Statistics

332. A. Field (Ed.), Discovering Statistics Using IBM SPSS (4th ed.), SAGE Publications Ltd, London, California, New Delhi (2013), IBM CorpIBM SPSS Statistics for Windows, Version 21.0IBM Corp, Armonk, NY (2012)
333. K.D.S. YoungBayesian diagnostics for checking assumptions of normality, J. Stat. Comput. Simul., 47 (3–4) (1993), pp. 167-180
334. A. Cicchetti, V. DomenicGuidelines, criteria, and rules of thumb for evaluating normed and standardized assessment instruments in psychology, Psychol. Assess., 6 (4) (1994), pp. 284-290,
335. D.G. Altman, J.M. BlandMeasurement in medicine: the analysis of method comparison studies, Statistician, 32 (1983), pp. 307-317,

XIII. Work of Breathing

336. Cabello, Belen, and Jordi Mancebo. "Work of breathing." *Intensive care medicine* 32.9 (2006): 1311-1314.
337. Banner, Michael J., MARC J. Jaeger, and ROBERT R. Kirby. "Components of the work of breathing and implications for monitoring ventilator-dependent patients." *Critical care medicine* 22.3 (1994): 515-523.
338. Otis, Arthur B. "The work of breathing." *Physiological reviews* 34.3 (1954): 449-458.
339. Mancebo, J., et al. "Comparative effects of pressure support ventilation and intermittent positive pressure breathing (IPPB) in non-intubated healthy subjects." *European Respiratory Journal* 8.11 (1995): 1901-1909.
340. Zakynthinos, S., and C. Roussos. "Oxygen Cost of Breathing." *Tissue Oxygen Utilization*. Springer, Berlin, Heidelberg, 1991. 171-184.
341. Campbell, E. J. M., E. K. Westlake, and R. M. Cherniack. "Simple methods of estimating oxygen consumption and efficiency of the muscles of breathing." *Journal of applied physiology* 11.2 (1957): 303-308.
342. Campbell, Edward James Moran. *The respiratory muscles and the mechanics of breathing*. Lloyd-Luke, 1958.
343. Peters, Richard M. "The energy cost (work) of breathing." *The Annals of thoracic surgery* 7.1 (1969): 51-67.

XIV. Physiology of the Airway

344. Wilson WC, Benumof, Bunumof and Hagburg's Airway Management 3rd, Chapter 5 - Physiology of the Airway Edition, Elsevier *2013, Pages 118-158*
345. Coleman L, Zakowski M, Gold JA, Ramanathan S, Bunumof and Hagburg's Airway Management 3rd Edition, Chapter 1 - Functional Anatomy of the Airway, Elsevier 2013, Pages 3-20

XV. Myth Busters

346. Green NDC. Long duration acceleration. In: Gradwell DP, Rainford DJ, editors. Ernsting's Aviation and Space Medicine. 5th ed. Boca Raton: CRC Press; 2016.
347. Pollock RD, Tank H, Edwards F, Stevenson AT. Cummulative +Gz exposure and its effects on acceleration atelectasis. 89th Annual Scientific Meeting Aerospace Medicine Association; 6-10th May 2018; Dallas TX 2018.
348. Smith AM. Health status review of F/A-18F Super Hornet aircrew. IAM Report 2015-006-CR. . Adelaide: RAAF Institute of Avition Medicine.; 2015.
349. Fong KL, Fan SW. An overview of the physiological effects of sustained high +Gz forces on human being. Annals of the Academy of Medicine, Singapore. 1997;26(1):94-103.
350. Frerichs I, Dudykevych T, Hinz J, Bodenstein M, Hahn G, Hellige G. Gravity effects on regional lung ventilation determined by functional EIT during parabolic flights. Journal of applied physiology (Bethesda, Md : 1985). 2001;91(1):39-50.
351. Green ND. Lung volumes during +Gz acceleration and the effects of positive pressure breathing and chest counter-pressure. Journal of gravitational physiology : a journal of the International Society for Gravitational Physiology. 1994;1(1):P41-4.
352. Haswell MS, Tacker WA, Jr., Balldin UI, Burton RR. Influence of inspired oxygen concentration on acceleration atelectasis. Aviation, space, and environmental medicine. 1986;57(5):432-7.
353. Tacker WA, Jr., Balldin UI, Burton RR, Glaister DH, Gillingham KK, Mercer JR. Induction and prevention of acceleration atelectasis. Aviation, space, and environmental medicine. 1987;58(1):69-75.
354. Air and Space Interoperability Council (ASIC). Minimum physiological requirements for aircrew demand breathing systems. Air Standard 61/101/6A. Washington DC: Air and Space Interoperability Council (ASIC); 2000.
355. Military Specification MIL-D-85520, Design and Installation of On Board Oxygen Generating Systems in Aircraft, General Specification for, of 10 Mar1983
356. NAVAIRWARCENACDIV Warminster's Dynamic Flight Simulator ("F/A-18 Breathing System Analysis, Phase II - Breathing Requirements Evaluation", NADC-87061-60)
357. Coyne K, Caretti D, Scott W, Johnson A, Koh F. Inspiratory flow rates during hard work when breathing through different respirator inhalation and exhalation resistances. J Occup Environ Hyg. 2006 Sep;3 (9):490-500.
358. Whitley PE, Pilot performance of the anti-G straining maneuver: respiratory demands and breathing system effects, Aviat Space Environ Med, 1997 Apr;68(4):312-6
359. Harding R. Human respiratory responses during high performance flight. Neuilly-sur-seine, France: AGARD. AGARD-AG-312,1987.
360. Macmillan AJF, Patrick GA, Root DE. Inspiratory flow and pulmonary ventilation in aerobatic flight. Washington, DC: Air Standardization Coordinating Committee: Aerospace Medical and Life Support Systems Report of the Seventeenth Meeting of Working Party 61, Vol. 2:265-76, 1976.
361. White JT, Morin LME. Anti-G straining maneuver incompatibility with tactical aircraft oxygen, Aviat Space Environ Me1988; 59:176-7.

Additional References

362. G Effects on the Pilot During Aerobatics, S. R. Mobler, M.D., FAA-AM-72-28.
363. G Incapacitation in Aerobatic Pilots: A Flight Hazard, W. R. Kirkham, M.D., Ph.D., S. M. Wicks, and D. L. Lowrey, FAA-AM-82-13

364. Newman DG. High G Flight. In. *High G Flight: Physiological Effects and Countermeasures.* Farnham, UK: Ashgate, 2015: 1-268.
365. Convertino VA, High sustained +Gz acceleration: physiological adaptation to high-G tolerance, J Gravit Physiol, 1998 Jul;5(1):P51-4
366. Voge V. Comparison of several G-tolerance measuring methods at various seatback angles. Aviation, Space, and Environmental Medicine. 1978;49(2):377-383
367. [34] Burton R. Mathematical models for predicting G-duration tolerances. Aviation, Space, and Environmental Medicine. 2000;71(10):981-990
368. [35] Protection Against the 'G' [Internet]. Aviation Medicine: Aerospace Medicine. Available from: http://www.avmed.in/2012/06/protection-against-the-g/ [Accessed: Oct 1, 2017]
369. [36] Wood E. Development of anti-G suits and their limitations. Aviation, Space, and Environmental Medicine. 1987;58(7):699-706
370. [37] Wood E, Code C, Baldes E. Partial supination versus Gz protection. Aviation, Space, and Environmental Medicine. 1990;61(9):850-858
371. [38] Burns J, Ivan D, Stern C, Patterson J, Johnson P, Drew W, et al. Protection to +12 Gz. Aviation, Space, and Environmental Medicine. 2001;72(5):413-421

XVI. Appendix One References

1. Air standardization Coordination Committee. Air Std 61/101/6A. Minimum Physiological Requirements for Aircrew Demand Breathing Systems. Air Std 61/101/1C Minimal Protection for Aircrew Exposed to Altitudes above 50,000 Ft. 1988 Washington DC
2. Balldin, UI Pressure Breathing and Acceleration Atelectasis. Raising the Operational Ceiling. A Workshop on the Life Support amd Physiolgical Issues of Flight at 60,000 and above, June 1995
3. Buick F., Porlier JAG, Oxyhemoglobin saturation following rapid decompression to 18,288 m preceded by diluted oxygen breathing. Aviat. Space Environ Med. 1991: 62:1119-26
4. Cook JP, Ikels KG, Adams JD, Miller RL RElation of Breathing Oxygen-Argon Gas Mixtures to Altitude Decompression Sickness, Aviat. Space Environ Med. 1980 51:537-541
5. Ernsting J Some Effects of Oxygen Breathing in Man, Proc. Roy. Soc. Med 1960; 53, 96-98
6. Ernsting J The Ideal Relationship between Inspired Oxygen Concentration and Cabin Altitude. Aerospace Med 1963; 34 991-997
7. Ernsting J, The Influence of Alveolar Nitrogen Concentration upon the Rate of Gas Absorption from Non Ventilated Lung. Aerospace Med 1965; 36. 948-955
8. Ernsting J, Some Effects of Raised Intrapulmonary Pressure in Man. AGARDograph 106 Maidenhead Technivision 1966
9. Ernsting J. Hypoxia and Oxygen Requirements in Aviation and Space Flight: In Payne JP & Hill DW (ed). A Symposium on Oxygen Measurements in Blood and Tissue: London: Butterworth 1975:231-247
10. Ernsting J Prevention of Hypoxia - Acceptable Compromises: Aviat. Space Environ Med 1978: 49, 495-502
11. Ernsting J An Advanced Oxygen System for Future Combat Aircraft In: Recent Advances in Aeronautical and Space Medicine. AGARD Conference Proceedings no: CP 265, 1979, 2-1 to 2-16

12. Ernsting J Operational and Physiological Requirements for Aircraft Oxygen Systems AGARD Report No 697,1984, 1-1 to 1-10
13. Ernsting J, Gedye JL, McHardy GJR, Anoxia subsequent to rapid decompression In: Human Problems in Supersonic and Hypersonic Flight (Ed Buchanan A, Whittingham HE) Oxford, 1962 Pergamon Press p359
14. Glaister DH, Acceleration Atelectasis - Some Factors modifying its occurrence and Magnitude. RAF IAM Report No 299, Farnborough, MODUK, 1970
15. Glaister, DH, Pulmonary gas Exchange During Positive Acceleration, Flying Personnel Research Committee, AirMinistry, 1963
16. Gradwell, DP, Tidley MG, Ernsting J Alveolar Oxygen measurements during Rapid Decompression to High Altitudes Breathing Gas Mixture Simulants of MSOC Product Gas, Aviat. Space Environ Med. 1994, 65, 454
17. Gree ID, Synopsis of Recent Work done on the Problem of Pulmonary Atelectasis Associated with Breathing 100% Oxygen and Increased Positive "G". RAF IAM Report No 230, Farnborough, MODUK, 1963
18. West JB, A Strategy for In-Flight Measurements of Physiology of Pilots of High Performance Fighter Aircraft, Jor Appl Phys, Jul 2013, 115 (1) 145-149
19. Browne, D. R. G., Rochford, J., O'Connell, V., and Jones, J. G. (1970). The incidence of post-operative atelectasis in the dependent lung following thoracotomy: the values of added nitrogen. Br. J. Anatsth., 42, 340.
20. Burger, E. J., and Macklem, P. T.(1966). The effect on the lungs of breathing 100% oxygen near residual volume. Fed. Proc., 25,566.
21. Caro, C. G., Butler, J., and DuBois, A. B. (1960). Some effects of restriction of chest cage expansion on pulmonary function in man: an experimental study. /. Ctin. Invest., 39, 573.
22. Cotes, J. E. (1968). Lung function. Assessment and Application in Medicine. Oxford: Blackwell.
23. Dale, W. A., and Rahn, H. (1952). Rate of gas absorption during atelectasis. Am. J. Physioi, 170, 606.
24. Dantzker, D. R., Wagner, P. D., and West, J.B. (1975). Instability of lung units with low VA/(J ratios during C*2 breathing. J. Appl. Physioi, 38, 886.
25. Dery, R., Pelletier, J., Jacques, A., davet, M., and Houde, J. (1965). Alveolar collapse induced by denitrogenation. Can. Anaesth.Soc.J.,\2, 531.
26. Douglas, N. J., Drummond, G. B., and Sudlow, M. F. (1981). Breathing at low lung volumes and chest strapping: a comparison of lung mechanics. /. Appl. Physioi., 50,650.
27. Du Bois, A. B., Turaids, T., Mammen, R. E., and Nobrega, F. T. (1966). Pulmonary atelectasis in subjects breathing oxygen at sea level or at ninwlati-H altitude. /. Appl. Physioi., 21, 828.
28. Gariinkel, F., and Fitzgerald, R. S. (1978). The effect of hyperoxia, hypoxia and hypercapnia on FRC and occlusion pressure in human subjects. Rap. Physioi., 33,241.
29. Green, I. D. (1967). The pathogenesis and physiological effects of pulmonary collapse induced by breathing oxygen and increased gravitational force. PH.D. Thesis, London University.
30. Henderson, R., Horsfield, K., and Cumming, G. (1969). Intersegmental collateral ventilation in the human lung. Rtsp. Physioi.,6,128. 824 BRITISH JOURNAL OF ANAESTHESIA

31. Langdon, D. E., and Reynolds, G. E. (1961). Post-flight respiratory symptoms associated with 100% oxygen and G-forces. Aerotp. Mtd., 32,713.
32. Levine, B. E., and Johnson, R.P. (1965). Effects of atelectasis on pulmonary surfactant and quasi-static lung mechanics. /. Appl. Physiol., 20, 859.
33. Logan, D. A., Spence, A. A., and Smith, G. (1977). Postoperative pulmonary function. Anaesthesia, 32, 3.
34. Manco, J. C , and Hyatt, R. E. (1975). Relationships of air trapping to increased lung recoil pressure induced by chest cage restriction. Am. Rev. Rapir. Dis., 111,21.
35. Mead, J., Whittenberger, J. L., and Radford, E. P. jr (1957). Surface tensions as a factor in pulmonary volume-pressure hysteresis. /. Appl. Physiol, 10,191.
36. Morrison, S. C , Stubbing, D. G., Zimmerman, P. V., and Campbell, E. J. M. (1982). Lung volume, closing volume and gas exchange. /. Appl. Physiol., 52,1453.
37. Morton, A. P., and Baker, A. B. (1978). r.linir-ai review: postoperative respiratory dysfunction. Anaesth. Intens. Care, 6,56.
38. Nunn, J. F., Coleman, A. J., Sarhirhannn Hanj T., Bergman, N. A., and Laws, J. W. (1965). Hypoxaemia and atelectasis produced by forced expiration. Br. J. Anaesth., 37, 3.
39. Payne, J. P. (1962). Hypoxaemia after general anaesthesia. Lancet,2, 631.
40. Williams, I. P., Jones, J. G., Hewlett, A.M., Hulands, G. H., and Minty, B. D. (1978). Detection and reversal of pulmonary absorption collapse. Br. J. Anaesth., 50, 91.
41. Prys-Roberta, C , Nunn, J. F., Dobson, R. H., Robinson, R. H., Greenbaum, R., and Harris, R. S. (1967). Radiologically undetectable pulmonary collapse in the supine position. Lancet, 2, 399.
42. Rahn, H., and Farhi, L. E. (1963). Gaseous environment and atelectasis. Fed. Proc., 22, 1035.
43. Stubbs, S. E., and Hyatt, R. E. (1972). Effect of increased lung recoil pressure on maiimal expiratory flow in normal subjects. /. Appl. Physiol., 32, 325.
44. Sybrecht, G. W., Garrett, L., and Anthoniscn, N. R. (1975). Effect of chest strapping on regional lung function. /. Appl. Physiol., 39, 707.
45. Wagner, P. D., Laravuso, R. B., Uhl, R. R., and West, J. B. (1974). Continuous distributions of ventilation-perfusion ratios in normal subjects breathing air and 100% Oj. /. CUn. Invest., 54, 54.
46. Webb, S. J. S., and Nunn, J. F. (1967). A comparison between the effect of nitrous oxide and nitrogen on arterial POj. Anaesthesia, 22, 69.
47. Wildsmith, J. A. W., and Masson, A. H. B. (1974). Some effects of maintaining pulmonary nitrogenation during anaesthesia.

Technical Section 8: Non-PBA Aircraft Analysis and Lessons of PBA Data for Other Breathing Systems

8.0 Introduction

Throughout the project, PBA (Pilot Breathing Assessment) developed a database for assessing the pilot/aircraft interaction to identify relative stresses on the pilot. PBA was specifically designed to minimize the number of independent variables by only considering the two different LOX aircraft in two different breathing system variants (USN configuration with the CRU-103 regulator and the USAF configuration with the CRU-73 regulator). The USN configuration was a demand system that provided 100% O_2 and the USAF configuration was a diluter-demand system that supplied 100% O_2 mixed with cabin air. Regardless of the system, the pilot wears a tightly fitting mask that ideally allows no gas to enter or leave except through the inhalation or exhalation valves. The inhalation port on the mask is connected to the breathing gas supply and the exhalation port exhausts exhaled gas to the cabin (through the VigilOX system for PBA flights).

This section generalizes the lessons learned from the restricted PBA dataset to consider various aircraft with different breathing systems, most notably those with other gas delivery systems (OBOGS). Because of the lack of data on other aircraft, this section is, at times, more speculative and qualitative. Where data is available, however, it is used for direct comparison and discussion. These results show that the pathfinding PBA dataset and analysis techniques can be extrapolated/generalized to what is experienced in other aircraft with respect to fundamental aspects of breathing. Of particular concern is having two pilots breathing off the same plenum in an OBOGS jet and having to breath off of a variable supply pressure plenum while the cabin pressure is simultaneously varying (NESC-RP-17-01205, F/A-18 and E/A-18 Fleet Physiological Episodes).

Also discussed is using the PBA dataset and analysis techniques to diagnose different mask and/or valve failure mechanisms that are common to all aircraft. The PBA data show that the detailed VigilOX data can diagnose common mask failure modes.

8.1 Valve Malfunction

Proper pilot breathing occurs when the breathing system responds quickly and proportionally to pilot demand and the valves open and close in the proper sequence. When that does not occur, breathing can become uncomfortable and/or difficult and in the extreme lead to adverse physiological problems.

8.1.1 Breathing Fundamentals

The following sequence occurs during an idealized pilot breath cycle (inhale followed by exhale) for a pilot breathing on either the USN or USAF system. Possible malfunction in the mask and/or valves by each step where appropriate.

1. The pilot initiates inhale by reducing airway pressure (expanding the chest cavity and contracting the diaphragm).
2. This demand from the pilot gets transmitted to the mask and its pressure decreases.
3. The inhalation valve opens.
    a. A valve malfunction can occur if either valve fails to transition quickly and the demand from the pilot does not get instantly transmitted to the regulator

4. The decrease in mask pressure gets transmitted to the outlet of the regulator where the inhale line pressure decreases.
    a. If there is any dynamic loss between the mask and the regulator, due to an obstruction or turbulent flow, the demand from the pilot is delayed in getting to the regulator and not proportionally delivered.
5. The regulator starts to flow. In an idealized breathing system steps 1 thru 5 occur very quickly. The demand from the pilot gets transmitted instantly to the regulator outlet. In addition, regulator ideally produces a flow that is in proportion to the demand, the higher the differential pressure, the higher the flow. The demand signal to the regulator is the outlet pressure referenced to the cabin ($\Delta P_{(l-c)} = P_{line} - P_{cabin}$).
    a. There can be a delay in the response of the regulator to the demand signal. PBA data shows that there is little delay in the USAF configuration and significantly more delay in the USN configuration.
6. During a typical inhale, the pressure will decrease quickly, and the regulator will respond proportionally. The pressure will reach a minimum value and the flow a maximum value (ideally the minimum pressure and maximum flow occur at the same time) after which the pressure increases and the flow decreases.
    a. In an ideal breathing system, the relationship flow is monotonically proportional to the pressure and that relationship is consistent and predictable.
    b. The regulator responds to the line or regulator outlet pressure referenced to the cabin. PBA data show that cabin pressure oscillations on the order of the demand signal and at frequencies on the order of the pilot respiration rate can impact the regulator response.
7. At the end of the inhale, the mask pressure reaches its nominal value (approximately 0.0 and 3.0 mmHg for the USAF and USN configurations, respectively) and the inhalation valve closes. The inhalation flow stops and for the USN configuration the regulator ideally maintains the inhale line at the safety pressure.
    a. There can be times when both the inhalation valve and exhalation valve are open simultaneously
8. The pilot initiates exhale by increasing the airway pressure above the mask pressure. The pressure attempts to close the inhalation valve first if it was not fully closed in step 7 (e.g., limp or obstructed inhalation valve). Once the inhalation valve is closed, the regulator communicates the safety pressure to the exhalation valve via the compensation tube and bladder. The inhale line pressure applies a back force on the exhalation valve and the stability of the inhale line pressure directly impacts the pressure required to open and push exhale gas out of the mask.
    a. If the regulator cannot maintain a constant pressure the force exerted on the exhalation valve will vary and can make exhale difficult.
    b. The compensation bladder can malfunction (sticky, slow or torn) or the compensation tube that connects the inhale line to the exhalation valve can leak, break or become obstructed.
9. The exhale flow starts when the mask pressure exceeds either the cabin pressure (USAF configuration) or the safety pressure (USN configuration) and the exhalation valve opens.
    a. The exhalation valve can stick in which case the pressure required to open the valve will be in excess of the nominal pressure to open the valve.

b. If the inhalation valve fails to close before the exhalation valve opens, the increase in mask pressure will be transmitted to the inhale line. This increase in inhale line pressure gets transmitted to the exhalation valve requiring more than the nominal pressure to open.

10. Once open the mask pressure and exhale flow will increase, reaching a peak pressure and flow after which the pressure and flow decrease. Ideally the peak flow is coincident in time with the peak pressure and the flow is proportional to the pressure.
11. As the pressure decreases to the cabin (USAF) or safety (USN) pressure flow decreases and when the exhalation flow stops, the exhalation valve closes, and the process repeats as the pilot initiates the next breath.

8.1.2 Valve Function Metrics

The valve malfunctions each possess a unique 'signature' in the VigilOX data. There are a number of metrics derived from these data signatures that can track the functionality of the mask, and by extension the breathing system.

A. $\Delta P_{(l - c)}$ during exhalation. The inhale line pressure or regulator outlet pressure (referenced to the cabin) during exhalation sets the safety pressure of the system. During exhalation, this pressure is ideally constant, and the mean value determines the safety pressure. The mean and standard deviation of this differential pressure during exhalation are a measure of the safety pressure and its variation. The mean is ideally constant throughout a mission and the standard deviation should be very low. Using VigilOX this is a derived parameter estimated as the inhale line pressure minus the exhale line pressure.

B. $\Delta P_{(m - sp)}$ during exhalation. In a properly functioning mask/regulator system, the exhalation valve will open when the mask pressure exceeds the value required to overcome the spring holding the valve shut (~ 0.8 mmHg) in USAF configuration or the mask pressure exceeds the safety pressure (~ 3.0 mmHg) plus the added pressure to compress the two springs holding the valve shut (~ 0.8 mmHg) in USN configuration. The safety pressure is set by the regulator during exhalation since the static line pressure at the outlet of the regulator (assuming no inhalation flow) applies a back force on the exhalation valve through the compensation tube and the compensation bladder (Section 1.3.2). To initiate exhale flow, the mask pressure must exceed this safety pressure. If there is exhalation flow and the mask pressure is below the safety pressure plus the spring pressure, there is a malfunction in the mask/regulator system. The average value of $\Delta P_{(m - sp)}$ during exhalation is a measurement of the actual value of the safety pressure. Ideally this value is constant and equal to 3.0 mmHg for a properly functioning system. The variability of safety pressure during exhalation is judged simply by the standard deviation of $\Delta P_{(m - sp)}$ about its mean value.

C. Comparing $\Delta P_{(m - sp)}$ to $\Delta P_{(m - c)}$ during exhalation. Tracking the deviation of the mask pressure from the safety pressure during exhalation is critical in understanding mask valve functionality. This functionality is tracked as the average deviation of the mask pressure from the safety pressure during exhalation ($\Delta P_{(m - c)}$ - $\Delta P_{(m - sp)}$), the standard deviation of this differential and the maximum and minimum values. Finally, a critical metric is the fraction of time the mask pressure is lower than the inhale line differential pressure.

D. $\Delta P_{(m-c)}$ $\Delta P_{(l-c)}$ correlation. During idealized exhalation (not inhalation) the line differential pressure is constant and there is no relationship or correlation between the mask pressure and the differential line pressure. Because of valve handover (between inhalation and exhalation) and non-ideal system behavior the line differential pressure is not constant and some of the variation will correspond to variations in mask pressure. The correlation is defined below. Values closer to 0.0 indicate no correlation and values closer to 1.0 indicate highly correlated values. Negative values indicate positive changes in mask pressure are correlated to negative changes in line differential pressure.

$$\chi = \frac{1}{n} \sum_{i=exhl.\ start}^{exhl.\ end} \frac{\left(\Delta P^{i}_{(l-c)} - \mu_{\Delta P_{(l-c)}}\right)\left(\Delta P^{i}_{(m-c)} - \mu_{\Delta P_{(m-c)}}\right)}{\sigma_{\Delta P_{(l-c)}}\ \sigma_{\Delta P_{(m-c)}}}$$

For reference, Figure 8.1.1 and Table 8.1.1 show three minutes of good breathing during a PBA flight (FLT-045 fore seat) and the associated valve function metric, respectively.

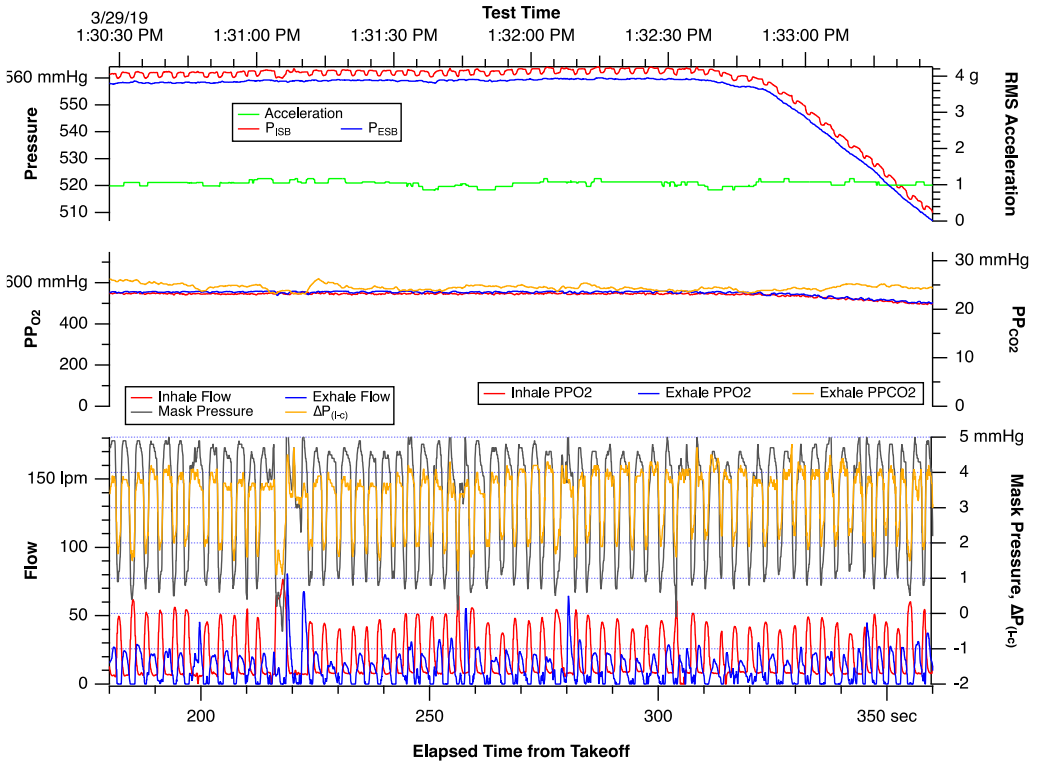

Figure 8.1.1. 3-minute Time Slice of Raw VigilOX Data for PBA Flight FLT-045 (fore seat) Starting 3 minutes After Take-Off

The ISB and ESB RMS acceleration and line and cabin pressures are on the upper axes, the ISB and ESB O_2 and CO_2 partial pressures on the middle axes and the ISB and ESB flow, mask pressure and line-cabin differential pressure on the lower axes. The line-cabin differential pressure is derived by subtracting the ISB line pressure from the ESB line pressure.

The first two lines in the table are the start and end times of the region of interest. The next two lines are the mean and standard deviation of the line-cabin differential pressure during exhalation during this region. The mean is taken to be the value of the safety pressure during this time. The next four rows are the relevant statistics of the value of the deviation between the mask pressure and safety pressure during exhalation in this time period. The second to the last row is the

fraction of time the mask pressure is lower than the safety pressure during exhalation in this time period. The last row is the value of the correlation between the mask pressure and safety pressure during this time period.

Table 8.1.1. Values of Relevant Mask Function Parameters for Time Segment of PBA FLT-045 (fore seat) in Figure 8.1.1

Parameter	**Region 1**
Region Start Time (s)	180
Region End Time (s)	360
Average ΔP(l-c), safety pressure (sp)	3.848
Std. Dev. ΔP(l-c)	0.245
Avg. Dev. ΔP(m-sp)	0.497
Std. Dev. ΔP(m-sp) (mmHg)	0.361
Maximum ΔP(m-sp) (mmHg)	1.47
Minimum ΔP(m-sp) (mmHg)	-0.93
Fraction ΔP(m-c) < sp	0.067
ΔP(l-c) <-> ΔP(m-c) correlation	0.324

Figure 8.1.1 shows that there is timely handoff between the inhale and exhalation valves and the valves appear to open and close as designed. Table 8.1.1 shows the relevant parameters during this time period. The safety pressure is at an appropriate value (possibly a little high, but that could be an artifact of deriving the differential pressure from two absolute pressures) and its variation during exhalation is relatively low (standard deviation). The mask pressure is consistently above safety pressure with only a few minor times when the mask pressure is below the safety pressure. Finally, there is almost no correlation between the mask and line differential pressures indicating there is little communication between the valves.

8.2 Valve Failure Modes

Examination of the PBA data showed a range of non-ideal valve behavior and valve failures. In this subsection, the data signatures associated with each of these failure modes are identified. The first failure mode appears as exhalation hysteresis and does not use the metrics described above. The remaining failure modes use the metrics described above.

8.2.1 Sticky/Delayed Valve Opening or Closing

There were PBA flights that showed either a sticky or delayed valve opening or closing. The predominant Figure 8.2.1 shows a 20 second time slice for a PBA flight (FLT-083) that exhibited a persistent sticky or delayed-opening/closing exhalation valve for a significant portion of the flight. The plot shows the relevant raw VigilOX data along with the derived line-cabin differential pressure, $\Delta P_{(l-c)}$. Figure 8.2.2 shows three consecutive exhalation breaths during the time period in Figure 8.2.1 with the exhale flow as a function of mask pressure for each breath. As exhale starts, mask pressure begins to increase, but the valve opening is delayed resulting in a higher mask pressure to open or crack the valve. Once open, flow increases quickly and reaches the peak value as the valve is fully open. The exhalation flow decreases, but the valve appears to remain open, especially for the first breath in Figure 8.2.2 as the flow (the data use a threshold flow of 0.20 lps indicated by the dashed line in Figure 8.2.2) continues to a mask pressure below which the valve should normally close. The end result is that a relatively large value of the exhalation hysteresis (shown in the red line in the first breath in Figure 8.2.2).

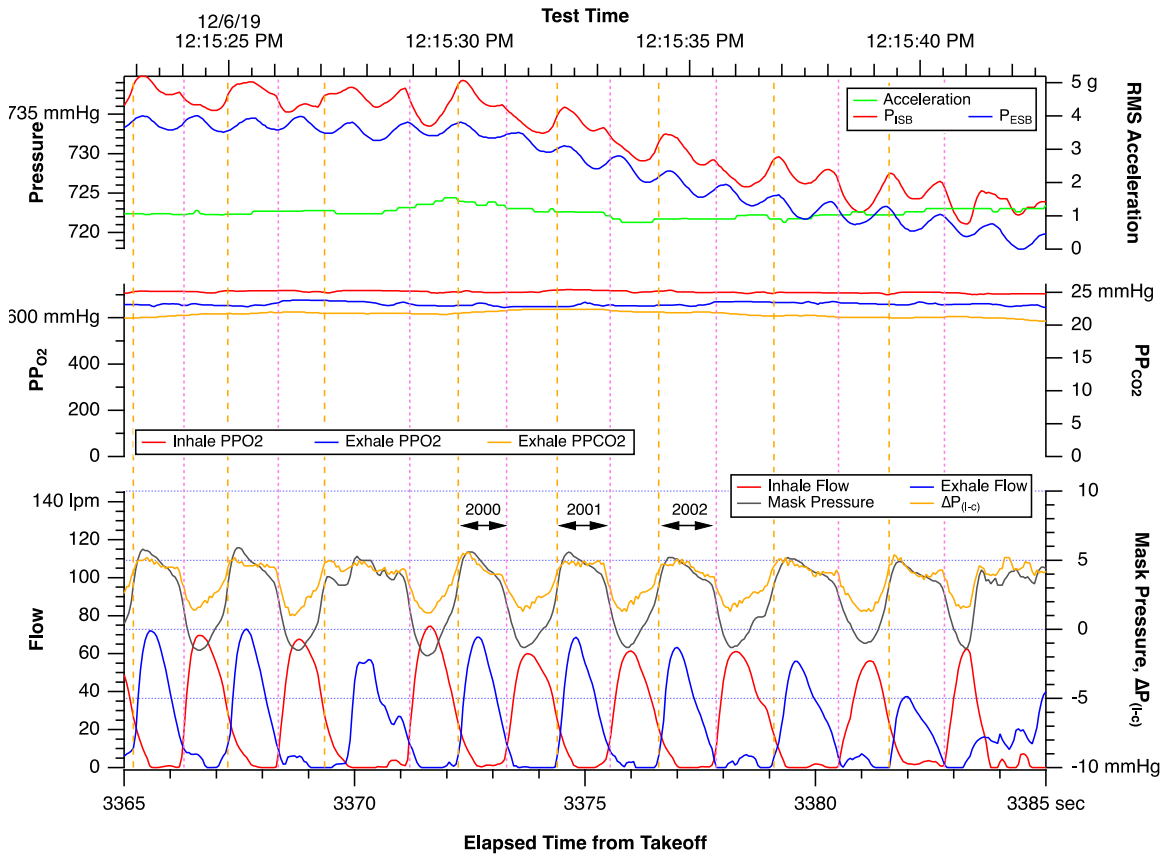

Figure 8.2.2. Raw VigilOX Data for 20-second Time Slice in PBA FLT-083
The plot also includes the derived line-cabin differential pressure, $\Delta P_{(l-c)}$. This PBA flight exhibited a consistent sticky or delayed opening exhalation valve. The vertical lines indicate the beginning and end of an inhale or exhale and the numbers reference the breaths in Figure 8.2.2.

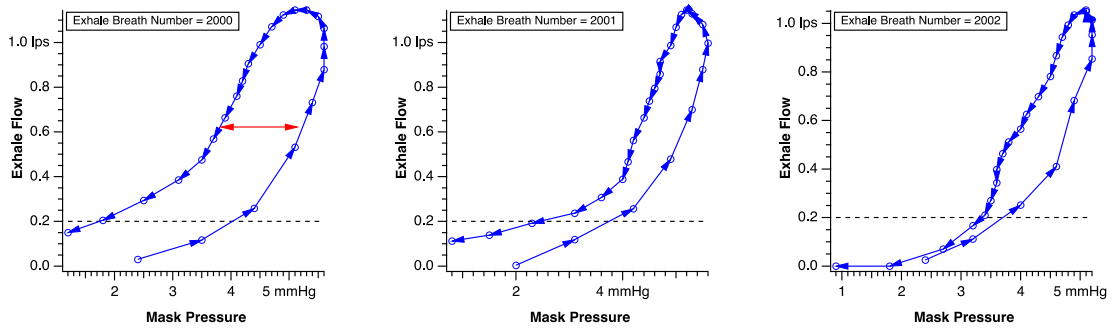

Figure 8.2.3. Exhale Flow as Function Mask Pressure for Three Consecutive Exhalation Breaths During PBA FLT-083 During Time Period in Figure 8.2.1
The arrows trace the time sequence of the exhale in 0.05 second increments. The graph shows that the valve opens at a higher pressure and then re-closes at a lower pressure (taken as the mask pressure when the flow exceeds 0.20 lps). The red line in the first breath (2000) indicates the value of the exhalation hysteresis for that breath.

Table 8.2.1 shows the values of the valve function metrics for a 3-minute segment in FLT-083 containing the breaths in Figures 8.2.1 and 8.2.2. The results show that the value and variation of the safety pressure as measured by the mean and standard deviation of $\Delta P_{(l-c)}$ during

exhalation is higher than the reference data. Further, mask pressure is lower than the safety pressure during exhalation for a significant fraction of time and there is relatively large correlation between the line differential and mask pressures during exhalation compared to the reference data.

Table 8.2.1. Comparison of Valve Function Metrics of FLT-109 with Reference Data in Table 8.1.1

Parameter	Reference Data	FLT-083
Region Start Time (s)	180	3220
Region End Time (s)	360	3400
Average ΔP(l-c), safety pressure (sp)	3.848	4.474
Std. Dev. ΔP(l-c)	0.245	0.474
Avg. Dev. ΔP(m-sp)	0.497	0.040
Std. Dev. ΔP(m-sp) (mmHg)	0.361	0.909
Maximum ΔP(m-sp) (mmHg)	1.47	4.234
Minimum ΔP(m-sp) (mmHg)	-0.93	-2.666
Fraction ΔP(m-c) < sp	0.067	0.529
ΔP(l-c) <-> ΔP(m-c) correlation	0.324	0.731

Another failure mode is a sticky (or lazy) inhalation valve. In this failure mode, the mask pressure drops coincident with the start of inhalation. The inhalation valve is then slow to open or slow to open completely and the demand from the mask is delayed reaching the outlet of the regulator. In the data this presents as a difference between the hysteresis measured using the line cabin differential pressure and that measured using the mask pressure.

Figure 8.2.4 shows the inhalation flow versus the line-cabin differential pressure (left) and mask pressure (right) for a breath where there is no hysteresis measured using either differential pressure.

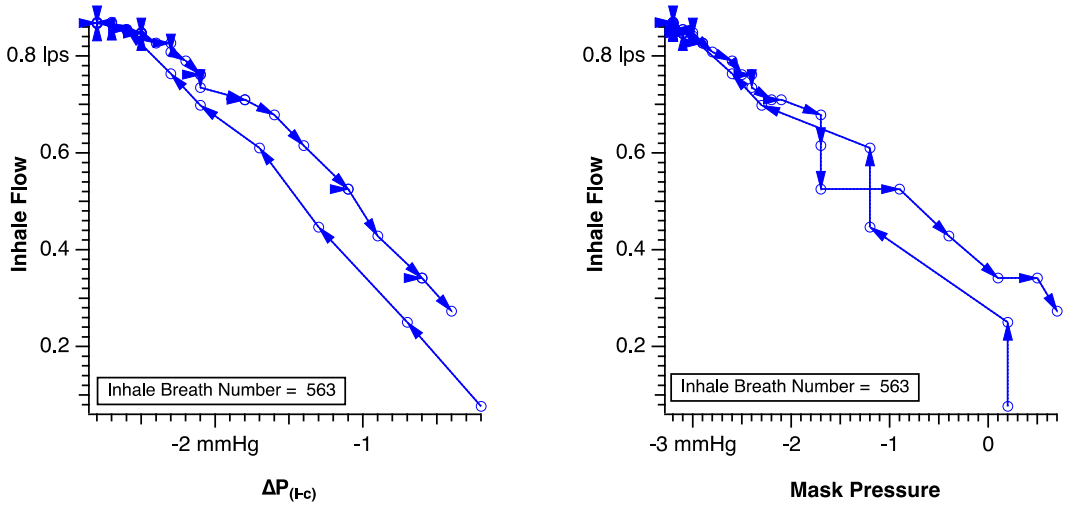

Figure 8.2.4. The Inhalation Flow as Function of Line-Cabin Differential (left) and Mask (right) Pressures
For this breath the hysteresis measured using each differential pressure is near zero (FLT-058). The arrows indicate the time progression with each datum point representing a 0.05 sec increment in time.

Figure 8.2.5 shows an example of a single breath where the hysteresis is not zero and the mask hysteresis is a bit higher. A close examination of the data shows that mask pressure drops below

the safety pressure for a fraction of a second before flow starts. As the mask pressure drops, however, the line-cabin differential pressure remains constant and there is no flow. The line-cabin differential pressure responds instantly once it sees the demand signal – the demand signal is simply delayed getting to the regulator.

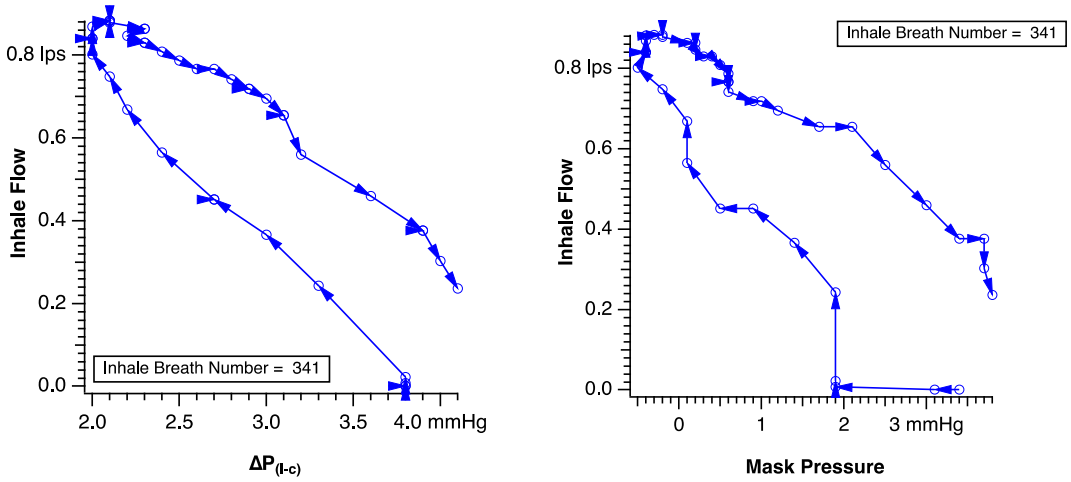

Figure 8.2.5. The Inhalation Flow as Function of Line-Cabin Differential (left) and Mask (right) Pressures
For this breath the hysteresis measured using the line-cabin differential pressure is low (but greater than zero) and the hysteresis measured using the mask is higher (FLT-060).

Figure 8.2.6 shows the histograms for the hysteresis measured using both the line-cabin differential (left) and mask (right) pressures for this flight. The data show the breath pattern in Figure 8.2.5 was prevalent throughout the flight. Finally, note that while the inhalation valve is, in the PBA team's view, the likely cause of the discrepancy, any flow obstruction between the mask and regulator could cause this behavior. The inhalation valve is likely the weak link in the chain though.

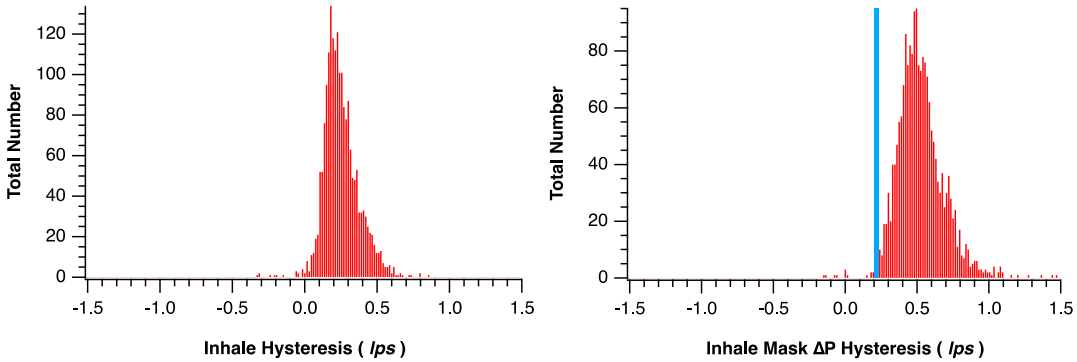

Figure 8.2.6. The Hysteresis Histograms for PBA FLT-060 Measured Using Line-Cabin Differential (left) and Mask (right) Pressures
The blue line on the mask hysteresis histogram represents the mean line-cabin differential pressure hysteresis.

8.2.2 Faulty Exhalation Valve Case Study — PBA FLT-109

PBA FLT-109 was a Profile H flight in USN life support gear. Quick examination of the VigilOX data showed significant ESB DFRL errors and so it is not included in much of the

summary statistics data in this report. The pilot did not report any breathing problems, and in fact reported that breathing was easier than usual for a USN configured flight. Close examination of the VigilOX data from the flight, presented below, led the PBA team to seek a post-flight examination of the valve set by USN personnel to determine their functionality. That examination showed that the exhalation valve was not properly compensating. The compensation diaphragm on the exhalation valve would not immediately return to the fully inflated position after being depressed. The likely result of this problem was that the compensation diaphragm would be slow to return to full compensation. A second problem was that the as the diaphragm would return to its fully compensated position, it would "chatter" repeatedly. Finally, the inhalation valve on the north side, was slightly limp and may have caused it to not seal properly during exhalation (particularly early in exhalation).

Figure 8.2.7 shows a 60-second time window of raw VigilOX data that highlights how the valve issues manifested in the data. The data show prolonged periods where the mask pressure is below the line-cabin differential pressure during exhalation (e.g., 1210 seconds after take-off in Figure 8.2.7). In other words, the mask pressure during exhalation was below the safety pressure which should not occur in a properly functioning breathing system. As described previously and shown in Figure 8.2.9 (lower left image), in order for exhalation flow to begin in a safety pressure system the mask pressure must exceed the safety pressure as set by the inhale line-cabin differential pressure (~ 3.0 mmHg) and the pressure required to compress the small springs in the exhalation valve (~ 0.80 mmHg). Therefore, the minimum mask pressure during exhalation should be close to 1 mmHg higher than the safety pressure in a properly functioning breathing system.

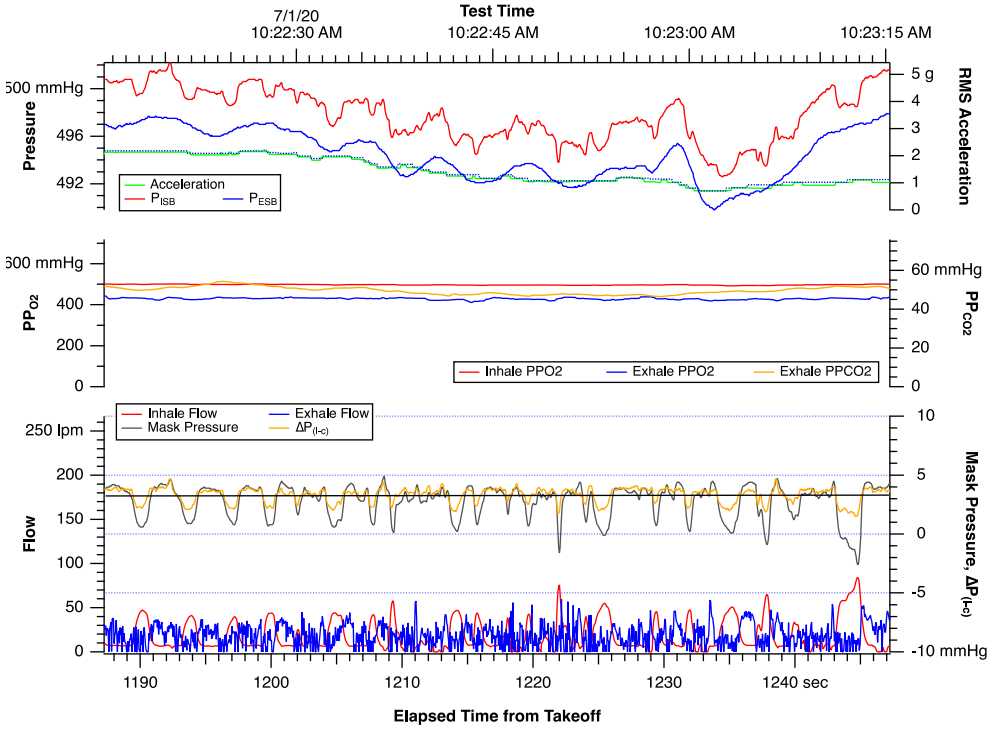

Figure 8.2.7. VigilOX Data for 60-second Segment of PBA FLT-109
The ISB and ESB O_2 and CO_2 partial pressures on the middle axes and the ISB and ESB flow, mask pressure and line-cabin differential pressure on the lower axes. The line-cabin differential pressure is derived by subtracting the ISB line pressure from the ESB line pressure.

Figure 8.2.8 shows how the loss of safety pressure impacts the breathing system in more detail. This particular segment was during higher G-levels which places additional stress on the pilot and breathing system. During this 60 second slice of time the mask pressure drops below the safety pressure by more than 1 mmHg. When this happens, the inhalation valve can open and allow regulator flow through the inhalation valve during exhalation (Figure 8.2.9, lower-center image). Figure 8.2.8 shows that during exhalation, there is a regulator flow of approximately 10 to 20 lpm. This flow value is consistent with that observed in independent USN testing of masks and regulators with a deliberate mask leak (breathing data courtesy of NSWCPCD/J. Camperman). The only time the regulator flow decreases to close to zero is when the mask pressure increases to approximately the same value of the safety pressure at which time the inhalation valve can close.

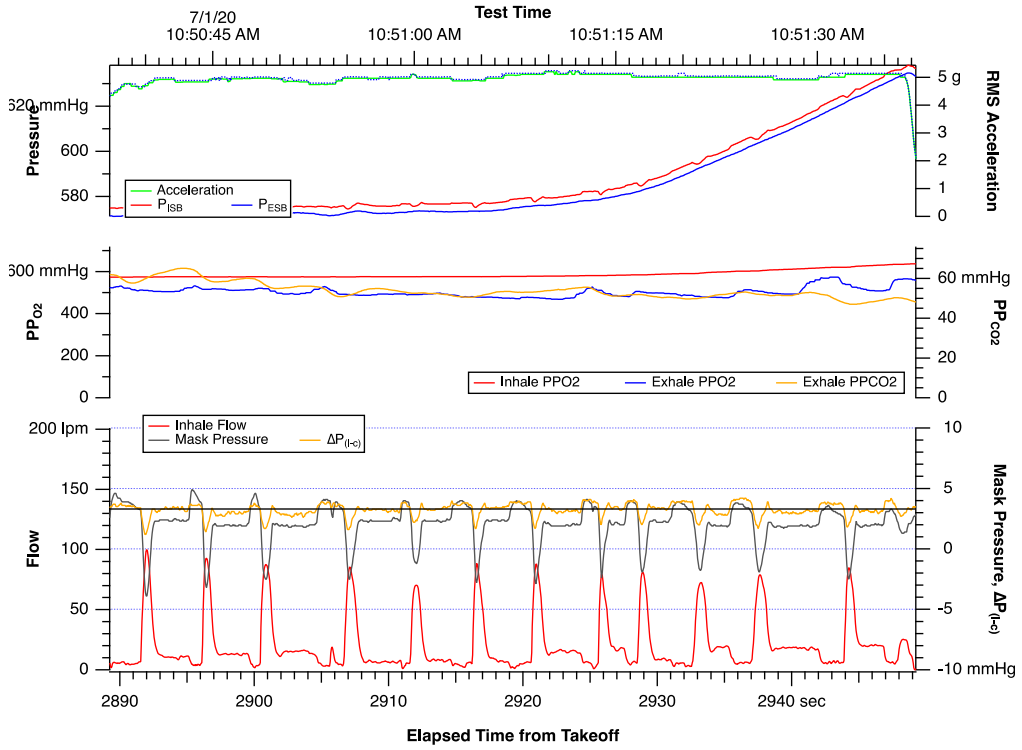

Figure 8.2.8. Raw VigilOX Data from 60-second Time Segment during PBA FLT-109 showing mask pressure more than 1 mmHg lower than the line-cabin differential (safety) pressure during exhalation. The RMS acceleration and ESB and ISB line pressures are on the upper axes. The ISB and ESB O_2 and CO_2 partial pressures on the middle axes and the ISB and ESB flow, mask pressure and line-cabin differential pressure on the lower axes. The line-cabin differential pressure is derived by subtracting the ISB line pressure from the ESB line pressure.

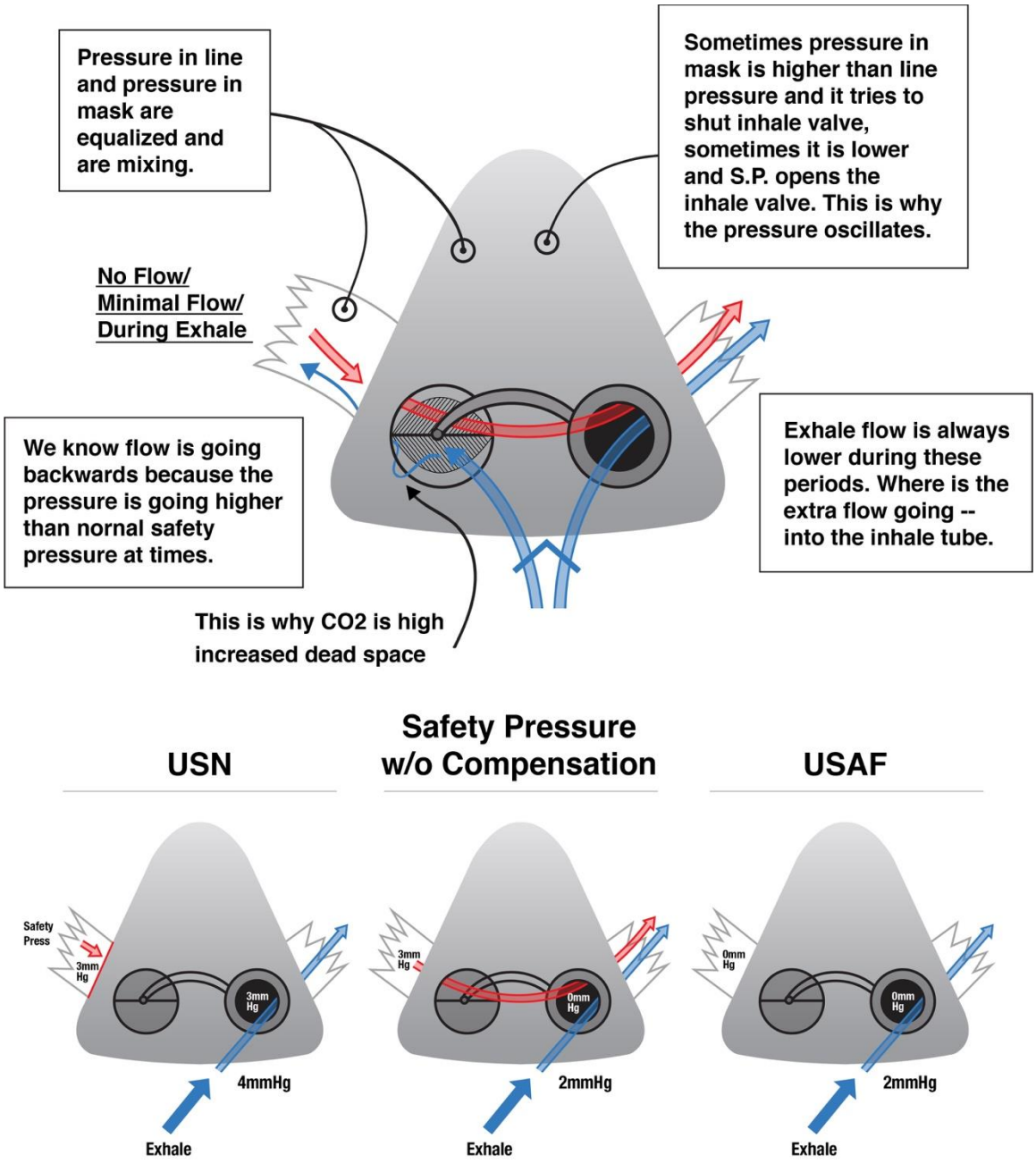

Figure 8.2.9. Schematic of Mask Valve Functioning in Properly Functioning Safety Pressure System (left) Malfunctioning Safety Pressure System (center) and Non-Safety Pressure System.

The loss of safety pressure observed in the data is consistent with the pilot observation of relatively easy breathing on the USN safety pressure system. The results of the valve set inspection (particularly the exhalation valve), the pilot observation and the VigilOX data all suggest a failure of the exhalation valve safety pressure compensation mechanism. The loss of mask pressure could be partially explained by a poor mask seal, but the pilot did not report a significant mask leak (and was specifically asked); any mask leak would likely have been small. To produce the VigilOX data observed, the mask leak would likely have been quite large and persistent throughout the flight. Thus, the failed exhalation valve is likely responsible.

The VigilOX data further show that the mask pressure and line-cabin differential pressure 'track' each other or the oscillations in the mask pressure match pressure oscillations in the line-cabin differential pressure. In a properly functioning breathing system this should not occur as the line-cabin differential pressure should be constant and variations in the mask pressure should be isolated from inhale line pressure domain.

Table 8.2.2 shows how the valve function metrics discussed in Section 8.2.2 for FLT-109 compared to the reference time segment in Table 8.1.1. The highlighted values are the ones the most indicate valve malfunction in FLT-109. The regulator appears to be functioning properly as the safety pressure set-point is the appropriate value and shows little deviation. The average deviation between the mask and line-cabin differential is problematic as the mask pressure is on average below the safety pressure during exhalation which is an indicator of malfunction. This is also borne out in the fraction of time the mask pressure is below the safety pressure during exhalation. Ideally, this value is close to zero as it is in the reference flight. In FLT-109, however, the mask pressure is below the safety pressure almost half the time, indicative of valve malfunction. Finally, the correlation between the mask pressure and safety pressure is nearly 0.60, nearly twice as large as the reference time segment.

Table 8.2.2. Comparison of Valve Function Metrics of FLT-109 with Reference Data in Table 8.1.1

Parameter	Reference Data	FLT-109
Region Start Time (s)	180	0
Region End Time (s)	360	5000
Average ΔP(l-c), safety pressure (sp)	3.848	3.59
Std. Dev. ΔP(l-c)	0.245	0.313
Avg. Dev. ΔP(m-sp)	0.497	-0.026
Std. Dev. ΔP(m-sp) (mmHg)	0.361	1.09
Maximum ΔP(m-sp) (mmHg)	1.47	26.71
Minimum ΔP(m-sp) (mmHg)	-0.93	-3.99
Fraction ΔP(m-c) < sp	0.067	0.499
ΔP(l-c) <-> ΔP(m-c) correlation	0.324	0.562

The data from the flight further show that the failure of the compensation mechanism is not benign. While the pilot did not report any breathing difficulty, the data show a physiological compensation to the failing valve set – namely a significantly increased CO_2 concentration on exhale. The VigilOX data also show that the $PPCO_2$ data were unusually high for this flight (Figure 8.2.10). While the values are not physiologically unrealistic, they are the highest observed over the course of an entire flight during PBA. Figure 8.2.10 shows that the $PPCO_2$ was high for the entire flight with long periods close to 60 mmHg. For reference the same pilot had $PPCO_2$ values of approximately 25 mmHg in his previous two flights (similar flight profiles).

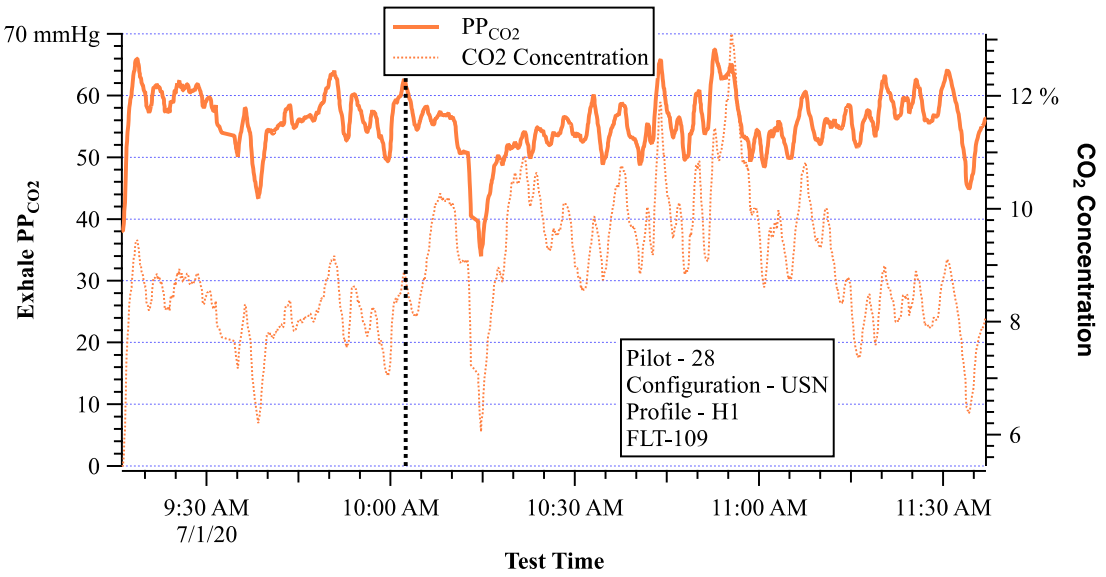

Figure 8.2.10. Exhale $PPCO_2$ and CO_2 Concentration as Function of Time for Entire PBA FLT-109 Test The exhale CO_2 is much higher than that of a typical PBA flight.

While the $PPCO_2$ data from the VigilOX could be in error, it is noted that the same VigilOX ESB unit in the previous and subsequent flights recorded nominal $PPCO_2$ values for the pilot during the entire flight, so the problem was not a systemic drift of the $PPCO_2$ sensor in the ESB. Also note that the $PPCO_2$ values recorded prior to mask DON were near zero and the sensor was returning to a zero reading after mask DOFF (the VigilOX was turned off before it returned to zero). Another note is the specific ESB CO_2 unit in FLT-109 flew on a subsequent flight where the pilot's mask had the new in-mask CO_2 sensor. The CO_2 readings from both units were consistent with each other reducing the likelihood that the high CO_2 reading in FLT-109 was the result of a sensor drift or malfunction. Thus, all indications are that the sensor operated correctly during the flight and that the $PPCO_2$ reading is physiological and not the result of a sensor error. Nevertheless, the PBA team did not specifically verify proper sensor functionality immediately before and after the flight, so the sensor error cannot be ruled out.

The $PPCO_2$ values from FLT-109 are significantly larger than those observed for most PBA flights even if they are not physiologically unrealistic. If the sensor readings are correct, then the question is if there is a mechanism associated with the valve failure that could cause the increased $PPCO_2$. One possibility is that the limp inhalation valve noted by the inspector and the fact that the mask pressure and line-cabin differential pressure seem to track each means that exhaled breath could be going through the inhalation valve and into the supply line (Figure 8.2.9 upper picture). While one would expect the total volume of exhalation flow that would backflow up the inhalation line to be small, if in fact the volume is closer to the pilot's tidal volume, the pilot would then inhale a volume of CO_2-enriched gas. If this is the case, one would expect higher CO_2 levels on exhale as the metabolically produced CO_2 in a breath would mix with the CO_2-enriched gas already inhaled resulting in higher than expected CO_2 on exhale. That is precisely what the ESB CO_2 sensor data show, although there is no data to conclusively this mechanism.

All the evidence from the data to the pilot report to the valve inspection indicate a malfunctioning mask and/or leaking mask seal. All signs point to a consistent pattern of an

exhalation valve failing to properly compensate during flight, intermittently working and intermittently failing giving a unique contrast to understand this failure mode. PBA data has patterns similar to this on occasion, sometimes more than others, so having a firm understanding of this dynamic case study is invaluable.

Given that this is a common failure in USN aircraft and that it may not present as breathing difficulty, it is likely happening more frequently than believed. But the data show that it is not a benign problem. Physiological changes due to the valve failures may reduce the pilot's ability to adapt to either a more challenging flight environments or could be a contributing factor to a PE. Two malfunctions that would not individually result in a PE could, if they happen simultaneously, potentially result in an episode (e.g., exhalation valve malfunction in conjunction with OBOGS degrade)

8.2.3 Inhalation Valve Case Study

There was one PBA flight that appeared to have a significant inhalation valve malfunction for the entire flight. This particular failure mode has been documented in great detail[1]. The significant difference between this flight (PBA FLT-022) and FLT-109 was that the exhalation valve safety pressure compensation worked properly for this flight. In the analysis, the exhalation valve failure to compensate was the driving factor even though the inspection showed a mildly limp inhalation valve and the data suggested that the inhalation valve was open during inhalation.

In this valve failure mode, the inhale proceeds normally. When the pilot begins to exhale, the mask pressure begins to increase. The inhalation valve, however, remains at least partially open (the opening only needs to be very small) and the pilot begins to pressurize the air supply line since the mask and inhale line are not isolated by the closed valve. This increase in pressure then gets applied to the exhalation valve, effectively increasing the pressure required to open the exhalation valve. This results in a pressure spike at the beginning of exhale associated with the increased force required to open the exhalation valve (Figure 8.2.11).

The data show a pressure spike during exhalation in the inhale line and mask. The RMS acceleration and ESB and ISB line pressures are on the upper axes. The ISB and ESB O_2 and CO_2 partial pressures on the middle axes and the ISB and ESB flow, mask pressure and line-cabin differential pressure on the lower axes. The line-cabin differential pressure is derived by subtracting the ISB and ESB line pressures.

[1] Pilot Oxygen Mask Valve Degradation and Physiological Episodes In agile aircraft (T-6, T-45, F-18, F-22, F-35), NASA Pilot Breathing Assessment Face to Face New Orleans, 28 January 2020, From COPE Fighter Summit 19B presentation, 11 Dec 2019, John Camperman, PhD, PE, Diving and Life Support Senior Scientist, Naval Surface Warfare Center Panama City Division, Sponsors: NAVAIR PMA 265, PMA 273

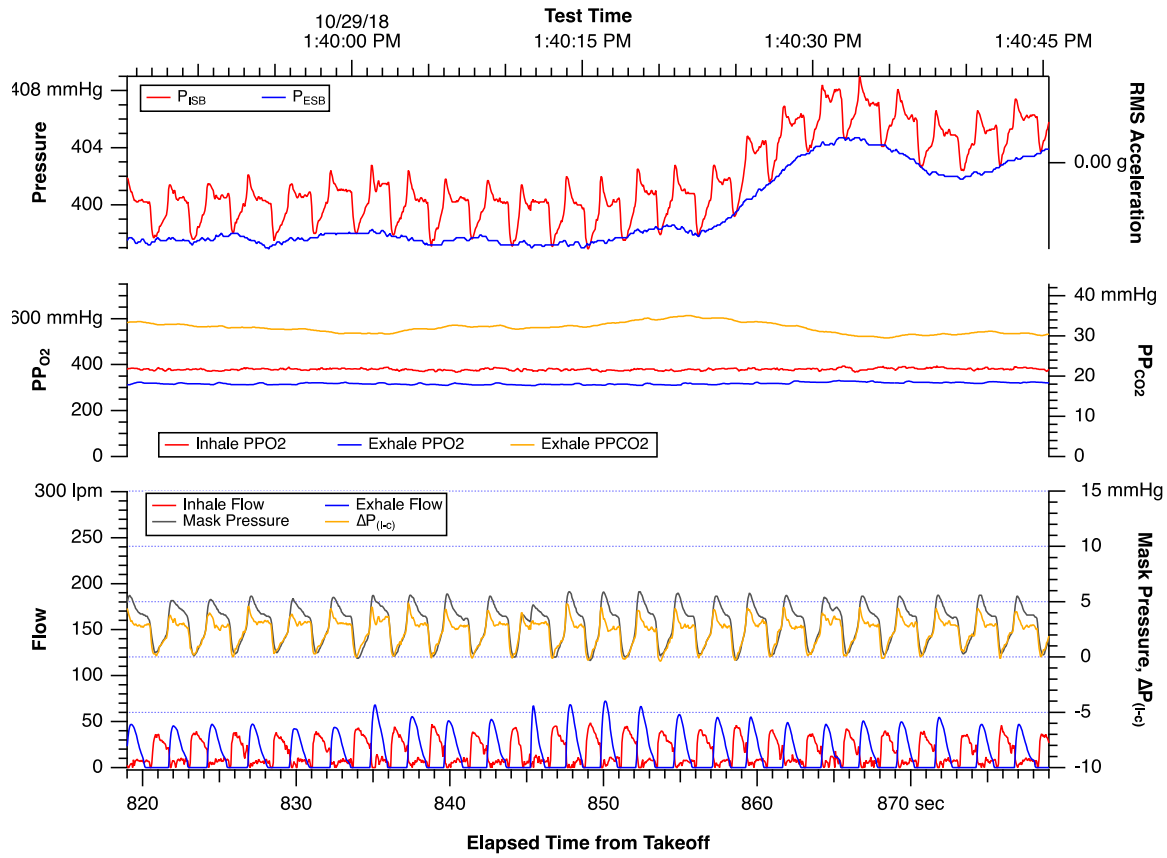

Figure 8.2.11. Raw VigilOX Data for Representative 60-second Time Period during PBA FLT-022

Table 8.2.3 presents the valve function metrics for the first 1000 sec of PBA FLT-022 (before the ESB DFRL errors became prominent) to the reference data in Table 8.1.1. Again, the markers that indicate significant valve malfunction are highlighted. The safety pressure for both flights is reasonable. The data indicate a much higher variation of the safety pressure in FLT-022 consistent with the pressure spike as a result of the valve not closing completely. The other metric that is significantly different is the correlation between the line and mask. Because the inhalation valve is open during exhalation, one would expect the two domains to be correlated and the data show precisely that, a much higher correlation between line-cabin differential and mask pressure variations.

Table 8.2.3. Comparison of Valve Function Metrics of FLT-022 with Reference Data in Table 8.1.1

Parameter	Reference Data	FLT-022
Region Start Time (s)	180	0
Region End Time (s)	360	1000
Average ΔP(l-c), safety pressure (sp)	3.848	3.19
Std. Dev. ΔP(l-c)	0.245	0.671
Avg. Dev. ΔP(m-sp)	0.497	1.477
Std. Dev. ΔP(m-sp) (mmHg)	0.361	0.834
Maximum ΔP(m-sp) (mmHg)	1.47	4.907
Minimum ΔP(m-sp) (mmHg)	-0.93	-1.193
Fraction ΔP(m-c) < sp	0.067	0.039
ΔP(l-c) <-> ΔP(m-c) correlation	0.324	0.644

To understand the physiological implications of this valve failure, a flight comparison between PBA FLT-022 and FLT-050 was performed. Both flights had the same pilot flying the same flight Profile A with the same life support equipment in F-18 aircraft (different tail numbers) in relatively close proximity (in date) to each other. While this type of comparison is not statistically rigorous, it is useful to consider the possible physiological implications of this type of valve failure. It is worth noting that the pilot did not mention breathing difficulty in either flight.

Figures 8.2.12 (FLT-022) and 8.2.13 (FLT-050) show the relevant physiological metrics derived from the VigilOX data for the two PBA flights. PBA FLT-050 did not exhibit the inhalation valve malfunction that was evident on FLT-022. The data show two striking differences. First, the average tidal volume is significantly lower for the entire test on the flight that exhibited the valve malfunction. The three-minute averaged tidal volume on FLT-050 starts at slightly over 0.80 l and then decreases after take-off while at the high altitude, reaching a minimum of approximately 0.60 l. This behavior is consistent with PBA Profile A flights, particularly Profile A flights. The 3-minute averaged tidal volume for FLT-022 is slightly above 0.50 l. The decrease at altitude is less but decreases to over 0.40 l towards the end of the flight.

The second notable difference is that exhale $ppCO_2$ is considerably higher on FLT-022 than FLT-050. The increased CO_2 with decreased tidal volume is logical if the CO_2 output for both flights was approximately constant.

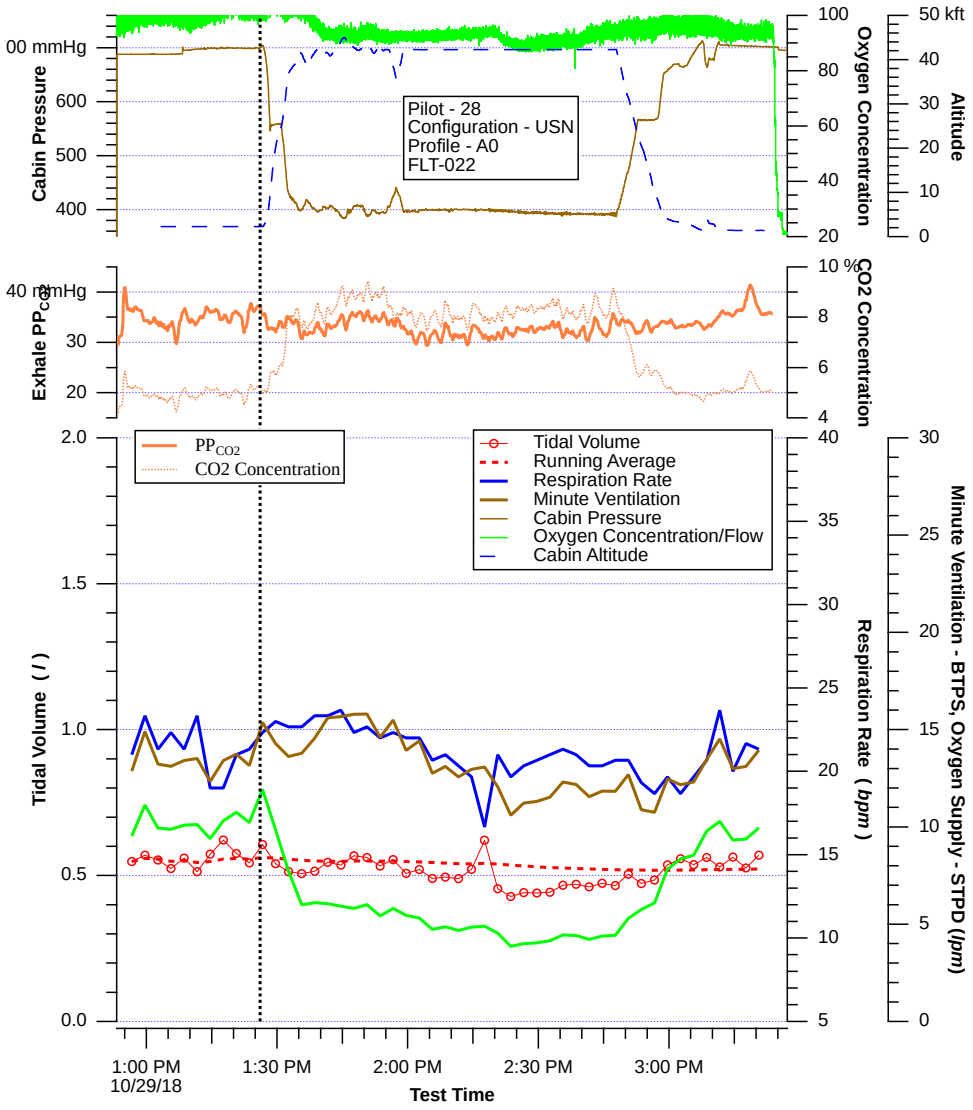

Figure 8.2.12. Relevant Physiological Data Extracted from VigilOX System for FLT-022 The upper axes are for the aircraft altitude, cabin pressure and inhalation O_2 concentration. The middle axes are the exhalation CO_2 concentration and partial pressure. The lower axes are the 3-minute averaged tidal volume (the shading represents plus and minus one standard deviation), the running average, the respiration rate and the minute ventilation (BTPS conditions) and O_2 supply rate (STPD conditions).

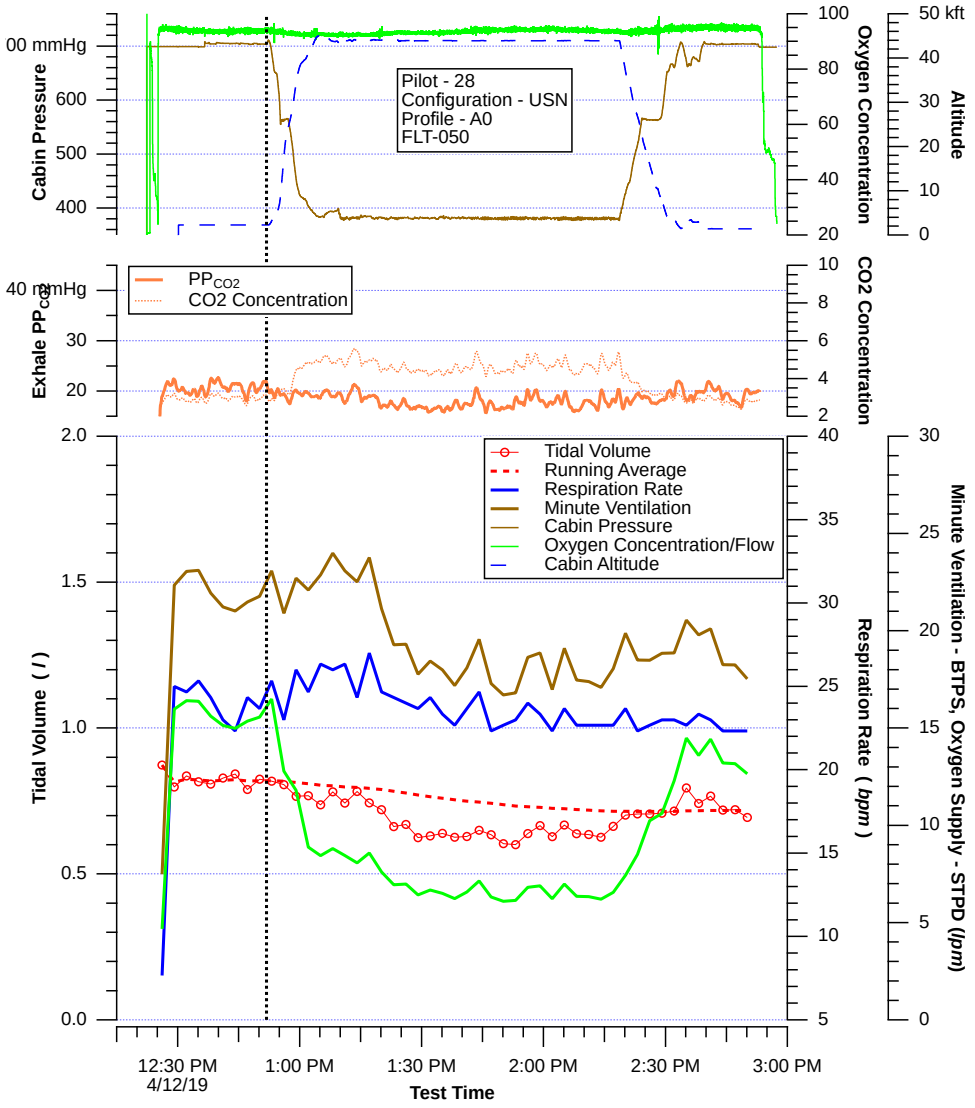

Figure 8.2.13. Relevant Physiological Data Extracted from VigilOX System for FLT-050 The upper axes are for the aircraft altitude, cabin pressure and inhalation O_2 concentration. The middle axes are the exhalation CO_2 concentration and partial pressure. The lower axes are the three-minute averaged tidal volume (the shading represents plus and minus one standard deviation), the running average, the respiration rate and the minute ventilation (BTPS conditions) and O_2 supply rate (STPD conditions).

Figure 8.2.14 shows the exhale peak pressure histograms for the two flights. As expected, the pilot required a higher peak pressure (to move a significantly lower volume) on the flight with the inhalation valve malfunction. The data show how a small valve malfunction can significantly pilot physiology even when there were no complaints of difficulty breathing.

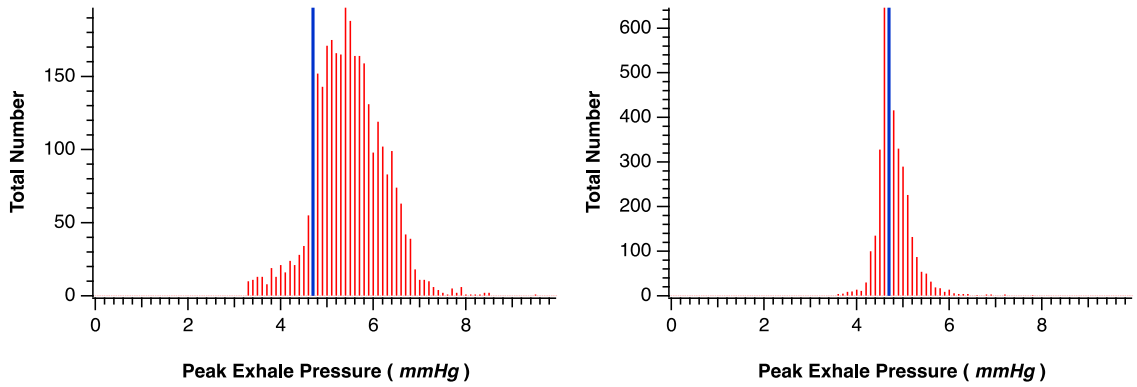

Figure 8.2.14. Exhale Peak Pressure Histograms for FLT-022 (left) and FLT-050 (right) The blue line in both histograms is a reference line at 4.7 mmHg, the approximate mode of the distribution for FLT-050.

8.2.4 Valve Malfunction Summary

The PBA was not a project to systematically study valve failures in pilot masks. As such, there are no tests or series of tests where the PBA team deliberately induced a specific valve failure mode for a number of pilots in different flight conditions to measure the effect on pilot breathing. During the course of the PBA, however, data signatures are noticed on several PBA flights that are consistent with different valve failure modes. While the project was fortunate that these malfunctions did not result in any adverse, reportable problems with breathing, that meant that the discovery of potential problems only occurred when looking at the VigilOX data (and once the PBA team knew what to look for), sometimes days, weeks or even months after the flight. With the exception of FLT-109, that meant that the valves were not removed, inspected or tested after flight as would have been the case if the PBA team were specifically inducing and studying valve malfunction.

These cited cases are specific cases where the valve failures persisted for the entire flight. Of the slightly over 100 sorties, there were persistent valve failures on at least 4 PBA flights. In addition, there are at least 20 PBA flights that had instances of periodic valve failures that could be as small as a few scattered breaths over the entire flight to longer periods of many breaths that were more frequent in a flight. Therefore, the VigilOX data show that valve failures were not uncommon and that persistent valve failures while not common, were also not rare or unusual.

The data further show that the valve failures are not benign events and can cause quantifiable changes in pilot physiology and breathing. While none of these events rose to the level of a documented PE, they did cause quantifiable changes to pilot breathing and/or physiology that, in conjunction with another failure mode, could contribute to a PE.

Because the PBA study did not specifically examine valve failures, the data do not represent a rigorous or statistically significant investigation into mask valve failures and their implications. The PBA team believes; however, the data are compelling and point to (1) the utility of VigilOX data to quantify valve function, and (2) show that valve failures are not benign events and merit further study to understand the implications to the pilot.

8.3 Fundamental Differences between Aircraft for Consideration

8.3.1 OBOGS versus LOX

Different configurations for aircraft O_2 system supplies include OBOGS and LOX. OBOGS is a regenerable swing-bed type concentrator system which uses chemical sorbent beds to differentially concentrate O_2 out of ambient air collected from engine bleed, with this concentrated O_2 then being supplied to the pilot. A LOX system consists of a LOX dewar tank which is gradually evaporated to create a continuous supply of gaseous O_2 to the pilot. OBOGS systems have become more common in recent use because, being regenerable and gathering O_2 from the ambient atmosphere, OBOGS systems can support long-duration mission operations. LOX tanks, being consumable, support shorter mission durations. LOX requires a depot supply of O_2 to re-fill the dewar tank at a ground station, whereas OBOGS does not. In terms of aircraft performance, OBOGS is fundamentally different from LOX due to the inherent pressure and concentration swings created by the pumping action of the regenerating beds, which can result in O_2 pressure and concentration fluctuations in the downstream supply to the pilot. LOX supplies a relatively constant pressure and concentration of O_2 to the pilot.

8.3.2 Individual versus Shared Plenum (One/Two seat aircraft)

Aircraft breathing systems often use a plenum volume between the pilot's gas supply and the regulator to the breathing mask. The plenum volume serves as a buffer between the gas supply and the pilot's regulator, helping to even flow and gas constituency through to the cyclic demand of a pilot's breathing. Specific plenum volume varies between models of aircraft, but the plenum volume is typically equivalent to only a few (i.e., 2-3) full breaths of volume for an adult male breathing heavily. In a dual-seat aircraft, the designed plenum volume may stay the same as carried over from a single-seat aircraft variant, meaning that there are now two aircrew drawing from the same buffer volume that serves a single pilot in a single-seat aircraft. In the case of a dual-seat aircraft, the proportionally smaller plenum volume may lead to issues as two aircrew under high breathing demand may be able to temporarily out-breathe/deplete the gas supply feeding the plenum volume.

8.3.3 Safety (SP) versus Non-Safety (NOSP) Pressure Regulator

Some aircraft, notably the USN fighter aircraft whose configurations were analyzed in this study, use "safety pressure" regulator configuration. In a safety pressure system, the regulator delivers a continuous, constant pressure baseline flow, even when the pilot is not inhaling, and no demand is being placed on the regulator. The use of safety pressure results in a constant positive-pressure air flow delivered through the pilot's mask, regardless of pilot breathing.

It should be noted that the PBA was unable to determine the initial requirement or locate reference to consistent technical basis for the use of safety pressure, despite research into the issue. Possible explanations for the use of safety pressure offered in interviews and indirectly discussed in literature included:

1) Maintaining positive flow so that an unconscious pilot may continue to receive breathing gas even if they temporarily stopped breathing.
2) Maintaining a positive pressure so that gaseous warfare agents and other potential contaminants may be continually flushed from the pilot's mask.
3) Maintaining a positive pressure to the pilot's mask in the event of a water ditching, to aid the pilot's breathing while momentarily submerged.

Although variations of these explanations were repeatedly offered, the reference was always anecdotal, and there appears to be no technical basis or written baseline requirement documenting the implementation and use of safety pressure. The PBA team recommends additional investigation into the continued use of safety pressure regulator systems, as noted in the findings and recommendations attached to this report.

For testing purposes in the context of PBA, USN aircraft configurations generally used safety pressure, while USAF aircraft configurations generally did not use safety pressure. NASA test aircraft used in the PBA study were likewise configured with safety pressure regulators in the USN equipment configuration and non-safety pressure regulators in the USAF equipment configuration.

8.3.4 Diluter-Demand versus Demand Regulator

Two regulator types analyzed by the PBA study are the pressure demand (sometimes called simply "demand") and diluter demand regulators. A pressure demand regulator delivers a constant stream of pure pressurized O_2 to the pilot's mask when the pilot inhales. A diluter demand regulator delivers O_2 partially diluted by mixing in ambient air from the aircraft cabin. Diluter demand regulators operate on a schedule as described in the next section.

F.8-1*. *Pilot subjective reports indicate diluter demand regulators as easier to breathe which is supported by breathing effort analysis. Regulators that deliver breathing gas at neutral pressure (mask pressure the same as cabin pressure) exhibit less phase shift with current mask/regulator design, especially during high volume/high velocity breathing.*

R.6-10. Subjective reports of breathing difficulty from pilots should be trusted as a significant indication of breathing system performance and followed up in a methodical manner including assessment with objective data. ***(F.6-20, F.8-1)***

8.3.5 100% Oxygen versus Scheduled Oxygen

As previously discussed, pressure demand regulator systems typically deliver pure 100% O_2 to the pilot's mask, while diluter demand systems deliver O_2 diluted with ambient cabin air according to a schedule. With a diluter demand system, the supplied concentration of O_2 increases (dilution decreases) as the aircraft ascends and the relative cabin altitude increases, until the concentration eventually reaches 100% O_2. OBOGS also operate according to a schedule, supplying higher O_2 concentrations to the pilot at higher cabin altitudes. In different aircraft configurations, the function of O_2 concentration scheduling may be delegated to either the OBOGS or the regulator as required.

8.4 Case Study – USN T-45

A case study of a two-seat USN T-45 where the aft pilot experienced a near-PE

8.4.1 Flight Summary

On August 23, 2018 a USN T-45C two-seat aircraft at Air Test and Evaluation Squadron TWO THREE (VX-23) flew out of Naval Air Station Patuxent River Maryland. The flight was conducted as part of the Root Cause and Corrective Action (RCCA) investigation of the T-45. The aircrew executed a variety of maneuvers (e.g., stalls, elevated-G wind-up turns, basic fighter maneuvers, high altitude decent) during the 1.4-hour flight. Both aircrew were equipped with VigilOX ISB and ESB units. Both units appeared to function properly, and a post-flight

characterization of the unit was performed by NAVAIR personnel (VigilOX Engineering Investigation from T-45 Flight Test on August 23rd, 16 September 2018).

The goal of this mini-study was to apply the analysis tools developed as part of the PBA to the T-45 data supplied to the PBA team by the USN. The results of the analysis, presented below, show clear differences between the fore and aft pilots and provide independent verification of the validity of the PBA approach to the analysis of pilot breathing by examining a different aircraft equipped with an OBOGS (as opposed to the PBA LOX systems). This is, however, only an analysis of a single flight of a single aircraft with two (fore and aft) pilots wearing different masks and flight gear. The analysis is not intended, nor should it be used, to draw definitive, generalized conclusions about the aircraft and/or pilots.

While both pilots were equipped with both ISB and ESB VigilOX units, there were differences between the hardware and software between the two pilots. Given the developmental status of VigilOX at the time of the flight, changes in either hardware or software could affect the data quality, analysis and resulting conclusions. The ISB units on both pilots was identical with respects to both hardware and software. Therefore, any analysis/conclusions from ISB data ie expected to be reasonable. This includes tidal volume, respiration rate, minute ventilation, inhale to total time ratio, inhale hysteresis measured from line pressure and relative time to 50% volume.

The ESB units (both hardware and software) was different for the two pilots. The ESB for the aft pilot in particular was subject to random bit collisions that caused random spikes in the different data channels. The primary ESB data the analysis relies on is the mask pressure and therefore, any analysis and conclusions that rely on mask pressure (or any other ESB data) come with the caveat that the hardware and software between the two ESB units was different. This includes inhale mask hysteresis, exhale hysteresis, the valve function metrics and the determination of the spectral content of the pilot breathing. Further, the analysis does use mask pressure for breath discrimination (determining the beginning/end of inhalation/exhalation). Close examination of the breath-by-breath data shows that the breath discrimination did not appear to be significantly affected by the bit collision problem. The breath discrimination was influenced, however, by the fact that the mask would consistently loose the safety pressure for the aft pilot. This was not a problem with the data, but rather represented differences between the pilot/breathing system interactions of the two pilots.

Despite the differences between the instrumentation of the two pilots and the noted possibility of bit collision errors on the aft pilot's ESB unit, the data and analysis show clear differences between the fore and aft pilots and highlight the potential of PBA analysis techniques to provide insight into the differences of the interaction of the pilots with the breathing system during flight.

8.4.2 Summary Physiological Data

Figures 8.4.1 and 8.4.2 show the summary physiological data for the fore and aft pilots, respectively. The data show that the mean tidal volumes before take-off for each pilot are nearly equal. The fore pilot experiences a decrease in mean tidal volume consistent with that observed for most PBA pilots, especially in Profile A flights. The mean tidal volume of the aft pilot also decreases but has periods where it increases briefly to the pre-flight value. The respiration rates for the two pilots are also nearly equal.

While the tidal volumes and respiration rates are, as expected somewhat different for each pilot, they are within the normal range for PBA flights. The data do show that the aft pilot has a larger fraction of large breaths as evidenced by the shading around the mean tidal volume in Figures 8.4.1 and 8.4.2.

There is some difference in the CO_2 data for the two pilots. Specifically, the fore pilot $PPCO_2$ gradually decreases after take-off reaches a minimum midway through the flight before gradually increasing until the end of the flight. The aft pilot experiences a similar trend in $PPCO_2$, but with much larger and longer-duration fluctuations. In addition, the $PPCO_2$ for the aft pilot was considerably higher for the entire flight. Whether this is significant or not is not apparent but is a distinct difference between the two pilots.

The data in Figures 8.4.1 and 8.4.2, in contrast to the PBA data, clearly show how important the O_2 supply is to the breathing system. The O_2 supply for this T-45 flight was an OBOGS as opposed to the LOX in PBA tests. The O_2 data for both pilots is consistent (minimizing the possibility of sensor error) and shows swings in O_2 concentration from 50% to near 90%. The PPO_2 data show swings in the range of 300 to 500 mmHg. During the final (presumably low power) descent, the O_2 concentration continuously decreases from nearly 90% to 60%. The PPO_2, however, increases during this time as the cabin pressure increases.

While the tidal volume and respiration rates for the fore and aft pilots are similar, there are physiological metrics that are significantly different. Figures 8.4.3 and 8.4.4 show the inhale time to total breath time ratio as a function of time for the fore and aft pilots, and the respective histograms of the inhale to total breath time distributions. The data show that for the fore pilot, with the notable exception of the high G-level period, the ratio for the fore pilot is much less than 0.40 for the entire flight. The values are consistent with those expected for relaxed breathing in air (no breathing system). The aft pilot has different values for this ratio. Shortly after take-off, the ratio is approximately 0.40 and remains closer to 0.50 for the entire flight until the end of the flight where it drops below 0.40.

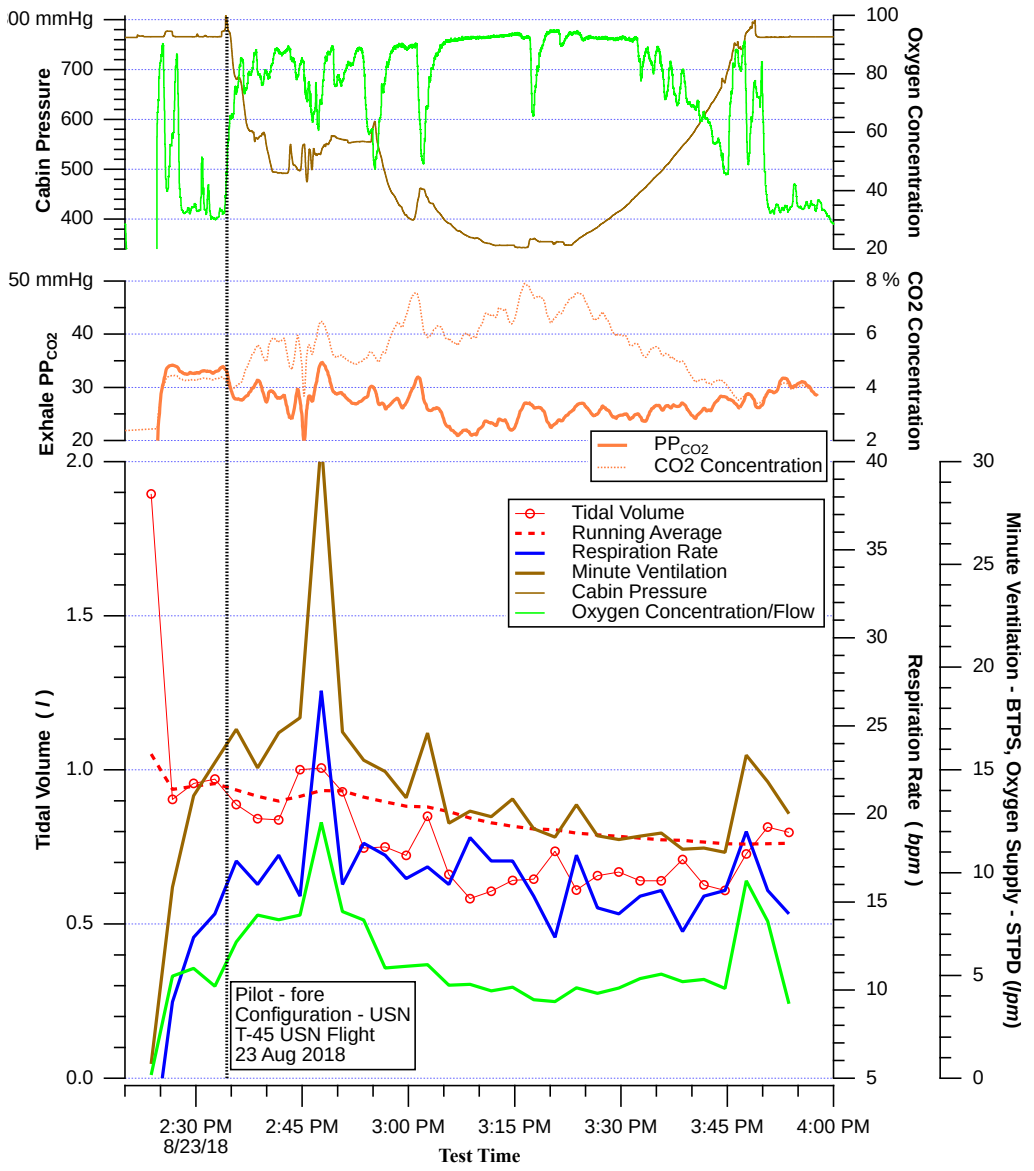

Figure 8.4.1. Summary Metabolic Data for Fore Pilot

The lower axes show the 3-minute averaged tidal volume (the shading represents plus/minus one standard deviation of the mean), respiration rate and minute ventilation (computed from the ISB flow) and O_2 supply. The middle axes show the CO_2 partial pressure and concentration and the upper axes the cabin pressure and O_2 concentration. The dashed vertical line indicates take-off.

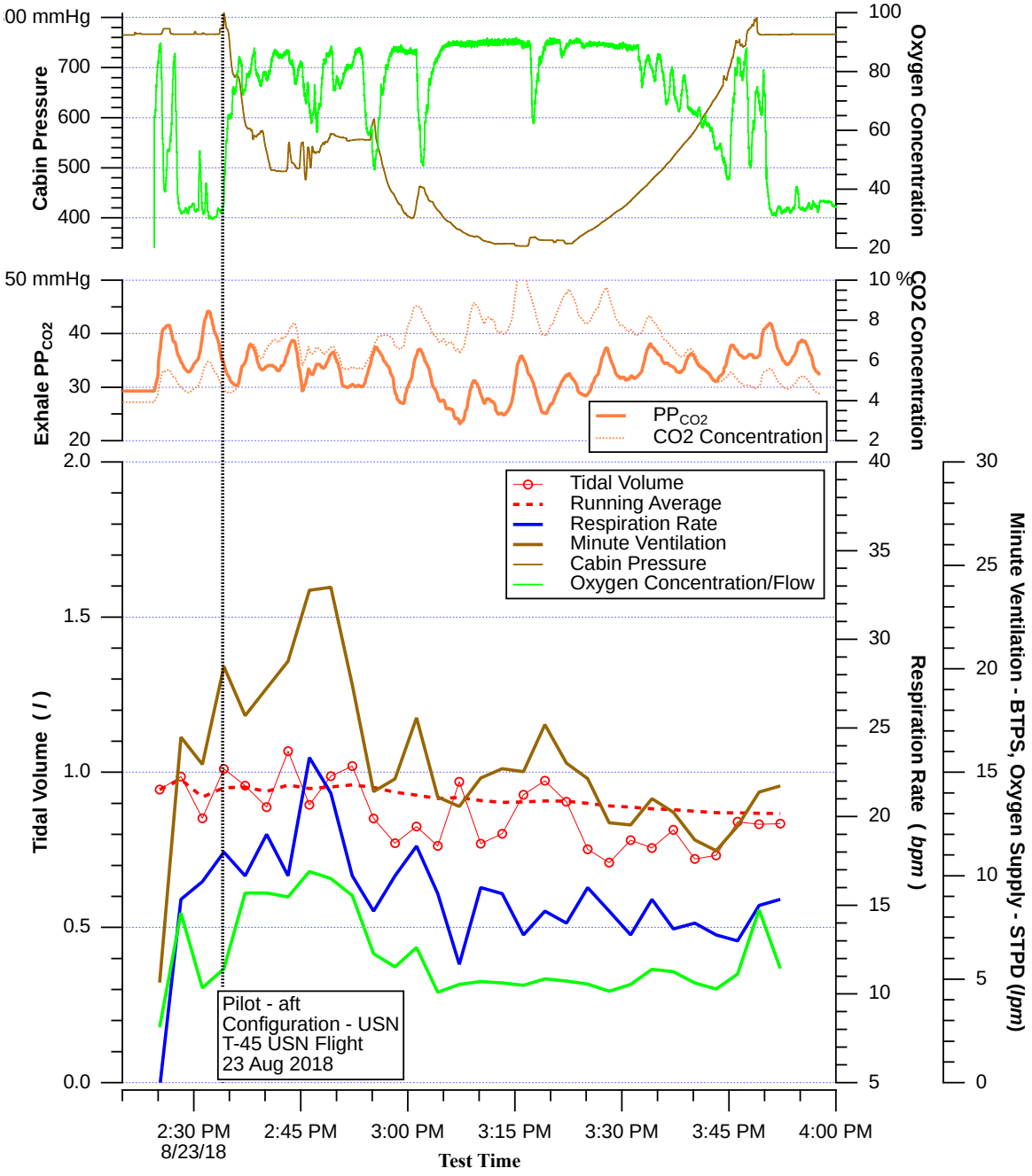

Figure 8.4.2. Summary Metabolic Data for Aft Pilot

The lower axes show the 3-minute averaged tidal volume (the shading represents plus/minus one standard deviation of the mean), respiration rate and minute ventilation (computed from the ISB flow) and O_2 supply. The middle axes show the CO_2 partial pressure and concentration and the upper axes the cabin pressure and O_2 concentration. The dashed vertical line indicates take-off.

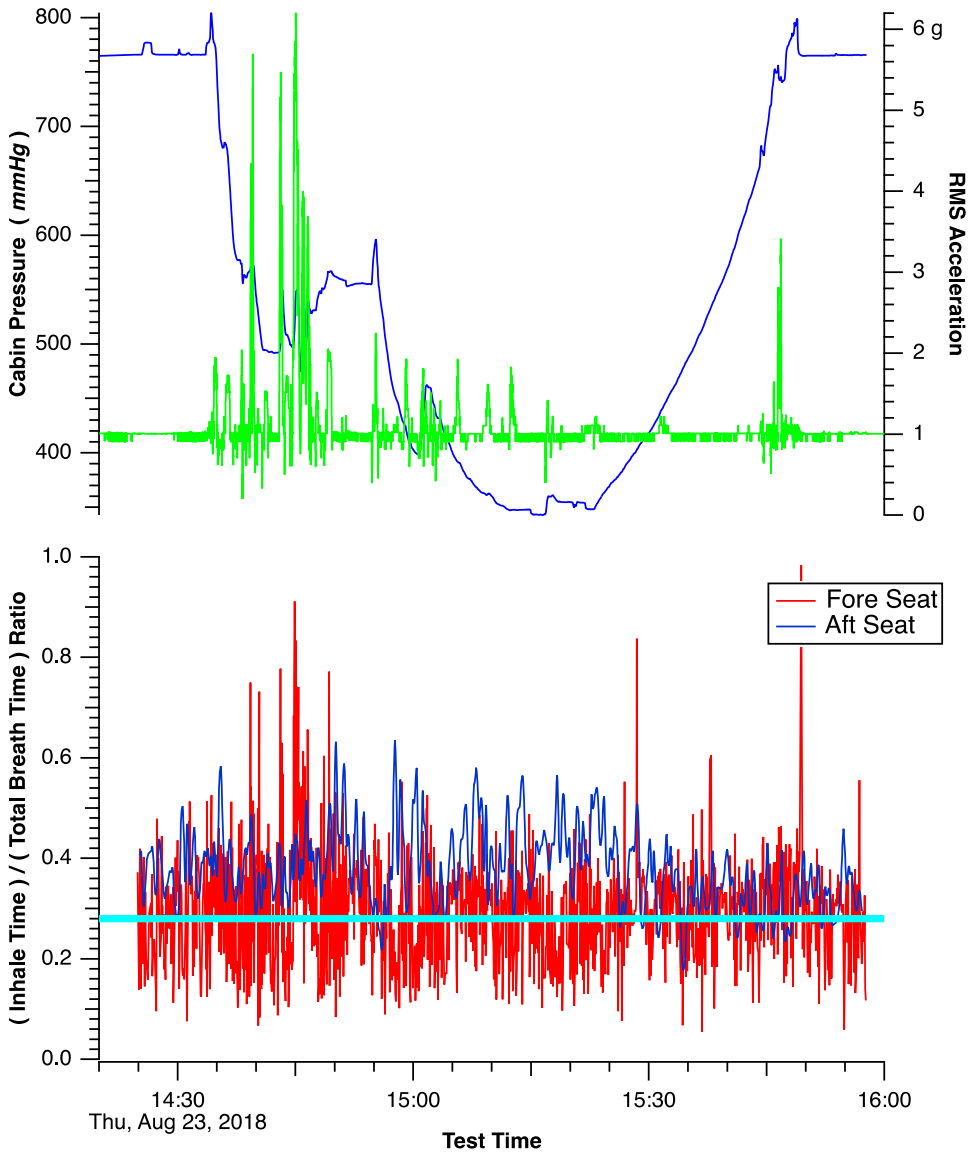

Figure 8.4.3. Inhale Time to Total Breath Time Ratio as Function of Time for Fore and Aft Seat Pilots The horizontal line at a ratio of 0.28 represents the mean ratio for the five PBA pilots during normal breathing (no breathing system).

Section 7 presented the results of ground spirometry tests of the PBA pilots. During this testing, the pilots performed relaxed, normal breathing for three minutes while the Spirodoc recorded volumetric flow data. These data provided baseline data that allowed direct comparison of relaxed, normal breathing on the ground (no breathing system) to that in the aircraft during flight while breathing on the breathing system. The ground spirometry testing also provided insight into the pre-flight breathing metrics of the seated pilot, seated with the harness and then with the harness in the ejection seat. These data are not available for this study. The metrics such as respiration rate, tidal volume and peak inhale and exhale flows can vary from pilot-to-pilot, and also whether the pilot was in gear and/or seated in the aircraft. Certain metrics were independent of pilot, gear/no gear and seated in the aircraft or in the ready room. One such metric was the

inhale to total time ratio. The approximate mean value for all of the PBA pilots was 0.28 and had a tight distribution around this value with individual breaths rarely exceeding 0.33.

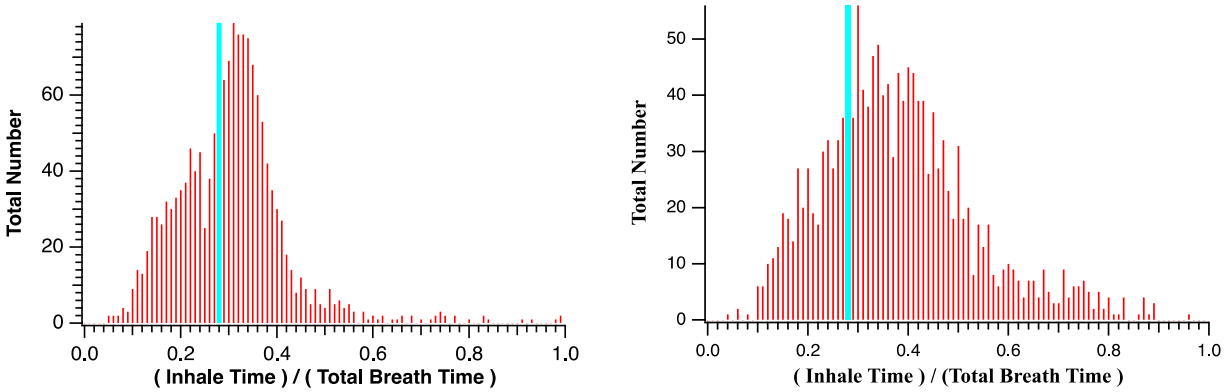

Figure 8.4.4. Inhale to Total Breath Time Distribution Histograms for Fore (left) and Aft (right) Seat Pilots
The vertical blue lines on the plots are the mean value for the PBA pilots during normal, relaxed breathing (no breathing system).

The data for the T-45 pilots show that the fore seat comes much closer to the ground breathing data for the PBA pilots than the aft pilot. The fore seat pilot values are typically slightly larger than the PBA pilot ground baseline. The aft pilot, however, had much larger deviations from PBA pilot data baseline indicating a much more significant physiologic adaptation to the aircraft breathing system than the fore pilot.

8.4.3 Summary Pilot/Breathing System Supply Data

While some of the metabolic data for the two pilots is similar, exhibiting similar values and trends with time, the data for the interactions between the pilot and the breathing system are significantly different for the two pilots. Figure 8.4.5 shows the histograms for the line and mask hysteresis for both the fore (left) and aft (right) pilots. The data for the histograms is numerically tabulated in Tables 8.4.1 and 8.4.2 for the fore and aft pilots, respectively.

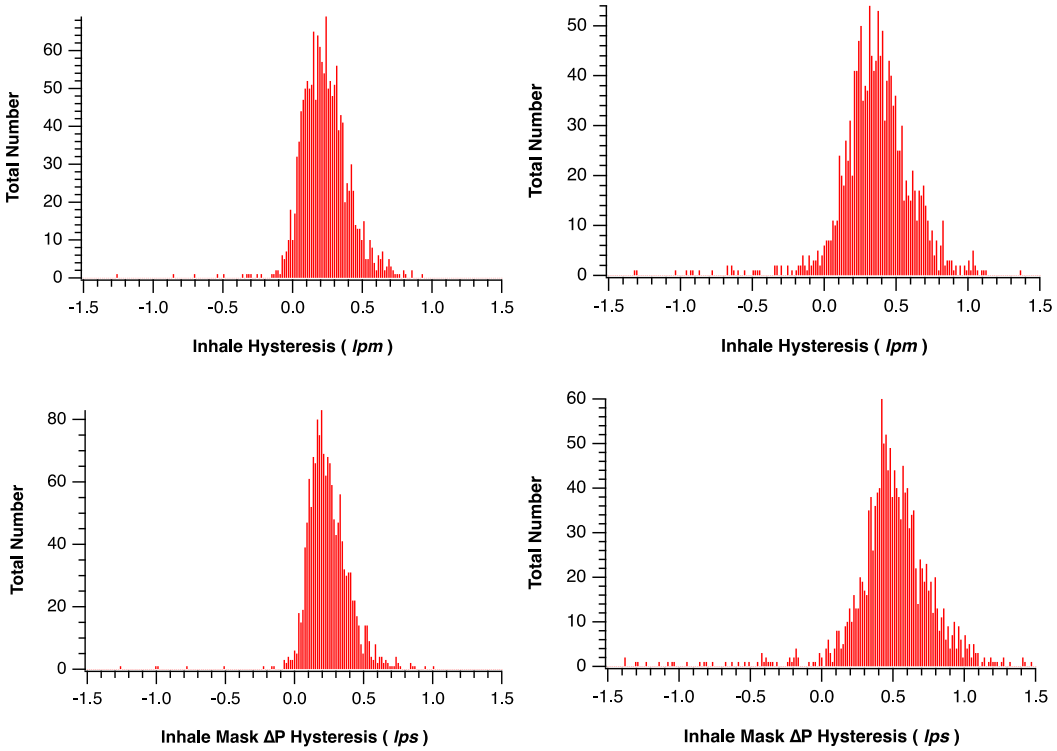

Figure 8.5.5. Line and Mask Inhale Hysteresis Histograms for Fore and Aft Pilots
The fore pilot histograms are the leftmost two and the aft pilot are the rightmost two.

Table 8.4.1. Tabulated Data for Fore Pilot Line and Mask Histograms of Figure 8.4-5
This table shows the mean, standard deviation, and fractions above 0.50, 0.75 and 1.0 lps.

	Line Hysteresis	Mask Hysteresis
Mean Hysteresis (lps)	0.24	0.25
Standard Deviation (lps)	0.18	0.16
Fraction > 0.50 lps	0.07	0.06
Fraction > 0.75 lps	0.01	0.01
Fraction > 1.00 lps	0.00	0.00

Table 8.4.2. Tabulated Data for Aft Pilot Line and Mask Histograms of Figure 8.4-5
This table shows the mean, standard deviation, and fractions above 0.50, 0.75 and 1.0 lps.

	Line Hysteresis	Mask Hysteresis
Mean Hysteresis (lps)	0.37	0.50
Standard Deviation (lps)	0.25	0.29
Fraction > 0.50 lps	0.25	0.51
Fraction > 0.75 lps	0.05	0.15
Fraction > 1.00 lps	0.01	0.03

The data in Figure 8.4.5 and Table 8.4.1 show that the value of the line hysteresis is low (good) for a safety pressure system. In addition, the value of the standard deviation and the fraction above the critical values of 0.50, 0.75 and 1.0 lps indicate that the regulator is consistently responding proportionally to the demand signal it receives and rarely undersupplies or

oversupplies during a breath. In addition, the mask hysteresis is nearly identical to the line hysteresis (the mean, standard deviation and fractions above 0.50, 0.75 and 1.0 lps) indicating that the pilot demand is being transmitted to the regulator proportionally and without delay.

The data in Figure 8.4.5 and Table 8.4.2, however, show that the interaction between the pilot and the breathing system for the aft pilot is not ideal. The mean line hysteresis is more than 50% higher than the fore pilot and the standard deviation is also nearly 50% higher. While value of the mean hysteresis is consistent with PBA data for a safety pressure system there are five times more breaths at values greater than 0.75 lps which is a significant number.

In addition, the mean mask hysteresis is more than 33% higher than the line hysteresis and the standard deviation is also higher. A substantial fraction of the breaths have values greater than 0.75 lps. The fact the mask hysteresis is larger than the line hysteresis implies that the pilot demand is not getting transmitted to the regulator either proportionally or without delay. This coupled with the poorer response of the regulator to its demand signal means that the, relative to the fore pilot, the aft pilot is experiencing a significantly degraded interaction with the breathing system.

While the summary statistics show a large discrepancy, the time dependence of the hysteresis is even more illuminating. The fore seat hysteresis showed almost no substantial variation of the hysteresis with time, remaining near the mean value for the entire flight. Figure 8.4.6 shows the time variation of the aft seat hysteresis. The data show that there are periods of time, notably during the OBOGS descent where the mask hysteresis has high values with local averages in the vicinity of 0.80 lps. The PBA data suggest that clusters of breathing with hysteresis this large are indicative of a lack of harmony between the pilot and the breathing system.

This disparate interaction between the aft pilot and breathing system manifests in the relative time to get 50% of inhale volume (Figure 8.4.7 and Table 8.4.3). The data shows the fore pilot has a mean value slightly less than 0.50. By contrast, the aft pilot had a higher average value, a larger standard deviation and, perhaps most importantly, a significant fraction of the breaths with values greater than 0.60. Similar to large hysteresis values, PBA data suggest that a substantial number of breaths with values of the relative time to 50% volume greater than 0.60 indicates a significant lack of harmony between the pilot and the breathing system.

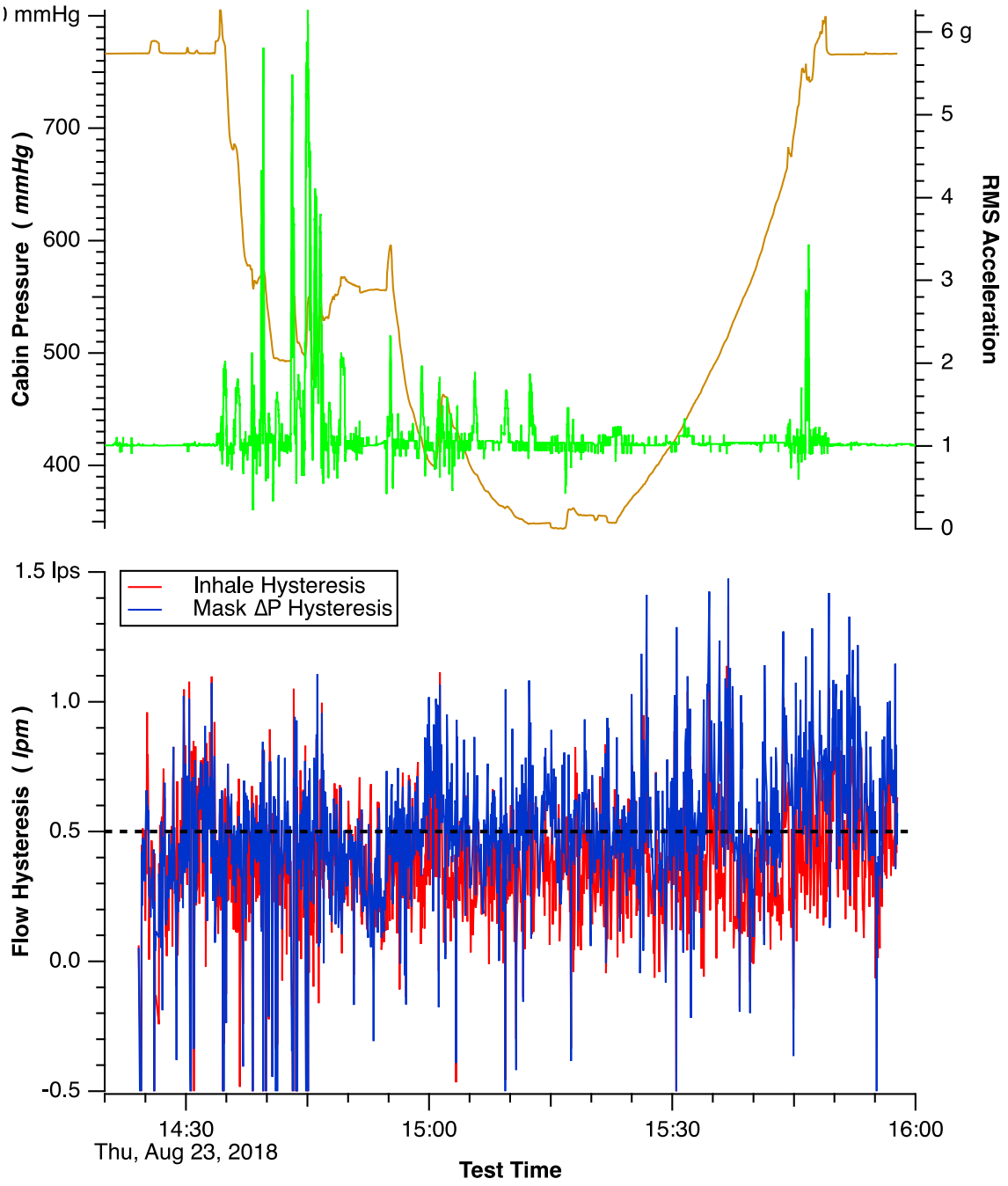

Figure 8.4.6. Line and Mask Hysteresis for Each Breath as Function of Time (lower axes) for Aft Seat in T-45 Test
The upper axes are the cabin pressure and RMS acceleration as a function of time.

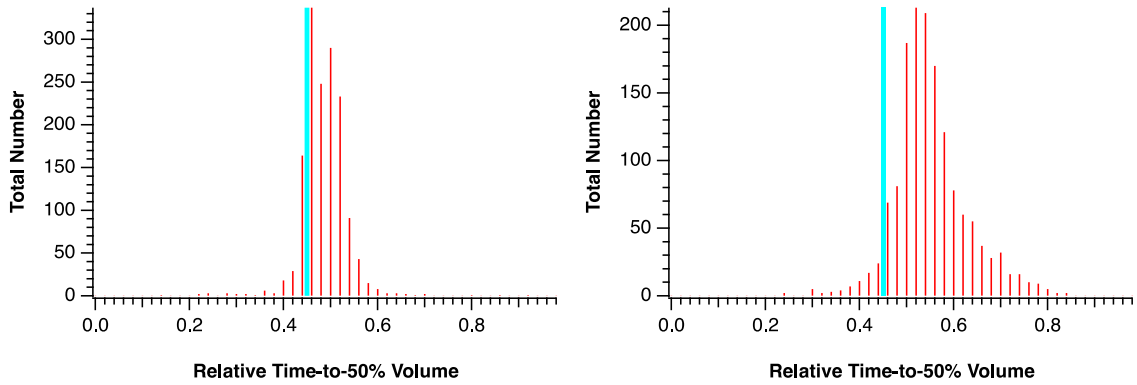

Figure 8.4.7. Histograms of Relative Time to Achieve 50% of Inhale Volume for Fore (top) and Aft (bottom) Pilots
The vertical blue lines represent the mean value of the metric for normal, relaxed PBA pilot breathing (no breathing system).

Table 8.4.3. Summary Statistics for Relative Time to 50% Volume Distributions Shown in Figure 8.4.7

	Fore Pilot	Aft Pilot
Number of breaths	1504	1475
Mean Value	0.50	0.56
Standard Deviation	0.044	0.078
Total Breaths > 0.50	691	1250
Fraction Breaths > 0.50	0.459	0.847
Total Breaths > 0.60	19	350
Fraction Breaths > 0.60	0.013	0.237
Total Breaths > 0.70	3	92
Fraction Breaths > 0.70	0.002	0.062

The relative time to 50% volume metric is another metric that for relaxed, normal pilot breathing is relatively invariant to pilot, gear/no gear and in/out of aircraft. The value of this metric was computed for each PBA pilot during the three-minute relaxed breathing data of the ground spirometry testing. With the exception of one PBA pilot whose value was less than 0.40, all the PBA pilots had values of the relative time to 50% volume that were clustered around a mean value of 0.45 with values for individual breaths rarely, if ever, exceeding 0.50.

Comparisons of the relaxed breathing data of PBA pilots to T-45 data show that the fore pilot had values that were somewhat larger (mean value 0.50 compared to the PBA ground breathing mean of 0.45) and are consistent with data from PBA flights with no breathing issues. The values highlight that there is some physiological adaptation of the pilot to even a good breathing system.

The aft seat pilot shows a much greater deviation from the PBA ground breathing mean (0.56 versus 0.45) indicating a much greater change in pilot inhalation pattern. Even more concerning is that the PBA pilot ground breathing data rarely, if ever, had values in excess of 0.50 while the aft seat pilot had a substantial fraction of the breaths (nearly 25%) with values in excess of 0.60, and a small fraction with values in excess of 0.70 – a value indicative of severe inhale dysfunction.

R.6-6. Measure and track phase shift, hysteresis, and PNF (Pressure – No Flow) when evaluating aircraft system health – especially during times of peak breathing. ***(F.6-1, F.6-12)***

F.8-2. MIL STD 3050 uses a "trumpet curve" format to describe, define, and specify pilot breathing requirements. Trumpet curve profiles are inadequate as they only define peak pressure/flow relationships but do not provide any information about timing, sequence, or synchronization/disharmony within the breath.

R.8-1. Hysteresis and PNF (Pressure – No Flow) analysis methods are recommended augmentations to evaluate flow, pressure, and timing/sequence anomalies related to breathing air delivery. (F.8-2)

F.8-3. Pilot breathing patterns are altered, and effort of breathing increases when there are a series of breaths with high peak breathing demands, and the pilot breathing system delays the supply of air.

F.7-2*. *PBA spirometry found that the Aircrew Flight Equipment (AFE) and being harnessed to the seat reduced measured available lung volume prior to flight. Functional Vital Capacity (FVC) measurements taken from PBA pilots just prior to take off revealed a large decrease in FVC mean from baseline.*

F.7-3*. *PBA spirometry found further decreased Functional Vital Capacity (FVC) in PBA pilots immediately after landing as compared to the respective immediate pre-flight measurements.*

8.4.4 Summary Pilot Exhale Data

The previous section focused on the interaction between the pilot and air supply system, showing significant differences between the fore and aft pilots. This section shows that there are significant differences between the exhale dynamics for the fore and aft pilots.

Figure 8.4.8 shows three consecutive exhales for the same segment of time for the fore (top) and aft (bottom) pilots. The graphs show the exhale flow as a function of mask pressure. The fore pilot data show very consistent exhales where the exhalation valve opens (cracks) and closes (seals) at nearly the same pressure for each breath and the crack and seal pressures are the same breath-to-breath. In contrast, the crack pressure is considerably higher than the seal pressure for all three breaths for the aft pilot (for the last breath the crack and seal pressures are close). In addition, while the seal pressure for the fore and aft pilot are very close, the crack pressure for the aft pilot is considerably higher.

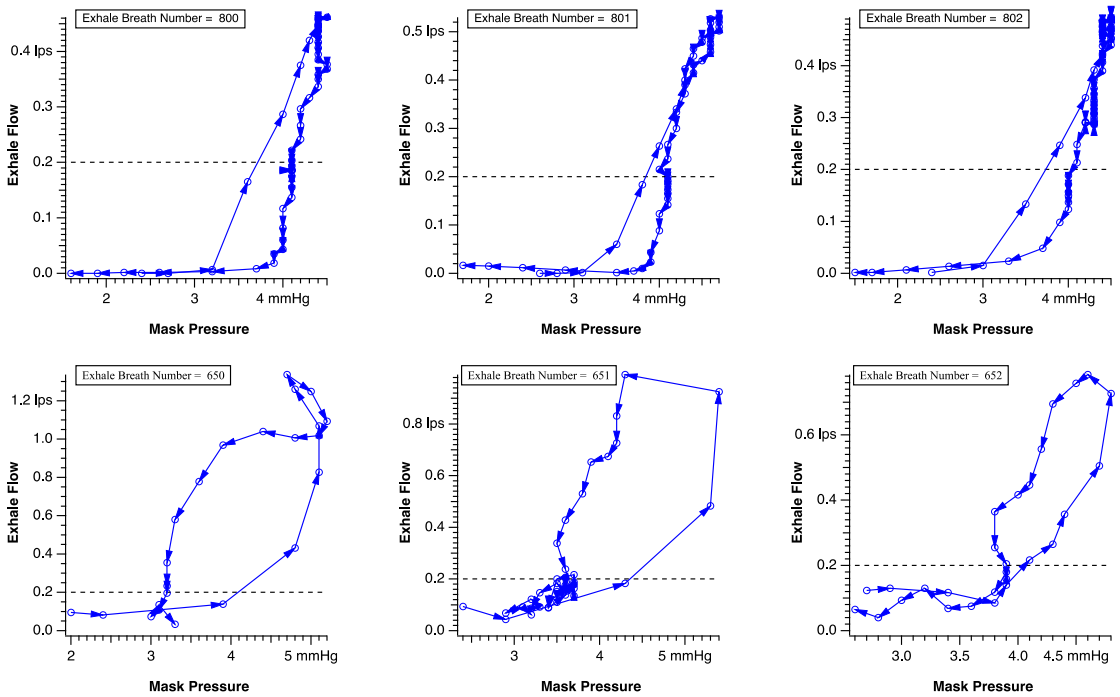

Figure 8.4.8. Three Consecutive Breaths from Same Segment of Time for Fore (top row) and Aft (bottom row) Pilot
The plots show the exhale flow versus the Mask Pressure.

The graphs show that nominal opening and closing of the exhalation valve for the fore pilot. The plots for the aft pilot show that the valve requires excessive pressure to open and nominal closing (the exhalation exhibits hysteresis).

These differences are apparent by examining the crack and seal pressure histograms for the two pilots (Figure 8.4.9). There is scatter in the data representing the difficulty in estimating these pressures with the VigilOX hardware. The data indicate that for the fore pilot the valve crack and seal pressures are similar. For the aft pilot, the crack pressure is considerably higher than the crack pressure for the fore pilot and higher than the seal pressure.

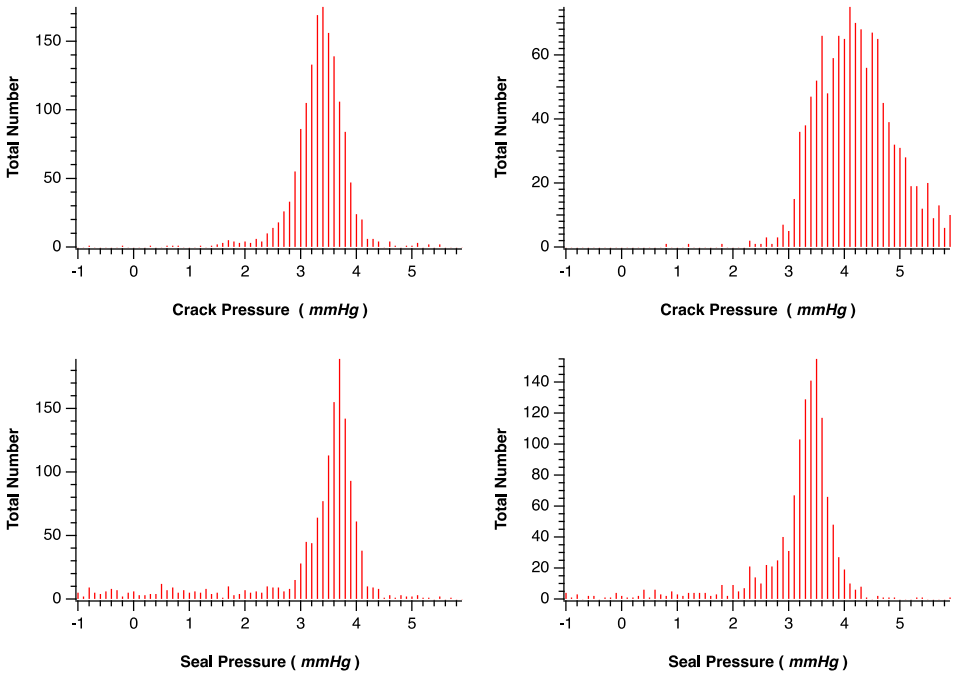

Figure 8.4.9. Exhalation Valve Crack (top row) and Seal (bottom row) Pressure Histograms for Fore (left column) and Aft (right column) Pilots

8.4.5 Valve Function Metrics

Figures 8.4.10 through 8.4.13 show the raw VigilOX data for two 1-minute windows for each pilot, one during the initial ascent and the other during the final OBOGS descent. Table 8.4.4 shows the valve function metrics for the two windows in time for each pilot. Surprisingly, the value of the safety pressure increased substantially for both seats from the initial ascent to the final descent, with the fore seat exhibiting the largest increase. Whether this increase is real, particularly for the fore seat, or an artifact of deriving the differential pressure from the absolute ISB and ESB line pressures is unknown and needs further study. Ideally, the inhalation line pressure measurement would be a differential pressure measurement like the mask pressure.

As a result of the increase in safety pressure, the fraction of time where the mask pressure is below the safety pressure during exhalation increases substantially (from near 0 to almost 80%) for the fore seat. The mask pressure is lower than the safety pressure for nearly 40% of the time during the initial ascent and essentially all of the time during the final descent.

The RMS acceleration and ESB and ISB line pressures are on the upper axes. The ISB and ESB O_2 and CO_2 partial pressures on the middle axes and the ISB and ESB flow, mask pressure and line-cabin differential pressure on the lower axes. The line-cabin differential pressure is derived by subtracting the ISB line pressure from the ESB line pressure.

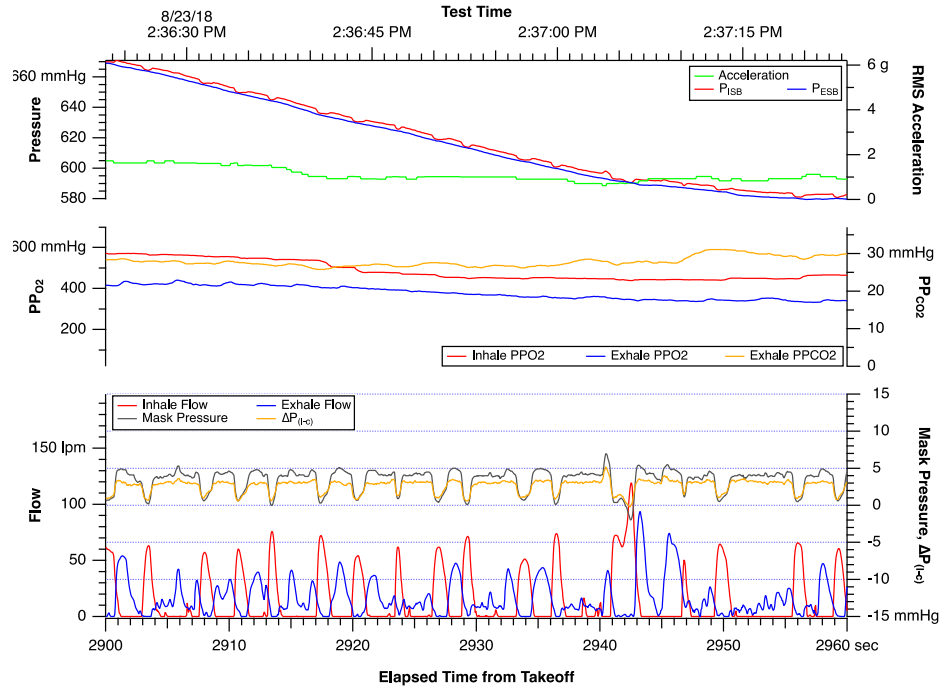

Figure 8.4.10. Raw VigilOX Data for 60-second Window of Fore Seat Pilot During Initial Ascent After Take-Off

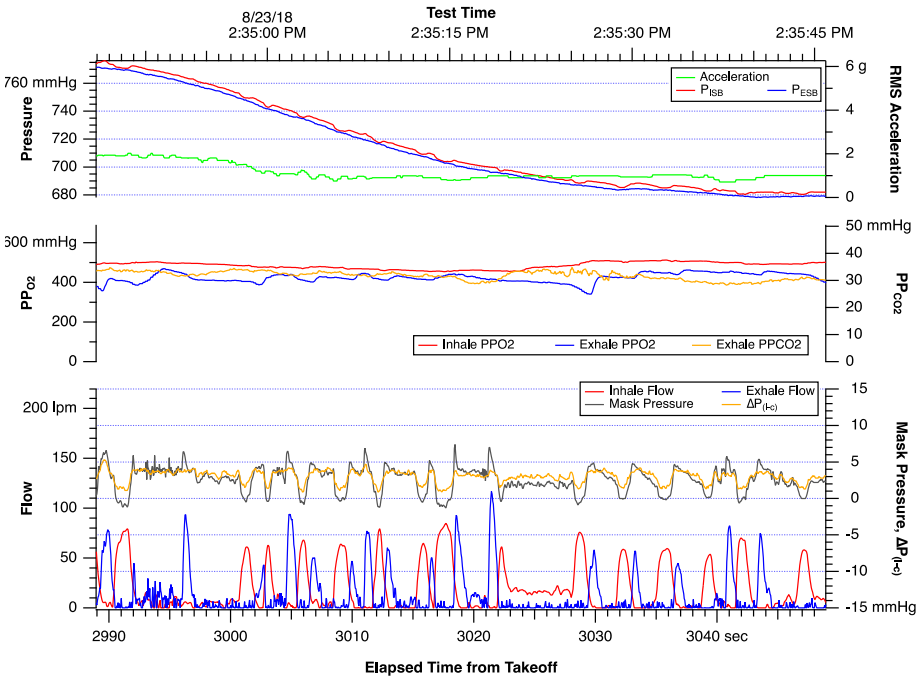

Figure 8.4.11. Raw VigilOX Data for 60-second Window of Aft Seat Pilot During Initial Ascent After Take-Off

The RMS acceleration and ESB and ISB line pressures are on the upper axes. The ISB and ESB O_2 and CO_2 partial pressures on the middle axes and the ISB and ESB flow, mask pressure and line-cabin differential pressure on the lower axes. The line-cabin differential pressure is derived by subtracting the ISB line pressure from the ESB line pressure.

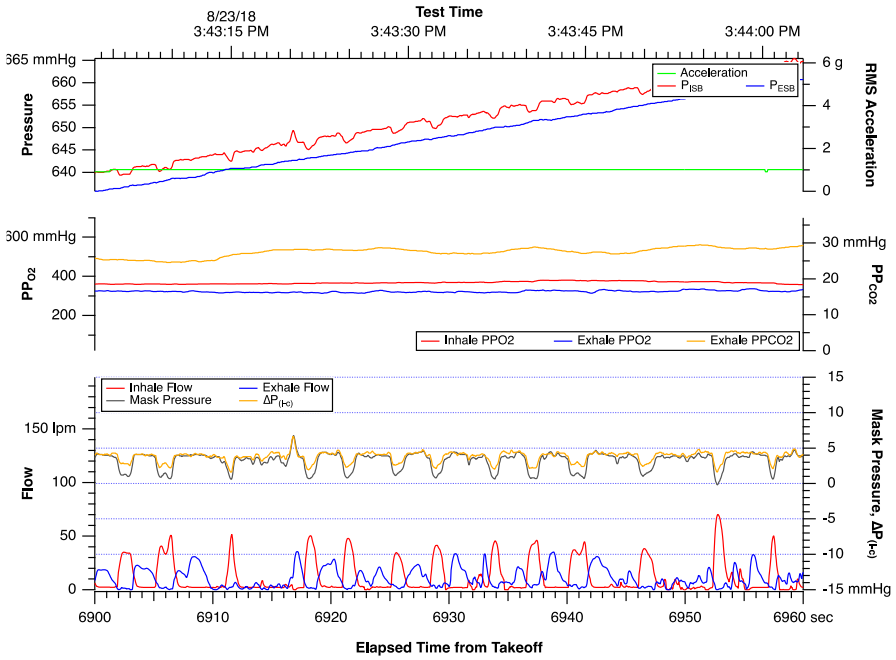

Figure 8.4.12. Raw VigilOX Data for 60-second Window of Fore Seat Pilot During Final OBOGS Descent

The RMS acceleration and ESB and ISB line pressures are on the upper axes. The ISB and ESB O_2 and CO_2 partial pressures on the middle axes and the ISB and ESB flow, mask pressure and line-cabin differential pressure on the lower axes. The line-cabin differential pressure is derived by subtracting the ISB line pressure from the ESB line pressure.

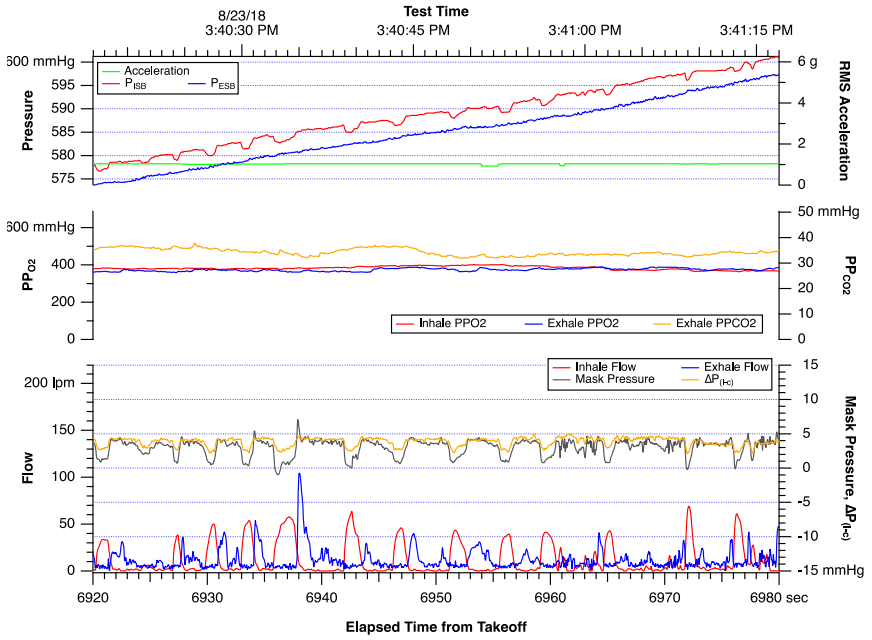

Figure 8.4.13. Raw VigilOX Data for 60-second Window of Aft Seat Pilot During Final OBOGS Descent

The RMS acceleration and ESB and ISB line pressures are on the upper axes. The ISB and ESB O_2 and CO_2 partial pressures on the middle axes and the ISB and ESB flow, mask pressure and line-cabin differential pressure on the lower axes. The line-cabin differential pressure is derived by subtracting the ISB line pressure from the ESB line pressure.

Table 8.4.4. Tabulated Values of Valve Function Characteristics During Flight Segments Shown in Figures 8.4.10 to 8.4.13.

	Fore Seat	**Aft Seat**	**Fore Seat**	**Aft Seat**
Region Start Time (s)	2900	2990	6900	6920
Region End Time (s)	2960	3050	6960	6980
Average ΔP(l-c), safety pressure (sp)	3.141	3.569	4.176	4.121
Std. Dev. ΔP(l-c)	0.243	0.347	0.336	0.390
Avg. Dev. ΔP(m-sp)	0.452	-0.072	0.037	-0.286
Std. Dev. ΔP(m-sp) (mmHg)	0.443	0.865	0.446	0.569
Maximum ΔP(m-sp) (mmHg)	3.157	3.104	2.957	1.404
Minimum ΔP(m-sp) (mmHg)	-0.743	-2.096	-1.443	-2.796
Fraction ΔP(m-c) < sp	0.003	0.361	0.792	0.876
ΔP(l-c) <-> ΔP(m-c) correlation	0.524	0.497	0.757	0.367

Finally, Table 8.4.5 shows the valve function characteristics for the window of time from take-off to landing. The metrics for the average deviation from safety pressure and fraction of the time the mask pressure is below safety pressure all indicate exhalation valve malfunction and a loss of safety pressure in the aft seat. The fore seat has less than ideal behavior, but the increase in safety pressure complicates (real or an instrument artifact) the interpretation of the numbers.

Table 8.4.5. Tabulated Values of Valve Function Characteristics During Entire Flight Portion (before take-off and after landing excluded)

	Fore Seat	**Aft Seat**
Region Start Time (s)	2700	2950
Region End Time (s)	7200	7450
Average ΔP(l-c), safety pressure (sp)	3.843	3.896
Std. Dev. ΔP(l-c)	0.619	0.354
Avg. Dev. ΔP(m-sp)	0.252	-0.173
Std. Dev. ΔP(m-sp) (mmHg)	0.450	0.700
Maximum ΔP(m-sp) (mmHg)	11.157	11.904
Minimum ΔP(m-sp) (mmHg)	-3.343	-4.596
Fraction ΔP(m-c) < sp	0.239	0.590
ΔP(l-c) <-> ΔP(m-c) correlation	0.080	0.382

8.4.6 Mask Pressure Fluctuations

The mask pressure data in Figures 8.4.10 to 8.4.13 shows substantially larger mask pressure oscillations that appear to be visually larger for the aft seat pilot. Figure 8.4.14 is the power spectral density (PSD) of the mask pressure for both the fore and aft pilots during flight. For reference, the graph also shows PBA data for a test with the 12P mask that, at least visually,

showed the smoothest mask pressure during flight. As such, the PBA team used this to represent the frequency content of mask pressure due solely to breathing.

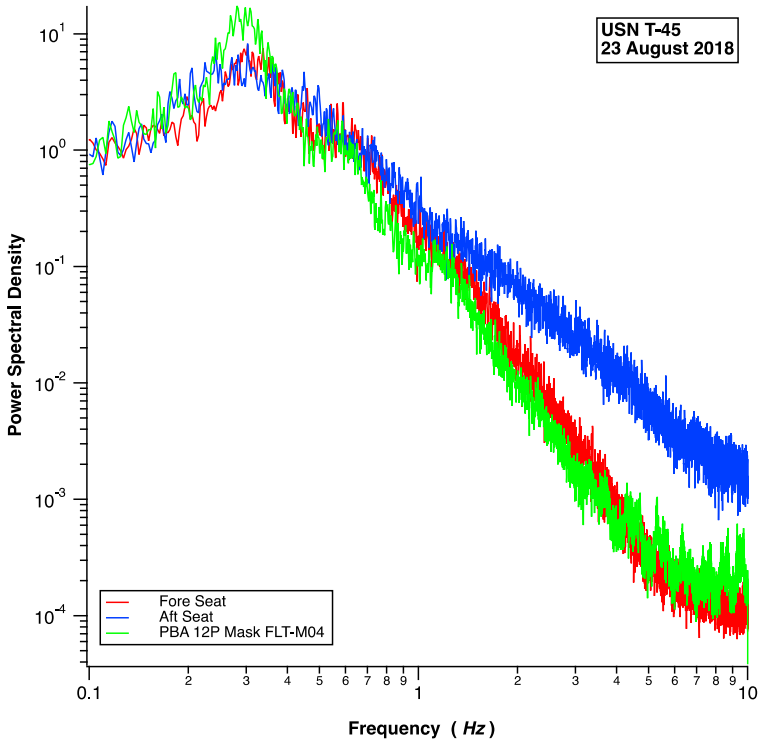

Figure 8.4.14. Power Spectral Density (PSD) for Mask Pressure During Flight Phase (before take-off and after landing excluded) of USN T-45 Flight
The reference data is a PBA flight with the 12P mask that exhibited (visually) the smoothest mask pressure variations and thus represents, as closely as possible, the frequency composition due solely to breathing.

All of the data in Figure 8.4.14 show a peak in the vicinity of 0.25 Hz or the nominal respiration rate of 15 bpm in Figures 8.4.1 and 8.4.2. The decay in the fore seat pilot and PBA 12P mask flight show a similar decay in PSD with increasing frequency. Purely sinusoidal breathing would have a single frequency, but pilots do not breath in a sinusoid. Breathing has spectral content at frequencies lower and higher than the respiration rate. The PSDs for the fore seat pilot and 12P mask pilot imply that their mask pressure frequency content is the frequency content caused by the pilot.

The PSD for the aft pilot is significantly higher at frequencies above 1 to 2 Hz. The additional energy at these higher frequencies then represents mask pressure oscillations caused by the breathing system and are thus not caused by the pilot but imposed on the pilot by the aircraft breathing system.

F.8-4. PBA found that pilots do not breathe at a constant flow rate with a sinusoidal breathing pattern but demonstrate high variability. Standard bench tests of regulators at constant flow conditions do not appropriately approximate in-flight conditions. (8.4.6)

F.2-1. Pilots subconsciously adjust their breathing to accommodate to changes in the mechanical supply system.

F.6-12.* *Key physiological parameters of the breathing system are pressure, flow, volume and timing of supplied air. Systematic disharmony of the system can be measured by breathing hysteresis and breathing phase shift, which are new PBA methods of measuring BSDs. Instances of Pressure No Flow (PNF) was also an indicator of systematic disharmony of the system*

R.6-6 Measure and track phase shift, hysteresis, and PNF (Pressure – No Flow) when evaluating aircraft system health – especially during times of peak breathing. ***(F.6-1, F.6-12)***

Technical Section 9: Sensor Status and Future Development

9.0 Introduction

As discussed in Technical Sections 1 and 2, the Cobham VigilOX system provided the primary method of breathing data collection for the Pilot Breathing Assessment. Technical Section 5 showed the value of these measurements in linking pilot response and aircraft flight parameters. However, detailed analyses also showed that the VigilOX system remains a developmental system that is still undergoing efforts to resolve some technical challenges. The three primary needs are improving TRL with relation to hardware durability and suitability for an operational field environment, adaptation of the physical interface to fit different existing pilot breathing hardware configurations and automating synchronization of sensor time-bases with aircraft sensor systems. These issues are currently being addressed with collaborative efforts among Cobham, NASA, and the military services. Progress has been sufficient to provide robust sensor data-streams for the PBA study.

The one remaining technical challenge revolves around the measurement of exhaled O_2, CO_2 and water vapor (H_2O) concentrations in the ESB. Although the existing sensors provide proper measurements, their placement is approximately 12 in downstream from the pilot's mask and so the O_2, CO_2 and H_2O concentrations at the sensor are affected by dilution, delay, and flow variability during the normal breathing cycle. As such, the ESB provides time integrated information, which has some value to assess metabolic mass balance and potential to leaks in the system, but does not provide the within-breath profiles that could be useful to understand real-time issues with hypoxia-like symptoms, hypercapnia (CO_2 retention), hyperventilation, and O_2 uptake.

These observations during the PBA study lead to the efforts to develop a better sensing system for O_2, CO_2 and H_2O. The consensus from the NASA NESC team was that accurate within breath profiling would be an important addition to the PE diagnostic toolbox. Furthermore, the PBA team proposed that real-time feedback to the pilot regarding anomalous CO_2 concentrations would provide a form of early warning for onset of PEs.

From a technological perspective, CO_2 and H_2O can be measured using a single mid-infrared laser detector at ~2600 nm (2.6 μm). O_2 would require a separate laser operating at ~760 nm in the near-infrared, which are a bit more exotic. In addition, CO_2 and H_2O are of primary concern from a physiological/metabolic perspective. As such, it was decided to initially focus on CO_2 and H_2O to streamline the development.

The PBA team embarked on a separate effort to develop sensors to directly measure CO_2 and H_2O that could be inserted directly at the nose/mouth source within the pilot's mask. A major challenge was to combine high-frequency measurements with a sufficiently small hardware format to be unobtrusive to the pilot and to avoid a major redesign of existing mask architecture. This was accomplished using a mid-IR laser detector.

9.1 NASA-JPL "In-Mask CO_2 and Water Vapor Sensor" (IMCWS) Project

9.1.1 Purpose and Intent

The purpose and intent of this project was to implement a sensor system specifically to support PBA and potential future pilot breathing measurement campaigns. Measuring gas composition inside the mask avoids observed dilution, delay, and flow variability in the existing sensor

systems during the normal breathing cycle. Specifically, the intent was to gain access to the actual breathing slope profiles at beginning, the middle, and the end of each exhaled breath. The technical requirements implemented for the IMCWS system were set to match the goals for the PBA measurements to detect and acquire at a frequency fast enough to detect changes in gas composition during exhalation, with dynamic range, accuracy and detection limits sufficient to make physiological interpretations of the CO_2, water vapor, and pressure profiles.

NASA's Jet Propulsion Laboratory (JPL) in Pasadena, CA was selected to develop the IMCWS; their sensor group, led by Dr. Lance Christensen, had proven long-term expertise for making these kinds of measurements. The JPL group had already developed a CO_2 sensor system that was compact, sensitive, and fast acting for space suit applications that were thought to be directly applicable to jet-fighter pilot breathing gear.

Initial design concepts considered measuring O_2 and exhalation velocity in addition to CO_2, water vapor, and mask pressure. Because the O_2 and velocity sensors were less mature, and development time was limited, the IMCWS focused on measuring CO_2, water vapor, and pressure inside the mask.

The original intent of making the measurements was entirely related to pilot physiology. Early prototypes of the sensor demonstrated that a very sensitive, fast acting pressure measurement could also provide insight into hardware performance. Pressure signals can track inhalation valve and exhalation valve sequencing and help diagnose hardware anomalies. This unintended (but favorable) consequence may prove to be significant and helpful.

The purpose and intent of the sensor can be summarized by listing some of the key requirements for the IMCWS system:

- The IMCWS shall be reviewed in accordance with AFRC practices and declared to be airworthy
- The IMCWS shall measure CO_2, water vapor, and pressure inside the pilot's mask
- The IMCWS shall have a measurement frequency of 60 Hz or greater (the measurement frequency in the final design is 83 Hz)
- The CO_2 measurement range shall be from 200 ppm to 20% by volume.
- The CO_2 sensor noise shall be less than 200 ppm (at 83 Hz)

9.1.2 IMCWS Configuration

The IMCWS system has three main elements: 1) the sensor components located on the inside of the mask, 2) an external power box with a battery power supply, sensor signal processing hardware, data storage, power switches, and status light, and 3) the cable that connects the mask components to the external power box. Figure 9.1 is a photograph of the IMCWS that shows the mask, cable, and power box.

Figure 9.1. Photograph of IMCWS Configuration Showing Mask, Cable, and External Power Supply Box

The external power box is similar and size and shape to the VigilOX ESB and is mounted to the pilot's suit using the same trapezoidal mounting bracket. The box is configured so the power toggle, status light, and event marker have similar positioning to the VigilOX system and are accessible to the pilot. The cable uses standard connection fixtures like those used previously in AFRC flight tests. The cable connection to the Gentex mask uses a mounting location that has been used for a cable pass-through in other applications.

The assembled configuration of the IMCWS is shown in Figure 9.2. The photograph was taken shortly before a windblast test. The IMCWS configuration is similar to VigilOX ISB and ESB because the external power box uses the same mounting bracket, but the windblast profile is smaller, because the windblast cross section of the cable is smaller than the windblast cross section of the exhalation hose. IMCWS does not affect pilot range of motion.

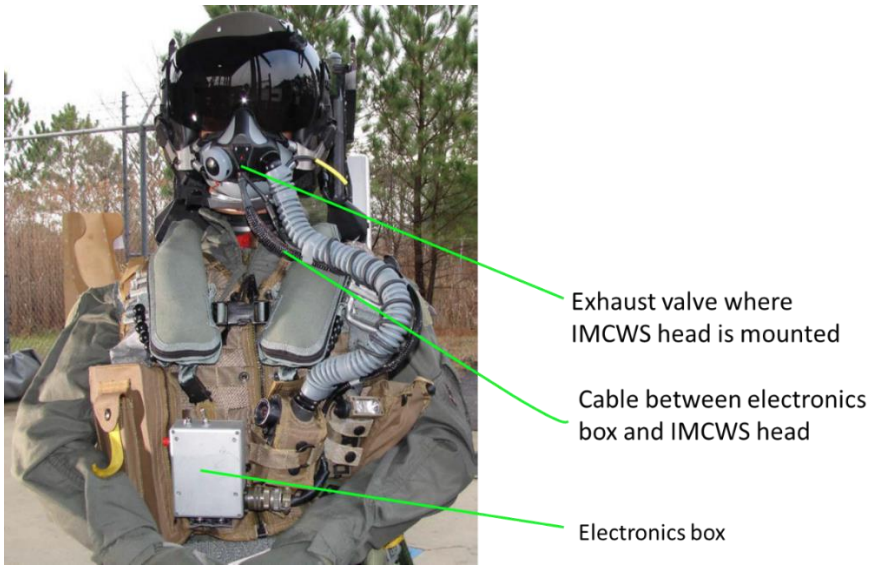

Figure 9.2. Photo of AMCWS, Mounted onto Mannequin Outfitted with Air Crew Equipment in USN Configuration
Electronics box is mounted with a trapezoidal mounting bracket that has been used for VigilOX mounting. Cable is routed to follow the inhalation hose.

9.2 ICMS Sensors Hardware

The IMCWS has two sets of sensor hardware that measure four parameters in aggregate. A pressure-temperature sensor measures mask pressure and local temperature. A laser-detector system measure CO_2 and H_2O concentration. The laser is integrated with a heat sink for thermal control. The laser/heat sink, the P-T sensor, and the detector are all structurally mounted onto a single mounting fixture. The mounting fixture is attached to the outside structure of the exhalation valve. The mounting fixture does not block the flow of airflow through the exhalation valve, and it does not affect valve function in any way. The mounting fixture positions the CO_2 – H_2O sensor system measure gas concentration in the region immediately above the exhalation valve port. The spectral design has a single pass "pitch and catch" configuration. The CO_2 – H_2O spectroscopic measurement requires a measurement of the pressure and the temperature. The P-T sensor is located close to the CO_2 – H_2O sensor, but for packaging reasons, the P-T sensor is not located immediately adjacent to the CO_2 – H_2O sensor hardware. An exploded view of the sensor components, mounting fixture, and mask exhalation valve is shown in Figure 9.3.

Photographs of the individual sensor elements is shown in Figure 9.4. Optical sensor elements have a standard interface; a cylindrical mount 8 mm in diameter. The CO_2 – H_2O laser, the IR detector, and the P-T sensor each have a cylindrical shape and are mounted in a housing with an 8 mm diameter.

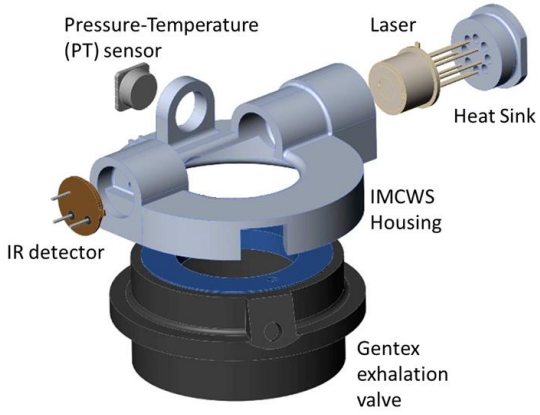

Figure 9.3. Exploded View Diagram Showing Configuration of Sensor Elements, Structural Housing, and Mask Exhalation Valve

Figure 9.4. Photographs of Laser, Detector, and Pressure Sensor
The nominal diameter of each of the components is 8 mm.

9.3 Flight Design requirements:

The IMCWS had to address a set of flight design requirements; some of these issues are entirely related to use as a sensor worn by a pilot in a test flight, some of these issues are common to all sensor systems. The sections below describe how each of the following issues were addressed: 1) fit, 2) windblast compliance, 3) Rapid decompression compliance, 4) Mask integration, 5) laser safety, 6) thermal management, 7) structural integrity, 8) electromagnetic interference, and 9) electromagnetic susceptibility.

9.3.1 Fit

The IMCWS went through three major prototype/fit check iterations. After each of the three prototypes were built, they were evaluated by AFRC test pilots. The first iteration prototype needed fairly significant redesign – the microphone for the radio could not be positioned properly, and the structural housing of the CO_2 – H_2O sensor physically contacted the pilot's face. The second iteration was substantially smaller – the microphone could be positioned, and the sensor did not contact the pilot's face, but the wire harnessing took more space than necessary. The third and final configuration used smaller gauge wires, and a more efficient routing pattern. All prototypes used the narrow version of the Gentex mask, to ensure fit for all mask sizes.

9.3.2 Wind Blast Compliance

Items worn by the pilot need to pass a windblast test before they can be declared airworthy. If there is an ejection seat event, items attached to the pilot's flight suit must maintain integrity. It would not be acceptable, for instance, if a one end of the cable were to break off, and the cable was free to whip about, flogging the pilot.

VigilOX hardware was subjected to a specific set of wind speed, wind direction, and seat angle test conditions. IMCWS was tested under the same test conditions as the VigilOX; 450 KEAS, 22º seat angle, ±30º yaw. The windblast test was performed by the USN, using their Windblast test facility located at Patuxent River NAS. A series of high-pressure gas storage tanks store compressed air. A set of large valves release the air through a blast nozzle with a pressure rake, then the air is routed through a set of flow straightening devices. Air velocity profiles are measured, and mannequin mounted test articles are inspected before and after the windblast event.

A pre-test photo of the IMCWS hardware, its test configuration, is shown in Figure 9.5. The largest IMCWS component that had exposure to windblast loads was the external power box. This box is similar in size, shape, and location to VigilOX ISB and ESB, and the external box is attached with the identical hardware. The cable is attached and routed with the inhalation hose. The cable has a relatively small windblast profile. The cable connecting the mask to the electronics box uses a Glenair connector 880-001PA-K19M-M020J5-48. Two tests were performed in early February 2020. The tests were nominal and uneventful – there were no signs of any structural failure. Details of the testing can be found in a NAVAIR test report dated February 10, 2020.

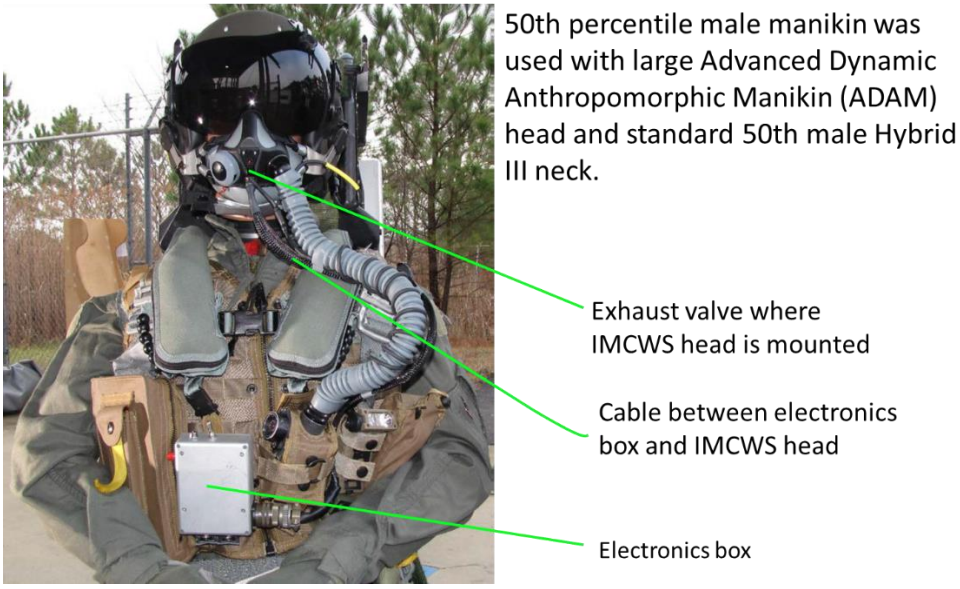

Figure 9.5. Photo of IMCWS Test Hardware, Immediately Prior to Windblast Test
Exposed IMCWS hardware includes the cable between the mask and electronics box, and the external electronics box.

9.3.3 Rapid Decompression Compliance

Another standard test required for airworthiness evaluation is a test of Rapid Decompression. There is a concern that hardware may have closed and sealed elements that may rupture if subjected to sudden changes in environmental pressure. The test profile is graphically described in Figure 9.6. The test was performed at labs managed by KBR-Wyle in San Antonio, Texas.

- Ascend to 60k ft at 5k fpm
- Descend to 22k at 5k fpm; hold 2 min
- Rapid ascent to 60k ft (90 % of decompression in ≤ 0.1 s).
- Slowly pressurize chamber to ambient at 5k fpm.

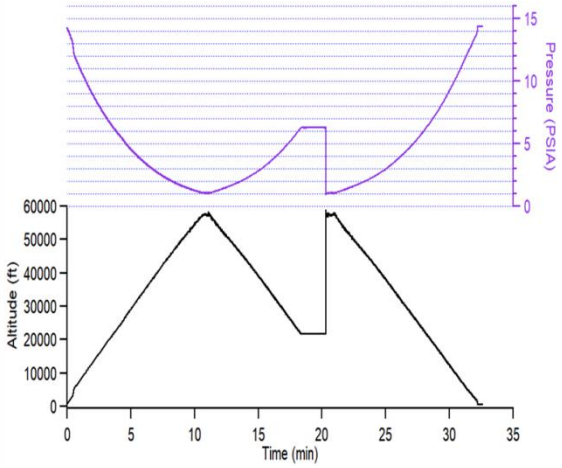

Figure 9.6. Rapid Decompression Test Profile to Assess Pressure Safety

Prior to the test, some small vent holes were added to the design of the electronics box – out of an abundance of caution. The test results were entirely nominal and unremarkable. Tests were performed with the hardware unpowered. The hardware was unaffected by rapid changes in pressure. A photo of the test articles in pre-test configuration is shown in Figure 9.7.

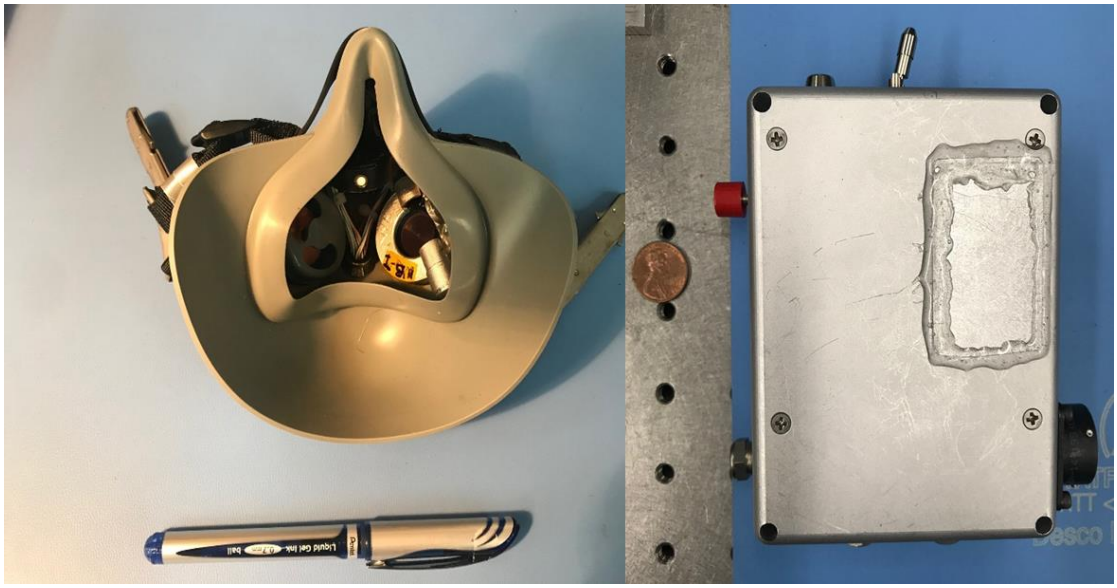

Figure 9.7. IMCWS Test Articles Immediately Prior to Rapid Decompression Testing

9.3.4 Mask Integration

Integration of the IMCWS sensor system into the pilot's mask cannot adversely affect any aspect of the mask. Several aspects of mask integration were considered. These issues are described in this section, and other sections. The wire pass-through used a Glenair connector which was mounted in a location that was previously designated for this purpose. Different versions of this mask have a connector in this location installed at Gentex facilities. The connector, and all other IMCWS components were assembled and structurally attached to the mask at JPL.

Flow through the exhalation valve was not affected by the addition of the sensor housing. This was verified by inspection of the design and test. Added weight caused by addition of sensor is small, less than 40 grams. O_2 flammability and materials compatibility were assessed in a materials compatibility memo (See Appendix 5). Materials used, including epoxies and coatings were determined to be compatible with use for human-systems and mask materials requirements.

9.3.5 Laser Safety

The IMCWS uses a tunable diode laser (TDL) emitting at a wavelength of 2683 nm. The laser tunes over a part of the spectrum that has strong absorption features for both CO_2 and H_2O. The laser is driven by control electronics that sweep the laser emission over the spectral range of interest at a rate >86Hz. The system was assessed for laser safety. The maximum emitted power is 9.5 mW at the laser, but Figure 9.8 illustrates that the output power into the mask volume is <500 µW. An aperture restricts the majority of the laser energy from entering the mask open volume. During the laser safety evaluation, the mounting hardware was coated black to provide an extra level of control over laser light reflecting off a surface. The laser was rated as Class 1, safe to use without any special warnings, labels, or operational constraints.

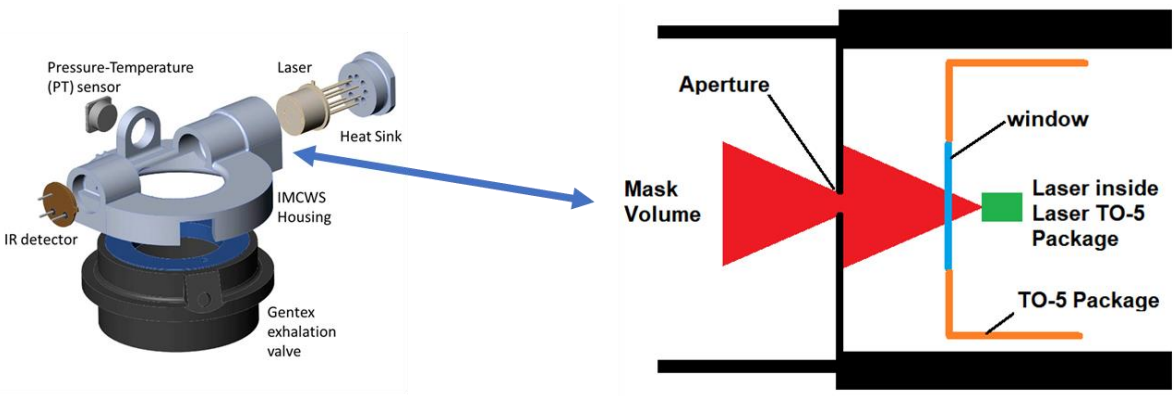

Figure 9.8. Graphical Illustration of Aperture Limiting Laser Power in Mask Open Area

9.3.6 Thermal Management

Multiple, redundant controls are provided to prevent inadvertent overheating inside the mask System power is limited to be less than 5W. Small elements in the laser system are connected to a heat sink. There is a specific temperature control circuit that measures sensor temperature, and cuts power if the temperature approaches 50C. Thermal hazards and overtemperature controls were reviewed and approved by the AFRC Technical Brief panel. It should be made clear that the 50C temperature limit applies to a relatively small (rice grain size) component which was assessed to pose no significant burn or injury hazard to the pilot.

9.3.7 Structural Integrity

Structural integrity of the IMCWS was analyzed; results are detailed in a structural analysis memo (See Appendix 5). The structural analysis memo considered the possibility of any of the sensor components coming loose if the sensor was subjected to an impact load. Structural analysis considered the greatest impact load that was survivable by a pilot, and conservatively analyzed load cases with greater impact. Sensor components are small and have a low mass. They are secured in a structural housing that provides a large contact surface, relative to the size of each component. Additionally, each component is secured using strong epoxy. The detailed analysis is provided in a dedicated structural analysis report. The AFRC Tech Brief Panel reviewed and approved the report and there is no credible hazard of having loose bits inside the mask due to lack of structural containment.

9.3.8 Electromagnetic Interference

Electromagnetic interference tests were performed at the JPL EMI facility on February 20, 2020. Tests included a range from 100 MHz to 18 GHz and followed MIL-STD-461G. The instrument was powered on during the test. For emissions, RE-102 with “fixed-wing internal, <25 meters nose to tail” was used as the evaluation criteria. The IMCWS does not emit EMI that interferes with other equipment, nor does it violate any aspect of MIL-STD-461G. There are no safety issues related to EMI for IMCWS.

9.3.9 Electromagnetic Susceptibility

Test results from the EMI tests performed at the JPL EMI facility on February 20, 2020, are shown in Figure 9.9. At the lowest frequencies, there are some over-guideline measurements. Subject matter experts who were brought in to evaluate these data found that these kinds of signatures are fairly common, and the greatest risk is that there are some data drop-outs. This

does not cause a safety issue but only increases the risk that data is not properly recorded. The IMCWS project chose to accept the risk of data dropout, with the support of PBA project management.

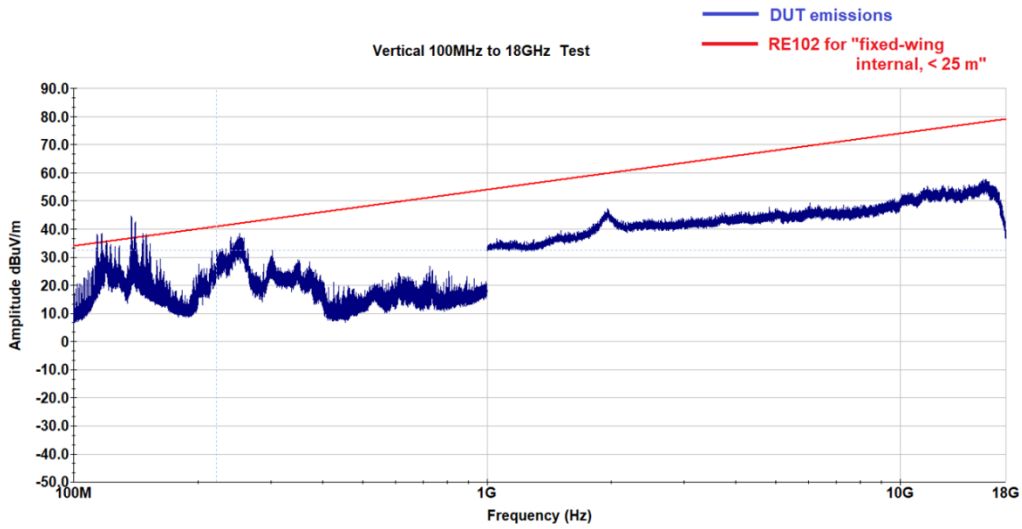

Figure 9.9. EMI Test Results for Electromagnetic Susceptibility Showing Stability Against Fixed Wing Standard

9.4 System Sensor Performance

IMCWS sensor performance was evaluated in the lab prior to any flight tests. Data plots shown below can highlight some of the key aspects of system performance. Figure 9.10 plots the CO_2 levels recorded for three breaths, collected in a lab environment. Sensor range captures the breathing profile, and sensor response (83 Hz) captures the most dynamic changes at the beginning of the exhaled breath.

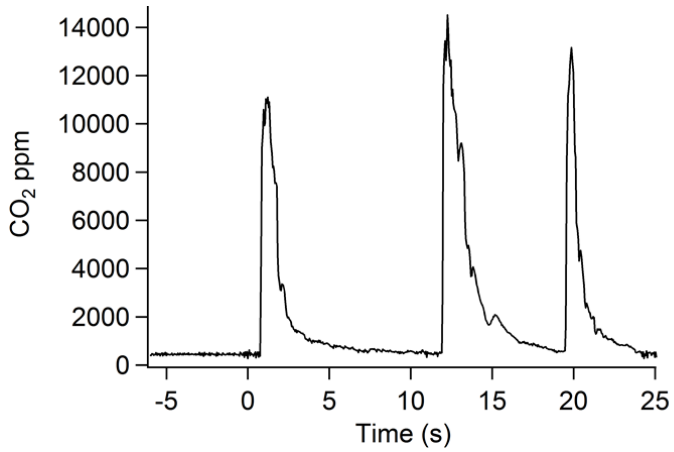

Figure 9.10. CO_2 Profiles for Three Breaths, Collected in Lab Environment; Profile Demonstrate Excellent Resolution for Tracking Within-Breath Profiles

Figure 9.11 plots the temperature, pressure, water vapor, and CO_2 traces for six breaths, as measured in a lab environment. The time resolution of each of these four traces captures the most dynamic events, and features in one trace can be correlated to features of another trace. Note that the pressure trace is the most complex pattern. Pressure trends can indicate the precise timing of inhalation and exhalation valve function.

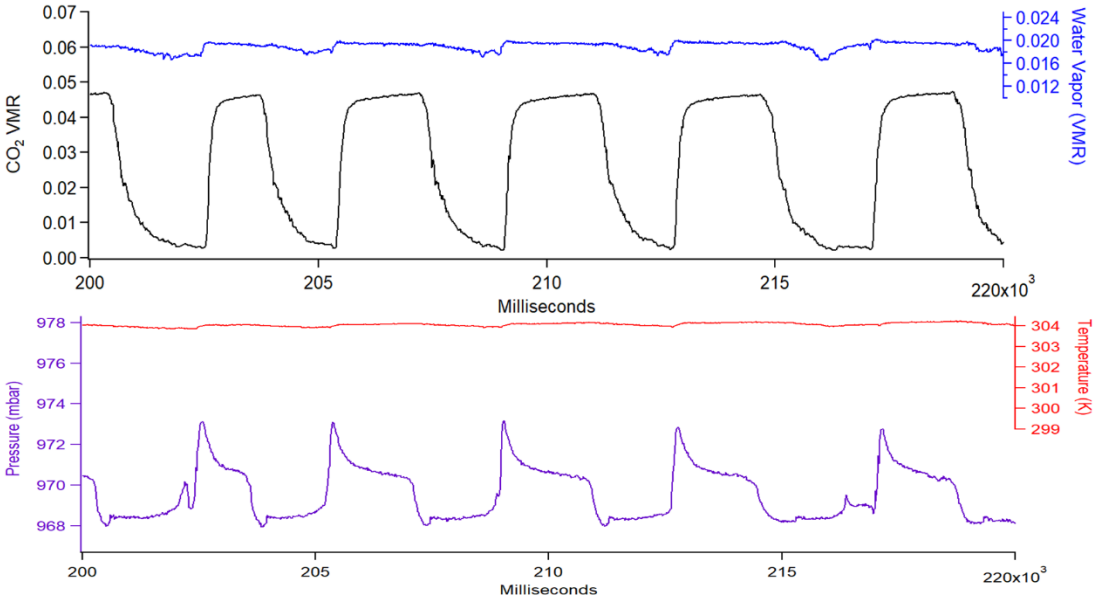

Figure 9.11. Plots of Water Vapor, CO_2, Temperature, and Pressure for 6 Breaths for Data Collected in Laboratory Environment Demonstrating Overall Correlation Among Sensors Resolution and response are capable of tracking within-breath changes for pilot physiology and mask performance needs.

Figure 9.12 focuses on just the pressure and CO_2 trends of a single breath. Focusing on just one breath can highlight some of the characteristics of breathing in a mask. The mask pressure rises for 185 ms, before there is sharp drop in pressure and a sharp rise in CO_2. This shows the amount of time between the start of the exhalation and the opening of the exhalation valve. At the end of the exhaled breath, there are some fluctuations in the CO_2 levels. This signature is found consistently synchronized with a pressure fluctuation indicating that the CO_2 trends are connected to valve actuation.

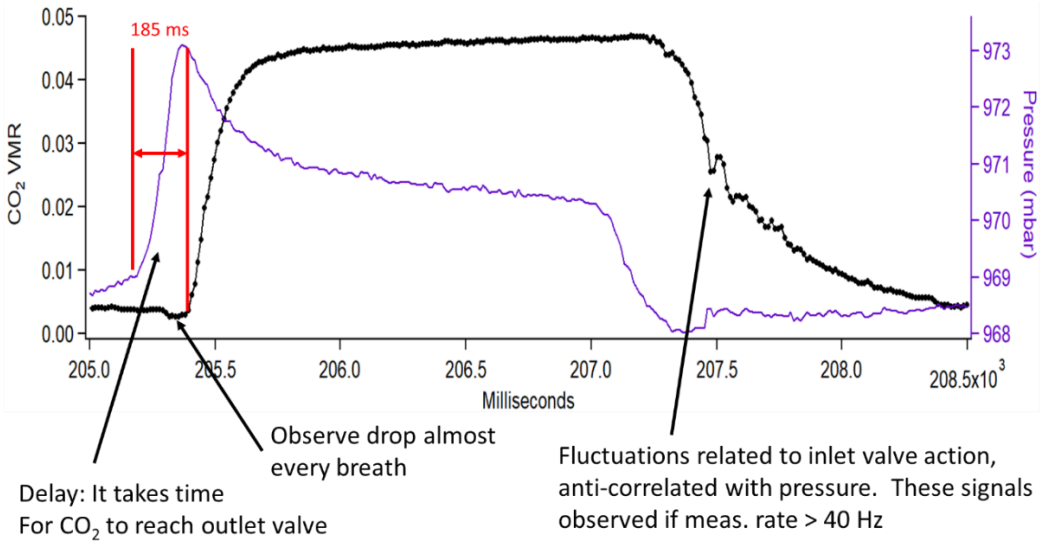

Figure 9.12. Overlay Plots of CO_2 and Pressure, Collected During Single Exhaled Breath Collected in Lab Environment
Graphs are annotated to show important features of correlation.

9.5 Performance Benefits of Capnography

Rather than accumulated CO_2 with the VigilOX, the JPL sensor offers a tool that can be diagnostically physiologically and may have insight mechanically. The JPL sensor seems to offer time based capnography. The measurement of CO_2 is not an accurate physiological measure of metabolic and lung function. This is a combined volume of

a. Physiological dead space
b. Mechanical dead space
c. Normal inhaled portion
d. Retained portion from the stagnant area in the mask in front of the face

Capnography is exceptional both for its utility physiological testing and also in patient care in EMS and hospitals. It has been applied in many uses to assess ventilatory and metabolic physiological of breathing systems. The essential mechanism of capnography was originally grounded on the property that CO_2 absorbs infrared radiation. When the patient exhales, a beam of infrared light is passed over the gas sample on a sensor. The presence or lack of CO_2, is inversely indicated by the amount of light that passes through the sensor. High CO_2 levels are indicated by low infrared, and low CO_2 levels result in high amounts of light. Electrochemical sensors may incorporate long averaging times, 20 or more seconds, for large, abrupt changes in O_2 concentration. Laser diode technology offers short response times to be a more immediate reading without delay. Laser diodes are now being incorporated into sensor platforms for physiological monitoring. The CO_2 levels are then displayed on an IR detector and overlap water, thus can cause some confusion if not accounted for. This is less likely with laser platforms.

What is measured by the capnograph is known as the End Tidal CO_2 ($ETCO_2$) or the amount of (or partial pressure of) the CO_2 released at the end of expiration, an essential component of measuring cardiac output.

Figure 9.13 shows a normal capnography waveform.

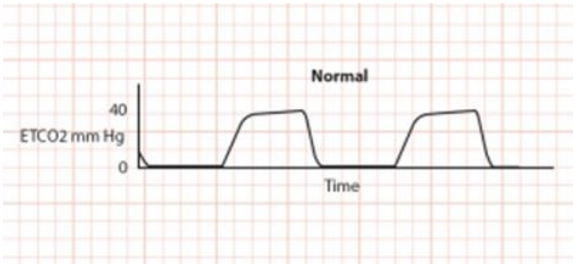

Figure 9.13. Normal Capnography Waveform

The length of the wave represents the time, while the height of the wave represents the amount of CO_2 in the exhaled breath. Thus, faster breathing is represented by a relatively short duration of the waveform, whereas slower breathing is shown with longer waveforms. On the other axis, the taller the waveform, the more $ETCO_2$ is in the breath. Inspiration, therefore, is shown on the waveform by a drop of the CO_2 levels to zero.

The process is relatively simple, as is the equipment. There are two types of capnography, mainstream and sidestream. Mainstream capnography is characterized as invasive and non-diverting, meaning that the measurement of the $ETCO_2$ is done at the airway, or the sample site, thus providing a real-time measurement of the CO_2 pressure. Sidestream, on the other hand, is

non-invasive and diverting. This means that the gas sample is transported from the sample site through a plastic tube and analyzed in a sample cell. This results in a couple seconds delay of the analysis and a possible distortion of the analysis, which can be consequential in an emergency situation.

In the situation where a person is breathing normally, the non-invasive nature of sidestream capnography means that it can be easily used on non-intubated patients. Mainstream capnography is used with the invasive forms of monitoring, such as with an intubated patient (a tube is inserted to breath for a person). Mainstream capnography is less prone to technological and monitoring difficulties. Ultimately, capnography is a simple process that is useful both in emergency settings, in hospitals, and with physiological testing. See Figure 9.14.

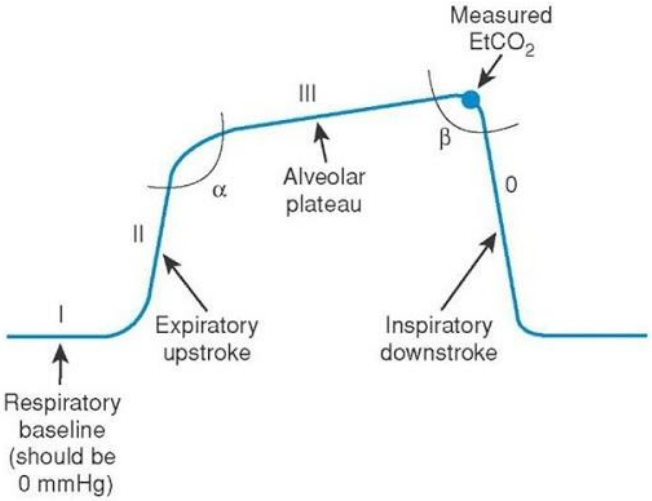

Figure 9.14. Capnography Cycle
http://www.emdocs.net/interpreting-waveform-capnography-pearls-and-pitfalls/

The expiratory segment of a time capnogram is divided into three phases: I, II, III. Occasionally, at the end of phase III, a terminal upswing, phase IV, may occur. Phase I represents the CO_2-free gas from the airways (anatomical dead space and apparatus dead space). Phase II consists of a rapid S-shaped upswing on the tracing (due to mixing of dead space gas with alveolar gas – the gas exchange units). Phase III consists of an alveolar plateau representing CO_2-rich gas from the alveoli. It almost always has a positive slope, indicating a rising $ppCO_2$. This rise is due to continued excretion of CO_2 into the alveoli and then into the airways. It also can be due to a late emptying of alveoli if there are lower ventilation/perfusion ratios. This represents under ventilated alveoli resulting in a relatively higher $ppC0_2$. The angle between phases II and III, which has been referred to as the alpha (ά) angle, increases as the slope of phase III increases. The alpha angle is thus an indirect indication of V/Q status of the lung. After phase III is complete, the descending limb makes an almost right angle turn and rapidly descends to the base line. This represents the inspiratory phase during which the fresh gases (CO_2 -free gases) are inhaled and CO_2 concentration falls rapidly to zero. The nearly 90 degrees angle between phase III and the descending limb has been termed as the beta (β) angle. This can be used to assess the extent of rebreathing. Rebreathing in a mask is secondary to retained in a mask system. During rebreathing, there is an increase in beta angle from the normal 90 degrees. As rebreathing increases, the horizontal baseline of phase 0 and phase I can be elevated above normal.

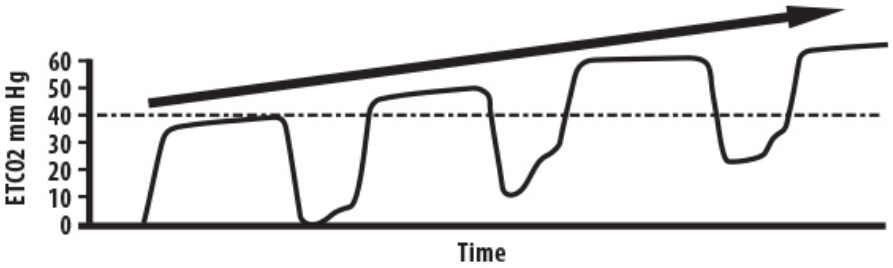

Figure 9.15. Elevating baseline

In looking at mechanical function, capnography can have some insight into specific malfunctions. If a ventilator has an inspiratory valve not closing properly, it will result in a flip in the plateau at the beginning of inspiration, see the red line in Figure 9.16.

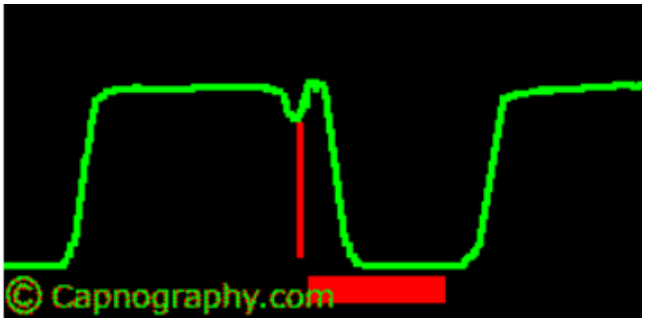

Figure 9.16. Red-line Indicating Improperly Closing Inspiratory Valve (Source: From Capnography.com)

In a patient on a ventilator, the presence of the disconnection or incompetent valve, the inspiratory portion of the capnogram is unchanged. During expiration, the initial high expiratory flow rate will be sufficient to close the inspiratory valve and allow exhaled gas to flow through the CO_2 analyzer giving rise to the normal looking expiratory plateau. However, if an exhalation valve is partially incompetent or floppy, a portion of expiratory gases exit through the valve representing a leak. This reduces the expired tidal volume. As the expiratory flow rate decreases, leak flow will cause pressure to decrease in the mask, allowing the expiratory valve to close prematurely and facilitate flow of inspiratory gases. The flow of fresh gases flow from the inspiratory limb reduces the measured CO_2 at the analyzer. As the fresh gas flow causes pressure to rebuild in the mask, the expiratory valve will reopen, allowing the further movement of alveolar gases pass through the CO_2 analyzer.

If the Inspiratory valve is displaced or totally incompetent it will result in rebreathing and the following pattern; see the red sections in Figure 9.17.

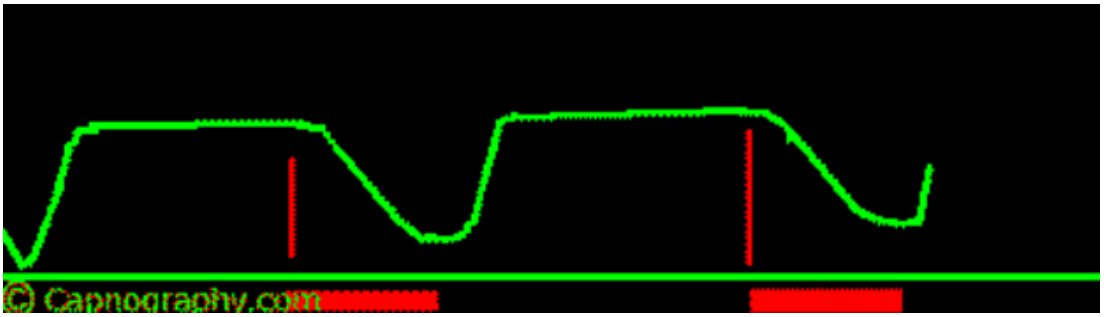

Figure 9.17. Red-marked Sections Indicating Incompetent Inspiratory Valve

If the expiratory valve is incompetent, it can result in a prolonged phase II, slanting of descending limb of inspiration, and possible rebreathing indicated by baseline elevation, see Figure 9.18.

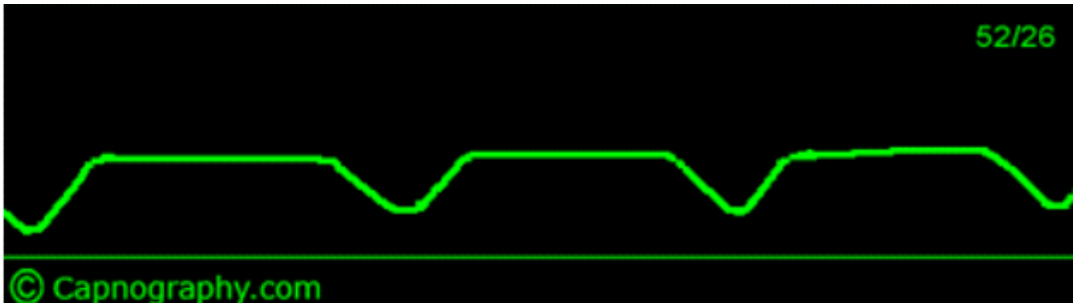

Figure 9.18. Elevated Baseline Typical of Rebreathing Caused by Incompetent Expiratory Valve

Since the JPL sensor is in the mask in the expiratory steam, this offers near mainstream accuracy in measurements. Further refinement can be done to examine this in detail and develop algorithms to aid in this analysis.

As an example, some sections of flight 100 Hz data from the JPL In-Mask-Sensor (IMS) allows for some minute details to be analyzed from the $ppCO_2$, revealing clues indicative of physiological states or mechanical interactions.

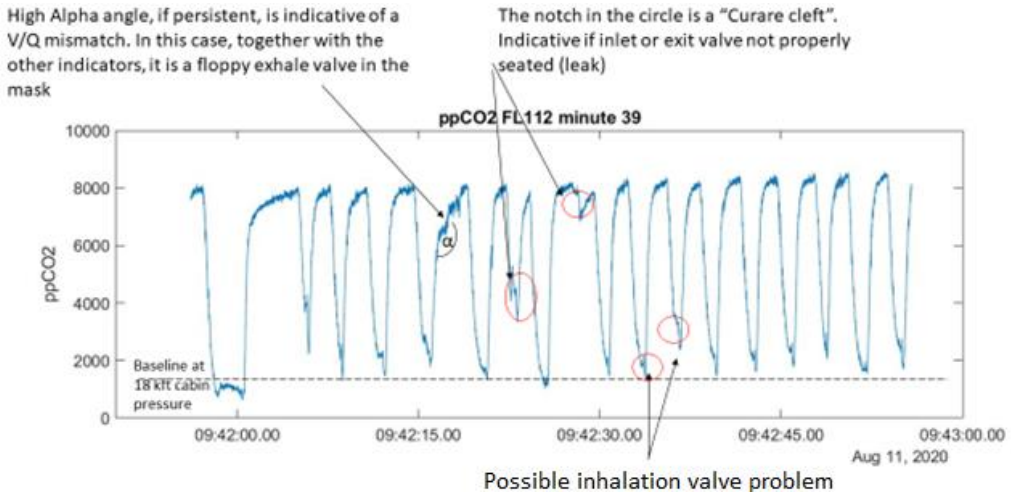

Figure 9.19. Example Capnography Profile, with Labeled Artifacts

As was stated, a high ά angle can be an indirect indication of a V/Q mismatch in the lung. It also can indicate a decreased flow to the CO_2 sensor, so looking at other segments to localize a problem is in order. If there is solely an isolated and continuous ά angle opening or increasing, then a V/Q mismatch should be suspected. This would indicate decreased tidal volumes to the mask and pilot are occurring. Specifically, an inspiratory line obstruction or incompetent valve will result in phase II and phase III being prolonged and ά angle (angle between phase II and phase III) is increased.

Also, notable here is the "Curare cleft". As mentioned, the "curare cleft" seen in the alveolar plateau in clinical medicine is actually a patient making an attempt to breath. With a weak inspiratory effort, some fresh gas sucked from the ventilator tubing and past the capnometer, generates this pattern. With an aircrew breathing system the pilot is awake and thus is the result

of a mechanical failure. In the presence of a partially incompetent exhalation valve, the inspiratory capnogram is unchanged. During expiration, the initial high expiratory flow rate will be sufficient to close the inspiratory valve and allow exhaled gas to flow to the CO_2 analyzer giving rise to the normal looking expiratory plateau. However, a portion of expiratory gases exit through a leak created by the incompetent valve. This reduces the measure expired tidal volume. As the expiratory flow rate decreases, leak flow will cause pressure to decrease in the mask, allowing expiratory valve to close prematurely and facilitate flow of inspiratory gases. The flow of fresh gases flow from the inspiratory limb reduces the measured CO_2 at the analyzer. As the fresh gas flow causes pressure to rebuild in the circuit, the expiratory valve will reopen, allowing the further movement of alveolar gases pass to the CO_2 analyzer.

Also, one should note there appears to be an elevation of the baseline and phase I of the capnogram. This may be a mechanical retention of gases (CO_2) or due to an alteration in the mask barometric pressure. This may or may not be retained and rebreathed by the pilot. If the β angle is also opening to greater than 100º, this likely may represent a physiological retention.

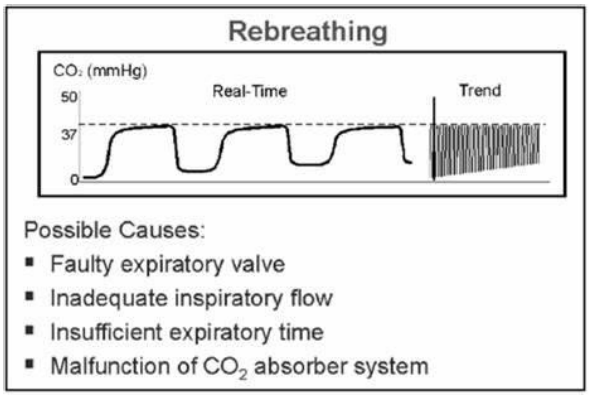

Figure 9.20. Elevated Baseline Typical of Rebreathing
From http://kidocs.org/tag/co2/

There is also a small notch at the base of phase IV that usually indicates an inhalation or sometimes an exhalation valve problem with retention.

Figure 9.21. Notches in Capnography Profile
From: https://iiimedical.com/?msclkid=e1ca6a562163170a7b1635dbc35670fa

In another segment of the flight, the following was recorded.

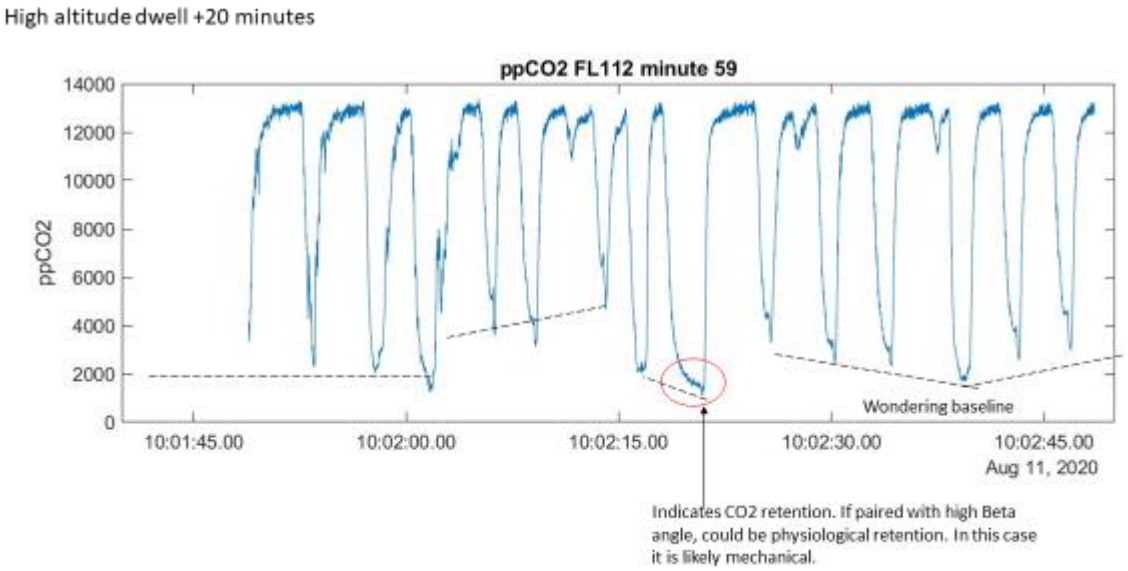

Figure 9.22. Example Recorded Capnography Data

Notable in the segment (Figure 9.22) is a wandering baseline and phase I of the capnogram. This indicates a sensor with varying amounts of CO_2 recorded. This is likely due to an intermittent or "floppy" mask valve malfunction with varying amounts of air being retained in the mask. If the β angle also opens up, then a physiological retention should be suspected accompanying the mechanical retention. Possible rebreathing of the retained gas in the mask should be considered.

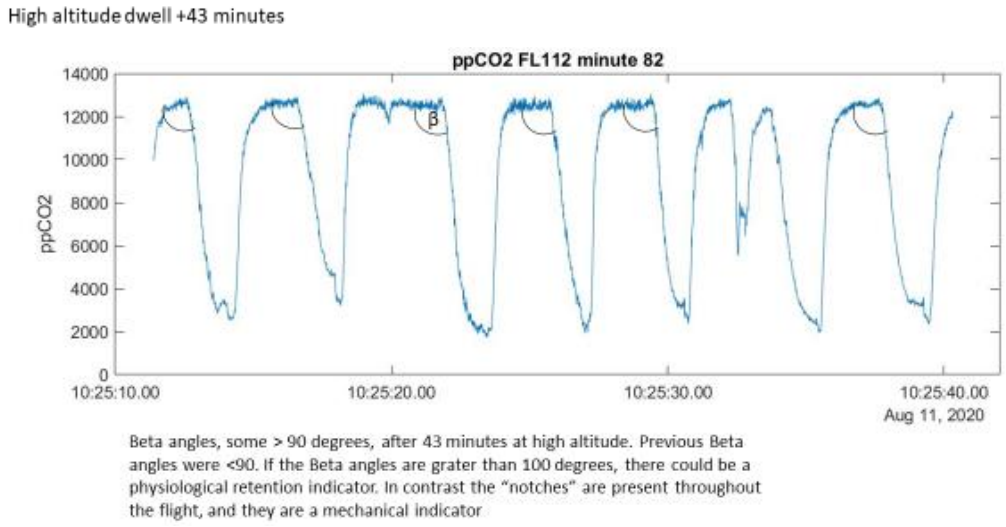

Figure 9.23. Capnography Data Indicating Beta Angles β

Now looking at the Beta (β) angles, Figure 9.24 shows the following.

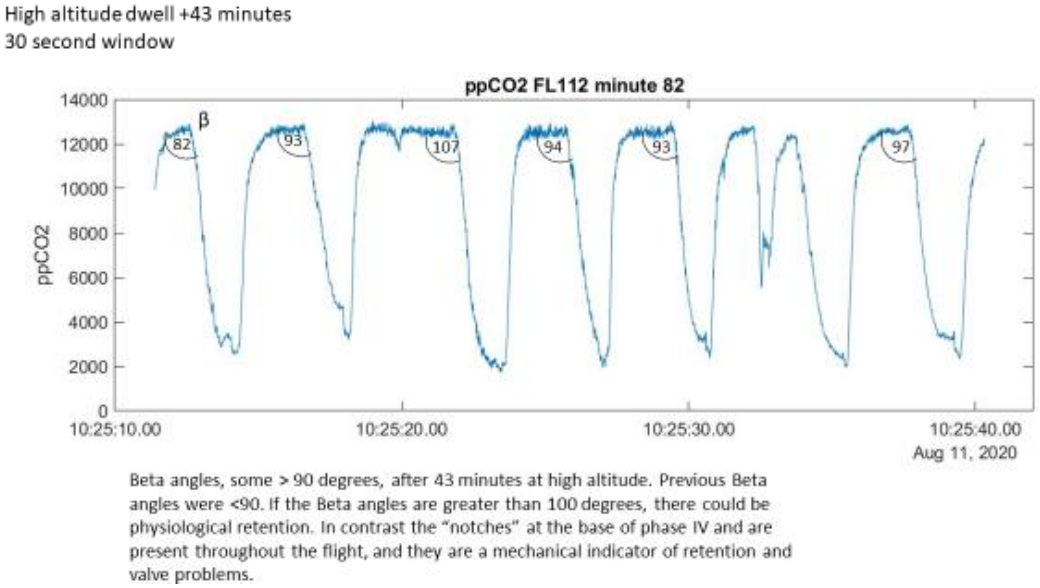

Figure 9.24. Capnography Data with Labeled Beta Angles (β)

Looking at the capnogram in Figure 9.24 as whole, there are indications of valve dysfunctions with mechanical retention. Use of the JPL sensor can be used with mask flow and pressure to isolate the particular valve dysfunctions. If used solely, the JPL may be used as an early warning or as a diagnostic tool for the mask.

F.9-1. An in-mask CO_2 sensor offers significant new capability for identifying pilot O_2 processing ("metabolic cost of flying" assessment) by producing high resolution data for system diagnostics.

9.6 Physiological Relevance

The benefits from having a CO_2 measurement at the mouth and mask exhalation valve are substantial. This setup prevents long hoses attached to the exhale port and subsequent dilution of gasses within the long tube and with cabin air. In addition, the frequency response allows the possibility of resolution of physiologically relevant metrics that relate to the performance of small airway and air exchange functions in the lung. The shape of the CO_2 curve has potential to give insight into pilot lung physiology and potentially indicate degraded function in real time from common pathologies such as absorption atelectasis. These features do not currently exist in any other sensor. High fidelity data with insight as close to the mouth as possible of pressure, valve function, and CO_2 is a revolution in pilot sensor capability.

9.7 Development Status

At the time this section is being written, the IMCWS has been reviewed by the AFRC Tech Brief committee and approved for use in flight test. Flight testing of the IMCWS was successfully completed in August 2020.

9.8 Conclusions

The NASA-JPL IMCWS increases the value of integrated data collection and evaluation techniques available to assess pilot performance in real time. The primary importance is the high-resolution within- and between-breath profiles that allow medical evaluation of breathing

perturbations including hyperventilation, hypercapnia, and O_2 metabolism, as well as tracking mask valve and regulator response perturbations.

As technical progress continues, the IMCWS may offer real opportunity for additional field applications across a wide range of aircraft platforms and use environments, including other occupational fields employing artificial atmospheres such as firefighting and technical (military) diving.

Technical Section 10: Development of a Diagnostic Test of In-Flight Breathing System Performance

10.0 Motivation for Developing an In-Flight Diagnostic Test

September 26, 2017, marks the origin of this section of the report, and the entire PBA project. On that date the NESC presented the results of its independent assessment of the causes of PEs affecting pilots flying USN F/A-18 aircraft. The NESC team presented their findings to a delegation that included Admiral Sara Joyner. At the conclusion of the presentation, Admiral Joyner thanked the NESC team for their work – she also issued a challenge. Admiral Joyner told the NESC team that there were specific aircraft that were involved in multiple PE incidents, but none of the existing USN diagnostic tests could find the source of the problem. Admiral Joyner issued a significant challenge to the NESC team – develop a diagnostic test that could identify precisely what was wrong with the "bad actor" jets.

In September of 2017, the NESC team had nothing helpful to offer. The central recommendation was that pilot breathing should be directly measured in-flight, but the NESC had no detailed recommendations about the specific test procedures, measurement equipment, or data analysis techniques. In September of 2017, all NESC could offer was a general recommendation.

In March of 2018, Clint Cragg presented a plan to the NESC Review Board (NRB) recommending a program to develop a standard method of measuring pilot breathing in the cockpit of F-15 and F/A-18 jets operated by NASA and flown from NASA Armstrong Flight Research Center. This program, called Pilot Breathing Assessment, began with an admission that measuring pilot breathing in a cockpit of a military jet would be difficult. It would require measurement equipment that was not available in any flight qualified, validated form. It would require new flight test procedures, and new data analysis techniques. NESC is structured to address complex technical problems that require subject matter experts from multiple different disciplines from multiple different organizations – and have them work together as a team. NESC teams are structured to solve one specific problem.

Part of the NRB process to start a new project involves defining the scope of the project and declaring exit criteria. PBA was <u>not</u> scoped to find the causes of PEs. The scope of PBA was to develop a standard method of measuring pilot breathing. This scope was defined with Admiral Joyner's challenge in mind – NESC would do the work to develop a standard test – Admiral Joyner's organizations would perform the tests.

The PBA team had lots of false starts and logistical problems – especially in the beginning of the project. SMEs did not know what kinds of measurements would be useful. When NESC received the first data sets from the early flights, data analysts had no context for the measurements, so there was not easy to identify which measurements represented nominal conditions, and which measurements identified unusual conditions. Some unusual characteristics in the data were measurement error, caused by quirks in the measurement equipment. Some unusual characteristics in the data were clear signs of breathing system disharmony – but for most measurements, there was not enough contextual data, or sufficient understanding of breathing system interactions to correctly interpret the data.

Slowly, incrementally, the understanding of the PBA data improved. With increasing numbers of flights, the PBA data analysts could begin to see trends. Because PBA was structured to

collect data from tightly scripted flights with repeatable maneuvers, segments from one flight could be compared to segments from a different flight.

Many of the test flights were nominal and ordinary, with pilot reports of easy breathing. A few flights resulted in pilot reports of difficulty breathing. During two flights, the breathing difficulties were so significant that the pilot discontinued tasks. The PBA was not designed to fly near the edges of the envelope, and pilots were instructed to limit their maneuvers if breathing became difficult.

The differences in PBA data between nominal flights and flights with pilot reports of breathing difficulties is stark. Flight 29 was unlike any previous flight. Flight 29 triggered an investigation into its causes, and a report of findings was presented to USN and USAF stakeholders. The initial interpretation about the causes of flight 29 – targeting mask components – is likely correct, but also likely incomplete. In January 2019, when flight 29 was first evaluated, the PBA team had a new appreciation for mask components, but no real insight into system level interactions or system level responses.

Since January 2019, the PBA team has made one key insight. This insight came slowly and incrementally, as flights continued and new data was analyzed, the central insight about the causes of breathing difficulties became more apparent:

Pilot breathing systems need to operate in a time-coordinated way. If individual components in a pilot breathing system cycle early, or cycle late – breathing sequence insults can result. Breathing sequence insults can alter pilot breathing, cause pilots to become aware of their breathing, and trigger pilot perceptions of breathing difficulty. Listed below are a series of statements breathing system timing and sequence – and resulting consequences:

- If a pilot inhales and receives the correct amount of air, at the correct pressure, with the correct flow rate, at the correct time – breathing is smooth and easy.
- If a pilot inhales and receives the correct amount of air, at the correct pressure, with the correct flow rate, but at the wrong time – breathing is difficult and the amount of breathing can be reduced.
- If a pilot exhales, and exhalation valves open at the proper time, exhalation is smooth, and breathing is smooth and easy.
- If a pilot exhales and the exhalation valve opens late, exhalation is difficult, breathing is difficult, and the amount of breathing can be reduced.
- If a demand regulator acts in perfect harmony with the pilot's inhalation/exhalation sequence, pilot breathing is smooth and easy.
- If the demand regulator delivers air at the wrong phase of the inhalation/exhalation sequence, breathing is difficult, and the amount of breathing can be reduced.
- Individual components can meet all acceptance test criteria, but if they cycle at the wrong time, out of sequence with the other components in the breathing system, breathing is difficult, and the amount of breathing can be reduced.
- If the pilot inhalation/exhalation sequence sets the timing of the breathing system, pilot breathing is smooth and easy.
- If the system sets the inhalation/exhalation sequence, and the pilot needs to adjust their rhythm to meet the timing of the mechanical system, breathing is difficult, and the amount of breathing can be reduced.

Consider the 2017 challenge from Admiral Joyner - devise a test to identify exactly what is wrong with the bad actor jets. In 2017, the NESC team did not have anything specific or helpful, just a general recommendation to measure pilot breathing. In 2020, the PBA team meets Admiral Joyner's challenge, and meets the PBA exit criteria. This chapter describes a flight test that can identify and isolate problems affecting bad actor jets. This test plan includes:

- Identification of a New Set of Diagnostic Mechanisms. Breathing sequence insults and breathing sequence timing mishaps were not recognized by the NESC team in 2017. In 2020, we recognize their importance. It is also understood why components can pass bench tests and diagnostics tests, only to cause breathing difficulties on the jet – timing, sequence, and response rate are important, and these bench tests cannot measure timing, sequence, or response rate.
- Test Equipment. VigilOX is still not fully validated, but >100 flights with the equipment has resulted in a substantial increase in maturity. The JPL developed sensor system is very new, with just 6 flight tests, but its ability to measure CO_2, humidity, temperature and pressure directly inside the mask gives it great potential for diagnosing problems in flight.
- Flight Profile. PBA has flown scripted test flights – the PBA pilots and analysts have used this experience to develop a flight script (referred to as Profile H) to provide a consistent set of breathing system challenges, and serve as a general screen to identify potential "bad actor" jets before they cause a PE.
- Data Analysis. PBA has developed a standard method for statistical analysis and flight segment to flight segment comparison
- Data Set for Comparison. Data from early PBA flights lacked context. Data archived in the Pilot Breathing Almanac provides a reference for comparison.
- Data Interpretation. PBA analysts have made many insights and have developed characteristic signatures for many different system interactions. The most significant ones involve breathing sequence, and system level timing. PBA analysts have developed two quantitative measures of system level timing – breathing system hysteresis and breathing system phase shift.

10.1 Objectives for the In-Flight Diagnostic Test

Operational flights are conducted with an essentially no measurements of pilot breathing. Many times, the first record of a problem with the breathing system is a PE. PE rate of occurrence range from 1/1000 to 1/2000. Recording and documenting PEs can identify the worst breathing system out of 1000 flights, but it cannot identify the worst breathing system out of 100 flights, or 50 flights, or 10 flights.

The objective for the in-flight diagnostic test is to identify the worst breathing system out of 100 flights and identify the worst breathing system out of 50 flights and identify the worst breathing system out of 10 flights. If small problems can be identified, corrective actions can be taken before breathing system problems reach the level of causing a PE. If small problems can be spotted, trends can be identified. If small problems can be spotted, the effects of corrective actions can be tracked.

The scoring method is designed to match the objectives to identify:

- The worst breathing system out of a group of 10
- The worst breathing system out of a group of 50
- The worst breathing system out of a group of 100

The scoring method tries to simplify a complex breathing system interactions into simple summary scores, and a color coded classification of Green, Yellow, and Red. A flight with a few "yellow card" scores can be considered to be well within the normal range, but a series of "yellow card" scores with one or more "red card" scores can indicate a more serious problem.

"Test like you fly" (TLYF) is a familiar adage to those who work with aircraft and aerospace systems. Another related adage – "fly like you test and test like you fly" reinforces the concept that the connection between test and flight goes in both directions. Tests need to be conducted in a flight environment, or the results are not valid. Operational profiles should be restricted to the envelope where valid test data is available. A pilot breathing system is a complex system, with interactions that only occur in the flight environment. The intent of this diagnostic test is to measure breathing system performance in a realistic environment, and to accurately measure the effects of system interactions. The objective for this test is to meet the criteria – "fly like you test and test like you fly."

Another important objective for this test is to be simple enough to effectively conduct the test, analyze the data, and determine a single score that is easy to assess. To meet this objective, the test is restricted to a single flight, the data analysis is restricted to 10 categories, and the example pilot questionnaire can be completed in a few minutes.

The final objective is that the test results in a single score, so results can be easily interpreted.

10.2 Structure of the In-Flight Diagnostic Test

The details will be provided in subsequent sections, but it is helpful to begin with a general overview of the In-Flight Diagnostic Test structure and process. The test an assessment process has 7 main steps:

1. Outfit the pilot with the VigilOX breathing system.
2. Outfit the plane with instrumentation that measures cabin pressure, supply pressure, altitude, airspeed, and G levels.
3. Record the test configuration.
4. Fly Profile H.
5. Ask the pilot about the flight.
6. Conduct a standard numerical assessment of the data
7. Issue a summary score for the flight

Each of these steps is described in greater detail in the sections below:

10.2.1 Outfit the Pilot with the VigilOX breathing system

There are other methods for measuring pilot breathing. The JPL In-Mask Sensor has potential for making more sensitive measurements and identifying breathing system problems that VigilOX cannot identify. In 2020, VigilOX offers the best operational solution, because VigilOX has greater operational maturity and because results can be compared to the PBA database.

10.2.2 Outfit the Plane with Instrumentation

Understanding pilot – plane system interactions requires data about the pilot and data about the plane. These two different datasets need to be time synchronized and put into a common datafile for analysis. The two most important measurements from the aircraft are cabin pressure, and line supply pressure. Information about aircraft altitude, airspeed, and G-levels can help determine if the flight profile was followed, and it can help break a complex flight into smaller flight segments. The PBA used Madgetech instrumentation, but other instruments can be used to measure cabin pressure and line pressure.

10.2.3 Record the Test Configuration

Test configuration should be documented for real time analysis, and to search for trends in the data when there is test data from a substantial number of in-flight diagnostic tests. A recommended list of test configuration records includes:

1. Aircraft type, configuration and tail number
2. Regulator type and serial number
3. Mask type and serial number
4. Aircrew equipment configuration
5. Seat position (FCP/RCP)
6. Sensor serial numbers/software version

10.2.4 Fly Profile H

Profile H was developed late in the PBA flight test program, after more than 80 test flights had been conducted, and a substantial amount of data analysis had been performed. It was developed precisely for in-flight diagnostic purposes. The intent of Profile H is to provide as comprehensive a flight test environment as practically possible – given the requirements that the test is completed within a single flight, and different aircraft have different fuel limitations.

Flight Profile H was flown on six different test flights. It was demonstrated to be operationally effective, but there is not enough flight experience with flight Profile H for PBA to use only test results from this flight as the reference database. The larger PBA database will be used as a reference of comparison. To make these comparisons more accurate, analyses will use data from specific flight segments.

Note that Flight Profile H involves some sections that will complicate automated data analysis techniques. Section 4 involves mask-off/mask-on procedures. This is an instructive diagnostic section, but this portion of the flight needs to be removed from the database if automated data analysis is performed. Modifications to flight Profile H may be required if automated data processing for the entire flight is performed.

A summary of Flight Profile H is shown in Figure 10.1.

PROFILE H:STANDARDIZED BREATHING FCF

Card	DESCRIPTION	ALT	KCAS
1	Ground Block	--	--
2	Takeoff & Mil Power Climb	A/R	A/R
3	15K Level Systems Operations	15K	250
4	Mask-On / Mask-Off Comparison	15K	250
5	15K Talking Script	15K	250
6	Mil Power Climb	15K – 30K	A/R
7	OBOGS Descent	30K – 7K	250
8	Mil Power Climb	7K – 25K	A/R
9	25K Level Systems Operations	25K	250
10	Combat Descent	25K - 7K	325 - 420
11	Zoom Climb	7K – 12K	A/R
12	Level Accel/Decel	12K	A/R
13	G-Exercise	12K	400 - 450
14	High G Maneuvering	12K – 7K	450
15	Max AB Climb	7K – 30K	A/R
16	30K Level Systems Operations	30K	250
17	Cruise Descent	30K – 20K	300
18	Spiral Descent / "Defensive" BFM	A/R	A/R
19	RTB	A/R	A/R
20	Ground Block	--	--

Figure 10.1. Summary of Flight Profile H

10.2.5 Ask the Pilots about the Flight

Pilot feedback is essential. Pilots are aware of the system as a whole and can notice things that are not detected with a simplified data processing script. The combination of pilot reports and numerical analysis can be powerful for diagnostics.

PBA used a set of pilot debrief records and pilot questionnaires that were not designed specifically for an in-flight diagnostic test. PBA recommends that each group performing the in-flight diagnostic test develop a set of pilot questions that meet the needs of their specific aircraft type and pilot population.

The PBA team can offer some general recommendations, and an example set of questions. The questions should be easy to answer in a few minutes. The questions should specifically call out systems of interest, but there should be an opportunity for the pilot to make general comments. Some of the questions should prompt the pilot to grade a category with a simple three-level (green, yellow, red) score. Some of the questions should allow the pilot to make note specific observations.

An example set of questions is listed below:

At a minimum, queries should include targeted questions covering the following four general areas, with optional opened ended responses. These questions should not be viewed as prescriptive. These questions were not used during PBA. It is strongly recommended for each aircraft community to develop their own set of questions based on tailored study and known aircraft issues, these questions are provided as an example or a starting point only.

1. On a scale of 1-3 (1 is great, 2 is minor issues, 3 is something was noticeably wrong) – How did the breathing systems perform as expected during this flight? If specific segments of the flight had perceptible impact on any part of the breathing systems, please identify the segment and describe.
2. On a scale of 1-3 (1 is great, 2 is minor issues, 3 is something was noticeably wrong) - How did the breathing system perform when breathing in? If specific phases (beginning, middle, or end) of inhale were distinct or noticeable, please identify the phase and describe.
3. On a scale of 1-3 (1 is great, 2 is minor issues, 3 is something was noticeably wrong) - How did the breathing system perform when breathing out or talking? If any change in effort during exhalation was noticeable, please identify the change, the phase (beginning, middle, end) and describe.
4. Do you have any notes to share about the breathing system performance during this flight, observations about any of the breathing components, comparisons with other experiences, comments, or concerns about a specific segment of the flight?

The goal is to help pilots methodically think about breathing in a structured manner since breathing challenges and breathing sequence insults occur frequently at a noticeable but nearly subconscious level. Methodical questions help with recall of issues that otherwise would not be captured and should be tailored after careful study to the individual aircraft community.

10.2.6 Conduct a Standard Numerical Assessment of the Data

Data analysis must balance the need to be comprehensive, with the need to be simple enough to be operationally effective. PBA analysts considered the needs of a single flight, in-flight, diagnostic test, and developed a set of numerical analyses. They are listed below, and then described in greater detail:

1. Inhalation Hysteresis
2. Inhalation Flow
3. Exhalation Hysteresis
4. Exhalation Flow
5. Inhalation O_2
6. Exhalation CO_2
7. Inhalation Phase Shift
8. Exhalation Phase Shift
9. Inhalation Correlation
10. Exhalation Correlation
11. Cabin Pressure Fluctuation

Inhalation hysteresis is a measure of timing and sequence during inhalation. Inhalation hysteresis is measured for each inhalation throughout the flight. The maximum difference in flow (lps) between the amount of flow from an early part of inhalation, and the amount of flow from a late part of inhalation (when delta pressure is the same) is inhalation hysteresis. A perfect score is 0, a severely degraded score is >0.5. This category has four different scoring criteria: 1) the mean value for inhalation hysteresis for every breath during the flight, 2) the percentage of breaths that are slightly degraded, 3) the percentage of breaths that are moderately degraded, 4) the number of breaths that are severely degraded. The inhalation flow is a measure of the pressure-flow relationship for each inhalation. Much like the trumpet curve, it compares the greatest pressure for each inhalation to the greatest flow. This score does not assess timing – it assesses if enough flow was delivered. Inhalation flow has two scoring criteria: 1) the fraction of breaths where there is slightly less flow than expected, 2) the fraction of breaths with significant flow shortages. A perfect score is 0, where none of the breaths have flow shortages, a severely degraded score is >0.25, where a quarter of the breaths have flow shortages.

Exhalation hysteresis is measured in pressure (mmHg). It is the greatest pressure difference (for equivalent flows) between early stage of exhalation and late exhalation. If there is a stuck exhalation valve, for instance, the initial pressure difference early in the exhalation would be greater than normal, and mask pressure late in exhalation would be less than normal. In this case, the exhalation hysteresis would be large. There are two scoring categories: 1) the mean hysteresis value for every breath during the flight, 2) the fraction of breaths with substantial exhalation hysteresis.

The exhalation flow score matches inhalation. It is a measure of whether the maximum flow corresponds to the expected value, based on the maximum pressure. There are two scoring criteria: 1) the fraction of breaths with slightly less flow than expected, 2) the fraction of breaths with significantly less flow than expected. A perfect score is 0.0, where there are no flow shortages, a severely degraded score is >.25, where a quarter of the breaths suffer flow shortages. Exhalation flow score is related to “trumpet curve” pressure/flow relationships.

Inhalation O_2 score is a measure of O_2 levels in the supply air. Inhalation O_2 scoring criteria is platform specific. The USN configuration uses a LOX O_2 supply, a demand regulator, and pilots nominally breathe 100% O_2 throughout the flight. If O_2 levels drop, that is a sign of in-leakage. For the USN configuration, the scoring criteria is the mean percentage of the 25 breaths with the lowest O_2 during the flight (above 95% is expected for a well-functioning system). The USAF configuration uses a diluter-demand system, ppO_2 is used to score O_2 for this configuration. Mean ppO_2 greater than 180 mmHg is expected for a well-functioning system. Jets with OBOGS O_2 supply systems will need a new scoring criteria for O_2 – PBA recommends a scoring category to evaluate O_2 fluctuation, and a scoring category to evaluate for excess amounts of O_2 as well as insufficient amounts of O_2.

Exhalation CO_2 is a check for two conditions: 1) if exhalation is difficult, CO_2 rebreathing of exhaled breath can occur and CO_2 levels will be higher than nominal, 2) if there is a valve malfunction and supply air continuously flows through the mask, CO_2 levels will be lower than nominal. Average $ppCO_2$ level throughout the flight is used to score this category.

Inhalation phase shift is a measure of the relative timing of maximum pressure and maximum flow during inhalation. It is measured in degrees. An example of nominal phase shift

(a slight delay in flow nominal in a pilot breathing system) and an example of "red" levels of phase shift are shown below. There are three scoring criteria for phase shift: 1) the number of breaths in a flight with positive phase shift, 2) the number of breaths in a flight with phase shift between -20 and -50 degrees, 3) the number of breaths in a flight with phase shift <-50 degrees. A perfect system has 0 for all three categories.

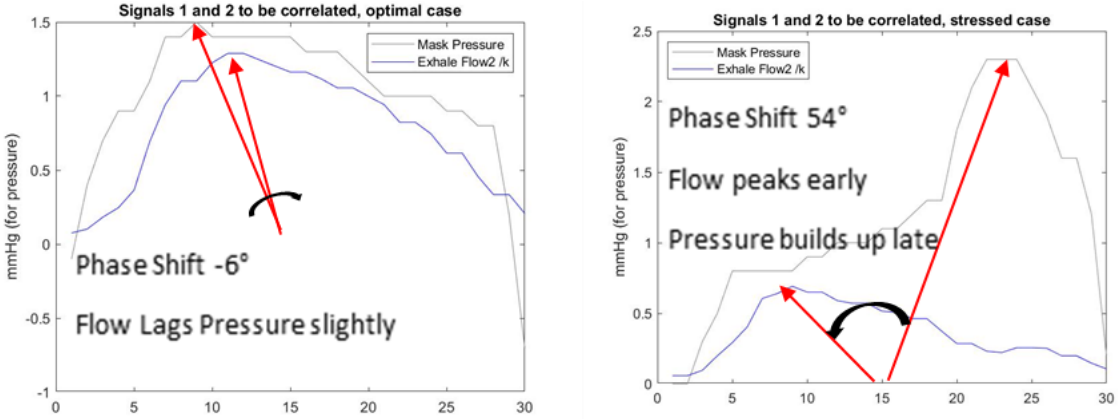

Figure 10.2. Examples of Nominal Phase Shift (left), and Severe Phase Shift (right)

Exhalation phase shift makes the same time correlation between peak pressure and peak flow as inhalation phase shift, and it uses the same scoring criteria. There are three scoring criteria for phase shift: 1) the number of breaths in a flight with positive phase shift, 2) the number of breaths in a flight with phase shift between -20 and -50 degrees, 3) the number of breaths in a flight with phase shift <-50 degrees. A perfect system has 0 for all three categories.

Inhalation correlation and exhalation correlation compare the pressure to flow. In both cases, ideal breathing has perfect pressure-flow correlation, and a correlation score of 1.0. Severely degraded breathing systems can have correlation scores <0.8.

The cabin pressure fluctuation score evaluates the number of cabin pressure fluctuations that occur at a frequency similar to breathing cadence. Low frequency cabin pressure fluctuations occur over the course of several breaths. The regulators can mask can re-set every breath, so low frequency cabin pressure fluctuations can be compensated for. Extremely high frequency cabin pressure fluctuations have small amplitude – there is insufficient time to change cabin pressure substantially. The cabin pressure fluctuations in the 0.2 – 0.4 Hz range can have adverse interactions with the rest of the breathing system. There are two scoring criteria for cabin pressure fluctuation: 1) portion of cabin pressure fluctuations that are in the 0.2 – 0.4 Hz frequency range (less than 0.03 is ideal), and 2) the separation between the maxima pilot breathing frequency and the maxima cabin pressure fluctuation frequency (>0.2 Hz is ideal).

Different breathing systems need different scoring criteria. PBA flew two main configurations: referred to as USN and USAF. Scoring criteria for these two systems are shown in the tables below, as an example of specific "green/yellow/red" scoring criterial. Notice that the scoring criteria demonstrates that it is significantly easier to breath in the USAF configuration.

Table 10.1. Scoring Table for USN Configuration with Positive Pressure

Diagnostic Flight Test Scoring Table: USN Configuration AFE				
		Green	Yellow	Red
1	Inhalation Hysteresis			
	Mean (lps)	<0.4	between	>0.5
	Fraction of breaths >0.5	<0.2	between	>0.4
	Fraction of breaths >0.75	<0.1	between	>0.2
	Fraction of breaths >1.0	<0.01	between	>0.03
2	Inhalation Flow			
	Fraction slightly degraded (0.1-0.2)	<.15	between	>.25
	Fraction of breaths severely degraded (>0.2)	<.02	between	>.05
3	Exhalation Hysteresis			
	Mean (mmHg)	<0.75	between	>1.5
	Fraction >1.0 mmHg	<0.1	between	>.25
4	Exhalation Flow			
	Fraction slightly degraded (0.1-0.2)	<.15	between	>.25
	Fraction severely degraded (>0.2)	<.02	between	>.05
5	Exhalation CO_2			
	Flow-thru, low CO_2 (mmHg)	>25	between	<20
	Rebreathe, high CO_2 (mmHg)	<40	between	>45
6	Inhalation O_2			
	mean PPO_2 percentage	>95%	between	<90%
7	Inhalation Phase Shift			
	Number of breaths with phase shift (>0)	<5	between	>50
	Number of breaths, phase shift (-20 to -50)	<25	between	>100
	Number of breaths, phase shift (<-50)	<5	between	>50
8	Exhalation Phase Shift			
	Number of breaths with phase shift (>0)	<5	between	>50
	Number of breaths, phase shift (-20 to -50)	<25	between	>100
	Number of breaths, phase shift (<-50)	<5	between	>50
9	Inhalation Pressure - Flow Correlation			
	Correlation score	>0.82	between	<0.72
10	Exhalation Pressure – Flow Correlation			
	Correlation score	>0.82	between	<0.72
11	Cabin Pressure Fluctuations			
	Fraction of fluctuations (0.2 – 0.4 Hz)	<0.03	between	>0.10
	Spacing between peak cabin frequency and peak breathing peak	>0.2	between	<0.1

Table 10.2. Scoring Table for USAF Configuration

Diagnostic Flight Test Scoring Table: USAF Configuration AFE				
		Green	Yellow	Red
1	Inhalation Hysteresis			
	Mean (lps)	<0.3	between	>0.4
	Fraction of breaths >0.5	<0.10	between	>0.2
	Fraction of breaths >0.75	<0.05	between	>0.1
	Fraction of breaths >1.0	<0.01	between	>0.02
2	Inhalation Flow			
	Fraction slightly degraded (0.1-0.2)	<.15	between	>.25
	Fraction of breaths severely degraded (>0.2)	<.02	between	>.05
3	Exhalation Hysteresis			
	Mean (mmHg)	<0.5	between	>1.0
	Fraction >1.0 mmHg	<0.1	between	>.25
4	Exhalation Flow			
	Fraction slightly degraded (0.1-0.2)	<.15	between	>.25
	Fraction severely degraded (>0.2)	<.02	between	>.05
5	Exhalation CO_2			
	Flow-thru, low CO_2 (mmHg)	>25	between	<20
	Rebreathe, high CO_2 (mmHg)	<40	between	>45
6	Inhalation O_2			
	mean PPO_2 (mmHg)	>200	between	<170
7	Inhalation Phase Shift			
	Number of breaths with phase shift (>0)	<5	between	>25
	Number of breaths, phase shift (-20 to -50)	<25	between	>75
	Number of breaths, phase shift (<-50)	<5	between	>25
8	Exhalation Phase Shift			
	Number of breaths with phase shift (>0)	<5	between	>25
	Number of breaths, phase shift (-20 to -50)	<25	between	>75
	Number of breaths, phase shift (<-50)	<5	between	>25
9	Inhalation Pressure - Flow Correlation			
	Correlation score	>0.90	between	<0.8
10	Exhalation Pressure – Flow Correlation			
	Correlation score	>0.84	between	<0.74
11	Cabin Pressure Fluctuations			
	Fraction of fluctuations (0.2 – 0.4 Hz)	<0.03	between	>0.10
	Spacing between peak cabin frequency and peak breathing peak	>0.2	between	<0.1

10.2.7 Issue a Summary Grade for a Flight

Each flight should have a single summary grade that is easy to interpret. The recommended scoring criteria is:

Every pilot comment noted as a minor problem:	+10 points
Every pilot comment notes as a major problem:	+20 points
Every yellow grade in the data table:	+5 points
Every red grade in the data table:	+10 points

The higher score, the more problems with the breathing system.

10.2.8 Examples of a Diagnostic Test Scoresheet

Two example scoresheets from PBA flights are shown below. Both flights have USN configuration. Flight 84 is an example with good performance. Flight 17 is an example of a flight with no pilot reports of breathing difficulty, but diagnostic scores indicate that the breathing system did not perform as well as 84.

Table 10.3. Scoring Table for PBA Flight 84

Diagnostic Flight Test Scoring Table: PBA Flight 84, USN Configuration AFE				
		Green	Yellow	Red
1	Inhalation Hysteresis			
	Mean (lps)	0.355		
	Fraction of breaths >0.5	0.111		
	Fraction of breaths >0.75	0.008		
	Fraction of breaths >1.0	0.000		
2	Inhalation Flow			
	Fraction slightly degraded (0.1-0.2)		.238	
	Fraction of breaths severely degraded (>0.2)	.011		
3	Exhalation Hysteresis			
	Mean (mmHg)	0.60		
	Fraction >1.0 mmHg	.079		
4	Exhalation Flow			
	Fraction slightly degraded (0.1-0.2)		No data	
	Fraction severely degraded (>0.2)		No data	
5	Exhalation CO_2			
	Flow-thru, low CO_2 (mmHg)	27.2		
	Rebreathe, high CO_2 (mmHg)	27.2		
6	Inhalation O_2			
	mean PPO_2 percentage	100%		
7	Inhalation Phase Shift			
	Number of breaths with phase shift (>0)		12	
	Number of breaths, phase shift (-20 to -50)		38	
	Number of breaths, phase shift (<-50)		22	
8	Exhalation Phase Shift			
	Number of breaths with phase shift (>0)	0		
	Number of breaths, phase shift (-20 to -50)	15		
	Number of breaths, phase shift (<-50)	0		
9	Inhalation Pressure - Flow Correlation			
	Correlation score	.87		
10	Exhalation Pressure – Flow Correlation			
	Correlation score	.86		
11	Cabin Pressure Fluctuations			
	Fraction of fluctuations (0.2 – 0.4 Hz)	.02		
	Spacing between peak cabin frequency and peak breathing peak	.27		

Total Breathing Problem Score: 20

Table 10.4. Scoring Table for PBA Flight 17

Diagnostic Flight Test Scoring Table: PBA Flight 17, USN Configuration AFE				
		Green	Yellow	Red
1	Inhalation Hysteresis			
	Mean (lps)			0.751
	Fraction of breaths >0.5			0.880
	Fraction of breaths >0.75			0.497
	Fraction of breaths >1.0			0.134
2	Inhalation Flow			
	Fraction slightly degraded (0.1-0.2)		.28	
	Fraction of breaths severely degraded (>0.2)		.05	
3	Exhalation Hysteresis			
	Mean (mmHg)		.755	
	Fraction >1.0 mmHg			.261
4	Exhalation Flow			
	Fraction slightly degraded (0.1-0.2)		No data	
	Fraction severely degraded (>0.2)		No data	
5	Exhalation CO_2			
	Flow-thru, low CO_2 (mmHg)	35.7		
	Rebreathe, high CO_2 (mmHg)	35.7		
6	Inhalation O_2			
	mean PPO_2 percentage	98%		
7	Inhalation Phase Shift			
	Number of breaths with phase shift (>0)	0		
	Number of breaths, phase shift (-20 to -50)		36	
	Number of breaths, phase shift (<-50)	0		
8	Exhalation Phase Shift			
	Number of breaths with phase shift (>0)		15	
	Number of breaths, phase shift (-20 to -50)		38	
	Number of breaths, phase shift (<-50)		10	
9	Inhalation Pressure - Flow Correlation			
	Correlation score	.84		
10	Exhalation Pressure – Flow Correlation			
	Correlation score	.87		
11	Cabin Pressure Fluctuations			
	Fraction of fluctuations (0.2 – 0.4 Hz)	.02		
	Spacing between peak cabin frequency and peak breathing peak	.26		

Total Breathing Problem Score: 85

10.2.9 Additional Figures to Illustrate Phase Shift and Cabin Pressure Fluctuations:

Phase shift and cabin pressure fluctuations are complex concepts. Additional figures that graphically present these concepts can help explain the concepts. Two examples of phase shift

histograms can compare the differences between nearly perfect flights and problem flights. Flight 76 provides an example of a flight that exhibits exemplary inhalation phase shift behavior. Essentially every breath has a slight negative phase shift. Flight 29 provides an example of a flight that exhibits phase shift problems. Notice the color coding of the histogram bars – with phase shift between 20 degrees and 50 degrees shown in yellow and phase shift greater than 50 degrees shown in red.

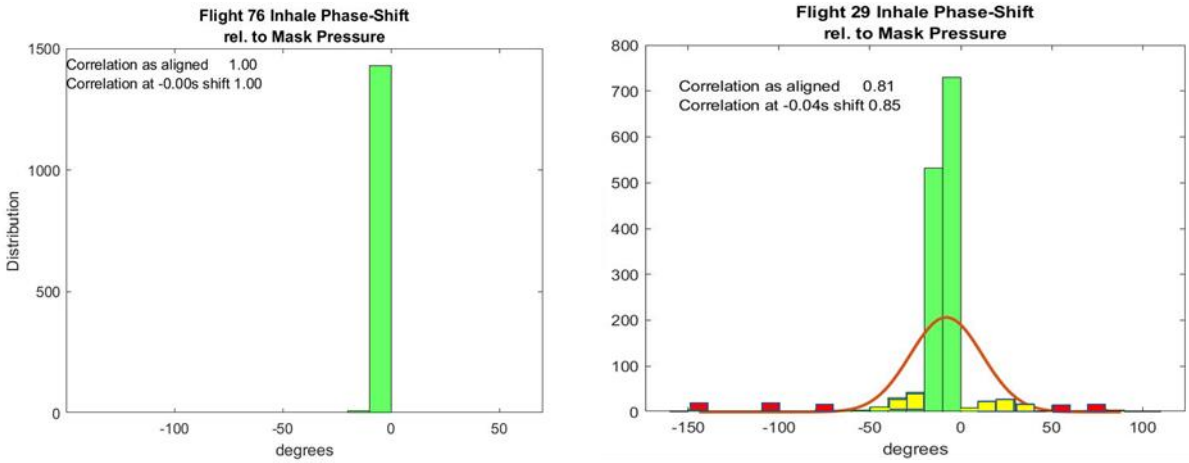

Figure 10.3. Examples of Exemplary Breathing (left) and Problem Breathing (right)

Figures 10.4 through 10.7 offer examples of pressure fluctuation frequency distributions for cabin pressure fluctuations and breathing pressure fluctuations. Seeing a series of these distribution plots can provide a context for the range of possible outcomes.

Figure 10.4 offers an example of exemplary phase shift behavior, from PBA flight 84. Notice that the vast majority of cabin pressure fluctuations had frequencies ranging between 0 and 0.07 Hz. Notice that the frequency distribution of mask pressure clusters in the 0.2 – 0.4 Hz frequency range. Notice that the primary cabin pressure fluctuation frequency is distinct, and substantially different than the primary mask pressure frequency set by breathing rates.

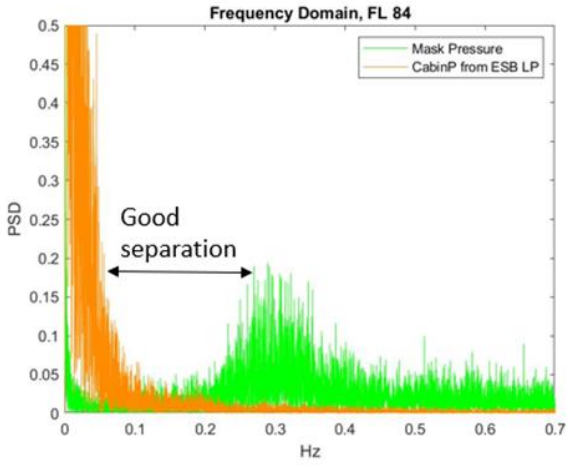

Figure 10.4. Example of Exemplary Cabin Pressure Fluctuation Performance

Figure 10.5 provides an example of a flight with substantial interference and overlap between mask pressure fluctuations caused by breathing, and cabin pressure fluctuations. Flight 29 has a

substantial overlap and interference in the 0.17 to 0.33 Hz frequency range. Note, in contrast to flight 84, how many times the pilot had to adapt and change their breathing through the course of Flight 29, as evidenced by the multitude of green frequency component peaks.

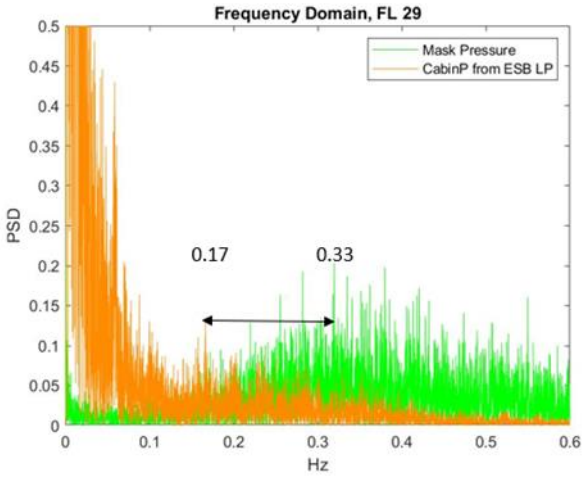

Figure 10.5. Example of Flight with Cabin Pressure Fluctuations that Can Interfere with Breathing

Figure 10.6 provides an intermediate example. Flight 102 has a significant amount of cabin pressure/mask pressure interference in the 0.2 – 0.4 Hz frequency range, but the amount of interference is not as great as flight 29.

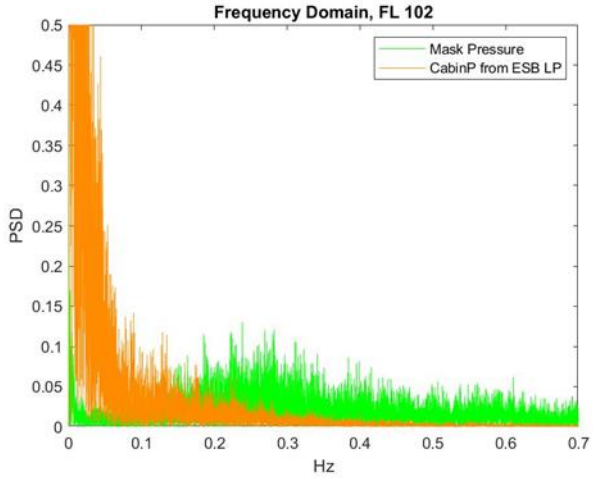

Figure 10.6. Example of Flight with Intermediate Amounts of CabinP/MaskP Interference

F.10-1*. *F-Project-1. Test methods developed and demonstrated in PBA were an effective means to quantify complex system interactions between the pilot and aircraft leading to deeper insight into problems in the aircraft Breathing Gas System (BGS).*

F.10-2*. *F-DM-1. A simple and objective scoring rubric was developed and implemented to identify faults in the components of the breathing gas system that could be applied to standardized profiles to compare aircraft.*

Technical Section 11: Almanac of Pilot Breathing

11.1 Introduction and Scope

The PBA has captured pilot in-flight baseline breathing metrics from F/A-18 (and some F-15) LOX equipped jets, set in either USN or USAF configuration. For the USN configuration, the PBA installed the CRU-103 regulator. This provides a small amount (~3 mmHg) of positive pressure, intended to aid in inhalation. On the exhale side, the pilot needs to push air past the positive pressure. The USAF configuration provides no positive pressure on the F/A-18 and is a diluter-demand system (CRU-73). The PBA finds it important to capture this body of work, as many subject matter references and system tests are based on ground (not in-flight, human-in-the-loop) tests.

Additionally, as fighter pilots execute a variety of maneuvers under different G-strains, pressures, dynamic conditions and durations, the PBA has catalogued breathing metrics (such as rate of breathing, tidal volume, minute ventilation, air supply peak pressure and flow, etc.) tied to aircraft and flight conditions. The motivation that fueled publishing this data in an Almanac form is to share it with pilots to provide an improved cockpit experience and inform decision makers and ECS engineers with a true basis of life support (supply pressure, maximum flow rate over duration, maximum range of volume used in a minute) requirements.

Suggested use of the Almanac Tables 11.2 and 11.3 includes comparison of mask breathing metrics such as driving pressure with and without positive pressure systems, as the tables are separated per USAF–like configuration (Table 11.2) with diluter demand and no safety pressure (NOSP), and USN-like configuration (Table 11.3) with 100% O_2 and safety pressure (SP). Paired with the Aircraft Parameters (Table 11.4), the tables can answer not only by how much liter-per-minute instantaneous flow rate increases in certain segments like high-G, but also how the air supply volumetric demand increases in the recovery periods provided in the Almanac, or if inverted maneuvers have any effect on air supply or breathing. It can provide information, so sorties are designed well balanced (recovery breathing built in). The Almanac provides corner-of-the-envelope metrics via the Maximum Breathing entry, in which volumetric intake increase 400% just after 3 breaths – could the system handle extended periods of such breathing? The Almanac provides as-flown metrics for to inform the next generation of breathing system requirements.

Flight profile instructions are prescribed on flight cards. These can include maneuver altitude, starting and ending velocities, and in case of PBA even breathing or talking exercises. Careful and precise descriptors on the flight card ensure repeatability of the test segment when executed by multiple pilots. The special VigilOX instrument enabled the pilots to push-button mark the start of segments of interest, which made flight segmentation easier for the analysts. PBA analysts collaborated with the pilots on defining these segments, which are described in Table 11.3.

11.2 Definitions of Flight Segments

Table 11.1. Flight Segment Definitions Encompass Wide Variety of Maneuvers In-Flight Pilot Breathing Almanac

Segment	Descriptions
Ground	On tarmac, Mask On, mostly pre-flight, sitting with gear on in the cockpit
Takeoff	From Weight-off-wheels to 2.1 kft AGL
Mil Power Ascent	Post Take-off, 5.5 kft per minute, 27 deg max pitch
Max AB Climb	12.6 kft per minute with After Burner, 47 deg pitch
Pop Pattern	Climb to Altitude, then drop 3,000 ft; pull up
Low Boom dive	14 kft dive, with the purpose of reaching > Mach 1
HighG	Criteria > 3.5 G's. Max measured 5.2 G's
PostG	Recovery, first 2-3 minutes after G breathing
40 Kft	High Altitude, low pressure, long 1 hour duration
Sonic	Criteria > 0.9 Mach, to as high as 1.3 Mach
OBOGS Descent	Long duration descent from 40 kft, > 10 minutes
Post OBOGS descent	Recovery period of 2 minutes, immediately following OBOGS descent
Combat Descent	Fast descent at 45 deg, dropping 17 kft/minute
Airline Descent	Slow descent, 11 degrees, 3 kft/minute
Flight Baseline	<1.5 G's, 500 ft ALT delta, <7 deg Pitch
Talking Script	Pilots talked in-flight with mask on, following 2x 30 second scripts
Max Breath	Scripted as 3 Max Breaths, Taken during Velocity < 300 KCAS, straight and level

11.3 In-Flight Pilot Breathing Almanac

Table 11.2. Pilot Breathing Almanac of Flight Segments Flown on Aircraft w/o Safety Pressure (NOSP) Colors represent a heat map.

Segment	Front Safety Pressure	mean BPM	mean Peak Inhale Mask Pressure	mean Peak Inhale Flow LPM	mean Peak Exhale MaskP	mean Peak Exhale Flow LPM	mean Minute Ventilation	mean Tidal Vol mean	mean of Max Gs	min Cabin Pressure mmHg	max Cabin Pressure mmHg	mean Duration min
Ground	NOSP	11	-2.30	32.12	1.90	23.96	11.76	1.12	1.00	706.80	706.90	0.94
Takeoff	NOSP	18	-6.96	66.30	3.44	49.45	16.18	0.91	2.22	657.30	717.1	1.67
Mil Power Ascent	NOSP	17	-6.11	55.73	3.67	38.57	14.06	0.83	2.30	387.00	722.70	6.01
Max AB Climb	NOSP	21	-6.79	57.58	3.88	44.36	17.54	0.84	3.17	482.30	697.2	1.84
Pop Pattern	NOSP	18	-7.00	68.12	4.56	64.42	13.38	0.8	4.43	627.2	716.8	0.77
Low Boom	NOSP	17	-5.15	43.07	2.33	29.75	18.21	1.07	3.98	431.50	572.4	0.44
HighG	NOSP	25	-6.55	51.59	3.49	46.89	15.34	0.66	4.83	531.50	578.8	0.49
PostG	NOSP	20	-8.43	70.52	4.12	59.40	19.99	1.00	2.83	551.90	586.8	1.35
40 Kft	NOSP	17	-7.50	50.69	4.37	41.22	13.34	0.82	1.71	369.80	389.9	63.94
Sonic	NOSP	18	-8.00	64.56	4.94	50.85	17.00	1.02	3.66	361.30	568.5	5.12
Combat Descent	NOSP	17	-6.39	56.80	2.95	40.83	15.43	0.93	2.72	507.70	685.3	1.67
Post Combat Desct	NOSP	18	-3.42	65.07	5.49	43.67	16.68	0.94	1.82	556.70	669.4	1.50
OBOGS Descent	NOSP	15	-5.37	51.88	3.70	49.40	11.63	0.76	1.94	345.40	656.5	10.55
Post OBOGS Descent	NOP	16	-5.92	67.90	3.54	52.08	11.95	0.74	1.38	637.30	667.80	2.00
Airline Descent	NOSP	16	-5.92	59.67	3.01	41.92	12.58	0.81	1.46	571.70	689.70	5.06
Flight Baseline	NOSP	16	-7.25	70.75	3.63	46.65	15.27	0.94	1.23	682.30	709.60	2.00
Talking Script	NOSP	17	-9.30	71.18	3.05	40.23	13.91	0.84	1.32	561.00	651.20	1.28
Max Breath	NOSP	19	-22.79	113.22	15.88	111.95	56.87	3.20	1.04	405.70	407.30	0.20

Notes for Table 11.2:

- ***a.*** *NOSP = No Safety Pressure air supply, synonymous with USAF configuration. The "front" designates front-seater pilot data*
- ***b.*** *Volume is transformed into Standard Temperature, Pressure, Dry (STPD)*
- ***c.*** *"mean" = average across segments. In "mean of mean" first the segment mean is calculated, then the average across segments. The flight matrix was designed so all PBA pilots are represented in all segments*
- ***d.*** *BPM = Breaths Per Minute*
- ***e.*** *MaskP = Inhale and Exhale mask pressure in mmHg (mm of Mercury). Steady state is at 0, negative occurs during inhalation, and positive during exhalation*
- ***f.*** *Flow = Liter per Minute (lpm) rate. This is the unit of measure provided by VigilOX, and it is the instantaneous flow rate*
- ***g.*** *Minute Ventilation = BPM x Tidal Volume (of 1 breath), expressed in Liters*

Table 11.3. Pilot Breathing Almanac of Flight Segments Flown on Aircraft with Safety Pressure (SP)

Segment	Front Safety Pressure	mean BPM	mean Peak Inhale Mask Pressure	mean Peak Inhale Flow LPM	mean Peak Exhale MaskP	mean Peak Exhale Flow LPM	mean Minute Ventilation	mean Tidal Vol mean	mean of Max Gs	min Cabin Pressure mmHg	max Cabin Pressure mmHg	mean Duration min
Ground	SP	12	-0.03	41.56	4.60	22.31	12.78	1.04	1.00	731.60	732.40	0.77
Takeoff	SP	18	-2.78	73.76	6.49	66.51	17.04	1.00	2.01	633.60	713.30	1.28
Mil Power Ascent	SP	18	-1.86	63.2	6.27	53.35	15.31	0.86	2.05	380.80	710.10	4.66
Max AB Climb	SP	21	-2.13	59.97	5.93	46.60	16.98	0.82	2.72	510.90	700.40	1.94
Pop Pattern	SP	19	-1.45	65.59	5.99	55.37	16.94	0.94	4.27	625.7	722.4	0.74
Low Boom	SP	19	-0.54	39.12	5.02	31.66	17.06	0.95	4.25	398.70	532.30	0.42
HighG	SP	24	-2.55	64.92	6.57	47.64	23.03	0.98	4.82	566.80	583.20	0.42
PostG	SP	20	-2.88	77.09	7.72	63.85	21.52	1.07	2.71	597.50	703.90	1.79
40 Kft	SP	19	-2.20	48.24	7.25	42.63	16.83	0.91	1.64	374.10	391.60	42.41
Sonic	SP	20	-2.40	60.81	6.16	46.62	15.46	0.81	3.53	358.20	557.10	7.62
Combat Descent	SP	18	-2.48	71.47	5.63	47.03	16.81	0.93	2.71	381.90	563.50	1.61
Post Combat Desct	SP	17	-4.78	62.39	4.16	42.80	15.49	0.97	2.22	560.20	697.00	1.50
OBOGS Descent	SP	16	-2.32	75.78	6.65	52.64	13.43	0.86	1.47	380.20	644.60	8.11
Post OBOGS Descent	SP	17	-2.24	73.2	5.96	44.17	14.4	0.91	1.58	644.6	671.9	1.88
Airline Descent	SP	15	-2.84	69.29	5.61	47.63	12.19	0.82	1.46	560.90	677.60	5.23
Flight Baseline	SP	18	-2.43	63.04	4.92	44.66	17.50	1.07	1.28	673.40	707.10	1.89
Talking Script	SP	18	-3.91	77.69	5.69	40.54	15.36	0.89	1.21	604.2	654.8	1.2
Max Breath	SP	15	-11.77	126.5	17.66	109.72	44.01	3.12	1.06	558.50	561.50	0.20

Notes for Table 11.3:

a. *SP = Safety (Positive) Pressure air supply, synonymous with USN configuration. Flown with CRU-103 regulator. The mode of the Positive Pressure is 3 mmHg*

b. *Volume is transformed into Standard Temperature, Pressure, Dry (STPD)*

There is great variation in air supply demand between segments, some segments doubling (e.g., High-G/Post-G) or even quadrupling (i.e., 3 Max Breaths) the air demand compared to on-the-ground baseline.

Table 11.4. Aircraft Parameters During Segments Reported in Tables 11.2 and 11.3 Define Physical Characteristics of Respective Flight Segments

Segment	mean Altitude delta kft	mean Max Velocity Knots	mean Min Velocity Kts	Mean Roll degrees	Max Roll degrees	Mean Pitch degrees	Peak Pitch degrees
Ground	0	1.06	0	1.04	1.36	-0.24	-0.63
Takeoff	2.17	477.40	0	17.80	77.31	6.64	37.24
Mil Power Ascent	27.38	682.85	180.23	9.22	164.21	9.88	25.90
Max AB Climb	25.84	619.37	327.19	9.32	178.33	20.45	47.88
Pop Pattern	-3.48	514.7	335.88	44.88	174.29	4.8	42.33
Low Boom	-14.04	736.43	461.89	65.38	179.98	-29.63	-64.1
HighG	-0.37	650.63	331.77	68.35	179.84	2.36	89.41
PostG	1.82	609.83	279.93	17.81	167.81	4.37	31.06
40 Kft	-0.06	616.93	323.86	9.41	63.66	4.61	10.18
Sonic	-1.48	797.00	514.05	14.97	179.98	3.13	-61.23
Combat Descent	-24.49	637.37	309.50	10.70	95.10	-15.04	-44.35
Post Combat Descent	3.44	516.23	244.62	12.37	179.70	6.96	34.6
OBOGS Descent	-31.89	523.85	245.41	9.52	72.82	-1.57	-10.51
Post OBOGS Descent	-0.63	349.60	137.71	10.62	66.83	4.28	10.02
Airline Descent	-15.72	491.17	296.30	7.39	75.10	-1.99	-10.65
Flight Baseline	-0.63	443.36	136.45	4.91	44.30	2.80	6.52
Talking Script	-0.38	588.03	203.58	8.8	58.62	3.23	-14.41
Max Breath	0	453.97	265.77	5.45	32.16	4.53	8.24

Notes on Table 11.4 column headers

- Mean – The PBA averaged summary statistics from segments extracted from 65 flights and 8 different profiles.
- Altitude delta kft – Reports the altitude change during the segment in thousands of feet (kft) is important because it shows the differences between certain descents (e.g., the long duration OBOGS Descent encompassed a 32,000 ft change. This was still a LOX flight as all PBA flights; it is named to mimic the long duration descent on OBOGS aircraft which crosses both pressure schedule-change regimes). Most of the high-G maneuvers were level turns. The numbers in this column also reflect the PBA philosophy of de-coupling compound effects, and exercises such as dwelling at "40 kft" (40,000 ft altitude), "Post OBOGS Descent" recovery, "Flight Baseline" normal breathing, "Talking Script" and taking 3 "Max Breaths" were all executed as close to straight and level as possible.
- Max and Min Velocity – Shows the maximum and minimum velocities in knots for each segment, to highlight how dynamic the segment is. This is especially useful for the "sonic" segment and "Low Boom" segment.
- Mean and Max Roll Degrees – These are absolute degrees as the aircraft reports +/- according to right or left roll. The Mean Roll Degrees calculates the average for the segment, then calculates the mean across all segments in the group. The mean roll gives an

idea of the body's relative orientation during the segment, while the Max Roll of 179 degrees indicates inversion.

- Mean and Peak Pitch Degrees – Here the +/- sign is indicative of ascent or descent respectively, and it delineates the differences between the different types of ascents or descents. Compound maneuvers result in a near-0 mean. For the Peak Pitch, the positive and negative maxima was calculated, and the greater of the 2 is listed. As not all PBA instrumentation included true angle-of-attack (AOA) measurements, the Roll and Pitch were contributors to the dynamic pressure studies. For example, the Combat Descent at –44 degree pitch followed by a 34-degree pull-up has triggered cabin pressure oscillations which could affect air supply.

11.4 Baseline Normal Breathing –in-flight and on the ground

The ambitious PBA flight profiles were scripted so densely, that finding an un-eventful 2 minutes of flight, with no taxing maneuver as a predecessor, was difficult. To find these rare segments to serve as baselines for in-flight breathing, the PBA analysts used the following methodology:

- 10 aircraft parameters were selected: altitude, pitch, roll, heading, power lever angle, velocity, acceleration per 3 axes, and composite acceleration (G3).
- Summary statistic was computed as the sum of normalized values for the range (max value – min value) of each parameter in the data segment.
- The 2-minute segment providing a minimum sum was designated the "quietest" period in the flight and a potential baseline candidate.
- No significant aircraft activity (such as high-G maneuvers) was allowed to have occurred in the one minute preceding the start of that segment.

Establishing a good flight baseline is important, so life support equipment decision makers can have a true basis of metrics regarding flow and volume requirements.

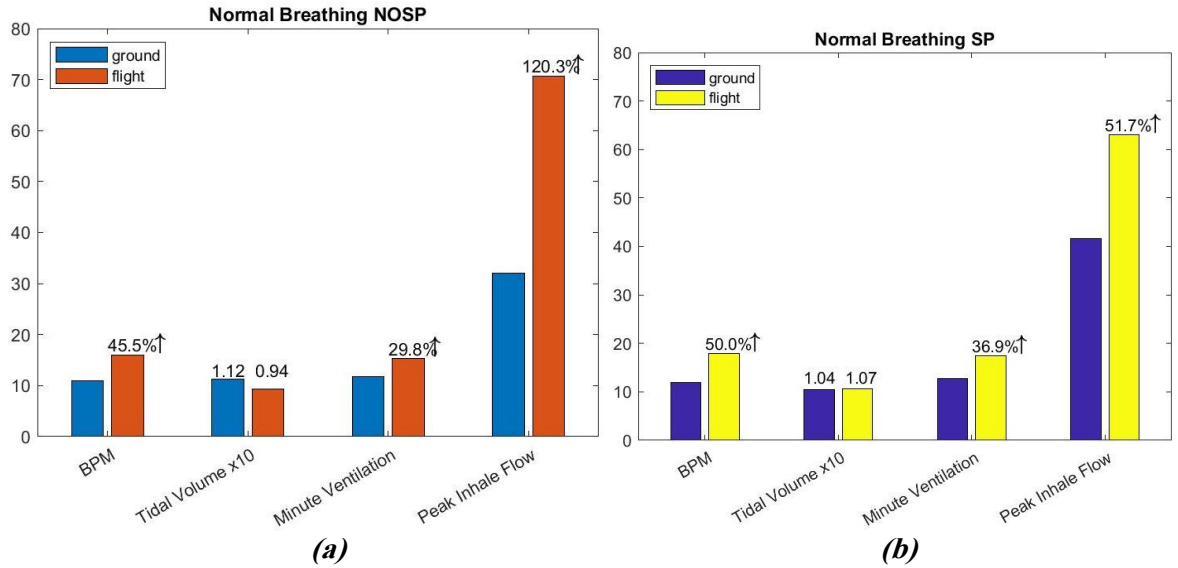

(a) *(b)*

Figure 11.1. PBA Data Show In-Flight Breathing Differs Greatly from On-Ground Breathing , (52 to 120% increase in Peak Inhale Flow Rate) (even with a mask on and sitting in the cockpit) Tidal Volume and Minute Ventilation are (L); Flow is in (lpm).

- BPM increases in flight by 45-50% compared to ground for No Safety Pressure (NOSP) and SP cases.
- Volume per Breath (TV) decreases by 16% in the NOSP configuration and increases by 3% with SP. TV values are on the order of 1 L as labeled in Figure 11.1, while for visualization purposes only Tidal Volume is plotted at 10 times its value.
- Due to higher BPM and significantly higher Peak Inhale Flow, the Minute Ventilation increases 30-37% in flight vs. ground.
- The breathing parameter with the greatest change is the Instantaneous Peak Inhalation Flow Rate in lpm with a **120% increase in flight vs. ground (NOSP).** The in-flight Peak Flow Rate is 60-70 lpm for the two configurations.

11.5 Breathing under G's versus Baseline Normal Breathing –in-flight and on the ground

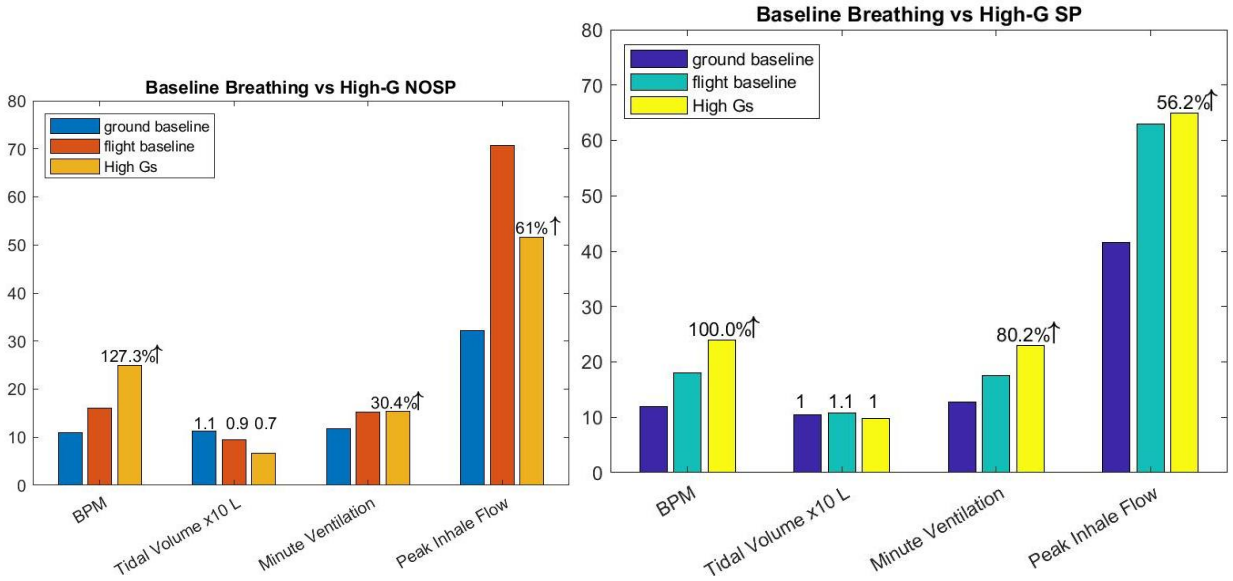

(a) ***(b)***

Figure 11.2. BPM Increase Under G's for Both Configurations
The Safety Pressure (SP) configuration (b) allows for greater peak inhalation flow, which is contributing to higher minute ventilation (compared to NOSP).

- *Percentages displayed are between High-G breathing vs Ground baseline. "High-G" for the PBA is defined as 3.5 to 5+ G's*
- *For the NOSP setup, the pilots kept the Minute Ventilation the same during G's as during baseline flight, by increasing their rate of breathing (BPM), and conditions resulting to a lower Tidal Volume (Liters per breath). The width of an inhale is narrower (shorter time) under High-G breathing.*
- *For the SP setup, the pilots increased Minute Ventilation by increasing their rate of breathing (BPM) by 100%, and they were able to increase the Peak Inhale Flow Rate as well.*

11.6 Post G Breathing Recovery

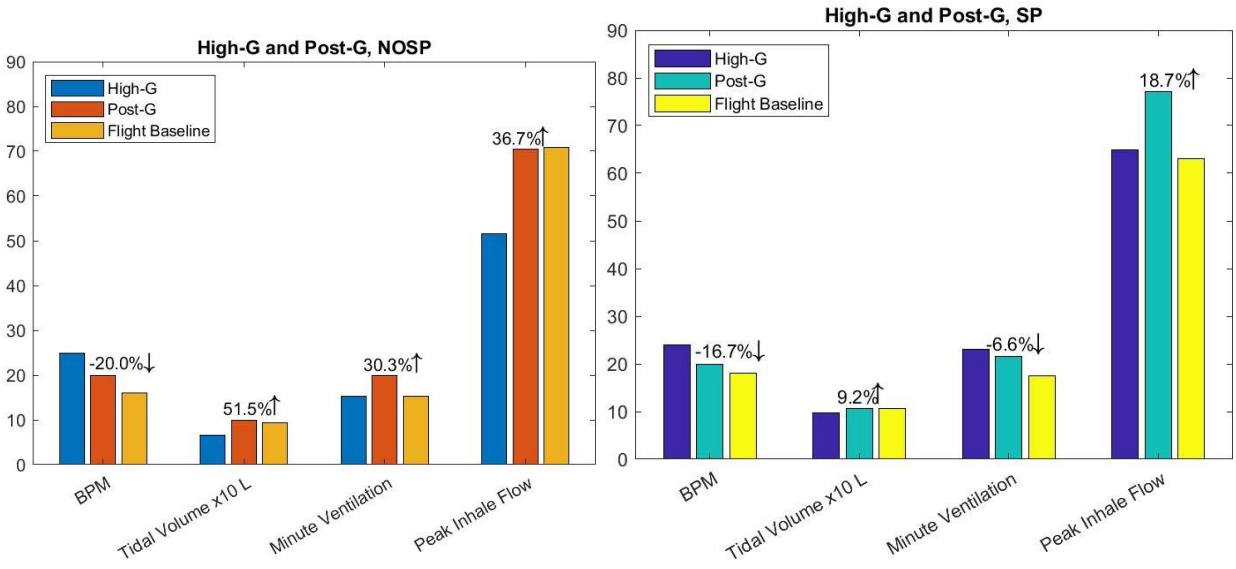

(a) ***(b)***

Figure 11.3. During Post-G Recovery BPM Reduces in Both Configurations, and Tidal Volume Increases

- *Percentages displayed are between Post-G recovery vs breathing under high G's. "High-G" for the PBA is defined as 3.5 to 5 G's*
- *As BPM reduces, inhale time increases, thus the Tidal Volume increases. This is more dramatic in the NOSP case, due to the greater increase in Peak Inhale Flow rate (compared to the G segment)*

11.7 Descents

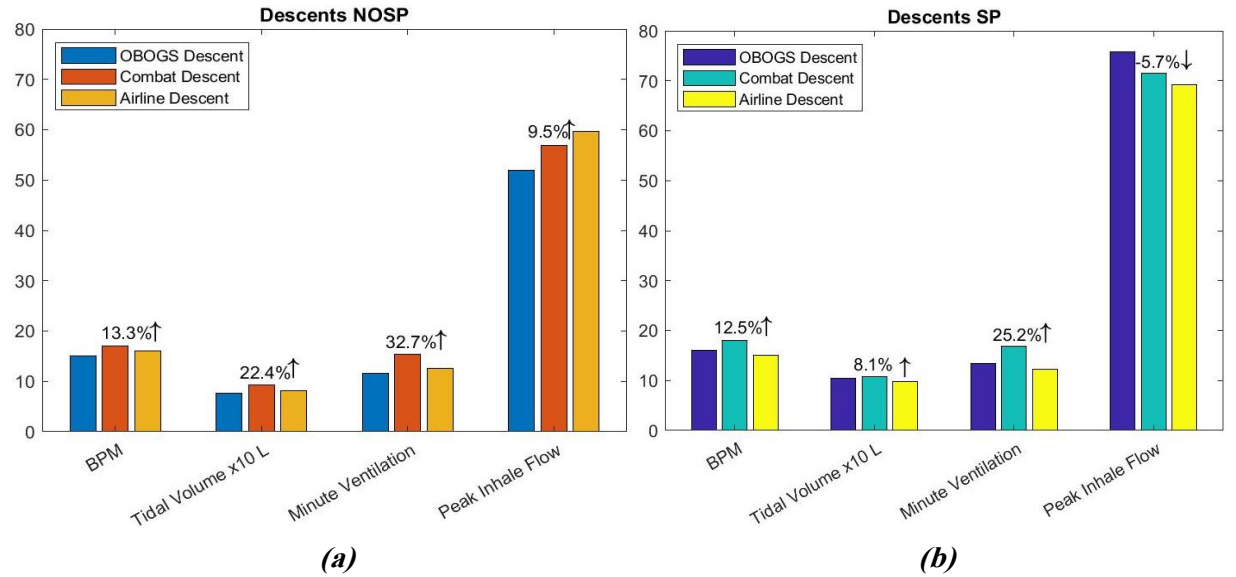

(a) ***(b)***

Figure 11.4. In all 3 Descent Types, Minute Ventilation is Similar in NOSP and SP Configuration even though Peak Inhale Flow Rates are higher in Safety Pressure (SP) flights than NOSP

- *Percentages displayed are between Combat Descent vs OBOGS descent. "OBOGS" descent comes from testing an OBOGS system by crossing the pressure schedule change zones (in and out of Isobaric region). The PBA flew LOX supplied jets, but to study the effects of pressure zones, the OBOGS descent Altitude delta was 32 kft*

Continuing with Descents, Combat Descents having a steep downward pitch angle of –44 degrees were the most problematic for cabin pressure regulation, as PBA data often shows cabin pressure oscillation commencing and not resolving at times for a minute. The PBA team was interested not just in the dynamic events, but also in the post-event follow-on, or recovery breathing. In the case of Combat Descent, the complexity of environmental changes continues into the recovery, as a steep downward nose is followed by a +30 degree pull up, so there are lots of changes the pressure breathing system needs to keep adjusting to. The sudden and constant reference pressure change leads to pressure-flow mismatch in this section, as seen in Tables 11.5 and 11.6. The heat map colors are imported from Tables 11.2 and 11.3.

Table 11.5. Mismatch Of Colors (circled) Shows Pressure-Flow Disharmony During Post Combat Descent, SP
Here a low pressure-draw (green) results in medium-high flow (light red)

Segment	Front Safety Pressure	mean BPM	mean Peak Inhale Mask Pressure	mean Peak Inhale Flow LPM	mean Peak Exhale MaskP	mean Peak Exhale Flow LPM	mean Minute Ventilation	mean Tidal Vol mean
Combat Descent	NOSP	17	-6.39	56.80	2.95	40.83	15.43	0.93
Post Combat Descent	NOSP	18	-3.42	65.07	5.49	43.67	16.68	0.94

Table 11.6. Shows Unexpected Pressure-Flow Relationship During Post Combat Descent, SP
A large pressure draw returns a lower than expected flow rate.

Segment	Front Safety Pressure	mean BPM	mean Peak Inhale Mask Pressure	mean Peak Inhale Flow LPM	mean Peak Exhale MaskP	mean Peak Exhale Flow LPM	mean Minute Ventilation	mean Tidal Vol mean
Combat Descent	SP	18	-2.48	71.47	5.63	47.03	16.81	0.93
Post Combat Descent	SP	17	-4.78	62.39	4.16	42.80	15.49	0.97

Flow is dependent on pressure change. As mask pressure (absolute) magnitude changes, so should Peak Flow rate. In Table 11.5 (no safety pressure), there is disharmony in Post Combat Descent: the pilots exert less effort (do not draw down as much, i.e., -3.42 mmHg), but reach higher Peak Inhale Flow.

In the Safety Pressure setup, Table 11.6, there is also disharmony. There is pressure draw from +3 to -4.78 mmHg, a large change of almost 8 mmHg, yet the Peak Inhale Flow is less, when compared to the No-Safety Pressure group. Data from this segment suggests that the inhalation is easier without safety pressure and the exhalation is easier with Safety Pressure, which is the reverse of observations made from other segments in general.

11.8 Maximum Metrics

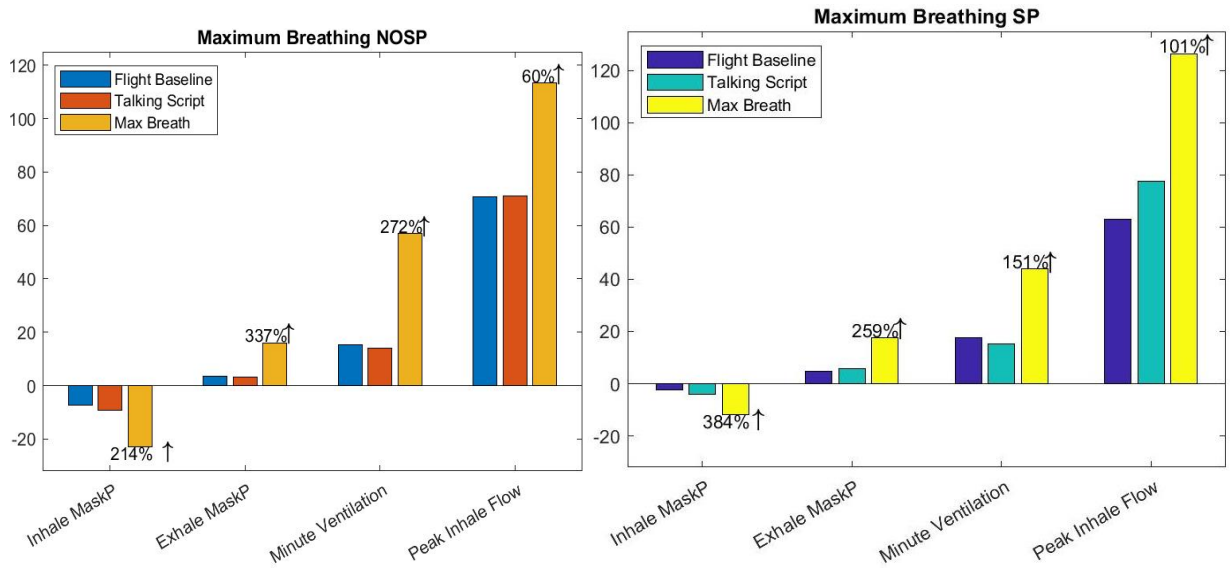

(a) ***(b)***

Figure 11.5. Shows Pilots' Baseline only uses 20 to 30% of Maximum Pressure Draw They are Able to Exert
Note: percentages shown are for Max breathing compared to baseline.

Takeaways:

1. Even though Inhale Pressure during Max Breathing increases by 214% and 384% in both configurations, the resultant Peak Inhale Flow only increase 60% to 101%. It is important to observe that after a threshold, one gets diminished return, no matter how hard one tries to draw an inhale.
2. Exhale Mask Pressure during Max Breathing is able to increase far greater with No Positive Pressure. Inhale on the other hand is enabled to increase more when executed with a Positive Pressure system.
3. Talking with a mask, and specifically exhaling, has been reported as more difficult to push through the positive pressure
4. Individual differences will have an amplified effect, especially during Max breathing

F.11-1. Segmentation allows comparisons of like segments from different profile flights, and can help identify an outlier or unexpected behavior, which otherwise would be washed out if looking at the entire flight. The Almanac provided in Section 11 provides a good baseline for breathing on F/A-18 legacy aircraft with LOX air supply, under different regulator configurations.

Technical Section 12: Oxygen Transport Model (OTM)

12.1 OTM in 2017

This section re-introduces the OTM that was first presented in the F/A-18 NESC Independent Assessment Final Report, and then updates the OTM, to emphasize additional in-flight data obtained by PBA, and the additional understanding of pilot breathing system interactions. This newfound understanding of pilot breathing system interactions is a direct result of PBA in-flight measurements. The OTM was drafted in 2017 for the NESC Independent Assessment of PEs affecting USN pilots flying F/A-18 aircraft. Figure 12.1 shows the OTM as it was in the 2017 final report.

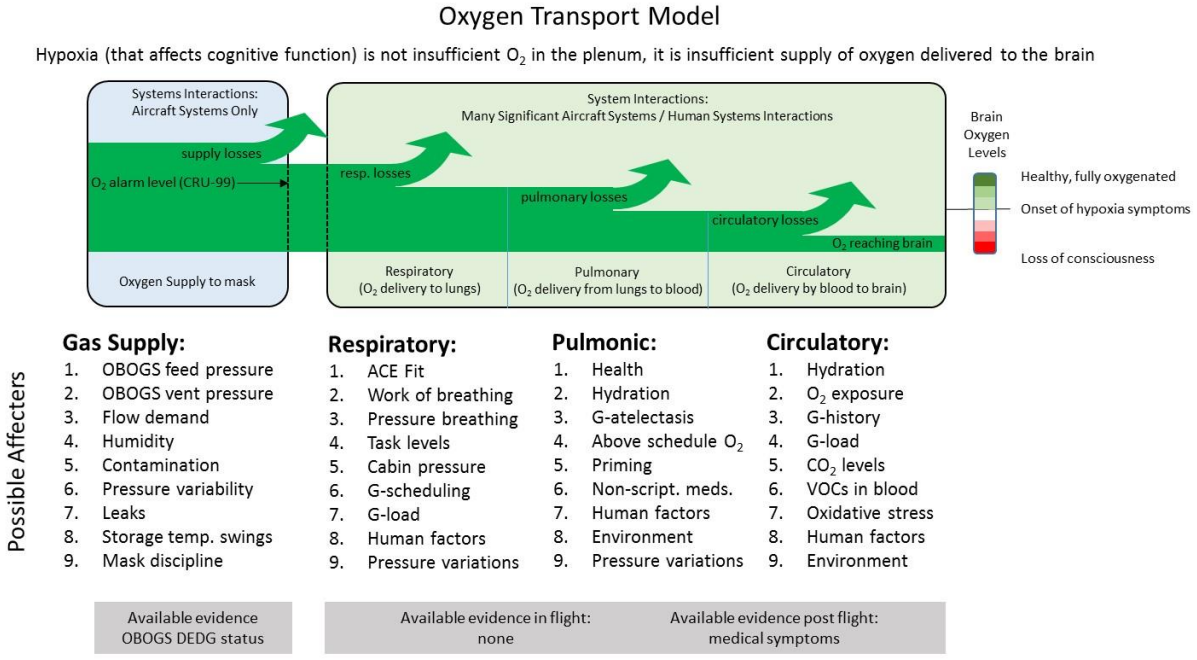

Figure 12.1. OTM in 2017 F/A-18 Final Report

The OTM attempts to graphically illustrate several different concepts in a single graphic. These concepts included:

- O_2 travels through a pilot breathing system that transports O_2 from a supply line to the tissues in the pilot's brain.
- The pilot breathing system is complex and contains many different elements.
- In-flight data about the performance of these elements is extremely limited.
- For many PE events, data about O_2 transport through the pilot breathing system was limited to status records of the jet's onboard 'OBOGS degrade' sensor, and medical diagnostics collected by a physician after the PE incident.
- There are a multitude of possible factors that could contribute to a PE, but without in-flight data of pilot breathing, it is difficult to identify which contributing factors are most significant.

The number one recommendation listed in the 2017 F/A-18 final report was to collect pilot breathing measurements in a flight environment. The most significant aspect of the 2017 OTM was a listing of available data – and a listing of missing data. Figure 12.2 repeats the 2017 OTM,

with the graphical displays describing available information (and missing information) highlighted in red.

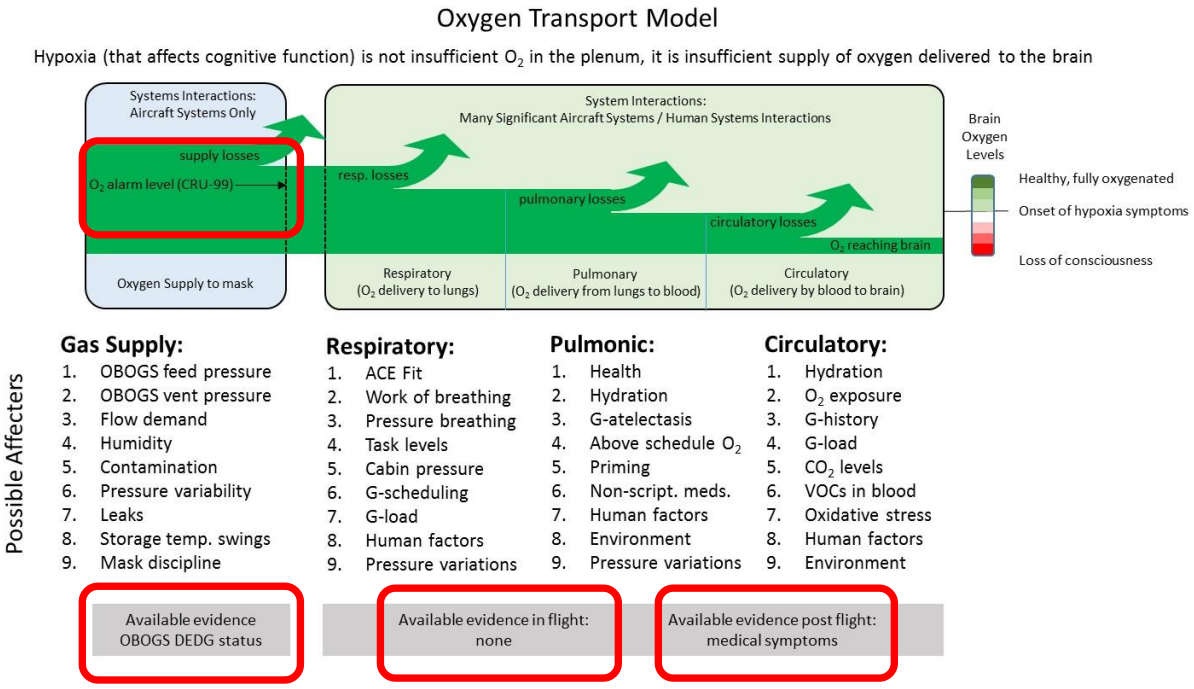

Figure 12.2. 2017 OTM with Notes About Available Data Outlined with Red Boxes

12.2 OTM in 2018

The OTM was used to describe the purpose, intent, and structure of the PBA, when the PBA was initially proposed. When the PBA was first proposed to the NESC, lack of flight data about pilot breathing was stressed. Additionally, the importance of understanding system interactions within the pilot breathing system was also stressed. Figure 12.3 describes the key concepts of O_2 transport as they were understood in 2018, when PBA was proposed, approved, and initiated. Figure 12.3 graphically describes the level of understanding of how a pilot breathing system performs in flight, and data collection goals for PBA:

- Recognize that O_2 transport is carried out by a pilot breathing system.
- Recognize that the pilot breathing system is complex and has many complex system interactions.
- Recognize that in 2018, the pilot breathing system needed to be treated as a "black box" system, with no in-flight data about the internal workings of the system.
- PBA goals are to collect the best possible data about aircraft, pilot, and systems at the aircraft-pilot interface, and to identify and evaluate the system interactions that occur inside the "black box".

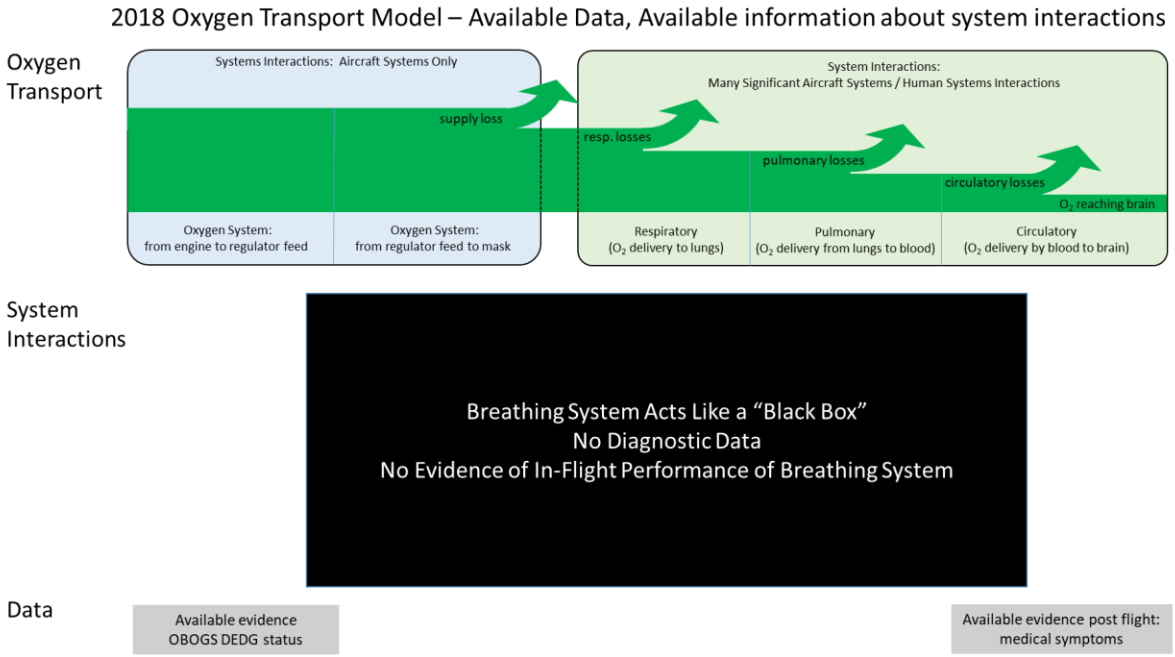

Figure 12.3. Key Concepts in OTM as They Were Understood in 2018

12.3 OTM in 2020

The PBA successfully collected pilot breathing data in-flight. As much as practically possible, evidence about operational performance was collected for every element in the pilot breathing system. In 2020, a more accurate graphical representation of the pilot breathing system would contain three elements (not two as it was in 2017). One section involves aircraft and aviation elements, one section involves elements at the aircraft-pilot interface, and one section involves the pilot and the pilot's physiological systems. Data about the in-flight performance of the aircraft/aviation part of the pilot breathing system is limited but compared to the other two sections – this part of the system has the most available data. PBA provided new quantitative data about pilot breathing, and human-machine system interactions. Pilot breathing occurs at the interface of the aircraft and human parts of the system. Pilot breathing is affected by the aircraft parts of the system, and by the human parts of the system.

The 2017 version of the OTM had a large list of possible contributing factors to PEs. There was insufficient data to assess which of these many factors are the most significant. PBA has developed quantitative measurement techniques to measure timing and sequence in-flight. PBA discovered that system interactions disrupt the timing and sequence of breathing, and data suggest this disruption is significant. Figure 12.4 updates the earlier OTM graphic to emphasize three key things:

The pilot breathing system has three specific sections. One involving aircraft/aviation systems, one section at the aircraft-pilot interface (performance is affected by both the aircraft and the human parts of the system) and one involving the pilot and human physiology.

- System interactions involving timing and sequence of the pilot breathing system are especially significant.
- In 2020, there are quantitative measurements of timing and sequence. These measurements were not available in 2017.

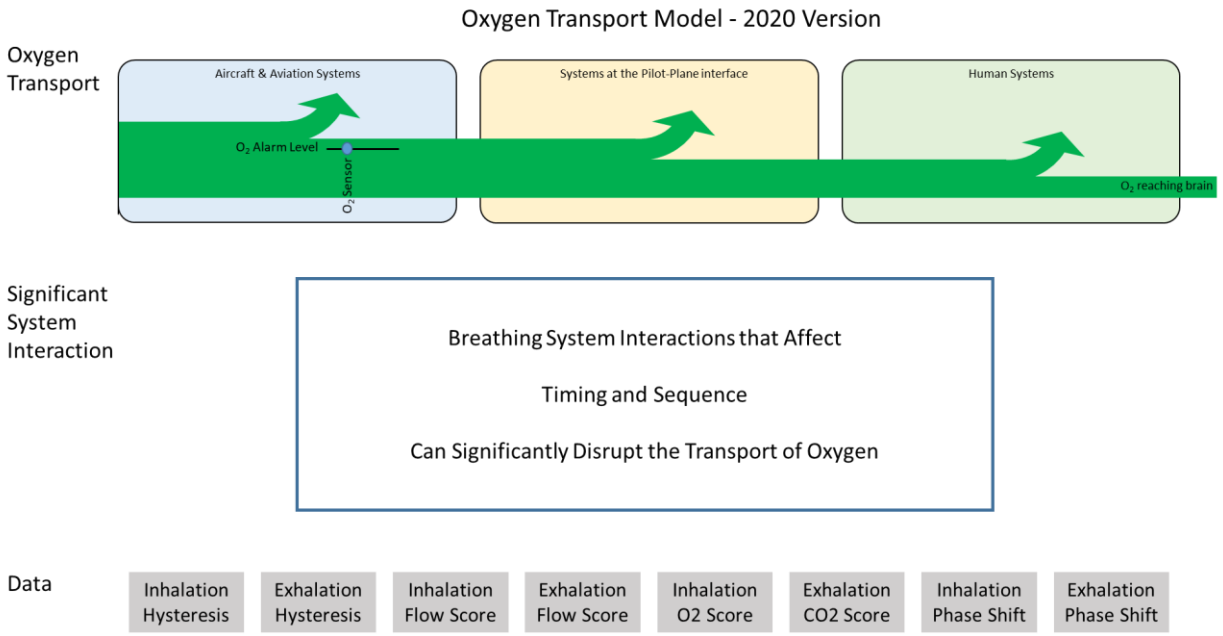

Figure 12.4. Key Concepts of OTM as They Are Understood in 2020

Figure 12.4 provides a general description of the key concepts of O_2 transport and identifies timing and sequence as a general class of system interaction. PBA has identified three system interactions that have occurred simultaneously:

1. Hysteresis causing symptoms of inadequate air supply
2. Safety pressure component delays
3. Cabin pressure surges triggering exhalation disharmony

Figure 12.5 provides a graphical description of a system interaction between regulator timing, and pilot breathing. When regulators deliver air with a timing and sequence that is unexpected, pilots change their breathing patterns to adapt. It the mismatch between the timing and effort of breathing and the timing and quantity of realized inhalation air is too great, the pilot becomes aware of this mismatch. The pilot is interacting with the mechanical elements of the breathing system and affecting timing and sequence – the mechanical elements of the breathing system are affecting the breathing profile of the pilot – the timing of the mechanical elements is not matched with the timing of pilot breathing, and the pilot is aware of the disharmony.

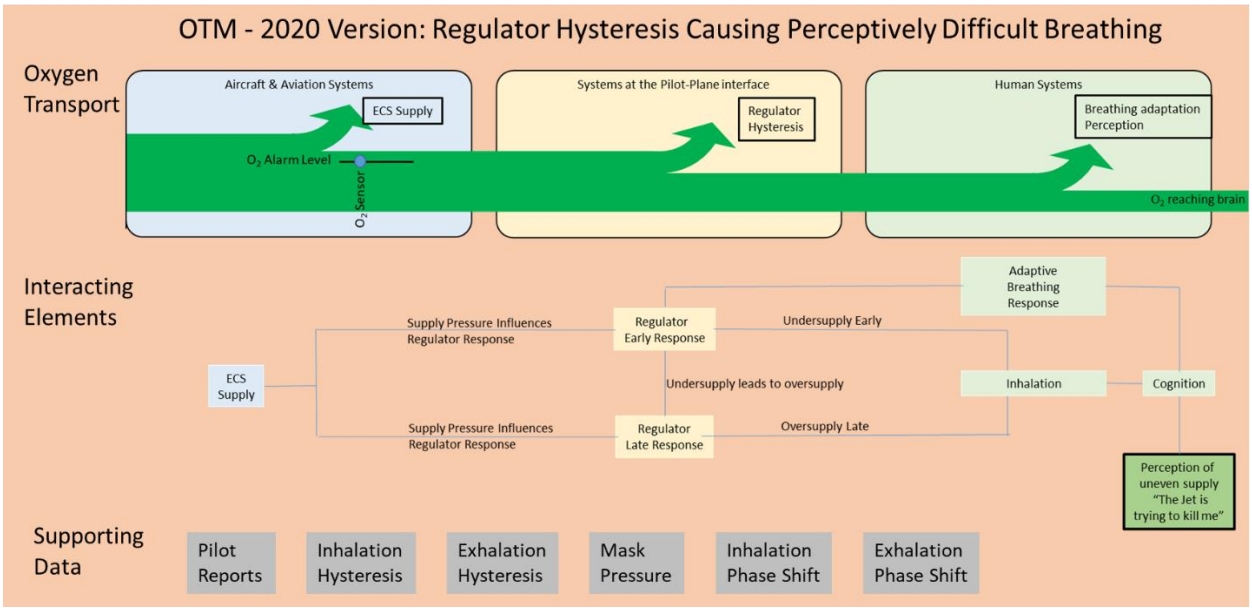

Figure 12.5. Graphical Description of System Interactions Involving Unexpected Regulator Timing and Pilot Breathing Adaptations

The most significant data about this system interaction comes from pilot reports. Pilot interviews would document a phenomenon where the pilot would be trying to take a regular breath, but early in the inhalation the pilot would get no air. Later in the breath, the system would overcompensate and, in the words of one pilot, "shove air down my throat." Pilots flying many different types of aircraft would make similar reports, but F-35 pilots would report this situation most frequently. One pilot described the situation with the words, "the jet is trying to kill me." Note that disharmony between the pilot and the mechanical elements of the breathing are perceived by the pilot. Humans are constantly changing their breathing patterns to receive the necessary amount of inhalation for the minimum physical effort. Usually, a person is not aware that their breathing patterns, but if the mismatch between effort and received air is great enough – the person becomes cognitively aware of the mismatch. Human factors subject matter experts stress the importance of eliminating cognitive distractions, so pilots can focus on piloting.

Pilot reports of shortness of breath or other symptoms can be attributed breathing system hysteresis – receiving too little inhalation air early in the breath and too much air late in the inhalation – were not previously linked to timing and sequence problems. PBA has supplied quantitative measures of breathing that place pilot reports in the context of specific and measurable system interactions. PBA measurements of inhalation hysteresis, exhalation hysteresis, mask pressure, inhalation phase shift, and exhalation phase shift has documented the phenomena, and helped identify specific causal mechanisms. Regulators can be tuned to produce a tolerable and repeatable system response to pilot breathing demands. The pilot inhales, line pressure drops, there is a delay in the supply of air early in the inhalation event, but the regulator is tuned to slightly oversupply later in the breath. The pilot learns to adjust. If there is a change in the system; such as a change in the line supply pressure, the tuning (i.e., regulator response rate) changes. If the difference in response time is sufficient to be perceptible to the pilot – a symptom of inadequate breathing or struggling to breathe results.

The combination of pilot reports and hysteresis and phase shift measurements documents this system interaction. PBA measurements have validated that this system interaction occurs, and it has developed a quantitative measurement so the severity of this interaction can be quantitatively measured.

The second breathing system interaction related to timing and sequence is graphically described in Figure 12.6.

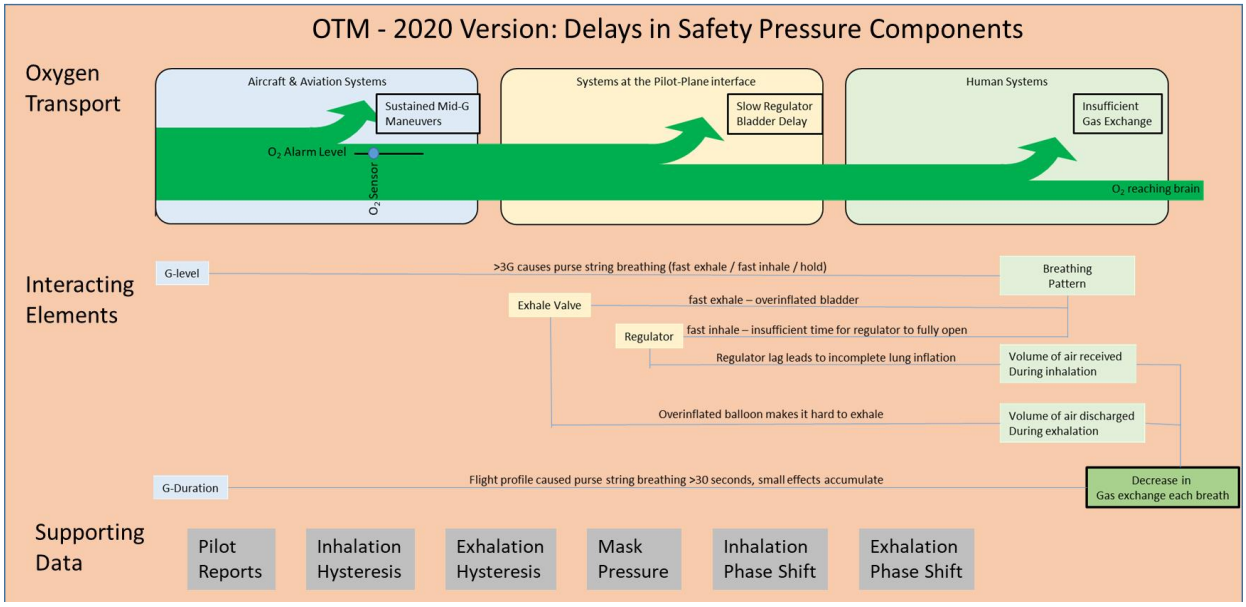

Figure 12.6. Graphical Description of Delays in Safety Pressure Components

This mechanism was described in detail, in the 2019 presentation describing Flight 29. Breathing systems that maintain safety pressure, have an additional set of components that require timing, sequence, and coordination with the rest of the breathing system. Flight 29 measurements document a condition where large, abrupt, breathing patterns associated with anti-G straining maneuver (sometimes referred to as purse string breathing) causes sudden changes in the breathing cadence. Pressure compensation in the exhalation valve is delayed, because it takes time to transfer air through the small pressure compensation tube to inflate the pneumatic bladder in the exhalation valve. The pressure compensation changes are delayed relative to the pilot breathing cadence. The demand regulator response is also delayed. The combination of delays in regulator flow and delays in exhalation valve response creates a condition where the volume of gas exchange decreases with each subsequent breath.

This timing/sequence system interaction has been documented by PBA and can be quantitatively assessed using measurements that include spirometry, inhalation hysteresis, exhalation hysteresis, inhalation flow score, exhalation flow score, inhalation phase shift and exhalation phase shift. The exhalation phase shift score is an especially helpful diagnostic parameter for recognizing this system interaction.

The third breathing system interaction that relates to timing and sequence is graphically shown in Figure 12.7. Cabin pressure fluctuations can trigger timing and sequence disharmony.

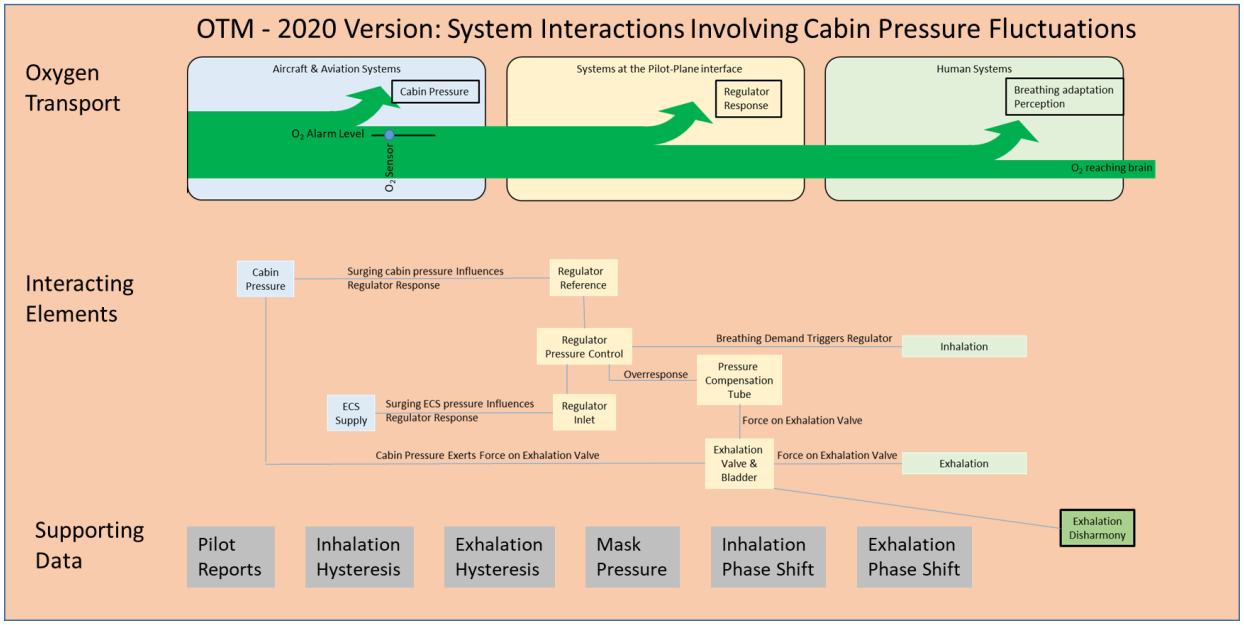

Figure 12.7. System Interactions Involving Cabin Pressure Fluctuations

Cabin pressure fluctuations can trigger timing and sequence disharmony in breathing systems. The cabin pressure fluctuations have a direct effect on regulator timing, because the regulator including the exhalation valve, is referenced to cabin pressure. Pilots adjust their inhalation and exhalation, to try to adapt to the changes in the breathing system. Many times, these adjustments are made subconsciously – in conditions of severe disharmony, pilots become aware of their breathing and aware of their changes in breathing. These adaptations can result in changes in exhalation volume, exhalation pressure profile, and the volume of subsequent breaths.

System interactions involving cabin pressure fluctuations have been documented by PBA. PBA has developed a set of quantitative measurements of the timing and sequence disharmony. Measurements of mask pressure, cabin pressure, inhalation hysteresis, exhalation hysteresis, exhalation flow score, inhalation phase shift and exhalation phase shift can quantify the extent of the system interactions.

Cabin pressure fluctuations should be emphasized, and described in greater detail for several reasons:

- In 2017, cabin pressure fluctuations were evaluated only for their possible impact on severe barotrauma and decompression sickness. Small magnitude pressure fluctuations (those of 10 mmHg or less) were discounted because fluctuations of this magnitude cannot result in severe barotrauma or DCS. In 2020, with recognition of cabin pressure fluctuation impact on breathing system sequence – cabin pressure fluctuations take on greater significance.
- It has been observed that some jet's capability to maintain consistent cabin pressure degrades with age resulting in increased cabin pressure fluctuations. These small fluctuations timed correctly can lead to BSD. A diagnostic test of the breathing system could have identified the cabin pressure fluctuations earlier, before they became severe.
- At least one pilot has been chronically injured and permanently grounded because of a severe e PE. Evidence suggests that cabin pressure fluctuations were involved (described in greater detail in Appendix 7).

The specific effect of cabin pressure fluctuation on pilot breathing is graphically described in Figure 12.8.

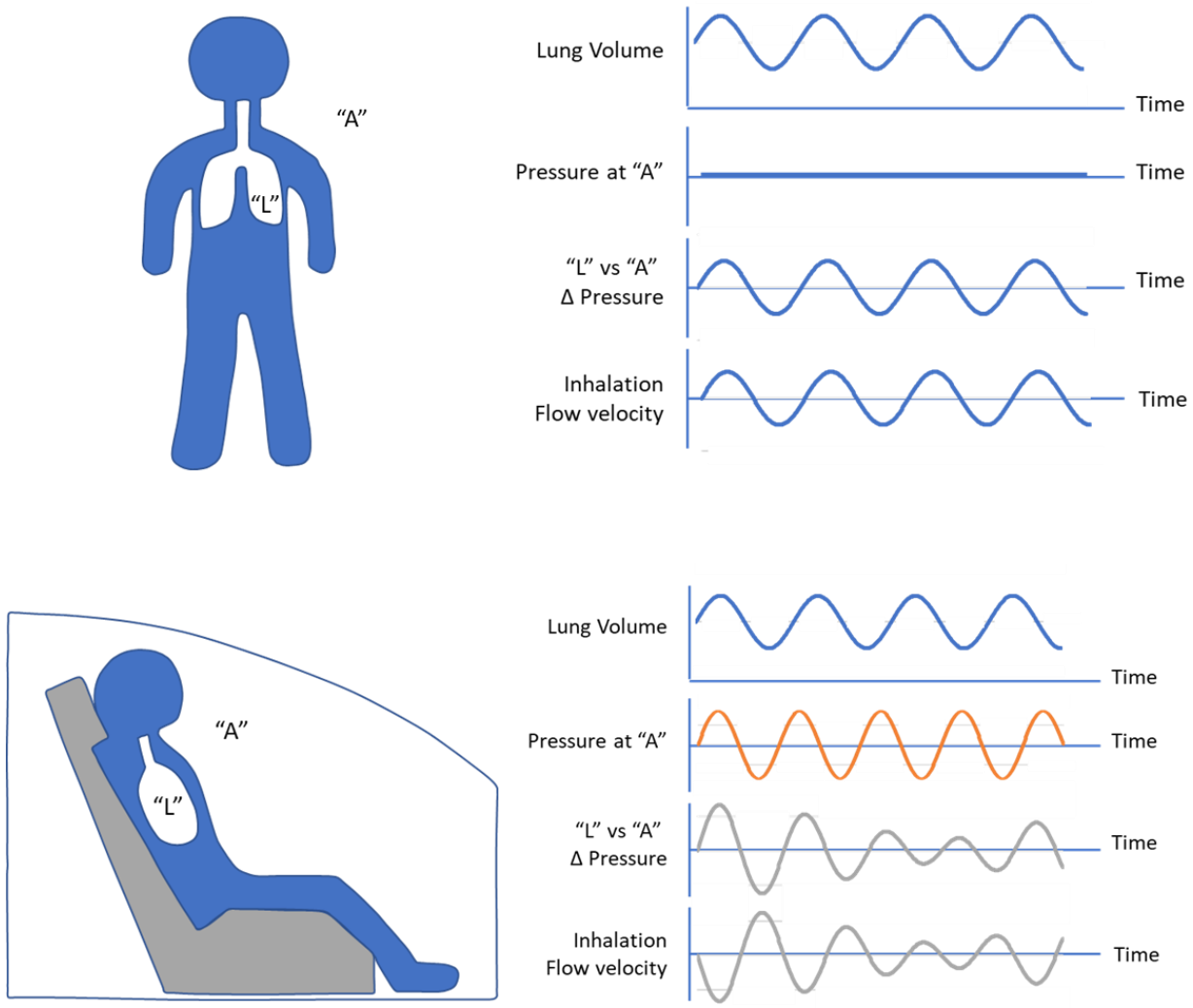

Figure 12.8. Effects of External Environmental Pressure on Breathing

Figure 12.8 illustrates the effects of external environmental pressure on breathing. In the example at the top of the figure, a person in a nominal external environment is breathing regularly. The person moves the diaphragm and intercostal muscles to expand the chest cavity – which increases lung volume – which decreases lung pressure. Then the person relaxes and contracts their diaphragm and intercostal muscles which contract the chest cavity – which decreases lung volume – which increases lung pressure. In this example, the external environment maintains a constant pressure. Diaphragm muscles cause lung volume changes, which is directly related to lung pressure changes, which is directly related to the different in pressure between lung pressure at "L" and atmosphere pressure at "A". Air flow related to inhalation and exhalation is directly controlled by the difference in pressure between "L" and "A". There is a direct connection between muscle work and breathing - the relationship between muscle movement and inhalation flow is direct and predictable. Note that for nominal breathing, the magnitude of these pressure changes is small – lung pressure variations of 2-4 mmHg drive nominal breathing.

The example at the bottom of Figure 12.8 describes pilot breathing in a jet with cabin pressure fluctuations. In this example, the magnitude of the lung pressure fluctuations are 2-4 mmHg, and the frequency of the fluctuations is 20 BPM. Cabin pressure fluctuations have similar magnitude and similar frequency. PBA data indicate that cabin pressure fluctuations on the order of 2-4 mmHg, at a frequency of 15-30 pressure fluctuations per minute are relatively common. The pilot moves the diaphragm and intercostal muscles in a smooth, regular fashion, creating a smooth regular expansion/contraction pattern of chest cavity and lung volume. The delta pressure between lung "L" and atmosphere "A" follows a much more complex trend. The two pressure profiles combine additively, sometimes increasing in magnitude, and sometimes cancelling out. Inhalation flow and exhalation flow are driven by the delta pressure between "L" and "A". In this example, the pilot makes smooth, regular muscle movement and increases/decreases lung volume in a smooth regular way, but the resulting inhalation flow and exhalation flow results in three breaths with progressively decreased volume. PBA has recorded pressure and flow measurements that have followed this pattern. Pilots move their muscles in accordance with smooth and regular breathing – but receive chaotic and irregular inhalation and exhalation flows. The disconnect between the timing of pilot muscle movement and resultant airflow is an example of a BSD.

Figure 12.9 repeats this example – in simplified form – to emphasize and stress the significance of this system interaction.

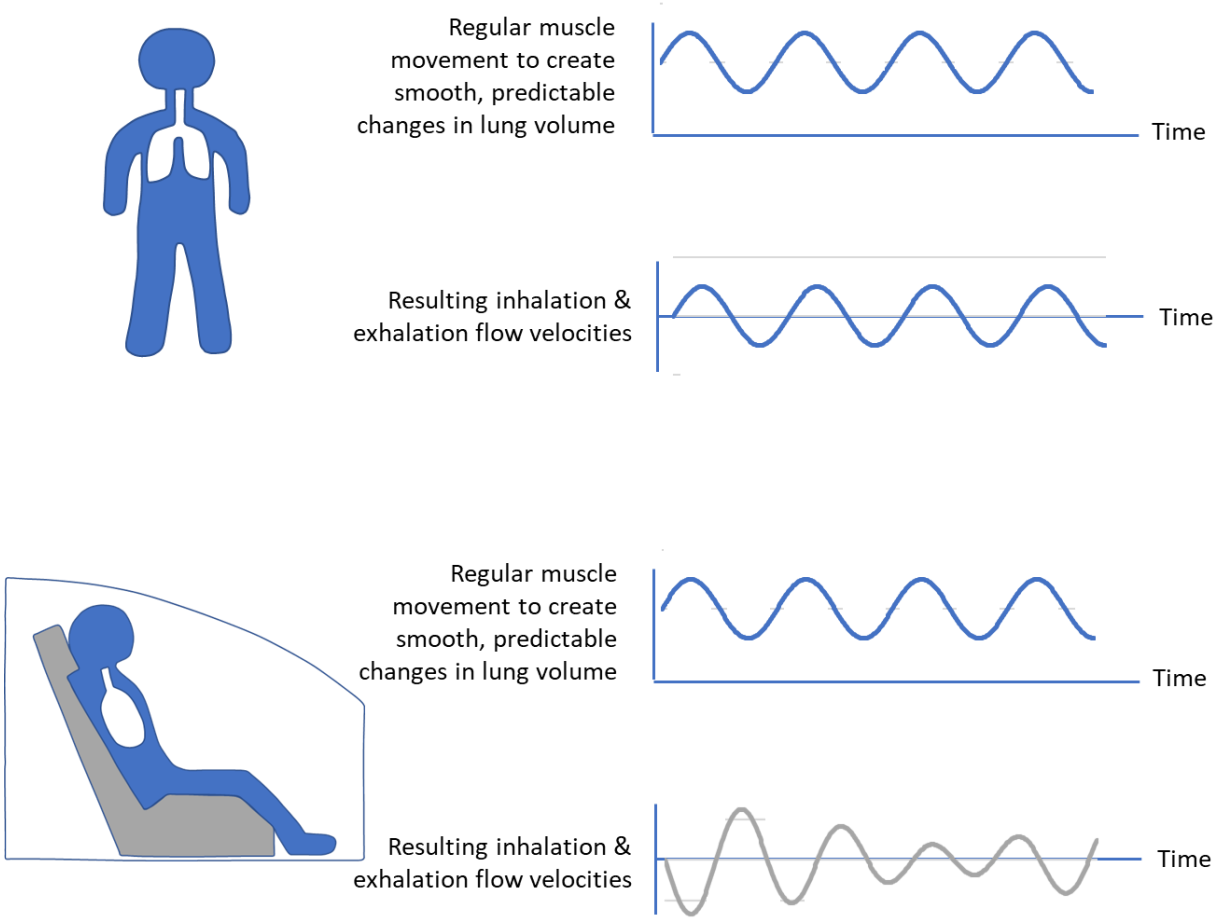

Figure 12.9. Comparison of Muscle Movement and Resulting Inhalation/Exhalation Flow Velocities

The 2017 OTM stressed what was not known; there was very little data about pilot breathing in-flight, so the pilot breathing system had to be treated as a black box.

The 2020 OTM stresses the importance of breathing system interactions related to timing and sequence – and the measurement tools to quantify timing and sequence problems.

12.4 A Chronology of Available Evidence, Consensus Opinions about Causes of PEs, and the Impact of the OTM and BSDs on the Evaluation of Available Evidence

Disclaimer: This section includes a simplified list of available evidence, and a simplified assessment of consensus opinions about the causes of PEs. These simplifications are made for reasons of clarity.

2009 – F-22 Pilot Reports Suggest Hypoxia

The NASA NESC F-22 team was formed in 2012 and was briefed by USAF and Boeing SMEs. These briefings described early investigations about PEs affecting F-22 pilots and described a process that initially focused on O_2 supply systems. Medical diagnostics suggested hypoxia – the most likely cause of hypoxia was attributed to low levels of O_2 in the pilot breathing gas – caused by an intermittent (but otherwise undescribed) problem with the OBOGS. Diagnostic efforts were focused on the OBOGS. In 2009, PE investigations were not structured as a comprehensive Root Cause Corrective Action (RCCA) process. PE investigations were targeted troubleshooting efforts that focused on OBOGS hardware.

2009 F-22 Pilot Reports

Consensus opinion about the probable cause of PEs	probably hypoxia, probably OBOGs related
Available evidence	pilot reports
Recognition of OTM	none
Recognition of BSD	none

2010 – No Clear Signs of Problems with F-22 OBOGS

The performance and reliability of the F-22 OBOGS was carefully reviewed as part of 2010 troubleshooting efforts. The OBOGS was evaluated and tested as an isolated piece of equipment, not as a component in a complex system with many system interactions. The performance of the OBOGS was solid – the OBOGS was meeting performance specifications, and there was no indication of latent defect or component failure. The F-22 OBOGS was working as specified.

2010 No Clear Problems with F-22 OBOGs

Consensus opinion about the probable cause of PEs	OBOGs working nominally Perhaps there is contamination
Available evidence	OBOGs test data (lab data)
Recognition of OTM	none
Recognition of BSD	none

2011 – No Clear Signs of Contamination in F-22

The USAF conducted an extensive test campaign to search for chemical contamination. The OBOGS was subjected to contaminant challenge tests. Chemical measurements throughout the Environmental Control System (ECS) were made, both in-flight and post-flight. There was no clear indication that pilots were exposed to toxicologically significant levels of chemical contamination – not nearly enough to match reported symptoms. There were a few isolated cases of chemical contamination, but as a rule, these isolated cases also had clear signs of a mechanical failure. Note, it is hard to prove the absence of something – there was many chemical measurements made – taken as a whole there was compelling evidence that widespread chemical contamination was not occurring – but it is hard to use this data to prove that chemical contamination did not occur on a flight where no measurements were taken.

2011 No Clear Signs of F-22 Contamination

Consensus opinion about the probable cause of PEs	We don't know Perhaps many smaller factors
Available evidence	Lots of chemical measurements
Recognition of OTM	none
Recognition of BSD	none

2012 – C2A1 Filter was Added - then PE rates Increased

In 2012, the F-22 configuration was changed to install the C2A1 chemical protection filter on all flights. The intent of the filter was to protect the pilots from chemical contamination. When the C2A1 filters were in use, the rates of reported PEs increased substantially, and pilots reported difficulty breathing. C2A1 filters were removed and rates of reported PEs dropped.

2012 C2A1 Filter added and PE rates increased

Consensus opinion about the probable cause of PEs	We don't know No consensus opinion
Available evidence	PEs increase when C2A1 installed PEs decrease when C2A1 removed Pilots report difficulty breathing
Recognition of OTM	none
Recognition of BSD	none

2012 – UPG Valve Inflates Vest During Inhalation

In 2012, centrifuge tests of the F-22 pilot breathing system were conducted. These were new tests; a complete breathing system had not been tested in a centrifuge environment before. The tests involved an OBOGS, Breathing Regulator/Anti-G (BRAG) regulator, a pilot wearing a complete set of AFE gear, including a UPG with a UPG valve. Tests were conducted under different G-loads. The UPG valve actuated with a sequence directly opposite the pilot inhalation/exhalation sequence. At the beginning of pilot inhalation, the vest would inflate – making in more difficult to inhale. The UPG was quickly removed, and PE rates dropped. Eventually, the UPG valve was fixed and the UPG was re-introduced to the F-22 configuration but tailored to be used only during profiles where pressure breathing for altitude would potentially be required, thus removing extra AFE bulk for missions where it was not required. PE rates continued to stay low.

2012 UPG Valve Inflates During Inhalation

Consensus opinion about the probable cause of PEs	UPG valve failure was a major contributor to F-22 PEs
Available evidence	Compelling centrifuge test data System level testing
Recognition of OTM	none
Recognition of BSD	None In 2020 – this is classic BSD In 2012 – this was a faulty valve

2017 – T-6 and T-45 Instructor Pilots Go on Strike

In 2017, more than 100 instructor pilots refused to fly in the T-6 trainer aircraft. T-45 instructor pilots also reported problems with their pilot breathing system and refused to fly. The USAF and

USN did extensive testing for chemical contamination – there was no evidence of widespread contamination. Investigations identified a specific flight condition of low ECS "muscle pressure" during idle descent. Operations were changed to increase power levels during descent. From a 2020 perspective, the correlation between seat location and severity of breathing problems suggests a BSD. The back seat instructor, with a longer breathing hose, suffered a longer delay between the start of muscle movement to expand chest volume – and the initial delivery of inhalation air.

2017 T-45 Instructor Pilots Go On Strike

Consensus opinion about the probable cause of PEs	Underpowered ECS System More throttle = better breathing
Available evidence	Back seat instructors had more problems Instructors had longer hoses Pilots reported difficulty breathing
Recognition of OTM	none
Recognition of BSD	None In 2020 – this is classic BSD

2017 – F/A-18 PE Rates Track with OBOGS DEGD

Statistics were collected for reported PE rates, sorted by in-flight data parameters. One of the data parameters with the greatest interest was OBOGS DEGD, a fault condition that can be caused by low O_2 levels in the breathing gas. Reported PE rates were 10 times greater under OBOGS DEGD conditions, but the majority of the PEs occurred under "OBOGS OK" conditions. In 2017, this confused many analysts; the thinking at the time was "if the PEs are hypoxia related, the majority of the PEs should occur under OBOGS DEGD conditions because hypoxia requires low levels of O_2 in the pilot breathing gas. From a 2020 perspective, this correlation makes sense. There are several ways to create an environment that results in hypoxia. One way is to deliver pilot breathing gas with insufficient O_2. This will cause an OBOGS-DEGD condition; it makes sense that flights with OBOGS DEGD conditions are more likely to result in reported PEs. Another way to create an environment that results in hypoxia is a timing/sequence disruption.

Consider this hypothetical example:

- 1% of flights have OBOGS DEGD conditions
- The chance of a hypoxia PE caused by insufficient O_2 is 1 in 10
- 50% of flights have BSDs
- The chance of a hypoxia PE caused by BSD is 1 in 100
- After 1000 flights, there would be 1 PE under OBOGS DEGD and 5 PEs under "OBOGS OK"

2017 F/A-18 PE Rates Increase with OBOGs DEGD

Consensus opinion about the probable cause of PEs	No consensus
Available evidence	>99% of flights: OBOGS OK <1% of flights: OBOGS DEGD Most PEs – OBOGS OK 10 times more likely OBOGS DEGD
Recognition of OTM	none
Recognition of BSD	None In 2020 – this is classic BSD

2017 – Mask Discipline Training

In 2017, when the NESC team was conducting its independent assessment, mask discipline and mask discipline training provided one of the most significant pieces of evidence that was mostly overlooked (at the time). Compared to the general population, pilots are disciplined people who follow procedures. When there is a widespread prevalence of pilots breaking training and not following procedures – the disconnect between training and practice should be recognized as a clear sign that the pilot breathing system can be difficult to breathe through at times. In 2017, it was recognized that many pilots regularly drop their masks. A training program was instituted to reinforce the importance of wearing masks at all times.

2017 F/A-18 Mask Discipline Training

Consensus opinion about the probable cause of PEs	No consensus
Available evidence	Pilots generally follow procedures Pilots are instructed to wear mask Pilots regularly drop their mask
Recognition of OTM	none
Recognition of BSD	None

2017 – The OTM

The OTM provides no new evidence. The OTM does not describe a mechanism for the specific causes of PEs. The OTM can be helpful in one respect; it can help people out of a logic trap. In 2017, many people were stuck in a logic trap: if hypoxia is caused by insufficient O_2, and "OBOGS OK" verifies that there was sufficient O_2 in the breathing gas during a flight with a PE, then the cause of the PE cannot be hypoxia related. This is not true – the OTM points out that hypoxia relates to O_2 concentration in tissues in the brain, and CRU-99 measures O_2

concentration in the pilot breathing gas. There are many possible disruptions downstream of the CRU-99 that could delay the transport of O_2 and cause hypoxia. OTM provides a framework to consider evidence about the pilot breathing system as it relates to hypoxia.

While the OTM does not define a PE in terms of mechanism, or evidence, it does identify potential causes. The OTM as a functional model of the entire pilot breathing system can help an investigator (or engineer, designer or maintainer) understand and evaluate system interactions and performance. Combined with an understanding of how the breathing system interacts temporally with its environment, an investigator can identify BSD issues. There are many possible ways to disrupt the flow of O_2 from a source to where it is needed and when it is needed. The OTM provides a framework to gather and evaluate evidence and identify causes of hypoxia in the complex and dynamic tactical jet environment.

2017 Oxygen Transport Model

Consensus opinion about the probable cause of PEs	No consensus OTM provides a framework to suggest hypoxia may be widespread
Available evidence	No evidence Lack on in-flight breathing data is pointed out
Recognition of OTM	First time in 2017
Recognition of BSD	None

2018 – First Measurements of Hysteresis and Phase Shift

In 2018, PBA was collecting its first sets of in-flight measurements of breathing using VigilOX. The flight tests were conducted in "discovery mode". Everything was new, there were no standard ways to review or analyze the data. One of the many ways to analyze pressure/flow/time relationships is hysteresis. Inhalation hysteresis compares the pressure/flow relationship early in the inhalation, to the pressure/flow relationship later in the inhalation. Another new method of analyzing VigilOX data is Phase Shift. Phase shift compares the time of peak flow to the time of peak pressure within a single inhalation/exhalation cycle. The significance of these measurements was not recognized in 2018 – they were simply new ways to look at the data. In 2018, the PBA team did not recognize the importance of timing and sequence in the pilot breathing system. The tools to measure timing and sequence – hysteresis and phase shift – were new and had not been applied to a sufficient number of test flights.

2018 First Measurements of Hysteresis and Phase Shift

Consensus opinion about the probable cause of PEs	No consensus
Available evidence	In flight breathing data New measurement – hysteresis New measurement – phase shift
Recognition of OTM	Yes – OTM is 1 year old
Recognition of BSD	None

2019 – Hysteresis Measurements from F-35

The PBA team had heard F-35 pilots reported difficulty breathing, but this difficulty was not fully appreciated until the hysteresis data from the limited ground measurements was compared to hysteresis data from PBA flight tests conducted at AFRC. Suddenly, the system interactions, and the pilot's attempts to adjust to chaotic breathing gas supply all made sense. Pilot comments "the jet is trying to shove air down my throat" makes sense when you see the hysteresis data. This data also teaches the PBA team about the importance of timing and sequence. Getting a sufficient amount of air – but at the wrong time in the inhalation/exhalation cycle can be disruptive. Viewed in the context of the OTM, BSD is an example of a way to diminish the delivery of O_2 to tissues in the brain – even if the breathing gas has sufficient O_2.

2019 Hysteresis Measurements of F-35

Consensus opinion about the probable cause of PEs	No consensus
Available evidence	Profound hysteresis levels in a breathing system
Recognition of OTM	Yes – OTM is 1 year old
Recognition of BSD	New/Emerging awareness of BSD

2019 – Assessment of PBA Flight 29 Data

Flight 29 had problems with the pilot breathing system. The pilot reported that it was difficult to breathe on several occasions throughout the flight. Pilot breathing measurements were collected throughout the flight. Hysteresis and phase shift are standard PBA data analysis techniques by the time Flight 29 occurs. The PBA team recognizes that the pilot breathing system is complex – there are many internal system interactions and timing and sequence are important. For Flight 29, the most significant system interactions that disrupt the timing and sequence relate to the mask components that regulate safety pressure.

2019 Assessment of PBA Flight 29 Data

Consensus opinion about the probable cause of PEs	No consensus
Available evidence	In-flight measurements of timing and sequence disruptions, especially mask, exhalation, and safety pressure
Recognition of OTM	Yes – OTM is 2 years old
Recognition of BSD	Strengthened awareness of BSD

2020 – Measurements of Oxygen Levels in Pilot's Blood

Hypoxia is the inadequate supply of O_2 to the tissues. Hypoxemia (low arterial O_2) is a marker that the supply of O_2 to the tissues is deficient and thus results in hypoxia (low O_2). The O_2 saturation was used as a measure of the O_2 in the blood. It was found that O_2 saturations were lower after donning flight crew equipment and strapped into the aircraft. Oximetry (saturations) measured after flight (mean 94.86%, range of 91-98%) was lower than baseline and the pre-flight measurements (mean 96.14%, range 93.62-99%). Levels lower than 95% represent mild hypoxia without symptoms. The O_2 saturation level of less than 98% seen in USN configuration after flight is alarming in the regime of breathing > 95% O_2 in flight. These values represent a significant physiological decrement that would degrade the physiological reserve and lower the threshold for developing uncompensated symptomatic hypoxia in flight.

2020 Measurements of Oxygen Saturations in Blood

Consensus opinion about the probable cause of PEs	Hypoxia a major factor for PEs
Available evidence	Measurements of blood oxygen levels in pilot's blood immediately after flight
Recognition of OTM	Yes – consistent with OTM
Recognition of BSD	Yes – consistent with BSD

12.5 What does this all mean? A 2020 review of available evidence in light of the OTM and BSDs

The list of available evidence can be re-examined, in 2020, with an awareness of the OTM and BSDs. What does all of this evidence suggest?

- F/A-18 pilots, and F-22 pilots, T-6 pilots, and T-45 pilots likely suffer BSDs that contribute to hypoxia PEs. PBA provides the tools to learn the details and fix the problems.

Why hasn't this been recognized before?

- It is hard to put the pieces together without a system model
- Prior to 2018, there was very little in-flight data on pilot breathing. The breathing system could not be evaluated as a system with system interactions and timing/sequence issues. Prior to 2018, the breathing system had to be treated as a black box.
- In-flight breathing measurements were not collected at a large scale in a systematic way until PBA
- The importance of breathing system timing and sequence was necessary. The significance of BSDs was not appreciated until 2019.
- A quantitative measure of timing and sequence was necessary – hysteresis and phase shift provides a quantitative measure of timing and sequence

A re-evaluation of available evidence with 2020 vision and understanding of OTM and BSD:

- F-22 pilots reported symptoms matching the pattern of hypoxia as early as 2008. The evidence was there from the start, but not a framework in which to understand it.
- Review of the OBOGS performance correctly noted that the OBOGS did not suffer any latent mechanical defects. From a 2020 perspective, the F-22 specifications were incomplete. Too much O_2 can contribute to hypoxia. Oscillating levels of O_2 can contribute to hypoxia. Anecdotes that pilots were less prone to hypoxia with LOX systems are likely true – but not because the F-22 OBOGS was suffering mechanical failures. LOX systems may be less prone to hypoxia PEs because LOX systems are less prone to BSDs.
- The F-22 breathing gas did not contain levels of contamination that were toxicologically harmful. As a fault tree exercise – if PEs occur, and PEs related to contamination are unlikely, hypoxia PEs caused by previously unrecognized mechanisms (fluctuations in O_2 levels, BSDs) should be considered.
- The C2A1 filter likely caused a BSD. It was not recognized at the time, but the C2A1 filter almost certainly changed pilot breathing system timing and sequence. The effect of C2A1 on breathing sequence can be directly tested.
- The UPG valve actuation likely caused a BSD. When the pilot moved their muscles to expand their chest cavity and initiate inhalation, the breathing system response was to direct flow to the vest. In 2012, the correlation between UPG valve malfunction and increased rates of PEs was attributed to work of breathing. In 2020, the diagnosis is more complex – work of breathing may be a factor – BSD may also be a factor.
- The T-45 and T-6 trainers have at least two system interactions that relate to hypoxia, that can be described using the concepts of the OTM and BSDs:

1. When ESC supply pressure is low, regulator timing and sequence will change.
2. When one pilot has a short breathing hose, another pilot has a longer breathing hose, they use the same regulator, and the regulator is not tuned and tested as a dynamic system the system is prone to BSDs. There is limited (but compelling) data to confirm this.

- F/A-18 PE statistics suggest that hypoxia is common, and BSDs are major contributors.
    1. If PEs are 10 times more likely under OBOGS DEGD error status, this suggests that hypoxia is a cause of PEs – low O_2 levels is one (of several) factors that contribute to hypoxia.
    2. If the vast majority of flights occur under OBOGS OK conditions, this suggests that there are other ways to create hypoxia - like a BSD. An awareness of the connection between BSDs and hypoxia PEs can explain the F/A-18 PE statistics.
    3. The two factors are not mutually exclusive: if a specific flight has a BSD, and low O_2 levels, a hypoxia PE is considerably more likely.
- Mask discipline is an extremely strong indicator of BSDs. Pilots adjust their breathing patterns to find a "solution to their breathing needs". If the breathing system is out of sequence, and the pilot cannot take a full deep breath – they will find a solution to their breathing problems – they will drop their mask. Pilots follow procedures unless there is a compelling reason not to. The number of occurrences of pilots dropping their masks indicates the severity and commonality of BSDs.
- The OTM puts all of the evidence in context. There is a complex breathing system that needs to work properly – or the pilot can suffer hypoxia. Even if there is no lack of O_2 in the breathing air.
- Hysteresis and Phase Shift provides a quantitative way to measure timing and sequence problems. These are essential tools to pinpointing exactly which aspects of a breathing system are causing the most disruption. PBA evidence of the effects of safety pressure is one example showing the power of hysteresis and phase shift. PBA evidence of the differences between a demand regulator and a diluter demand regulator is another example showing the power of hysteresis and phase shift.
- The hysteresis measurements taken in the F-35 (limited data, ground measurements only) give a compelling example of what a severe BSD can look like.
- Flight 29 shows what happens when cabin pressure fluctuations combine with OTM transport model, this is a specific breathing system interaction that disrupts timing. It is not related to the amount of O_2 in the breathing air – it is related to timing and sequence.
- Blood o O_2 xygen measurements demonstrate that the conditions of flight stress pilot physiology. Even when pilots have no symptoms, their physiological wellness can be diminished.

Technical Section 13: Case Example Application – The F-35 Lightning II

As the PBA team compiled results from the study reported here, an opportunity presented to apply the methods described to look at reported concerns with the F-35 Lightning's breathing system. The case study is analogous to how a physician listens to her patients, takes some summary measurements and compares those against past experiences, reports, and a large body of established metrics to decide a course of action. While it must be stated up front that the F-35 data available is very limited when compared to the compressive PBA study, two key aspects remain:

1. The limited, objective data sets on two F-35A jets is evaluated against the substantial knowledge generated during the PBA assessment. This enabled metrics of breathing taken during two F-35 ground runs to be compared to metrics of breathing established during the PBA. In the cases evaluated, the F-35 breathing metrics were the most deviant when compared to normal human breathing.
2. As documented and supported in this NESC PBA report, and previously in the NESC's F/A-18 report, pilot reports of breathing challenges should not be ignored. Five F-35 pilots were interviewed on their in-flight experiences. All of them reported experiencing breathing difficulties in the F-35.

Taken alone, the two F-35 limited data sets and five pilot reports cannot be used to draw *statistically significant* conclusions, as was the case with PBA, but these data do support findings that *suggest* the possibility of significant systemic design, integration or performance deficiencies in the F-35 LSS. More importantly, the evidence, taken together, fully supports a strong recommendation that additional data and pilot experience be collected to fully understand the situation and implement corrective actions, as necessary.

Pilots report that breathing system difficulties force them to think about their breathing in the F-35. Interviewees state that this is a cognitive distraction that divides attention away from mission tasks. Additionally, pilots report different breathing experiences in different F-35 jets. A disturbing observation is that some pilots reported organizational concerns over protecting the F-35 program resulted in pressure to ascribe breathing problems to pilots instead of the hardware.

Data were analyzed using the techniques previously described. In the F-35 case, the divergence from normal breathing patterns established during PBA are so distinct, that the shape of some hysteresis waveforms is unrecognizable compared to other aircraft.

The PBA team analyzed VigilOX data from two short ground tests of F-35 aircraft from Hill AFB. The data were taken using the same pilot and two different aircraft, one qualitatively judged by the pilot to be a 'good' breather and the other a 'bad' breather. Figure 13.1 shows the inhalation flow as a function of line-cabin differential pressure for three consecutive resting breaths on NASA PBA aircraft in USAF configuration (top), USN configuration (center) and one of the F-35 aircraft (bottom).

The data show that the breaths of the pilots in the USAF configuration are smooth, consistent and repeatable. Breathing in the USN configuration exhibits some hysteresis where flow does not trace the same path with pressure in the beginning as it does at the end of the breath. The within-breath relationship between pressure and flow is still smooth, consistent and repeatable. The F-35 breaths are completely different. No discernable relationship exists between flow and

pressure. Note than although the F-35 is an OBOGS aircraft and the PBA F-15 and F-18 jets were LOX-based, the key comparisons here are on pressure and flow timing compared to the normal human breathing experience.

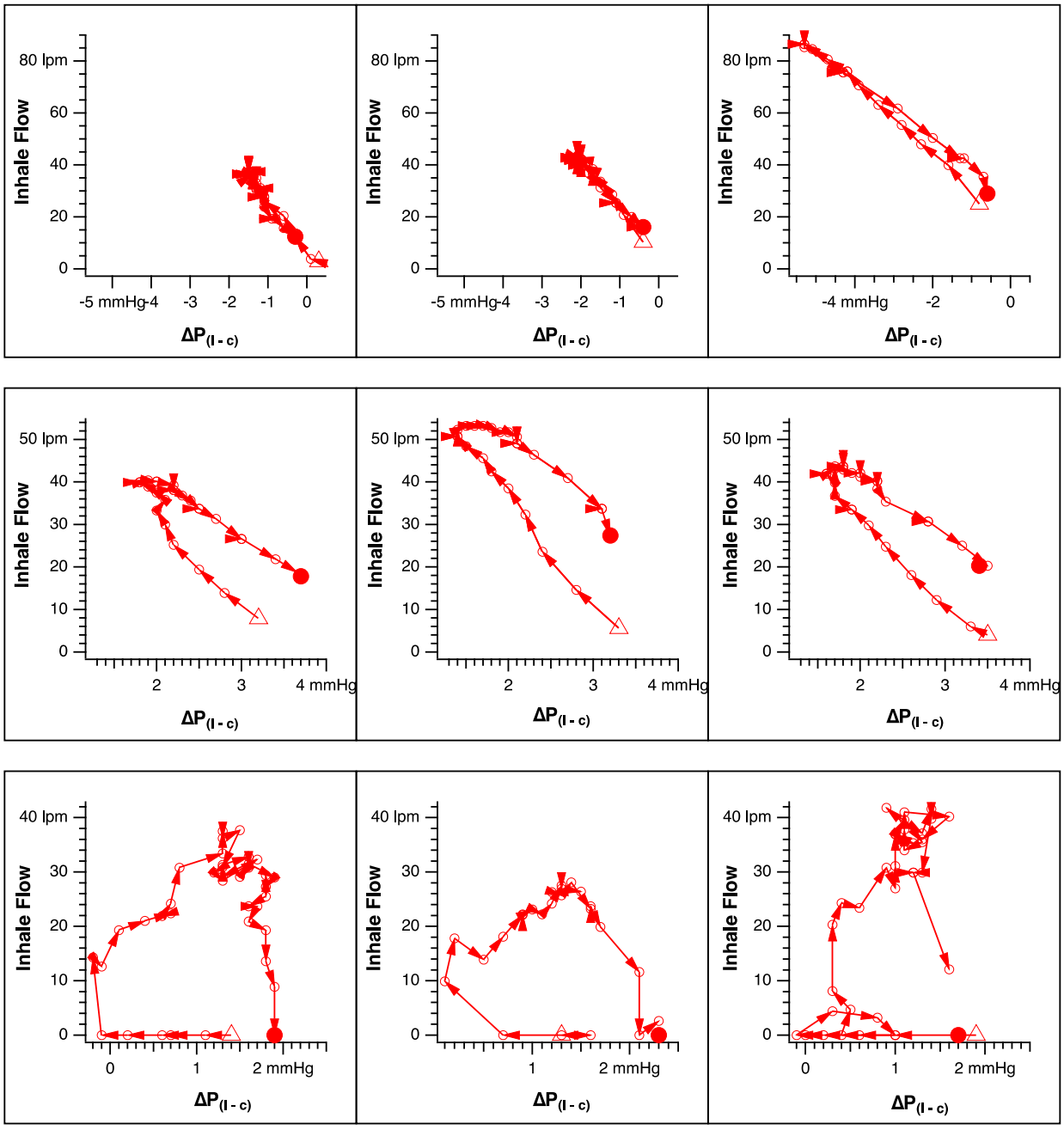

Figure 13.1. Three Consecutive Resting Breaths on PBA Aircraft in USAF (top), USN (center) and one F-35 Aircraft
The arrows trace the time history of the breaths.

The breaths for the PBA flights in the USAF configuration suggest a linear relationship between pressure and flow. Figure 13.2 shows the histograms for the slope of the flow versus pressure curves in Figure 13.1 for all of the breaths in each test (USAF, left; USN, center; F-35, right). The results for the USAF (PBA FLT-058) show a histogram that is narrowly distributed,

emphasizing that the breathing system is behaving consistently and repeatably. Figure 13.3 shows the correlation coefficient of the linear fit, a value of 1.0 indicates a perfect fit while a value of 0 shows no correlation between flow and pressure. The correlation coefficient data for the USAF in Figure 13.3 (left) shows an excellent fit for virtually all of the breaths in the test.

The data for the slope and correlation coefficient for all of the breaths of the PBA test (FLT-045) in the USN configuration (center graphs on Figure 13.2 and 13.3) show that the slope is slightly lower (indicating, on average, less flow per unit of demand) as is the correlation coefficient. This is consistent with hysteresis in the within-breath flow versus pressure data.

The F-35 histogram for slope (Figure 13.2, right) is, on average, in the opposite direction (positive slope) indicating that, on average, flow decreases with increasing demand. Furthermore, the histogram for the correlation coefficient (Figure 13.3, right) shows that flow and pressure are essentially not correlated.

These results combined with pilot reports suggest that severe BSDs may be commonplace on the F-35. As a result, the PBA team initiated a detailed study of the F-35 ground test data. The details of the F-35 analysis are found in Appendix 7.

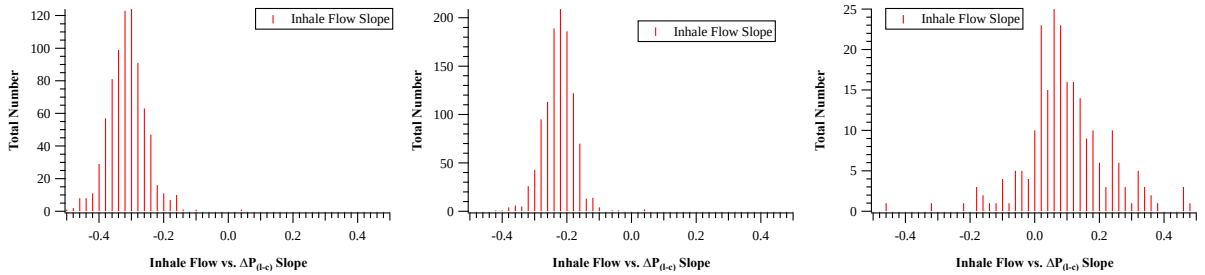

Figure 13.2. Histogram of Slope of Flow versus Pressure Curve (Figure 13.1) for PBA Test in USAF (FLT-058, left), USN (FLT-045, center) Configuration and F-35 (right)

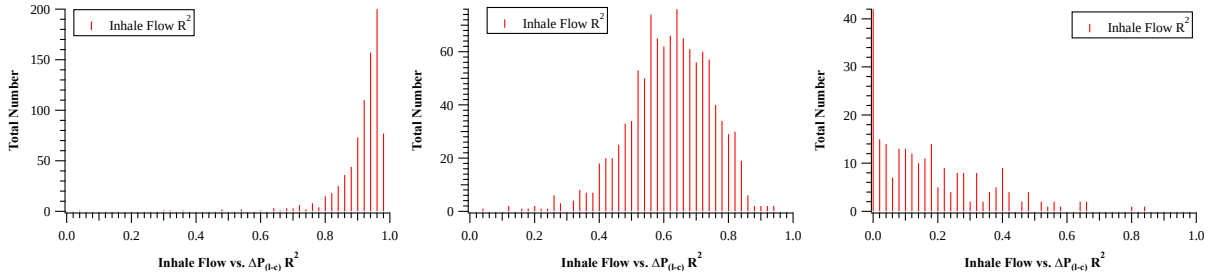

Figure 13.3. Histogram of Correlation Coefficient of Linear Fit to Flow versus Pressure Curves (Figure 13.1) for the PBA test in USAF (FLT-058, left), USN (FLT-045, center) configuration and the F-35 (right)

The F-35 data are consistent with patterns of severe BSDs. These can induce physiological responses which are further corroborated by F-35 pilot interview reports of coughing fits, significant post-flight fatigue, lightheadedness, nausea, and other physiological symptoms. These incidents were disruptive and detectable to the pilots but were not reported as PEs. This is particularly concerning as excessive pressure delivered at the wrong time in the breathing cycle can cause alveolar overdistention, potentially resulting in 'micro-tears' of lung tissue and result in cumulative loss of function over time. One instance of an F-35 pilot being medically disqualified from service following a PE is documented.

13.1 F-35 Discussion

Pilot perception of breathing difficulty, breathing dynamics, and breathing disharmony are not directly related to mask pressure. Low mask pressures and lower swings in mask pressure are usually thought to denote a system that is performing well, but that is not necessarily true when a flow restriction is present. Conversely, high mask pressures and higher mask pressure swings are traditionally considered to denote a poorly performing system, but pilots did not perceive those pressures as either large or objectionable when the flow adequately responds to large demands. In both cases, pilot perception of breathing performance was not correlated directly with mask pressure magnitude. Rather, pilot perception of breathing dynamics appeared to depend upon receiving a flow commensurate with the pilots breathing demand and without delay. This suggests that mask pressure and flow should be viewed synergistically, not independently, when considering pilot perceptions of breathing dynamics. Specifically, the proportional relationship and timing between mask pressure and flow with respect to each other should be questioned and addressed in careful detail when communicating with (test) pilots about any perceived difficulty in breathing.

For exhalation measurements made during PBA flights, there is a consistent relationship between pressure and flow. This pressure-flow relationship is linear or near-linear with a slight time lag, which can be characterized by hysteresis and phase shift.

The divergence from normal breathing patterns in the F-35 is so distinct that the shape of some hysteresis waveforms is unrecognizable compared to other aircraft. The mechanical and human elements of the breathing system are profoundly out of sequence. In the F-35, the pressure and flow peaks often diverge more than 30 degrees (phase shift) apart. Mechanical elements of the breathing system act like inhalation during exhalation. The human element of the breathing system is unable to control unpredictable and inconsistent pressures. These BSDs are not currently measured on any bench test, and no requirements exist to measure or prevent excessive disruptions.

This pattern should be considered highly concerning, as it demonstrates that the airflow supplied from the F-35 life support system is inconsistent, variable, and does not align the pilot’s breathing demands. Attenuated inhalation, delayed exhalation, reduced exhalation, and difficulty exhaling are demonstrated in hysteresis plots, with phase shift being a simple measure of that BSD.

Furthermore, there are surges in airflow late in the inhalation sequence demonstrated by hysteresis plots and characterized by negative inhale phase shift. These surges in airflow can cause limited tidal volumes and ineffective ventilation due to delayed flow and the natural protective compensation of the body (see additional discussion in Appendix 7, Section 8).

Dynamics are important to the proper functioning of these complex systems. Large or abrupt changes lead to system disharmony. Systems are bench tested with smooth and linear breathing systems which do not resemble the environment they experience in flight. Neither the inhalation nor exhalation valve appear to be designed to function in the presence of the observed frequency or magnitude of pressure oscillations observed in the F-35 breathing system. Valves require a finite time to function and when the valves are not tuned or working properly, they can have an adverse impact on breathing dynamics. The interrelationship between pilot and aircraft deserve more consideration than is typically given in during design and system integration.

F-35 Aircraft 1 was identified subjectively as a “Bad Breather” and the limited data support that assertion. Furthermore, F-35 Aircraft 2 also showed “bad breather” behavior to a lesser extent but was still found to be distinct from the more normal breathing characteristics seen in the PBA analysis of other aircraft.

13.2 F-35 Specific Findings

The limited F-35 data, when compared to the comparatively larger body of PBA data and corresponding pilot experience reports is supportive of the following findings:

F-35.1 The measured pressure, flow, and timing response of the breathing system is inconsistent. For a given pressure, the amount of flow at the beginning, middle, and end of the breath is unpredictable, and can be chaotically different.

F-35.2 Mask pressure changes depict sawtooth patterns. Ideal mask pressure changes are smooth and synchronous as with unencumbered breathing in open air. Sharp, sudden, frequent pressure variations as seen in the F-35 cannot be physiologically produced by a person, therefore, these are caused by elements of the F-35 breathing system.

F-35.3 Measured mask pressure swings exceed MIL-STD 3050 limits.

F-35.4 Breathing supply line pressure oscillations are evident resulting in mask pressure oscillations that exceed AIR-STD 4039 limits.

F-35.5 Breathing gas oxygen concentrations varied by 20 to 40% over one-minute intervals. Large breaths produced drops in breathing gas oxygen concentration.

F-35.6 Changes to environmental controls or G-suit connections affected measured pilot respiratory patterns differently between the two aircraft tested. Tidal volume, respiration rate, and minute ventilation changed by physiologically significant amounts.

Findings F-35.7 through F-35.12 specifically address the pilot experiences documented during structured interviews. F35.7 through F-35.10 are discussed more fully in the context of pilot symptom and perception cluster analysis detailed in Appendix 7, Section 2.2.2, and Appendix 7.2, along with many direct quotes from the pilot community.

F-35.7 Pilots perceive that the F-35 breathing environment and physiological experience is dissimilar to a) other aircraft flown and b) non-aircraft situations. The F-35 breathing system noticeably discourages normal breathing function via high-pressure, pressure surges, and hyperoxia.

F-35.8 Pilots perceive the there is a distinct breathing system disparity across F-35 aircraft with no clear explanation or solution.

F-35.9 Pilots perceive that the symptoms experienced by F-35 pilots in-flight are frequent and variable among pilots and tend to mimic pilot-specific hypoxia symptoms. However, there are additional individual symptoms that are F-35 specific and learned exclusively from flying the F-35 that suggest additional pathophysiology.

F-35.10 Pilots perceive that the hypoxia recognition training as it currently exists is not a sufficient match with the respiratory environment in the F-35 when compared to the symptom exhibition and mitigation needs experienced during actual flight.

F-35.11 Breathing system recovery after mask removal is inconsistent between the two aircraft sampled, with excessive inhalation effort needed to restart the flow of breathing gas.

F-35.12 Pilots report that exhalation and verbal communication can be difficult in the F-35, including reports of being cutoff mid-speech by mask pressure fluctuations, while talking.

F-35.13 Pilots report differences in their breathing experience between different F-35 jets.

Given the potential significance of these findings, if further corroborated by additional data, the NESC recommends that the following actions be taken by the stakeholder organizations responsible for production and operation of F-35 LSS systems and components.

R.F-35.1 Read the statements and quotes given by the pilots in their own words documented throughout Appendices 7 and 7.1 ***(F-35.7-13)***

R.F-35.2 Take action to investigate and validate the observed breathing system anomalies with special emphasis on understanding F-35 system dynamics that lead to BSDs and oxygen concentration changes. ***(F-35.1-4, 7-13)***

R.F-35.3 Measure F-35 breathing metrics in-flight***. (F-35.1-4)***

R.F-35.4 Measure pilot respiratory capacity pre- and post-fight with spirometry. ***(F-35.9)***

R.F-35.5 When investigating PEs, consider BSDs as a hypothesis when oxygen concentrations have been verified as adequate. ***(F-35.1, 2, 4, 5)***

R.F-35.6 Address policies and procedures that may have inadvertently exacerbated normalization of deviance***. (F-35.7-13)***

R.F-35.7 Collect additional (and regular) pilot experience reports to identify common complaints for further investigation. ***(F-35.7-13)***

Technical Section 14: PBA Findings and NESC Recommendations

PBA Findings (* represents a Key Finding)

Technical Section 2- Fundamentals of Pilot Breathing

F.2-1. Pilots subconsciously adjust their breathing to accommodate to changes in the mechanical supply system.

F.2-2*. *Lung pressure changes of 2-3 mmHg drive normal inhalation and exhalation. Cabin pressures can change up to 5 mmHg during the course of a single inhalation and can have a profound effect on breathing.*

Technical Section 5: Summary Information and Statistical Analyses based on 1-min Data Compilations

Part 1. Summary Statistics and Data Visualization

F.5-1. Q-Q plots and heat maps are valuable visualization tools to quickly identify flight segments that contain breathing anomalies.

F.5-2. Higher breathing rates (BPM) are associated with aggressive aerobatic maneuvers.

F.5-3. The highest observed values of mean inspiratory flow rates in PBA pilots occurred in aerobatics profiles and some of the lowest observed values occurred in high altitude flights.

F.5-4. Highest values of peak inspiratory flow rate (maximum instantaneous flow) observed in PBA pilots under stress are below that of typical adult exertion stress tests observed in the laboratory. PBA profiles were limited to an aircraft maximum G-force of approximately 5.

F.5-5. Observations of PBA pilot tidal volume per flight minute are similar to those found in typical adults at low to moderate levels of aerobatic exercise.

F.5-6. PBA evaluated mask pressure variation to identify flight minutes with high oscillations and developed the Standard Deviation Mask Pressure (st. dev. MP) metric for use in the detection of potential breathing stress including those caused by mask valve dysfunction.

F.5-7. Heat maps of PBA flight minute data can be used to quickly identify outliers of the dependent breathing variables and flight segments recommended for further detailed analyses.

F.5-8. With the exception of breathing rate, flight minute pilot breathing data are lognormally distributed and must be treated as such in summary statistics and modeling evaluations.

Part 2. Mixed effects models

F.5-9. Mixed effects models of six dependent pilot physiological response metrics indicated that most variability was likely due to flight/equipment related factors, with the exception of breathing rate which was due to individual factors.

F.5-10. Breathing rate: 61% of total breathing rate variance is attributable to individual differences in PBA pilots indicating that breathing rate is more strongly dependent on individual pilot physiology than on external flight factors.

F.5-11. Inhalation Flow Variance (mean): Approximately 18% of total measurement variance is attributable to PBA individual pilot physiological differences indicating larger effect of flight/equipment on mean flow.

F.5-12. Inhalation Flow Variance (max): Approximately 10% of measurement variance is attributable to PBA individual pilot physiological differences indicating larger effect of external stimuli on sudden rapid inhalations.

F.5-13. Breath Volume Variance: Approximately 19% of total breath volume variance is attributable to PBA individual pilot physiological differences indicating a larger effect of flight/equipment on breath volume.

F.5-14. Differential Mask Pressure (DMP) Variance: Approximately 9% of Differential Mask Pressure (DMP) variance is attributable to PBA individual pilot physiological differences. Factors affecting DMP variation are experienced similarly by all PBA pilots.

F.5-15. Standard Deviation of Mask Pressure Oscillations: Only 17% of Standard Deviation of Mask Pressure Oscillations variance is attributable to PBA individual pilot physiological differences indicating larger effects of flight/equipment.

F.5-16. Aircraft velocity, delta cabin pressure (max – min cabin pressure within a 1-min window), and G-force are significant predictors of Breathing Rate, Differential Mask Pressure, and Standard Deviation Mask Pressure.

F.5-17. Peak inspiratory flow is not strongly correlated with aircraft velocity, delta cabin pressure, or G-force, but rather with differences in flight profile.

F.5-18. G-force is a significant predictor for all six PBA pilot breathing response metrics.

F.5-19. A mixed-effects model analysis showed that VigilOX hardware and software updates throughout the PBA study were a significant predictor for 4 of the 6 dependent variables but did not affect the interpreted conclusions.

F.5-20. Mixed-effects model results indicate that the main sources of variability in PBA pilot breathing parameters are imposed by aircraft flight activities and breathing gear, rather than by individual PBA pilot physiology.

Technical Section 6: Engineering Analysis of Pilot Breathing

F.6-1*. *Phase shift analysis is a numerical tool to quantify disharmony between pilot breathing demand and the breathing system delivery. The test results are corroborated by independent pilot observations.*

F.6-2. PBA quantified aspects of flight that affect the human breathing system function and Air Crew Breathing System interactions.

F.6-3*. *PBA found systematic disharmony between pilot breathing demand and breathing system delivery as indicated by magnitudes and timing of the pressure and flow data channels.*

F.6-4. A NASA machine learning Inductive Monitoring System can detect Mask Pressure-No-Flow (PNF) situations. In the sample ingested, 5x more positive IDs were found in the USN-like configurations with positive pressure and no diluter-demand. Even a short (less than 1s) PNF can correspond to a pilot perception of difficulty inhaling.

F.6-5*. *When PBA pilots reported subjective perceptions of difficulty breathing or experienced physiological symptoms, these were corroborated by in-flight objective measurements.*

F.6-6. The pressure, flow, and timing response of the USAF configured diluter demand breathing system is consistent throughout the breath; for a given pressure there is a 1:1 relationship to the resulting flow.

F.6-7. Safety pressure, as defined by continuous pressure above ambient, and as used on USN aircraft, exacerbated or induced vast majority of the adverse breathing system interactions identified by PBA.

F.6-8. The supply of the pilot breathing system can cause BSDs by 1) misalignments in time relative to demand, 2) excessive inspiratory and/or expiratory pressure impeding inhalation and/or exhalation, 3) flow restriction of inhalation and exhalation volumes especially under dynamic conditions.

F.6-9. The frequency components of cabin pressure oscillations (situational or continuous) are close in frequency to pilot breathing, with a mode at 0.3 Hz. The cabin pressure oscillations and breathing frequency combine and affect pilot air supply and pilot breathing.

F.6-10. PBA routinely measured cabin pressure changes between 500-1000 ft equivalent pressure altitude due to dynamic pressure in all cabin pressure regimes. Importantly, these pressure changes were documented even in isobaric regions where the aircraft should deliver constant cabin pressure.

F.6-11. PBA identified cabin pressurization issues due to increase of dynamic pressure (affected by airspeed, G's, maneuvers, throttle position, and system settings). These changes also affect the entire breathing system.

F.6-12*. *Key physiological parameters of the breathing system are pressure, flow, volume and timing of supplied air. Systematic disharmony of the system can be measured by breathing hysteresis and breathing phase shift, which are new PBA methods of measuring BSDs. Instances of Pressure No Flow (PNF) was also an indicator of systematic disharmony of the system.*

F.6-13. BSDs (deviations from normal linear pressure flow relationships) are not measured as part of acceptance testing or routine maintenance of aircrew breathing systems and no requirements exist to prevent excessive BSDs.

F.6-14. BSDs, as measured by breathing phase shift and hysteresis, can result in attenuated inhalation volume, delayed exhalation, reduced exhalation, and resistance in exhalation.

F.6-15. Despite using LOX breathing supply systems which are considered to be stable, PBA found regulator and mask performance anomalies.

F.6-16. PBA has determined that large regulator supply pressure variations are possible. The largest regulator supply pressure drop was 50 PSI (e.g., USN configuration, level flight, after 3 deep breaths). Frequent 20 PSI drops were observed (e.g., at the onset of 5 G turns).

F.6-17. Breathing system performance can be evaluated by quantitative analysis of mask pressure changes. Ideal mask pressure changes are smooth and match the pressure changes of breathing in open air. Sharp, sudden, frequent pressure variations are not produced physiologically, therefore, these variations are the result of the breathing system or the environment and require pilot compensation.

F.6-18. Pressure compensated masks, like the MBU-20/P, in combination with the CRU-103 regulator, can suffer adverse system interactions under certain dynamic breathing conditions.

F.6-19. PBA documented a delay of flow at the start of inhalation due to the regulator's (i.e., CRU-103) inability to maintain the prescribed safety pressure. This timing delay between pilot demand and regulator supply presents as a BSD.

F.6-20. PBA found subjective breathing difficulty reported in flight correlated to objective measurements of breathing system performance.

F.6-21. Even small amplitude cabin pressure oscillations (e.g., a few mmHg) will impact the regulator reference pressure and response. The severity of the combined effect determines the impact to pilot breathing.

F.6-22. When an aircraft cannot maintain steady cabin pressure, the regulator has a harder time adjusting. This lag is especially pronounced in a dynamic profile (rapid altitude changes, G's at 4 G's or higher).

F.6-23. Cabin pressure fluctuations affect the reference pressure for safety pressure regulators and cause BSDs and adversely affect the delivery pressure, flow, and timing of the breathing system response.

F.6-24. PBA discovered that aircraft cabin pressure fluctuates in a manner which can have both a primary impact to the pilot's physiology, and a secondary impact through oscillatory fluctuation in reference pressure for the pilot's breathing regulator, resulting in complex impacts to pilot breathing.

F.6.25. Minute ventilation is greatest during the post-G recovery segment.

Technical Section 7: Pilot Physiology and Medical Outcomes

F.7-1. As designed, current mechanical regulators cannot effectively respond to the full dynamic range of all breathing profile conditions during in-flight operation.

F.7-2*. *PBA spirometry found that the Aircrew Flight Equipment (AFE) and being harnessed to the seat reduced measured available lung volume prior to flight. Functional Vital Capacity (FVC) measurements taken from PBA pilots just prior to take off revealed a large decrease in FVC mean from baseline.*

F.7-3*. *PBA spirometry found further decreased Functional Vital Capacity (FVC) in PBA pilots immediately after landing as compared to the respective immediate pre-flight measurements.*

F.7-4. PBA found Oxygen Saturation (SpO_2) measurements were lower than baseline (seated in flight suit, not in aircraft) in all subsequent observations, including recovery.

F.7-5*. *PBA found Oxygen Saturation (SpO_2) did not return to baseline by the time of the recovery measurement taken at approximately 1 hour post-flight.*

F.7-6*. *Numerous instances of mild hypoxia (SpO_2 < 95%) were indicated in both the post flight and post doffing observations as measured by pilot Oxygen Saturation.*

F.7-7*. *PBA found pilot Oxygen Saturation (SpO_2) measurements taken immediately after flight were below the < 93.5% cutoff indicating critical physiological impacts due to hypoxia. Especially problematic is that the vast majority of the lowest SpO_2 readings are found in the 100% supplied oxygen configuration (CRU-103) throughout the flight. There were no pilot subjective reports of hypoxia symptoms.*

F.7-8. FVC and Oximetry post-flight measurements of the PBA pilots indicated the presence of impaired in-flight lung gas exchange indicative of lung and circulation mismatches (Ventilation-perfusion Mismatches - V/Q Mismatch).

F.7-9. PBA pilots reported a concern that high temperature exposure was enough to induce adverse physiological responses with some mission impact.

Technical Section 8: Non-PBA Aircraft Analysis and Lessons of PBA Data for Other Breathing Systems

F.8-1*. *Pilot subjective reports indicate diluter demand regulators as easier to breathe which is supported by breathing effort analysis. Regulators that deliver breathing gas at neutral pressure (mask pressure the same as cabin pressure) exhibit less phase shift with current mask/regulator design, especially during high volume/high velocity breathing.*

F.8-2. MIL STD 3050 uses a “trumpet curve” format to describe, define, and specify pilot breathing requirements. Trumpet curve profiles are inadequate as they only define peak pressure/flow relationships but do not provide any information about timing, sequence, or synchronization/disharmony within the breath.

F.8-3. Pilot breathing patterns are altered, and effort of breathing increases when there are a series of breaths with high peak breathing demands, and the pilot breathing system delays the supply of air.

F.8-4. PBA found that pilots do not breathe at a constant flow rate with a sinusoidal breathing pattern but demonstrate high variability. Standard bench tests of regulators at constant flow conditions do not appropriately approximate in-flight conditions.

Technical Section 9: Sensor Status and Future Development

F.9-1. An in-mask CO_2 sensor offers significant new capability for identifying pilot oxygen processing (“metabolic cost of flying” assessment) by producing high resolution data for system diagnostics.

Technical Section 10: Development of a Diagnostic Test of In-Flight Breathing System Performance

F.10-1*. *F-Project-1. Test methods developed and demonstrated in PBA were an effective means to quantify complex system interactions between the pilot and aircraft leading to deeper insight into problems in the aircraft Breathing Gas System (BGS).*

F.10-2*. *F-DM-1. A simple and objective scoring rubric was developed and implemented to identify faults in the components of the breathing gas system that could be applied to standardized profiles to compare aircraft.*

Technical Section 11: Almanac of Pilot Breathing

F.11-1. Segmentation allows comparisons of like segments from different profile flights, and can help identify an outlier or unexpected behavior, which otherwise would be washed out if looking at the entire flight. The Almanac provided in Section 11 provides a good baseline for breathing on F/A-18 legacy aircraft with LOX air supply, under different regulator configurations.

PBA Recommendations (* represents a Key Recommendation)

Applicable to all US Military and High-performance aircraft manufacturers

R.5-1*. *Quantitative measures of pilot breathing should be used in the creation of hardware and system specifications to meet pilot physiological needs and used to validate that individual integrated systems meet pilot physiological needs throughout all relevant flight envelopes."* ***(F.5-1, F.5-7, F.5-8. R-1)***

R.5-2. Use of visualization tools: QQ-plots and Heat maps should be used to evaluate pilot – aircraft interactions, and implemented for integrated system testing/maintenance of jetfighters. ***(F.5-7, F.5-8. R-2)***

R.5-3. Mixed-effects model results indicate that the main sources of variability in PBA pilot breathing parameters are imposed by aircraft flight activities and breathing gear, rather than by individual pilot susceptibilities. Mitigation of pilot stress is more likely achieved by modifying the aircraft and gear parameters. ***(F.5-9, F.5-11 to F.5-18)***

R.6-1. For flights where both mask pressure and flow are available, apply phase shift analysis for early detection of equipment issues or validation of pilot reports. Collapse flights or segments into bins or single numbers of Phase Shift Mean, ± standard deviation, lag (time) and correlation coefficients. ***(F.6-1)***

R.6-2. Aircrew life support breathing system stakeholders should take actions to investigate, validate, and correct systems that lead to physiological symptoms and have corresponding anomalous pilot breathing patterns. ***(F.6-5)***

R.6-3. In light of unexplained PEs and data pointing to disharmony between pilot and air-system, Re-evaluate the risk/benefit trade-off of the use of Safety-Pressure 100% of the time. Minimize safety pressure magnitude and duration of use where possible. ***(F.6-7)***

R.6-4. Cabin pressure fluctuations at a frequency that require pilot compensation should be monitored and mitigated to ensure smooth and predictable breathing gas delivery. ***(F.6-8)***

R.6-5. Perform Fast Fourier Transform analysis of unfiltered and un-smoothed cabin pressure (and pilot mask pressure, when possible). Use a prominent cabin pressure frequency as a trigger for maintenance check of systems that affect cabin pressure (e.g., control valve or exit valve). ***(F.6-9)***

R.6-6*. *Measure and track phase shift, hysteresis, and PNF (Pressure – No Flow) when evaluating aircraft system health – especially during times of peak breathing.* ***(F.6-1, F.6-12)***

R.6-7*. *Perform standardized flight test procedures to establish and evaluate an aircraft's pilot breathing system performance.* ***(F.6-12)***

R.6-8. Air delivery systems should be capable of delivering 5 lps for 3 seconds per pilot. (F.6-16)

R.6-9. Investigate pressure compensated mask/regulator system interactions, their effects on pilots, and correct as necessary. ***(F.6-18)***

R.6-10*. *Subjective reports of breathing difficulty from pilots should be trusted as a significant indication of breathing system performance and followed up in a methodical manner including assessment with objective data.* ***(F.6-20, F.8-1)***

R.6-11. Regulators should be bench tested with pressure and flow rate changes commensurate with an operational flight environment. ***(F.6-20)***

R.6-12. Develop and deploy a cabin pressure sensor that can measure the absolute magnitude of the cabin pressure and is also capable of measuring sub-mmHg pressure oscillations about the absolute pressure in the 0.01 to 10 Hz range. ***(F.6-24)***

R.7-1. Prior interviews with PBA, F-35, and F/A-18 fleet pilots indicate heat exposure is a common hazard. Appropriate mitigations for heat-stress should be identified and deployed. ***(F.7-9)***

R.8-1. Hysteresis and PNF (Pressure – No Flow) analysis methods are recommended augmentations to evaluate flow, pressure, and timing/sequence anomalies related to breathing air delivery. ***(F.8-2)***

F-35 Specific Findings

The limited F-35 data, when compared to the comparatively larger body of PBA data and corresponding pilot experience reports is supportive of the following findings:

F-35.1. The measured pressure, flow, and timing response of the breathing system is inconsistent. For a given pressure, the amount of flow at the beginning, middle, and end of the breath is unpredictable, and can be chaotically different.

F-35.2. Mask pressure changes depict sawtooth patterns. Ideal mask pressure changes are smooth and synchronous as with unencumbered breathing in open air. Sharp, sudden, frequent pressure variations as seen in the F-35 cannot be physiologically produced by a person, therefore, these are caused by elements of the F-35 breathing system.

F-35.3. Measured mask pressure swings exceed MIL-STD 3050 limits.

F-35.4. Breathing supply line pressure oscillations are evident resulting in mask pressure oscillations that exceed AIR-STD 4039 limits.

F-35.5. Breathing gas oxygen concentrations varied by 20 to 40% over one-minute intervals. Large breaths produced drops in breathing gas oxygen concentration.

F-35.6. Changes to environmental controls or G-suit connections affected measured pilot respiratory patterns differently between the two aircraft tested. Tidal volume, respiration rate, and minute ventilation changed by physiologically significant amounts.

Findings F-35.7 through F-35.12 specifically address the pilot experiences documented during structured interviews. F-35.7 through F-35.10 are discussed more fully in the context of pilot symptom and perception cluster analysis detailed in Appendix 7, Section 2.2.2, and Appendix 7.1, along with many direct quotes from the pilot community.

F-35.7. Pilots perceive that the F-35 breathing environment and physiological experience is dissimilar to a) other aircraft flown and b) non-aircraft situations. The F-35 breathing system noticeably discourages normal breathing function via high-pressure, pressure surges, and hyperoxia.

F-35.8. Pilots perceive there is a distinct breathing system disparity across F-35 aircraft with no clear explanation or solution.

F-35.9. Pilots perceive that the symptoms experienced by F-35 pilots in-flight are frequent and variable among pilots and tend to mimic pilot-specific hypoxia symptoms. However, there are additional individual symptoms that are F-35 specific and learned exclusively from flying the F-35 that suggest additional pathophysiology.

F-35.10. Pilots perceive that the hypoxia recognition training as it currently exists is not a sufficient match with the respiratory environment in the F-35 when compared to the symptom exhibition and mitigation needs experienced during actual flight.

F-35.11. Breathing system recovery after mask removal is inconsistent between the two aircraft sampled, with excessive inhalation effort needed to restart the flow of breathing gas.

F-35.12. Pilots report that exhalation and verbal communication can be difficult in the F-35, including reports of being cutoff mid-speech by mask pressure fluctuations, while talking.

F-35.13. Pilots report differences in their breathing experience between different F-35 jets.

Given the potential significance of these findings, if further corroborated by additional data, the NESC recommends that the following actions be taken by the stakeholder organizations responsible for production and operation of F-35 LSS systems and components.

R.F-35.1. Read the statements and quotes given by the pilots in their own words documented throughout Appendices 7 and 7.1. ***(F-35.7-13)***

R.F-35.2. Take action to investigate and validate the observed breathing system anomalies with special emphasis on understanding F-35 system dynamics that lead to BSDs and oxygen concentration changes. ***(F-35.1-4, 7-13)***

R.F-35.3. Measure F-35 breathing metrics in-flight. ***(F-35.1-4)***

R.F-35.4. Measure pilot respiratory capacity pre- and post-fight with spirometry. ***(F-35.9)***

R.F-35.5. When investigating PEs, consider BSDs as a hypothesis when oxygen concentrations have been verified as adequate. ***(F-35.1, 2, 4, 5)***

R.F-35.6. Address policies and procedures that may have inadvertently exacerbated normalization of deviance. ***(F-35.7-13)***

R.F-35.7. Collect additional (and regular) pilot experience reports to identify common complaints for further investigation. ***(F-35.7-13)***

Technical Section 15: Acronyms and Abbreviations

ΔP	Differential Pressure
AB	Afterburner; also Air Crew Equipment (see also AFE and ALSE)
ACAT	Aeromedical Crisis Action Team
ACE	Angiotensin-Converting Enzyme
ACE	Air Crew Equipment
ACES	Advanced Concept Ejection Seat
ACM	Air Combat Maneuvering
ACM	Air Cycle Machine
ACS	Automatic Pilot Control System
ACSC	Air Conditioning System Controller
ADRAC	Altitude Decompression Sickness Risk Computer
AF	Air Force
AFB	Air Force Base
AFB	Airframe Bulletin
AFC	Air Frame Change
AFCE	Automatic Flight Control Equipment in the USAF
AFE	Aircrew Flight Equipment (see also ACE and ALSE)
AFRC	Armstrong Flight Research Center or Air Force Reserve Command
AGARD	Advisory Group for Aerospace Research and Development
AGE	Arterial Gas Embolism
AGL	Above Ground Level
AGSM	Anti-G Straining Maneuver
AI	Artificial Intelligence
ALS	Amyotrophic Lateral Sclerosis
ALSE	Aircrew Life Support Equipment (see also ACE and AFE)
ALSS	Aviation Life Support Systems
AMB	Aviation Mishap Board
AMPSS	Aircrew Physiologic Monitoring Sensor Suite
AMSO	Aeromedical Safety Officers
ANN	Artificial Neural Network
AOA	Angle of Attack
AOS	Aircrew Oxygen System
ARC	Ames Research Center
ARWG	Aeromedical Reference and Waiver Guide
ASCC	Air Standardization and Coordination Committee
ASD	Atrial Septal Defect
ASL	Arterial Spin Labeling
ASME	Aeromedical Subject Matter Expert
ASO	Aviation Safety Officer
ASRS	Aviation Safety Reporting System
ASTM	American Standard Test Method
ATAGS	Advanced Tactical Anti-G Suit
ATC	Air Traffic Control
ATP	Adenosine-5’-triphosphate
ATPD	Ambient Temperature and Pressure Dry

AV	Alternobaric Vertigo
AVR	Alveolar Ventilation Rate
BE	Board-Eligible
BFM	Basic Fighter Maneuvering (USN) Basic Fighter Maneuvers (USAF)
BGS	Breathing Gas System
BLUF	Bottom Line Up Front
BOS	Back-up Oxygen System
BPM	Breaths Per Minute
BR	Breathing Rate
BRAG	Breathing Regulator/Anti-G
BSD	Breathing Sequence Disruption
BUMED	Bureau of Medicine and Surgery
BUNO	Bureau Number
CAPR	Cabin Air Pressure Regulator
CAST	Combined Aircrew Systems Tester
CBF	Cerebral Blood Flow
CI	Cardiac Index
cmH_2O	Centimeters of Water Column
$CMRO_2$	Cerebral Metabolic Rate Of Oxygen
CNAL	Commander, Naval Air Force, U.S. Atlantic Fleet
CNS	Central Nervous System
CO	Cardiac Output
CO	Carbon Monoxide
CO_2	Carbon Dioxide
CP	Cabin Pressure
CPAP	Continuous Positive Airway Pressure
CPAP	Continuous Positive Airway Pressure
CPCS	Cabin Pressure Control System
CPETL	Cockpit Pressurization Engineering Test Laboratory
CPG	Clinical Practice Guideline
CPS	Cabin Pressurization System
CRM	Crew Resource Management
CRU-##	Oxygen Regulators
CSV	Cabin Safety Valve
CT	Continuation Training
cv	Coefficient of Variation
CVA	Cerebral vascular attack; cerebrovascular accident, a “Stroke
DAA	Denitrogenation Absorption Atelectasis
DCI	Decompression Illness
DCS	Decompression Sickness
DEGD	Degraded Ability to Display Cautions
DFF	Deep Feed-Forward
DFRL	Internal Fault Code
DHA	Docosahexaenoic acid
DL	Diffusing Capacity of the lung
DLCO	Diffusing Capacity of the Lung for Carbon Monoxide

DLP	Delta Line Pressure
DMO	Dive Medical Officer
DMP	Differential Mask Pressure
DoD	Department of Defense
DODAF	Department of Defense Architecture Framework
DUMBELS	Diaphoresis and Diarrhea; urination; miosis (constricted pupils); bradycardia, bronchospasm, bronchorrhea; emesis; excess lacrimation; and salivation
e	Amount of Error
EBN	Exhale Breath #
ECLSS	Environmental Control and Life Support System
ECS	Environmental Control System
EEG	Electroencephalography
EGT	Exhaust Gas Temperature
EI	Engineering Investigation
EMER	Emergency
EMI	Electromagnetic Interference
EOS	Emergency Oxygen Subsystem
EPA	Environmental Protection Agency
ERV	Expiratory Residual Volume or Expiratory Reserve volume
ERV	Expiratory Residual Volume
ESB	Exhalation Sensor Block
$ETCO_2$	End Tidal Carbon Dioxide
ETR	Expected Thrust Request
F	Flow Rate
FCF	Functional Check Flights
FCP	Front Cockpit
FEV	Forced Expiratory Volume
FFT	Fast Fourier Transform
FiO_2	Fraction of Inspired Oxygen or Inhaled Oxygen
F_IO_2	Fractional Inspired Oxygen Content
FIV	Forced Inspiratory Volume
FIVC	Forced Inspiratory Vital Capacity
FL	Flight Level
FLYT	Fly Like You Test
fMRI	flow Magnetic Resonance Imager/Imaging
FOD	Foreign Object Damage
FOQA	Flight Operations Quality Assurance
FOR	Findings, Observations and NESC Recommendation
FPA	Flight Path Angle
fpm, FPM	feet per minute, Flight Path Marker
FPV	Flight Path Vector
FRC	Functional Residual Capacity
ft	Foot
ft/s	Feet per Second
ft/s^2	Feet per Second Squared

FVC	Forced Vital Capacity or Functional Vital Capacity
FWHM	Full Width at Half Maximum
G	Gravity
G_3	Acceleration Vector
GC-MS	Gas Chromatography – Mass Spectrometry
GE	General Electric
GFE	Government Furnished Equipment
GGU-12	Slimline Oxygen Concentrator (Manf: Cobham)
GLM	Generalized Linear Model
G-LOC, GLOC	Gravity-induced Loss Of Consciousness
Gz	rate of change of vertical gravity (gz) with height (z) - vertical gravity gradient
H_2O	Water
HAZREP	Hazard Report
HbCO	Carboxyhemoglogin
HBO	Hyperbaric Oxygen
HBOT	Hyperbaric Oxygen Treatment
HEI	Human Error Identification
HF	Human Factors
HFACS	Human Factors and Classification System
HFE	Human Factors Ergonomics
HMAPS	Holistic Modular Aircrew Physiologic Status Monitoring System
HPW	Human Performance Wing
HSI	Human System Integration, Horizontal Situation Indicator
HUD	Heads-Up Display
Hz	Hertz
I/O	Input/Output
I:E	Inspiratory Expiratory Ratio
IC	Inspiratory Capacity
ICAWS	Integrated Cautions and Warnings System Can also stand for Intersection Collision Avoidance Warning System
ICD	Interface Control Documents
ICU	Intensive Care Unit
ID	Identity or Identification
iDMP	instantaneous Delta Mask Pressure
IETM	Interactive Electronic Technical Manuals
IMCWS	In-Mask Carbon Dioxide and Water Vapor Sensor
IMS	In-Mask-Sensor
IMS	Inductive Monitoring System
INS	Inertial Navigation System
IP	Instructor Pilots
IPT	Integrated Project Team
IR	Infrared
IRV	Inspiratory Reserve Volume
ISB	Inhalation Sensor Block
ISST	In-Service Support Team

IVC	Inferior Vena Cava or Inspiratory Slow Vital Capacity
JCAST	Joint Combined Aircrew Systems Tester
JDRS	Joint Defense Reporting System
JPL	Jet Propulsion Laboratory
JPO	Joint Program Office
JSF	Joint Strike Fighter, the F-35
KCAS	Knots Calibrated Airspeed
kft	Kilofoot
kft/minute	Kilofeet per Minute
LAM	Laser Air Monitor
LED	Light Emitting Diode
LOC	Loss of Consciousness
LOX	Liquid Oxygen
LPM or lpm	Liters per Minute
LPS or lps	Liters Per Second
LS	Life Support
LSS	Life Support Specialist
M	Meter
MASES	MAsk SEnsor System
MaskP	Sum of Cabin Pressure and Mask Pressure
MAX	Maximum
MBU	Mask Breathing Unit
MDS	Mission Design Series
MEG	Magnetoencephalography
MFI	Microvascular Flow Index
MICROS	Miniature Integrated Circuits Reporting Overall Status
MIL-STD	Military Standard
min	Minute
M_{IPO}	Maximal Inspiratory Pressure
MIR	Medical International Research
mJ	Millijoule
ML	Machine Learning
mL	Milliliter
mm	Millimeter
mmHg	Millimeters of Mercury (pressure)
MP	Mask Pressure
Mpbs	Megabits per second
MRI	Magnetic Resonance Imaging
ms	Millisecond
MSL	Mean Sea Level
MSOGS	Molecular Sieve Oxygen Generation System
MSP	Maintenance Status Panel
MU	Memory Unit
MURS	Memory Unit Rosetta Stone
MV	Minute Volume
MV	Minute Ventilation

mW	Milliwatts
NACES	Navy Aircrew Common Ejection Seat
NAMI	Naval Aeromedical Institute
NAMP	Naval Aviation Maintenance Program
NAMRL	Navy Aeromedical Research Laboratory
NAMRU-D	Naval Medical Research Unit - Dayton
NAS	Naval Air Station
NATEC	Naval Air Technical Data and Engineering Service Center
NATOPS	Naval Air Training and Operating Procedures Standardization
NAVAIR	Naval Air Systems Command
NAVFLIR	Naval Aircraft Flight Record
NAVSAFECEN	Naval Safety Center
NESC	NASA Engineering and Safety Center
NIBP	Noninvasive Blood Pressure
NIOSH	National Institute for Occupational Safety and Health
NMPHC	Navy and Marine Corps Public Health Center
NOSP	No Safety Pressure
N_R	Reynolds Number
NSP	No Safety Pressure
NSTI	Naval Survival Training Institute
NWW	Nose Wheel Well
O_2	Oxygen
OBOGS	On-Board Oxygen Generation System
OEM	Original Equipment Manufacturer
OFP	Operational Flight Program
OPNAV	Operations-Navy
ORM	Operational Risk Management
OSHA	Occupational Safety and Health Administration
OTM	Oxygen Transport Model
PA	Pressure Altitude
P_ACO_2	Partial Pressure Of Carbon Dioxide, or Blood Carbon Dioxide
P_AO_2	Partial Pressure of Oxygen; Minimum Alveolar O_2 Pressure; Arterial Oxygen Level
PAO_2	Alveolar Oxygen Level
PBA	Pilot Breathing Assessment
PBA	Pressure Breathing for Altitude
PBG	Pressure Breathing for G
PCHIP	Piecewise Cubic Hermite Interpolating Polynomial
PCM	Personal Computer Memory
pCO_2	Concentration of Carbon Dioxide
PE	Physiological Episode
PE IPT	Physiological Episodes Integrated Project Team
PEAT	Physiological Episode Action Team
PEEP	Positive-End Expiratory Pressure
PEF	Positive end-expiratory pressure
P_{ESB}	Cabin Pressure

PFO	Patent Foramen Ovale
PFT	Pulmonary Function Test
pH	Acidity
PHYSIO	Physiologic Health Status of Isolated Personnel
Pi	Perfusion Index
PIC	Pilot Interface Connection, also Pilot in Command
PIF	Peak Inspiratory Flow
PIO	Pilot-in-the-Loop Oscillations
PIP or P_{IP}	Peak Inspiratory Pressure
P_{ISB}	Inhalation Pressure
PNF	Pressure-No-Flow
PNIAF	Peak Nasal Inhalation Flow
pO_2	Concentration of Oxygen
PO_2	Partial Pressure of Oxygen
PPB	Positive Pressure Breathing
$ppCO_2$	Partial Pressure of Carbon Dioxide
ppO_2	Oxygen Partial Pressure
ppO_2 or PPO_2	Partial Pressure of Oxygen
PPV	Proportion of Perfused Vessels
PR	Pulse Rate
PSA	Pressure Swing Adsorption
PSD	Power Spectral Density
PSI	Pounds per Square Inch
PSVD	perfused small vessel density
PTMS	Power and Thermal Management System
PTT	Press to Test
PUFA	Polyunsaturated Fatty Acid
PVD	Perfused Vessel Density
PVi	Pleth variability index
Q	Perfusion
Q	Supplied Turbulent Flow
QQ-plot	Quantile-Quantile Plot
R	Normalized Correlation
R	Respiratory quotient
r^2	goodness of fit
RAAF	Royal Australian Air Force
RAC	Risk Assessment Code
RAF	Royal Air Force
RAM	Residence in Aerospace Medicine
RCCA	Root Cause Corrective Action
RCM	Reliability Centered Maintenance
RCP	Rear Cockpit
RD	Rapid Decompression
Re	Reynolds Number
REML	Restricted Maximum Likelihood
RMS	Root Mean Square

ROBD	Reduced Oxygen Breathing Device
ROC	Rate of Change
ROS	Reactive Oxygen Species
RQ	Respiratory Quotient
RR	Respiration Rate
RRa	Acoustic Respiration Rate
RTB	Return to Base
RV	Residual Volume
s.d. MP	standard deviation Mask Pressure
S/N	Serial Number
SAD	Servo Air Dryer
SaO_2	Arterial Oxygen Saturation
SCUBA	Self-Contained Underwater Breathing Apparatus
SECNAV	Secretary of the Navy
SI	Stroke Index
SIR	Safety Investigation Report
SLL	Static Lung Loading
slpm	Standard Liter Per Minute
SLUDGE	Salivation, Lacrimation, Urination, Diarrhea, GI upset, Emesis
SME	Subject Matter Expert
SOD	Superoxide Dismutases
SOPs	Standard Operating Procedures
SP	Safety Pressure
SpHb	Total Hemoglobin
SpO_2	Oxygen Saturation or peripheral hemoglobin saturation
st. dev. MP	standard deviation Mask Pressure
STPD	Standard Temperature Pressure Dry
SVRI	Systemic Vascular Resistance Index
T	True Value
TCP	Tricresyl Phosphate
TDL	Tunable Diode Laser
te	Exhale time
ti	Inhale time
TIR	Technical Independent Review
TLC	Total Lung Capacity
TLYF	Test-Like-You-Fly
TM	Tympanic Membrane
TRL	Technology Readiness Level
TS0, TS1	Technical Section (within report)
TTC	Teletronics Technology Corporation
t-tot	Total breath time
TUC	Time of Useful Consciousness
TV	Tidal Volume
UMO	Underwater Medical Officers
UPE	Unknown Physiological Event – usually due to hypoxia symptoms
UPG	Upper Pressure Garment

UPT	Undergraduate Pilot Training
URTI	Upper Respiratory Tract Infection
USAF	United States Air Force
USAFSAM	USAF School of Aerospace Medicine
USN	United States Navy
USNAC	US Naval Aeromedical Conference
UTC	Coordinated Universal Time
V	Ventilation Ratio
V/Q	Ventilation/Perfusion Ratio
VA/Q	Flow Rate Calculation (can be used to measure V/Q mismatch)
VC	Vital Capacity
VCM	Vital Capacity Maneuver
VCNO	Vice Chief of Naval Operations
VGE	Venous Gas Emboli
VO_2	Muscle Oxygen Consumption
VOC	Volatile Organic Compound
V_T	Tidal Volume
WESS	Web-Enabled Safety System
WFF	Wallops Flight Facility
WOB	Work Of Breathing
WSO	Weapons Systems Operator
X	Observed Value
ΔP	Differential Pressure
β	Beta
μm	Micrometer
μW	Microwatts

Appendices (Volume II)